Energy & Environments: Geology in the "Nether World" of Indiana County, Pennyslvania

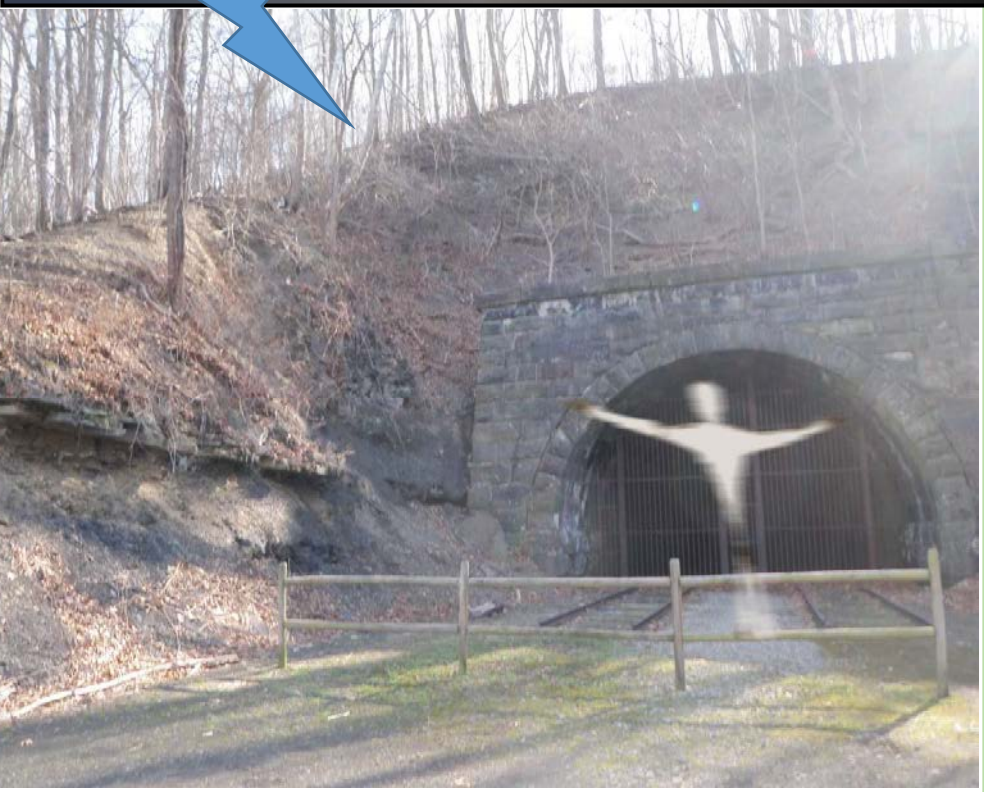

Hosts:

Pennsylvania Geologic Survey

University of Pittsburgh at Johnstown

Geoscience Department of Indiana University of Pennsylvania

October 6th – 8th 2016

81st Annual Field Conference of Pennsylvania Geologists

SYSTEM	SERIES	GROUP OR FORMATION	FORMATION OR MEMBER	MAJOR BEDS
PENN.-PERMIAN	UPPER PENNSYLVANIAN/ LOWER PERMIAN	DUNKARD GROUP (PART)	GREENE FORMATION	
			WASHINGTON FORMATION	Upper Washington limestone Washington coal bed
			WAYNESBURG FORMATION	Waynesburg "A" coal bed Waynesburg coal bed
? PENNSYLVANIAN	UPPER	MONONGAHELA GROUP	UNIONTOWN FORMATION	Uniontown coal bed
			PITTSBURGH FORMATION	Sewickley coal bed Redstone coal bed Pittsburgh coal bed
		CONEMAUGH GROUP	CASSELMAN FORMATION	Morgantown sandstone Skelley marine zone
			GLENSHAW FORMATION	Ames marine zone (prominent) Pittsburgh red shale Noble marine zone (less prominent) Upper Bakerstown coal bed Carnahan Run marine zone (less prominent) Woods Run marine zone (prominent) Lower Bakerstown coal bed Nadine marine zone (less prominent) Pine Creek marine zone (prominent) Brush Creek marine zone (prominent) Brush Creek coal bed Mahoning sandstone (Big Dunkard*) Zone of brackish-water fossils Mahoning coal bed (F)
	MIDDLE	ALLEGHENY FORMATION		Upper (E) } Freeport coal beds Lower (D) } Upper Kittanning (C') coal bed Johnstown limestone Middle (C) } Kittanning coal beds Lower (B) } Vanport limestone Clarion (A') and Brookville (A) coal beds
		POTTSVILLE FORMATION		Homewood sandstone (First Salt sand*) Upper } Mercer coal beds Lower } Upper Connoquenessing sandstone (Second Salt sand*) Quakertown coal bed Lower Connoquenessing sandstone (Third Salt sand*) Sharon coal bed
	? LOWER			
MISSISSIPPIAN	UPPER	MAUCH CHUNK FORMATION		Mauch Chunk red beds
			LOYALHANNA MEMBER	Loyalhanna Limestone (Big lime*)
		POCONO FORMATION		Burgoon Sandstone Shenango sandstone

GUIDEBOOK FOR THE
81ST ANNUAL FIELD CONFERENCE OF PENNSYLVANIA GEOLOGISTS
OCTOBER 6 — 8, 2016

ENERGY AND ENVIRONMENTS:
GEOLOGY IN THE "NETHER WORLD" OF INDIANA COUNTY, PENNSYLVANIA

Editor

Robin Anthony, Pennsylvania Geological Survey, Pittsburgh, PA

Field Trip Organizers, Leaders and Guidebook Contributors

Joan Hawk, CME Management, LLC
William A. "Bill" Bragonier, coal geologist, retired

Field Trip Leaders and Guidebook Contributors

John A. Harper, Joseph R. Tedeski,
Pennsylvania Geological Survey, retired

Neil Coleman, Uldis Kaktins, Christopher Coughenour, Stephen R. Lindberg, Ryan Kerrigan,
University of Pittsburgh – Johnstown

Karen Rose Cercone, Indiana University of Pennsylvania

Harold Rollins, University of Pittsburgh

Frank J. Vento, Anthony Vega
Clarion University of Pennsylvania

David "Duff" Gold, Alan Davis, Chuma Mbalu-Keswa
Penn State University

Ryan Mathur, Juniata College

Collin Littlefield, Shippensburg University

Stephanie Wojno, NW Missouri State University

Michael C. Rygel, SUNY Potsdam

Jeff Zick, Shawn Simmers
Cambria Cogeneration

Gary Merritt, Northern Star Generation Services Company LLC

John St. Clair, Rosebud Mining Company

Jackie Ritko, Cambria County Conservation District

Jacqueline Hockenberry, J Hockenberry Environmental Services, Inc

Jack D. Beuthin, Weatherford Laboratories

Todd Coleman, Minetech Engineers Inc.

Gareth D. Mitchell, EMS Energy Institute

Arnold G. Doden, GMRE, Inc.

Hosts

The Pennsylvania Geologic Survey, The University of Pittsburgh at Johnstown, The Geoscience Department of Indiana University of Pennsylvania

Headquarters

Park Inn by Radisson, 1395 Wayne Avenue, Indiana, PA 15701

Cartoons

John Harper

Cover

Railroad tunnel through Bow Ridge, near Conemaugh Dam

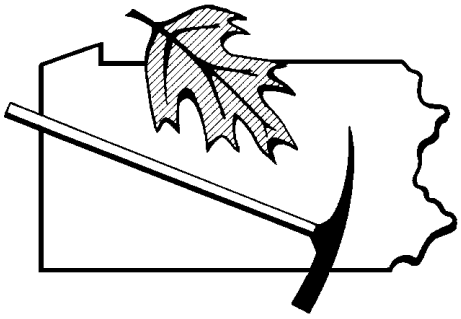

TABLE OF CONTENTS

STRATIGRAPHIC COLUMN ..... inside front cover
ACKNOWLEDGMENTS v
IN MEMORIAM–Emeritus Professor Uldis Kaktins, University of Pittsburgh at Johnstown vi
INTRODUCTION 1
Reference 2
STRUCTURAL GEOLOGY OF THE SOUTHWESTERN SECTION OF THE APPALACHIAN PLATEAU 3
Introduction 3
General Geology 3
Formation 5
Intra-Plateau Structural Front 6
Silurian Salina Group 6
Folds 7
Laurel Hill anticline 7
Chestnut Ridge anticline 8
Lineaments 8
Summary 9
References 9
LUCERNE COAL REFUSE SITE – CAMBRIA RECLAMATION CORP, CENTER TOWNSHIP, INDIANA COUNTY: RECLAMATION VIA COAL REFUSE FIRED ELECTRIC GENERATION UNITS 11
Executive Summary 11
Pennsylvania's Abandoned Mine Land Problem including Coal Refuse Sites 13
Land 13
Water 13
Air 13
PURPA 14
Fluidized Bed Combustion Technology 15
Introduction - Lucerne Coal Refuse site 17
Lucerne's Location 19
History of the Lucerne Mine Complex 20
Geologic and Groundwater Overview of the Lucerne Coal Refuse Site 21
The Mining Operation 23
Summary and the Dilemma 24
References 24
ROSEBUD MINING AND THE ST. MICHAEL DISCHARGE WATER TREATMENT PLANT, ST. MICHAEL, PENNSYLVANIA – TOPPER RUN DISCHARGE 25
Introduction 25
Background History 27
The "Berwind Mine Pool" 27
Topper Run Water Chemistry 28
Components of the Treatment Plant 29
Conclusion 30
References 30
A PRELIMINARY ANALYSIS OF AN UPPER PENNSYLVANIAN FLUVIAL CHANNEL COMPLEX OF THE CASSELMAN FORMATION (CONEMAUGH GROUP) EXPOSED ALONG US-22 NEAR BLAIRSVILLE, PA 31
Introduction 31
Methodology 33
Casselman Formation in the study area 33
Facies descriptions and interpretations 34
Facies Fl (fine-grained, laminated) 35
Facies Shr (sandy, horizontal to ripple-laminated) 35
Facies Fm (massive mudstone/siltstone) 36
Facies Shm (very sandy, horizontal to faint lamination) 36
Facies Se (sandy scours with crude bedding and intraclasts) 38
Facies St (sandy, trough cross-bedding) 38
Facies Sl (sandy, low-angle cross-bedding) 39
Local coal and claystone 40

Architectural elements: 40
Interpretation of fluvial style 43
Conclusion 44
References: 44
SOME GEOLOGICAL CONSIDERATIONS OF THE MARINE ROCKS OF THE GLENSHAW FORMATION (UPPER PENNSYLVANIAN, CONEMAUGH GROUP) 47
The Glenshaw Formation 47
Glenshaw Cyclothems: Allocyclicity versus Autocyclicity 48
Glenshaw Marine Zones 50
Brush Creek Marine Zone 50
Pine Creek Marine Zone: 51
Cambridge (Nadine) Marine Zone 52
Woods Run Marine Zone 53
Bakerstown Marine Zone 53
Ames Marine Zone 54
A Note on Casselman Formation Marine Zones 54
Problems and Resolutions of Identity and Correlation 55
References 57
Plates 60
PINE CREEK MARINE ZONE, US 422 BYPASS, KITTANNING 63
Introduction 63
Glenshaw Formation 64
Pine Creek Marine Zone 65
Correlation 65
Lithology 66
Fossils 68
Other Marine Zones 70
On The Nature of Lower Conemaugh Unconformities 71
References 73
STRATIGRAPHY, LITHOLOGY, AND SEA-LEVEL HISTORY OF THE BRUSH CREEK MARINE DEPOSITS OF THE GLENSHAW FORMATION 75
Introduction and History 75
Lithology and Petrology 76
Discussion of sea-level and regional events 79
References 83
EVIDENCE OF A SINGLE-EVENT DEPOSIT OVERLYING THE UPPER FREEPORT COAL SEAM IN CENTRAL WESTERN PENNSYLVANIA 87
Abstract 87
Introduction 87
Draw Rock Characteristics 88
Thickness Distribution 88
Influence on Mining 88
Lithology 90
Organic Content 91
Arguments for a Single-Event Deposit 92
Paleontological 92
Sedimentological 94
Regional Setting 96
Conclusions 99
Acknowledgements 100
References 100
STRATIGRAPHY OF FLINT CLAYS OF THE ALLEGHENY AND POTTSVILLE GROUPS, WESTERN PENNSYLVANIA 101
Introduction 101
Physical Properties 101
Definitions and Nomenclature 103
Stratigraphic Relationships 109
Genesis 110
Introduction 110
In-Situ Leaching 112

The Effects of Organics 113
Differential Colloidal Flocculation 113
Brecciation 115
Conclusions 117
References 117
THE ROGUE KIMBERLITE DIKES IN INDIANA COUNTY, PENNSYLVANIA
part 1. UNUSUAL INTRUSIVE HABIT OF KIMBERLITE DIKES IN COAL SEAMS 121
Abstract 121
Introduction 122
History and Previous Studies 124
The Barr Slope/Dixonville Mine Kimberlite 125
The Tanoma Mine Kimberlite 125
The Ernest Mine Kimberlite 127
The Sandy Ridge Kimberlite 129
Spatial and Thermal Nature of the Intrusions 129
Habit, Temperature, and Intrusive Mode 129
Geology of the Dixonville Dike 131
Geology of the Tanoma Dike 132
Mineralogy and Petrology 137
Olivine 140
Pyroxene 140
Ilmenite 141
Phlogopite 142
Garnets 143
Spinels 143
Micro-veins 143
Emplacement Depth and FO_2 Considerations 143
Tectonic Setting and Age of Emplacement 144
Summary and Conclusions 147
Acknowledgements 147
References 148
THE ROGUE KIMBERLITE DIKES IN INDIANA COUNTY, PENNSYLVANIA
part 2. COKED COAL MARGINAL TO KIMBERLITE INTRUSION IN THE TANOMA MINE 151
Introduction 151
Evaluation of Thermal History 152
Samples (see Part 1, Figure 12) 153
Analytical Protocol 154
Results and Discussion 155
Laboratory Carbonization Experiments 157
Conclusions 159
References 159
PALEOSOL DEVELOPMENT ALONG THE MISSISSIPPIAN-PENNSYLVANIAN UNCONFORMITY NEAR JOHNSTOWN, PENNSYLVANIA 161
Abstract 161
Introduction 161
Stratigraphic Setting 163
The Route 56 Paleosol 164
Outcrop Description 164
Micromorphology and Petrography 165
Bulk Mineralogical and Geochemical Features of the Boundary Mudstone 167
Discussion 170
Evidence of Intense Pedogenesis 170
A Polygenetic History 170
Relationship to the Mississippian-Pennsylvanian Unconformity 172
Conclusions 172
Acknowledgments 173
References Cited 173
GENETIC STRATIGRAPHY: LATE PLEISTOCENE THROUGH THE HOLOCENE PALEOCLIMATES AND PALEOENVIRONMENTS OF PENNSYLVANIA 177

Introduction ... 177
Introduction to Genetic Stratigraphy ... 177
Methodological Application and Implementation of Genetic Stratigraphy-Pennsylvania and the Middle Atlantic Region ... 184
(1.) Stratigraphic Sections: ... 186
(2.) Paleosols as Allogenic Units: ... 186
(3.) Initial Assumption of Allogenicity: ... 186
(4.) A and B Horizons in Alluvial Sequences: ... 191
(5.) Floating Sections and Use of Marker Horizons: ... 192
Stratigraphic Disconformities over the Last 12,000 Years ... 192
Paleoclimatology and Paleoenvironments ... 194
Pleistocene to Holocene Transition ... 194
The Last Glacial Maximum (22,000-14,000 BP. ... 197
The Bolling-Allerod Interstadial (LGM to 11,200 BP.) ... 202
The Younger Dryas (11,000 BP. - 10,100 BP.) ... 204
The Pre-Boreal (10,100-9100 BP.) and Boreal (9100-8000 BP.) ... 208
Holocene Environments ... 210
Pre-Boreal Climatic Episode (10,100 BP. - 9000 BP.) ... 210
Boreal Climatic Episode (9000 BP. - 8000 BP.) ... 211
Atlantic Climatic Episode (8000 BP. – 4200 BP.) ... 213
The Sub-Boreal Climatic Episode (4200 BP. - 3000 BP.) ... 215
The Sub-Atlantic Climatic Episode (3000 BP. - 1750 BP.) ... 219
Scandic (1750 BP. - 1250 BP.) ... 220
Neo-Atlantic (1100 BP. - 750 BP.) ... 220
Little Ice Age (Neoglacial) 750 BP. - 150 BP. ... 221
Modern (150 BP. - present) ... 222
Current Stratigraphic Practices in Geoarchaeology ... 223
References ... 223
DAM-BREACH HYDROLOGY OF THE JOHNSTOWN FLOOD OF 1889 CHALLENGING THE FINDINGS OF THE 1891 INVESTIGATION REPORT *(selected excerpts)* ... 231
Abstract ... 231
1. Introduction ... 231
2. Background ... 232
2.1 Changes made to the South Fork dam ... 232
[See full paper for details on the development of the following figures] ... 237
5. Discussion ... 240
6. Conclusions ... 242
Acknowledgements ... 244
References ... 244
APPENDIX A: ARIPPA White Paper on Coal Refuse ... 247
What is coal refuse? ... 247
Where was and is coal refuse placed? ... 247
What problems do unreclaimed coal refuse sites cause? ... 248
Land ... 248
Water ... 249
Air ... 250
What is Pennsylvania's experience with reclaiming coal refuse sites? ... 251
What must be considered in the reclamation of coal refuse piles? ... 252
Alternative Solution for reclaiming coal refuse impacted areas ... 253
What processes do coal refuse-fired units use to solve the problems associated with abandoned coal refuse sites? ... 255
What is the air emission profile of a coal refuse-fired CFB boiler? ... 256
What are coal ash or Coal Combustion Residuals (CCR) and how can they be beneficially used for reclamation of coal refuse sites? ... 257
Are there examples of the benefits provided by this reclamation? ... 257
Revloc, Pennsylvania ... 258
Maple Coal Site ... 259
APPENDIX B: PETROGRAPHY OF THE TANOMA AND ERNEST KIMBERLITES ... 263
SPONSORS ... inside back cover

ACKNOWLEDGMENTS

We extend special thanks to FCOPG officers, Katie Schmid, Kristen Hand, Stephen Shank and Connie Cross; trip organizers Joan Hawk and Bill Bragonier, stop leaders, guidebook contributors and volunteers,

and

- The bus company, Butler Motor Transit, Inc., for working with us to access even the least accessible outcrops
- The US government, for creating the interstate highway system that has given geologists the roadcuts to study these rocks, and flesh out the "Nether World" of Indiana County
- The traffic flagging service, Area Wide Protective, for keeping those roadcuts safe for geologists to examine

and

- Bill Bragonier, retired coal geologist, for his exhaustive work on the road log and his many fine articles discussing the relationship of the coal measures to the surrounding lithologies
- Dr. Frank Vento, Professor Emeritus, Department of Geology, Clarion University of Pennsylvania and President of Quaternary Geological and Environmental Consultants LLC, for speaking at our banquet
- John A. Harper, Pennsylvania Geologic Survey, retired, for continuing to provide "comic relief" on the blank pages of the roadlog and guidebook
- Thomas Whitfield, for his roadlog maps, and Michael Moore, for his cooperation
- Robin Anthony, for her patience and dedication editing the roadlog, stop descriptions and guidebook, and Katie Schmid, for standardizing the amazingly variable "references" format
- Joan Hawk, CME Management LLC, for relentlessly chasing down all the loose ends to pull this conference together

and especially

- **Lucerne Mines, for allowing us access to their bony pile and describing their operations**
- **Mr. Scott Steele, for allowing us access to the quarry on his land**
- **Mr. Polka, for allowing us access to his land**
- **Allied Van Lines, for allowing us to park our buses on their property**
- **John & Kathy Starr, for property access**
- **Conemaugh Valley Conservancy, for property access**

IN MEMORIAM

EMERITUS PROFESSOR ULDIS KAKTINS

UNIVERSITY OF PITTSBURGH AT JOHNSTOWN

Uldis Kaktins, long-time attendee of our field conference, passed away at his home on July 2nd after surviving cancer for three years. He was born in war-torn Riga, Latvia, at the height of WWII, and his family made their way to the United States while he was a child. He grew up in Boston where the family put down new roots, and he worked hard to get an education. The Vietnam War interrupted Uldis' graduate studies when he was deployed to Vietnam. He wrote a thesis by hand on the floor of his Bachelor Officer's Quarters. He began teaching in Pitt Johnstown's Department of Earth & Planetary Science in 1975 and retired after a long career in 2008.

Emeritus Professor Uldis Kaktins is a beloved professor who touched the lives of thousands of students and inspired hundreds to pursue careers in geology, hydrology, and other fields in the earth sciences. Hydrology and flood studies were his passions, always focused on fieldwork. He was lead author of a 2013 paper about the 1889 Johnstown flood, published in the Pennsylvania History Journal. His latest paper on the 1889 flood was published in the journal Heliyon on June 16, 2016, the result of more than five years of research. Excerpts from that paper may be found in this conference guidebook. Uldis summarized the findings in an interview with a Johnstown reporter just days before his passing. "You still hear all of the time that there was supposedly so much rain that their dam would've been over-topped no matter what. That's simply not the case – and now we have the scientific facts to prove it."

You will also find in the older 1989 guidebook an article Uldis wrote with the late Hal Fry of UPJ about the three historic floods that have struck Johnstown, in 1889, 1936, and 1977. We will visit the site of the South Fork dam on the second day of the conference to learn more about the latest research on the Johnstown flood of 1889. This year's visit to the Johnstown Flood memorial is dedicated to Emeritus Professor Kaktins.

INTRODUCTION

JOAN HAWK, CME MANAGEMENT LLC

I have been asked why the Field Conference is being held in Indiana, "What of geological significance is there to see in Indiana County?" they ask. The sub-title, "Geology in the Netherworld of Indiana County" is apt…and historically correct. P. Lesley, in his preface to the Report of Progress in Indiana County, volume HHHH (1878) states,

> "Connections between the geology of the Allegheny River, worked out by the first Survey previous to 1841, and the geology of the counties bordering on the Allegheny Mountain and the Maryland State line, have hitherto been unsatisfactory because imperfect; the almost unexplored region of Indiana and West Armstrong counties acting as a barrier over which none of our vague hypotheses of identification could pass either way. Covered as this region is with the Barren Measures, and large parts of it being until recently an almost unbroken forest, mine exposures have always been wanting, and natural exposures difficult to find, and when found hard to collate. The first geological survey of Pennsylvania therefore passed to the right and left of Indiana County, and nothing of account was done in subsequent years to discover its minerals and explain its geology…" The survey now happily completed by Mr. W. G. Platt places the geology of Indiana in clear light".

Several important observations were made to place the stratigraphic units of Indiana County in proper context with those of adjacent counties. One of these observations was that the earlier surveys of Cambria and Somerset counties in 1875-7 had "revealed the startling truth that there were several other important and persistent limestone horizons in the lower coal measures and in the barren measures, not one of which could be made to correspond properly with the Ferriferous Limestone (Vanport) and Buhrstone iron of the Allegheny region" (Lesley, 1878).

The presence of multiple limestone beds had resulted serious stratigraphic miscorrelation between the western and eastern sides of Pennsylvania's third Coal Basin during the First Geological Survey. During the Second Survey, Platt was unable to find the Ferriferous Limestone at its expected position in Indiana County east of the Indiana anticline. Another observation was that of an extensive sandstone "fault" in the Pittsburgh Coal, described by Platt as "representing a line of ancient (stream) erosion in the old swamps and lagoons in which the vegetation for the formation of the coal was collected."

The Pittsburgh Coal outcrops in the valley of the Conemaugh River at Blairsville and on the southern valley wall, above remnants of the Pennsylvania canal, collapsed workings on the Pittsburgh Coal can be seen. The coal is overlain by the massive Pittsburgh Sandstone. The face of the exposed sandstone is coated with an efflorescence of alum that "blossoms" out of the strata that gives the cliff face a pitted and "honeycomb" pattern. This outcrop, known as Alum Hill" is best accessed from the Conemaugh River at Blairsville.

Regardless of Lesley's proclamation, Indiana County retained geologic puzzles into the 20th and 21 centuries and corrections to second survey work were made during subsequent investigations by the Pennsylvania Geological Survey and others. Road cuts, railroad cuts, surface

mines, and deep mines exposed stratigraphic enigmas that would not have been otherwise brought to light.

The exploration programs of the former Rochester & Pittsburgh Coal Company and a recent roadcut in Indiana County revealed what shouldn't be—the Upper Freeport Coal transitioning into flint clay and limestone. A buried log jam revealed in the roof of an Upper Freeport Coal deep mine in Indiana County, seen by only a few, remains hidden from view. In adjacent Armstrong County, a similar phenomenon on the Upper Freeport Coal occurs at the surface exposure; however, this outcrop will disappear into the "mists of time" because after this year's field conference views it, the landowner is placing it off limits to further visitations. The Pennsylvania Department of Environmental Protection requires that surface mines are to be backfilled soon after mining ceases and PennDOT has a similar mindset. However, sometimes a particularly striking outcrop, such the Morgantown Sandstone along the ramps at the intersection of Routes 22 and 119 near Blairsville, escapes the plague of crown vetch or other plant that is used as a "cloaking device". Several Indiana County coal mines revealed the presence of Jurassic Age dikes intruding into Pennsylvanian Age coal beds. We won't get to see them because there are no known surface exposures; however, this year's guidebook contains a body of current work that synthesizes the current state of knowledge and photodocumentation that will guide future work.

The theme of energy and environments is appropriate for this year's field conference, although perhaps not in the most obvious way. Indiana County has an abundance of energy resources – coal and gas. At the time of the second survey publication HHH, gas was barely mentioned. If only Lesley could see a map of the gas wells that have been drilled since the publication of Volume HHHH. Coal and gas are one source of energy. The other "energy" is that of the paleoenvironments preserved in the rock record. We will see in outcrop the preserved remnants of high energy paleo-rivers and their associated strata low energy environments. Unfortunately as soon the stratigraphy of the county is exposed, it is almost covered up again, or made inaccessible. The geology of Indiana County has been preserved, uncovered and hidden again—will we ever be able to decipher the geologic past here with only such fleeting glimpses?

Reference

Platt, W.G., 1878, Report of Progress in Indiana County: Pennsylvania Geological Survey, 2nd ser., vol HHHH, 316 p.

STRUCTURAL GEOLOGY OF THE SOUTHWESTERN SECTION OF THE APPALACHIAN PLATEAU

RYAN KERRIGAN, DEPARTMENT OF ENERGY AND EARTH RESOURCES, UNIVERSITY OF PITTSBURGH AT JOHNSTOWN, 450 SCHOOLHOUSE ROAD, JOHNSTOWN, PA 15904

Introduction

The Appalachian plateau is the westernmost province of the Appalachian mountain belt and stretches from Alabama to New York. The Appalachian plateau is characterized by broad, low, open folds with dips ranging from 20° to less than 5°. Wavelengths of the folds range from 5 to 20 miles and the structural relief can be a few hundred to greater than 3,500 feet. The structural trends show fold amplitudes that decrease from the eastern margin to the western margin. Various structural lineaments, or cross-strike structural discontinuities, cross-cut the Appalachian plateau generally perpendicular to fold axes. The structural development of the Appalachian plateau ranges from Precambrian age, with Grenvillian basement structural features influencing lower stratigraphic levels, to Permian age with Allegheny orogeny development of décollement slip and folds. Much debate has occurred to determine the timing of fold development and the influence of the basement of the Appalachian plateau. This paper will focus on the key structural features of the Appalachian plateau in southwestern Pennsylvania.

General Geology

The Pennsylvania state portion of the Appalachian Plateau can be broken up into several sub-provinces or sections (Figure 1-1). This brief structural geology summary will focus on literature covering the Pittsburgh Low Plateau Section and the Alleghany Mountain Section. The plateau province comprises almost entirely sedimentary rocks in gentle folds with large wavelengths and amplitudes that decrease to the northwest. Most folds are asymmetrical with the steep flank dipping to the southeast. Anticlines commonly have dips ranging from 3° to 12° on their northwestern flanks and from 4° to 20° on their southeastern flanks, however, larger dips have been measured throughout the plateau at scattered localities (Hickok and Moyer, 1971; Harper, 1989; Beardsley et al., 1999). Fold axes are generally arcuate and remain parallel to sub-parallel to the arcuate trend of the Appalachian mountain range seen in central Pennsylvania. Folds generally trend northeast to southwest and plunge 1° to 2° to the northeast (Iranpanah and Wonsettler, 1989). Overall the plateau is characterized by generally level surface with some rolling hills which are at an altitude great enough to permit erosion of deep valleys by streams.

The general stratigraphy is Pennsylvanian through Cambrian sedimentary units deposited on a metamorphic Precambrian basement. Most models of the plateau show anticlines and synclines extending down to a décollement surface within salts of the Silurian Salina Group. The Appalachian plateau is often cited as the type example of broad zone, layer-parallel shortening with subordinate splay faults in the hanging wall of the detachment sheet (Gwinn, 1964; Rodgers, 1964; Scanlin and Engelder, 2003). Layers of rock above the décollement are referred to as the Appalachian plateau detachment sheet and were folded above the décollement by a variety of mechanisms. Using seismic reflection data Scanlin and Engelder (2003) were able to discern the following three-tiered mechanical stratigraphy: a thin basal detachment zone in Upper Silurian

strata, an imbrication zone within Upper Silurian through Lower/Middle Devonian strata, and a wedge zone within Upper Devonian and Mississippian strata.

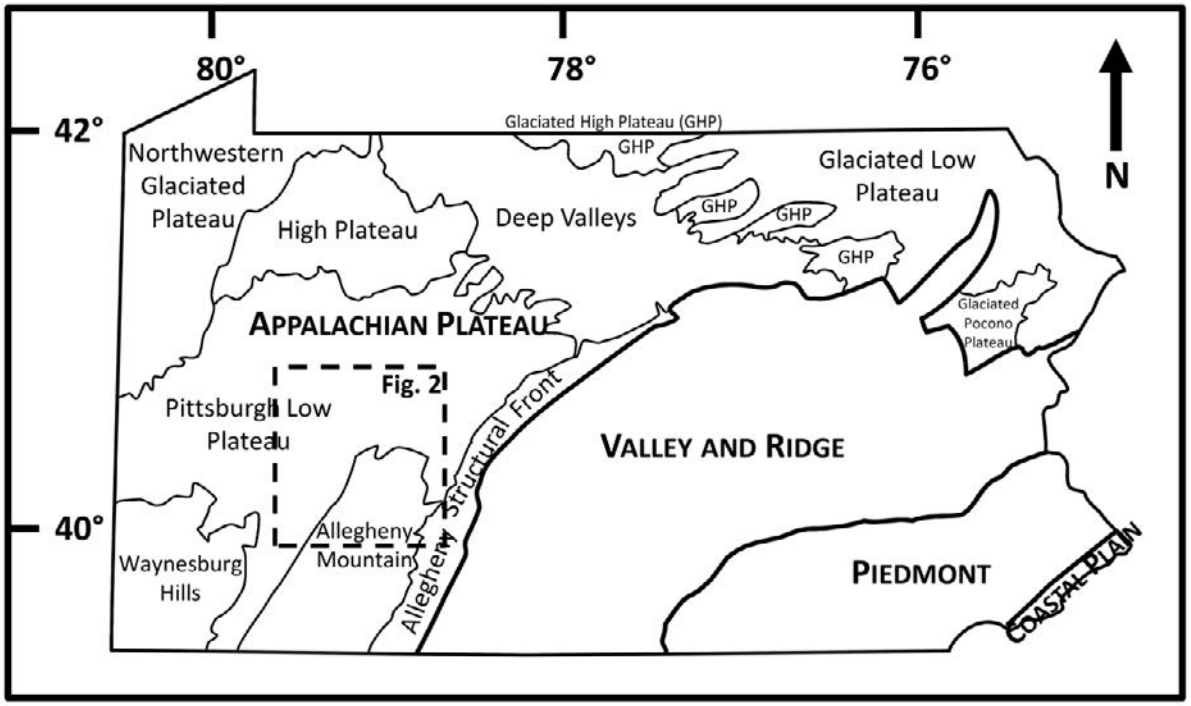

Figure1-1. Generalized physiographic provinces of Pennsylvania with province sections for the Appalachian Plateau (Berg et al., 1980)

Above the detachment zone, at the core of plateau anticlines, seismic data support the presence of imbricated thrusts of splay faults that exhibit fault-propagation folds, fault-bend folds, and kink banding morphology (Scanlin and Engelder, 2003; Gillespie et al., 2015). These imbrications are observed to cut the Lower/Middle Devonian units which are composed of carbonates (Tully, Onondaga, and Helderberg limestones) and interbedded clastics (Marcellus shale and Oriskany sandstone). Above the imbrication zone is an area that exhibits wedge thrusts with a combination of foreland and hinterland thrust directions (Scanlin and Engelder, 2003).

Proximity to the Allegheny structural front and variation of thickness of the salt detachment appears to control the variation of subsurface structural style and structural relief (Wiltschko and Chapple, 1977). Detachment and translation occurred during the Pennsylvanian-Permian Alleghenian Orogeny. Mount (2014) estimated the shortening necessary to create observed structural is approximately 1-2%. However, Scanlin and Engelder (2003) note that movement along the salt décollement alone is insufficient to account for the fold amplitude in the Bedford-Pittsburgh region and that additional mechanisms are required for full anticlinal growth. It is postulated that some salt doming within the Salinas Group has contributed to folding (Wiltschko and Chapple, 1977). When examining the folds within the context of buckle fold mechanisms, relatively modest length to spacing ratios are predicted (Biot, 1961). However, the anticlines of the Allegheny plateau have large aspect ratios which are more akin to forced folds centered on basement involved faulting indicating that there are important footwall structures involved in fold development (Scanlin and Engelder, 2003). Evidence appears to suggest that the evolution of the Appalachian plateau folds are a complex intermingling of mechanisms including:

décollement slip and buckling; hanging wall thrusts, imbrications, and wedging; kink banding; salt doming; pervasive layer-parallel shortening; and footwall faulting in basement rocks.

Formation

The classic model for the Appalachian plateau detachment sheet involves periodic buckling above a detachment in salt (Wiltschko and Chapple, 1977). There are two hypotheses for the formation of the large-scale folds of the Allegheny Plateau: folds are the result of thin-skinned tectonics which deformed the upper layers without basement deformation (Rodgers, 1949, 1953, 1964; Gwinn, 1964); folds are the result of deep basement faulting that passively folded the upper layers (Cooper, 1964).

The Grenvillian basement in the plateau has various décollement ramps, tear faults, and transform faults from the Grenville orogeny (~1 Ga) that were later reactivated to influence folding throughout the plateau (Beardsley et al., 1999). These Grenvillian structures initiated a large graben (the Rome Trough) and growth faults within the overlying Cambrian strata during tensional stress related to rifting in the Cambrian. The Appalachian plateau region was primarily a sedimentary basin during much of the Paleozoic which facilitated deposition of thick sedimentary sequences that were shed from the eastward Taconic and Acadian mountain belts. The Paleozoic sedimentary sequence is occasionally punctuated by limestone units. Throughout the Taconic orogeny (480-440 Ma) the plateau underwent compression stresses which created a series of monoclinal flexures across the old growth-faulted terrane (Beardsley et al., 1999). During the Acadian/Caledonian orogenies (~390 Ma) down-warping of monoclinal flexures occurred. Stresses imposed by the Alleghenian orogeny (~260-340 Ma) pushed strata along a basal detachment creating the Appalachian Plateau detachment sheet and induced thrusting and folding within the detachment sheet creating much of the structure present in the plateau today.

Examination of several types of strain indicators (e.g., deformed fossils, solution cleavage, and mechanically twinned calcite grains), studies have been able to show that there has been approximately 10% layer-parallel shortening throughout the Appalachian plateau (Nickelsen, 1966; Engelder and Engelder, 1977; and Engelder, 1979). Strain indicators are oriented at right angles to the northwestward movement of the orogenic front and suggest that layer-parallel shortening occurred prior to folding (Gillespie et al., 2015). Recent estimates of the shortening needed to create the folding present in the Appalachian plateau are approximately 1-2% (Mount, 2014).

Asymmetry of folds (i.e., shallow northwesterly limbs and over-steepened southeasterly limbs) in the Appalachian plateau has been the source of much debate. This asymmetry in the folds of the plateau is the exact opposite trend seen in the Valley and Ridge province to the east. Sherrill (1934) proposed that the asymmetry was caused by an overall southeasterly regional dip at the time of deformation and the southeasterly thickening of the folded sequence. Others have suggested that the asymmetry was developed by basement-driven, deep-seated underthrusting of northwest limbs by the southeast limbs (Cathcart and Myers, 1934). Gwinn (1964) developed a complex model of splay faulting shearing off the décollement and translating wedges of material northwest into the northwesterly limbs of the folds reducing the northwestern limb dips and over-steepening the southeasterly limbs. Seismic interpretations conducted by Mount (2014)

suggest that fold asymmetry is created by mechanically pinched out salt at synclinal locations at the décollement level buttressing the folds and accentuating asymmetry.

Intra-Plateau Structural Front

Gwinn (1964) identified significant decrease in structural relief going toward the foreland which he subdivided into the Inner plateau, to the east, and the Outer plateau, to the west, along an intra-plateau structural front (Figure 1-2). The Intra-Plateau Structural Front is a demarcation within the plateau where a change in the character of folding is apparent. The Intra-Plateau Structural Front is present on the west side strike parallel to the Chestnut Ridge anticline and separates the relatively more intense folding of the southeastern portion of the plateau from the gentler, less intense folding of the northwestern portion of the plateau (Gwinn, 1964). The broad gentle folds of the Outer plateau region commonly have dips less than 5° on their limbs whereas the Inner plateau often has dips from 5° to 20° on their limbs.

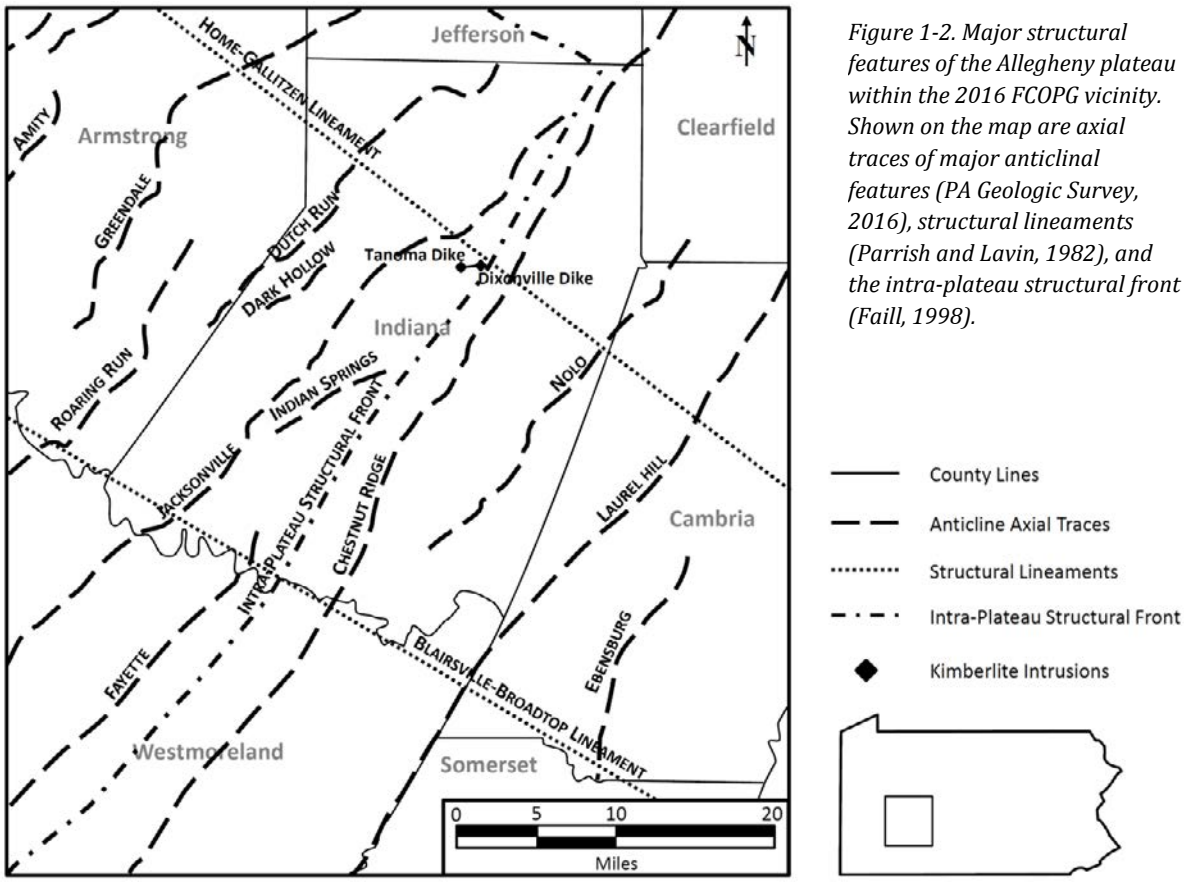

Figure 1-2. Major structural features of the Allegheny plateau within the 2016 FCOPG vicinity. Shown on the map are axial traces of major anticlinal features (PA Geologic Survey, 2016), structural lineaments (Parrish and Lavin, 1982), and the intra-plateau structural front (Faill, 1998).

Silurian Salina Group

Most models for the plateau folds suggest detachment along the Silurian Salina salts with overlying imbrication zones within the incompetent Devonian shales punctuated by limestones, folding the units above. In southwestern Pennsylvania the Salina Group generally consists of: the Vernon formation, a unit of red and green shale, and the Syracuse formation, an interbedded dolomite, anhydrate, and salt. Along with two other minor formations, the Camillus and Bertie

formations, the overall thickness of the Salina Group is approximately 650 meters (Heyman, 1977). There are at least six major salt units within the Salina Group designated "A" through "F". Two notable salt layers within the Syracuse formation, the F-2 and F-3 salts have been measured to exceed 50 meters in thickness. However, the F-2 and F-3 salts are not regionally continuous and therefore are unable to accommodate the full décollement of the plateau (Heyman, 1977). It believed that the Vernon shales must accommodate some of the detachment (Scanlin and Engelder, 2003). In northwestern Pennsylvania the folds die out, this is attributed to a reduction of stress but also the pinching out of the Salina salts (Frey, 1973).

Folds

Numerous folds transect the plateau region (Figure 2) and two major folds within this region, the Laurel Hill anticline and the Chestnut Ridge anticline, are further examined. Both folds are broad, open, slightly asymmetric folds with accurate axial trends that are approximately 030°. The folds plunge 1° to 2° to the northeast and both folds extend for over 125 miles. The Laurel Hill and Chestnut Ridge anticlines lie within the Inner plateau region of the Appalachian plateau with the northwestern margin of the Chestnut Ridge anticline serving as the limits of the Inner plateau region.

Laurel Hill anticline

The Laurel Hill anticline is an open, slightly asymmetrical fold with dip on southeastern limb ranging from 10° to 15° and 8° to 10° on the northwestern limb (Iranpanah and Wonsettler, 1989). The anticline, on average, is 8 miles wide and generally has a flat broad top that can be up to 2 miles wide. The amplitude of the Laurel Hill anticline to the adjacent synclines, the Ligonier syncline to the northwest and the Johnstown syncline to the southeast, is as much as 1,800 ft (Hickok and Moyer, 1971). However, the northwest limb of the Laurel Hill anticline has been uplifted slightly more than the southeast limb giving the northwest limb slightly less structural relief (Hickok and Moyer, 1971).

The Conemaugh River cuts through the Laurel Hill anticline just west of Johnstown creating the Conemaugh Gorge. The creation of the Conemaugh Gorge is thought to be from an antecedent river that existed before the surface expression of the Laurel Hill anticline (Iranpanah and Wonsettler, 1989). The Conemaugh Gorge is approximately 1,500 ft in relief, trends 330° and provides a well exposed cross-section of Pennsylvanian, Mississippian, and Devonian strata (Iranpanah and Wonsettler, 1989).

Scanlin and Engelder (2003) subdivide the subsurface of the Laurel Hill anticline into three tiers: an Upper Devonian wedge zone, a Silurian through Lower/Middle Devonian imbrication zone with central triangle structures, and a Silurian detachment zone. Thrust wedges within the wedge zone of the Laurel Hill anticline have been measured to be approximately 1,400 ft thick (Scalin and Engelder, 2003). There is evidence for basement involved faulting beneath the Laurel Hill anticline in the form of monoclinal bends that show little indication of detachment in seismic reflection, however, the seismic data show some deep high angle faults (Scalin and Engelder, 2003).

Chestnut Ridge anticline

The Chestnut Ridge anticline is an open, slightly asymmetrical fold with dip on southeastern limb are up to 15° to 20° and on the narrower northwestern limb approximately 10° or less (Shumaker, 2002). The anticline is about 8-10 miles wide with a generally flat broad top. Unlike the Laurel Hill anticline, the southeast limb of the Chestnut Ridge anticline has been uplifted slightly more than the northwest limb (Hickok and Moyer, 1971). The asymmetry of uplift provides varied structural relief with respect to the adjacent synclines. On the northwest limb of the Chestnut Ridge anticline, adjacent to the Uniontown syncline, structural relief is as much as 3,400 ft. The southeast limb of the Chestnut Ridge anticline, adjacent to the Ligonier syncline, structural relief is as much as 1,700 ft (Hickok and Moyer, 1971). Approximately 25 miles northeast of Indiana, near Johnsonburg, the Jacksonville anticline (also referenced as the Grapeville-Kinter Hill anticline) merges with the Chestnut Ridge anticline forming a broader Chestnut Ridge anticline which continues another 35 miles northeast.

Subsurface structure of the Chestnut Hill anticline displays the same three tier structure as Laurel Hill anticline as reported by Scanlin and Engelder (2003). Seismic reflection data shows that the Chestnut Ridge anticline has a thickened Upper Silurian section with doubly vergent blind thrusts at the level of the Lower/Middle Devonian section (Scanlin and Engelder, 2003). Passive concentric folding is accommodated above the blind splay faults in the Upper Devonian unit above the Lower/Middle Devonian faulted units. The footwall ramp can be seen in the reflection data cutting the F-2 and F-3 salt of the Syracuse formation at an angle of 25°. Additionally, thickening of the Vernon shale is seen by Scanlin and Engelder (2003) which fills some of the fold volume.

The change in structural styles between the southwest and northeast portions of the Chestnut Ridge anticline correlates to sub-detachment structures. Scanlin and Engelder (2003) used seismic data to suggest that, along the axis, changes in structural styles of the Chestnut Ridge anticline are due to the presence of the Rome Trough in the southwest portion which appears absent in the northeast portion of the Chestnut Ridge anticline. The southwestern portion of the Chestnut Ridge anticline subsurface exhibits extensive wedge thrusting at depth (Scalin and Engelder, 2003). Using a combination of well logs and seismic profiles along the southwest portion Shumaker (2002) identified subsurface structure that is more akin to faulted folds rather than traditional imbrications. The northeast portion of the Chestnut Ridge anticline seismic reflections indicate larger-scale imbrication in the imbrication zone leading to more coherent concentric folding throughout the Devonian section (Scanlin and Engelder, 2003).

Lineaments

Structural lineaments in this area have been identified using gravity, magnetic, structural, and Landsat data and represent fracture zones which penetrate deeply into the crust (Lavin et al., 1982). Using these data sets, several structural lineaments have been identified by observing the following: terminations and displacements in gravity and magnetic surveys; terminations of fold axes; high fracture densities; linear topographic depressions; zones of anomalous hydrocarbon leakage; and valley and stream alignments on Landsat images (Gold, 1999). Additionally, these fracture zones are occasionally visible in the field with the presence of: 0.3 to 1.2 miles wide zones of increased fracture density, geometrically related faulting and jointing, and Pb-Zn and Cu mineralization (Lavin et al., 1982). Where the lineaments intersect plateau

folds there is often a rapid decrease in the amplitude of folding, as much as 900 ft in some locations (Parrish and Lavin, 1982). The lineaments may represent fossil transform faults that have been later reactivated (Gold, 1999).

The Allegheny plateau is thought to be part of the Lake Erie-Maryland crustal block. This rectangular crustal block is thought to be approximately 60 miles wide and 350 miles in length and bound in the plateau region by the Tyrone-Mt. Union lineament to the northeast and the Pittsburgh-Washington lineament to the southwest (both trending approximately 320-330°). These two larger lineaments are considered to extend at least into the Precambrian basement, if not into the mantle (Lavin et al., 1982). Displacement along the Pittsburgh-Washington and Tyrone-Mt. Union lineaments has been identified and is thought to be as much as 35 miles left-lateral movement on the Pittsburgh-Washington lineament and 60 miles right-lateral movement on the Tyrone-Mt. Union lineament resulting in northwest translation of the Lake Erie-Maryland block during continental collisions (Lavin et al., 1982).

Two structural lineaments, the Blairsville-Broad Top and Home Gallitzin lineaments (Figure 2), are present within the 2016 Field conference vicinity and are considered to be within the Lake Erie-Maryland crustal block. Gravity and magnetic data for the Blairsville-Broad Top and Home Gallitzin lineament lack strong reflectance which compelled Parrish (1978) to suggest that they are confined to the sedimentary section and upper basement. Additionally, Parrish (1978) found no apparent evidence of major displacement suggesting that they are undisturbed within the block but interrupted or terminated along the deep crustal fractures beneath the bounding lineaments (i.e., the Pittsburgh-Washington and Tyrone-Mt. Union lineaments).

Summary

The structural geology of the Appalachian plateau can be deceptively complex when examining only the subtle features expressed at grounds surface. Debate about the exact mechanisms of deformation has engaged geologists for over a century. The recent wealth of seismic profiles related to increased petroleum hydrocarbon exploration in the plateau is providing the opportunity for more detailed research of subsurface features responsible for the architecture of the Appalachian plateau. As more data becomes available, it is apparent that this region will spur debate for years to come.

References

Beardsley, R.W., Campbell, R.C., and Shaw, M.A., 1999, Appalachian Plateaus, chap. 20 of Schultz, C.H., ed., The geology of Pennsylvania: Pennsylvania Geological Survey, 4th ser., Special Publication 1, p. 286-297.

Berg, T.M., Edmunds, W.E., Geyer, A.R., and others, compilers, 1980, Geologic map of Pennsylvania (2nd ed.): Pennsylvania Geological Survey, 4th ser., Map 1, 3 sheets, scale 1:250,000.

Biot, M.A., 1961, Theory of folding of stratified viscoelastic media and its implications in tectonics and orogenesis: Geological Society of America Bulletin, v. 72, p. 1595-1620.

Cathcart, S.H., and Myers, T.H., 1934, Gas in Tioga County, Pennsylvania: Pennsylvania Topographic and Geologic Survey, Bulletin 107, 42 p.

Cooper, B.N., 1964, Relation of stratigraphy to structure in the Southern Appalachians, in Lowery, W.D., ed., Tectonics of the Southern Appalachian Valley and Ridge: Virginia Polytechnic Institute, Department of Geological Sciences Memoir 1, p. 81-114.

Engelder, T., 1979, The nature of the deformation within the outer limits of the Central Appalachian foreland fold and thrust belts in New York State: Tectonophysics, v. 55, p. 289-310.

Engelder, T., and Engelder, R., 1977, Fossil distortion and décollement tectonics on the Appalachian plateau: Geology, v. 5, p. 457-460.

Faill, R.T., 1998, A geologic history of the north-central Appalachians, Part 3, The Allegheny orogeny: American Journal of Science, v. 298, p. 131-179.

Frey, M.G., 1973, Influence of Salina salt on the structure in New York-Pennsylvania part of the Appalachian Plateau: American Association of Petroleum Geologists Bulletin, v. 57, p. 1027-1037.

Gillespie, P., van Hagen, J., Wessels, S., and Lynch, D., 2015, Hierarchical kink band development in the Appalachian Plateau décollement sheet: American Association of Petroleum Geologists Bulletin, v. 99, p. 51-76.

Gold, D.P., 1999, Lineaments and their interregional relationships, chap. 22 of Schultz, C.H., ed., The Geology of Pennsylvania: Pennsylvania Geological Survey, 4th ser., Special Publication 1, p. 306-313.

Gwinn, V.E., 1964, Thin-skinned tectonics in the plateau and northwestern valley and ridge provinces of the central Appalachians: Geological Society of America Bulletin, v. 75, p. 863-900.

Harper, J.A., 1989, Geology in the Laurel Highlands of Southwestern Pennsylvania Introduction, in: Harper, J.A., ed., Geology in the Laurel Highlands, southwestern Pennsylvania: Annual Field Conference of Pennsylvania Geologists, 54th, Johnstown, Pa., Guidebook, p. 1-5.

Heyman, R., 1977, Tully (Middle Devonian) to Queenston (Upper Ordovician) correlations in the subsurface of western Pennsylvania: Pennsylvania Geological Survey, 4th ser., Mineral Resource Report 73, 16 p.

Hickok, W.O., and Moyer, F.T., 1971, Geology and Mineral Resources of Fayette County, Pennsylvania: Pennsylvania Geological Survey County Report 26, 530 p.

Iranpanah, A. and Wonsettler, S.C., 1989, Structural Geology, in Harper, J.A., ed., Geology in the Laurel Highlands of Southwestern Pennsylvania: Annual Field Conference of Pennsylvania Geologists, 54th, Johnstown, Pa., Guidebook, p. 6-22.

Lavin, P.M., Chaffin, D.L., and Davis, W.F., 1982, Major Lineaments and the Lake Erie-Maryland crustal block: Tectonics, v. 1, p. 431-440.

Mount, V. S. 2014, Structural style of the Appalachian Plateau fold belt, north-central Pennsylvania: Journal of Structural Geology, v. 69, p. 284-303.

Nickelsen, R.P., 1966, Fossil distortion and penetrative rock deformation in the Appalachian Plateau: Pennsylvania: Journal of Geology, v. 8, p. 924-931.

Parrish, J.B., 1978, The relationship of geophysical and remote sensing lineaments to regional structure and kimberlite intrusions in the Appalachian Plateau of Pennsylvania: University Park, Pennsylvania State University, M.S. thesis, p. 65.

Parrish, J.B., and Lavin, P.M., 1982, Tectonic model for kimberlite emplacement in the Appalachian Plateau of Pennsylvania: Geology, v. 10, p. 344-347.

Pennsylvania Geological Survey, 2016, PaGEODE—Pennsylvania Geologic Data Exploration: Pennsylvania Geological Survey, http://www.gis.dcnr.state.pa.us/geology/index.html [accessed June 2016].

Rodgers, J., 1949, Evolution of thought on structure of middle and southern Appalachians: American Association of Petroleum Geologists Bulletin, v. 33, p. 1643-1654.

Rodgers, J., 1953, Geologic map of east Tennessee with explanatory text: Tennessee Division Geology Bulletin 58, 168 p.

Rodgers, J., 1964, Basement and no-basement hypotheses in the Jura and the Appalachian Valley and Ridge, in Lowery, W. D., ed., Tectonics of the Southern Appalachian Valley and Ridge: Virginia Polytechnic Institute, Department of Geological Sciences Memoir 1, p. 71-80.

Scanlin, M.A. and Engelder, T., 2003, The basement versus the no-basement hypotheses for folding within the Appalachian Plateau Detachment Sheet: American Journal of Science, v. 303, p. 519-563.

Shumaker, R.C., 2002, Reinterpreted Oriskany structure at the North Summit field, Chestnut Ridge anticline, Pennsylvania: American Association of Petroleum Geologists Bulletin, v. 86, p. 653-670.

Sherril, R., 1934, Symmetry of Appalachian foreland folding: Journal of Geology, v. 42, p. 225-247.

Wiltschko, D.V. and Chapple, W.M., 1977, Flow of weak rocks in Appalachian Plateau folds: American Association of Petroleum Geologists Bulletin, v. 61, p. 653-670.

LUCERNE COAL REFUSE SITE

CAMBRIA RECLAMATION CORP – CENTER TOWNSHIP, INDIANA COUNTY RECLAMATION VIA COAL REFUSE FIRED ELECTRIC GENERATION UNITS

SHAWN SIMMERS, PE, ENVIRONMENTAL HEALTH AND SAFETY, CAMBRIA COGENERATION
JEFF ZICK, PE, FUELS MANAGER, CAMBRIA COGENERATION AND IPAC COLVER
TODD COLEMAN, PE, PRESIDENT, MINETECH ENGINEERS INC.
GARY MERRITT, PG, NORTHERN STAR GENERATION SERVICES COMPANY LLC

Executive Summary

Coal Mining was a critical economic factor in the industrial development of Pennsylvania tied directly to the iron and steel industry. As a result, the underground deep mines from the late 1800's through the mid 1980's were directly connected. The metallurgical coal needed to produce coke was a key ingredient to the manufacturing and production of steel.

The Lucerne Coal Mines in Indiana County, Pennsylvania, were developed to support the production of coke. In fact, there were large beehive coking batteries (Lucernemines Coking Works) that were an integral part of their operations.

Associated with the coal mining and coke production activities was the disposal of the waste produced by the coal mining and processing operations. The Lucerne Coal Refuse Site is one example. There were over 8.7 million tons of coal refuse (in the form of coarse rejects and fines/slurry placed on two areas of the property. This material was simply placed on the land with no environmental restrictions (in other words dumped on the land to burn and leach creating air, water and land pollution) at that point in time.

As a result, the Federal Surface Mining Control and Reclamation Act (P.L. 96-87) accomplished two major things: (1) regulated the disposal of coal refuse, and (2) established an Abandoned Mine Land Reclamation Program funded by fees.

In 1978, the Public Utility Regulatory Policy Act (PURPA) was passed. The Act was designed to encourage alternative generation in terms of Qualifying Facilities (either cogeneration or small power produce). This required Utilities to enter into Power Purchase Agreements, which was the financial vehicle to allow these plants to be designed, financed, constructed and operated. The Act and the FERC regulations encouraged the use of alternative fuels including waste fuels. FERC recognized that coal refuse was a waste fuel. These plants were limited in size with the larger small power production facilities capped at about 125 MW.

At this time, there was a new clean coal technology developed in Europe and brought to the United States and improved. The technology allowed for the burning of lower Btu, high ash waste (coal refuse) in a Fluidized Bed Combustor. The emissions were controlled by injecting limestone into the boiler to be fired with the coal refuse to control SO_2 emissions (90% to 95% capture in the boiler), control Filterable Particulate Matter through the use of baghouses, and control NOx through the combustion process and in some cases the use of Selective Non-Catalytic Reduction (SNCR) technology. Mercury has always been controlled to limits below the 1.2 lbs/TBtus.

Coal refuse-fired plants provide an important public-private partnership to address critical pollution and safety issues through removal, remediation and reclamation of polluting coal refuse piles. Acid mine drainage (AMD) from mine affected lands, including coal-refuse piles, is a major source of water pollution in Pennsylvania with over 3,300 miles of streams being impacted. The coal refuse piles have burned (as evidenced by the "red-dog"), are burning and will burn in the future. While burning, these sites emit uncontrolled toxic air pollutants. They are also major contributors of fugitive dust.

In Pennsylvania, coal refuse-fired plants have removed more than 214 million tons of coal refuse for use as fuel and remediated millions more tons of coal refuse through the use of the resulting beneficial use ash. Thousands of acres of land have been remediated and reclaimed through these operations. (See Appendix A)

Land, water and air pollution are permanently eliminated which results in an improved environment and a higher quality of life for all members of the public. Remediation of coal refuse sites has energized local watershed groups to prioritize their clean-up efforts in the same watersheds. Significant local, county and state emergency services costs are avoided by the removal of coal refuse piles.

In general, the coal refuse fired plants have controlled their emissions of SO_2, NOx, and PM. They have been some of the lowest emitters of Mercury and PM. In fact, 8 of the coal refuse fired units were in the EPA floor calculations to determine the emission rate for SO_2.

The ability of these plants to comply with the acid gas aspects of MATS is a function of the sulfur content of the fuel. Plants located in the anthracite area burn low sulfur fuel whereas the sulfur content of the fuel in the bituminous area is high. This allows the plants in the anthracite area to comply with the SO_2 surrogate of 0.2 lb/MMbtu as they only need to capture approximately 90% of the sulfur in the boiler. Whereas, the coal refuse fired units in the bituminous area would have to achieve 98+% capture of the sulfur in the boiler.

The Lucerne site is an old abandoned coal refuse pile where the mining and coal processing wastes from the Lucerne Deep Mines Complex was placed. There was a total of 8.7 million tons of coal refuse of varying quality and size. The quality of the pile varies in Btus from 5000 to 8000 and sulfur content from 1 to 6%

The site was un-reclaimed, discharging acid and iron to Yellow Creek and one of its unnamed tributaries, as indicated by seeps and discharges from the areas where coal refuse was placed. Silt laden runoff was also discharging into the stream. In addition, there have been times when the pile was burning in the past as evidenced by "red dog".

The project mines and blends the coal refuse, ships the material to Cambria and Colver plants as well as shipping some material to Seward. Coal combustion residuals from both Colver and Cambria are returned as part of the site reclamation. Cambria Reclamation permitted and bonded the site and conducts the mining and reclamation operations.

It is projected that upon completion, this should reduce the discharge load to the stream by 261,000 lbs of acidity a year and 59,000 lbs of iron a year.

Pennsylvania's Abandoned Mine Land Problem including Coal Refuse Sites

Pennsylvania's coal miners have extracted approximately 16.3 billion short tons of anthracite and bituminous coal from the state's mines since commercial mining began in 1800. While mines permitted under the 1997 Surface Mining Control and Reclamation Act (SMCRA) are required to be reclaimed after the coal is extracted and processed, many pre-SMCRA mines were abandoned without any reclamation. These sites are referred to as Abandoned Mine Lands (AML).

In Pennsylvania, there are more than 5,000 abandoned, unreclaimed mining areas covering approximately 184,000 acres. The estimated cost to address these problems is between $15 and $16 Billion.

What are the impacts from abandoned, unreclaimed coal refuse sites? There are three basic areas of impact: Land, Water, and Air.

Land

The coal refuse piles are scattered across the landscape next to communities, rivers and streams and sometimes fill entire valleys. These piles are unsightly and scar the landscape and some areas look like moonscapes. The piles also tend to attract dumping and other activities, increasing the potential for nuisances such as starting the coal refuse piles on fire. Abandoned coal mines and coal refuse piles cause many adverse impacts to surrounding land. Unstable coal refuse piles may collapse and threaten the safety of nearby communities and the scenic and recreational quality of the landscape is ruined. Properly reclaimed coal refuse sites can and have returned the land to productive uses including wildlife habitat, recreational opportunities and commercial development.

Water

More than 3,300 miles of streams in Pennsylvania are impacted by Acid Mine Drainage (AMD), according to the United States Geological Survey (USGS). This is the result of AMD from both mine discharges and acid runoff from coal refuse piles. The run-off from precipitation, in addition to being acidic and contaminated by metals, contains silt, which is also a pollutant. This acidic contaminated discharge creates water pollution and negatively affects the ability of a stream to support aquatic life.

Air

Coal refuse sites historically and currently catch fire. Coal refuse fires typically start as a smoldering, oxygen starved fire that produces the necessary oxygen from the generation of steam created by moisture in the coal refuse. Slowly, as the fire continues to develop, avenues for oxygen migration through the refuse expand, resulting in flames. Combustion of the coal refuse emits uncontrolled toxic air pollutants and greenhouse gases into the atmosphere. The toxic air pollutants are a particular health and safety problem in the proximity of the coal refuse fires.

Coal refuse disposal piles have been burning and causing air pollution since coal mining first started (Sussman and Mulhern, 1964).

The oxidation of pyrites produces an exothermic reaction that produces heat, which causes the carbonaceous material in the coal refuse pile to ignite and burn. The temperature within a coal refuse pile (or portions of a pile) will increase when more oxygen is available to cause oxidation but the amount of air circulating in the pile is insufficient to provide for the dissipation

of heat. The temperature of the refuse increases until the ignition temperature of the carbonaceous material in the refuse is reached. At this point the coal refuse pile spontaneously combusts, releasing various uncontrolled pollutants into the air of the near-by community.

Pennsylvania Department of Environmental Protection has identified 42 coal refuse piles that are currently burning and at some point will need to be addressed. This does not include underground mine fires.

Pennsylvania was the first state to pass a law to address the air pollution associated with coal refuse disposal, entitled "The Coal Refuse Disposal Control Act, Act of September 24, 1968, P.L. 1040, No. 318." This has allowed the Commonwealth to address active coal refuse pile fires and to attempt to prevent additional coal refuse piles from catching fire. While the efforts have met with success, new coal refuse fires continue to occur.

The EPA (1978 Study) identified the uncontrolled emissions from burning coal refuse piles. The following pollutants were listed:

(1) criteria pollutants (total particulates, respirable particulates, nitrogen oxides, sulfur dioxide, sulfur trioxide, hydrocarbons, carbon monoxide, and mercury);
(2) non-criteria pollutants (ammonia, hydrogen sulfide, polycyclic organic materials); and
(3) trace elements (arsenic, boron, silicon, iron, manganese, magnesium, aluminum, calcium, copper, sodium, titanium, lead, tin, chromium and vanadium)

The money needed to address Pennsylvania's Abandoned Mine Land problems is not available at this time. It was projected that Pennsylvania would receive over $1 Billion from the Federal AML Fund. This represents less than 7% of the money needed to address the problem. Pennsylvania recognized this and has pushed for remining previously mined areas in order to reclaim the land. The remining was tied to the mining of coal, not coal refuse.

There were efforts in the 1980s to have coal refuse piles reprocessed and reclaim the coal mixed in the piles. This had marginal success, but more often than not resulted in many coal refuse sites being partially mined, not reclaimed, which forfeited bonds.

Pennsylvania's Coal-Refuse Fired EGUs became the most effective tool for reclaiming abandoned coal refuse piles. This program has resulted in over 200 million tons of coal refuse fired as fuel and 1000's of acres of land reclaimed. This industry was a result of the Public Utility Regulatory Policy Act of 1978 (PURPA).

PURPA

While it was recognized that the Federal AML Program would not be able to address the AML problem in many of the States, what was unforeseen was the potential of PURPA to help address the problem. PURPA established a program requiring states to contract for power from qualifying facilities (QF). QF status was accorded to types of projects: Cogeneration and/or Small Power Production Facilities.

FERC would certify the facilities as being cogeneration and/or small power production QFs. FERC certified small power production facilities as QFs if the facility was burning waste (coal refuse), and if the waste provided 75% of the heat input to the boiler and had no value. Further,

in the case of coal refuse (waste coal), FERC certified the coal refuse fuel sources as waste coal and later established the criteria for coal refuse to be classified as waste in its regulations.

As a result of the QF certification, the Utility in the area was required to enter into contracts for purchasing power from these facilities at their avoided costs.

Pennsylvania Administrations embraced PURPA and more specifically bought into utilizing coal refuse (waste coal) in these facilities. They saw two basic benefits: (1) economic development in these areas that were distressed economically; and (2) environmental remediation and clean up. There were 15 QF facilities in Pennsylvania burning coal refuse, of which 2 have ceased operations. In addition, the Seward Facility (an Electric Wholesale Generator) also burns coal refuse and is larger than the other 4 bituminous coal refuse fired QFs (525 MW vs 320 MW).

The coal refuse fired PURPA QF facilities utilized Fluidized Bed Combustion Technology.

Fluidized Bed Combustion Technology

Fluidized Bed Combustion (Circulating Fluidized Bed Combustion (CFB)) Technology is a clean coal technology developed in Europe. The technology allows low Btu high ash coal refuse to be the fuel (Figure 1).

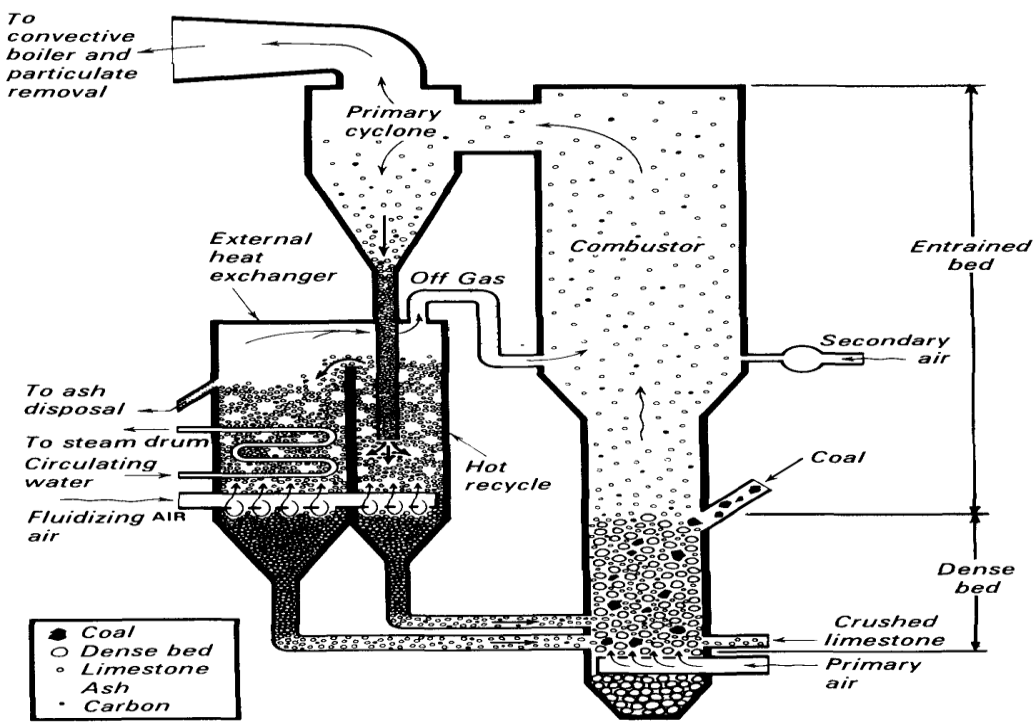

Figure 1. Cross Section of a Circulating Fluidized Bed Combustor

There are four coal refuse fired CFB electric generating units within a 30-mile radius of the site and a total of 14 plants in Pennsylvania (Figure 2). They are: Cambria Cogeneration, IPAC-Colver, Ebensburg Power (which were QFs) and Seward (an Electric Wholesale Generator). These plants vary in size and age. While the CFB Technology is basically unchanged, with design

modifications these plants have grown in size (electrical output) and the ability to control their emissions. The basic aspects of a CFB is that the fuel (coal refuse) is co-fired with injected limestone to control SO_2 emissions, use combustion and/or emission control technology to reduce NOx emissions, and bag-house to control particulate emissions.

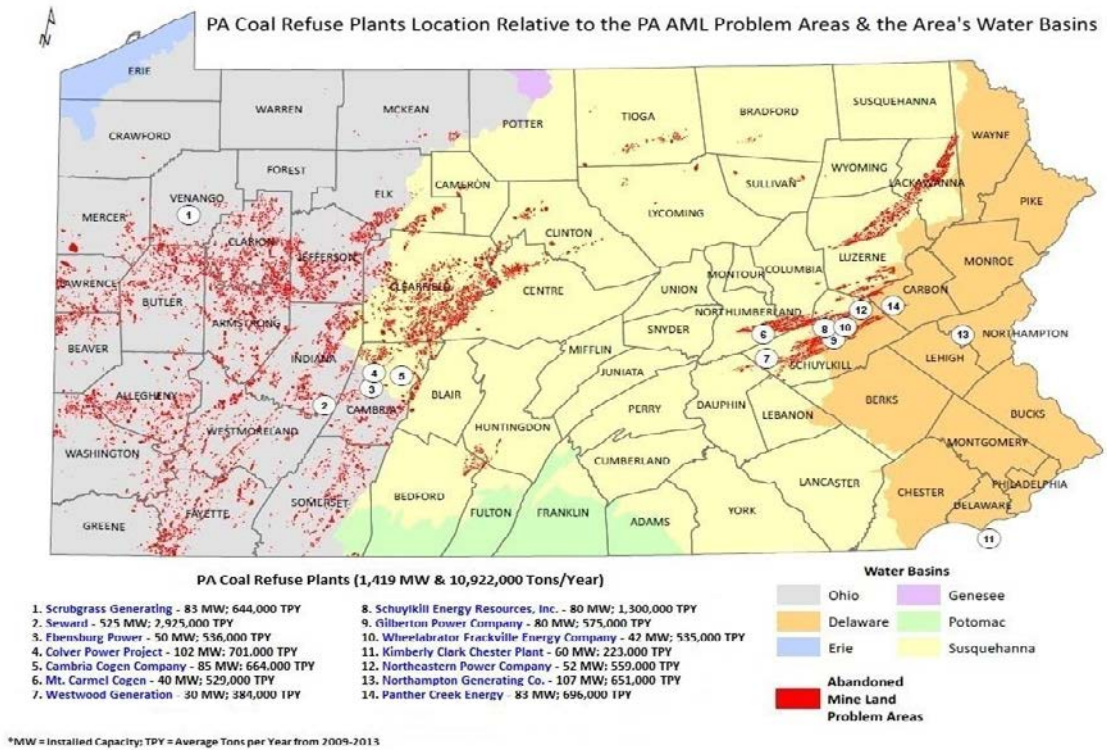

Figure 2. Map Showing Coal Refuse Plant Locations

Unlike coal fired units, these facilities have been controlling their emissions effectively. These facilities control SO_2 emissions from the fuel between 90% and 95%, control their mercury emissions at levels at or below the new EPA standard, and control PM emissions below the EPA standards, while cleaning up the environment by eliminating coal refuse sites as existing and future uncontrolled air emission sources, ameliorating, if not eliminating water pollution, from these sites, and returning the property back to a productive use and establishing vegetation.

These plants are very low emitters of mercury and filterable particulate matter (per the baghouse technology). They have controlled SO_2 emissions from the day operations were commenced. These plants inject both limestone and coal refuse in the boiler. The temperatures in the boiler allow the limestone to calcine and the resulting lime oxide to react with the sulfur dioxide (SO_2) in the boiler, reducing the emissions of SO_2 from 90% to 95%. To achieve the 98% reduction that the Mercury Air Toxic Rule (MATS) will impose on the plants will place a major technical and financial burden on the ability of a coal refuse facility to survive.

The sulfur content of the bituminous coal refuse varies from lows in the 1% range to over 6% and generally falls in the range of 2.5% to 4%. The Lucerne site has this level of variability, whereas anthracite coal refuse is usually around 1%. Thus, coal refuse fired units in the

anthracite area have the ability to meet the MATS rule. The bituminous meets all but the SO_2 limits in the MATS rule, but must bring their units into compliance with the acid gas aspects of MATS by April of 2019.

Because of the calcinations of the limestone, fluidized bed combustion units have a higher level of CO_2 emissions than a coal fired boiler.

It should be pointed out that if the coal refuse sites are not used as fuel, they remain un-reclaimed and a source of air pollution (fugitive dust and air toxics from burning); water pollution (silt laden runoff to acid mine drainage); and the land is unproductive (none to minimal vegetation).

Each new generation of CFB coal-refuse fired units has been able to reduce SO_2 emissions by increasing limestone consumption. (It should be noted that the upgrades to the newer plants are not able to be applied to the older plants.) These plants have been able to control their mercury emission significantly (~99% reductions) and are low emitters of mercury per the EPA Mercury and Air Toxics Rule. The plants have used baghouse to control Particulate Matter (PM) emissions at levels below that required by the MATS rule. These plants are either low emitters of PM or are very close to the low emitter limits. They are low emitters of NOx emissions which results from either use combustion control or Selective Non-Catalytic Reduction Technology. Further, these plants are low emitters of Nitrogen Oxides (N_2O). These facilities have a higher footprint for Carbon Dioxide Emissions resulting from burning the coal refuse and the calcining of the limestone to control SO_2 emissions.

The smaller, earlier Coal-Refuse Fired CFB (>130 MW) have a problem meeting the HCl emission rate or its SO_2 surrogate. These units would need to achieve either 98% capture of the HCl or SO_2. The economics of controlling these emissions at that level in today's electric market is problematic let alone having the technology to control or the cost of said technology.

Introduction - Lucerne Coal Refuse site

The Lucerne Coal Refuse Site represents the coal refuse aspect of Pennsylvania's Abandoned Coal Mine Legacy. The Lucerne Coal Refuse Pile resulted from the disposal of coal refuse from the Lucerne Mines that were developed in 1907, with the mines ceasing operations in 1929 (Lucerne Mine No.1), 1943 (Lucerne Mine No. 2) and 1967 (Lucerne Mine No. 3). The mine complex covered over 14,000 acres. Through the years (until 1948), the coal was delivered to the breaker where it was crushed and sized. At the breaker, men were employed to pick slate, rock, and sulfur from the conveyors for disposal. The operations slowly transitioned to mechanical separation with the construction and operation of the Lucerne Coal Cleaning Plant in 1948. (Mountjoy, IUP Website).

The coal refuse disposal was placed on 125 acres of a 397 acre property of which 286 acres have been permitted. The process of coal refuse to energy is leading to the Lucerne site being reclaimed. This process is summarized in Figure 3.

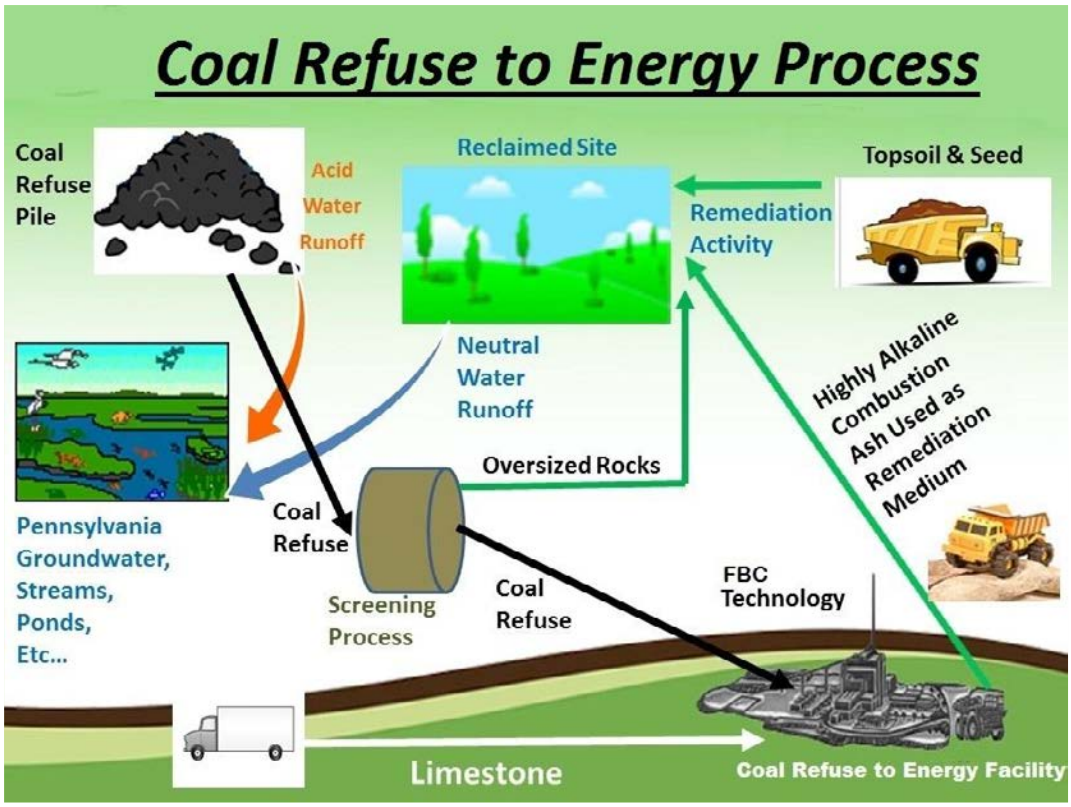

Figure 3. Coal Refuse to Energy Process *(Source - www.wpcamr.org)*

The Lucerne Site has burned in the past, as is evidenced by "red-dog" (burnt coal refuse) present within the pile. The area is unreclaimed with no vegetation, which creates fugitive dust, sediment laden run-off and acid mine drainage pollutional discharges.

Since the site was not permitted (nor required to be permitted) at the time it was in operation, it was subsequently abandoned with no one required to reclaim the site. The reclamation fell to the Commonwealth, but with no funding available to reclaim, it remained in the unreclaimed state.

The Federal AML Program was designed to provide monies for addressing abandoned mine problems in the States through a federal reclamation fee assessed against each ton of coal mined. These monies were to be used to reclaim priority 1 and 2 sites first. In the case of Pennsylvania, most of these sites would fall into either priority 3 or 4. (With Pennsylvania's AML program needing over $15 Billion to address its AML problem, and projected to receive $1 Billion dollars, with most of the sites being classified as priority 3 or 4, it is doubtful that these sites will be reclaimed.)

As such, the Commonwealth will not be able to fully address its priority 1 or 2 sites so it remains very doubtful that it can address the coal refuse sites.

Lucerne's Location

The Lucerne Coal Refuse pile is located in Center Twp., Indiana County, PA, adjacent to Homer City Borough, and near the communities of Lucerne Mines and Tide, just off US 119 and Township Road T-840 (Tide Road) (Figure 4).

The coal refuse disposal was placed on 125 acres of a 397 acre property of which 286 acres have been permitted. The 125 acres is comprised of two specific areas of the property (Figure 4). Area 1 was primarily coarse coal refuse (the main site for mining operations) and Area 2 (sludge/coal slurry) as the coal cleaning process improved.

The reject from the coal cleaning plant was delivered by conveyor to the Lucerne coal refuse site (Figure 5). There was over 8,700,000 tons of coal refuse placed on the site.

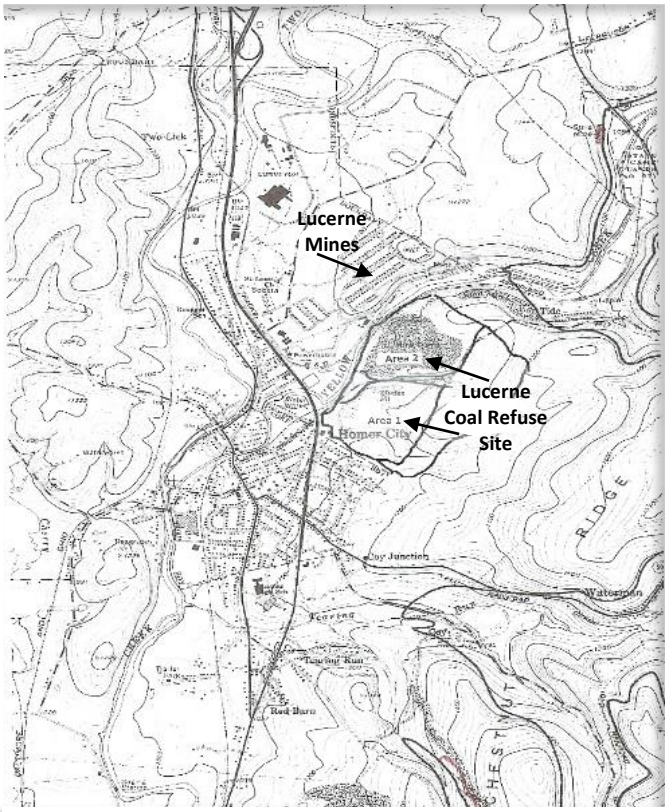

Figure 4. Location of Lucerne Coal Refuse Site (Area 1 & Area 2) and Lucerne mines, Indiana County

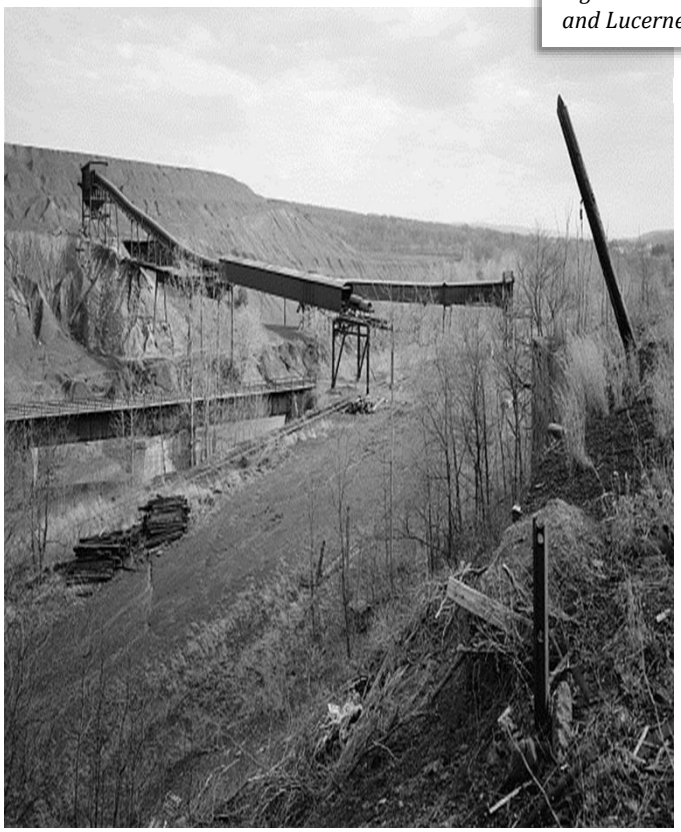

Figure 5. Library of Congress Photo showing boney pile (coal refuse) and Conveyor at Lucerne

History of the Lucerne Mine Complex (Mountjoy, IUP Website)

The Rochester and Pittsburgh Coal and Iron Co. (R&P) opened the Lucerne Mines operation and patch town in 1907. Within 15 years, Lucerne had three mine openings, steel tipple, and central power house (Figure 6) making Lucerne one of the largest and most complete mining plants in the United States.

Over the course of the next 60 years, R&P played an important role of electrifying mines when in 1899, R&P began to convert the haulage systems at each of its mines to electric from animal. Starting in 1903, R&P began to construct power plants at its mine with Ernest being one of the first. However, due to the high-line losses, R&P built a centralized power plant at Lucerne and placed it into operation in 1911.

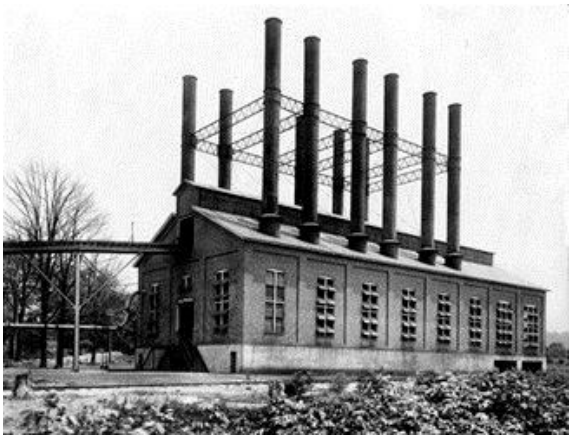

Figure 6. The Lucerne power plant

At this time, R&P was testing electric cutting machines at Lucerne which led to R&P electrifying all their mines using electric cutting machines.

With the centralized power plant, R&P began to run power lines to its various mines in Indiana and Armstrong County. The Ernest Mine was the first mine to be powered by the Lucerne Power Plant.

The Lucerne power house was furnishing electricity to all R&P mines in Indiana County as well as to the Indiana Street Railway system near Lucerne by 1920. The Lucerne Power Plant was modernized by replacing a number of the old boilers with two large ones, building the first tall stack in 1937, and additional turbogenerators were placed in operation 10 years later along with additional boilers and a tall stack.

By 1948, Lucerne had brought on line a new coal cleaning plant which over time was upgraded to improve coal quality. The resulting coal refuse and silt from the cleaning plant were conveyed over to the Lucerne Coal Refuse Site.

In 1952, R&P had a battery of 264 beehive coke ovens built at Lucerne furnishing high quality coke for the iron and steel industry until 1972 (Figure 7).

Figure 7. General perspective view of coke ovens looking east (264 block beehive ovens) - Lucernemines Coke Works, Coke Ovens, 0.5 mile East of Lucerne, adjacent, Lucerne Mines, Indiana County, PA.

Photos from Survey HAER PA-264-A

In 1964, R&P made the decision not to upgrade the power plant and to purchase electricity from the Pennsylvania Electric Company.

The original mines at Lucerne closed down with Lucerne No. 1 Mine ceasing operations in1929; No. 2 closed in 1943 and No. 3 ceased operations after 60 years of production in 1967.

Today, the Lucerne coal refuse site is providing fuel to serve Coal Refuse Fired Circulating Fluidized Bed Facilities resulting in the energy stored in the coal refuse at the site to be utilized to generate electric power. Further, the coal ash produced from a CFB Unit is highly alkaline and meets the State regulatory requirement for its use in mine land reclamation.

Geologic and Groundwater Overview of the Lucerne Coal Refuse Site

This portion of Indiana County is underlain by the Pennsylvania Conemaugh and Allegheny Group (Figure 8).

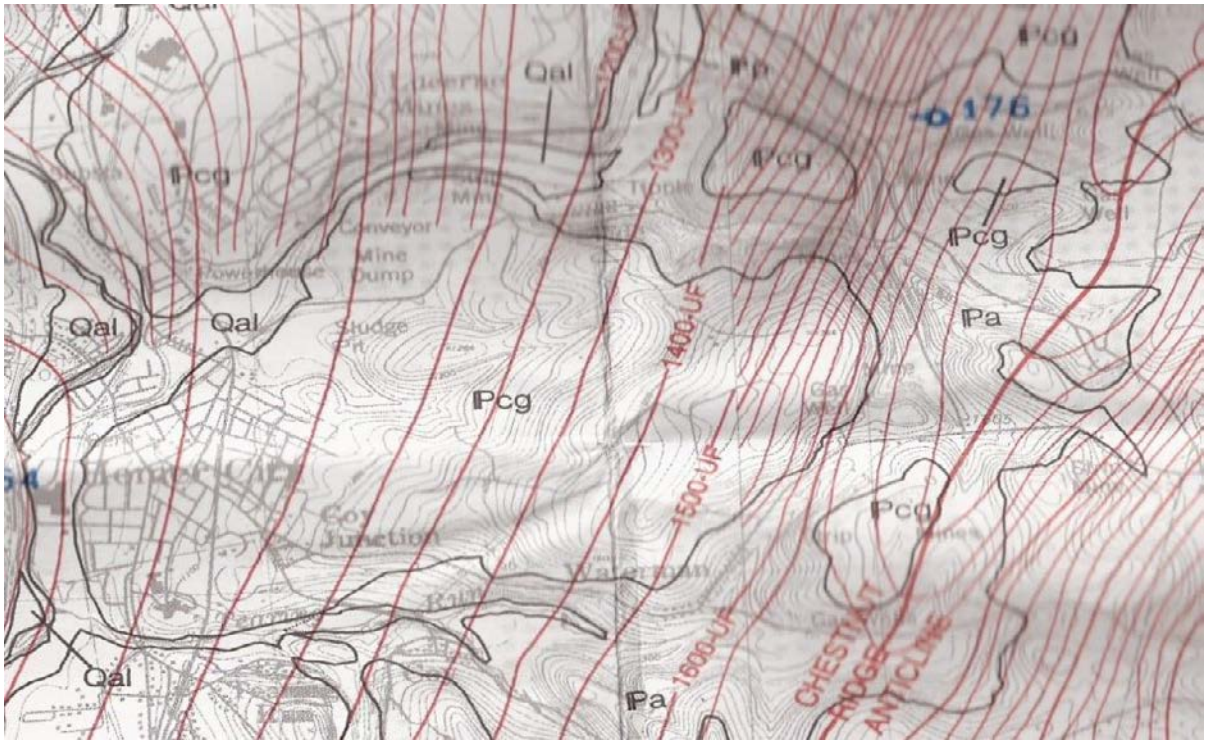

Figure 8. Geologic Map with Structural Contours (Williams and McElroy, 1997)

The Lucerne Coal Refuse Site is located approximately 1.4 miles southeast of the Latrobe Syncline and 2.0 miles northwest of the Chestnut Ridge Anticline. The area beneath the mine site had been extensively deep mined with the mine complex being over 14,000 acres extending from the Lucerne area to the Ernest area.

The coal refuse area (identified as the conveyor mine dump) and the slurry impoundment (identified as the "Sludge Pit") is underlain by the Pennsylvanian Conemaugh Group (the Glenshaw Formation (Pcg)). The Glenshaw Formation has been described as being olive-gray to dark-gray, thinly bedded fossilferous, limestone and clay shales, red claystone, locally massive fine to coarse-grained sandstone near the base, fresh water limestone, and thin, non-persistent coal (Williams and McElroy, 1997).

The Upper Freeport Coal (Allegheny Group) underlies the area and has been extensively deep mined, as was the Upper Kittanning Coal (Allegheny Group) by Rochester and Pittsburgh Coal and Iron Company from 1907 to ~1972. (Bragonier and Glover, 1996) (Figures 9 and 10).

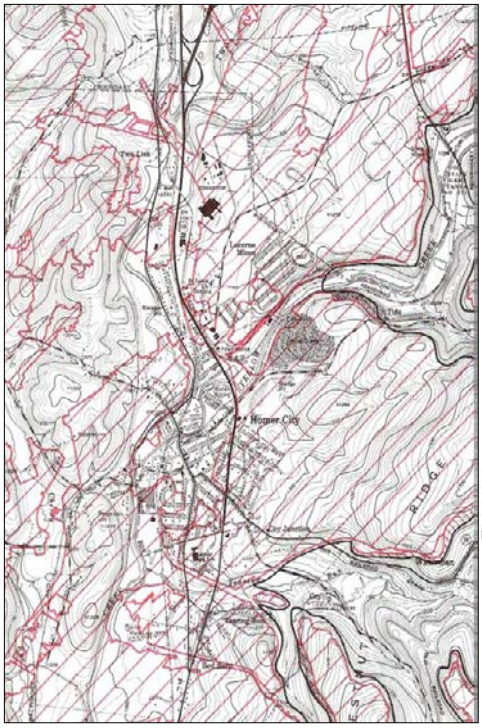

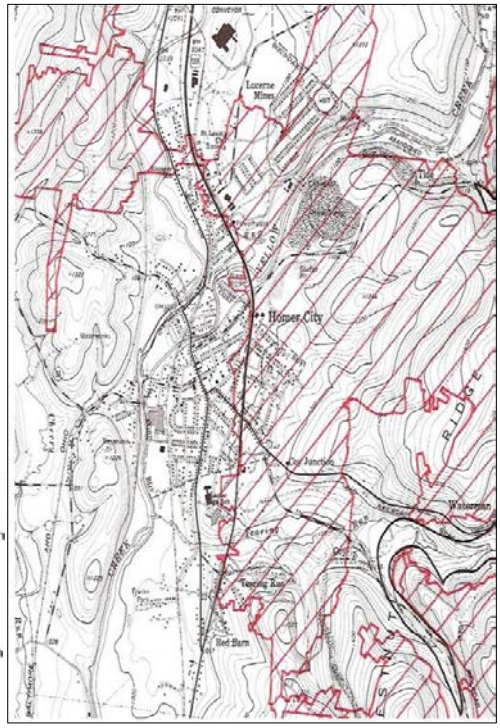

Figure 9. Mining in the Upper Freeport Coal

Figure 10. Mining in the Lower Kittanning Coal (Bragonier and Glover, 1996)

The coal refuse was placed on the sites with minimal considerations (not having legislation or regulation dealing with stability or environmental issues. In 1952, the Lucerne Mines constructed and operated a coal preparation and cleaning facility across the stream from the coal refuse site and sludge pit. Waste from the Lucerne Preparation Plant was transported to the coal refuse site, where it was dumped on the ground with minimal compaction. Later, the sludge pits was established to dispose of slurry from the preparation plant. Both the coal refuse site and the slurry sites were placed on the ground surface.

The valley adjacent to the coal refuse site has Quaternary Age Alluvium (Qal) deposits.

The pre-1972 deep mining and coal refuse disposal has impacted groundwater quality and surface water quality in the area. In general, the groundwater system within the permit area consists of one or more perched water tables with the regional water table at the level of Yellow Creek. However, the extensive deep-mining of the Upper Freeport and the Lower Kittanning has had a major impact on ground and surface water in the area. The Upper Freeport Deep Mine is flooded to an elevation of 1040 feet to >1070 feet. The mining in this area has been to the rise, resulting in additional head allowing deep mine discharges at the 1040 and 1070 foot elevation. In addition, the extensive deep-mining has probably led to subsidence issues allowing the mine to dewater the shallow perched water groundwater.

The Lucerne Coal Refuse Site is being remined and used as a fuel source for Cambria, Colver, and Seward. The coal refuse and slurry located on the sites has been certified by FERC as waste coal.

The Mining Operation

There are two distinct areas of mining based on the past coal refuse and coal slurry disposal operations. The intent is to remine the site, using the coal refuse as fuel for the coal-refuse fired electric generating units, eliminate the piles as source of acid mine water and sediment laden runoff, use the alkaline ash beneficially to reclaim the site, eliminate the potential for the site to burn in the future and restore the land to a productive use.

The site has been permitted to be mined. The permit includes a mining plan and abatement plan to reduce or eliminate the pre-existing pollution emanating from the site, as well as full-cost reclamation bonding. A key aspect is burning the coal refuse and replacing it with an alkaline coal ash as a beneficial use in the mine reclamation.

The site will be monitored for a period of 10 years from the day the last coal ash is placed on the site before the site is eligible for final bond release.

The mining operations commenced in Area 1, in order to develop this portion of the site to accept ash when mining coal refuse in Area 2. As part of the development of this portion of the site, some of the slurry/silt was moved and stockpiled on the coarse refuse site. This was needed in order to manage coal ash from the Cambria Cogeneration facility. This coal ash, approved for beneficial use in coal mine land reclamation, is being placed in that area. The active coal refuse mining activities are being conducted on the coarse refuse site (which also has areas of silt/slurry). At this time, no ash is being placed in this area, as the site needs to be developed in a manner that maximizes the recovery of the coal refuse. In mining this area, the variability in fuel quality, based on wide swings in Btus and sulfur percentage, requires the development of 'coal refuse "highwalls"'. The coal refuse is shipped to the plants on a daily basis by trucks loaded with coal refuse from the different highwalls that are mixed and blended at the plants to achieve a more uniform Btu and sulfur content. This procedure:

(1) allows for mining of the coarse refuse to maximize recovery without it being limited by being ash bound,
(2) insures that the acid producing material is burned and neutralized,
(3) the site will not catch fire in the future and
(4) water quality from the site will improve.

The site was un-reclaimed causing acid and iron discharges to Yellow Creek and one of its unnamed tributaries as indicated by seeps and discharges from the areas where coal refuse was placed. There was silt laden runoff that was also discharging to the stream. In addition, there have been times when the pile was burning in the past as evidenced by "red dog". It is projected that upon completion, this should reduce the discharge load to the stream by 261,000 lbs. of acidity a year and 59,000 lbs. of iron a year.

Summary and the Dilemma

In summary, the remining of the Lucerne Coal Refuse Site allows for the coal refuse to be used as a fuel in coal-refuse fired electric generating units in Indiana and Cambria County. As a result of the mining effort, the site will be reclaimed, the potential for future fires eliminated, and in the process eliminate 261,000 lbs. of acidity and 59,000 lbs. of iron from being discharged into Yellow Creek and one of its unnamed tributaries, improving the overall water quality.

The dilemma is that the Coal Refuse Fired EGUs have proven they are able to generate power, meet reasonable environmental regulations, and clean up the piles through the Coal Refuse to Energy Process (Figure 3). In the process, they have minimized or eliminated the mine drainage from these sites, eliminated the future potential of these sites to burn, and returned the land to a productive use with the **vegetation becoming a carbon sink**. Without these sites, there is no economical means to reclaim the sites to standards for regulated coal mining. The dilemma is the need to keep these types of electric generating units operational so that they can continue to be an economic tool in the region and more importantly clean up the pollution associated with the abandoned coal refuse sites.

References

Bragonier, William A. and Glover, Albert D., 1996, Coal Resources of Indiana County, Pennsylvania: Pennsylvania Geologic Survey, Mineral Resources Report 98 Part 1, 4 pages and maps.

Mountjoy, Eileen, The Company Town of Lucerne, IUP website [accessed 8/2/2016]: http://www.iup.edu/archives/coal/mines-and-company-towns/the-company-town-of-lucerne/

Sussman, Victor H. and Mulhern, John J., 1964, Air Pollution from Coal Refuse Disposal Areas, Journal of the Air Pollution Control Association, 14:7, 279-284, DOI: 10.1080/00022470.1964.10468282

Western Pennsylvania Coalition for Abandoned Mine Reclamation, www.wpcamr.org

Williams, Donald R. and McElroy, Thomas A, 1997, Water Resources of Indiana County, Pennsylvania: U.S. Geological Survey, Water Resources Investigation Report 95-4164, 105p.

For more information on Coal Refuse, see Appendix A.

ROSEBUD MINING AND THE ST. MICHAEL DISCHARGE WATER TREATMENT PLANT, ST. MICHAEL, PENNSYLVANIA – TOPPER RUN DISCHARGE

JACQUELINE HOCKENBERRY P.G., J HOCKENBERRY ENVIRONMENTAL SERVICES, INC.
JACKIE RITKO, CAMBRIA COUNTY CONSERVATION DISTRICT
JOHN ST. CLAIR, ROSEBUD MINING COMPANY

Introduction

The South Fork Branch of the Little Conemaugh River Watershed has been home to a long history of both surface and deep coal mining. For decades, beginning in the early 1900's, the coal mining industry established its presence, created jobs and spurred development of municipalities such as St. Michael, Beaverdale, Sidman, and South Fork located outside of Johnstown, Pennsylvania. This industry in turn supported the steel industry.

The remnants of the past mining have etched many faces on the surface in the form of old company housing, railroads, bony piles, un-reclaimed and reclaimed surface mine areas, mine openings, shafts and mine discharges that were accepted as a part of life and landscape.

For decades, the South Fork Branch and its tributaries have received mine discharges into their corridors from closed or abandoned mines, creating a quagmire of water chemistry and landscapes of brown, red, and white within their channels.

Fast forward to 2010, and mining has a new mission and a new perspective to mining coal in this area. The Rosebud Mining Company presented a proposal to the Pennsylvania Department of Environmental Protection, the United States Environmental Protection Agency, local municipalities and countless other interested parties to substantially remove the acid mine drainage load to the largest pollution contributor within the Little Conemaugh Watershed in exchange for a permit to deep mine coal reserves that were flooded by both past mining and geological conditions.

What has been referred to as "out of the box" thinking, Rosebud has entered into an agreement with the regulatory agencies to substantially reduce the metal loading to the South Fork Branch of the Little Conemaugh River by pumping and treating the worst discharge in the Little Conemaugh Watershed in exchange for the ability to continue mining – Mine 78 (Upper Kittanning – C')

Rosebud Mining Company committed to fund and construct the now functioning $15 million dollar water treatment facility and pay treatment expenses during the active mining of "Mine 78." In addition, Rosebud will contribute another $15 million to establish a fully funded perpetual treatment trust fund. The construction of the treatment plant has been completed the treatment of the water commenced in 2013.

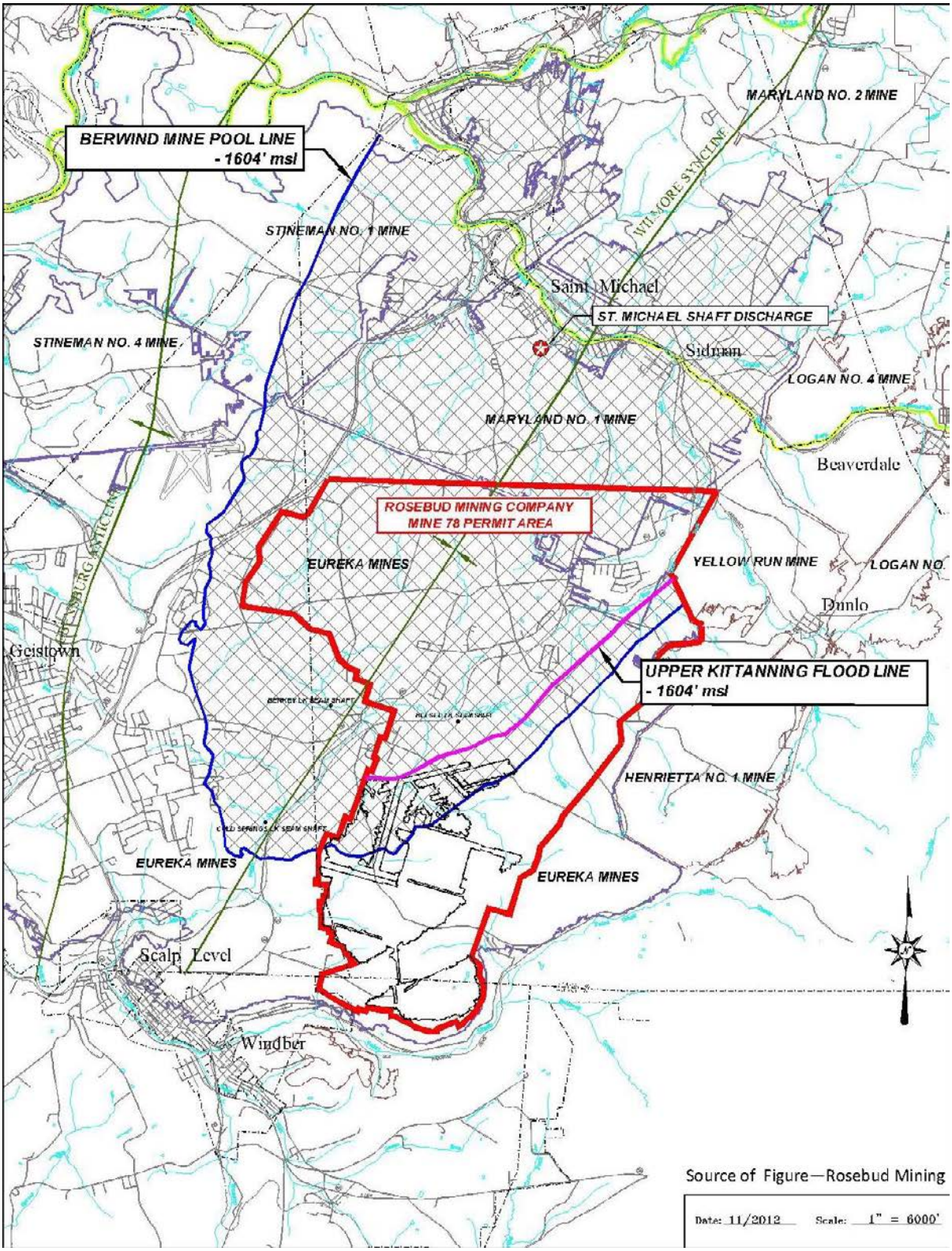

Figure 1. Map showing the geological structure of the area as it relates to the Berwind Mine pool (outlined in blue), limit of flooded area of the Upper Kittanning C–coal seam (pink line), and the St. Michael shaft discharge. The Rosebud Mining Company Mine 78 permit area is outlined in red. Source of figure – Rosebud Mining.

Background History

One of mining companies who established a mine operation in the St. Michael area around the 1900's time was the Maryland Coal Company of Pennsylvania. The company, based out of New York City established the Maryland Shaft & Collieries circa 1908-1910. The mine was established in the Topper Run Watershed (tributary to the South Fork Branch of the Little Conemaugh). When this mine opened, a shaft was constructed 670-ft deep, which at the time was the deepest shaft of all bituminous mines in Pennsylvania. This mine operated under the Maryland Coal Company until 1932 when it was sold to the Berwind-White Coal Company. Berwind operated the mine until 1958 when the mine was closed. Berwind ceased pumping the shaft in July 1962 and the shaft became the infamous discharge in December 1963.

Since that time, the shaft had been discharging untreated acid mine drainage water progressively into Topper Run, to the South Fork Branch of the Conemaugh, Stonycreek River, the Conemaugh, Kiskiminetas River to the eventually to the Lower Allegheny River. The Maryland Shaft (St. Michael) discharge is the largest single source of acid mine drainage pollution within the Little Conemaugh River, producing 29.2% of the total acid mine drainage pollution load on the river. Average flow rates approximate the discharge as 2, 067 gallons per minute to as high a 3,656 gallons per minute. The discharge originates from a 36-inch pipe at the top of the shaft.

The shaft was evaluated for integrity as part of the design for the treatment plant. The shaft was considered to be in good condition despite its construction date of 1908-1910 era.

The "Berwind Mine Pool"

The discharge and subsurface conditions have created the "Berwind Mine Pool" which in the subsurface have flooded substantial areas above the Lower Kittanning "B" prohibiting the mining of the Upper Kittanning coals (C') (Figure 2).

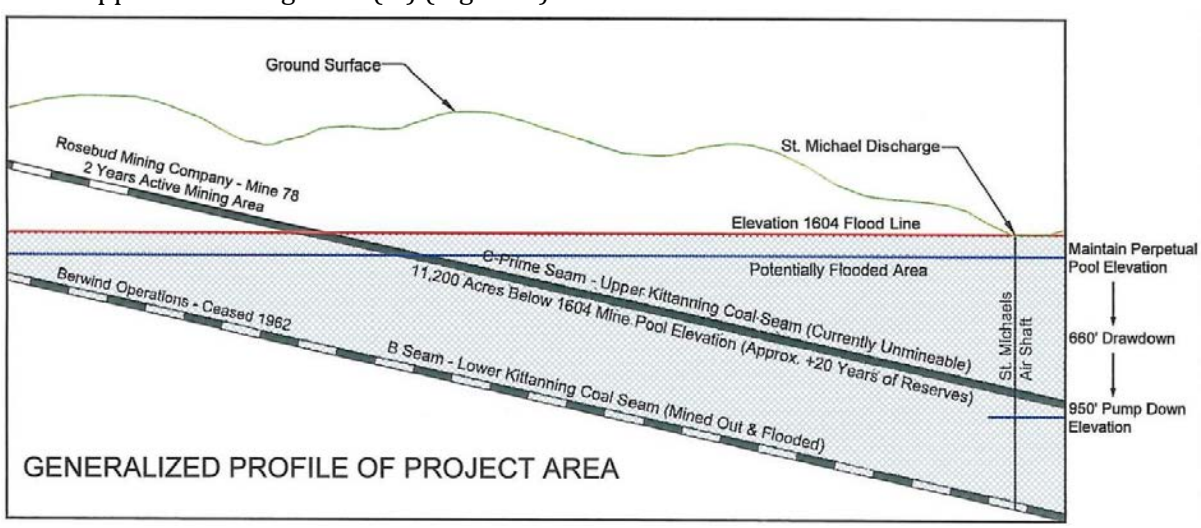

Figure 2. The Upper Kittanning coal seam (seam being extracted by Mine 78) is approximately 100 feet above the Lower Kittanning coal seam (seam extracted in the early 20th century) and they are hydraulically connected. No mining can be conducted at Mine 78 below an elevation of 1604' msl until the area is dewatered by pumping the Berwind mine pool at the St. Michael Shaft. The pumping and treatment facilities will allow 20 plus years of additional mining and eliminate 30% of the AMD loading on the Little Conemaugh Watershed. Upon completion of the mining activities at Mine 78, the mine pool will be allowed to rise but be maintained below the current discharge elevation. Source of figure – Rosebud Mining.

The mine pool developed resultant of the structural geology of the area. Ground water in the vicinity traverses towards the Wilmore syncline, which plunges in the direction of the St. Michael/ Maryland Shaft (Figure 3). The groundwater fills the synclinal feature and the shaft becomes the discharge point for the mine pool. This elevation is approximately 1604 feet. Rosebud will pump the mine pool to an elevation of 950-feet allowing the deep mining of Mine 78 to continue for 20+ years. Upon completion of the mining, the mine pool will rise, but will be maintained below the 1604 discharge elevation. Treatment will continue after mining is completed via use of the established trust funds.

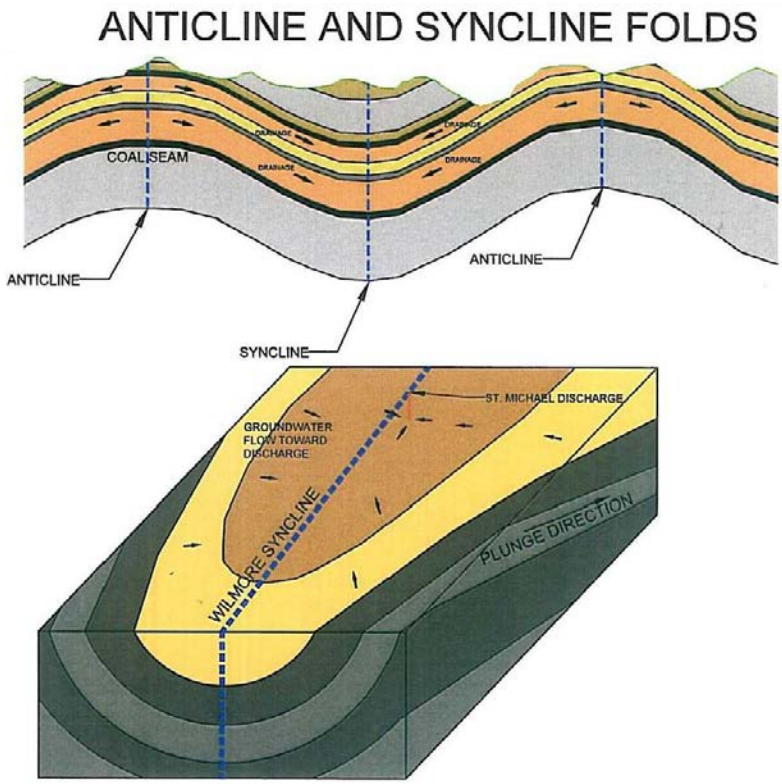

Figure 3. Water enters the subsurface near stratigraphic high areas known as anticlines. Groundwater then travels down gradient toward the axis of stratigraphic lows known as synclines. The Wilmore Syncline plunges toward the St. Michael Shaft where the groundwater fills a bowl-like structure to form the Berwind Mine Pool. St. Michael Shaft is the discharge point of the mine pool. Source of figure – Rosebud Mining.

Topper Run Water Chemistry

Significant interest in this watershed has spurred the initiation of several studies. Many organizations have donated time and resources in attempts to improve the watershed. These studies have sought to identify the discharges that plaque this watershed. Some of these studies commenced twenty to thirty years ago and served as a basis to identify and inventory the discharges in the watershed. The studies were conducted to determine the total impact of the acid mine drainage to the watershed and to observe changes in waterways resultant of other land-use activities. The historic record of inventory and chemical analysis is reflective of the interest in the community to reduce pollution in these waterways. The overall conclusion is that many of these discharge flow rates prohibit any type of treatment except for chemical, which as presented with the St. Michael/Maryland Shaft discharge is very costly.

In a comprehensive watershed study conducted by the Cambria County Conservation District in 2000, Topper Run was recognized as being the largest source of acid mine drainage in the watershed. The study notes that Topper Run is contaminated with 100-150 mg/l ferrous iron with a field pH of 4.91. Comparing the iron content of the discharge with the Pennsylvania Maximum Contaminant Level for drinking water in Pennsylvania of 0.3 mg/l puts the extent of the pollution in perspective.

Other contaminant levels for this discharge included:

Sulfates:	132 mg/l
Manganese:	4.46 mg/l
Aluminum:	0.717 mg/l

This chemistry equates to a load of 31,141 pounds per day and 3700 tons of acid mine drainage annually.

The Rosebud/ St. Michael Water Treatment Project which is now operational treats an average flow rate of 3,656 gallons per minute, and draw down pump capacity is up to 10,000 gallons per minute.

This treatment facility significantly improves the water quality of Topper Run, however, refuse piles located contiguous to the stream, which are situated upgradient of the treatment facility, leach pollution to Topper Run.

Sulfur Creek, another tributary to the South Fork Branch, is ranked as the second most significant acid producer to the South Branch of the Little Conemaugh River, contributing a load of 11,418 pounds per day, and attributes to 10.71 % of the pollution in this watershed. A visit to Sulfur Creek closely depicts the condition of Topper Run prior to the treatment. The Sulfur Creek landscape is dominated by the considerable accumulation of iron mounds, created from the deposition of the iron and other metals. It is a stark display of the magnitude of how acid mine drainage distresses the environment. In addition to the visual characteristics, these affected areas are extremely hazardous, due to the instability of the iron mounding and water chemistry associated with these site(s).

Components of the Treatment Plant

The Rosebud/ St. Michael Water Treatment Project which is now operational treats an average flow rate of 3,656 gallons per minute, and draw down pump capacity is up to 10,000 gallons per minute.

Some of the major components of the treatment facility include:

- Installation of 266-H-piles and 6,560 cubic yards of concrete for the foundation for 2, 210-feet diameter thickener tanks
- Construction of 2-35-diameter tanks, reactor tanks and mixers
- Construction of a 525 ft. long concrete retaining wall
- Construction of a treatment plant building, with 2-120 ton silos, motor control center, lime slakers, sludge transfer pumps, grit bunkers, various pumps and flow measuring devices

- Installation of caissons, steel platform for the installation of 2-800 horsepower mine dewatering pumps
- Installation of the 36-inch discharge piping and outlet structure

Conclusion

Acid mine drainage issues will continue to affect South Fork Branch of the Little Conemaugh River, but this project is a substantial step forward in removing pollution from these waterways.

This project is an effective of how industry and the regulatory agencies can work together to bring environmental and economic outcomes that benefit this area.

References

St. Michael Discharge Water Treatment Facility

Rosebud Mining: St. Michael Discharge Water Treatment Plant Power Point Presentation

Cambria County Conservation District, 2000, South Fork Branch of the Little Conemaugh River Watershed Comprehensive Plan; funded through the Pennsylvania Department of Environmental Protection, Watershed Restoration and Assistance Program Grant

Internet Web Sites:

http://patheoldminer.rootsweb.ancestry.com/cammarylandsh.html

http://www.cjmerlo.com/index.php?page=saint-michaels-acid-mine-draining-treatment-plant

Personal Communication:

John St. Clair: Rosebud Mining Company
Jacqueline Ritko: Cambria County Conservation District

A PRELIMINARY ANALYSIS OF AN UPPER PENNSYLVANIAN FLUVIAL CHANNEL COMPLEX OF THE CASSELMAN FORMATION (CONEMAUGH GROUP) EXPOSED ALONG US-22 NEAR BLAIRSVILLE, PA

CHRISTOPHER COUGHENOUR, UNIVERSITY OF PITTSBURGH-JOHNSTOWN
JOAN HAWK, CME MANAGEMENT LLC

Introduction

In 2001 the Pennsylvania Department of Transportation began work on highway improvements to portions of US-22 and US-119 in Indiana County. These improvements included lane widening, straightening and, two miles east of Blairsville, construction of a ramp linking US-22 W to US-119 N (Figure 1). On the north side of this exit ramp an extensive roadcut reveals a complex of fluvial deposits in the Casselman Formation (Conemaugh Group, Virgilian) that measures 300 meters laterally and up to 6 meters vertically (Figure 2). The south side of the ramp offers a similar, but slightly less extensive vantage point. Just below the ramp, the interchange provides more exposures that are nearly orthogonal to the east-west trending sections of the ramp, facilitating a three-dimensional perspective of the unit and its architecture. Accordingly, this represents one of the largest and most accessible outcrops of its kind in Indiana County.

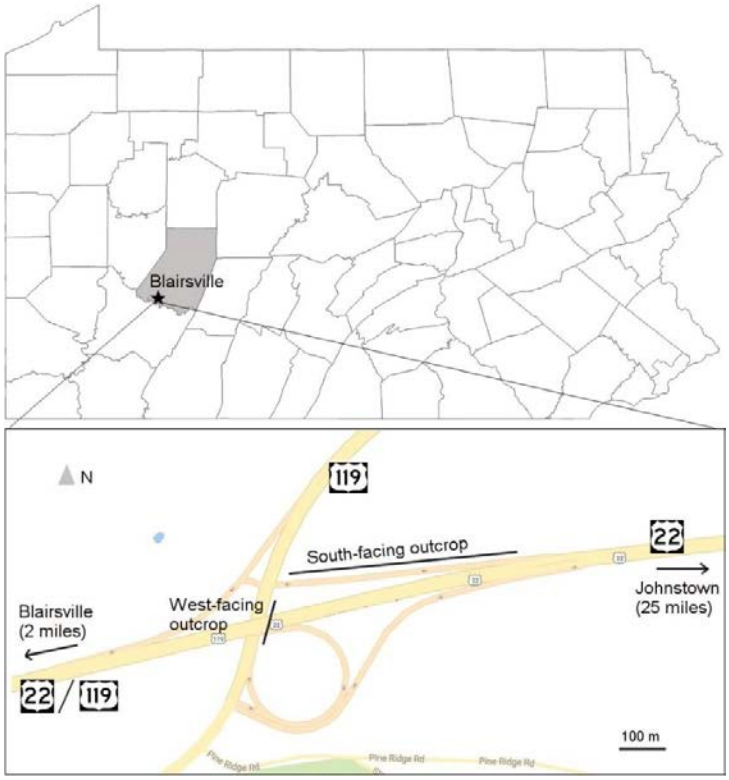

Figure 1. Map of the study locality near Blairsville, Indiana County (highway map from Google Maps)

The locality lies at the western edge of the northeast trending Chestnut Ridge, one of the more prominent structural and geomorphic features of the Appalachian Plateau in western Pennsylvania. This results in structurally controlled dips of around 6.3° (11%) to the northwest (Bragonier and Glover, 1996). Stratigraphic units near the interchange and its vicinity have been mapped as belonging to the Casselman Formation of the Conemaugh Group (Berg and Dodge, 1981).

The Conemaugh Group (Upper Pennsylvania, upper Missourian and Lower Virgilian) is a clastic sequence dominated by siltstone, claystone, shale and sandstone (Edmunds et al., 1999). Early Pennsylvania geologists called this series of rocks the "Lower Barren Measures" due to the lack of economically important coal beds that characterize the underlying Allegheny and the

overlying Monongahela series. That changed in 1865 when Franklin Platt renamed it "Conemaugh" after exposures along the Conemaugh River in adjacent Cambria County (Shaffner, 1958). The Conemaugh is bounded by the Upper Freeport coal at the base and the Pittsburgh coal at the top. The Conemaugh Group was divided into the Glenshaw and Casselman Formations by Flint (1965) in his survey of southern Somerset County based on the last occurrence of marine units. The unit dividing the two formations is the marine Ames limestone, which caps the Glenshaw Formation.

Figure 2. A typical section of the south-facing exposure along the US-22 W exit ramp. Sand sheet bodies predominate and generally lie above higher order bounding (erosional) surfaces and silty-sandy overbank deposits. Jacob's staff is 1.83 m in height.

The Casselman Formation is devoid of marine units with the exception of the non-persistent Skelly Marine Zone in the lower Casselman, which in Somerset County to the southeast is represented by a marine shale on the Federal Hill Coal and in Pittsburgh to the west by the Birmingham shale on the Duquesne Coal (Edmunds et al., 1999). By early Virgilian time the sea had retreated completely from this area and the Casselman Formation was deposited as alluvial sediments, often ascribed to upper deltaic environments (Edmunds et al., 1979). Although Pennsylvanian formations are composed of somewhat cyclic sequences of sedimentary lithologies, the concept of an idealized cyclothem as applied to the mid-continent falls apart for the Central Appalachians. Unlike the mid-continent, there is little vertical or horizontal lithic continuity in the Central Appalachians (Edmunds et al., 1979). In fact, the Glenshaw Formation thins from approximately 128 meters (420 feet) in Somerset County to approximately 85 meters (280 feet) in the very western part of Pennsylvania; the Casselman thins in a similar fashion from 148 meters (485 feet) in southern Somerset County to 70 meters (230 feet) in westernmost Pennsylvania. The Casselman Formation is one of the least studied formations of the Pennsylvanian, primarily because of its lack of economic resources and paleontologically significant fossil zone (Edmunds et al., 1999).

Methodology

To begin this reconnaissance study, the authors and several colleagues walked the US-22/US119 interchange and determined the most extensive outcrops were 1) the extensive south-facing roadcut along the US-22 W exit ramp and 2) the west-facing roadcut at the end of the ramp (Figure 1). The outcrops were then each divided into 10-meter sections. Each section was analyzed and photographed at 2.5 meter intervals. Where possible, fresh portions of the outcrop were sampled to observe grain size, color, composition and structure. Where sampling was not possible (due to height), deposit grain size and texture had to be visually inferred.

Determination of stratigraphic position within the Casselman Formation was explored via previously published literature and analysis of logged drill core data from the Rochester & Pittsburgh Coal Company (R&P). These cores were taken between 1.5 and 3 km from the study area. Drill core data also permitted determination of group and formation thicknesses and other local trends.

Casselman Formation in the study area

The Morgantown sandstone occurs in the approximate middle of the Casselman Formation and is often bounded by redbeds; Clarksburg red clay above and the Birmingham shale below (Figure 3). With limited exposures available, Shaffner had estimated the top of the Morgantown sandstone to lie approximately 64 meters (210 feet) below the base of the Pittsburgh Coal. Prior to the construction of the current interchange, Shaffner (1958) documented an occurrence of the Morgantown sandstone located just north of this outcrop along the original alignment of U.S. Route 119. In addition, he found a highly weathered outcrop of the Ames limestone along the original section of US. Route 22 (now Old William Penn Highway) near the current Chestnut Ridge Golf Club (400 m from the interchange) consisting of weathered limestone nodules 6 to 8 inches in diameter. This supports the notion that this outcrop is the Morgantown sandstone.

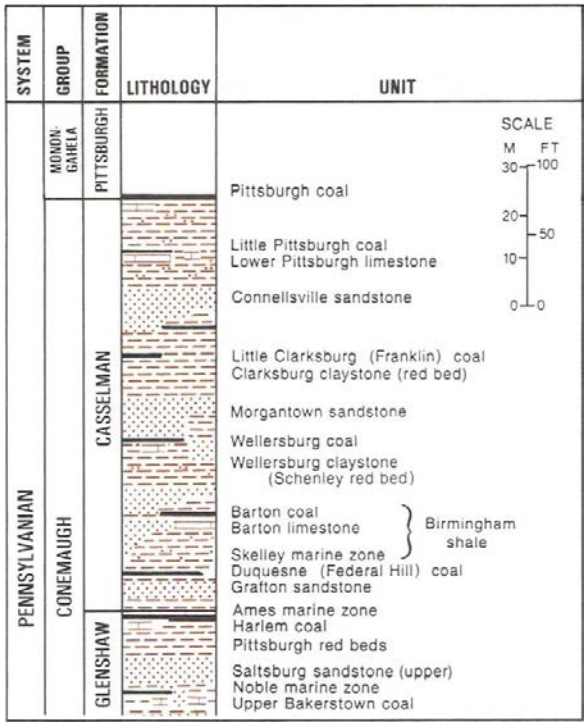

Figure 3. Simplified stratigraphic column for the Casselman Formation (Conemaugh Group) modified from Edmunds et al. (1999)

Three exploration drill holes from the archives of the Rochester & Pittsburgh Coal Company, IND-D-HELN-B0009, IND-D-HELN-B0011 and IND-D-HELN-B0012 show the total thickness of the Conemaugh to be approximately 222 meters (730 feet) with the Glenshaw approximately 375 thick and the overlying Casselman approximately 108 meters (355 feet) thick. These holes lie between approximately 1.5 kilometers (5,000 feet) and 3 kilometers (10,000 feet) from the outcrop. Two of the drill holes (B009 and B0011) were advanced through strata starting above

the Pittsburgh Coal in the overlying Monongahela Group and extending through the Lower Kittanning Coal in the underlying Allegheny Group. The third drill hole, B0012, was advanced through strata starting at what is correlated to the Connellsville sandstone. These drill hole logs are included in Appendix (digital guidebook).

The lack of lateral continuity of lithic units comprising the Casselman Formation is illustrated by these drill holes. Correlations among the drill holes indicate that the top of the Morgantown Sandstone lies approximately 60 meters (200 feet) below the base of the Pittsburgh Coal. The base of the Morgantown sandstone lies approximately 40 meters (130 feet) above the top of the Ames limestone. However, 5 meters (18 feet) of sandstone, correlated to the Morgantown sandstone is present at one location, bounded by red shale, whereas at a second location, the sandstone is not present, but its horizon is marked by 11 meters (36 feet) of sandy shale overlain by red shale, and underlain by the fossiliferous dark gray shale of the Skelley marine zone. At a distance of 27 meters (90 feet) above the Ames Limestone in the third hole there is no sandstone or sandy shale, but 9 meters (30 feet) of light grayish green shale bounded by red shale. In this same hole, at a height of approximately 45 meters (150 feet) above the Ames Limestone, there is 6 meters (20 feet) of light grayish green sandy fireclay, directly overlain by the Connellsville sandstone. The intervening strata are composed of shale and thin limestone. This may represent a merging of the Connellsville Sandstone with the representative of the Morgantown Sandstone horizon at this location. At the location where the Skelley marine zone is present there is no Ames fossil zone identified; however, the underlying Harlem coal is present, which is not present in the other holes.

Facies descriptions and interpretations

Primary lithofacies observed were described according to the scheme of Miall (1981), which provides standardized descriptions for commonly encountered fluvial lithologies. Overall, there are seven basic facies that occur throughout the study area (Table 1). The outcrops display a narrow grain size distribution, with nearly all sediment between the silt and medium sand size classes (save for a few, local gravels). The sands predominate over the silts. Horizontal, planar internal stratification (with minor ripple cross-lamination) is most common, with trough cross-stratification also common. In the sand-sized fraction, there is a broad degree of similarity in texture and color throughout the exposures. These sands are strongly quartzose, with some dark clasts, possibly tourmaline, also present (Orsborn, 2015). Mica content is variable, ranging from minor, small clasts to large flecks. The color is consistently medium-light gray with a slight light brown hue (unweathered). In some places, it simply appears to be a sandier gradation of Fl, while in other locations it shows distinct ripple lamination. Contorted strata, overturned strata, and flame structures were observed in this facies and Fl.

Gravels, which are rare on the south-facing outcrop, are common in some particular sand bodies along other exposures. Gravels consist almost entirely of mud rip-up clasts, save for rare isolated pebble conglomerate bodies. Diagenetic siderite concretions are commonly present. There is little evidence of widespread pedogenesis or biological activity in the outcrops examined, aside from some thin (< 1 cm) stringers of woody material/low-grade coal. Small occurrences of bioturbated claystone and coal were observed at the lowest stratigraphic position in the study.

Table 1. Codes and descriptions for basic lithofacies observed in the study (modified from Miall, 1981)

FACIES CODE	LITHOFACIES	SEDIMENTARY STRUCTURES
Fl	Silt (>50%), with some fine sand	Fine lamination (some heterolithic), small ripple cross lamination
Shr	Sand (>50%), fine to med with prominent silt	Horizontal lamination or ripple cross lamination
Fm	Mud	Massive, often with evidence of deformation
Shm	Sand (>80%), fine to coarse, with minor silt	Internal planar, horizontal lamination, sometimes with only thin, discontinuous silt (some appear internally massive on weathered surfaces)
Se	Sand, fine to coarse with intraclasts	Crude cross-bedding and/or massive appearance
St	Sand, fine to coarse	Solitary or grouped trough cross-beds
Sl	Sand, fine	Low angle (<10°) internal cross-stratification

Facies Fl (fine-grained, laminated)

A common unit observed, particularly along the south-facing outcrop, is a dark gray micaceous siltstone that is variably heterolithic, and commonly exhibits (internal) planar to wavy (small ripple) lamination that alternates between the dominant, dark silt size fraction and buff-colored sands of fine to medium size. This facies is designated as 'Fl' (Figure 4.A). In many places this facies is in contact with sandier zones that exhibit similar planar stratification. Disconformities and subtle angular discordances are not uncommon within this facies, particularly at contacts with sandier laminae. Identification of fine, millimeter-scale structures was greatly aided by the remnant blast drill holes used to excavate the cut. This facies commonly occurs in sets that are thick (some exceeding 2 meters) and laterally continuous over tens of meters. Facies Fl is most extensive in the south-facing outcrop in the first 60 meters of the section (much of the rest of the outcrop has a distinctly sandier character). There is little bioturbation or evidence of pedogenesis.

Facies Fl is interpreted as originating from overbank processes. Similar facies have been ascribed to floodplain deposition (see Bridge and Demicco, 2008) and passive fill of abandoned channels associated with overbank sedimentation (Li and Bhattacharya, 2014). Geometry of the body can help differentiate specific sub-environment (see Table 2).

Facies Shr (sandy, horizontal to ripple-laminated)

Facies Fl is closely associated in space/arrangement with a sandier unit (Shr) that exhibits horizontal planar lamination and some current-ripple lamination (Figure 4.B). These sandier bodies may represent particularly high-amplitude flood events (i.e. sheet floods), also in the overbank/floodplain environment. Facies Fl and Shr feather out and are often cut into by channel elements. The micaceous silt fraction was likely deposited from suspension when deeper water conditions prevailed or late in a waning flow, while the fine sands likely represent traction

transport produced during strong flows. Current-ripple lamination and preserved 2-D ripples are further evidence that traction transport was occurring.

Soft-sediment deformation is commonly observed in both Fl and Shr, likely the result of strong shear stresses induced by traction currents as overlying sands were laid down. Sometimes this occurs under basal channel scour, such as in the outcrop along US-119. Along the exit ramp, it occurs under trough and low-angle cross-beds (see below).

In these facies, there is a general lack of root casts, bioturbation, and plant fossils with the exception of limited zones of carbonified woody material and thin, low-grade coals. A paucity of pedogenic features indicates soil-forming processes were inhibited by relatively frequent delivery of sediment from active channels. Unfavorable climate conditions for pedogenesis may have also prevailed during this time, although typical arid climate indicators such as desiccation cracks, gypsum pseudomorphs, or adhesion ripples associated with aeolian transport were not observed (Wilson et al., 2014).

Facies Fm (massive mudstone/siltstone)

Another finer-grained facies present is a dark gray siltstone (in places, mudstone) that often does not display evident stratification or significant sand (in a few places it does resemble folded Fl). This facies often possesses an irregular, almost hackly appearance and displays jointed surfaces. It is locally fissile. It most commonly occurs in irregular tabular bodies up to 2 meters in thickness, but is also present in a large lobe and a ribbon body. It almost ubiquitously underlies sandstone deposits of facies Shm and St. This facies is designated as 'Fm' and is most common on the south-facing 'exit ramp' outcrop. (Figure 4.C)

The irregular surfaces of Fm, some perhaps accentuated by late diagenetic jointing, may indicate syndepositional or very early diagenetic deformation. In several outcrops, the beds are noticeably tilted and contain contorted beds. Its occurrence under channel sandstone facies and its geometric relation to channel forms suggests a relation to channel deposition. It is easily denoted (top and bottom) by bounding surfaces, implying three possible scenarios: 1) shear deformation of saturated Fl/Shr facies owing to precipitation and stresses of channel incision (or sheet flows where it occurs under Shr), 2) deposition at the bottom of an (initially) abandoned channel (Li and Battacharya, 2014) or 3) deposition during later-stage channel abandonment. For most of the Fm facies (occurring as irregular tabular bodies) we interpret scenario 1. An extreme case of scenario 2 occurs at the east end of the exit ramp, where a complete channel body is filled with Fm, forming a mud plug (Figure 5). This body is a "ribbon", possessing a width of 60 m and a maximum thickness of 4 m, yielding a W/T = 15 (Gibling, 2006). If the facies is more linear, or perhaps, slightly concave-down in character, scenario 3 is interpreted.

Facies Shm (very sandy, horizontal to faint lamination)

As sand content is further increased and silt becomes a minor component, the laminations become more linear and, in some cases, difficult to distinguish. These overwhelmingly sandy facies are denoted 'Shm' (Figure 4.D). These are often bounded by erosional surfaces and comprise sand bodies a few tens of meters long. This facies is the second most common facies observed (after Shr) and generally occurs in sand bodies bounded by high-order erosional surfaces (often concave-up).

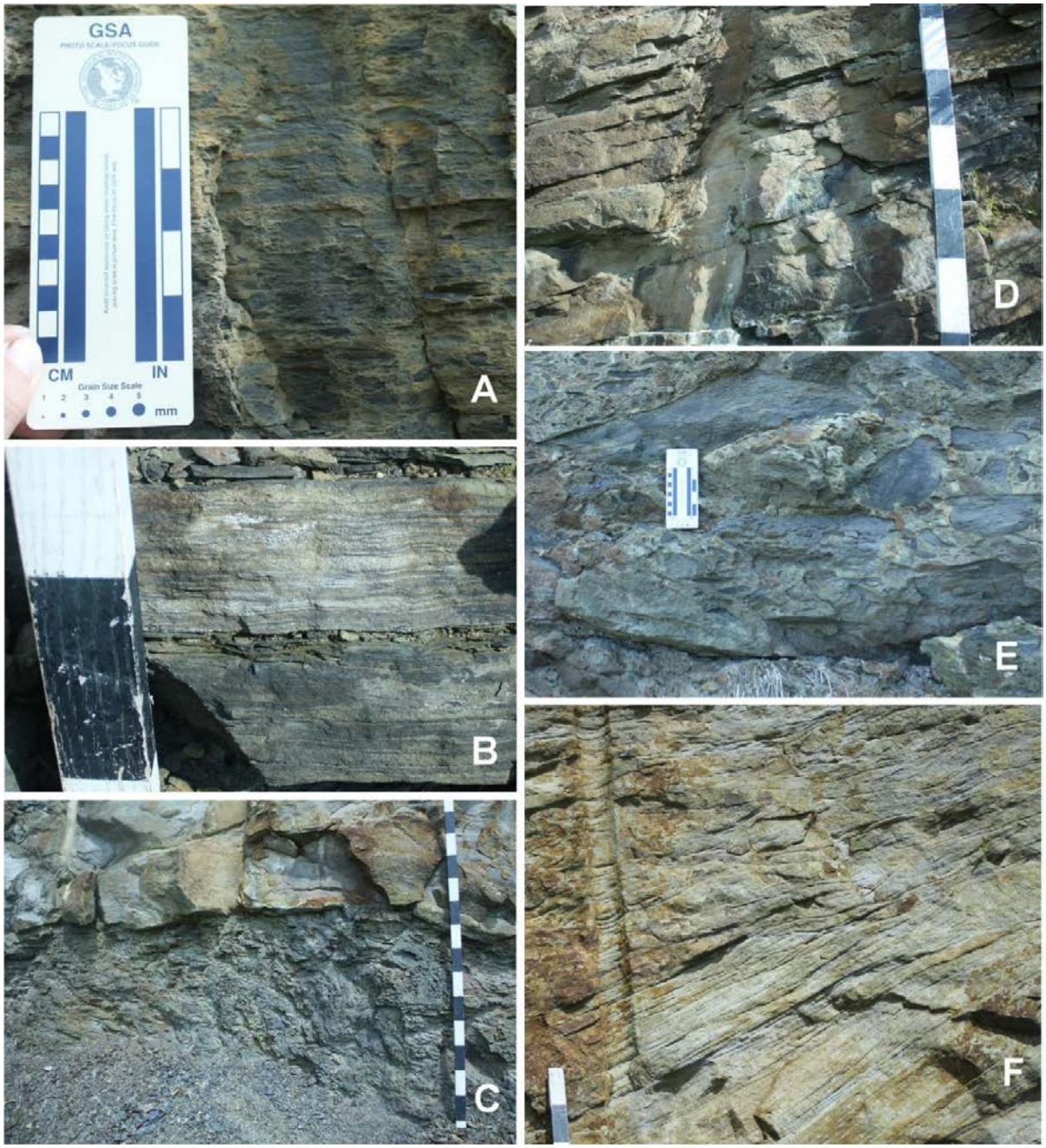

Figure 4. Examples of the primary facies observed: A) Fl, B) Shr, C) Fm, D) Shm, E) Se, and F) St (composed of superposed trough cross-bed sets on larger-scale inclined strata). Jacob's staff marked in decimeter increments.

Facies Shm is prominent in many sand bodies that are bounded by concave-up erosional surfaces. As such, we interpret these as channel bodies. In many of these sand bodies, there is prominent large-scale stratification (decimeter-scale), with the cumulative thickness of the sets generally 1-2 m. Beds are often boundary conformable, or nearly so. Dips are overwhelmingly to the west. Superposed on the larger-scale stratification is internal (mm-cm scale) horizontal stratification and, possibly, some trough cross-bedding.

These channel-fill bodies represent accretion, with several possible styles: vertical, downstream, or lateral. Li et al., (2015) interpreted similar deposits as resulting from channel filling after abandonment. Overbank sedimentation from active channels would supply sediment. Others have interpreted similar boundary-conformable arrangements as related to downstream unit-bar migration (e.g. Lowe and Arnott, 2015). Neither of these interpretations, nor the bulk of the visible outcrop evidence suggest widespread occurrence of lateral accretion elements, such as point bars. Weathering and relative height on the outcrop may be obscuring some of finer-scale features and important diagnostics (see example from Morrison Formation in Miall, 1996).

In some cases, thin (dm-scale) bodies of sand extend laterally from the channel forms. These are interpreted as levee deposits (Gibling, 2006). They are typically composed of Shm, often with only faintly observable silt stringers.

Facies Se (sandy scours with crude bedding and intraclasts)

Many of the sandstones observed along US-119 (the west-facing outcrop) display prominent mud rip-up clasts forming a matrix-supported conglomerate. A number of these rip-ups are composed of facies Fl. Most of the units bearing intraclasts show little/no readily apparent signs of stratification within the sandstone, although the intraclasts do exhibit a preferred long-axis orientation. This facies is designated as 'Se' (Figure 4.E). The geometry of the bodies containing Se is somewhat variable. Along US-119, a concave-up base is formed with lateral tapering with a single channel containing most of the Se facies there. Along the south-facing outcrop, bodies of Se have steep margins that seem to feather into laminated and siltier Shr facies.

Facies Se indicates rapid, sediment-choked flow (Hjellbakk, 1997). An apparent ball-and-pillow structure along US-119 and a sandy, almost massive nature, suggest rapid deposition. Rip-up conglomerates often lie near the base and appear to be sourced from immediately underlying Shm and Fl facies. This denotes avulsion into overbank environments. This close relation to overbank facies, the rather limited overall appearance of Se, and its apparent feathering into siltier Shr facies implies possible crevasse and splay processes.

Facies St (sandy, trough cross-bedding)

Other sandstones, generally sans intraclasts, are cross-bedded (internally). The predominant internally cross-bedded facies is designated as 'St' (Figure 4.F). Larger-scale bedding, several meters in thickness, frequently occurs with nested internal stratification (generally, trough and horizontal). These larger-scale strata are strongly unidirectional and most are oriented broadly to the west. In at least one location (along US-119), festoon trough cross-bedding of sands is visible with set thicknesses of 0.5 - 1 m (Figure 6).

Facies St is interpreted as representing subaqueous dune migration. This likely would occur as a result of lower flow regime currents of moderate depth (Lowe and Arnott, 2016). St was observed from several vantage points. Along the south-facing outcrop, several sets with high-angle dipping beds indicate paleoflow was broadly to the west during that cycle. In other places decimeter-scale sets of trough cross-beds were superposed with oblique flow onto larger-scale, westward dipping accretion surfaces. This one of the few visible indications that compound bar migration was occurring producing lateral or downstream accretion (see Gibling, 2006). Rotating perspective by 110° and looking along the west-facing outcrop, festoon trough cross-

bedding indicates a roughly flow-parallel view into the outcrop (east-west paleoflow) related to sinuous mesoform migration (Figure 6).

Figure 5. Abandoned channel mud plug observed at the east end of the US-22 exit ramp. This is a "ribbon" channel body.

Figure 6. Prominent festoon cross-bedding along US-119.

Facies Sl (sandy, low-angle cross-bedding)

Another cross-bedded sandstone is denoted 'Sl' when exhibiting low-angle (< 10°) cross-bedding (Figure 7.A). This facies is not as common as those described above, but is not uncommon along the south-facing cut.

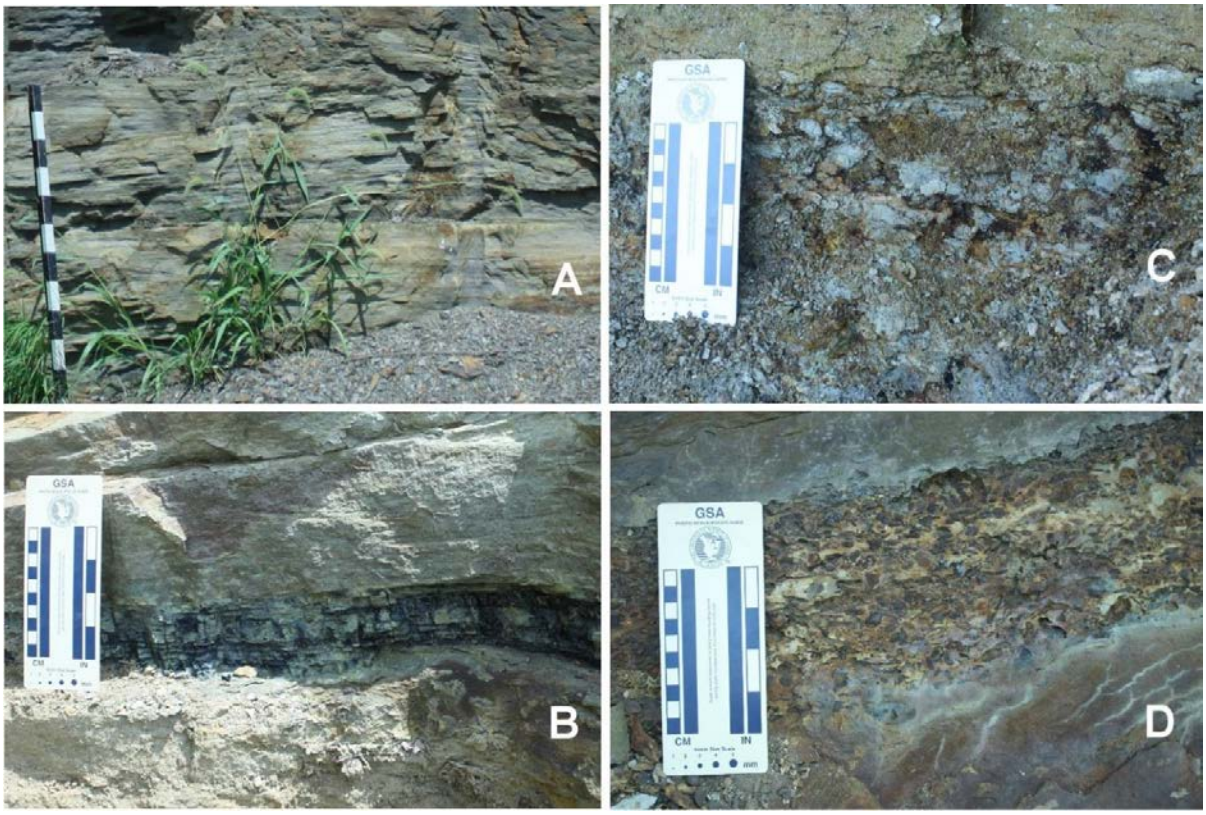

Figure 7. Secondary facies observed in the study area: A) Sl, B) coal, C) bioturbated claystone with apparent carbonized rootlets, and D) ferruginized conglomerate. Note that B-D were found near the bottom of the US-119 outcrop.

In a few places, silt-draped sandy laminae dipped sufficiently (< 10°) to warrant recognition of facies Sl. One interpretation for this facies is antidune/standing wave deposition (Fielding, 2006). This may have occurred on the floodplain with shallow depths promoting upper flow regime conditions, possibly during splaying (Wakelin-King and Webb, 2007). Contorted beds of Shr have been found under this deposit, suggesting rapid deposition and strong shear (Figure 8).

Local coal and claystone

At the lowest stratigraphic position of the pilot study, a 5 cm-thick coal bed was observed (Figure 7.B). In similar position several meters away was a bioturbated gray claystone (Figure 7.C). Just above these was a ferruginized pebble conglomerate. These were unique in that no similar units were found in the overlying 10-meters of sandstone and siltstones (Figure 7.D).

Near the bottom of the succession claystone and a thin coal were observed that suggest a different setting than that portrayed in the overlying sediments if, of course, these deposits are indicative of those in the subsurface. This could record a different fluvial/hydrogeologic regime that favored longer retention of near-surface water and/or a shift in paleoclimate.

Architectural elements:

All of the facies described above occur in association (except the basal coal and claystone). These facies can be further interpreted by recognizing "architectural elements" that "build" the overall system (see Miall, 1996). In this preliminary study, 5 elements were recognized (see Table 2). A typical section is annotated with its interpretation in Figure 9. A corresponding vertical log is provided in Figure 10.

Figure 8. Soft-sediment deformation showing internally contorted strata and overturning. Note that local shear would have been broadly toward the west (left on photo).

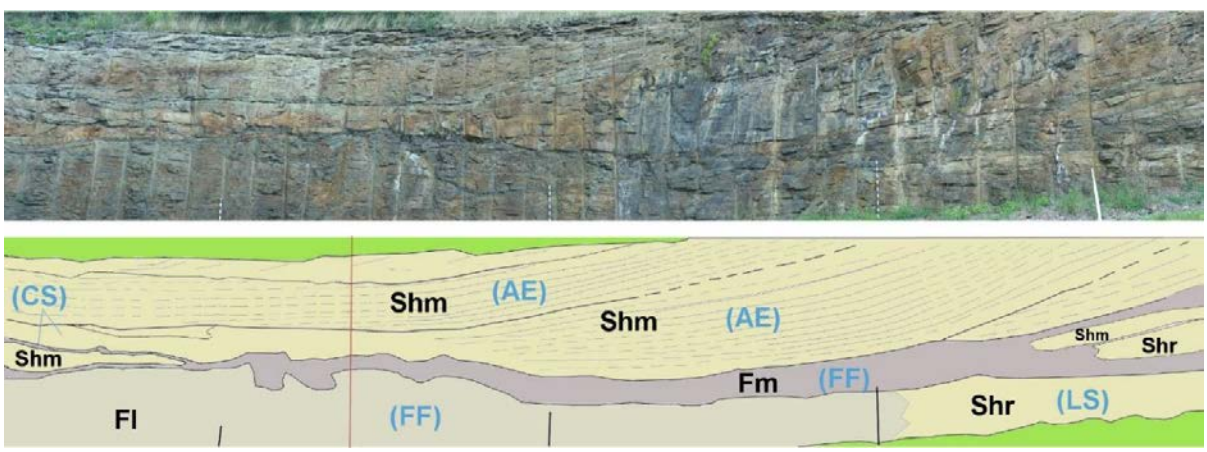

Figure 9. Photo of a section of the south-facing outcrop (top) with interpretation of the lateral profile (bottom). The staffs are 10 m apart. Lithofacies are denoted in black and architectural elements are in blue and parentheses (see Table 2 for element interpretations). The vertical red line denotes the location for the vertical log in Figure 10.

In the absence of other distinguishing criteria, or for simple channel fills, the channel element (CH) is invoked. A prominent CH element is noted at the extreme east end of the exit ramp and is interpreted as an abandoned channel fill (see Figure 5). It possesses a diagnostic concave-up basal surface, infill with muddy sediment (Fm), and lateral pinch-out. The accretion element (AE) is a more specific interpretation of channel deposits and filling. With further detailed

observations these may be broken down into vertical (often sandy bedforms), lateral, or downstream accretion elements (Miall, 1996).

The laminated sand sheet (LS), floodplain fines (FF), and crevasse splay (CS) elements are associated with overbank processes (at least relative to the trunk channel).

Table 2. Summary of lithofacies interpretations and architectural elements observed in the study

LITHO-FACIES	INTERPRETATION	ARCHITECTURAL ELEMENT(S)	COMMENTS	REFERENCE(S)
St	Within-channel migration of mesoforms (e.g. dunes)	AE (accretion element)	Generally observed on south-facing outcrop superposed with larger dipping surfaces. Strikes of set surfaces variable	Lowe & Arnott, 2016 Miall, 1996
Shr	Related to overbank traction transport and sheet flooding. Lower flow regime	LS (laminated sand sheet)	Second most common facies. Laterally extensive/unbounded geometry. Soft-sed deformation common	Bridge & Demicco, 2008 Wilson et al., 2014
Shm	Channel belt deposition by accretion	AE (accretion element)	Most common facies on south-facing outcrop. Bounded by concave-up basal surfaces. Note: some Shm are levee deps., denoted as CS elements	Li et al., 2015 Lowe & Arnott, 2016
Sl	Overbank, related to shallow depth promoted upper flow regime and antidune migration	LS (laminated sand sheet)	Grades from Shr. Often overlies soft-sediment deformation	Fielding, 2006 Wakelin-King & Webb, 2007
Se	Sediment dumping in channels. Scours due to avulsion (including crevasse channel cut)	CS (crevasse splay element) CH (channel element)	Intraclastic mud rip-ups and concave-up bases. Frequently exhibits steep margins that interfinger with Shr	Hjellbakk, 1997
Fl	Overbank (floodplain) primarily suspension	FF (floodplain fines element)	Often associated with Shr and laterally extensive/unbounded	Bridge & Demicco, 2008
Fm	Variously deformed/folded muds from floodplain shear and channel abandonment	FF (floodplain fines element) CH (channel element)	Most form thin (<1 m) irregular tabular bodies under channel sands. Prominent channel fill mud plug	Li & Bhattacharya, 2014

Interpretation of fluvial style

The large majority of sediments preserved in the system display evidence of bedload transport. Paleocurrent indicators observed were strongly unidirectional, particularly for larger-scale accretion surfaces, implying possible low sinuosity. Fluvial mechanics are interpreted here as probably that of a sandy bedload system (*sensu* Galloway and Hobday, 1996). Channel fills are dominantly sandy and floodplain deposits exhibit no/little bioturbation or pedogenesis and are sandy-silty in character. Furthermore, the sandy within-channel deposits volumetrically exceed interpreted overbank deposits. The above evidence suggests a medial position within the fluvial distributary system (Nichols and Fisher, 2007). Overall, the system appears to have been aggradational, with sand-body stacking and little evidence for terracing. Given the lateral extent of the sand bodies, it appears the system possessed a mobile channel belt. Braided, low-sinuosity, and meandering streams can occur in sandy, mobile belts (Gibling, 2006). An apparent lack of lateral accretion sets (epsilon cross-bedding), lack of divergent paleocurrent directions, and lack of oxbows or extensive "stable" floodplain seem to suggest the system was not meandering. Broadly similar architectural styles to those recorded at Blairsville have been observed in systems in which a sandy, braided style was interpreted (e.g. Wilson et al., (2014), Li et al., (2015), Lowe and Arnott (2016)). More observations, including more extensive paleocurrent data, are needed to more definitively elucidate fluvial style in the Blairsville outcrop.

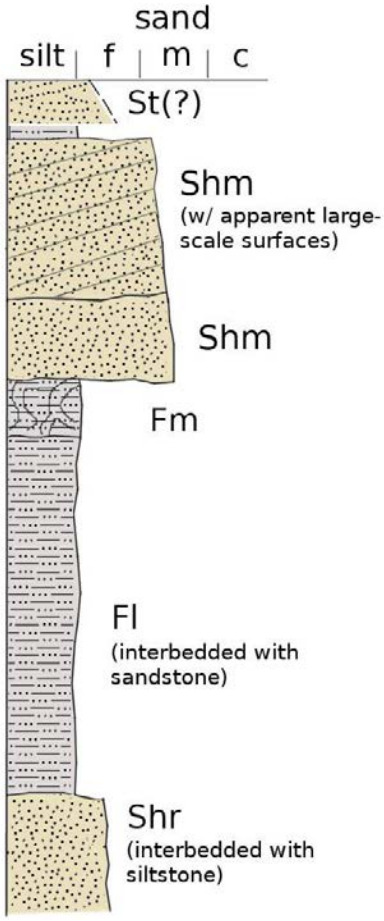

Figure 10. Representative vertical log for the south-facing outcrop. Note that a sandstone unit was present, but not in the outcrop photo in Figure 9.

Gibling (2006), in an exhaustive review of fluvial channel bodies and published literature, asserted that meandering streams appear to represent only a small fraction of styles preserved in the stratigraphic record. Hartley et al. (2015) noted that, in lateral profile, sandy fluvial deposits in the Morrison Formation resembled those often described/modeled as braided in style. This system, however, was exceptionally well-exposed in plan view in the Utah drylands, revealing a meandering planform. The key diagnostic for meandering streams, lateral accretion elements, composed less than 5% of the total outcrop.

The Upper Pennsylvanian Conemaugh Group is generally thought to denote the latter stages of a transition from marginal marine and coastal plain conditions, such as those predominating in the Middle Pennsylvanian, to more alluvial conditions such as those seen in the non-marine Casselman Formation (see Greb et al., 2009). The sandy bedload architecture and aggrading nature of the system preserved near Blairsville indicate at least strong, periodic fluxes of

sediment. Whether this was a function of proximity to sediment sources, tectonic forcing, or dry climate (or some combination thereof) remains for further study. A recent study of (lower) Casselman deposits and paleoecology prompted by the discovery of a temnospondyl amphibian (*Fedexia striegeli*, near Pittsburgh) reveals that this period of the Virgilian may have been fairly dry (Berman et al., 2010).

Conclusion

The US-22/US-119 interchange near Blairsville, PA preserves a laterally extensive record of the evolution of a mobile, sandy fluvial belt. The deposits here have been preliminarily assigned to the Morgantown sandstone member of the Casselman Formation. Extensive exposures like those seen at this roadcut offer a 3-D perspective and afford much greater information than data gathered from cores and borehole studies alone. More study of this unit and its correlatives in the region may reveal interesting evidence for basin-scale sedimentation dynamics and possible relations to tectonics, as well as regional paleoclimate.

References:

Berg, T.M. and Dodge, C.M., eds., Atlas of preliminary geologic quadrangle maps of Pennsylvania: Map 61, Bureau of Topographic and Geologic Survey, PA DCNR.

Berman, D.S., Henrici, A.C., Brezinski, D.K. and Kollar, A.D., 2010, A new trematopid amphibian (Temnospondyli: Dissorophoidea) from the Upper Pennsylvanian of western Pennsylvania: earliest record of terrestrial vertebrates responding to a warmer, drier climate: Annals of Carnegie Museum, v. 78, no. 4, p. 289-318.

Bridge, J. and Demicco, R., 2008, Earth surface processes, landforms and sediment deposits: Cambridge, England, Cambridge University Press, 815 p.

Bragonier, W.A and Glover A.D., 1996, Coal resources of the Indiana County, Part 1. Coal crop line, mined-out areas, and structure contours: Pennsylvania Geological Survey, 4th ser., Mineral Resource Report 98, 126 p.

Edmunds, W.E., Berg, T.M., Sevon, W.D., Piotrowski, R.C., Heyman, L., and Rickard, L.V., 1979, The Mississippian and Pennsylvanian (Carboniferous) Systems in the United States—Pennsylvania and New York, in, The Mississippian and Pennsylvanian Systems in the United States: U. S. Geological Survey Professional Paper 1110-A-L, p. B1-B33.

Edmunds, W.E., Skema, V.W., and Flint, N.K., 1999, Pennsylvanian, chap. 10 *of* Schultz, C. H., ed., The Geology of Pennsylvania: Pennsylvania Geological Survey, 4th ser., p. 15449-169.

Fielding, C.R., 2006, Upper flow regime sheets, lenses and scour fills: extending the range of architectural elements for fluvial sediment bodies: Sedimentary Geology, v. 190, p. 227-240.

Flint, N.K., 1965, Geology and mineral resources of southern Somerset County, Pennsylvania: Pennsylvania Geological Survey, 4th ser., County Report 56A, 267 p.

Galloway, W.E. and Hobday, D.K., 1996, Terrigenous Clastic Depositional Systems: Heidelberg, Springer Berlin, 489 p.

Gibling, M.R., 2006, Width and thickness of fluvial channel bodies and valley fills in the geological record: A literature compilation and classification: Journal of Sedimentary Research, v. 76, p. 731-770.

Greb, S.F., Chestnut, D.R., Eble, C.F., and Blake, B.M., 2009, The Pennsylvanian of the Appalachian Basin, *in* Greb, S.F. and Chestnut, D.R., eds., Carboniferous Geology and Biostratigraphy of the Appalachian Basin: Kentucky Geological Survey, Special Publication 10, p. 32-45.

Hartley, A.J., Owen, A., Swan, A., and others, 2015, Recognition and importance of amalgamated sandy meander belts in the continental rock record: Geology, v. 43, p. 679-682.

Hjellbakk, A., 1997, Facies and fluvial architecture of a high-energy braided river: the Upper Proterozoic Seglodden Member, Varanger Peninsula, northern Norway: Sedimentary Geology, v. 114, p. 131-161.

Li, Y. and Bhattacharya, J., 2014, Facies architecture of asymmetrical branching distributary channels: Cretaceous Ferron Sandstone, Utah, USA: Sedimentology, v. 61, p. 1452-1483.

Li, S., Yu, X., Chen, B., and Li, S., 2015, Quantitative Characterization of Architecture Elements and Their Response to Base-Level Change in a Sandy Braided Fluvial System at a Mountain Front: Journal of Sedimentary Research, v. 85, p. 1258-1274.

Lowe, D.G. and Arnott, R.W.C., 2016, Composition and Architecture of Braided and Sheetflood-Dominated Ephemeral Fluvial Strata in the Cambrian–Ordovician Potsdam Group: A Case Example of the Morphodynamics of Early Phanerozoic Fluvial Systems and Climate Change: Journal of Sedimentary Research, v. 86, p. 587-612.

Miall, A.D., 1981, Analysis of fluvial depositional systems: AAPG Education Course Note Series #20, 75 p.

Miall, A.D., 1996, The geology of fluvial deposits. Sedimentary facies, basin analysis, and petroleum geology: New York, NY, Springer-Verlag, 582 p.

Nichols, G.J. and Fisher, J.A., 2007, Processes, facies and architecture of fluvial distributary system deposits: Sedimentary Geology, v. 195, p. 75-90.

Orsborn, N., 2015, Deposition and Structural Features of the Basal Morgantown Sandstone of the Casselman Formation (Pennsylvanian) of the Greater Pittsburgh Region: Pittsburgh, Pa, University of Pittsburgh, Master's thesis, p. 111.

Shaffner, M.N., 1958, Geology and Mineral Resources of the New Florence Quadrangle, Pennsylvania: Pennsylvania Geological Survey, 4th ser., Atlas 57 p. 165.

Wakelin-King, G.A. and Webb, J.A., 2007, Upper-flow-regime mud floodplains, lower-flow-regime sand channels: sediment transport and deposition in a drylands mud-aggregate river: Journal of Sedimentary Research, v. 77, p. 702-712.

Wilson, A., Flint, S., Payenberg, T., Tohver, E. and Lanci, L., 2014: Architectural styles and sedimentology of the fluvial lower Beaufort Group, Karoo Basin, South Africa: Journal of Sedimentary Research, v. 84, p. 326-348.

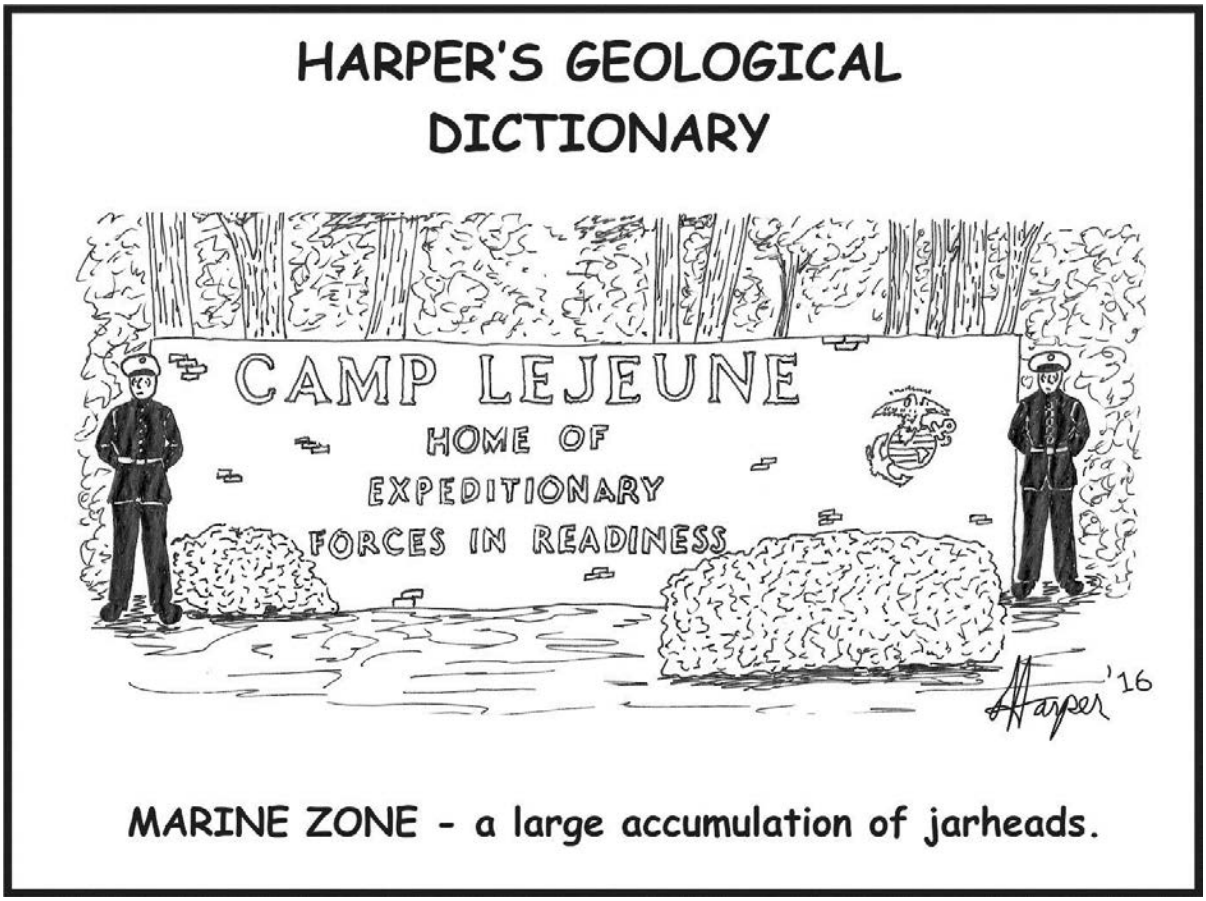
HARPER'S GEOLOGICAL DICTIONARY
CAMP LEJEUNE
HOME OF
EXPEDITIONARY
FORCES IN READINESS
Harper '16
MARINE ZONE - a large accumulation of jarheads.

SOME GEOLOGICAL CONSIDERATIONS OF THE MARINE ROCKS OF THE GLENSHAW FORMATION (UPPER PENNSYLVANIAN, CONEMAUGH GROUP)

JOHN A. HARPER, PENNSYLVANIA GEOLOGICAL SURVEY (RETIRED)

The Glenshaw Formation

When the first Geological Survey of Pennsylvania began its work in 1836, the series of rocks we now know as the Conemaugh Group was called the "Lower Barren Coal Measures" because of the perceived lack of economically mineable coal seams. This name remained in place until Platt (1875, p. 8) coined the term "Conemaugh series" to include all the rocks from the base of the coal, which cropped out along the Conemaugh River from Johnstown, Cambria County to Saltsburg, Indiana County. Woolsey (1906) later upgraded the name to Conemaugh Formation, and that nomenclature remained in place throughout most of the Appalachians until Flint (1965) subdivided the interval into a lower Glenshaw Formation, defined by the occurrence of numerous marine units, and an upper Casselman Formation that was mostly devoid of marine rocks. This action upgraded the Conemaugh to a group (although the Pennsylvania Geological Survey had been using that terminology for many years). The top of the marine Ames Limestone is the boundary between the two formations (Figure 1).

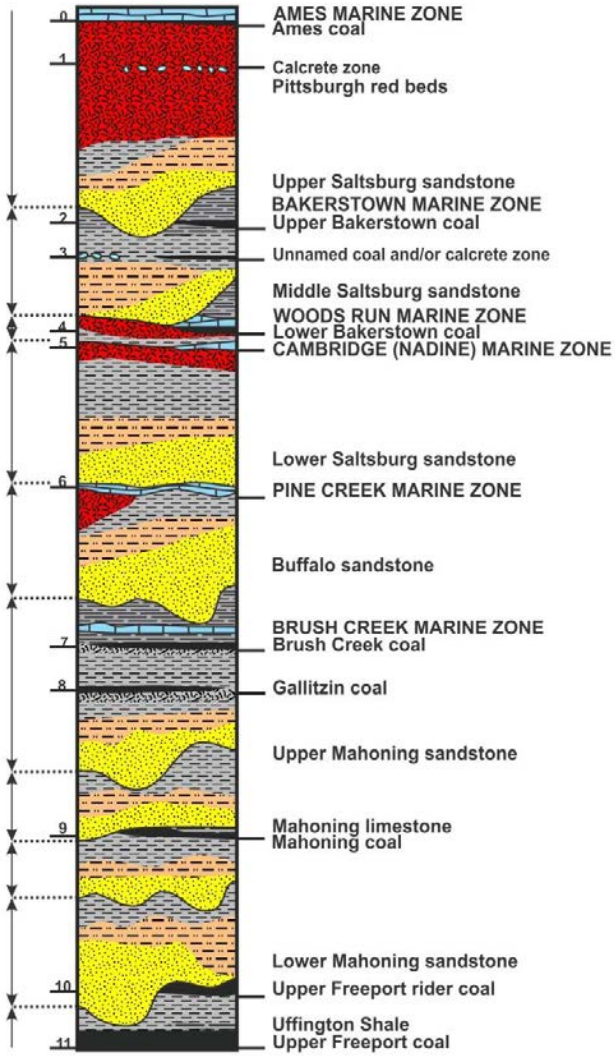

Figure 1. Generalized stratigraphic section of the Glenshaw Formation in western Pennsylvania (based on Busch and Rollins, 1984). The marine zones (in caps) are important marker horizons throughout the formation. Arrows between dashed lines indicate cyclothems based on the classic concept of Wanless and Weller (1932). Numbered intervals indicate transgressive surfaces or climate change surfaces separating 5th-order transgressive-regressive intervals (see Busch and Rollins, 1964).

The Glenshaw Formation in Pennsylvania ranges from about 280 ft (85 m) thick near the Ohio border to more than 400 ft (122 m) thick in Somerset and Cambria counties (Edmunds et al., 1999). It consists primarily of fluvio-deltaic siliciclastics that form a complex mosaic of interfingering channel, levee, overbank, and lacustrine deposits. These nonmarine

rocks are punctuated at intervals by thin marine zones of limestone and/or shale (Figure 1) that record six separate marine incursions of an epeiric sea that transgressed from the Midcontinent, probably through a seaway in southern Ohio and Kentucky (Donahue and Rollins, 1974a), onto a shelf formed by the detrital slope of the Appalachian highlands to the east during the Missourian through early Virgillian (late Westphalian D through Middle Stephanian global stages) (Heckel et al., 1998). The Glenshaw Formation contains few economically and stratigraphically important coals, but it makes up for that lack by the presence of the marine limestones, which have been used as key beds in physical (and temporal) correlation of outcrops and cores across western Pennsylvania and adjacent states. Despite a maximum thickness of only 1 to 3 ft (0.3-0.9 m), they are laterally extensive, and are known from western Pennsylvania, eastern Ohio, northern West Virginia, western Maryland, and even eastern Kentucky (Chesnut, 1981) (Figure 2). Two of the marine units, the Brush Creek and the Ames, tend to have the most continuous distribution of any sedimentary sequence within the Glenshaw. Because of their regional extent, unique lithologies, and fossil faunas, they are important marker beds for stratigraphic correlations within the Upper Pennsylvanian Series.

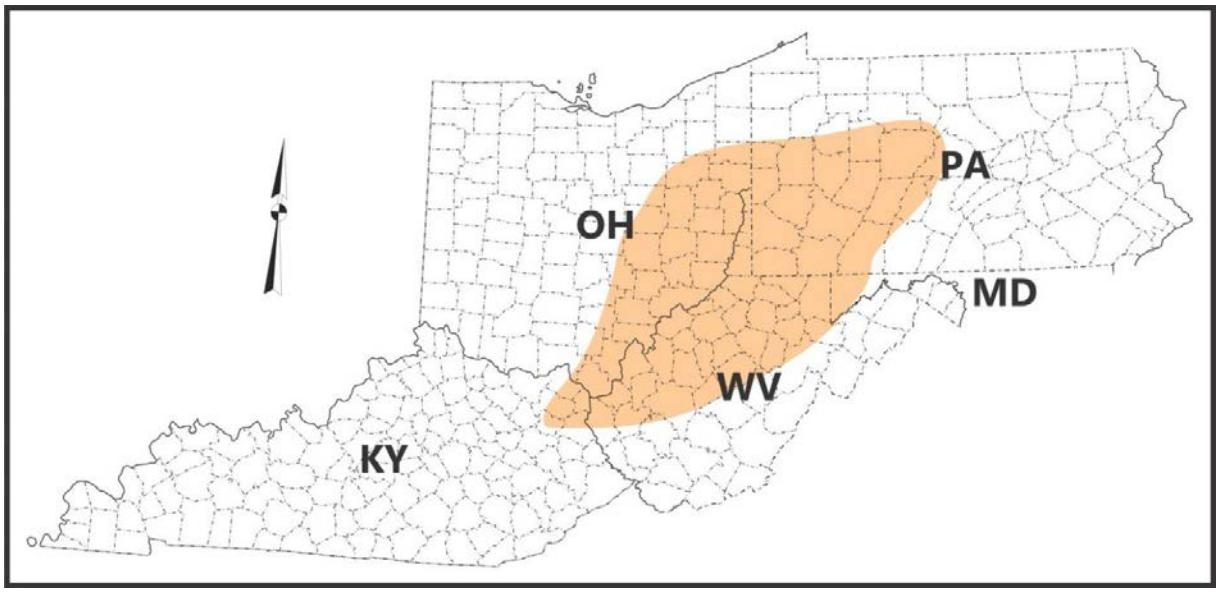

Figure 2. The sand-colored area denotes the approximate extent of the Glenshaw depositional basin (based on Busch and Rollins, 1984, and Martino, 2004).

Glenshaw Cyclothems: Allocyclicity versus Autocyclicity

Ever since the early 1930s, geologists have recognized cycles of deposition (cyclothems) throughout the Pennsylvanian strata of North America. Figure 3 illustrates an "ideal cyclothem" for the Appalachian Basin (compare Figure 3 with the cyclothem sequences in Figure 1). Twenty-six years after Wanless and Weller's classic paper on cyclothems (Wanless and Weller, 1932), Myron Sturgeon recognized eight cycles in the lower half of the Conemaugh Formation in Ohio (Sturgeon, in Sturgeon et al., 1958; Sturgeon and Hoare, 1968). Wanless and Shephard (1936)

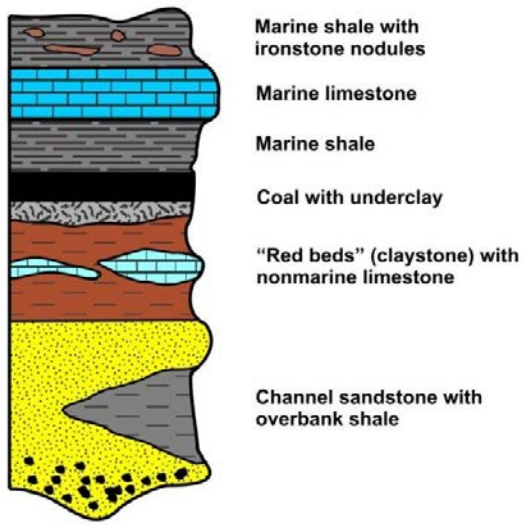

Figure 3. "Ideal cyclothem" for the Glenshaw (based on Donahue and Rollins, 1974a).

attributed these types of cycles to global sea level changes caused by glaciations in the southern hemisphere. Although not generally accepted at first, this concept became the standard explanation for the Appalachian Pennsylvanian cyclothems until the late 1960s and 1970s when work on depositional systems within the basin led some researchers to interpret Appalachian cyclothems as autocyclic, rather than allocyclic (e.g., Beerbower, 1964; Williams, 1964; Ferm, 1975; and others). Competing views of allocyclic versus autocyclic origins for Appalachian cyclothems were batted back and forth throughout the 1980s and 1990s. Busch (1984; also Busch and Rollins, 1984), Busch and West (1987), and Heckel (1995) among others, favored the allocyclic origin. In contrast, Klein and Willard (1989) and Klein and Kupperman (1992), among others, regarded Appalachian-type cyclothems as occurring in response to episodic thrust loading during orogenic events. According to this model, thrust loading caused the foreland basin to become deeper, generating transgressive facies in the basin. Regressive facies resulted when orogenic uplift caused increased sedimentation. More recently, Greb et al. (2008) found that, although glacial eustasy influenced Pennsylvanian deposition across the Appalachian Basin, the depositional cycles were influenced by changing paleoclimate, sediment flux, and changing rates of tectonic accommodation as well. So, the question of whether Pennsylvanian cyclothems are the result of allocyclic or autocyclic influences can be answered simply and succinctly: "yes!"

As marine units situated within a primarily terrestrial succession, the Glenshaw marine zones are valuable in assessing sea level cycles (e.g., Donahue and Rollins, 1974a; Busch and Rollins, 1984) and for use in correlating eustatic events between the Appalachian Basin and Carboniferous basins in Illinois and the Midcontinent (e.g., Heckel et al., 1998; 2011) (see below). Each of the Glenshaw marine intervals represents a sea level rise that inundated the deltaic margin and deposited marine shales and argillaceous limestone on the more typical fluvio-deltaic sandstones, non-calcareous shales, paleosols, and thin coals characteristic of Late Pennsylvanian sedimentation in the Appalachian Basin.

Martino et al. (1996; also Lebold, 2005) considered four of the Glenshaw marine zones, the Brush Creek, Pine Creek, Cambridge (Nadine), and Ames (Figure 1), to be widespread, major transgressions. Such transgressions established a variety of marine facies within the Appalachian Basin, allowing for numerous stratigraphic, sedimentologic, and paleoecologic studies since the late 1960s (Brant, 1971; Donahue et al., 1972; Donahue and Rollins, 1974a; 1974b; Shaak, 1975; Rollins and Donahue, 1975; Carother, 1976; Rollins et al., 1979; Al-Qayim, 1983; Brezinski, 1983; Busch, 1984; Saltsman, 1986; Caudill, 1990; Fahrer, 1996; Martino et al., 1996; Lebold and Kammer, 2006; Klasen, 2007; Heckel et al., 2011; and many others). Although the current stratigraphic framework is based on key beds (laterally persistent coal seams and

marine zones), several studies attempted to establish a sequence stratigraphic framework (Martino, 2004; Klasen, 2007).

Glenshaw Marine Zones

Busch (1984) recognized eight marine zones within the Glenshaw Formation in the Appalachian Basin. The lower two of these, apparently marine zones associated with the Upper Freeport and Mahoning cyclothemic sequences (Figure 1), are rarely, if ever, preserved and exposed in Pennsylvania, although they are exposed at places in Kentucky, Ohio, and West Virginia. Busch (1984) and Shaulis (1993) recognized a shale bearing lingulid brachiopods (brackish to marine) and plant fossils overlying the Mahoning coal near Lavansville, Somerset County. Busch (1984) referred to this as the "Uffington Shale". The type Uffington of West Virginia, however, is nonmarine and, where exposed, lies between the Upper Freeport coal and Lower Mahoning sandstone (Figure 1). The confusion results from a series of repeated misinterpretations: 1) Stevenson (1871) described, but did not name, a dark-colored, fine-grained, argillaceous shale containing marine fossils, identified by F. B. Meek, overlying the Upper Freeport coal; 2) White (1903), in describing and naming the Uffington, reported Meek's list of invertebrate fossils, even though he actually found only plant fossils in the formation, implying that Stevenson's shale and the Uffington were one and the same; and 3) until 1917, some authors (e.g., Raymond, 1910 and 1911) simply continued to consider the Uffington to be marine. Although Price (1917; also Hennen and Gawthrop, 1917) confirmed that the type Uffington was nonmarine, and that Stevenson's (1871) marine zone was actually Brush Creek, erroneous reports of the Uffington being a marine zone continued (e.g., Busch, 1984). Busch also made the error of placing the Uffington above the Mahoning coal, rather than above the Upper Freeport coal. If a marine zone actually associated with the Upper Freeport coal does exist, it apparently does not occur in Pennsylvania, and neither this nor the Mahoning marine zone will be addressed further here. The remaining six marine zones are widespread and typically preserved in many outcrops. In western Pennsylvania, these include, in ascending order, the Brush Creek, Pine Creek, Nadine, Woods Run, Bakerstown, and Ames.

Brush Creek Marine Zone

White (1878) named the Brush Creek limestone for a sequence of marine rocks exposed along Brush Creek in Cranberry Township, Butler County. He described it as:

> At times it is a black calcareous shale, 4 to 5 feet thick, and again we see it a very compact limestone, 1 to 2 feet thick. It often has a peculiar slaty and arenaceous aspect, and sometimes contains so much iron as to be used as an ore. It is usually fossiliferous, and the following species have been seen in it: *Chonetes mesoloba, Spirifer cameratus, Edmondia Aspenwalensis, Bellerophon montfortianus, Productus Prattenanus, P. longispinus, Nautilus occidentalus, and Lophophyllum proliferum*. (White, 1878, p. 34)

The names of those fossils have changed over the years, but all are recognizable to anyone who has collected Pennsylvanian fossils in the Appalachians. Plates 1 to 3 illustrate many of the marine invertebrate fossils that can be found in the Brush Creek and other Glenshaw marine zones in Pennsylvania. Busch (1984) described the Brush Creek as primarily black, gray, or olive marine shales containing common fossils and ironstone nodules. There is also a highly

fossiliferous, dark gray, argillaceous wackestone-packstone facies present within the shales at many localities, and in other localities the limestone is present but the marine shales are not.

For many years, any Glenshaw marine limestone sandwiched between dark-colored marine shales was considered to be the Brush Creek. Several classic localities in Allegheny (Sewickley locality), Armstrong (Cadet Restaurant locality), and Indiana (Shelocta locality) counties provided great fossil collecting opportunities for both weekend paleontologists and students anxious to write a Master's or Doctoral thesis on any number of paleobiological or paleoecological topics. Alas, many of these sites are now known to be Pine Creek localities, making the data and conclusions of those theses suspect. Some of the sites are now off limits, and others have been destroyed. In addition, certain localities in Fayette and Somerset counties considered Brush Creek because of appearance and fossil content (Piccolomini Strip Mine locality in Fayette County; Ursina locality in Somerset County) turned out to be Woods Run instead. This leads to the inevitable conclusion that, just because it looks like a duck, walks like a duck, and quacks like a duck doesn't mean it's a duck! Other "Brush Creek" localities (e.g., Donahoe and Youngwood in Westmoreland County) will remain Brush Creek until proven otherwise.

Pine Creek Marine Zone:

White (1878) named the Pine Creek limestone for exposures on the hill between Gourdhead Run and Pine Creek at Allison Park, Hampton Township, Allegheny County. The limestone was found on the property of J. A. Herron, lying 162.5 feet above Pine Creek (White, 1878, p. 161) (Figure 4). Some workers (e.g., Busch, 1984) and at least one website (Evans, 2003) mistakenly cited a classic exposure of the limestone on PA Route 8 in Etna, about 5 miles south of Allison Park, as the type locality, but White (1878) was quite specific.

The Pine Creek is a dark gray, argillaceous and arenaceous, fossiliferous wackestone that often carries phosphate granules (Busch, 1984). Like the Brush Creek, it commonly is sandwiched between dark gray or black marine shales carrying a well-preserved fauna. To the east, the Pine Creek grades into a dark gray, somewhat oolitic calcilutite surrounded by buff to reddish-colored clay shales with a few marine fossils. This phase of the Pine Creek marine zone is referred to as the Meyersdale red beds.

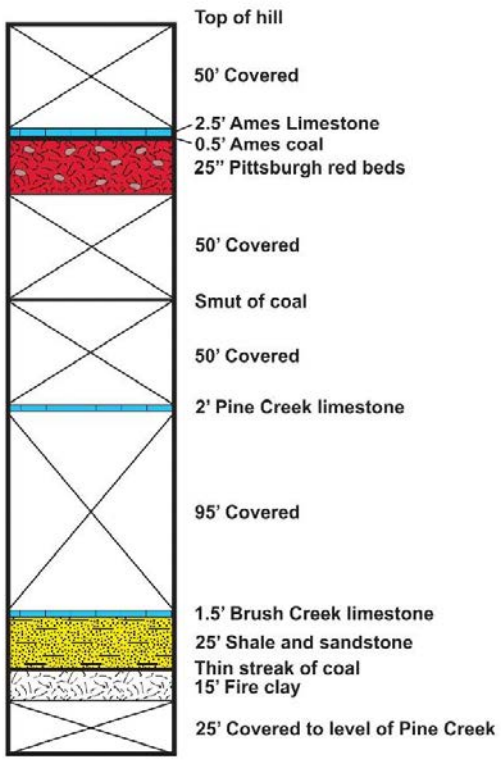

Figure 4. I. C. White's type section of the Pine Creek limestone near Allison Park, Allegheny County (modified from White, 1878).

The Pine Creek is also well known for including some large biogenic "mounds" in the New Kensington, Westmoreland County area, the Sewickley "Brush Creek" locality in Allegheny County (Figure 5A), and near Glouster, Ohio (Carothers, 1974a, 1974b, 1974c; Norton, 1974a). The lithology of the Pine Creek limestone within each mound is very similar to the intermound limestone beds (Figure 5B), except for vertical, bifurcating burrows in the central part of the mound. Carothers found the burrows in thin section were filled with either: 1) fossil fragments having a micritic or spar cement and 20 to 3 percent clay and silt-sized quartz; or 2) a drusy calcite fill with a micrite boundary separating the burrowed and unburrowed portions of the limestone. Both the unburrowed mound limestone and the intermound limestone have high clay and silt contents and contain fossils of foraminiferans, bryozoans, brachiopods, gastropods, and crinoids. The mounds typically are ice cream cone-shaped (Figure 5B), and display multiple truncation surfaces (compare Figures 5A and B). The highest truncation surface can be traced laterally into the intermound limestone throughout the outcrop. Carothers (1974c) and Norton (1974b) provided conflicting interpretations of the depositional environments for the mounds, but agreed that the burrows probably resulted from the activities of burrowing crustaceans.

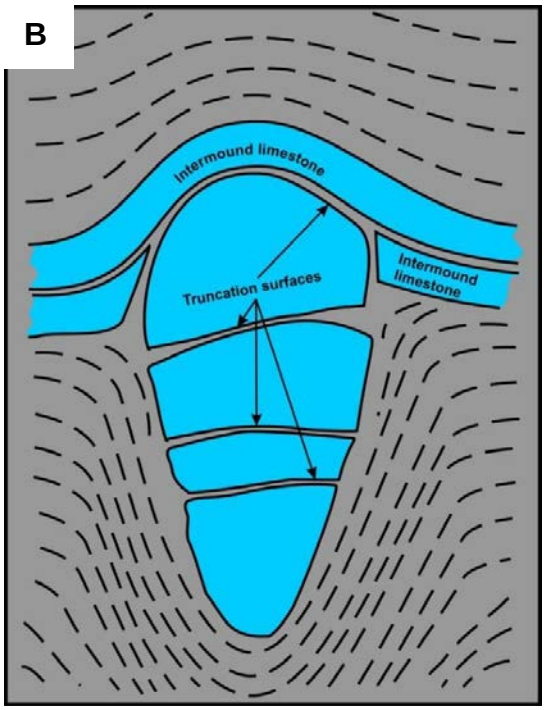

Figure 5. Pine Creek mounds. A – Photo of the mound at the Sewickley, Allegheny County, locality. This mound is now covered by talus and vegetation. B – Morphology of a typical mound (modified from Carothers, 1974c). The mound on which this was based was 10 ft (3 m) tall and consisted of a gray limestone cut by four truncation surfaces.

Cambridge (Nadine) Marine Zone

Andrews (1873) named the Cambridge Limestone, presumably for the abundant and excellent exposures in the Cambridge, Guernsey County, Ohio, area. For many decades, the Cambridge and Pine Creek were considered to be correlative (see below). Burke (1958) named the Nadine Limestone for a relatively pure, light to dark gray limestone 4 to 15 in (10 to 38 cm) thick that occurs on Allegheny River Boulevard near the intersection with Nadine Road in Allegheny County about 10 mi (16 km) northwest of downtown Pittsburgh. Previously, Johnson (1929) had noted the occurrence of this limestone, which he called the "lower bed" of the Woods Run limestone, in several places around the Pittsburgh area. Busch (1984, p. 34) described the Nadine as a thin, medium gray, crinoidal wackestone-packstone bearing allochthonous

phosphate granules and *in situ* phosphate nodules. Olive-colored marine clay shales occurring both above and below the limestone contain bivalve and chonetid brachiopod fossils. Burke (1958) noted the presence of "*Chonetina flemingi plebia*" (now *Chonetinella plebia*), and suggested it was a distinctive brachiopod within the fauna. Sturgeon and Hoare (1968) give the range for this brachiopod in Ohio as Brush Creek to Cambridge, so its presence in the Nadine, previously considered younger than Cambridge, should have been problematic. Now that we know the Nadine and Cambridge are the same marine zone, the brachiopod's presence in the Nadine should be expected.

Woods Run Marine Zone

Raymond (1910) named the Woods Run limestone for a fossiliferous marine limestone lying between the Pine Creek and Ames that, at one time, apparently was well exposed within the channel of Woods Run and along the roads in what is now the Woods Run neighborhood of Pittsburgh about 3 mi (5 km) north of the downtown area. He noted that the few fossils found in the limestone were common but low in diversity, with the horn coral *Lophophyllum* (now called *Stereostylus*) often the only fossil present in the rock.

Almost 50 years later, Burke (1958) named the Carnahan Run Shale for a 5-ft (1.5-m) thick, dark gray, fossiliferous shale cropping out in the vicinity of Carnahan Run, Parks Township, Armstrong County about 0.7 mi (1.1 km) north of the town of North Vandergrift. He stated that it was separated from the Woods Run limestone by 21.5 ft (6.6 m) of reddish-brown shale carrying plant fragments. Wells (1983), however, determined that the Carnahan Run was merely a shale facies of the Woods Run.

Busch (1984) described the Woods Run as an argillaceous, ferruginous wackestone, packstone, or grainstone with occasional phosphate granules and abundant macrofossils and microfossils. Dark gray to dark olive, platy shales with marine fossils commonly overly it. In Allegheny County, the few Woods Run outcrops I've seen were more mudstone than carbonate. In Fayette and Somerset counties, however, it often consists of a well-developed limestone sandwiched between dark colored shales (e.g., the Piccolomini Strip Mine and Ursina localities, respectively). It looks so much like typical Brush Creek that several reports erroneously used that name (Flint, 1965; Donahue et al., 1972) for what are now recognized as Woods Run outcrops.

Bakerstown Marine Zone

The Bakerstown marine zone is one of those anomalous units that went unrecognized for decades. It consists essentially of red, green, or black, platy to fissile shale with siderite nodules and a sparse marine or brackish water fauna (Busch, 1984) that lies above the Upper Bakerstown coal in a few places in western Pennsylvania. There are few or no occurrences of a bedded marine limestone associated with the zone in Pennsylvania, unless they occur in coal cores taken in the westernmost part of the state. The correlative Noble Limestone of Ohio (Murphy and Picking, 1967) is a white to gray, nodular limestone that is interbedded with greenish-gray, calcareous marine shales. In Ohio, the Noble itself grades laterally into a freshwater-to-brackish facies called the Rock Riffle Limestone, and to a calcrete zone called the Ewing Limestone.

Ames Marine Zone

Andrews (1873) named the Ames Limestone for exposures of a fossiliferous limestone, 1 to 5 ft (0.3 to 1.5 m) thick in Ames Township, Athens County, Ohio. This unit was, for many years, called the "crinoidal limestone" because of the abundance of crinoid ossicles, primarily columnals, scattered throughout. The Ames is a greenish-gray, argillaceous wackestone, packstone, or grainstone carrying abundant macrofossils. It is occasionally replaced by a dark gray to black, platy to fissile shale with wackestone nodules and a somewhat sparser fauna, but overall it is the most recognizable marine unit in the Glenshaw Formation. The Ames is, arguably, the most fossiliferous stratum in the Upper Pennsylvanian of western Pennsylvania. It has provided a plethora of familiar forms representative of most of the Late Paleozoic invertebrate phyla, as well as the occasional fish fossils (mostly "shark" teeth) and some species never before reported from Pennsylvania (Harper, 1986). A locality in northeastern Allegheny County, along PA Route 28 (the Allegheny Valley Expressway – Figure 6), in particular, provides a wealth of invertebrate fossils collected in a relatively short time (Harper, 1989).

Figure 6. Outcrop of Ames Limestone and Pittsburgh red beds along PA Route 28 near Creighton, Allegheny County.

The Ames has often been correlated with the Mill Creek Limestone of the anthracite area of northeastern Pennsylvania (e.g., White, 1903; Chow, 1951; Busch, 1984), but more recent analyses of the Mill Creek's conodont fauna indicates it is actually correlative with the Bakerstown/Noble marine zone (Merrill and Wentland, 1994; Heckel et al., 2011) (see below).

A Note on Casselman Formation Marine Zones

Two other marine zones occur above the Ames in the Appalachian Basin, within the lower Casselman Formation. The lower Gaysport marine zone does not occur in Pennsylvania, unless it is found in coal cores in the westernmost part of the state, but it probably correlates to the nonmarine Duquesne shale of the Pittsburgh area. The upper Skelley marine zone occurs in the Pittsburgh area as a brackish to marginal marine zone within the upper third of the Birmingham shale. Raymond (1909) first reported this from the railroad tracks below Kennywood Amusement Park in West Mifflin, Allegheny County, about 9 mi (14.5 km) southeast of downtown Pittsburgh. He found crinoid columnals, brachiopods, bivalves, gastropods, and a cephalopod at this locality, and mentioned the presence of fossils in this interval in several localities around the city, with the most common and best preserved at Kennywood, across the Monongahela River in East Pittsburgh, and farther east in Wilmerding. Brachiopods have also been found in the Birmingham shale in Washington County and in an outcrop adjacent to the Armstrong Tunnels beneath Duquesne University in Pittsburgh (H. B. Rollins, personal comm., 1970s). Price (1970) documented marine fossils in what he called the "green siltstone facies" at many localities in the Birmingham shale. He interpreted the fauna as representing a restricted marine environment

and noted that, although he did not find the "green siltstone facies" at all of the localities he visited, he believed that the restricted marine horizon was present over the entire study area.

Problems and Resolutions of Identity and Correlation

Of the six widespread Glenshaw marine units (Figure 1), the Brush Creek and Ames are the most recognizable in Pennsylvania, although, as pointed out above, several of the well-known Brush Creek localities are actually Pine Creek or Woods Run. These typically have well defined limestones sandwiched between dark-colored marine shales. The Cambridge (Nadine) has not been recognized in many places in Pennsylvania. It is often very thin with relatively small amounts of associated shale. The Woods Run in Allegheny County and adjacent areas is most often a punky brown, calcareous, argillaceous rock. The Bakerstown marine zone most often occurs as a dark-colored shale containing a few brackish-water fossils and rare truly marine species. One needs to have a very good handle on the stratigraphy of any particular sequence of Glenshaw rocks to have any chance of correctly identifying a marine zone.

Correlation of the marine zones across state lines has created even more numerous problems over the decades. In eastern Ohio, the Brush Creek was for many years considered to be divided into two parts of a single interval. Condit (1912), for example, described the Brush Creek limestone as consisting of two limestone units separated by 25 to 30 ft (7.5 to 9 m) of fossiliferous shale, resulting in a continuous series of fossiliferous beds 30 to 45 ft (9 to 14 m) thick. "Since the upper and lower limestones are so closely related it is best that they be included under the same name." (Condit, 1912, p. 49). As such, the limestones have been called Lower Brush Creek and Upper Brush Creek in Ohio and West Virginia for many years; these names were formalized by Sturgeon (in Sturgeon et al., 1958). A large part of the confusion resulted from White's (1903) referring to the Brush Creek and Pine Creek limestones in West Virginia with the names "Lower Cambridge" and "Upper Cambridge", respectively. Stevenson (1906) retained the name Brush Creek for the lower limestone but called the upper one Cambridge. Since the Cambridge Limestone had priority over Pine Creek, the name Pine Creek was abandoned in Ohio and West Virginia (and even in some parts of Pennsylvania – e.g., Butts, 1906). Although Pennsylvania retained the name Pine Creek, it was still considered to be correlative with the Cambridge Limestone for decades (e.g., Donahue and Rollins, 1974a; Carothers, 1976; Rollins et al., 1979). In fact, this was considered dogma until Busch (1984; also Busch and Rollins, 1984) showed the Pine Creek correlated with the Upper Brush Creek and the Cambridge correlated with the Nadine limestone (Figure 1). Thus, the Lower and Upper Brush Creek of Ohio and West Virginia are, respectively, the Brush Creek and Pine Creek of Pennsylvania.

The Friendsville marine zone of western Maryland, also once considered to be Cambridge (and therefore Pine Creek) equivalent (Swartz et al., 1919), is now correlated with the Woods Run, as is the Portersville marine zone of Ohio.

The Mill Creek Limestone of the anthracite area of northeastern Pennsylvania traditionally had been correlated with the Ames Limestone (White, 1903; Chow, 1951; Busch, 1984). Based on conodont content, however, Merrill and Wentland (1994) suggested that the Mill Creek correlated instead with the Noble Limestone of Ohio. Their analysis of Mill Creek conodonts showed that the fossil population was evolutionarily older than the conodont population found in the Ames. They concluded that the Mill Creek definitely is not equivalent with the Ames, and

was, in fact, actually older than the Noble Limestone in eastern OH. Although Merrill and Wentland (1994) determined that the Mill Creek could not be definitively correlated to any marine zone anywhere else in the Appalachian Basin, Heckel et al. (2011, p. 260) concluded that the dominance of *Streptognathodus firmus* in the Noble confirmed the correlation of that limestone with the Mill Creek.

In fact, the identification of conodonts in the Pennsylvanian marine zones of the Appalachian Basin has resolved most of the problems of identification that have cropped up over the last 120 years. Figure 7 illustrates our current understanding of the correlation of Upper Pennsylvanian marine zones from the Midcontinent to the Appalachian Basin, and Table 1 shows the conodont zonation of the Glenshaw Formation and correlative units. Any confusion of marine zones that might occur now and in the future should be able to be resolved by someone with enough expertise to sample for and identify the conodonts that occur within the Glenshaw marine zones.

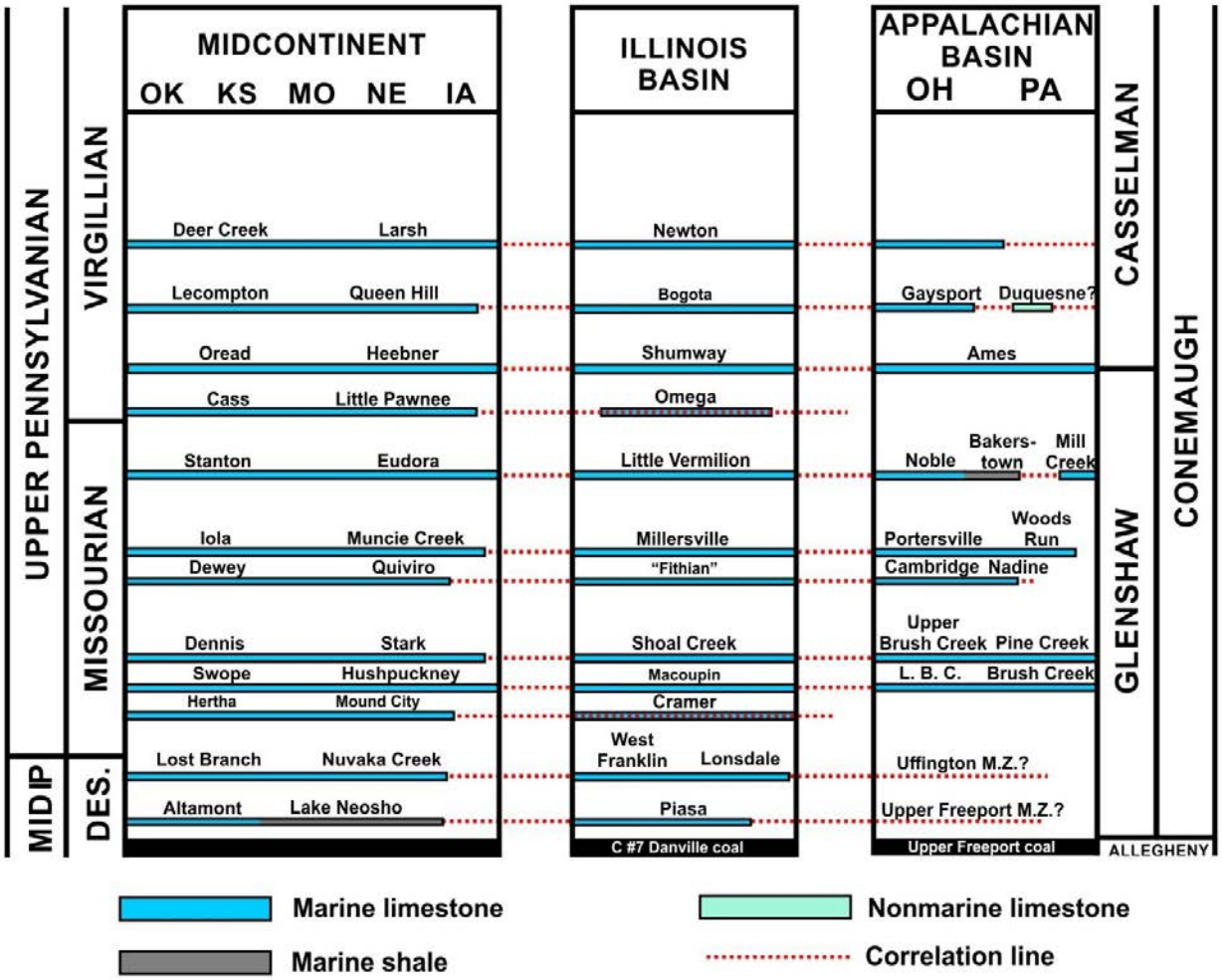

Figure 7. Correlation of Glenshaw marine zones with marine rocks in the Midcontinent and Illinois Basin (based on Heckel et al., 1998).

Table 1. Conodont zones associated with the Midcontinent and Illinois Basin marine zones and correlation with Glenshaw marine zones in the Appalachian Basin (from Heckel et al., 2011).

MIDCONTINENT	ILLINOIS BASIN	APPALACHIAN BASIN (Conemaugh Marine Units)	CONODONT ZONES
Oread/Heebner	Shumway	Ames	***Idiognathodus simulator***
Cass/Little Pawnee	"Omega"	?	***Streptognathodus zethus***
Stanton/Eudora	Little Vermilion	Bakerstown/Noble	***Idiognathodus eudoraensis***
Iola/Muncie Creek	Millersville	Woods Run/Portersville	***Streptognathodus gracilis***
Dewey/Quiviro	"Filian"	Nadine/Cambridge	***Streptognathodus gracilis***
Dennis/Stark	Shoal Creek	Pine Creek/Upper Brush Creek	***Idiognathodus confragus***
Swope/Hushpuckney	Macoupin	Brush Creek/Lower Brush Creek	***Idiognathodus cancellosus***
Hertha/Mound City	Cramer	"Mahoning"?	***Idiognathodus turbatus***
Lost Branch/Nuvaka Creek	West Franklin/Lonsdale	Upper Freeport?	***Idiognathodus eccentricus***

References

Al-Qayim, B.B., 1983, Facies analysis and depositional environments of the Ames marine member (Virgillian) of the Conemaugh Group (Pennsylvanian) in the Appalachian Basin: Pittsburgh, Pa., University of Pittsburgh, Ph.D. dissertation, p. 306.

Andrews, E.B., 1873, Geology of Athens County, Chapter X, in Report of the Geological Survey of Ohio, Part I, Geology: Ohio Geological Survey, Report of Progress, 2nd series, v. 1, p. 261-293.

Beerbower, J.R., 1964, Cyclothems and cyclic depositional mechanisms in alluvial plain sedimentation, *in* Symposium on Cyclic Sedimentation: Geological Survey of Kansas Bulletin, v. 169, p. 31-42.

Brant, L.A., 1971, A study of the faunal succession in the Brush Creek shale (Pennsylvanian) near Shelocta, Pennsylvania: University Park, Pa., Pennsylvania State University, M.S. thesis, p. 87.

Brezinski, D.K., 1983, Developmental model for an Appalachian Pennsylvanian marine incursion: Northeastern Geology, v. 5, p. 92-99.

Burke, J.J., 1958, New marine horizon in the Conemaugh Formation: Science, v. 128, p. 302.

Busch, R.M., 1984, Stratigraphic analysis of Pennsylvanian rocks using a hierarchy of transgressive-regressive units: Pittsburgh, Pa., University of Pittsburgh, Ph.D. dissertation, p. 427.

Busch, R.M. and Rollins, H.B., 1984, Correlation of Carboniferous strata using a hierarchy of transgressive–regressive units: Geology, v. 12, p. 471-474.

Busch, R.M., and West, R.R., 1987, Hierarchal genetic stratigraphy: A framework for paleoceanography: Paleoceanography, v. 2, p. 141-164.

Butts, C., 1906, Economic geology of the Kittanning and Rural Valley quadrangles, Pennsylvania: U. S. Geological Survey Bulletin 279, 198 p.

Carothers, M., 1974a, Stop #3, Mounds in Pine Creek marine event, *in* Donahue, J. and Rollins, H.B., eds., Conemaugh (Glenshaw) marine events: Third Annual Meeting of the Eastern Section, American Association of Petroleum Geologists and Eastern Section, Society of Economic Paleontologists and Mineralogist, April 20-21, Pittsburgh, PA, Field Trip Guidebook, p. 21-23.

Carothers, M., 1974b, Stop #4, Mounds in Pine Creek marine event, *in* Donahue, J. and Rollins, H.B., eds., Conemaugh (Glenshaw) marine events: Third Annual Meeting of the Eastern Section, American Association of Petroleum Geologists and Eastern Section, Society of Economic Paleontologists and Mineralogist, April 20-21, Pittsburgh, PA, Field Trip Guidebook, p. 23-25.

Carothers, M., 1974c, Origin of Pine Creek mounds and their significance as near-shore indicators, *in* Donahue, J. and Rollins, H.B., eds., Conemaugh (Glenshaw) marine events: Third Annual Meeting of the Eastern Section, American Association of Petroleum Geologists and Eastern Section, Society of Economic Paleontologists and Mineralogist, April 20-21, Pittsburgh, PA, Field Trip Guidebook, p. A-1 – A-6.

Carothers, M.C., 1976, Depositional environments of the Cambridge Limestone (Missourian, Pennsylvanian) of the Appalachian Basin: Pittsburgh, Pa., University of Pittsburgh, Ph.D. dissertation, p. 214.

Caudill, M.R., 1990, Lithostratigraphy of Conemaugh Group (Upper Pennsylvanian) marine zones; Steubenville, Ohio-Weirton, West Virginia: Southeastern Geology, v. 31, p. 173–182.

Chesnut, D.R., 1981, Marine zones of the Upper Carboniferous of eastern Kentucky, *in* Cobb, J. C., D. R. Chesnut, N. C. Hester, and J. C. Hower, eds., Coal and coal-bearing rocks of eastern Kentucky: Kentucky Geological Survey, ser. 11, p. 57-66.

Chow, M.M., 1951, The Pennsylvanian Mill Creek Limestone in Pennsylvania: Pennsylvania Geological Survey, 4th ser., General Geology Report 26, 36 p.

Condit, D.D., 1912, Conemaugh Formation in Ohio: Geological Survey of Ohio, 4th ser., Bulletin 17, 363 p.

Donahue, J. and Rollins, H.B., 1974a, Introduction, *in* Donahue, J. and H. B. Rollins, eds., Conemaugh (Glenshaw) marine events: Third Annual Meeting of the Eastern Section, American Association of Petroleum Geologists and Eastern Section, Society of Economic Paleontologists and Mineralogist, April 20-21, Pittsburgh, PA, Field Trip Guidebook, p. 1-14.

Donahue, J., and Rollins, H.B., 1974b, Paleoecological anatomy of a Conemaugh (Pennsylvanian) marine event, *in* Briggs, G., ed., Carboniferous of the southeastern United States: Geological Society of America Special Paper 48, p. 153-170.

Donahue, J., Rollins, H.B., and Shaak, G.D, 1972, Asymmetrical community succession in a transgressive-regressive sequence: 24th International Geological Congress, Montreal, v. 7, p. 74-81.

Edmunds, W.E., Skema, V.W., and Flint, N.K., 1999, Pennsylvanian, chap. 10 *of* Shultz, C.H., ed., The geology of Pennsylvania: Pennsylvania Geological Survey, 4th ser., Special Publication 1, p. 148-169.

Evans, M.A., 2003, Site: GLENS 8-2: Pine Creek Limestone type locality, Etna, PA. [Accessed online from http://www.geology2.pitt.edu/GeoSites/site%20GLENS%208-2new.htm, June, 2016]

Fahrer, T.R., 1996, Stratigraphy, petrography and paleoecology of marine units within the Conemaugh Group (upper Pennsylvanian) of the Appalachian Basin in Ohio, West Virginia and Pennsylvania: Iowa City, University of Iowa, PhD. Dissertation, p. 298.

Ferm, J.C., 1975, Pennsylvanian cyclothems of the Appalachian Plateau, a retrospective view: U.S. Geological Survey Professional Paper 853, Part II, p. 57-64.

Flint, N.K., 1965, Geology and mineral resources of southern Somerset County, Pennsylvania: Pennsylvania Geological Survey, 4th ser., County Report 56a, 267 p.

Greb, S.F., Pashin, J.C., Martino, R.L., and Eble, C.F., 2008, Appalachian sedimentary cycles during the Pennsylvanian: Changing influences of sea level, climate, and tectonics. Geological Society of America Special Papers 441, p. 235-248.

Harper, J.A., 1986, Diverse fauna at Beaver County fossil locality: Pennsylvania Geology, v. 17, no. 1, p. 13-16.

Harper, J.A., 1989, Abundant fossils at new Allegheny County locality: Pennsylvania Geology, v. 20, no. 1, p. 10-15.

Heckel, P.H., 1995, Glacial-eustatic base-level – Climate model for late Middle to Late Pennsylvanian coal-bed formation in the Appalachian basin: Journal of Sedimentary Research, v. 65, p. 348-356.

Heckel, P.H., Barrick, J.E., and Rosscoe, S.J., 2011, Conodont-based correlation of marine units in lower Conemaugh Group (Late Pennsylvanian) in Northern Appalachian Basin: Stratigraphy, v. 8, p. 253-269.

Heckel, P.H., Gibling, M.R., and King, N.R., 1998, Stratigraphic model for glacial-eustatic Pennsylvanian cyclothems in highstand nearshore detrital regimes: Journal of Geology, v. 106, p. 373-383.

Hennen, R.V. and Gawthrop, R.M., 1917, Braxton and Clay counties: West Virginia Geological Survey, p. 883.

Hoskins, D.M., Inners, J.D. and Harper, J.A, 1983, Fossil collecting in Pennsylvania: Pennsylvania Geological Survey, 4th ser., General Geology Report 40, 215 p.

Johnson, M.E., 1929, Geology and mineral resources of the Pittsburgh quadrangle, Pennsylvania: Pennsylvania Geological Survey, 4th ser., Atlas 27, 236 p.

Klasen, R.L., 2007, Sequence stratigraphic analysis of the Lower and Upper Brush Creek interval (Late Pennsylvanian), southeastern Ohio: Athens, OH, Ohio University, Ph.D. dissertation, p. 89.

Klein, G.D. and Kupperman, J.B., 1992, Pennsylvanian cyclothems: Methods of distinguishing tectonically induced changes in sea level from climatically induced changes: Geological Society of America Bulletin, v. 104, p. 166-175.

Klein, G.D. and D.A. Willard, 1989, Origin of the Pennsylvanian coal-bearing cyclothems of North America: Geology, v. 17, p. 152-155.

Lebold, J.G., 2005, Gradient and recurrence analyses of four marine zones in the Glenshaw Formation (Upper Pennsylvanian, Appalachian Basin): Morgantown, WV, West Virginia University, Ph.D. dissertation, p. 163.

Lebold, J.G. and Kammer, T.W., 2006, Gradient analysis of faunal distributions associated with rapid transgression and low accommodation space in a Late Pennsylvanian marine embayment: Biofacies of the Ames Member (Glenshaw Formation, Conemaugh Group) in the northern Appalachian Basin, USA: Palaeogeography, Palaeoclimatology, Palaeoecology, v. 231, p. 291-314.

Martino, R.L., 2004, Sequence stratigraphy of the Glenshaw Formation (Middle-Late Pennsylvanian) in the Central Appalachian Basin, *in* Pashin, J.C. and Gastaldo, R.A., eds., Sequence stratigraphy, paleoclimate, and tectonics of coal-bearing strata: AAPG Studies in Geology 51, p. 1-28.

Martino, R.L., McCullough, M.A., and Hamrick, T.L., 1996, Stratigraphic and depositional framework of the Glenshaw Formation (Late Pennsylvanian) in central Wayne County, West Virginia: Southeastern Geology, v. 36, p. 65-83.

Merrill, G.K. and Wentland, E.M., 1994, Conodont determination of the age of the Mill Creek Limestone: Carboniferous, northeastern Pennsylvania: Northeastern Geology, v. 16, p. 9-13.

Murphy, J.L. and Picking, L., 1967, A new marine member in the Conemaugh Group of Ohio: Kirtlandia 1, 7 p.

Norton, C.W., 1974a, Stop #10 (optional), Mounds in Upper Brush Creek marine event, *in* Donahue, J. and Rollins, H.B., eds., Conemaugh (Glenshaw) marine events: Third Annual Meeting of the Eastern Section, American Association of Petroleum Geologists and Eastern Section, Society of Economic Paleontologists and Mineralogist, April 20-21, Pittsburgh, PA, Field Trip Guidebook, p. 39-40.

Norton, W., 1974b, Biogenic mounds in the lower Conemaugh (Missourian, Pennsylvanian) of the Appalachian Basin, *in* Donahue, J. and Rollins, H.B., eds., Conemaugh (Glenshaw) marine events. Third Annual Meeting of the Eastern Section, American Association of Petroleum Geologists and Eastern Section, Society of Economic Paleontologists and Mineralogist, April 20-21, Pittsburgh, PA, variously paginated Field Trip Guidebook, p. B-1 – B-6.

Platt, F., 1875, Report of progress in the Clearfield and Jefferson District of the bituminous coal-fields of western Pennsylvania: Second Geological Survey of Pennsylvania, Report H, 294 p.

Price, M.L., 1970, The stratigraphy and environments of deposition of the Birmingham shale (Upper Pennsylvanian) of the Pittsburgh area: Pittsburgh, Pa., M.S. thesis, p. 103.

Price, W.A., 1917, The Uffington Shale of West Virginia and Its Supposed Marine Fauna: Science, New Series, V. 46, No. 1196, P. 540-542.

Raymond, P.E., 1909, Notice of two new horizons for marine fossils in western Pennsylvania: Science, new series, v. 29, p. 940-941.

Raymond, P.E., 1910, A preliminary list of the fauna of the Allegheny and Conemaugh series in western Pennsylvania: Annals of the Carnegie Museum, v. 7, p. 144–158.

Raymond, P.E., 1911, A preliminary list of the fauna of the Allegheny and Conemaugh series in western Pennsylvania: Pennsylvania Geologic Survey, 3rd ser., Report 1908-1010, p. 83-98.

Rollins, H.B. and Donahue, J., 1975, Towards a theoretical basis of paleoecology: Concepts of community dynamics: Lethaia, v. 8, p. 255-270.

Rollins, H.B., Carothers, M., and Donahue, J., 1979, Transgression, regression and fossil community succession: Lethaia, v. 12, p. 89–104.

Saltsman, A.L., 1986, Paleoenvironments of the Upper Pennsylvanian Ames Limestone and associated rocks near Pittsburgh, Pennsylvania: Geological Society of America Bulletin, v. 97 no. 2 p. 222-231.

Shaak, G.D., 1975, Diversity and community structure of the Brush Creek marine interval (Conemaugh group, Upper Pennsylvanian), in the Appalachian basin of western Pennsylvania: Florida State Museum Bulletin, Biological Sciences, v. 19, no. 2, 133 p.

Shaulis, J.R., 1993, Surface bedrock stratigraphy, *in* Shaulis, J.R., and others, eds., Geology of the southern Somerset County region, southwestern Pennsylvania: Annual Field Conference of Pennsylvania Geologists, 58th, Somerset, PA, Guidebook, p. 1-10.

Stevenson, J.J., 1871, A geological examination of Monongalia County, West Virginia, by J. J. Stevenson; with a list of fossils and descriptions, by F. B. Meek: West Virginia Board of Regents, Third Annual Report for the year 1870, Wheeling, WV, p. 40-73.

Stevenson, J.J., 1906, Carboniferous of the Appalachian Basin. Geological Society of America, v. 17, p. 65-228.

Sturgeon, M.T. and R.D. Hoare, 1968, Pennsylvanian brachiopods of Ohio: Ohio Geological Survey Bulletin 63, 95 p.

Sturgeon, M.T., Smith, G.E., and Flint, A.E., 1958, The geology and mineral resources of Athens County, Ohio: Ohio Division of Geological Survey, Bulletin 57, 600 p.

Swartz, C.K., Price, W.A., and Bassler, H., 1919, Coal measures of Maryland: Geological Society of America Bulletin, v. 30, p. 567-596.

Wanless, H.R. and Shephard, F.P., 1936, Sea level and climatic changes related to late Paleozoic cycles: Geological Society of America Bulletin, v. 47, p. 1177-1206.

Wanless, H.R. and Weller, J.M., 1932, Correlation and extent of Pennsylvanian cyclothems: Geological Society of America Bulletin, v. 4, p. 1003-1016.

Wells, K.E., 1983, Detailed correlation of paleogeographic development of the Woods Run and Carnahan Run marine units (Upper Pennsylvanian) in southwestern Pennsylvania (abs.): Geological Society of America, Abstracts with Programs, v. 15, no. 6, p. 717.

White, I.C., 1878, Report of progress in the Beaver River district of the bituminous coal fields of western Pennsylvania: Second Geological Survey of Pennsylvania, Report Q, 337 p.

White, I.C., 1903, The Appalachian coal field, the Conemaugh series: West Virginia Geological Survey, v. 2, p. 225-332.

Williams, E.G., 1964, The nature of cyclic sedimentation in the Carboniferous of western Pennsylvania *in* Williams, E.G., Ferm, J.C., Guber, A.L., and Bergenback, R.E., eds., Cyclic sedimentation in the Carboniferous of western Pennsylvania: Annual Field Conference of Pennsylvania Geologists, 29th, State College, Pa., Guidebook, p. 1-16.

Woolsey, L.H., 1906, Economic geology of the Beaver quadrangle, Pennsylvania: U.S. Geological Survey Bulletin 286, 132 p.

Plates

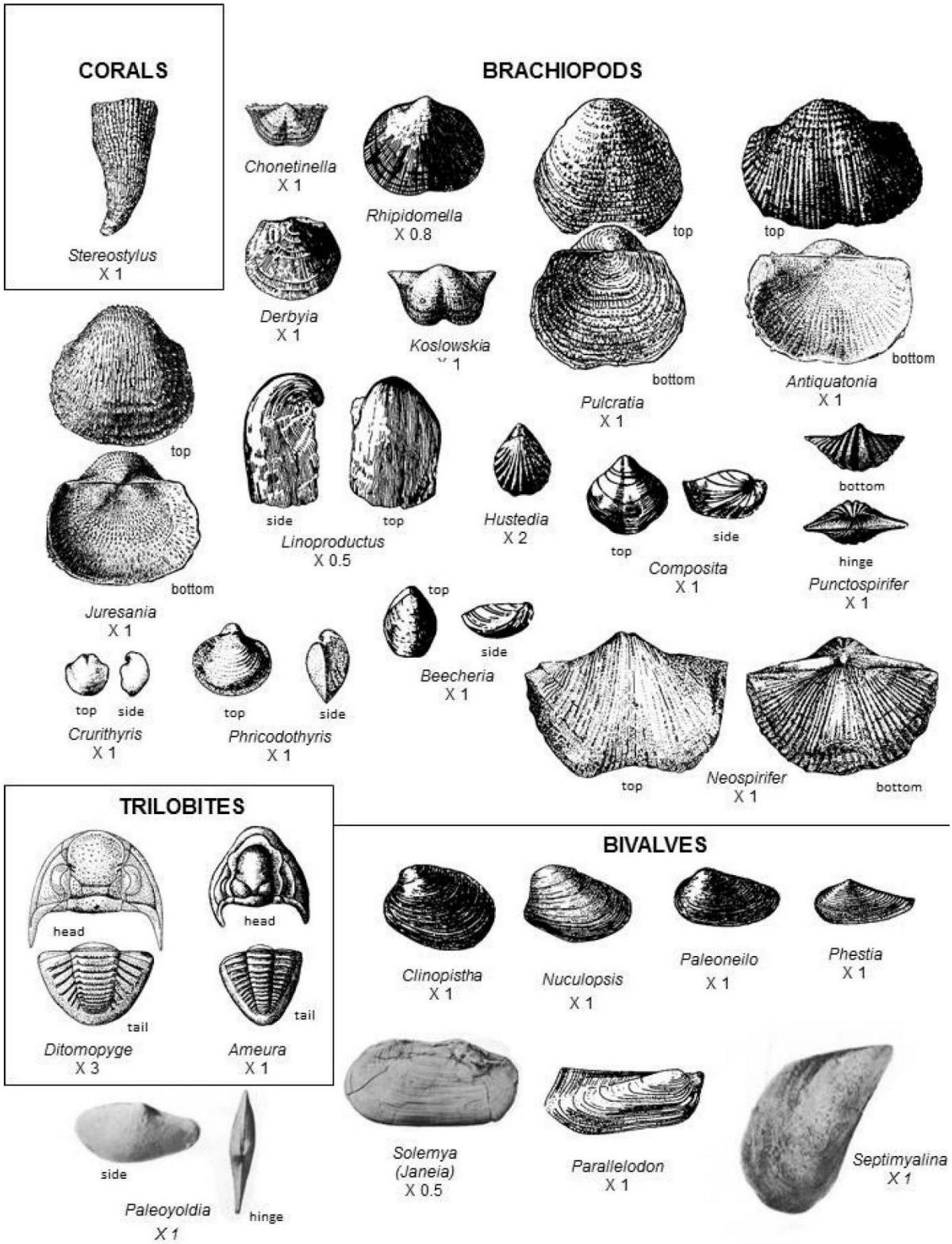

Plate 1. Illustrations of some fossils commonly found in the marine rocks of the Glenshaw Formation (from Moore et al., 1952; Hoskins et al., 1983; and a variety of other sources).

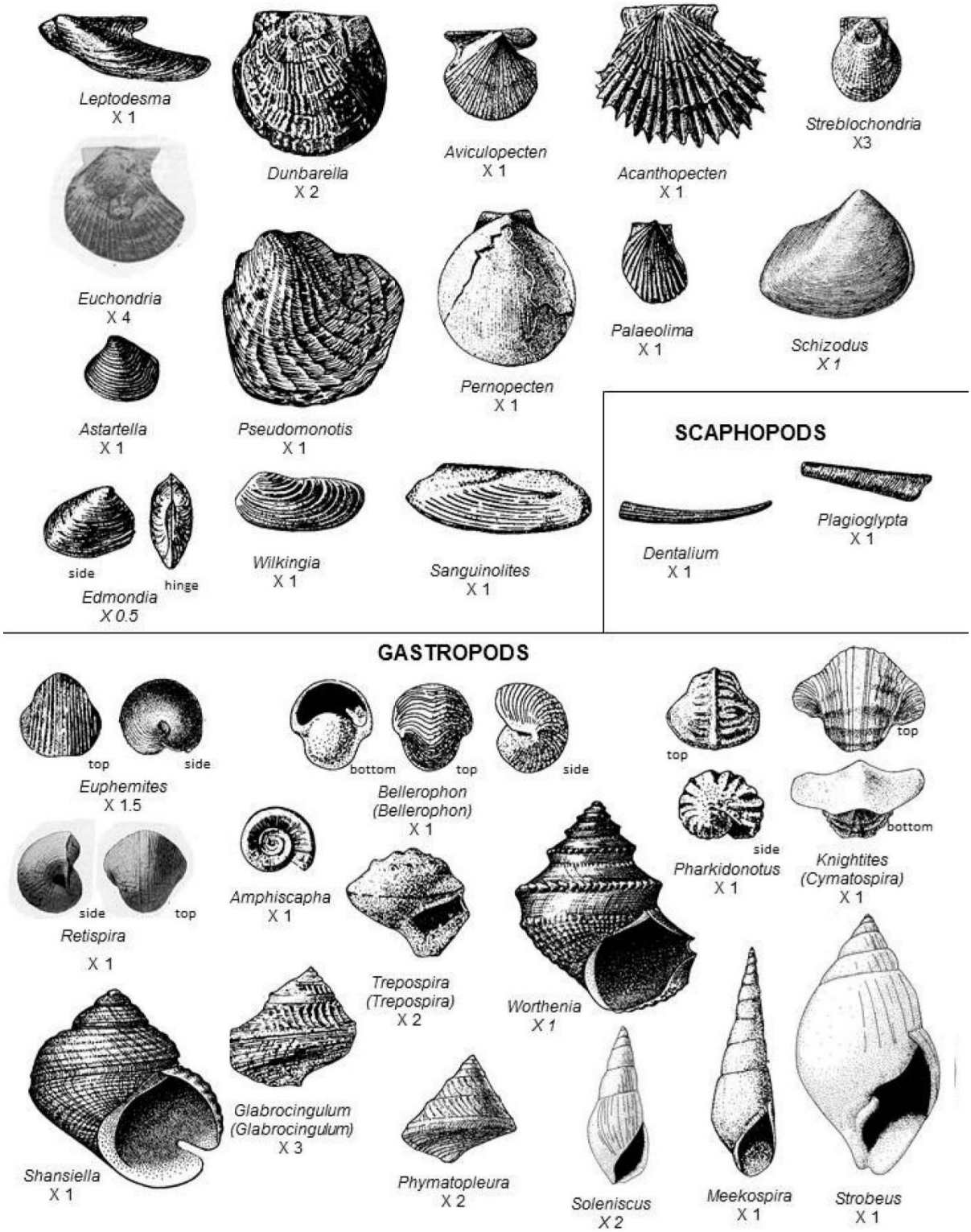

Plate 2. Illustrations of some fossils commonly found in the marine rocks of the Glenshaw Formation (from Moore et al., 1952; Hoskins et al., 1983; and a variety of other sources).

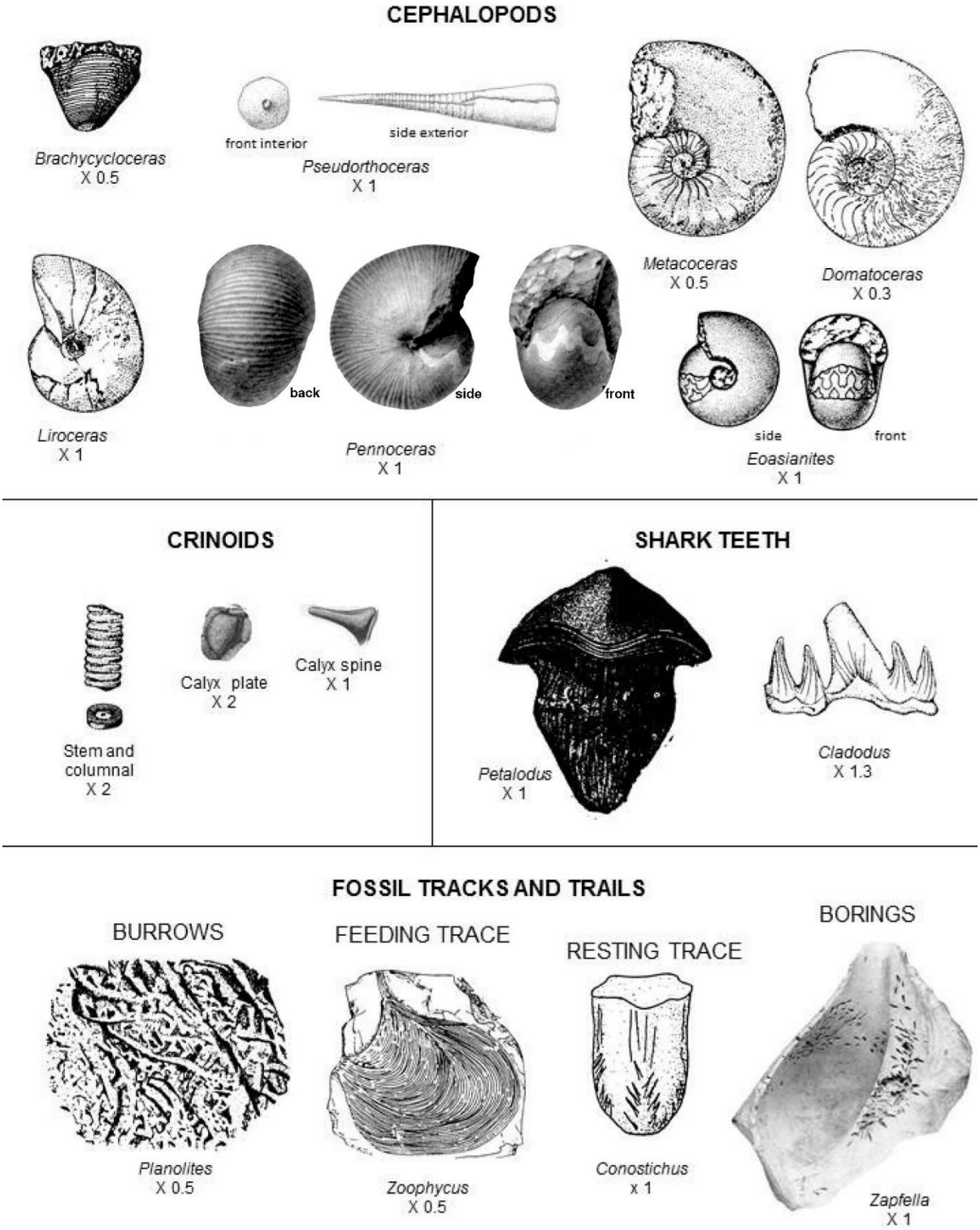

Plate 3. Illustrations of some fossils commonly found in the marine rocks of the Glenshaw Formation (from Moore et al., 1952; Hoskins et al., 1983; and a variety of other sources).

PINE CREEK MARINE ZONE, US 422 BYPASS, KITTANNING

JOHN A. HARPER, PENNSYLVANIA GEOLOGICAL SURVEY, RETIRED
BILL BRAGONIER, COAL GEOLOGIST, RETIRED

CAUTION: US 422 is a heavily traveled, high-speed, divided highway. Although, for the Field Conference, the stop will be protected by relatively wide berms and Flagger Force, caution should be taken while studying the outcrops and collecting fossils. Stay as far off the road and as close to the roadcuts as you can.

Introduction

Stop 5 occurs on the onramp from PA 28/66 (from New Bethlehem) to US 422 East (Figures 1 and 2A). This stop will give conferees the opportunity to examine the Pine Creek marine zone and its adjacent strata, as well as view other Glenshaw marine zones above and below the Pine Creek. A nearby outcrop, along the onramp from PA 28/66 to US 422 West, also exposes the Pine Creek marine zone at a lower level (Figure 2B), but the sharp curve of the onramp prohibits safe viewing.

Figure 1. Location of Stop 5 at the US 422 bypass around Kittanning and other locations mentioned in the text.

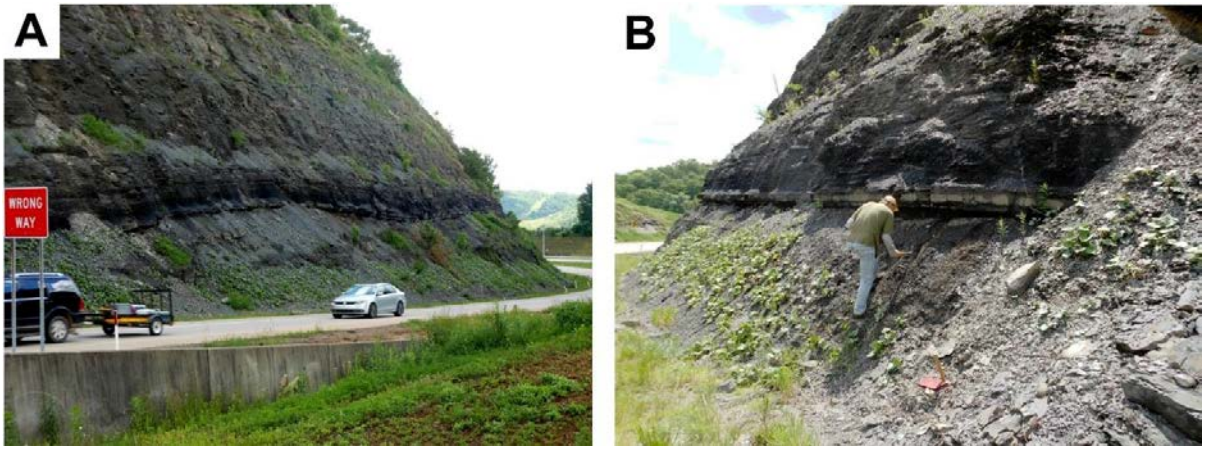

Figure 2. Photos at Stop 5 of the Pine Creek limestone and associated rocks. A – Outcrop along the onramp to US 422 East showing paleotopography beneath the limestone. B – Outcrop along the onramp to US 422 West.

In the 1970s, US 422 bypasses were built around New Castle, Kittanning, and Indiana. Sections of the Indiana bypass remained incomplete until 1995 and the Kittanning bypasses were completed in 2000. In 1982, the Kittanning Bypass opened from the Allegheny Valley Expressway (PA 28) to PA 66 and a median installed from there to Kittanning. The project cost $39 million and opened on December 13, 2001. Officials from state and local agencies as well as PennDOT and Federal Highway Administration officials cut the ribbon signaling the opening of the highway.

> "This is truly a monumental day for Armstrong County and it is a great pleasure for me to share in this celebrated opening of the A-15 Kittanning Bypass with you," said Pennsylvania Secretary of Transportation Bradley L. Mallory. "It is days like today that make this job worthwhile. And sharing these moments with hardworking Americans like the people of Armstrong County reminds me of why this country is great." (Kitsko, 2016).

Glenshaw Formation

The rocks exposed in the roadcuts at Stop 5 are part of the Glenshaw Formation, the lower unit of the mostly Late Pennsylvanian Conemaugh Group (Figure 3). Platt (1875, p. 8) first used the name "Conemaugh series" to include all the rocks from the base of the Pittsburgh coal to the top of the Upper Freeport coal. The Conemaugh later became a formation (Woolsey, 1906) and that nomenclature remained in effect throughout the Appalachian Basin until Flint (1965) subdivided it into the lower Glenshaw Formation and the upper Casselman Formation. Flint delineated the Glenshaw by the occurrence of numerous marine units, whereas the Casselman is mostly devoid of marine rocks. The top of the marine Ames Limestone is the boundary between the two formations. Although Busch (1984; also Busch and Rollins, 1984) recognized eight marine zones within the Glenshaw, the lower two are so rarely exposed that for all intents and purposes the Glenshaw has six regionally extensive marine zones. In Pennsylvania, these include, from oldest to youngest, the Brush Creek, Pine Creek, Cambridge (also called Nadine), Wood Run, Bakerstown, and Ames. The Casselman Formation also contains two marine zones, the Gaysport and Skelley, mostly restricted to eastern Ohio.

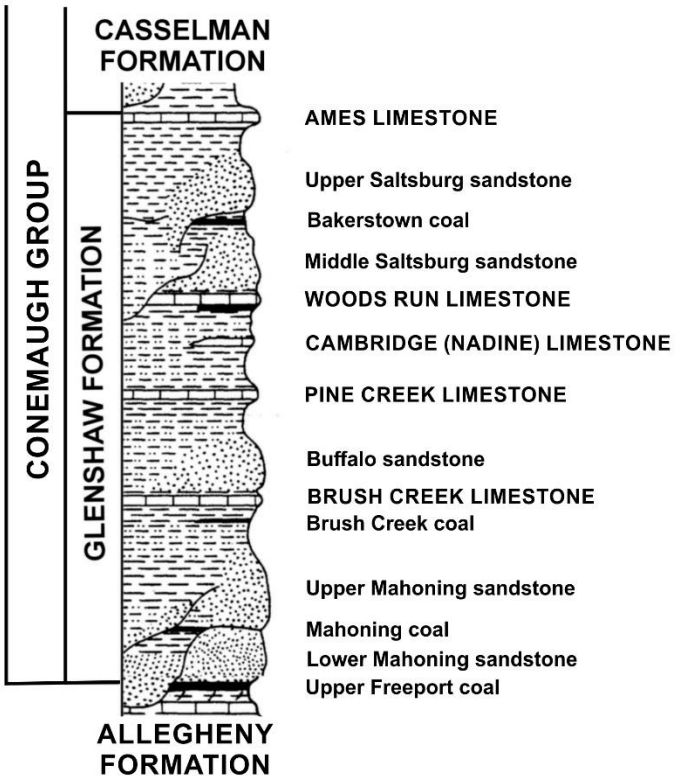

Figure 3. Generalized stratigraphic section of the Glenshaw Formation in western Pennsylvania. The marine intervals (in caps) are important marker horizons throughout the formation (modified from Harper and Laughrey, 1987).

The rocks exposed at Stop 5 include the Pine Creek marine zone and adjacent rocks. The Brush Creek marine zone (essentially, just the limestone) occurs near the base of the section along the bypass between the two onramps, and the Woods Run marine zone occurs near the tops of the higher knolls above the Pine Creek (see below).

Pine Creek Marine Zone

White (1878) named the Pine Creek limestone for a dark arenaceous and fossiliferous limestone bed about 2 ft (0.6 m) thick that crops out of the hillside between Gourdhead Run and Pine Creek in Allison Park, Allegheny County, PA. He described it as:

> "… quite variable; sometimes it is a compact light dove colored rock, and burns readily into a tolerably fair lime; but more generally it is quite arenaceous, and earthy, without close inspection would often be very readily mistaken for a stratum of sandstone. It is always fossiliferous, and generally more or less brecciated. In it were seen *Productus longispinus, P. Nebrascensis, Athyris subtilita, Chonetes mesoloba, Nautilus occidentalis, Orthoceras cribrosum,* and many stems and fragments of crinoids." (White, 1878, p. 32-33)

The names of the fossils have changed over the years, but the fossils themselves will be familiar to anyone who has collected from the Glenshaw marine zones around the Appalachian Basin. In its most recognizable form, the Pine Creek marine zone typically is a richly fossiliferous, shallow marine argillaceous limestone sandwiched between calcareous marine shales of various thickness.

Despite a maximum thickness of only about 3 ft (0.9 m) (Seaman, 1941), the Pine Creek limestone is laterally extensive. It is well known from western Pennsylvania, eastern Ohio, northern West Virginia, and western Maryland (Busch, 1984). It is possible that the Pine Creek also occurs in eastern Kentucky, as marine rocks above the Brush Creek and below the Ames occur there (Chestnut, 1981), but that particular name apparently has not been used. Because of its regional extent, lithology, and fossil fauna, it is an important marker bed for stratigraphic correlations within the Upper Pennsylvanian. As a marine unit situated within a primarily nonmarine succession, it also is valuable in assessing sea level cycles (e.g. Busch & Rollins, 1984) and for use in correlating allocyclic (eustatic) events between the Appalachian Basin and Carboniferous basins in the mid-continent (e.g. Heckel et al., 1998; 2011).

Correlation

White (1903) applied the names "Lower Cambridge" and "Upper Cambridge" to the two lower Conemaugh marine limestones in West Virginia. Stevenson (1906), realizing the lower of the two was the same as the Brush Creek of Pennsylvania, retained that name and restricted the name Cambridge to the higher of the two. Since the Cambridge Limestone, named by Andrews (1873, p. 262) for outcrops in Cambridge, Guernsey County, Ohio, had priority over the Pine Creek (White, 1878), the name Pine Creek was dropped in Ohio and West Virginia (and even in some parts of Pennsylvania; Butts, 1906, for example, called the marine zone "Cambridge (Pine Creek)" here in the Kittanning area). In fact, the Pine Creek was considered to be nothing more than Pennsylvania's name for the Cambridge Limestone for decades (e.g., Donahue and Rollins, 1974a; Carothers, 1976; Rollins et al., 1979) until Busch (1984) demonstrated that the Cambridge actually correlated with the Nadine Limestone, an otherwise insignificant marine zone above the

Pine Creek (Figure 3). The Pine Creek correlates instead with what Ohio and West Virginia call the Upper Brush Creek (see Harper, this guidebook, for additional details).

Lithology

The lithology of the Pine Creek marine zone varies considerably around the Appalachian Basin. It often occurs as a gray to greenish gray, argillaceous, sometimes arenaceous, skeletal mudstone and wackestone bearing allochthonous phosphate granules, and with the limestone sandwiched between dark gray to black, calcareous, clay shales containing marine fossils and siderite nodules. On a fresh surface the limestone typically is dark gray, whereas the weathered surface commonly is a buff color (Figure 4). Where it has been leached, sand grains can be so abundant that the rock seems to be more sandstone than limestone (Richardson, 1932). We measured the limestone on the US 422 West onramp adjacent to Stop 5 where it occurs at road level. The limestone was at 12 in (30.5 cm) thick, although it appears to vary across the outcrop. Internal stratification of the limestone, although not always readily apparent, is very apparent here. In most of the Glenshaw marine limestones, several layers can be discerned based on the presence of phosphatic nodules (lag deposits) and the presence of corals. At this locality, at least four separate layers can be distinguished within the Pine Creek limestone, separated on the basis of bedding, fissility, and frequency of fossils (Figure 5).

Figure 4. Pine Creek limestone at Stop 5 showing its weathered surface. U.S. quarter for scale.

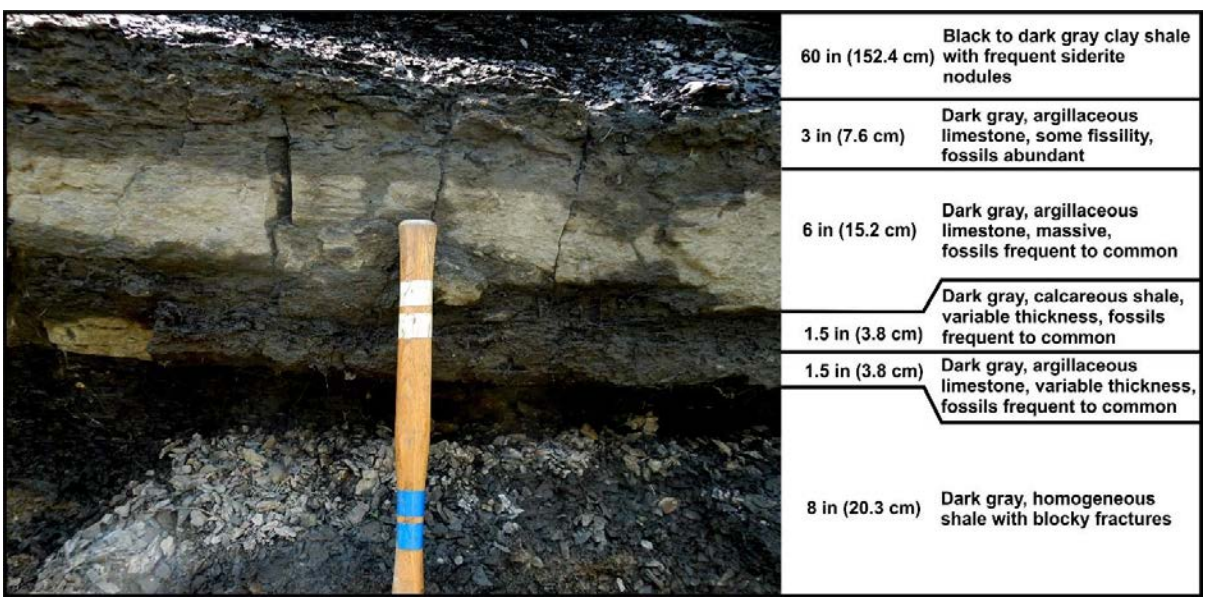

Figure 5. Details of the lithology of the Pine Creek marine zone at Stop 5. Hammer handle for scale; distance between blue and white tape = 6 in (15.24 cm).

The calcareous marine shales associated with the limestone can include compact nodules and sand lenses as well as siderite nodules and fossils. Besides the typical dark gray to black clay shales, other lithologies occur in different places. In Somerset County, for example, pale red- to buff-colored, platy to fissile clay shales occurring above and below the limestone, called the Meyersdale redbeds, grade laterally into typical Pine Creek lithologies farther west. Meyersdale shales can also occur in areas of "typical" Pine Creek. In southeastern Ohio, the shales are replaced locally by buff-colored spiculites (Busch, 1984). In many places, the lower marine shale interval is thin or absent and the limestone lies directly on the Buffalo sandstone interval. At Stop 5, the Buffalo interval consists of about 25 ft (7.6 m) of predominantly gray, silty shale containing thin layers of siderite nodules (Figure 6A). A thin, 2 ft (0.6 m) ledge of sandstone occurs at the top of this, followed by 22 in (55.9 cm) of light grayish green claystone (Figure 6B) and 8 in (20.3 cm) of dark gray, homogeneous shale displaying a blocky fracture pattern. The claystone is an underclay, but all evidence of coal is missing at this locality. Shaak (1975) measured the Pine Creek interval in the hillside behind the Cadet Restaurant, about 2,000 ft (610 m) south-southeast of Stop 5, where he documented a coal 22 ft (6.7 m) below the limestone (Figure 7), thereby showing one of the effects of paleotopography on the Pine Creek-Buffalo interval in the Kittanning area.

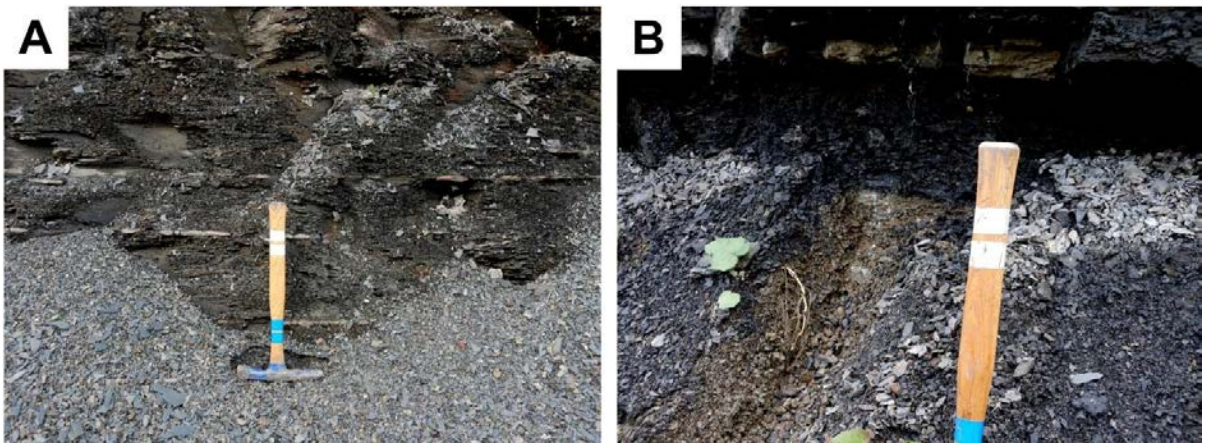

Figure 6. Photos of the rocks below the Pine Creek limestone at Stop 5. A - Siderite nodules are quite common in both the marine and nonmarine shales and siltstones above and below the limestone. B – Underclay 22 in (55.9 cm) thick occurs about 8 in (20.3 cm) below the limestone, but there is no evidence of coal. Hammer handle for scale; distance between blue and white tape = 6 in (15.24 cm).

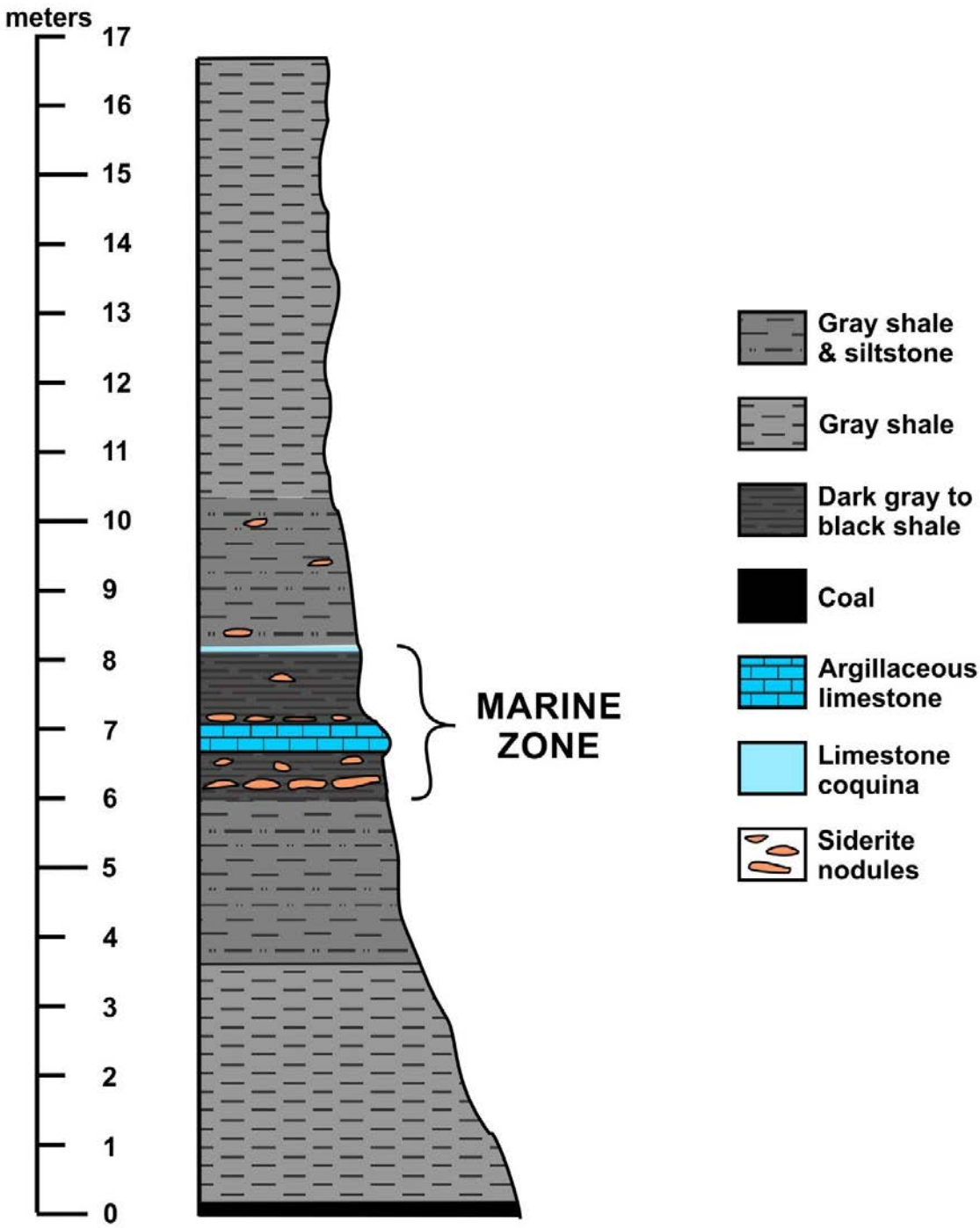

Figure 7. Stratigraphic column of Pine Creek and associated rocks exposed in the hillside behind the Cadet Restaurant on US 422 about 2,000 ft (610 m) SSE of Stop 5-2 (redrawn from Shaak, 1975; Shaak called this section Brush Creek).

Fossils

The Pine Creek marine zone can be a prolific fossil producer, yielding numerous excellent specimens, although no one group is dominant (Seaman, 1941). Where it is fossiliferous, the limestone commonly contains horn corals (*Stereostylus*), crinoid debris, a variety of brachiopods,

some cephalopods, and other fossils that lived in an open marine environment. Although some of the molluscs, particularly the gastropods (for example, *Meekospira, Amphiscapha, Shansiella*) and bivalves (for example, *Nuculopsis, Phestia, Astartella*), can be found in the limestone, they are far more commonly found in the shales because most were shallow water dwellers. *Meekospira*, in particular, appears to have been a mud snail that plowed through intertidal sediments looking for detrital organic material. Petalodontiform (*Petalodus*) and cladoselachid "shark" teeth (*Cladodus*) are not common, but they typically are found in the lower shales. Trace fossils also occur within the marine zone, including resting traces such as *Conostichus* and assorted burrows. We found a nice example of what appears to be *Asterosoma* (Figure 8A) lying along the side of the road at Stop 5. *Asterosoma* consists of bulbous to elliptical burrow chambers radiating out from a central burrow tube, probably made by some kind of worm or crustacean. Those with microscopes or good hand lenses might also be able to find ostracodes or agglutinating foraminifers attached to shells. Plates 1-4 illustrate many of the genera that have been found in Conemaugh marine deposits around the Appalachian Basin. Perhaps a few of these can be found at this locality (upon walking up to the outcrop at Stop 5 for the first time, Harper found two good specimens of the gastropod *Shansiella* just begging to be pulled out of the matrix. It took a few minutes to locate specimens of the brachiopod *Chonetinella* (Figure 8B), the resting trace *Conostichus*, and several badly preserved bivalves).

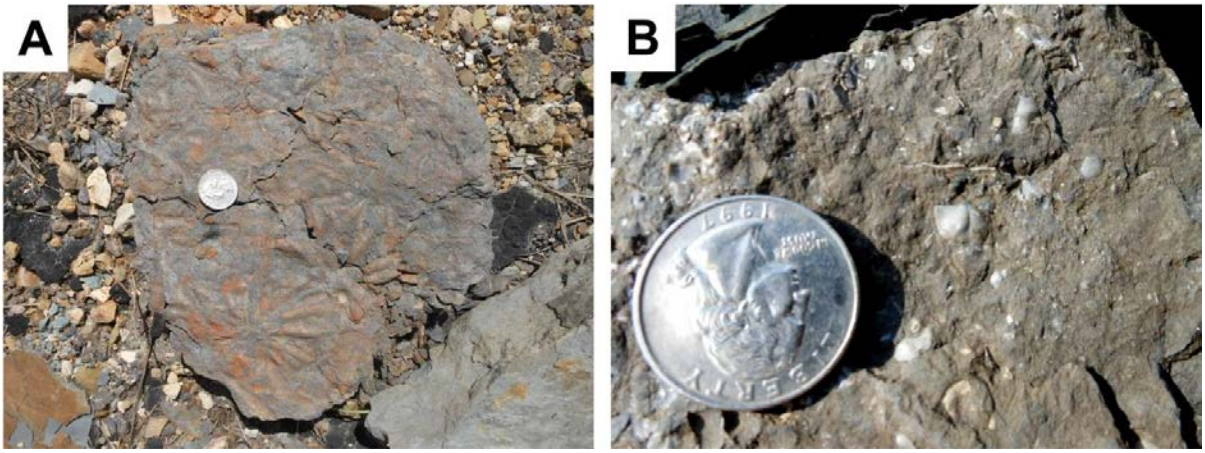

Figure 8. Photos of some Pine Creek fossils found at Stop 5. A – The trace fossil Asterosoma. B – Specimens of the brachiopod Chonetinella plebeian. Notice the white material on the rock. This is aragonite or high-magnesium calcite preserved by high organic content and hypoxic conditions in the rocks. US quarters for scale.

Some of the specimens lying around on the ground also showed evidence of preservation of original or near pristine shell material. The Pine Creek and, especially, Brush Creek marine zones are well known for having shell material preserved in near-pristine condition as primary aragonite and high-magnesium calcite (Cercone and others, 1989; Harper, 1992). Aragonite, a form of calcium carbonate that, in particular, most molluscs use to form their shells, is unstable under normal conditions. It tends either to recrystallize to calcite or dissolve completely after burial, resulting in internal and external molds. In unusual cases, however, such as in some Brush Creek and Pine Creek localities where the rock has a high organic content, the aragonite may be preserved in its original form and structure. Where abundant aragonitic shell material occurs in the Brush Creek or Pine Creek, there exists strong evidence for high organic content and hypoxic

conditions in the original muds. But the degree of preservation is not uniform across western Pennsylvania. At many localities the metastable carbonate components have undergone the normal stabilization to low-magnesium calcite. Whether the aragonitic shell material of molluscs at Stop 5 has been preserved will need to be tested. Keep an eye peeled. You might find some here.

Other Marine Zones

Although we will not be stopping to examine and collect from the other Glenshaw marine zones exposed at this stop, they deserves some mention. The Brush Creek limestone is exposed at the lower (northern) end of Stop 5 (Figure 9A) and along the west side of PA Route 66 just above road level south of the exit ramp to US 422 Eastbound (see Figure 1) where it is almost entirely obscured by talus. White (1878) named the Brush Creek limestone for 4 to 5-ft (1.2 to 1.5-m) thick sequence of fossiliferous, black, calcareous shale and 1 to 2-ft (0.3 to 0.6-m) thick, argillaceous or arenaceous, often ferruginous, and highly fossiliferous limestone. The Brush Creek quickly became so recognizable by its lithology and fossil content that, for many years, any Glenshaw marine limestone sandwiched between dark-colored marine shales was considered to be the Brush Creek, especially if only a limited section was exposed. Several classic "Brush Creek" localities in Allegheny, Armstrong, and Indiana counties provided numerous fossils used for a variety of paleoecological MS and PhD theses, but as it turned out these localities actually expose Pine Creek rather than Brush Creek, making the data and conclusions of those theses suspect. Where exposed in the vicinity of Stop 5, the Brush Creek limestone contains a relatively sparse marine fauna, mostly fragmented corals, crinoids, and brachiopods. The corals typically are exposed in either transverse or longitudinal cross section, and so are unmistakeable. Unlike most Brush Creek localities, the limestone is not sandwiched between dark-colored marine shales containing lots of fossils.

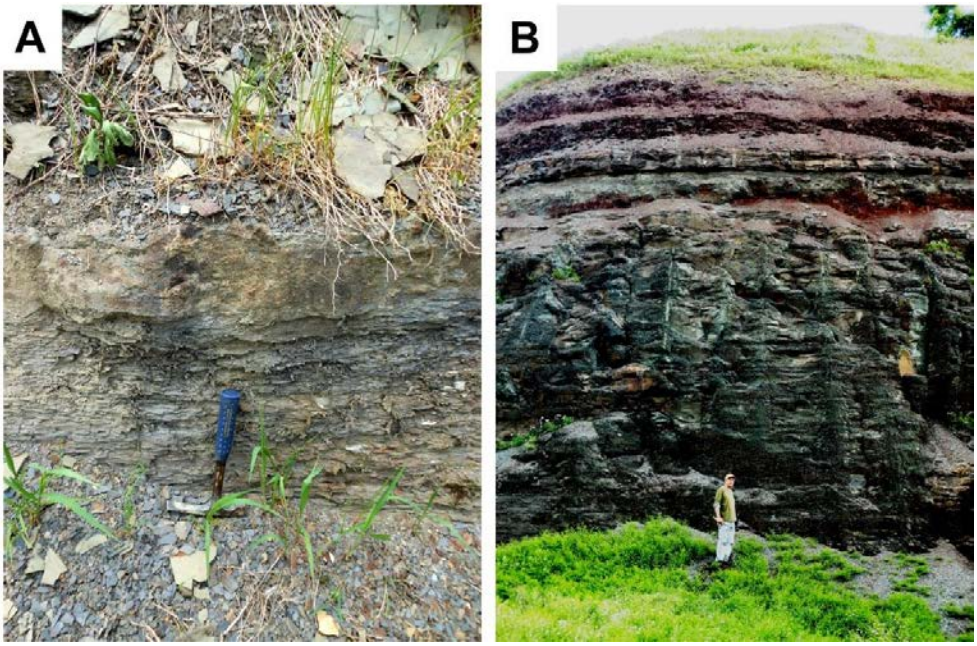

Figure 9. Other Glenshaw marine zones exposed at Stop 5. A – The Brush Creek limestone is exposed at the lower (northern) end of the onramp. Estwing rock hammer for scale. B – The Woods Run marine zone is exposed near the top of the roadcut, too high to get an accurate measurement. Notice the reddish or reddish-brown beds both above and below the limestone and its dark-colored marine shales. Geologist, 6 ft 2 in (1.9 m) tall, for scale.

In addition to the Brush Creek and Pine Creek marine zones, the Woods Run marine zone is also exposed near the top of the roadcut at Stop 5 (Figure 9B). Raymond (1910) named the Woods Run limestone for a fossiliferous marine limestone lying between the Pine Creek and Ames (Figure 1). He found only a few species of fossils in the limestone dominated by the coral *Stereostylus*. Busch (1984) described the Woods Run as an argillaceous, ferruginous limestone with occasional phosphate granules and abundant fossils. It is commonly overlain by dark gray shales with marine fossils. Burke (1958) named the Carnahan Run Shale for 5 ft (1.5 m) of dark gray, fossiliferous, marine shale separated from the Woods Run limestone by 21.5 ft (6.6 m) of reddish-brown shale carrying plant fragments. Wells (1983), however, determined that the Carnahan Run was merely a shale facies of the Woods Run. As you will see at Stop 5, the Woods Run marine zone is both underlain and overlain by reddish or reddish-brown beds (Figure 9B), probably the same beds Burke (1958) described as separating the Woods Run and Carnahan Run units.

On The Nature of Lower Conemaugh Unconformities

The on- and offramps to US 422 at Stop 5 provide an excellent three-dimensional exposure of the Pine Creek marine zone. One of the most significant features at this site is the undulating surface over which marine transgression strata were deposited. Immediately below the marine interval is a well-developed paleosol soil horizon that displays a high degree of lateral variability over a short distance. At the paleotopographic summit on the north end of the onramp, the clay is mottled red, green, and gray and contains abundant calcite nodules, mostly oriented parallel to the well-developed slickenlines within the clay. The red and green color disappears down the paleotopographic slope to the south, fading into light gray, but calcite nodules, still mostly aligned on slickensided surfaces, exist in the gray paleosol for some distance before disappearing downslope. In the lowest paleotopography visible at the site, the paleosol is a medium gray color and contains no visible calcite and minimal slickensides.

The mottled red and green and translocated calcite deposits are indicative of vertisols formed in dry-subhumid to semiarid climates (Cecil, 2003). Some degree of rainfall seasonality is required to form the slickensides. However the local paleotopography has obviously influenced paleosol development (i.e., a *paleocatena*). A paleocatena is a group of paleosols on the same buried land surface whose original soil properties differ owing to their different original landscape position and soil water regimes (Valentine and Dalrymple, 1975). The lateral changes in paleosol properties observable at this stop are best explained by lateral changes in soil moisture controlled by landscape position. Similarly, Fedorko (1998) equated lateral variations in Late Pennsylvanian organic and mineral paleosols over a 79-mi (127-km) long transect in northern West Virginia to a paleocatena. The underclay beneath the Pine Creek marine zone at Stop 5 fits the definition of a paleocatena on a micro scale, as well as the definition of a *toposequence*. A toposequence is a type of catena in which the differences among the soils result almost entirely from the influence of topography because the soils in the sequence all share the same parent material and have similar conditions regarding climate, vegetation, and time. The catena concept is similar to that of a toposequence, except that in a catena the member soils may or may not share a common parent material.

The maturity of soil development over an established paleotopographic surface prior to the Pine Creek transgression hints that Lower Conemaugh unconformities are temporally

substantial. In eastern Ohio, where the Mahoning coal has been extensively mined, it is common to see the undulating surface of the Brush Creek marine zone in pre-law Mahoning surface mines. The typical interval between the Mahoning and Brush Creek horizons is approximately 50 to 60 ft (15 to 18 m). However, drilling by the East Fairfield Coal Company in eastern Carroll and northern Jefferson Counties, Ohio, demonstrates the extreme variability of this interval. Figure 10 shows this interval in four closely spaced drill holes from northern Jefferson County where it varies from 60 ft (18 m) to over 100 ft (30.5 m). A 100-ft (30.5-m) Brush Creek-to-Mahoning coal interval requires the deposition and subsequent erosion of at least 40 ft 12 m) of sediment. In addition, as illustrated, one of the eroded deposits was a red paleosol over 13 ft (4 m) in thickness and another was a thin marine/brackish transgressive unit known as the Rock Camp marine zone. Additionally, Tim Miller, geologist for the East Fairfield Coal Company (personal communication), has mapped the Brush Creek-to-Mahoning interval immediately to the west of the cross section in Figure 10 and found that the interval *decreases* to as little as 19 ft (5.8 m), revealing a local relief of over 80 ft (24 m) after compaction and lithification.

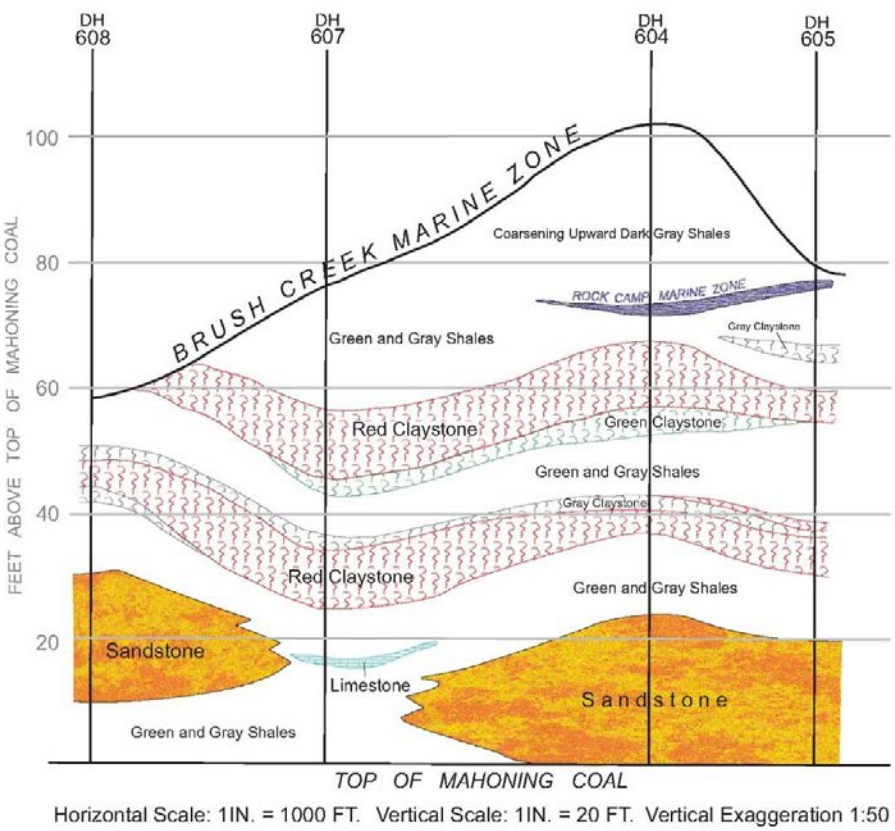

Figure 10. Cross-section defined by four diamond drill holes in Northern Jefferson County, Ohio, where the Brush Creek marine zone-to-Mahoning coal iterval increases from a normal interval of 50 to 60 ft 15 to 18 m) (DH 608) to over 100 ft (30.5 m). The uncomnmonly high interval exposes stratigraphic units normally eclipsed, suggesting the unconformable surface immediately beneath the Brush Creek transgression has substantial temporal significance.

The point of this discussion is that at least the two lowermost Glenshaw marine zones have transgressed over very mature erosional surfaces. The amount of relief on the Brush Creek surface in Ohio indicates that a formidable amount of material, including a thick soil horizon, was

deposited and eroded. It is suggested that the temporal interval involved was quite substantial. This insight is only possible due to the local "lifting off" of the Brush Creek marine zone, exposing rarely seen strata. What is not known, of course, is how much more strata were deposited and eroded for which there is no record.

References

Andrews, E. B., 1873, Geology of Athens County, Chapter X, *in* Report of the Geological Survey of Ohio, Part I, Geology. Ohio Geological Survey, Report of Progress, 2nd series, v. 1, p. 261-293.

Burke, J. J., 1958, New marine horizon in the Conemaugh Formation: Science, v. 128, p. 302.

Busch, R. M., 1984, Stratigraphic analysis of Pennsylvanian rocks using a hierarchy of transgressive-regressive units: Pittsburgh, Pa., University of Pittsburgh, Ph.D. dissertation, p. 427.

Busch, R. M. and Rollins, H. B., 1984, Correlation of Carboniferous stratigraphy using a hierarchy of transgressive-regressive units: Geology, v. 12, p. 471-474.

Butts, C., 1906, Economic geology of the Kittanning and Rural Valley quadrangles, Pennsylvania: U. S. Geological Survey Bulletin 279, 198 p.

Carothers, M. C., 1976, Depositional environments of the Cambridge Limestone (Missourian, Pennsylvanian) of the Appalachian Basin: Pittsburgh, Pa., University of Pittsburgh, Ph.D. dissertation, p. 214.

Cecil, C. B., 2003, The Concept of autocyclic and allocyclic controls on sedimentation and stratigraphy, emphasizing the climatic variable, *in* Cecil, C. B. and N. T. Edgar, eds., Climate Controls on Stratigraphy: SEPM Special Publication No. 77, p. 13–20.

Cercone, K. R., N. J. Durika, and J.F. Taylor, 1989, Taphonomy and geochemistry of the Brush Creek marine interval in Indiana, Armstrong, and Cambria Counties, *in* Harper, J. A, ed., Geology in the Laurel Highlands of southwestern Pennsylvania: Field Trip Guidebook, 54th Annual Field Conference of Pennsylvania Geologists, Johnstown, PA, p. 100-106

Chesnut, D.R., 1981. Marine zones of the Upper Carboniferous of eastern Kentucky, *in* Cobb, J.C., D. R. Chesnut, N. C. Hester, and J. C. Hower, eds., Coal and coal-bearing rocks of eastern Kentucky: Kentucky Geological Survey, ser. 11, p. 57-66.

Donahue, J. and H. B. Rollins, 1974a, Introduction, *in* Donahue, J. and H. B. Rollins, eds., Conemaugh (Glenshaw) marine events: Field Trip Guidebook, Third Annual Meeting of the Eastern Section, American Association of Petroleum Geologists and Eastern Section, Society of Economic Paleontologists and Mineralogists, April 20-21, Pittsburgh, PA, p. 1-14.

Fedorko III, N., 1998, Investigation of a paleocatena across a Late Pennsylvanian land-scape comprised of mineral and organic paleosols: Morgantown, WV, West Virginia University, MS thesis, p. 237.

Flint, N. K., 1965, Geology and mineral resources of southern Somerset County, Pennsylvania: Pennsylvania Geological Survey, 4th ser., County Report 56A, 267 p.

Harper, J. A., 1992, Life in a fossil shellfish community: an excellent outdoor classroom and a collector's paradise: Pennsylvania Geology, v. 23, no. 2, p. 9-14.

Harper, J. A. and C. D. and Laughrey, 1987, Geology of the oil and gas fields of southwestern Pennsylvania: Pennsylvania Geological Survey, 4th ser., Mineral Resource Report 87, 166 p.

Heckel, P. H., Barrick, J. E., and Rosscoe, S. J., 2011, Conodont-based correlation of marine units in lower Conemaugh Group (Late Pennsylvanian) in northern Appalachian basin: Stratigraphy, v. 8, p. 253-269.

Heckel, P. H., Gibling, M. R., and King, N. R., 1998, Stratigraphic model for glacial-eustatic Pennsylvanian cyclothems in highstand nearshore detrital regimes: Journal of Geology, v. 106, p. 373-383.

Kitsko, J. J., 2016, 422, Benjamin Franklin Highway: http://www.pahighways.com/us/ US422.html (accessed June, 2016).

Platt, F., 1875, Report of progress in the Clearfield and Jefferson District of the bituminous coal-fields of western Pennsylvania: Second Geological Survey of Pennsylvania, Report H, 294 p.

Raymond, P. E., 1910, A preliminary list of the fauna of the Allegheny and Conemaugh series in western Pennsylvania: Annals of the Carnegie Museum, v. 7, p. 144–158.

Richardson, G. B., 1932, Geology and coal, oil and gas resources of the New Kensington quadrangle, Pennsylvania: U.S. Geological Survey Bulletin 829, 102 p.

Rollins, H. B., M. Carothers, and J. Donahue, 1979, Transgression, regression and fossil community succession: Lethaia, v. 12, p. 89–104.

Seaman, D. M., 1941, The Cambridge (Pine Creek) limestone of western Pennsylvania: Pennsylvania Academy of Sciences Proceedings, v. 15, p. 60-65.

Shaak, G. D., 1975, Diversity and community structure of the Brush Creek marine interval (Conemaugh group, Upper Pennsylvanian), in the Appalachian basin of western Pennsylvania: Florida State Museum Bulletin, Biological Sciences, v. 19, no. 2, 133 p.

Stevenson, J. J., 1906, Carboniferous of the Appalachian Basin: Geological Society of America, v. 17, p. 65-228.

Valentine, K. W. G. and J. B. Dalrymple, 1975, The identification, lateral variation, and chronology of two buried paleocatenas at Woodhall Spa and West Runton, England: Quaternary Research, v. 5, p. 551-590.

Wells, K. E., 1983, Detailed correlation of paleogeographic development of the Woods Run and Carnahan Run marine units (Upper Pennsylvanian) in southwestern Pennsylvania (abstract): Geological Society of America, Abstracts with Programs, v. 15, no. 6, p. 717.

White, I. C., 1878, Report of progress in the Beaver River District of the bituminous coal-fields of western Pennsylvania: Second Geological Survey of Pennsylvania, Report Q, 337 p.

White, I. C., 1903, The Appalachian coal field, the Conemaugh series: West Virginia Geological Survey, v. 2, p. 225-332.

Woolsey, L. H., 1906, Economic geology of the Beaver quadrangle, Pennsylvania [southern Beaver and northwestern Allegheny Counties]: U.S. Geol. Survey Bull. 286, 132 p.

STRATIGRAPHY, LITHOLOGY, AND SEA-LEVEL HISTORY OF THE BRUSH CREEK MARINE DEPOSITS OF THE GLENSHAW FORMATION

CHRISTOPHER L. COUGHENOUR, UNIVERSITY OF PITTSBURGH-JOHNSTOWN

Introduction and History

The Brush Creek Limestone is a richly fossiliferous, shallow marine carbonaceous limestone in the Glenshaw Formation of the Conemaugh Group (Upper Pennsylvanian, Missourian). The unit and its associated calcareous marine shales are often known as the Brush Creek marine zone, which has a total thickness of around 15 feet (4.6 m) (White, 1878). This marine zone generally overlies the Brush Creek coal, which is a thin (1-2 feet), occasionally mined coal. As sea level receded in the basin, a terrestrial sandstone and siltstone unit, the Buffalo sandstone, was deposited. In some locations another marine unit, the Pine Creek limestone, is encountered directly above the Buffalo sandstone, indicating a relatively rapid return to marine conditions and the completion of a high-order (eustatic) transgressive-regressive cycle.

Despite a maximum thickness of only around 1 foot (0.3 m), the Brush Creek limestone is laterally extensive, as is the Pine Creek limestone (known as the upper Brush Creek limestone in Ohio and West Virginia), which attains thicknesses of several feet. These marine zones are known from western Pennsylvania, eastern Ohio, northern West Virginia, western Maryland (Wilmarth, 1938), and even eastern Kentucky (Chestnut, 1981) (Figure 1). Because of their regional extent, unique lithologies, and fossil faunas, they are important marker beds for stratigraphic correlations within the Upper Pennsylvanian Series. As marine units situated within a primarily terrestrial succession, they are also valuable in assessing sea level cycles (e.g. Busch & Rollins, 1984) and for use in correlating allocyclic (eustatic) events between the

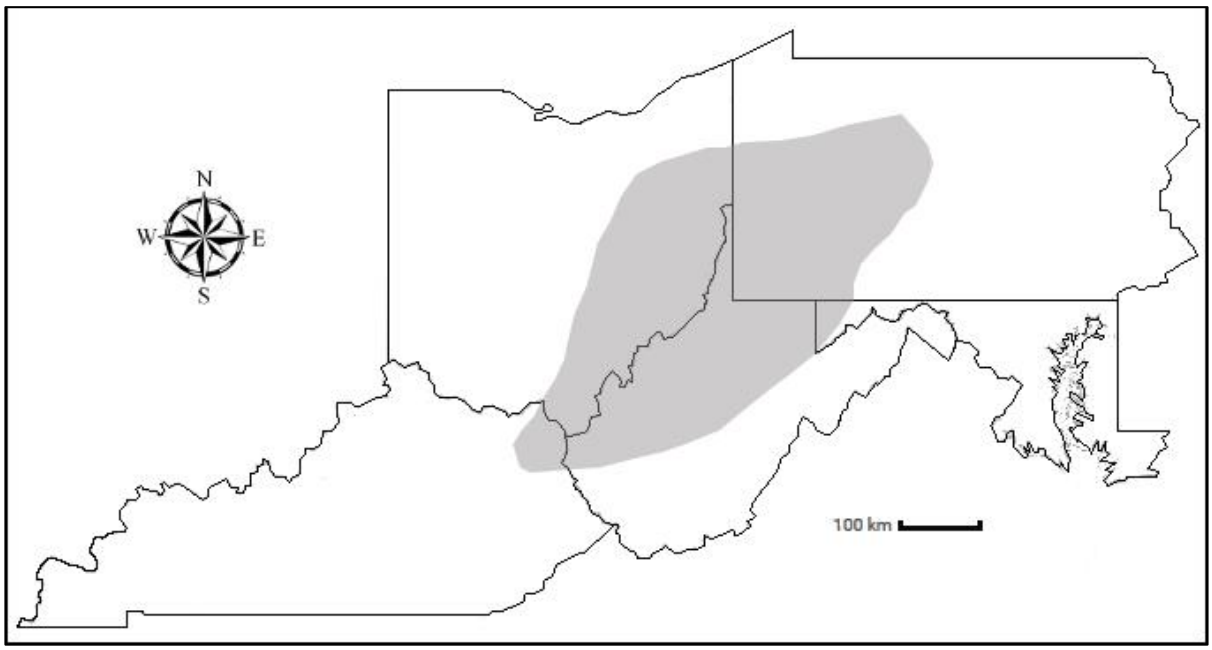

Figure 1. Shaded area denotes the approximate extent of the basin containing the Glenshaw Formation and Brush Creek and Pine Creek marine zones (after Busch & Rollins (1984) and Martino (2004)

Appalachian Basin and Carboniferous basins in the mid-continent (e.g. Heckel et al., 1998). Additionally, the units are prolific fossil producers, yielding relatively pristine gastropod fossils, including some that are still aragonitic (see discussion in Cercone and Taylor, 1989). The deposits also yield numerous bivalves and cephalopods.

The Brush Creek and Pine Creek limestones were first named by Israel Charles White in 1878, during the Second Geological Survey of Pennsylvania (White, 1878). White performed his mapping in the "Beaver River district" encompassing parts of Butler, Beaver, and Allegheny Counties. The Brush Creek limestone was described from an outcrop along Brush Creek in Cranberry Township, Butler County. The limestone and associated calcareous shales of the marine zone were all described within the "Lower Barren Measure Series". Franklin and William G. Platt, in a survey report from Cambria and Somerset Counties the previous year (1877), also delineated the "Lower Barren Measures" and within it described a Philson limestone. The Philson limestone correlates to the stratigraphic position of the Brush Creek limestone and has been synonymized with the Brush Creek limestone (although, technically 'Philson' has taxonomic priority). An underlying Gallitzin coal reported by Platt and Platt has, ultimately, been largely regarded as synonymous with the Brush Creek coal, after some uncertainty regarding a possible correlation to the isolated Humbert coal in southern Somerset County (see discussion in Shaulis, 1993). Both White and the Platts defined the Lower Barren Measures as all units occurring above the Upper Freeport coal and below the "Pittsburg" coal (in the second survey publications, Pittsburgh was spelled as 'Pittsburg'). Later, this section came to be known as the Conemaugh Formation (Woolsey, 1906) and, eventually, Conemaugh Group (see Wilmarth, 1938).

Later studies (Flint, 1965) divided the Conemaugh Group into the Glenshaw and Casselman Formations, with the Glenshaw extending from the upper contact of the Upper Freeport coal to the top of the Ames Limestone (Figure 2). The Brush Creek marine zone is the lowest marine unit in the Conemaugh Group. Flint (1965) noted the similarity of lithofacies between the Brush Creek shales and those associated with the Ames marine zone.

Moving up-section before one encounters the Pine Creek Limestone (White, 1878). In Ohio, a lower Brush Creek and upper Brush Creek limestone separated by around 20 feet of siliciclastic shale and sandstone have been recognized, along with the overlying Cambridge limestone (Wilmarth, 1938). Heckel et al (2011), using conodont relations, report that the Brush Creek limestone of Pennsylvania is biostratigraphically correlated to the lower Brush Creek limestone in Ohio, while the Pine Creek limestone is correlated to the upper Brush Creek limestone. The Cambridge limestone is not correlated to the Pine Creek/upper Brush Creek limestone.

Lithology and Petrology

The Brush Creek marine zone is composed of two basic carbonate lithofacies that overlie a 1-2 foot seam of bituminous coal. White (1878) described the lithologic heterogeneity in the carbonates overlying the coal, noting that "[a]t times it is a black calcareous shale, 4 to 5 feet thick, and again we see it a very compact limestone, 1 to 2 feet thick." The total thickness of the coal and carbonates is typically around 5 meters. In some localities (e.g. several road cuts in Indiana County), the coal is absent under the carbonates.

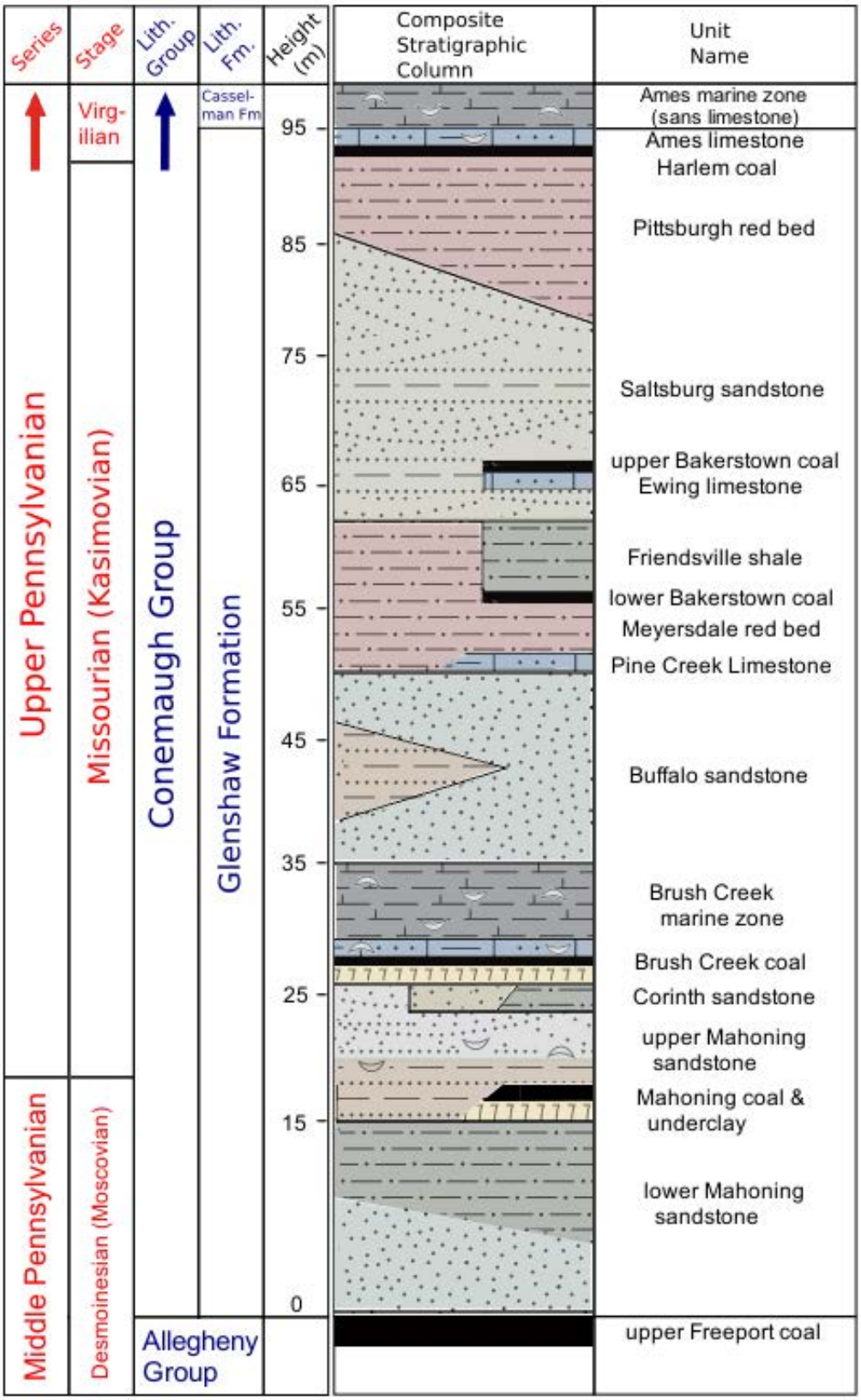

Figure 2. Composite stratigraphic column of the Conemaugh Group (for Cambria County) references: (White, 1878), (Phalen, 1910), and (Flint, 1965). Lithology symbols are those of USGS.

The Brush Creek limestone facies is a carbonaceous, often nodular limestone and its color at outcrop is dark gray (Munsell: Gley 1 3/N), with the calcareous shale facies being of similar color. The measured thickness of the limestone in the Johnstown area is 9-14 inches. Where it directly overlies the coal, it often forms an irregular, 'hummocky' contact. Stratification of the limestone, although not always readily apparent in situ, does become more apparent in broken hand sample. Thin, sub-mm, sub-parallel laminae are often present and the unit exhibits rather thick, flaggy partings under moderate shear (e.g. tapping with a hammer) that parallel the laminae. Few trace fossils are present in the marine zone.

Cutting and polishing of the limestone reveals several features not readily observed at outcrop. Numerous biogenic clasts become more visible (appear white when polished) that exhibit a wide variation in size (from sub-mm to several mm's). Photomicrographs reveal a biogenic clast-supported structure (Figure 3). Most of these clasts are fragmented mollusk shells that are sized as fine-medium sands. Overall, the Brush Creek limestone facies (as sampled in Johnstown) would be classed as a biomicrite in the Folk (1962) scheme and a packstone in the Dunham (1962) classification. In other localities, such as eastern Ohio, a wackestone lithology is also present (Klasen, 2007). Additionally, zones of golden colored iron sulfide become apparent. This is consistent with diagenetic pyritization observed in some gastropods collected in the unit. Iron is also present in other forms in the marine zone. Payne et al. (1981), working from thin sections, reported "many equant magnetite or titanomagnetite grains, generally less than 2 μm across." These were used in a paleomagnetic study that placed the magnetic pole during Brush Creek deposition in the area of the Yellow Sea (between the Korean Peninsula and China) (Payne et al., 1981).

Figure 3. Photomicrographs of polished hand sample of the Brush Creek limestone revealing biogenic clast-supported structure, iron sulfide zones (e.g. top, center), and dark, organic-rich matrix. The inset reveals the location of the photomicrograph at right.

The dark matrix that lends the shale and limestone its dark color is composed of significant terrigenous material, although micrite is also a component. Analysis of broadly similar "dirty" marine limestone and shale intervals from the Late Carboniferous of Nova Scotia revealed highly variable total organic content (several percent to over forty percent) that was primarily vitrinite and sporinite (Gibling and Kalkreuth, 1991), indicating input from relatively proximal forests/swamps. It is important to note that this does not denote a high influx of detrital sediment; in fact, the pyritization and skeletal make-up of the limestone (and to lesser degree shale) suggest sediment starvation and a period of slow deposition not affected by pulses of sediment from the Appalachian Highlands to the east that typify the period (Heckel, 1994).

The shale facies of the marine zone is fissile to platy and varies slightly in color from medium to dark gray. It overlies the limestone and in many outcrops also underlies it. The contact between the units is fairly abrupt. The shale facies possesses greater clay mineral content, and has calcareous mud content that is broadly similar in character, if not concentration, to the limestone. As with the limestone, marine gastropods, bivalves, and cephalopods are fairly common in the shales, although a rigorous comparison of the community compositions in the two facies has yet to be performed. Morris et al. (1973) reported the first known occurrence of a nearly complete ophiuroid (echinoderm) from the Upper Carboniferous (in Murrysville, PA). The specimen was found in the shale facies and the associated fauna there was described as "low in diversity". Overall, the shale indicates a deeper depositional setting than the limestone, with low energy and low oxygen waters. Unlike other basins in which these shales are more phosphatic, it appears that the Appalachian Basin shales were too shallow to allow the development of a pycnocline (usually at depths greater than several hundred meters) that would promote the accumulation of phosphates (Heckel, 1994).

Nodules are present in both the limestone and shale. Seaman and Hamilton (1950) report these as "clay-ironstone" concretions containing siderite, variable barite or calcite, pyrite, chalcopyrite, and several previously unknown polymorphs of the mineral Wurtzite (ZnS) present in shrinkage cracks (reported from near Shelocta, PA). Nodules are generally intermittent, but can form nearly linear (meters long) strands in the shales.

Discussion of sea-level and regional events

The Brush Creek limestone is the culmination of a high-order transgression that likely spanned only a few hundred thousand years and resulted from widespread glacially-driven changes in sea level, perhaps related to Milankovitch cyclicity (e.g. Bodek, 2006). An ideal example occurs at the outcrop exposed in Richland Township (behind Giant Eagle, along Eisenhower Blvd). A simple (high-order) transgressive-regressive (T-R) cycle typical of the Glenshaw Formation (but often obscured by talus or overburden) can be observed moving from the upper Mahoning sandstone to the Buffalo Sandstone. Moving up-section one encounters 1) interbedded sandstones and siltstones (regression/lower sea level), 2) underclay and coal, 3) the limestone and marine shales (transgression and highstand), and 4) the overlying siltstone and sandstone (regression).

This sequence mirrors, in fundamental form, the cyclical sedimentation described by Weller (1930) and Wanless and Weller (1932) during the development of the original cyclothem model. In fact, Weller (1930) makes explicit mention of the Brush Creek sediments and places units 1-3 from the cycle above within a 'cyclic formation' (later, 'cyclothem'). The cyclothem development was first

thought to be controlled by uplift/tectonic processes, although competing ideas that controls were related to fluctuations in global sea level were proposed soon after (see discussion in Heckel, 1994).

Later workers developed an alternative cyclic sedimentation model using the concept of a "punctuated aggradational cycle" (PAC) (Goodwin and Anderson, 1980; Busch and Rollins, 1984). A PAC is a rather abrupt, but low amplitude transgression that follows a period of relative stillstand and shallows upward (Goodwin and Anderson, 1985). The PAC concept was extended to relate to complete transgressive-regressive (T-R) units and cyclothems by the "cyclothemic PAC" model (Anderson and Goodwin, 1982). A cyclothemic PAC begins with the surface denoting the onset of transgression, often taken as the base of a widespread coal. The transgressive maximum is denoted by a marine limestone and the subsequent regression denoted by overlying marine mudstones and non-marine sandstones.

For example, units 2-4 (from the Johnstown outcrop) comprise a cyclothemic PAC, beginning with the base of the Brush Creek coal and terminating at the top of the marine zone shales. The Pine Creek limestone marks the beginning of the subsequent sequence. Busch and Rollins (1984) identified eleven cyclothemic PAC sequences in the Glenshaw Formation. The PAC hypothesis states that these represent time-stratigraphic units and allocyclic events that can be used for widespread correlation. Allocyclic controls denote mechanisms that originate outside of the basin, such as tectonic effects, climate change, or eustatic change, thus, occurrence of these events is of widespread chronostratigraphic significance. For example, with the aid of conodonts, the Brush Creek cyclothemic PAC (T-R unit) has been correlated to the Macoupin cyclothem in the Illinois Basin and the Swope cyclothem in the Midcontinent Basin (Heckel et al., 2011). Cyclothemic units with periods of several hundred thousand years are often ascribed to orbitally-driven (Milankovitch) changes in eustasy.

In considering transgressive-regressive processes, it is important to recall the hierarchical nature of stratigraphic cycles and their relevance in sequence stratigraphy (Figure 4). Temporal control is

Tectono-Eustatic/ Eustatic Cycle Order	*Sequence Stratigraphic Unit*	Duraction (my)	*Relative Sea Level Amplitude (m)*	*Relative Sea Level Rise/Fall Rate (cm/1,000 yr)*
First		>100		<1
Second	Supersequence	10-100	50-100	1-3
Third	Depositional Sequence Composite Sequence	1-10	50-100	1-10
Fourth	High Energy Sequence, Parasequence and Cycle Set	0.1-1	1-150	40-500
Fifth	Parasequence, High-Frequency Cycle	0.01-0.1	1-150	60-700

(From SEPM#40)

Figure 4. Stratigraphic cycle orders with corresponding duration and relative sea level parameters. From sepmstrata.org, reproduced from SEPM shortcourse notes by Kerans and Tinker (1997).

necessary for this task. Recent chronostratigraphic work places the Brush Creek units near the base of the Missourian Stage (ICS Kasimovian Stage) Ma (see summary in Greb and Chestnut, 2009). The Ames limestone at the top of the Glenshaw Formation is estimated at 301.5 Ma and the top of the upper Freeport coal is estimated at 305.5. Following Busch and Rollins (1984) in assuming 11 cyclothemic PACs in the Glenshaw Formation, the average duration of each cycle is then about 275,000 years. The Brush Creek marine zone then denotes a transgressive maximum within a 4th order T-R cycle (Figure 5). Using the definitions of Figure 3, Appalachian Basin cyclothems originally described by Weller (1930) are 4th order cycles (note that order definitions are not standardized).

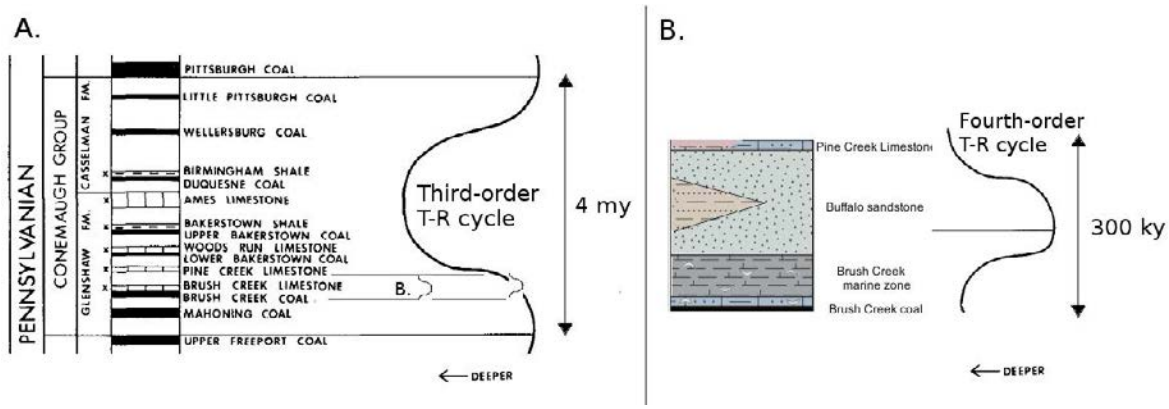

Figure 5. A. Depiction of the allocyclic (subsidence-controlled) third-order cycle of the Conemaugh Group (after Busch & Rollins, 1984). B. The allocyclic (eustatic-controlled) fourth-order cycle that is expressed between the Brush Creek coal and the Pine Creek Limestone.

The Brush Creek to Pine Creek 4th order interval can also be interpreted in terms of systems tracts (units defined by their deposition within a particular phase of sea level rise, fall, or relative stillstand). Systems tracts are the stacked depositional units that make up sequences. One model is that of a sequence composed of four systems tracts that span a complete T-R cycle (Figure 6). The four systems tracts are: lowstand systems tract (LST), transgressive systems tract (TST), highstand systems tract (HST), and falling stage systems tract (FSST). In many cases, however, delineating so many systems tracts and their boundaries is problematic at outcrop or with otherwise limited data. Accordingly, many workers group the HST, FSST, and LST into a single "regressive systems tract" (RST) (e.g. Johannessen et al., 1995).

Klasen (2007) performed a sequence stratigraphic analysis of the upper to lower Brush Creek interval in Ohio. The base of the Brush Creek coal, along with the underlying clay and upper Mahoning sandstone, is ascribed to a period of lower sea level, but with the overlying Brush Creek limestone, denotes a transition to marine facies. These units are interpreted to form the TST of sequence 1. It is thought deposits of the LST would not occur in the Appalachian Basin, but in correlatives in more westward basins (Klasen, 2007). Combined with the lithologic evidence of sediment starvation, the limestone has been interpreted as representing a condensed section where sedimentation rates were very low (often under 1 mm/yr) (Heckel, 1994). Condensed sections typically occur near the end of a TST as the rate of sea level rise and accommodation creation decrease, but water remains relatively deep.

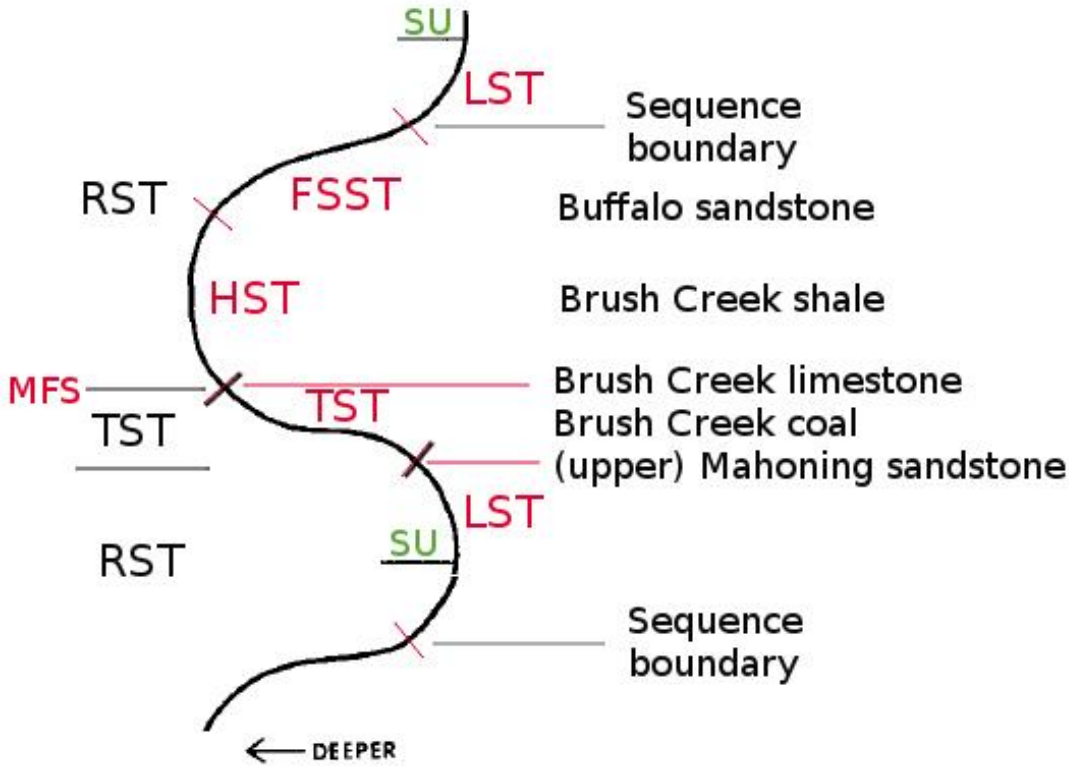

Figure 6. Model demonstrating systems tracts and their relation to relative sea level with approximate positions of the units of the lower Glenshaw Formation denoted. RST = regressive systems tract, TST = transgressive systems tract, MFS = maximum flooding surface, LST = lowstand systems tract, HST = highstand systems tract, FSST= falling stage systems tract, and SU = subaerial unconformity.

A maximum flooding surface (MFS), when sedimentation rates were very similar to the rate of increase in sea level (and accommodation), generally caps a condensed section and forms the boundary between the TST and HST. Accordingly, the MFS lies in the Brush Creek limestone. The transition to deeper marine calcareous shales is then ascribed to a HST (Klasen, 2007). This is the beginning of the RST. Sediment accumulation, while not very great here, exceeded the rate of sea level rise and creation of accommodation space, which become nearly zero. Subsequent to this was a period when sea level and accommodation space were decreasing and, eventually, reach a stillstand. This results in a seaward migration of depositional systems and, eventually, the onset of subaerial exposure, erosional surfaces, and sediment bypassing. Martino (2004) analyzed the Glenshaw Formation in a sequence stratigraphic framework, employing paleosols as important markers for systems tracts. The part of the RST corresponding to this "forced regression" would begin in the lower portions of the Buffalo sandstone, which does denote a prograding upper deltaic/fluvial system.

Martino (2016) notes that the Buffalo sandstone (in West Virginia) contains an incised valley fill cut during the RST and filled by the subsequent TST. This is consistent with Klasen (2007) in placing the Buffalo sandstone (and equivalents) within the RST. The overlying Pine Creek (or upper Brush Creek) limestone was not incised by this event, while some of the fill deposits aggrade up to the limestone (Martino, 2016). This indicates that the TST and the beginning of the next sequence is represented by the Pine Creek limestone. Thus, the TST of sequence 1 contain the upper Mahoning sandstone, the Brush Creek coal, underclay, and Brush Creek limestone. The RST of the sequence is composed of the Brush Creek shales and the Buffalo sandstone. Similar to the Brush Creek limestone, the Pine Creek limestone is thought to represent a condensed section and contain the maximum flooding surface.

The transgression represented by the Brush Creek deposits is nested within a larger transgressive trend that culminated in the thicker Ames limestone, and may represent a slower cycle related to foreland subsidence in that part of the basin (e.g. Ettensohn, 2008). Within the Conemaugh Group, the Ames marine zone is the thickest and most laterally extensive marine unit and is thus attributed to maximum transgression within the group. This transgression was preceded by the regressive maximum at the base of the upper Freeport coal and succeeded by the next regressive maximum at the base of the Pittsburgh coal. These coals are noted for having been locally removed by valley incision around times of low stand and subsequently filled (in part) with fluvial-estuarine sediments (see Martino, 2016 and discussion in Bragonier et al., 2007). The well-developed paleosols and fireclays underlying the coal also point to regression and long periods of subaerial exposure. Approximately 4 million years separate the upper Freeport coal from the Pittsburgh coal, thus, this interval represents a complete 3rd order T-R cycle (see Figure 5).

Interestingly, in Phalen's 1910 Johnstown Folio for the USGS, the author moves directly up-section from the Brush Creek (Gallitzin) coal to the Buffalo sandstone member with no mention of the Brush Creek marine zone above the coal, despite its known occurrence in the area, including the field stop in Richland Township (Phalen, 1910). Richardson (1936) noted the Brush Creek marine zone was almost entirely absent in quadrangles (Butler and Zelienople) neighboring the type locality of the Brush Creek Limestone. These episodic absences of the unit may be typical of high-shelf deposits that were dissected by erosion during subsequent high-order (4th order) regressions (Heckel et al., 1998).

References

Anderson, E.J. and Goodwin, P.W., 1982, Application of the hypothesis of punctuated aggradational cycles: Allocyclicity in the Helderberg Group, New York State: Abstracts of Belyea Conference on the Devonian System: Calgary, Alberta, Canadian Society of Petroleum Geologists.

Bodek Jr, R.J., 2006. Sequence Stratigraphic Architecture of Early Pennsylvanian, Coal-bearing Strata of the Cumberland Block: A Case Study from Dickenson County, Virginia: Blacksburg, Va., Virginia Polytechnic Institute and State University, Master's Thesis, p. 72.

Bragonier, W.A., Bohan, M.P. and Hawk, J.L., 2007, The monster channel complex of central-western Pennsylvania: Pennsylvania Geology, v. 37, p.2-13.

Busch, R.M. and Rollins, H.B., 1984, Correlation of Carboniferous strata using a hierarchy of transgressive-regressive units: Geology, v. 12, p. 471-474.

Cercone, K.R., Durika, N.J., and Taylor, J.F., 1989, Taphonomy and geochemistry of the Brush Creek marine interval in Indiana, Armstrong, and Cambria Counties, *in*: Harper, J. A. ed., Geology of the Laurel Highlands of Southwestern Pennsylvania: Annual Field Conference of Pennsylvania Geologists , 54th, Johnstown, Pa., Guidebook, p. 100-106.

Chestnut, D.R., 1981, Marine zones of the Upper Carboniferous of eastern Kentucky. Coal and Coal-Bearing Rocks of Eastern Kentucky. Annual Geological Society of America Coal Division Field Trip, pp.57-66.

Ettensohn, F.R., 2008, The Appalachian foreland basin in eastern United States: Sedimentary basins of the world, v. 5, p. 105-179.

Dunham, R.J., 1962, Classification of carbonate rocks according to depositional textures, *in* Ham, W.E., ed., Classification of Carbonate Rocks: American Association of Petroleum Geologists Memoir 1, p. 108-121.

Flint, N.K., 1965, Geology and mineral resources of southern Somerset County, Pennsylvania: Pennsylvania Geological Survey, 4th ser., County Report 56A, 267 p.

Folk, R.J., 1962, Spectral subdivision of limestone types, *in* Ham, W.E., ed., Classification of Carbonate Rocks: American Association of Petroleum Geologists Memoir 1, p. 62-84.

Gibling, M.R. and Kalkreuth, W.D., 1991, Petrology of selected carbonaceous limestones and shales in Late Carboniferous coal basins of Atlantic Canada: International Journal of Coal Geology, v. 17, p. 239-271.

Goodwin, P.W. and Anderson, E.J., 1980, Punctuated aggradational cycles: a general hypothesis of stratigraphic accumulation: Geological Society of America, Abstracts with Programs, v. 12, p. 436.

Goodwin, P.W. and Anderson, E.J., 1985, Punctuated aggradational cycles: a general hypothesis of episodic stratigraphic accumulation: The Journal of Geology, v. 93, p. 515-533.

Greb, S.F., Chestnut, D.R., Eble, C.F., and Blake, B.M., 2009, The Pennsylvanian of the Appalachian Basin, *in* Greb, S.F. and Chestnut, D.R. (Editors) Carboniferous Geology and Biostratigraphy of the Appalachian Basin: Kentucky Geological Survey, Special Publication 10, p. 32-45.

Heckel, P.H., 1994, Evaluation of evidence for glacio-eustatic control over marine Pennsylvanian cyclothems in North America and consideration of possible tectonic effects. Tectonic and Eustatic Controls on Sedimentary Cycles: SEPM, Concepts in Sedimentology and Paleontology, v. 4, p. 65-87.

Heckel, P.H., Barrick, J.E. and Rosscoe, S.J., 2011, Conodont-based correlation of marine units in lower Conemaugh Group (Late Pennsylvanian) in Northern Appalachian Basin: Stratigraphy, v. 8, p.253.

Heckel, P.H., Gibling, M.R. and King, N.R., 1998, Stratigraphic Model for Glacial-Eustatic Pennsylvanian Cyclothems in Highstand Nearshore Detrital Regimes: The Journal of Geology, v. 106, p. 373-384.

Johannessen, E.P., Mjos, R., Renshaw, D., Dalland, A., and Jacobsen, T., 1995, Northern limit of the "Brent Delta" at the Tampen Spur: a sequence stratigraphic approach for sandstone prediction, *in* Steel, R.J., Felt, V., Johannessen, E.P. and C. Mathieu, eds., Sequence Stratigraphy

of the Northwest European Margin: Norwegian Petroleum Society (NPF), Special Publication 5, p. 213-256.

Klasen, R.L., 2007, Sequence Stratigraphic Analysis of the Lower and Upper Brush Creek Interval (Late Pennsylvanian), Southeastern Ohio: Athens County, Ohio: Athens, Oh., Ohio University, Master's Thesis, p. 9.

Martino, R.L., 2004, Sequence stratigraphy of the Glenshaw Formation (middle-late Pennsylvanian) in the central Appalachian basin, *in* Pashin, J.C. and Gastaldo, R.A., eds., Sequence stratigraphy, paleoclimate, and tectonics of coal-bearing strata: AAPG Studies in Geology, v. 51, p. 1-28.

Martino, R.L., 2016, Sequence stratigraphy of fluvially dominated strata of the Mid-Late Pennsylvanian Conemaugh Formation, Central Appalachian Basin: International Journal of Coal Geology, v. 154-155, p. 136-154.

Morris, R.W., Rollins, H.B. and Shaak, G.D., 1973, A new ophiuroid from the Brush Creek shale (Conemaugh Group, Pennsylvanian) of western Pennsylvania: Journal of Paleontology, v. 47, p. 473-478.

Payne, M.A., Shulik, S.J., Donahue, J., Rollins, H.B. and Schmidt, V.A., 1981, Paleomagnetic poles for the Carboniferous Brush Creek limestone and Buffalo siltstone from southwestern Pennsylvania: Physics of the Earth and Planetary Interiors, v. 25, p. 113-118.

Phalen, W.C., 1910, Johnstown folio, Pennsylvania: US Geological Survey, no. 174, 15 p.

Platt, F. and Platt, W. G., 1877, Report of Progress in the Cambrian and Somerset District of the bituminous coal fields of western Pennsylvania; Part II Somerset: Pennsylvania Geological Survey, 2nd series, v. HHH, 348 p.

Seaman, D.M. and Hamilton, H., 1950, Occurrence of polymorphous wurtzite in western Pennsylvania and eastern Ohio: American Mineralogist, v. 35, p. 43-50.

Shaulis, J.R., 1993, Surface bedrock stratigraphy *in* Shaulis, J.R., Brezinski, D.K., Clark, G.M., and others, eds., Geology of the Southern Somerset County Region, Southwestern Pennsylvania, 58th, Somerset, Pa., Annual Field Conference of Pennsylvania Geologists, Guidebook, p. 1-20.

Wanless, H.R. and Weller, J.M., 1932, Correlation and extent of Pennsylvanian cyclothems: Geological Society of America Bulletin, v. 43, p. 1003-1016.

Weller, J.M., 1930, Cyclical sedimentation of the Pennsylvanian period and its significance: The Journal of Geology, v. 38, p. 97-135.

White, I.C., 1878, Report of progress in the Beaver River district of the bituminous coal fields of western Pennsylvania, with analyses of coal, cannel, coke, clay, limestone, and ore, from Butler and Beaver Counties, Pennsylvania by A.S. McCreath: Pennsylvania Geological Survey Report of Progress, 2nd series, v. Q, 337 p.

Wilmarth, M.G., 1938, Lexicon of Geologic Names of the United States (Including Alaska): USGS Bulletin 896, 1244 p.

Woolsey, L. H., 1906, Economic geology of the Beaver quadrangle, Pennsylvania [southern Beaver and northwestern Allegheny Counties]: U.S. Geol. Survey Bull. 286, 132 p.

Yes, but look at the bright side, Martha—
we don't live anywhere near Mt. St. Helens!

EVIDENCE OF A SINGLE-EVENT DEPOSIT OVERLYING THE UPPER FREEPORT COAL SEAM IN CENTRAL WESTERN PENNSYLVANIA

WILLIAM A. BRAGONIER, COAL GEOLOGIST, RETIRED

Abstract

The Toms Run Mine is a deep coal mine on the Upper Freeport coal seam operated by Rosebud Mining Company in southeastern Indiana County, Pennsylvania. A portion of the reserve area is overlain by *draw rock*, or rock in the immediate roof that falls as the coal is mined or soon after. The draw rock varies in thickness from nothing to over ten feet and the thickness has been mapped using available drill hole data and in-mine measurements. The draw rock is a clayey siltstone that typically has a churned, non-bedded appearance with a crude, color banding upward and contains numerous vitrainized plant fossils interpreted as logs and branches. Genetically, the argument is made herein that draw rock was emplaced catastrophically as a single depositional event. Paleontological and sedimentological evidence are provided to support the single-event hypothesis. The possibility of a more regional distribution of the draw rock, and, by extension, of the catastrophic single event, is also considered.

Introduction

The term *draw slate* or *draw rock* is a coal mining term that refers to an out-of-seam rock type which is usually a shale, coaly shale or bony shale in the immediate roof of a coal mine that falls either immediately or soon after the coal seam is mined. This is an undesirable type of roof rock since it becomes a contaminant in the run-of mine coal product and necessitates the need for coal beneficiation. The term commonly refers to rock less than two feet in thickness (McGraw-Hill, 2003) and the contact between coal and the overlying roof shale is often gradational.

Rosebud Mining Company's Toms Run Mine is a underground mine on the Upper Freeport coal seam located in Burrell Township, Indiana County Pennsylvania northeast of the town of Blairsville (Figure 1). The mine entrance is a drift off of the coal crop located on the northwest flank of the Chestnut Ridge anticline. The Upper Freeport coal averages approximately 50 inches in thickness over the reserve area. Most of the mining is slightly south and west of the mine entrance and extends down dip past the axis of the adjacent Latrobe Syncline, where the Upper Freeport coal acquires a cover of over 800 feet. Dips on the flank of the anticline exceed 10o but the coal is relatively flat on either side of the synclinal axis. Structural elevations within the mine range from 1160 feet to near 400 feet above mean sea level.

Figure 1 shows the final mine workings for the Tom's Run Mine. There is a large no-coal area west and slightly south of the mine defined by drill holes labeled *Flint Clay Area-No Coal*. The purple stippled area illustrates the extent of draw rock overlying the Upper Freeport coal in the Tom's Run reserve area. The area is largely defined by drill holes but also intersected by mine workings in several places.

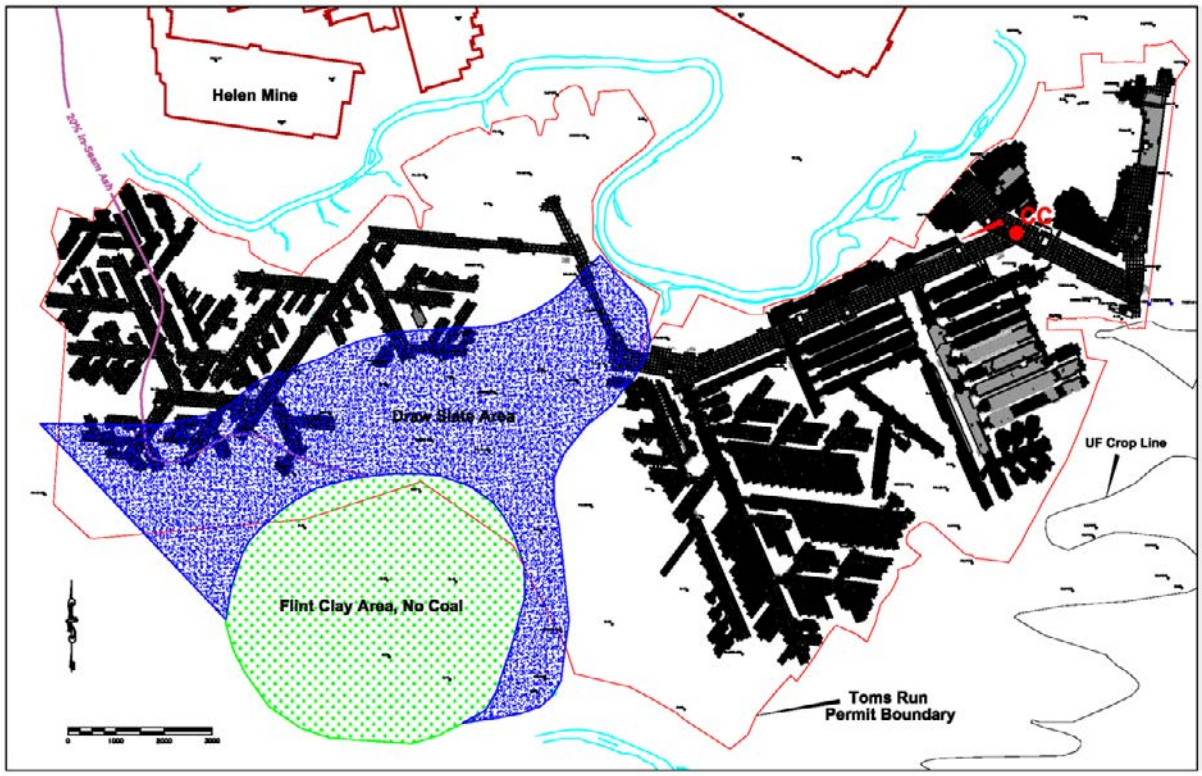

Figure 1. Map of Toms Run Mine showing the extent of the draw rock occurrence, the no coal (flint clay) area and areas of high (greater than 20%) in-seam ash.

Draw Rock Characteristics

Thickness Distribution

Figure 2 illustrates the thickness distribution in feet of the draw rock in the Tom's Run reserve area. The isopach map was constructed from drill hole data and in-mine thickness measurements. Several features are noteworthy. The distribution of the draw rock is geographically limited within the reserve area but thickens dramatically over short distances and achieves a maximum thickness of over 10 feet. Further, the draw rock thickness distribution appears center around the no-coal area south west of the Tom's Run reserve area.

Influence on Mining

The result of mining difficulties under the draw rock may be observed in the northeast corner of Figure 2. Note that the number of north-northwest trending mine headings under the draw rock has been reduced to three. The draw rock achieves a maximum thickness of over five feet above the mine workings as indicated on the isopach map. The heading reduction is due to the fact that the draw rock could not be supported and fell out immediately after the coal was mined and was consequently loaded with the coal. This area, designated as 'E Mains', was mined simply to provide an access to the coal on the northern side of the draw rock.

As noted above, draw rock is typically under a foot thick and commonly results from an upward gradational change from coal to shale. Figure 3 is a photograph taken in the eastern-most of the three headings in E Mains. The photo is facing northwest (i.e., inby). The contact between the coal and the overlying draw rock is obscured by rock dust but is visible on the right side of

the photograph about half way between the top and bottom of the entry. Note that the contact is ***not*** gradational, but a sharp line that separates the darker toned coal from the overlying lighter draw rock. The entry is approximately 18 feet wide and 10 feet high. The solid roof shale is shown at the top of the photograph and is supported with roof bolts.

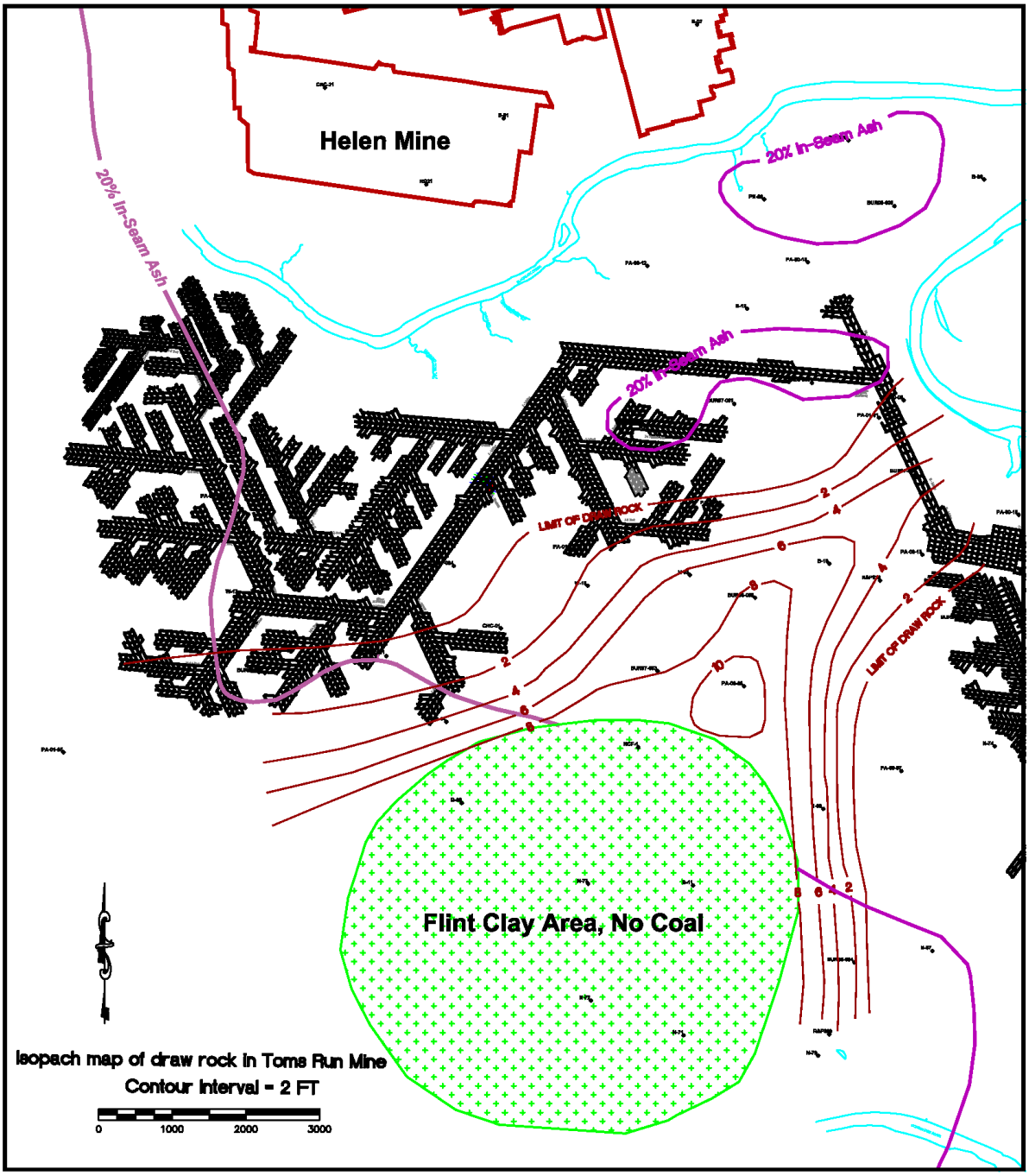

Figure 2. Isopach map of the draw rock overlying the Upper Freeport coal in the Toms Run reserve area. Thicknesses are in feet. Also shown are the no coal (flint clay) area and areas of high (greater than 20%) in-seam ash.

Lithology

Figure 4 shows the general texture of the draw rock in the Tom's Rum mine. In this image the draw rock is approximately 18 inches thick and can easily be distinguished from the underlying coal seam and the overlying roof shale. The striking difference between the roof shale and the draw rock is the bedding. While there is some semblance of bedding in the upper half of the draw rock, the lower half has a churned, non-bedded appearance. This stands in sharp contrast to the thin parallel laminae of the roof shale.

Figure 3. Image of the intake air heading in E Mains of the Toms Run Mine where over 5 feet of draw rock was mined. Rock dust obscures the deposit but the top of the coal is discernable just under half way up on the rib. The heading is approximately 18 feet wide and 10 feet high.

Figure 4. Image of draw rock showing vitrain streaks and numerous small slickensides. Compare the more chaotic texture of the draw rock with the laminae in the overlying Uffington shale. The distance between the blue and white tape on the hammer is 6 inches.

While not directly observable in Figure 4, the grain size of the draw rock is predominately silt but commonly intermixed with clay. The choppy appearance of the draw rock is in part due to slickensides indicative of the presence of clay. In Figure 5 the draw rock has a similar non-bedded appearance with obvious slickensides. Also, note the presence of dark fragments of plant material within the draw rock in both Figures 4 and 5.

Figure 5. Image of draw rock showing numerous slickensides and a chaotic texture. Note the difference in the texture of the draw rock with the laminae in the overlying Uffington shale. The distance between the blue and white tape on the hammer is 6 inches.

Figures 6 and 7 show another relevant aspect the draw rock. There is a crude color banding, most commonly restricted to the top half of the unit. Again, as in Figure 4 there is a distinct difference between the bedding in the draw rock and the finely laminated strata of the overlying roof shale visible at the very top of the image.

Figure 6. Image of draw rock showing vitrain streaks and a crude layering or color banding compared with the distinct laminations in the overlying roof shale. Note that the more defined layering in the draw rock is near the top of the deposit and is interpreted as an interference ripple effect of an initial strong wave pulse. The distance between the blue and white tape on the hammer is 6 inches.

Figure 7. Image of draw rock showing vitrain streaks, slickensides and a crude color layering as compared with the overlying roof shale at the top of the image. As in Figure 6, the more defined layering is in the upper half of the draw rock deposit, indicative of interference ripples after an initial strong wave pulse. The distance between the blue and white tape on the hammer is 6 inches.

Organic Content

Vitrified plant fragments, mostly parallel to sub-parallel with the bedding, may be seen in Figures 4 through 7. In many areas of the mine the vitrain fragments are not only more plentiful, but much larger than those in the above images. Figure 8 was taken in an area of the mine that is some distance from the working face where the rock has had time to 'weather.' Chemical weathering of the draw slate has produced yellow sulfur oxides that define vitrain fragments within the deposit, the obvious source of the sulfur. The vitrain fragments are interpreted to be tree branches and logs. In Figure 8 the organic fragments are sub-horizontal and generally follow bedding planes that are themselves sub-horizontal, but as shown in Figure 9, the plant material can occur at high angles to bedding.

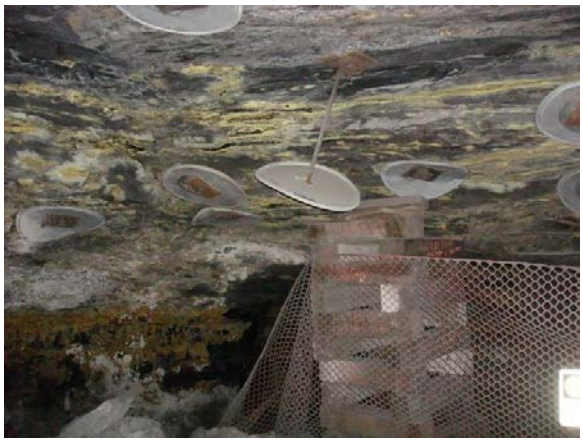

Figure 8. Exposure of draw rock in an outby heading of the Toms Run Mine where yellow sulfur oxides define vitrain within the deposit. The vitrain is interpreted to be flattened logs and/or branches. The circular roof bolt plates are 18 inches in diameter.

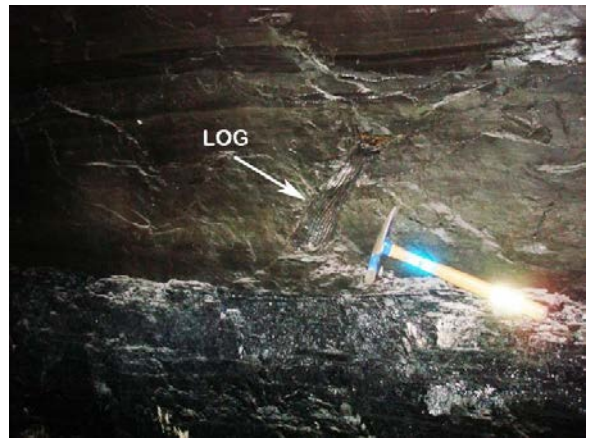

Figure 9. Exposure of draw rock showing a log deposited at a high angle to horizontal. As in Figures 6 and 7, note the crude color layering confined to the upper half of the draw rock deposit. The distance between the blue and white tape on the hammer is 6 inches.

In the center of Figure 10 there is an area of darker sediment that is completely surrounded by a layer of vitrain. This is interpreted as a compacted log that was partially filled with sediment and deposited within the draw rock. Several of these were noted in Toms Run mine and they demonstrate that plant material of considerable size exists within the draw rock.

Additionally, plant material of considerable size exists in the immediate roof of the Toms Run Mine, *but only in areas directly under or immediately adjacent to the draw rock*. Figures 11 through 14 illustrate not only the immense size of these logs, but their multi-directional distribution within the immediate roof.

Figure 10. Exposure of draw rock showing a dark area near the center of the image surrounded by vitrain. This is interpreted as a partially flattened log in cross section. Note that the sediment inside the log is darker than the surrounding sediment, indicating that it was partially filled with sediment and then transported. Also note the rock fragment near the top of the image. The distance between the blue and white tape on the hammer is 6 inches.

Figure 11. A large Sigillaria tree traverses the entire intake air entry in the Toms Run Mine. The entry is approximately 20 feet wide. Large tree fossils only occur directly over or near the peripheral edges of the draw rock. They are not present where the Uffington shale lies directly on the coal. The roof bolt plate is 6 inches square.

Figure 12. Flattened and randomly oriented fossil logs in the roof of Toms Run Mine. These logs occur only directly over or near the peripheral edges of the draw rock. They are not present where the Uffington shale lies directly on the coal. The roof bolt plate is 6 inches square.

Arguments for a Single-Event Deposit

Paleontological

A single event deposit with respect to the draw rock refers to the subaqueous deposition of a stratigraphic unit involving a high-energy flow regime triggered by a catastrophic event. The time of deposition would, in all probability, be measured in hours. The cause of such an event is unknown, but breaching of a natural dam, a storm or a tsunami are considered possibilities.

Figure 13. Flattened and randomly oriented fossil logs in the roof of Toms Run Mine. These logs occur only directly over or near the peripheral edges of the draw rock. They are not present where the Uffington shale lies directly on the coal. The roof bolt plate is 6 inches square.

The cross-sectional view of an entire compressed tree trunk in Figure 10 is arguably the most revealing testament to a single event deposit. Note that the sediment inside the compressed tree is darker than the surrounding sediment, indicating that the sediment inside the log existed prior to its deposition. The weight of a large tree partially filled with sediment would require a substantial amount of energy to transport. This is in stark contrast to the large trees shown in Figures 11 through 14 in the roof of the mine above the draw rock. With the possible exception of the large lycopsid in Figure 11, all of the logs in the roof images are, in taphonomic terms, transported compression assemblages, which contain a very minimal amount of sediment within the logs themselves. Furthermore, these logs have random orientations with respect to each other. There are two possible explanations for this. The trees could simply have died at different times and fallen over in different directions or they could have been washed in *en masse* and deposited as a logjam. The latter explanation is preferred since these trees only occur directly over or near the peripheral edges of the draw rock. It is

In genetic terms the thickness distribution, lithologic characteristics and organic content of the draw rock are all interpreted as indicative of a single event deposit. The nature of the organic content is the most striking manifestation of this explanation. As shown in Figure 8 a majority of the organic matter is fragments of vitrain ranging in size from six inches to two feet. These are interpreted as remnants of branches and/or tree trunk material and their abundance and size is indicative of a higher energy flow regime. Furthermore, while most of this plant material has been deposited sub horizontally, Figure 9 illustrates that a small percentage exists at high angles to bedding. Assuming compactional effects would reduce the angle of primary deposition, it may be argued that the original deposit contained plant material rather chaotically amassed.

Figure 14. Large flattened Sigillaria tree in the roof of Toms Run Mine. Large tree fossils only occur directly over or near the peripheral edges of the draw rock. They are not present where the Uffington shale lies directly on the coal. The round roof bolt plate is 18 inches in diameter.

suggested that sediment-laden logs were heavier and deposited within the draw rock while others simply floated and were deposited on top of the draw rock sediment only after floodwaters receded.

Sedimentological

The lithologic components described above are also suggestive of a single event deposit. Figures 4 and 5 illustrate the more jumbled, chaotic texture often seen in the draw rock, commonly highlighted by numerous small-scale slickensides. The distinction between the finely laminated roof shale and the more diffuse color banding of the draw rock has been noted (See Figures 5, 6 and 7). Note that the banding in Figures 6 and 7 is restricted to the upper half of the draw rock, which is typical of the deposit in general. Whereas, the genesis of the draw rock is being interpreted herein as a "single-event" deposit, a "single" onrush of sediment-laden water will produce "multiple" refraction waves within the area of deposition. The crude color banding observed in many exposures within the Tom's Run Mine, mostly restricted to, or at least more pronounced, in the upper portion of the deposit, is therefore interpreted as deposition from multiple refraction waves. Notice that within a single color-banded layer the color is darkest on the bottom and lightens up, which is also an indication of fining upward, as would be expected.

Finally, the areal distribution of the draw rock strongly suggests rapid deposition. Figure 2 defines the geometry of the draw rock over the Tom's Run reserve area. Several aspects of the distribution are noteworthy. First, the deposit is aerially restricted. Additionally, there is a thickness variation from zero to 10 feet and back to zero over a relatively short distance and the deposit exhibits a lineal geometry.

Note that the thickest draw rock is adjacent to the no coal area that is composed of flint clay. This requires a brief discussion of the genetic relationship between coal and flint clay. Upper Allegheny coals commonly grade into brecciated flint clays. Bragonier (1989) suggests that flint clays in close proximity to a coal seam form as a result of the swamp deepening into a shallow lake. The chemistry of the waters within lakes associated with Upper Allegheny coal seams would likely have a pH of neutral to alkaline since fresh water limestones commonly occur immediately beneath the underclays of these coal seams (and laterally adjacent lithologies). However, the pH near the peripheral margins of these lakes would likely be altered due to the presence of acidic swamp waters. The effect of organic acids on the flocculation of clay particles is well documented. [Hopkins (1898), Stout et. al., (1923), Hodson (1927), Schofield and Sampson (1954), Falla (1967), Keller (1968), Chukhrov (1970), Staub and Cohen (1978), and Keller (1981).] Consequently, as peat accumulates, flocculated flint clay correspondingly amasses along the lake margins and roughly approximates the thickness of the peat. However, the compaction ratio of peat is much greater than that of clay and numerous drill holes have demonstrated a much thicker flint clay section in close proximity to mineable upper Allegheny coals. (Bragonier, 1989).

Returning to the discussion of the draw rock distribution, it is quite conceivable that the Upper Freeport peat was either partially compacted prior to deposition of the draw rock (i.e., under its own weight) or was, in fact, compacted by the draw rock. This would result in the relatively uncompacted flint clay creating a topographic high that would act as a barrier to an onrushing torrent of sediment and logs, thus explaining the exceptional draw rock thickness juxtaposed to the flint clay.

Further evidence of high regime flow may be observed in an outby area of the Toms Run Mine. Figure 15 is an image of a current crescent located in sandstone roof at point CC on Figure 1. Current crescents are horseshoe shaped features formed as a current passes around a standing obstacle and causes sediment accumulations (in this case, sand) on the up-current side of the obstacle and on the both sides of the obstacle appearing as two wings formed by the stream flow deflected around the obstacle (Pye and Tsoar, 1990). As such, they are important current direction indicators. Although there are no apparent remains of the obstacle, vegetation is a likely candidate. (Rygel et. al., 2004). What is significant about the current crescent shown in Figure 15 is its immense size. Most current crescents are on the order of one or two feet. The mine post pictured in Figure 15 is over four feet in height (note hammer in lower right corner of image for scale). The long axis of the current crescent is approximately eleven feet. It is interpreted herein that the deposition of such a large feature must require an exceptionally strong current flow. The direction of the current flow is southwest at approximately the same angle as the main headings of the Toms Run Mine southwest of point CC (Note arrow direction on Figure 2). The southwesterly direction roughly aligns with the depositional strike of the draw rock shown in Figure 2, a feature not considered coincidental.

Figure 15. Exposure of a large horseshoe-shaped sandstone deposit in the roof of the Toms Run Mine. The sandstone is thickest near the apex of the bend and thins to nothing on both sides of the horseshoe. The deposit is interpreted to be a large current crescent created as sand was deposited around a stationary object such as a large tree. The current moved from right to left in the image. What is significant about the deposit is its size. The mine post is over 4 feet in height. Note hammer for scale. The size of the current crescent is interpreted as an indication of high-regime flow.

Regional Setting

Figure 16 illustrates some of the regional features associated with the Upper Freeport coal in central western Pennsylvania. Of particular interest is the northwest trending split seam area outlined in blue that traverses an area from northern Westmoreland County, through Indiana and Armstrong Counties and into eastern Butler County. The blue lines roughly define the 20% in-seam ash isopleth of the Upper Freeport coal. Within this area the coal obtains multiple "splits" or shale partings. In fact, some drill holes near the center of this area contain mostly shale with coal streaks and very little coal. This high ash zone is modified from Clark (1979).

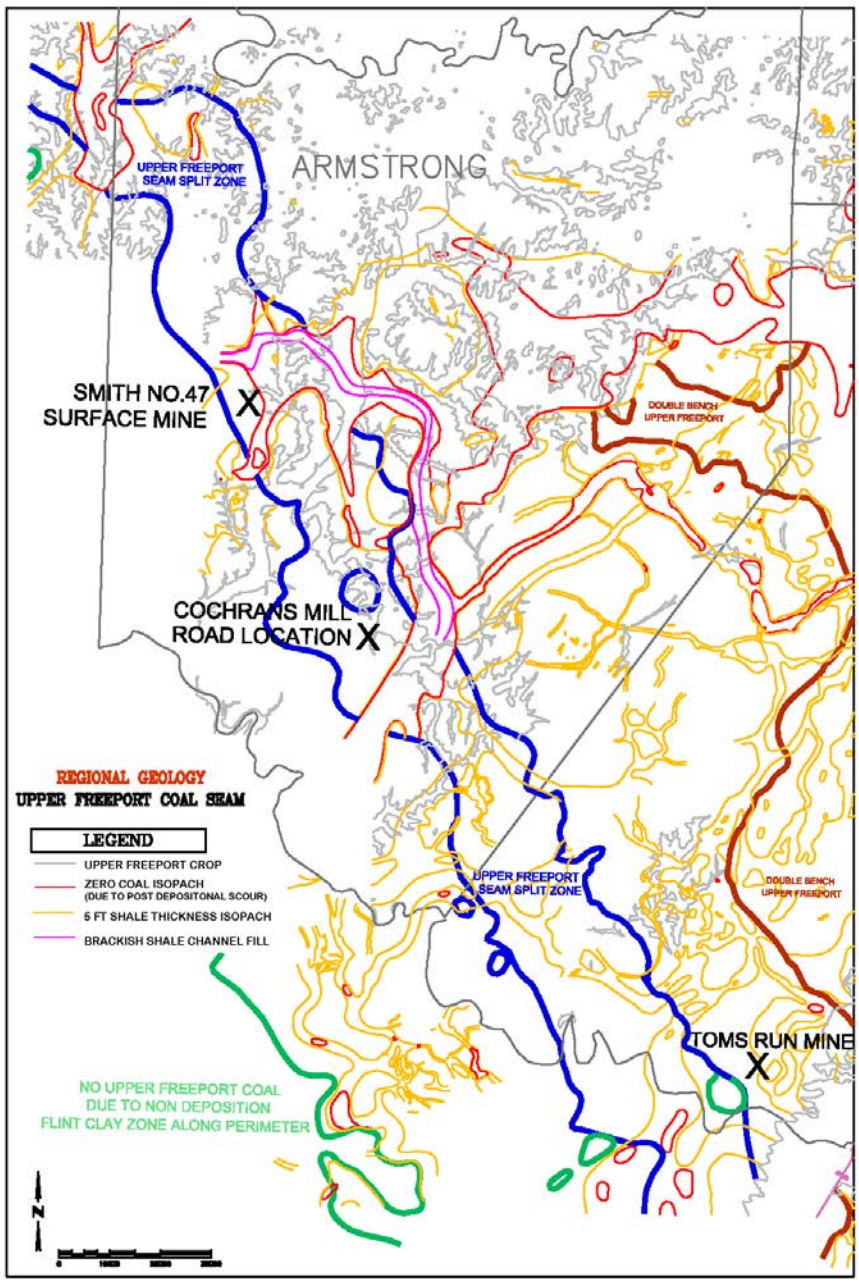

Figure 16. Map illustrating the paleogeography of the Upper Freeport seam split zone in a portion of central western Pennsylvania. The blue lines, which are modified from Clark (1979), roughly correspond to the 20% in-seam ash isopleth.

Between the lines the Upper Freeport coal contains numerous shale partings.

Also shown are the locations of the Toms Run Mine, the Cochrans Mill Road Upper Freeport exposure and the Smith No. 47 Surface Mine.

Figure 17 shows an exposure of the Upper Freeport high wall in the Smith No. 47 surface mine. As may be seen on Figure 16, the Smith No. 47 mine lies within the northwest striking in-seam split zone. The Upper Freeport in this area is near the perimeter of the high ash split zone, but numerous in-seam shale partings are visible in Figure 17. Also note in Figure 17 approximately one foot of soft clayey draw rock immediately above the coal. This lithology is strikingly similar to the draw rock in the Toms Run Mine. These two mines are roughly 30 miles from each other and the presence of draw rock in both prompted speculation that the single event deposit in Toms Run may be a more regional event somehow associated with the Upper Freeport split seam zone.

Figure 17. Exposure of the Upper Freeport coal at the Smith No. 47 surface mine in western Armstrong County approximately 30 miles northwest of the Toms Run Mine. The upper Freeport coal is within the in-seam split zone shown in Figure 16 and numerous shale partings are visible within the seam. Overlying the Upper Freeport coal is approximately 1 foot of a soft clayey draw rock that appears very similar to the draw rock in the Toms Run Mine.

This speculation was further encouraged by the presence of 47 inches of black and dark gray shale with plant fossils overlying the Upper Freeport coal at a natural exposure and road cut near the Cochrans Mill /Polka Hollow Road area in south central Armstrong County (location shown on Figure 16). Note that the latter location is more centrally located within the split seam zone.

There are numerous drill holes located within and adjacent to the Upper Freeport split zone and an attempt was made to develop an isopach map of the draw rock along the strike of the split zone. For various reasons the attempt was problematic. Many of the drill hole logs did not record the presence of coal streaks or plant fossils above the Upper Freeport seam even though they may have existed. Holes where a definite draw rock thickness could be determined were too few

to develop a consistent trend. In the central split seam zone many drill holes recorded sporadic thin coals rendering a clear definition of seam limits impossible. Post-depositional scouring of part or all of the seam added a further complication.

The attempt to develop an isopach map of the draw rock within and adjacent to the Upper Freeport seam split zone did yield several important generalizations including the following:

- There are numerous data points within the seam split zone that contain a lithology similar to draw rock overlying the split Upper Freeport seam.
- The thickness of the draw rock within the split zone increases toward the center.
- There is very little or no draw rock above the Upper Freeport coal adjacent to the split zone.
- The thickness of the draw rock decreases from southeast to northwest along the strike of the split zone.
- The width of the split zone thins substantially into Butler County (i.e. to the northwest).

The above observations suggest the Toms Run Mine draw rock has a more regional extent that is related to the northwest-striking seam split zone. However, based on the available data, which includes drill holes, deep mine observations and surface exposures, conclusions regarding depositional trends are difficult, if not contradictory. The large current crescent in Toms Run Mine and the thickest draw rock occurrence adjacent to and northeast of the no-coal flint clay area strongly suggest a flow direction from northeast to southwest. However the decreasing thickness of the draw rock in the Upper Freeport seam split zone from southeast to northwest suggests a southeastern source.

The exposures at the Cochrans Mill/Polka Hollow Road area in south central Armstrong County are also conflicting. Here a substantial thickness of draw rock (47 inches) overlies a split coal seam. In the streambed of an unnamed tributary of Crooked Creek that parallels Polka Hollow Road, hundreds of haphazardly oriented fossilized tree trunks are exposed that strongly resemble those in Figures 13 and 14. Genetically, there are two taphonomic mechanisms that will produce this configuration. One is the autochthonous model of water stressed conditions (including drowned, sub-aerially exposed, salinity variations and/or sediment influx); the "clastic swamp" of Gastaldo (1986, 1987). The other, the allochthonous model, assumes catastrophic deposition (i.e., a log jam). An argument for the latter has been made with respect to the Toms Run Mine draw rock and would seem, by extension, to apply to the draw rock at the Cochrans Mill/Polka Hollow site. However, there is a problem. The fossil rich partings within the split Upper Freeport seam are no different in appearance than the draw rock above the seam, yet they are intercalated with bands of apparently in-situ coal. The band thicknesses vary but generally increase toward the bottom of the seam. Within the split Upper Freeport seam, then, it may either be assumed there were multiple allochthonous events that interrupted a stable peat forming environment or a peat-forming swamp was intermittently subjected to water stressed conditions, resulting in multiple "clastic swamp" conditions. This amounts to a conundrum. Multiple layers of banded coal suggests the latter option seems more reasonable, that is, there were not multiple catastrophic events. However, the similarity of the draw rock in the Toms Run Mine, the Cochrans Mill/Polka Hollow exposure and the Smith 47 surface mine cannot be

summarily dismissed. In an established drainage channel, raging torrents are intermittently possible.

Conclusions

Evidence has been presented to demonstrate that the draw rock overlying part of the Toms Run Mine reserve area was deposited as the result of a single catastrophic event. Both sedimentological and paleontological features of the deposit suggest rapid deposition.

Site specific paleontological evidence includes:

- Abundant remnants of branches and/or tree trunk material scattered throughout the deposit (Figure 8). While most of this plant material is oriented sub horizontally, a small percentage exists at high angles to bedding.
- The cross-sectional view of an entire compressed tree trunk partially filled with dark sediment surrounded by lighter colored draw rock (Figure 10) indicating the log had to be transported.
- The existence of large, randomly oriented tree trunks in the roof rock overlying the draw rock deposit interpreted as a floating log jam that constituted the final depositional facet of the catastrophic event. These logs are restricted to areas in the mine roof either directly over or near the peripheral edges of the draw rock.

Site specific sedimentological evidence includes:

- The deposit is aerially restricted. There is a thickness variation from zero to ten feet and back to zero over a relatively short distance and the deposit exhibits a lineal geometry.
- A churned, chaotic texture of the draw rock highlighted by numerous small scale slickensides
- Color banding largely restricted to the upper half of the deposit interpreted as a result of diffraction waves created by an initial catastrophic deluge.
- The existence of a large-scale current crescent (indicative of high-regime flow) in an outby section of the Toms Run Mine, the current direction of which matches the lineal geometry of the draw rock deposit.

The presence of draw rock above the Upper Freeport coal seam in a surface mine approximately 30 miles northwest of the Toms Run Mine prompted the investigation of the possibility of a more regional extent of a single event deposit. From drill hole records within and adjacent to a previously identified northwest trending split seam zone in the Upper Freeport coal, it was determined that draw rock was, indeed, associated with the split seam zone. However, a definitive isopach map of the draw rock within the seam split zone was not possible to generate. Furthermore, conclusions regarding draw rock depositional trends were contradictory. A surface outcrop of the Upper Freeport coal within the split seam zone in south central Armstrong County revealed further contradictions. The draw rock exhibits all of the features of a transported compression assemblage, but similar exposed lithologies within the split Upper Freeport coal are intercalated with apparently in-situ layers of coal. Consequently, the distinction between allochthonous and autochthonous compression assemblages becomes problematic.

Acknowledgements

The author would like to express his appreciation to various personnel of the Rosebud Mining Company. Clifford Forrest, president of Rosebud Mining has generously consented to allow publication of this article. Ken Fletcher, mine foreman at the Toms Run Mine, and Jeff Gabster, mine clerk, provided valuable information regarding exposures of the draw rock as well as escorts into Toms Run Mine on several occasions. Craig Rinaman, Braden Hankey and Rob Higbee, Rosebud geologists, enthusiastically aided the author by providing drill hole data and digital mapping. The author would also like to thank William A. DiMichele of the Smithsonian Institution for his many suggestions regarding the context of the article.

References

Bragonier, W.B., 1989, Stratigraphy of flint clays of the Allegheny and Pottsville Groups, western Pennsylvania, *in*: Harper, J.A. ed., Geology of the Laurel Highlands of Southwestern Pennsylvania: Annual Field Conference of Pennsylvania Geologists, 54th, Johnstown, Pa., Guidebook, p. 69-88.

Chukhrov, F.V., 1970, Analogues of flint clay in Soviet literature: Clays and Clay Minerals, v. 18, p. 1-5.

Clark, W.J., 1979, An interfluve model for the Upper Freeport bed in part of western Pennsylvania: Columbia, SC, University of South Carolina, M.S. thesis, p. 54.

Falla, W.S., 1967, The petrology and geochemistry of the Clarion flint clay, western Pennsylvania: University Park, Pa., Pennsylvania State University, HS thesis, p. 84.

Gastaldo, R.A., 1986, Implications on the Paleoecology of Autochthonous Lycopods in Clastic Sedimentary Environments of the Early Pennsylvanian of Alabama: Paleogeography, Paleoclimatology and Paleoecology, v. 53, no. 2-4, p. 191-212.

Gastaldo, R.A., 1987, Confirmation of Carboniferous Clastic Swamp Communities: Nature, International Weekly Journal of Science, v. 326, p. 869-871.

Hodson, F., 1927, The origin of bedded Pennsylvanian fire clays in the United States: Journal of the American Ceramic Society, v. 10, p. 721-746.

Hopkins, T. C., 1898, Clays and clay mineral industries of Pennsylvania, Part I. Clays of western Pennsylvania: Appendix to the Annual Report of the Pennsylvania State College for 1897, p. 48-54.

Keller, W.D., 1968, Flint clays and a flint clay facies: Clays and Clay Minerals, v. 16, p. 113-128.

Keller, W.D., 1981, The sedimentology of flint clay: Journal of Sedimentary Petrology, v. 51, p. 233-244.

McGraw-Hill Dictionary of Scientific & Technical Terms, 6E, Copyright © 2003 by The McGraw-Hill Companies, Inc.

Pye, K. and Tsoar, H, 1990, Aeolian sand and sand dunes: London, Unwin Hyman, 416 p.

Rygel, M.C., Gibling, B.C. and Calder, J.H., 2004, Vegetation-induced sedimentary structures from fossil forests in the Pennsylvanian, Joggins Formation, Nova Scotia: Sedimentology, v. 51, p. 531-552.

Schofield, R. D., and Sampson, H. R., 1954, Flocculation of kaolinite due to attraction of oppositely charged crystal faces: Discussions of the Faraday Society, no. 18, p. 135-145.

Staub, J. R., and Cohen, A. D., 1978, Kaolinite-enrichment beneath coals; a modern analog, Snuggedy Swamp, South Carolina: Journal of Sedimentary Petrology, v. 48, p. 230-210.

Stout, W., Stull, R.T., McCaughey, W.J. and Demorest, D.J., 1923, Coal Formation Clays of Ohio: Geological Society of Ohio, ser.4 Bulletin 26, p. 109-150, 533-568.

STRATIGRAPHY OF FLINT CLAYS OF THE ALLEGHENY AND POTTSVILLE GROUPS, WESTERN PENNSYLVANIA

WILLIAM A. BRAGONIER, ROCHESTER & PITTSBURGH COAL COMPANY

Introduction

Keller (1968, p. 113) defined flint clay as a dominantly kaolinitic underclay that breaks with a conchoidal fracture and resists slaking in water. Flint clays occur between, or are associated with, most coal horizons of the Allegheny and Pottsville Groups of western Pennsylvania. An understanding of the coal-flint clay relationship is important to the prediction of clay occurrence, and also to coal stratigraphy.

Flint clays are physically, mineralogically, and chemically intermediate between plastic clays and high alumina nodule clays. They are commonly of local extent, brecciated, multicolored, hard and contain an abundance of well-crystallized kaolinite. Considerable attention has been devoted to an understanding of the origin of flint clays and the subject has not been without controversy. Late nineteenth and early twentieth century investigators into the origin of various types of Carboniferous clays rapidly found themselves polarized over the question of a residual versus a transported origin. The evolutionary outcome of this controversy, with respect to flint clay, involves the role of differential colloidal flocculation versus the processes of in situ residual leaching. Pottsville and Allegheny flint clays exhibit evidence of both petrogenetic mechanisms.

The purpose here is to describe the physical characteristics, stratigraphic relationships and origin of flint clays in the Allegheny and Pottsville groups of western Pennsylvania. A discussion of the relationship between flint clays and other lower Pennsylvanian clay types is necessarily included.

Physical Properties

The definitive megascopic properties necessary for flint clays are conchoidal fracture and a resistance to slaking. Another common characteristic is hardness (3 to 5 on Mohs hardness scale) the degree of which is broadly attributed to the amount of kaolinitic recrystallization (Patterson and Hosterman, 1960).

Flint clays occur in a great variety of colors including medium to dark gray (rarely black), light greenish gray to olive to green, tan to dark brown to red. Individual deposits are usually varicolored, although one color often predominates. Lower Allegheny and Pottsville clays are neutral to dark gray or brownish gray whereas Upper Allegheny clays are typically, tan, olive, greenish-gray and, rarely, red.

Ferm and Smith (1981) after examination of several hundred core samples, have subdivided flint clays into four categories based on physical appearance: massive, layered, brecciated and mosaic (see discussion, Figure 1). Oolitic flint clays occur in some Allegheny and Pottsville core samples. Patterson and Hosterman (1960, p. 186) note that “oolites are very abundant in some flint clay but they are not present at all in others." Similarly, some flint clays are root penetrated

and contain broken plant fragments whereas others are devoid of fossils. Slickensides are extremely rare in flint clay.

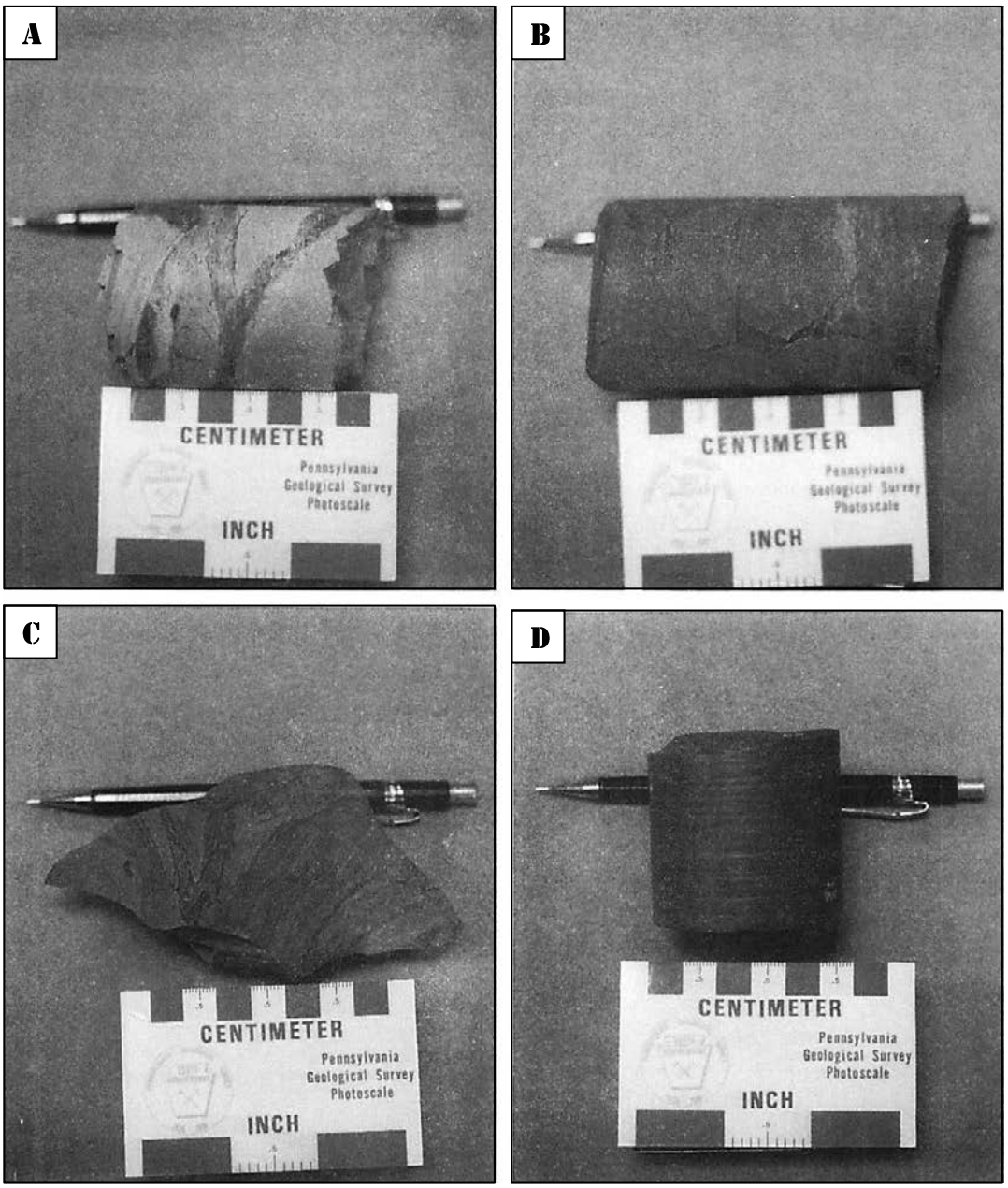

Figure 1. Photographs of various flint clays. (A) Brecciated semi-flint clay (Upper Freeport, Westmoreland Co.) composed of angular clay fragments in a sandy or silty matrix; volumetrically, this type of clay is disproportionately abundant. (B) Mosaic flint clay (Upper Freeport, Indiana Co.). "Mosaic" refers to a type of brecciation where the individual clay fragments may be seen to fit together if the matrix were removed. (C) Layered flint clay (Lower Mercer, Centre Co.) Less common; usually occurs as color laminations in brecciated fragments. Fracture is independent of layering. (D) Massive flint clay (Lower Mercer, Clearfield Co.). Also occurs as brecciated fragments, but may be represented as continuous lengths of core.

Definitions and Nomenclature

Flint clays are middle members of a physical, mineralogical, and chemical continuum ranging from illitic-rich plastic clays to aluminum-rich (boehmite, diaspore) nodule clays. Table 1 contains a summary of three generally recognized groups of clays.

Table 1. Properties of the Flint Clay Facies (from Smyth, 1980)

Data compiled from Patterson and Hosterman (1960, p. F52-F58), Keller (1968, p. 113-115), Keller (1976, p. 262), Keller (1978a, p. 15, 19), Keller (1978b, p. 239, 241), and Keller (1982, p. 150-151).

CHARACTERISTICS	CLAY TYPE		
	FLINT	SEMI-FLINT	PLASTIC
FRACTURE	Conchoidal	Rough, irregular approaching conchoidal	Rough, irregular
HARDNESS	3	2-3	Softer than semi-flint
GENERAL CLAY MINERALOGY	85% kaolinite 15% illite+ mixed layer clays	60-85% kaolinite	60% kaolinite 40% illite+ mixed layer clays
NATURAL PLASTICITY	Almost no plasticity unless very finely ground with water	Little plasticity unless finely ground with water	Considerable plasticity when wet
SLAKING CHARACTERISTICS	Resistant to slaking	Intermediate between flint and plastic clays	Breaks down rapidly into small particles in water
SLICKENSIDES	Very few	Abundant Diversely oriented	Abundant Becoming sealed upon weathering and clay becomes homogeneous in appearance
S.E.M. CHARACTERISTICS	Kaolinite plates or flakes can be seen to be well-developed, interlocking, inter-grown, dense and randomly oriented	Shows some swirl pattern composed of overlapping curved kaolinite flakes. Flakes are less curved than in plastic clays	Shows platy, anhedral bent, and twisted flakes with a swirl pattern

Plastic clays are characterized by a soft, plastic or shaly texture, are often internally slickensided, may be silty or sandy, and break down when mixed with water. Much of the nomenclature for plastic clays has evolved through common usage. To clarify the inherent ambiguity Table 2 (definitions) is included.

Table 2. Definitions of plastic and related clay types

CLAY TYPE	DEFINITION
Underclay	A layer of fine-grained detrital material, usually clay, lying immediately beneath a coal bed or forming the floor of a coal seam. It represents the old soil in which the plants (from which the coal was formed) were rooted and it commonly contains fossils of roots (esp. of the genus *Stigmaria*) (AGI Glossary, p. 676).
Seat Rock or Seat Earth	A British term for a bed of rock underlying a coal seam representing an old soil that supported the vegetation from which the coal was formed (AGI Glossary, p. 564).
Fireclay	1) A siliceous clay rich in hydrous aluminum silicates capable of withstanding high temperatures without deforming (either disintegrating or becoming soft and pasty), and useful to the manufacture of refractory ceramic products (such as crucibles or firebrick for lining furnaces). It is deficient in iron, calcium and alkalis, and approaches kaolin in composition, the better grades containing at least 35% alumina when fired (AGI Glossary, p. 230). 2) A clay that resists fusion or heat deformation below the arbitrarily defined pyrometric cone equivalent* 28 – customarily written PCE 28 (about 1615° C under specified conditions of heating). (Keller, 1975, p. 65-66). 3) A term formerly, but inaccurately, used for underclay. Although many fireclays commonly occur as underclays, not all fireclays carry a roof of coal and not all underclays are refractory (AGI Glossary, p. 230).
Ganister	In England, a highly siliceous seat earth (AGI Glossary, p. 252).
Tonstein	Originally meant an argillaceous rock, but has come to imply a number of additional characteristics including: association with coal seams, homogeneous mineral composition, usually kaolinite-rich, relatively thin (usually 2-3 inches), laterally persistent, and often considered a stratigraphic marker bed for correlation purposes (Moore, 1968, p. 108-109). Tonsteins are often of volcanic origin.

Underclays and seat earths commonly coarsen and lighten in color downward in the stratigraphic section. They are typically rooted, but despite the above definitions, it is often speculative as to whether the roots were from the plants that formed the overlying coal seam or from plants that pre-dated the coa1 seam.

Mineralogically, illite predominates in plastic clays, but subordinate amounts of kaolinite, mixed layer clay minerals and chlorite are common. Non-clay minerals, which can be abundant, are quartz, feldspar, mica, siderite, and calcite. Chemically, $Si0_2$ predominates (60 to 80 percent

by weight) and Al_20_3 comprises between 10 and 20 percent by weight. Minor oxides include K_20, MgO, Fe_20_3, Ti02 and CaO (Williams and others, 1968).

Semi-flint clays are a broad category of clays that contain properties intermediate between plastic and flint clays. Ideally, they are intermediate physically, mineralogically, and chemically. They are softer than flint clay (2 to 3 on Mohs hardness scale), possess a sub-conchoidal fracture, and are frequently slickensided. They may be strongly to weakly slaking or even non-slaking. The kaolinite range for semi-flint clay is between 60 and 85 percent (Smyth, 1980) with illite and mixed layer clay minerals comprising the bulk of the remainder. Chemically, semi-flint clays contain 35 to 37 percent Al_20_3 (Weitz, 1954). $Si0_2$ and the minor oxides present in plastic clays constitute the complementary chemical components.

The distinction between flint clay and higher grades of semi-flint clays can be problematic. The definition of flint clay incorporates both microscopic (percent kaolinite) and megascopic (conchoidal fracture and slaking) properties. Yet many clay types will satisfy only two of the three criteria for the definition of flint clay (and the term "sub-conchoidal" is ambiguous).

Table 3 shows chemical analyses and X-ray diffraction data of clays from the Allegheny and Pottsville Groups. All of these clays possess some degree of conchoidal fracture, and some are non-slaking, yet chemically they contain less $A1_20_3$ than Weitz's (1954) definition of semi-flint clay. Furthermore, Figure 39 illustrates X-ray diffraction data for four of twelve X-rayed samples of conchoidally fracturing clay from the Allegheny and Pottsville Groups. Note that the quartz (siderite in IND-D-3055) peaks are commonly more significant than the kaolinite peaks. Although these data are not directly quantitative, the implication is that there is a substantial quantity of quartz in rocks that are megascopically termed flint clays. Stricter definitions and/or nomenclatural expansion of the plastic/semi-flint/flint clay continuum appear to be warranted.

Hard clays are broadly subdivided into two categories; flint clays and nodule clays. Flint clays contain greater than 85 percent kaolinite and less than 15 percent illite and mixed layer clays (Smyth, 1980). Halloysite and chlorite may exist in minor amounts. Quartz, siderite, and feldspar are the most common non-clay minerals, although heavy minerals (tourmaline, rutile, and zircon) may occur in the form of sand size grains (Bragonier, 1970). Al_20_3 should be in the 38 to 40 percent-by-weight range (Weitz, 1954). The minor oxides occurring in plastic and semi-flint clays are also present in flint clay. Commercial quality flint clay must have a pyrometric cone equivalent (PCE) (see Table 2) of 32 (1700 °C in standard heating environment) or higher and a bulk density above 2, preferably 2.2 (Baumann and Keller, 1975).

Nodule clays are hard clays that contain rounded nodules of the aluminum hydroxide minerals boehmite ($HA10_2$) and diaspore (AlO OH). Nodule clays may contain only a few nodules in a kaolinite groundmass or be comprised almost entirely of aluminum hydroxide nodules. Gibbsite may be present in minor amounts. Nodule clays may be quite hard (greater than 5 on Mohs hardness scale) and contain up to 75 percent AL_20_3 by weight. In western Pennsylvania nodule clays are stratigraphically restr1cted to the Mercer horizon and geographically restricted to Clearfield, Centre, and Clinton Counties.

Table 3. Chemical analyses and x-ray diffraction results of flint and semi-flint clay samples from the Allegheny and Pottsville Groups of western Pennsylvania.

SAMPLE	CHEMICAL ANALYSES				X-RAY DIFFRACTION RESULTS		
	SiO_2	$Al2O_3$	FeO_2	PCE*	MAJOR MINERALS	CHARACTERISTIC PEAK	PEAK HEIGHT
Upper Freeport Westmoreland County	63.82	17.33	5.52	15-16			
Upper Freeport Westmoreland County	42.66	24.78	11.62	5			
Upper Freeport Westmoreland County	59.74	15.80	9.85	15			
Lower Freeport Westmoreland County	56.36	23.20	6.10	19	Quartz Kaolinite	4.26 Å 7.17 Å	65 24
Lower Freeport Westmoreland County	64.82	23.87	1.53	30			
Brookville Jefferson County	60.70	24.60	5.30	20-23			
Brookville Jefferson County	67.67	22.82	2.17	31.5-32	Quartz Kaolinite	4.26 Å 7.17 Å	45 50
Brookville Jefferson County	62.73	27.81	1.78	30-31			
Mercer Clearfield County	42.90	40.45	1.45	33			

*Pyrometric cone equivalent - a measure of the firing or melting temperature of the clay.

Lithologic names and descriptions used in the mining industry (Table 4) have been summarized by Foose (1944) and modified slightly by Weitz (1954). The descriptive terminology in Foose's classification is advantageous, but it is based on physical properties and has no petrographic significance. Weitz and Bolger (1951) advanced an alternative classification of fireclay types (Table 5). They used Foose's descriptions as their framework, but subdivided the high-alumina clay types on the basis of mineralogical composition. Erickson (1963) combined aspects of both previous classifications to produce a more systematic and moderately descriptive arrangement of fireclay types (Table 5).

The above classifications serve as workable instruments for the hard clay industry but all emphasize the more exotic but less common, nodule clay types. Furthermore, Weitz and Bolger (1951) and Erickson (1963) incorporate the problem of creating a field classification that is ultimately based on microscopic properties.

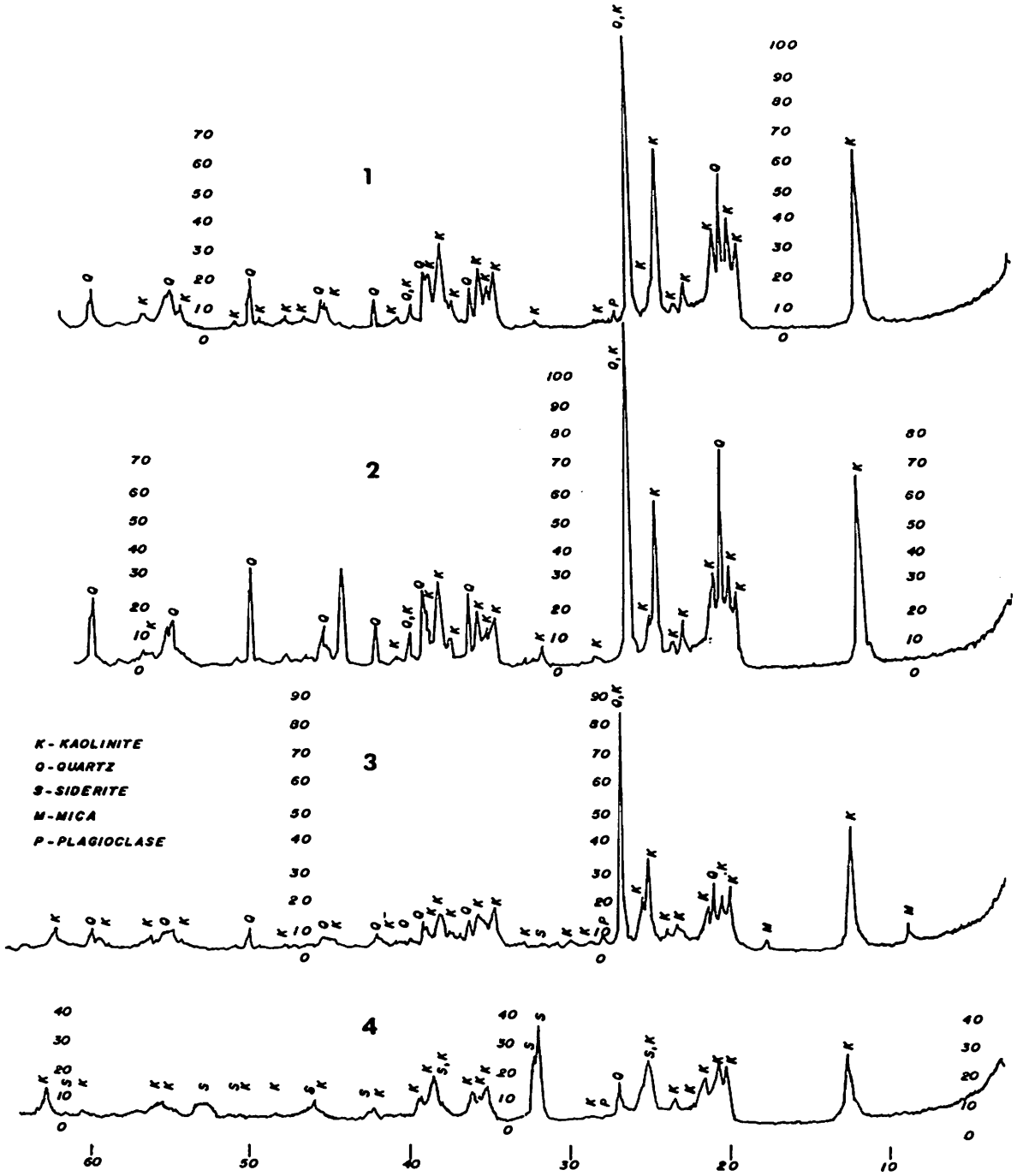

Figure 2. X-ray diffraction patterns of flint and semi-flint clays from the Allegheny and Pottsville groups of western Pennsylvania. (1) Lower Mercer, Centre Co. Hard, higher-grade flint clay. Note sharp, symmetrical and well-resolved nature of reflections. (2) Flint clay from Widman St. Exit, Johnstown, below Upper Kittanning coal. Well-resolved peaks indicate fairly high-grade flint clay, but quartz peaks more distinct than in (1). (3) Semi-flint clay from Lower Freeport horizon, drill hole in Conemaugh Twp., Indiana Co. Lower amounts of both kaolinite and quartz are present; peak heights and resolution not as well defined as in (1) and (2). Also note existence of mica, siderite, and plagioclase. (4) Siderite-rich semi-flint clay from above Upper Freeport coal, West Wheatfield Twp., Indiana Co. Note poor resolution.

Table 4. Nomenclature of fireclays as used in the mining industry
(from Weitz, 1954, modified from Foose, 1944)

CLAY TYPE	DESCRIPTION	APPROXIMATE % OF Al_2O_3
"Burnt" nodule clay	Gray to brown, porous, cindery appearance; usually nearly all diaspore; very rough fracture	65 – 75
Fine-grained (or blue) nodule clay	Homogeneous appearance; smaller nodules and harder than green nodule clay	60 – 65
Green nodule clay	Coarsely nodular; rough fracture; usually greenish cast	50 – 60
Nodule block clay	Gradational between green nodule and block clay; scattered nodules comprise less than half of the mass; rough, blocky fracture	40 – 50
Nodule flint clay	Gradational between green nodule and flint clay; scattered nodules comprise less than half of the mass; rough, conchoidal fracture	40 – 50
Flint clay	Very hard; smooth, conchoidal fracture with sharp edges and points; weathers into smaller jagged fragments; usually clear light or dark gray, but may contain dark spots or widely scattered nodules	38 – 40
Block clay	Hard; blocky fracture; weathers to rounder granules than flint clay; usually clear, light or dark gray, but may contain dark spots and widely scattered nodules	38 – 40
Semi-Flint clay	Gradational from flint clay to soft plastic clay; rough, irregular fracture, approaching conchoidal Associated nonrefractory clays include:	35 – 37
Slabby soft clay	Fracture slabby and irregular; slickensides common	
Soft (plastic) clay	Soft; irregular fractures; plastic when wet	
Shaly clay	Bedding evident; shaly fracture	

Table 5. Classification of high-alumina rock types
(modified from Erickson, 1963)

Composition	Weitz and Bolger's Classification	Equivalent Miner's Term	Erickson's Classification
Over 90% aluminum hydroxides	Diasporite	"Burnt" Nodule	Diasporite
Over 50% aluminum hydroxides	Argillaceous Diasporite	Fine-grained Nodule	Argillaceous (over 50% nodules)
		Green Nodule	Diasporite
Over 50% kaolinite	Diaspore Claystone	Nodule Flint Clay	Nodule Claystone (25-50% nodules)
		Nodule Block Clay	Nodule Block Claystone
			Flinty Nodule (5-25% nodules)
			Claystone
			Nodular Flinty (5% nodules)
			Claystone
Apparently all kaolinite	Flinty Claystone	Flint Clay	Flinty Claystone
	Blocky Claystone	Block Clay	Blocky Claystone
	Shaly Claystone	Shaly Clay	Shaly Claystone
	Soft (plastic) Clay	Soft (plastic) Clay	Soft (plastic) Clay

Stratigraphic Relationships

Flint clays occur at nearly all stratigraphic horizons in the (post-Connoquenessing) Pottsville and Allegheny Groups of western Pennsylvania. Smith and O'Brien (1965) have also reported flint clays as young as late Pennsylvanian, indicating that they formed throughout much of the Pennsylvanian. Nevertheless, they are much less common above the lowermost Conemaugh. Williams and others (1968) have demonstrated that there is an overall up-section increase in the illite: kaolinite ratios of underclays from the Mercer to Upper Freeport (consistent with data presented in Table 2. Keller (1975) also confirms that higher quality refractory clays are stratigraphically confined to the lower part of the Pennsylvanian system in the eastern United States. The Mt. Savage clay of western Maryland, the Olive Hill clay of Kentucky, the Cheltenham clay of Missouri and the Mercer of central Pennsylvania are examples of high quality refractory

clays that temporally represent the Lower and Middle Pennsylvanian. Keller suggests that they characterized "a particular geologic environment that was widely prevalent in the eastern United States during early Pennsylvanian time" Keller, 1975, p. 65). The Cheltenham and Mercer are the only clay deposits in the United States that contain the high alumina Diaspore/Boehmite facies and both are believed to rest unconformably on Mississippian sediments (Keller, 1975).

Non-plastic clays of the middle and upper Allegheny range from semi-flint to flint clay. Although many possess characteristic conchoidal fracture and brecciation, they are slightly to strongly slaking and marginally kaolinitic. Nevertheless, some Upper Allegheny flint clays are of refractory quality (e.g., the Bolivar flint clay of southwestern Indiana County).

Flint clays in the Allegheny Group usually occur in association with other "chemical'' rocks, specifically limestone and coal. Thin layers of flint clay have been found interbedded with the freshwater limestones beneath the Upper and Lower Freeport and Upper Kittanning coals, but are more characteristically found immediately beneath these limestones (Buswell, 1980). Williams and others (1968) demonstrated that flint clays are laterally equivalent to the Vanport Limestone in portions of Clarion County, Pennsylvania.

Figure 3 illustrates that flint clay is commonly the lateral equivalent of both coal and limestone. Coal equivalent with flint clay has been documented by Sturgeon (1958) for the Pittsburgh seam, by T. Miller (personal communication) for the Mahoning seam, by Smith and O'Brien (1965), Pedlow (1977), Clark (1979), and Hohos (1979) for the Upper Freeport, by Buswell (1980) for the Upper Kittanning, by Merrill (1952) for the Middle Kittanning and by Williams and others (1968) for the Scrubgrass (Clarion No. 3).

Genesis

Introduction

Despite numerous geochemical and petrologic investigations of flint clays, controversy still exists concerning their origin. Smyth (1980) has summarized the existing published theories of the origin of flint clays and related clay types. Her overall subdivision of theories into allogenic, authigenic, and combined recognizes a fundamental problem of flint clay origin -were they formed in-situ or transported?

Williams and others (1968) have demonstrated that although the illite/kaolinite ratios of underclays within the Pottsville and Allegheny Groups increase stratigraphically upward, the same is not true for shales immediately overlying the respective coal seams. Their conclusion is that "the composition of the sediments received from unknown source areas did not change in the stratigraphic interval examined" (Williams and others, 1968, p. 75). Their conclusion necessarily implies clay mineral alteration within the environment of deposition. This evidence stands in opposition to the theories proposed by Lovejoy (1925) Grim and Allen (1938) Greaves-Walker (1939), Schultz (1958) and Wilson (1965), all of whom invoke an external source area.

Formation of flint clays within the environment of deposition may be accomplished either by differential colloidal flocculation controlled by the chemistry of the depositional environment (Bolger and Weitz, 1952; Falla, 1967; and Williams and others, 1968) or by in situ leaching (Halm, 1952; Keller, 1952; Slatkine and Heller, 1960; Patterson and Hosterman, 1960; Smith and O'Brien, 1965; Goldberry, 1979; and Keller, 1981).

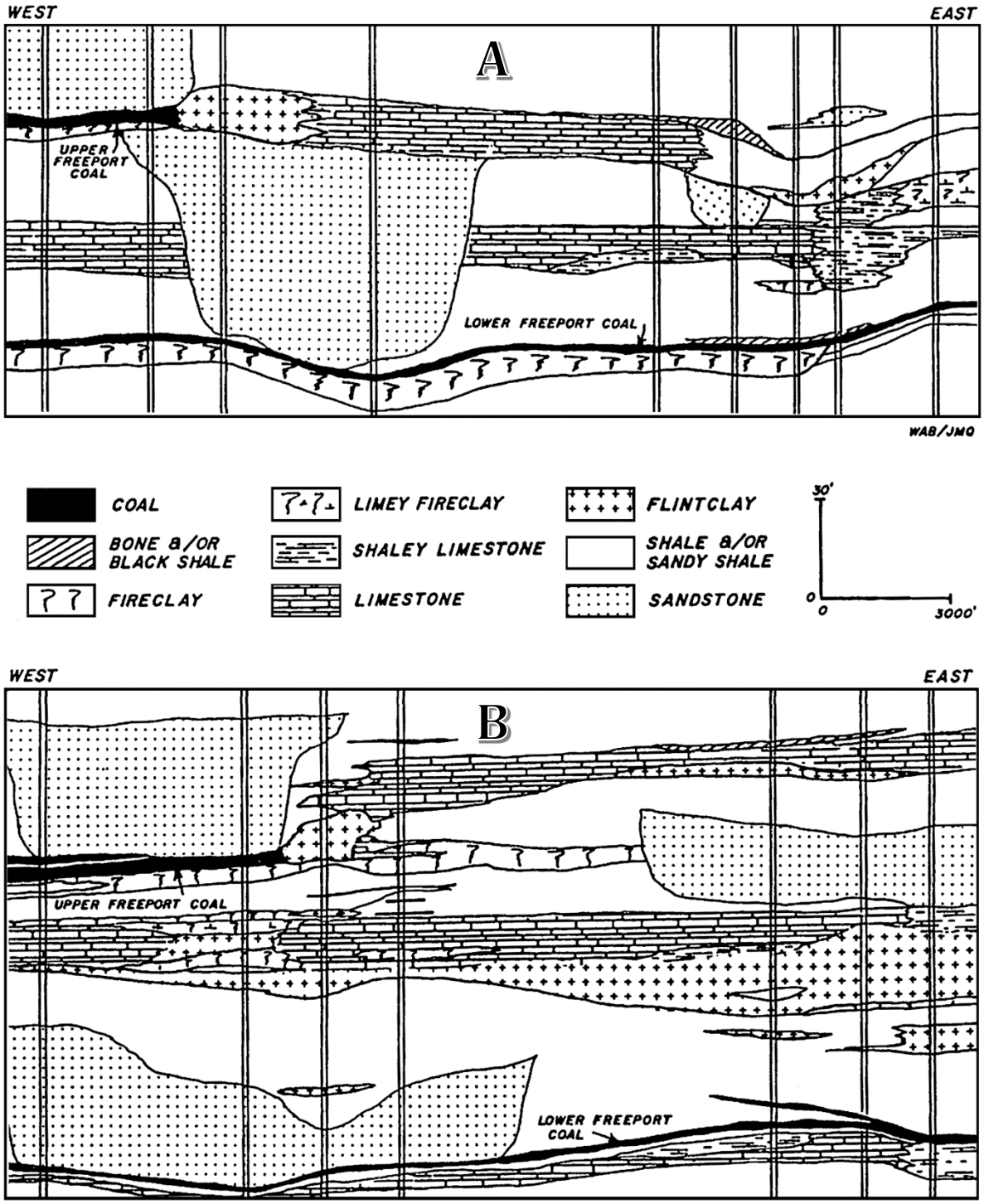

Figure 3. Cross-sections A (top) and B (bottom), showing lateral facies changes from coal to flint clay to fresh water limestone in the Upper Freeport horizon near Brush Valley, Indiana County. The datum is the top of the Upper Freeport limestone.

In-Situ Leaching

Keller (1981) provides one of the most complete accounts of in situ flint clay genesis. He interprets flint clay as a product of very early d1agenetic alteration of a parent alumina-silicate material. During a period of crustal stability in non-marine paludal/fluviatile environments, colloidal to fine-grained sediments accumulated in quieter, commonly plant-fringed, swamps. Removal of silica, iron, and alkaline and alkali earths presumably were the result of dialysis, hydrolysis, and the action of organic complexing compounds, organic acids, and silica accumulating plants. Keller (1968) suggests that acid swamp waters are the source of H^+ ions, which replace K^+ ions in illite, producing H-rich illite and kaolinite by structural rearrangement of the remaining silica and alumina. These processes could have been initiated in the fringing soil to produce colloidal kaolin. This, in turn, led to the formation of "a colloidal-chemical phase, possibly gel-like, having a composition essentially that of kaolin, from which the mineral kaolinite crystallized or crystallized into packets of inter-grown kaolinite crystals…" (Keller, 1981, p. 239). Other theories of in situ flint clay origin commonly incorporated the processes which Keller details, emphasizing various aspects for specific clay deposits.

Evidence which suggests in situ leaching is an important mechanism in flint clay genesis include the following:

Mineralogical: Vertical kaolinite enrichment within individual clay beds (both upward and downward kaolinite enrichment has been reported respectively by Smyth, 1980 and Keller, 1981).

Etching and complete dissolution of quartz grains (Patterson and Hosterman, 1960; Bragonier, 1970; Smyth, 1980).

Lack of feldspar (Patterson and Hosterman, 1960).

A change in kaolinite mineralogy from the outside of clay breccia fragments, where poorly crystalline kaolinite occurs in the cores of the breccia fragments surrounded by a well-crystallized kaolinite rim (Smith and O'Brien, 1965).

Kaolinite enrichment on paleotopographic highs (Holbrook and Williams, 1973).

Geochemical: Vertical alumina enrichment (Smyth, 1980; Keller, 1981).

Enrichment in titanium dioxide (Jaron, 1967; Williams and others, 1968).

Lack of Fe203 in the upper portions of some clays (Williams and others, 1968).

Iron and calcium concentrated in concretions or cracks in the lower portions of clays (Huddle and Patterson, 1961).

Upward loss of K20 (Holbrook and Williams, 1973).

General: Soil-like features in some clay deposits including cutans, clay-filled pores, ooliths, aggregates, spherulitic siderite, and mottled zones, roots, and soil profiles (Smyth, 1980).

The Effects of Organics

Keller's (1981) mention of organic complexing compounds, organic acids and silica-accumulating plants is important. Keller (1968, p. 122) notes:

> "The vegetation contributed to flint clay formation in several ways. Mechanically, it may have served as a filter that lined marshes and held out coarser clastics but allowed colloidal clay suspensions to pass. Plants growing in the clay extracted alkali and alkaline earth metals from the clay for growth and metabolism. These metal ions are easily leached out of leaves and stems after they fall from plants, thus mobilizing the flux ions for removal by solution. Silica likewise will be mobilized, thereby enriching the clay residue in alumina. Silica accumulating plants, such as reeds and bulrushes, live in this type of environment. If Equisetum was present, the aqueous solubility of silica could have been more than doubled relative to its value in freshwater as observed by Lovering (1959). Chelation by organic compounds and complexing by $C0_2$ from decaying organic matter could enhance the removal of fluxes and silica from the clay colloids and mud in the swamps. H^+ ions from organic acids would react with the silicates present to accelerate kaolinization."

The chemical effect of plants on the genesis of flint clays has been discussed by numerous authors including Hopkins (1898), Stout and others (1923), Hodson (1927), Chukhrov (1970), and Staub and Cohen (1978).

Furthermore, some tonsteins (see Table 2) associated with coal seams are believed to be volcanic ash deposits that owe their alteration to kaolinite almost entirely from the interaction with organic compounds and acids (Stach, 1950; Chalard, 1951; Bouroz and others, 1958; Bohor and Triplehorn, 1981). The influence of organic compounds on the recrystallization of kaolinite and the formation of diaspore and boehmite is also believed to be substantial (Bragonier, 1970; Keller, 1975).

Differential Colloidal Flocculation

Williams and others (1968) provide the most comprehensive argument for flint clay genesis via differential colloidal flocculation. They note that the Lower Kittanning flint clay in Clarion County is confined to an area laterally equivalent to the Vanport Limestone and an unnamed coal they also interpret as a lateral equivalent. They note that the distribution of illite/kaolinite ratios in the insoluble residue of the Vanport Limestone roughly correspond to the thickness distribution of the Vanport. They interpret this to suggest that the clay ratios parallel the Vanport shoreline. This reasoning is further supported by an overall agreement between the distribution of the illite/kaolinite ratios and the $Si0_2$:clay ratios and Fe_20_3 distribution within the Vanport insoluble residue.

Noting that Millot (1942) has shown colloidal flocculation is strongly affected by pH and electrolyte concentration, Williams and others conclude that flint clays are most likely to occur in areas where pH changes range from acid to basic, such as paludal-lacustrine environments that fringe a shallow sea. In such environments, if cation concentrations are low, colloidal alumina

would be more readily flocculated while silica would remain in solution to be flocculated in near-shore marine areas.

Williams and others (1968) propose a four-phase paragenesis for the flint clay as follows:

1) Flocculation of a colloidal gel in electrolytic solution forming interlocking kaolinite grains.
2) Recrystallization and shrinkage with water loss producing a brecciated appearance.
3) Resuspension of clay and quartz under more acid, swamp water conditions resulting in reprecipitation of the fine-grained groundmass, kaolinite books and quartz crystals.
4) Compaction and lithification.

Flint and semi-flint clays of the Allegheny Group illustrated in Figures 2 to 5 are believed to have originated from differential colloidal flocculation. Several stratigraphic relationships suggest this. Flint clay is commonly most abundant immediately adjacent to a coal seam, and appears to fringe the coal swamp. In the non-coal (basinward) direction flint clay is often laterally equivalent to freshwater limestone (a similar relationship observed by Williams and others, 1968 between the Vanport limestone and Kittanning flint clay). Near Trees Mills, in northern Westmoreland County, a black shale containing fresh water fossils (conchostracans and ostracods) appears to be the lateral equivalent of the Upper Freeport flint clay (Figure 4).

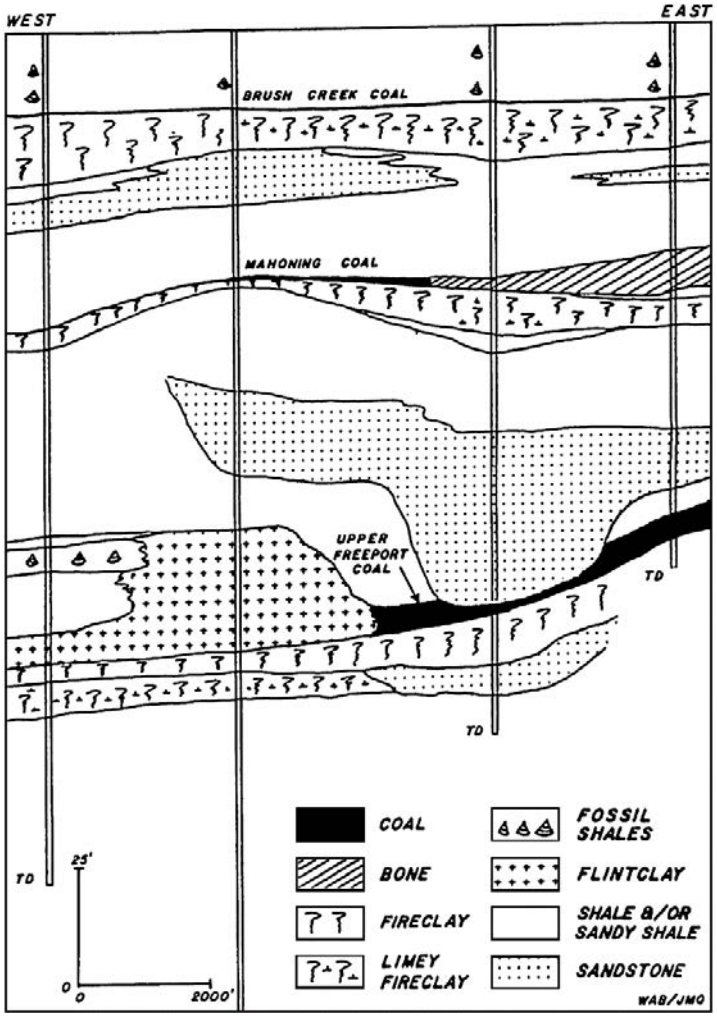

Figure 4. Cross-section showing lateral facies changes from coal to flint clay to black shale with fresh water fossils in the Upper Freeport horizon near Trees Mills, Westmoreland County. The datum is the overlying Brush Creek coal. Note position of coal relative to base of flint clay.

The genetic implication is that Upper Allegheny coal swamps were commonly adjacent to freshwater lakes. As peat accumulated, colloidal clays coming into contact with the acid swamp waters were flocculated. Staub and Cohen (1979) have documented the rapid flocculation of clay particles entering an acid environment in the modern Snuggedy Swamp of South Carolina. Schofield and Sampson (1954) note that acidity and a low cation concentration will cause edge-to-face (non-layered) flocculation of clay particles. The overall acidity of the lake would determine whether clay flocculation would be continuous across the lake or confined to the more acidic near-shore environments. Acidity, in turn, is strongly influenced by the size and shape of the lake, which controls internal circulation.

A further argument for a lacustrine flint clay origin-deposition in a paleotopographic low may be directly observed in the roadcut at the Widman Street exit (see description of Stop #10). Figure 5 illustrates a similar circumstance with a thicker coal and flint clay sequence (Upper Freeport). When the underlying Upper Freeport limestone is used as a datum, the Upper Freeport coal corresponds to a position near, but not at, the base of the adjacent flint clay. If the peat and clay accumulated at roughly the same rate, but the peat compacted four to five times more than the clay, this is the relationship to be expected.

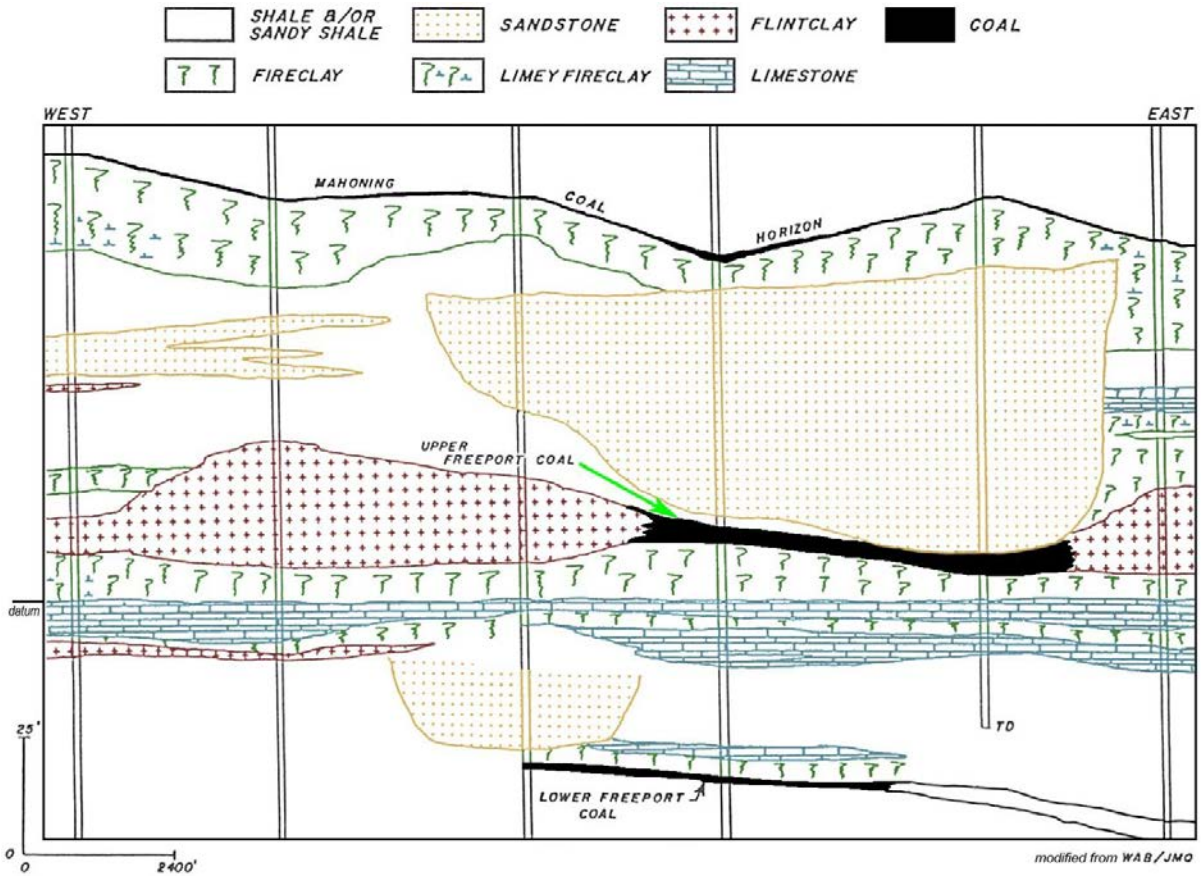

Figure 5. Cross-section of Upper Freeport coal and associated flint clay near Five Points, Westmoreland County. The datum is the top of the Upper Freeport limestone. Note vertical position of coal relative to the base of the flint clay.

The very fine laminae observed in many flint clays (Figure 1C) are also suggestive of sedimentation in a low energy environment. Such laminae have been observed in flint clay deposits believed to be of authigenic origin and may represent sedimentation of previously formed clay particles in localized depressions. Nevertheless, the presence of delicate, thin laminae, indicative of quiet water sedimentation, certainly does not preclude a lacustrine origin, especially for semi-flint clays.

Brecciation

The brecciation associated with many flint clays (Figure 1A) may, in fact, be related more to loading rather than shrinkage and drying as suggested by Williams and others (1968). The matrix for many of the brecciated flint and semi-flint clays is commonly not clay, but much coarser grained sand- and silt-sized material, often similar to the immediately overlying lithology. At

Cambridge, Ohio, a roadcut exposes brecciated semi-flint clay that is laterally equivalent to the Upper Freeport coal. Here, the material between the brecciated clay fragments is the same composition, color, and texture as the overlying lithology. Several large-scale slump blocks are also present, indicating that when the clay was loaded, it was structurally incompetent. The overlying material appears to have been oozed and slumped into the flint clay causing it to acquire a brecciated, fragmental appearance. The brecciation, of course, may be aided by the release of entrapped water. These conclusions are supported by evidence for early diagenetic slumping of flint clay at the Widman Street exit of Route 56 at Johnstown (see description of Stop #10). Figure 6 illustrates the hypothetical genetic model for deposition of the Upper Freeport flint clay and laterally equivalent facies prior to (6A) and after (6B) sediment loading.

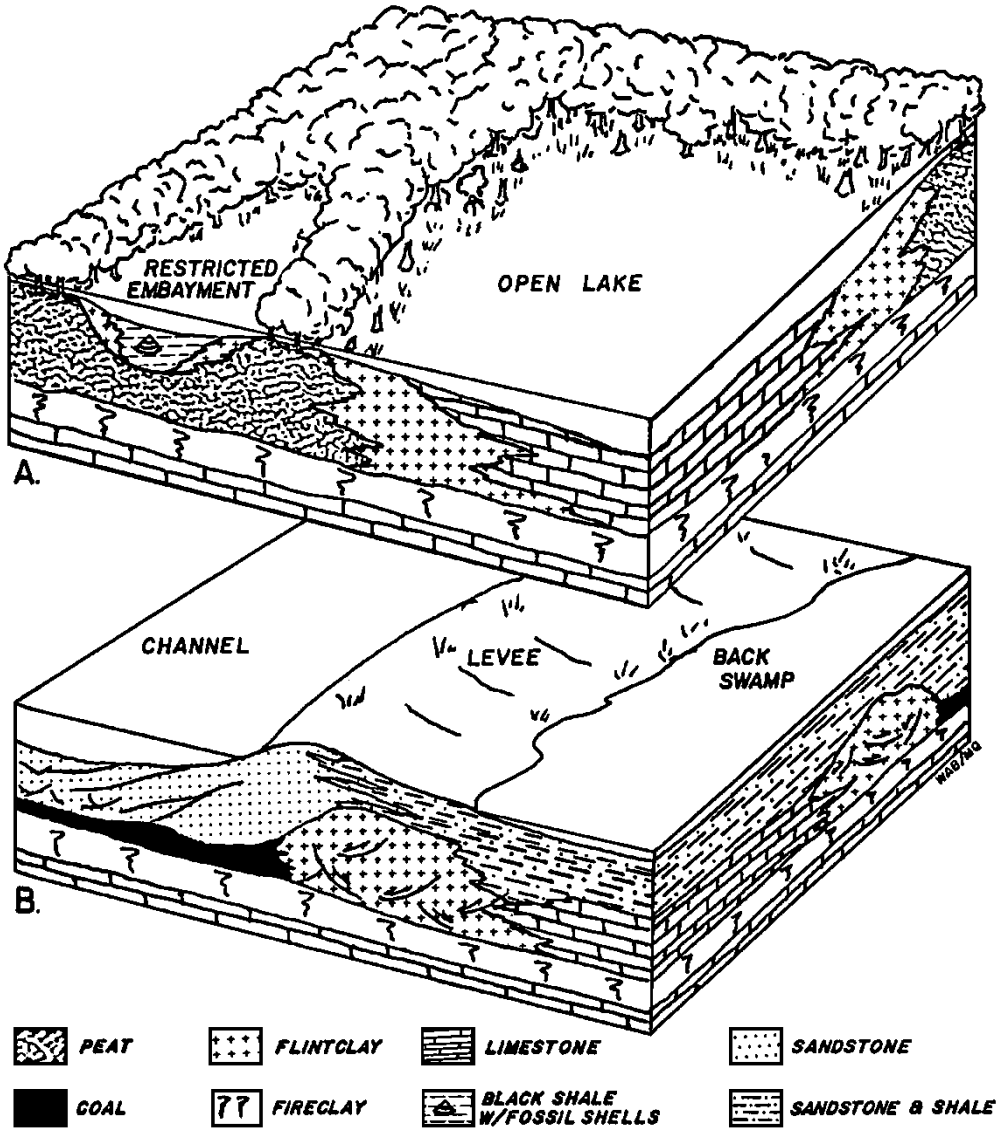

Figure 6. Depositional model and resultant compactional effects in the Upper Freeport sequence. (A) Depositional model for the Upper Freeport flint clay during deposition of the coal-flint clay-limestone sequence. (B) Resultant compactional effects of the Upper Freeport sequence after 10 to 20 ft. (3.1 to 6.2m) of loading by overlying sediments. Channel sandstones are commonly attracted to thick peat sequences (see Figures 3 to 5). Restricted embayment facies not shown in (B); presumed eroded by channel sandstone.

Conclusions

Geologic literature on the genesis of flint clay provides evidence that flint clays and related clay types may originate via three genetic mechanisms.

1) Leaching of an existing alumino-silicate deposit causing an alumina enrichment and the formation of kaolinite and/or aluminum hydroxide clay minerals.
2) Differential colloidal flocculation of kaolinite in shallow, low-energy, lacustrine or paludal environments.
3) The interaction of certain alumino-silicate deposits with organic compounds and acids. This mechanism is often supplementary but has been invoked exclusively to explain the genesis of tonstein deposits in coal seams.

In the Pottsville and Allegheny Groups, with few exceptions, higher grade flint clay {and nodule clay) occurs in the Pottsville and Lower Allegheny whereas less kaolinitic flint and semi-flint clay occurs in the Middle-to-Upper Allegheny {and Lowermost Conemaugh). Genetically, evidence such as dissolved and pitted quartz grains and boehmite enrichment on topographic highs strongly suggests that the Lower Mercer {Pottsville) flint and nodule clay was formed from intensive leaching over a long period of time, with the supplementary aid of organic compounds and acids. Other Lower Allegheny flint clays may have had a similar origin.

Upper Allegheny flint and semi-flint clays are thought to originate from differential colloidal flocculation in shallow paludal/lacustrine environments. This conclusion is supported by the following observations:

1) The association of flint clay with the perimeter of several coal seams.
2) The apparent distal equivalence of flint clay with limestone and/or other freshwater lacustrine rocks.
3) The paleotopographically lower position of flint clays relative to adjacent coal seams.
4) The occurrence of flint clay at the base of a coarsening upward sequence, laterally equivalent to black shale with coal streaks.
5) Very fine laminae observed in many fragments of brecciated flint clays.

The brecciation observed in many flint clays and formerly attributed to shrinkage and drying is believed to be caused at least partially by loading of the flint clay prior to complete lithification and possibly aided by the release of entrapped water. Incorporation of the immediately overlying lithology as the matrix material between brecciated flint clay fragments has been observed in drill holes and surface exposures. In the surface exposures it may be seen that the overlying material has been squeezed and slumped into the flint clay. It may also be demonstrated from surface exposures that sedimentary slumping occurred early after 12 to 15 ft. (3.7 to 4.6 m) of material had accumulated on top of the clay and that the flint clay was not sufficiently lithified at the time of slumping to incorporate underlying units in the slump.

References

Baumann, D., and Keller, W. D., 1975, Bulk densities of selected dried and fired kaolin clays: Clays and Clay Minerals, v. 23, p. 424-427.

Boher, B.F., and Triplehorn, D.M., 1981, Volcanic origin of the flint clay parting in the Hazard No. 4 (fire Clay) coal bed of the Breathitt formation in eastern Kentucky, *in* Cobb, J. C. and others,

eds., coal and Coal-Bearing Rocks of Eastern Kentucky: Kentucky Geological Survey, Lexington, KY, p. 49-53.

Bolger, R.C. and Weitz, J.H., 1952, Mineralogy and origin of the Mercer fireclay of north central Pennsylvania, in American Institute of Mining and Metallurgical Engineers, St. Louis Meeting (1951) Symposium Problems of Clay and laterite Genesis, York, PA, Maples Press Co., p. 81-93

Bouroz, A., Dolle, P., and Puirabuad, C., 1958, La aerie stratigraphique et les tonstein du Westphalian C du Sud-ouest de la concession de Noeux: Annales du Societe Geologique du Nord, v. 78, p. 108-123.

Bragonier, W.A., 1970, Genesis and geologic relations of the Mercer Fireclay, western Pennsylvania: University Park, Pa., Pennsylvania State University, M.S. thesis, p. 212.

Buswell, K.S., 1980, A depositional model for the Lower Freeport coal seam in central western Pennsylvania: Columbia, SC, University of South Carolina, M.S. thesis, p. 34.

Chalard, J., 1951, Tonstein du bassin houiller du Nord de la france: III Congress Intern. Stratigr. et Geol. du Carbonifere, Heerlen, p. 73-77.

Chukhrov, F.V., 1970, Analogues of flint clay in Soviet literature: Clays and Clay Minerals, v. 18, p. 1-5.

Clark, W.J., 1979, An interfluve model for the Upper Freeport bed in part of western Pennsylvania: Columbia, SC, University of South Carolina, M.S. thesis, p. 54.

Erickson, E.S., 1963, Mineralogical, petrographic and geochemical relationships in some high alumina and associated claystones from the Clearfield basin, Pennsylvania: University Park, Pa., Pennsylvania State University, PhD. Dissertation, p. 190.

Falla, W.S., 1967, The petrology and geochemistry of the Clarion flint clay, western Pennsylvania: University Park, Pa., Pennsylvania State University, HS thesis, 84 p

Ferm, J.C., and Smith, G.C., 1981, A guide to cored rocks in the Pittsburgh Basin: University of Kentucky and University of South Carolina Departments of Geology, 109 p.

Foose, P.M., 1944, High-alumina clays of Pennsylvania: Economic Geology, v. 39, p. 557-577.

Goldberry, R., 1979, Sedimentology of the Lower Jurassic flint clay bearing Mishhor formation, Makhtesh Ramon, Israel: Sedimentology, v. 26, p. 229-251.

Greaves-Walker, A.F., 1939, The origin, mineralogy and distribution of refractory clays of the United States: North Carolina College of Agriculture and Engineering, State College Record, v. 39, no. 4, 87 p.

Grim, R.D., and Allen, V.T., 1938, Petrology of the Pennsylvanian underclays of Illinois: Geological Society of America Bulletin, v. 49, p. 1485-1514.

Halm, L., 1952, Comparative study of American and French flint clays: American Ceramic Society Bulletin, v. 31, p. 79-84.

Hodson, F., 1927, The origin of bedded Pennsylvanian fire clays in the United States: Journal of the American Ceramic Society, v. 10, p. 721-746.

Hohos, E.F., 1979, Paleoenvironmental model of the Upper Freeport coal seam in parts of Indiana and Armstrong Counties, Pennsylvania: Columbia, SC, University of South Carolina, M.S. thesis, p. 59.

Holbrook, P.W., and Williams, E.G., 1973, Geologic and mineralogic factors controlling the properties and occurrence of ladle brick clays: Pennsylvania State University, College of Earth and Mineral Sciences University Park, PA, Special Publication 1-73, 89 p.

Hopkins, T.C., 1898, Clays and clay mineral industries of Pennsylvania, Part I. Clays of western Pennsylvania: Appendix to the Annual Report of the Pennsylvania State College for 1897, p. 48-54.

Huddle, J.W., and Patterson, S.H., 1961, Origin of Pennsylvanian underclay and related seat rocks: Geological Society of America Bulletin, v. 72, p. 1643-1660.

Jaron, M.G., 1967, A method for determining post-depositional alteration in underclays and associated lithologies: Pennsylvania Geologic Survey, 4th ser., Information Circular 57, 14 p.

Keller, W.D., 1952, Observations on the origin of Missouri high-alumina clays, in American Institute of Mining and Metallurgical Engineers, St. Louis Meeting, 1951, Symposium, Problems of Clay and Laterite Genesis: York, PA, Maple Press Co., p. 115-143.

------- 1968, flint clays and a flint clay facies: Clays and Clay Minerals, v. 16, p. 113-128.

------- 1975, Refractory clay in the lower part of the Pennsylvanian System, ~Paleotectonic Investigations of the Pennsylvanian System in the United States, Part 2: U.S. Geological Survey Professional Paper 853, p. 65-71.

------- 1976, Scan electron micrographs of kaolin collected from adverse origins - III. Influence of parent material on flint clays and flint-like clays: Clays and Clay Minerals, v. 24, p. 262-264.

----- 1978a, Classification of kaolins exemplified by their textures in scan electron micrographs: Clays and Clay Minerals, v. 26, p. 15-19.

----- 197Bb, flint-clay facies illustrated within one deposit of refractory clay: Clays and Clay Minerals v. 26, p. 237-243.

------ 1981, The sedimentology of flint clay: Journal of Sedimentary Petrology, v. 51, p. 233-244.

--- 1982, Scanning electron micrographs of claystone altering to flint clay: Clays and Clay Minerals, v. 301 p. 150-152.

Lovejoy, E., 1925, Theory of coal measure fire clays: Journal of the American Ceramic Society, v. a, p. 758-761.

Lovering, T.S., 1959, Significance of accumulator plants in rock weathering: Geological Society of America Bulletin, v. 70, p. 781-800.

Merrill, W.M., 1952, Replacement of the Middle Kittanning Coal by interfingering clastics in southeastern Ohio (abs): Geological Society of America Bulletin, v. 62, p. 1463.

Millott, G., 1942, Relations entre la constitution et la genese des roches sedimentaires *angi*leuses: Geol. Appliq. et. Prosp. Min., v. 2, 353 p.

Moore, L.R., 1968, Some sediments closely associated with coal seams, *in* Murchinson, D., and Westall, T.S., eds., Coal and Coal Bearing Strata: Oliver and Boyd, London, p. 105-123.

Patterson, S.H., and Hosterman, J.W., 1960, Geology of the clay deposits in the Olive Hill district, Kentucky, *in* Swineford, A., ed., Clays and Clay Minerals, Proceedings of the 7th National Conference: New York, Pergamon Press, p. 178-194.

Pedlow, G.W., 1977, A peat island hypothesis for the formation of thick coal: Columbia, SC, University of South Carolina, PhD. Dissertation, p. 104.

Schofield, R.D., and Sampson, H.R. (1954), Flocculation of kaolinite due to attraction of oppositely charged crystal faces: Discussions of the Faraday Society no. 18, p. 135-145.

Schultz, L.G., 1958, Petrology of underclays: Geological Society of America Bulletin, v. 69, p. 363-402.

Slatkine, A., and Heller, L., 1960, A petrological study of the flint clay from Makhtesh Ramon, Israel: International Geological Congress, 21st, International Commission for the Study of Clays, Proceedings, pt. 24, p. 88-107.

Smith, W.H., and O'Brien, N.R., 1965, Middle and Late Pennsylvanian flint clays: Journal of Sedimentary Petrology, v. 35, p. 610-618.

Smyth, A.L., 1980, Pedogenesis and diagenesis of the Olive Hill clay bed, Breathitt formation (Carboniferous) northeastern Kentucky: Cincinnati, OH, University of Cincinnati, M.S. thesis, p. 201.

Stach, E., 1950, Vulkanische Aschenreyen uber dem Steinkohlenmoor: Gluckauf, 86, p. 41-50.

Staub, J.R., and Cohen, A.D., 1978, Kaolinite-enrichment beneath coals; a modern analog, Snuggedy Swamp, South Carolina: Journal of Sedimentary Petrology, v. 48, p. 230-210.

----- 1979, The Snuggedy Swamp of South Carolina: A back barrier estuarine coal-forming environment: Journal of Sedimentary Petrology, v. 49, p. 133-144

Stout, W., Stull, R.T., McCaughey, W.J. and Demorest, D.J., 1923, Coal Formation Clays of Ohio: Geological Society of Ohio, ser.4 Bulletin 26, p. 109-150, 533-568.

Sturgeon, M.T., 1958, The geology and mineral resources of Athens County, Ohio: Ohio Geologic Survey Bull. 57, 600 p.

Weitz, J. H., 1954, The Mercer fire-clay in Clinton and Centre Counties, Pennsylvania: University Park, Pa., Pennsylvania State University, PhD. Dissertation, p. 107.

-------, and Bolger, R.C., 1951, Mineralogy and nomenclature of the Mercer fire-clay in north central Pennsylvania: Pennsylvania Academy of Sciences Proceedings, v. 26, p. 124-130.

Williams, E.G., Bergenback, R.E., Falla, W.S., and Udagawa, S., 1968, Origin of some Pennsylvanian underclays in western Pennsylvania: Journal of Sedimentary Petrology, v. 38, p. 1179-1193.

Wilson, M.J., 1965, The origin and geological significance of the South Wales underclay: Journal of Sedimentary Petrology, v. 35, p. 91-99.

THE ROGUE KIMBERLITE DIKES IN INDIANA COUNTY, PENNSYLVANIA
PART 1. UNUSUAL INTRUSIVE HABIT OF KIMBERLITE DIKES IN COAL SEAMS

DAVID (DUFF) GOLD[1], ARNOLD G. DODEN[2], CHUMA MBALU-KESWA [3]JOSEPH R. TEDESKI[4], AND RYAN MATHUR[5]

with contributions from: Robert C. Smith II, Viktoras W. Skema, Michael Moore, DCNR Bureau of Topographic and Geologic Survey, 3240 Schoolhouse Road, Middletown, PA 17057; Joseph Dague, 1296 Falling Spring Road, Chambersburg, PA 17272; Andrew Sicree, Adjunct, Penn State University and St. Francis University. 671 Boalsburg Road, Boalsburg, PA 16827; Barry Scheetz GMRE-Inc. 925 West College Ave., State College, PA 1680; Charles E. Miller Jr., 355 Carogin Drive, State College, PA 16803; Charles H. Shultz, Emeritus, Department of Geology, Slippery Rock University, Slippery Rock, PA

Abstract

Group II micaceous kimberlites have been recovered from underground workings in three coal mines in northern Indiana County, Pennsylvania. They occur as thin, relatively long dikes that exhibit a flow fabric, porphyritic texture with large phlogopite, chrome diopside and magnesian ilmenite phenocrysts/megacrysts, and exotic pyrope garnet xenocrysts. The apparent confinement of these intrusions to coal seams may be significant. The collinearity of the locations suggests the intrusions are part of an east-west trending dike system, but their continuity cannot be verified from surface exposures. They are mapped as long and narrow dikes with relatively few breaks along strike, and rarely split into multiple segments. Aberrations include minor bulbous sills, thin stringers and wedge-shaped apophyses, with both horizontal and steeply inclined terminations in the host coal seam. The former are described as oblate cylindrical sills, and the latter as bladed dikes. Clearly, the coal seam has influenced or controlled these bizarre intrusive habits. Samples examined are typical hypabyssal-facies, carbonate-rich kimberlite, with a poly-textured (agglomeratic) fabric. A passive expansion into the coal is apparent without the aggressive stockwork configuration of many intrusive contacts. Thermal metamorphism is restricted to 4-8 inches of coke in the coal, and is minimal in the underclay and overlying siltstone and shale. A high content of volatiles (±8 % H2O and 17.5 % CO2 in quenched whole rock) dissolved in the magma would promote crystallization and out-gassing at depth. We speculate that highly porous coal seams may have acted as a catalyst triggering crystallization, as well as a sink for outgassing phases, and is a likely scenario for hydraulic fracturing the favorable thicker coal seams. Unresolved questions include (a) whether their apparent confinement to coal seams is real, or is simply a sampling artifact linked to anthrogenic activity, (b) is there a tectonic significance to their off-craton setting in the Appalachian foreland basin, and (c) what is their potential to carry diamonds?

---

[1] Emeritus, Department of Geosciences, Penn State University, University Park, PA

[2] GMRE-Inc. 925 West College Ave., State College, Pa 16801

[3] 220 N Elms Avenue, Newtown, PA 18040

[4] 378 Garretts Run Road, Kittanning, PA 16201, Geological Scientist (retired), DCNR Bureau of Topographic and Geologic Survey, 400 Waterfront Dr, Pittsburgh, PA 15222-4745

[5] Department of Geology, Juniata College, Huntingdon, Pennsylvania, PA. 16652

Introduction

Kimberlites are rare, exotic ultramafic rocks whose name unfortunately conjures an unwarranted, but popular association with diamonds. Less than 10% of the 6974 localities known worldwide (De Wit, 2014) carry diamonds. Of these only 1% are economically viable (Coopersmith, 2014). To appreciate the rarity of diamonds one needs to consider that commercial operations express grades of diamonds in carats per 100 loads, where a load is approximately 16 cubic feet of broken rock, equivalent to ± 0.9 ton. Productive mine grades of 7 to 28 carats per 100 loads equate to 25 to 100 parts per billion (Gold, 1968).

Their tectonic association with old, cold cratons, similarities in texture, mineralogy and geochemistry between diverse types, and different ages "suggest kimberlite magmas are generated by a systematic and reproducible process" (Harris and Middlemost, 1969). They are the mavericks of volcanic rocks, with distinctive habits and various facies that reflect emplacement depth. They occur almost exclusively in steeply dipping fissures and narrow dikes (hypabyssal facies) that may expand into funnel-shaped pipes and vents (diatreme and crater facies) near the surface. Sills are extremely rare and none of the crater facies sites have demonstrable lava flows. These small intrusions (1 cm to meters scale for dikes; pipes rarely exceeding 1 km across) underscore their volumetric rarity in the crust, but overreach their petrological significance as the source of fist-sized samples of xenocrysts and up to boulder-sized xenoliths of the mantle. A signature mineralogy consisting of xenocrysts/phenocrysts of pyrope garnets, magnesian ilmenites and chrome diopsides is used as an exploration tool to locate eroded kimberlites from the heavy minerals in the stream sediment. Of the 10 groups of garnets found in kimberlites (Dawson and Stephens, 1975) only the G-9 and G-10 types correlate with diamonds.

Kimberlites are veritable windows to the upper mantle, where accumulations of fluid-rich magma migrate upward, cool and exsolve dissolved volatile phases, to generate a fluidized gas streaming system capable of rapidly moving kimberlite melt through small orifices over great distances. Their emplacement is envisaged as penetrative, rapid, and sufficiently cool to preserve the metastable phases of the upper mantle and lower crust. As such, kimberlites are composite assemblages of minerals and rocks from both the source and transit localities entrained during emplacement. A porphyritic texture implies an intermediate magma chamber, with growth time between eruptions, and disequilibrium between the phenocrysts and their kindred species in the matrix. We will not debate the subtle distinction between phenocryst and xenocryst here. We prefer to use non-generic terms based on crystal size of megacryst (>> matrix) to microcrysts that blend in with matrix). Fortunately, the polymineralic lithic inclusions (xenoliths) represent the equilibrium assemblages favored for petrogenetic studies.

We are fortunate in having three sites (Figure 1) in Indiana County, albeit all underground, linked by a common trend over a distance of approximately 9 miles. All were exposed by mining operations in at least two different coal seams (Lower Freeport and Lower Kittanning) (see Figure 2) and we are attempting to integrate their discovery into a coherent story. There is no known surface crop, nor has any magnetic anomaly, common to kimberlites, been detected in traverses over the projected surface locations. So far, a reconnaissance search for heavy minerals in the streams draining the potential crop sites failed to detect kimberlite signature (sputnik) minerals. They appear to represent an en echelon set of dikes with an approximately east-

northeasterly strike, and bulbous sills and wedged-shaped apophyses in the coal. A key question is whether there is a unique spatial relationship with the coal seams? Other issues include the source of excess argon in the phlogopites, the presence of an early melt phase in diopside and garnet megacrysts, the significance of G-9 garnets, and the emplacement temperatures inferred from the degree of coking in the coal.

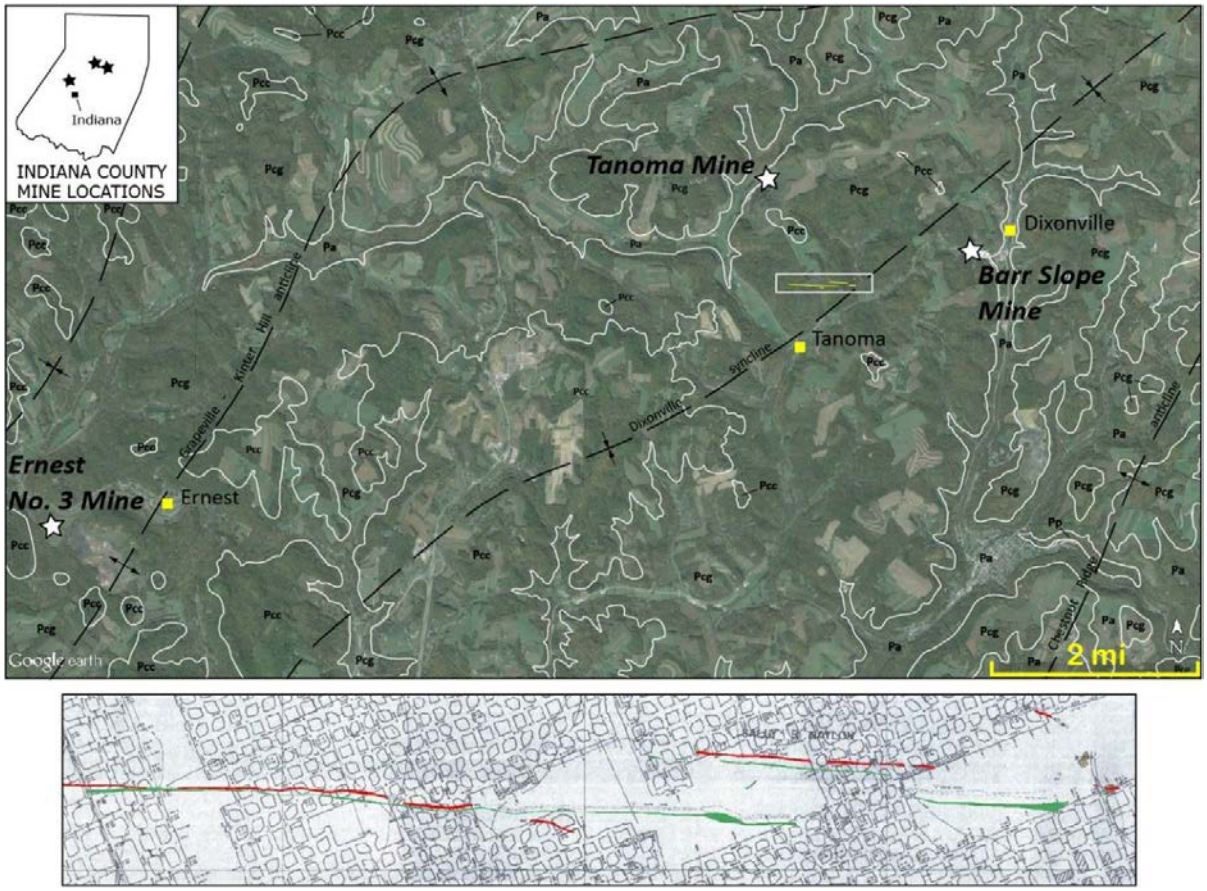

Figure 1. Map for part of Indiana County showing locations of the Ernest, Tanoma, and Barr Slope mines with white stars (Google Earth base image dated 10/11/2015, map scale in lower right corner). The Tanoma/Dixonville kimberlite dikes location is indicated with yellow lines in a white box, which corresponds to the detailed map below. Regional geology from Glover (1976a,b,c). Pennsylvanian age sedimentary units: Pp = Pottsville Group, Pa = Allegheny Group, Pcg = Glenshaw Group, and Pcc = Casselman Formation. Inset mine map provided by Michael Moore, PA DCNR, showing details of kimberlite dikes. Red lines portray the dikes exposed in the Lower Kittanning Coal of the Tanoma Mine and green lines show dike exposures in the Lower Freeport Coal in the Barr Slope Mine. The strike length of the red dikes is approximately 7200 feet.

It is gratifying that the geologic sleuthing skills of the discoverers (Honess and Graeber, Joseph and Jeanne Dague, Robert Smith, Viktoras Skema, and Joseph Tedeski) have led to follow-up studies and/or collections by Peter Deines, D. Dobransky, Peter Wyllie, David Gold, Charles Shultz, Robert Smith, John Barnes, Michael Moore, E. Law, Ryan Mathur, Andrew Sicree, Gareth Mitchell, Alan Davis, William Bragonier and Arnold Doden, as well as student theses by Max Borella (1997), Patrick Cassidy (2015), Chuma Mbalu-Keswa (1995), Susan Radomski (1995), and Pedro Faria (ongoing) and a number of abstracts and reports.

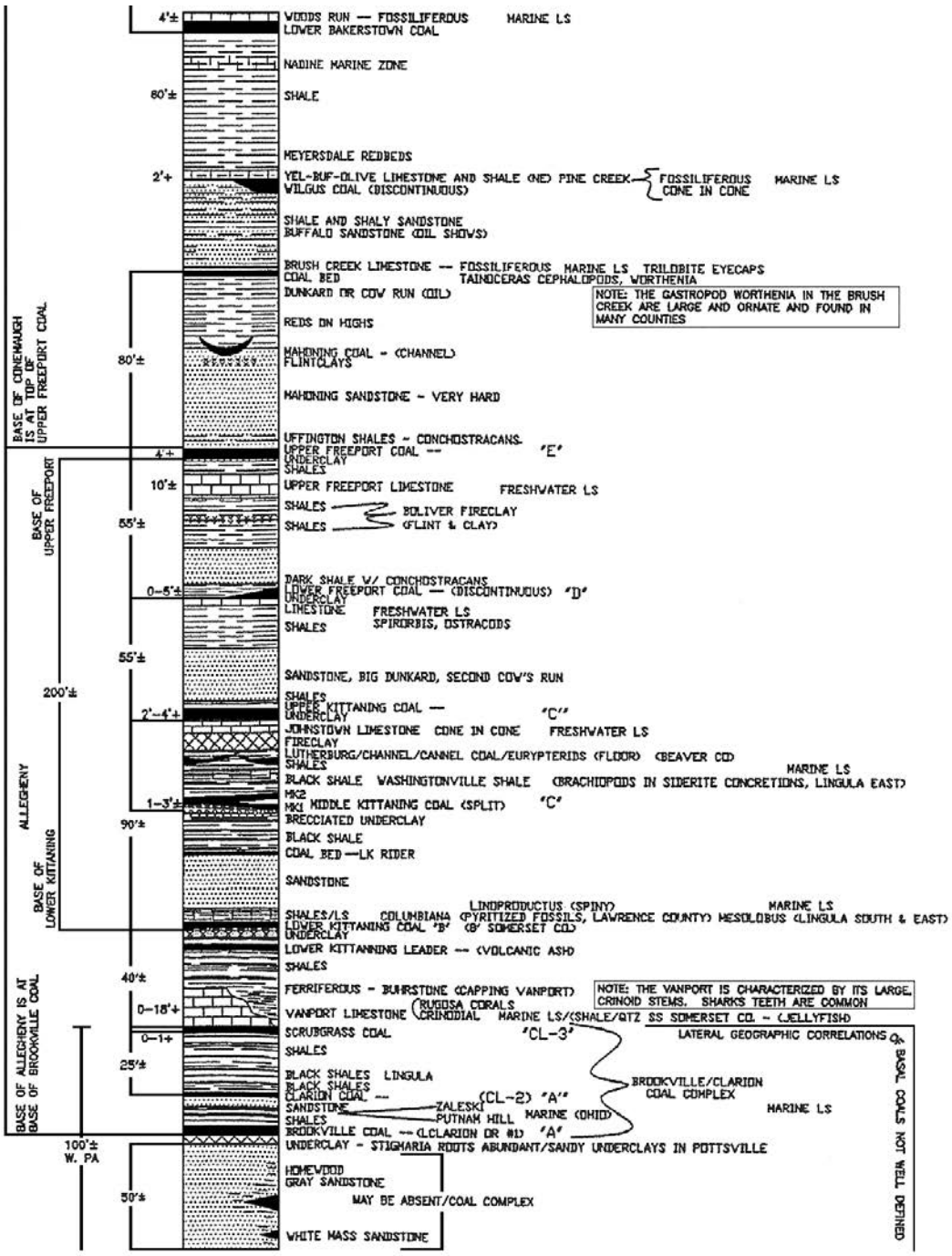

Figure 2. Generalized Stratigraphic Column for part of the Allegheny Section in western Pennsylvania. Not to scale. from W.J. Marks, 1999.

History and Previous Studies

There is a temptation to link Barr Slope, Tanoma and Ernest Mines with the surface trace of a line approximately 9 miles long, trending 255°. The link is more likely *en echelon* dikes striking 080° in Barr Slope Mine at a depth of approximately 200 feet in the Lower Freeport Coal, and the western end of the Tanoma Mine, where Tedeski (2002) recorded an attitude of 264°/84°,

complemented by 273° (1982) and 268° (1984) in Smith *et al*., (Pers. Comm., 2016) in the Lower Kittanning Coal. Neither the attitude nor location of the dike in the Ernest Mine is known, but it is suspected to intrude the Upper Freeport Coal in the crown pillar at No. 3 Portal.

The Barr Slope/Dixonville Mine Kimberlite

It is likely that miners were aware of the nature of the dikes in the area long before scientific recording of the mica peridotite dike at Dixonville in 1924 (Honess and Graeber, 1924). The Dixonville dike was encountered in at least four places along a strike of 080° (Honess and Graeber, 1926) in the underground workings of the Barr Slope Mine of the Clearfield Bituminous Coal Company, and correctly identified as a mica peridotite. They record a thickness of less than 2 feet near its ends to 45 feet in the middle. This greatly underscores the real extent, revealed during a search of archival mine maps by Michael Moore (Figure 3).

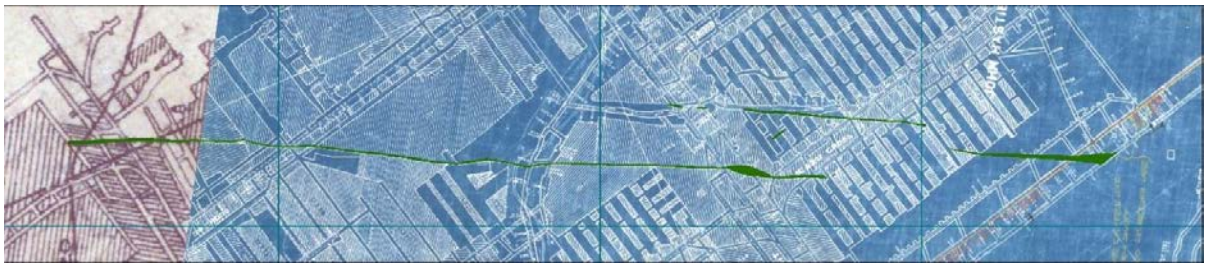

Figure 3. Barr Slope Mine map showing exposure of Dixonville Dike in the Lower Freeport workings. Map courtesy of Michael Moore (2016).

Unfortunately, samples archived at "The Pennsylvania State College", consist mainly of coke from the 8-inch thick metamorphic aureole. Stimulated by petrological investigations at Penn State on carbonatites and mantle carbonates during the late 1950's and early 1960's (Wyllie and Tuttle, 1960), Peter Wyllie acquired additional samples of the Dixonville dike from the Barr Slope Mine to study carbonate nodules. Part of this sampling (PJW 2 to 4), collected by graduate student Gil Franz, were given to Peter Deines, a graduate student in the Department of Geochemistry and Mineralogy (Pers. Comm., P.J. Wyllie, 2016) to examine the distribution of carbon and oxygen isotopes in carbonate inclusions (Deines, 1968). Unfortunately, there is no record of where these samples were collected. A systematic attempt to alert mine operators was initiated during 1964 and coordinated through Dave Snell, the Earth and Mineral Sciences Museum Director. Correspondence with R.C. Beerbower, Jr., of the U.S. Steel Corporation yielded an underground map of the Gates-Adah dike near Masontown. An August, 1964 letter to W.J. Shields of the Rochester and Pittsburgh Coal Company alludes to a kimberlite in the Ernest No. 3 Mine. Correspondence from the same period with J. L. Marshall of Imperial Keystone Mine, focused on the Dixonville dike in the Barr Slope Mine. During the mid- to late- 1960's, Penn State faculty (McKenzie Keith, David Gold, Peter Wyllie and Dave Snell) distributed kimberlite samples to mine operators in the region, along with a request to report similar findings in any of their operations.

The Tanoma Mine Kimberlite

Barnes and Tucker Coal Company opened the Tanoma Mine in 1982 to supply coal, for the South Korean market, from the 180-400 feet deep Lower Kittanning coal. "The slope and shaft for the Tanoma Mine were constructed in the pit of a Lower Freeport surface mine" (Moore, Pers.

Comm., 2016). The Tanoma Mine was developed 130 to 150 feet below the Barr Slope workings. The mapped exposures of the Tanoma kimberlite are shown in the mine map (Figure 4). A superposition of Figures 3 and 4 is shown in Figure 1. The traces of the dikes are an almost exact match if adjusted for the 84° dip separation. Hence, the Dixonville Dike and the Tanoma Kimberlite Dike are the same intrusion.

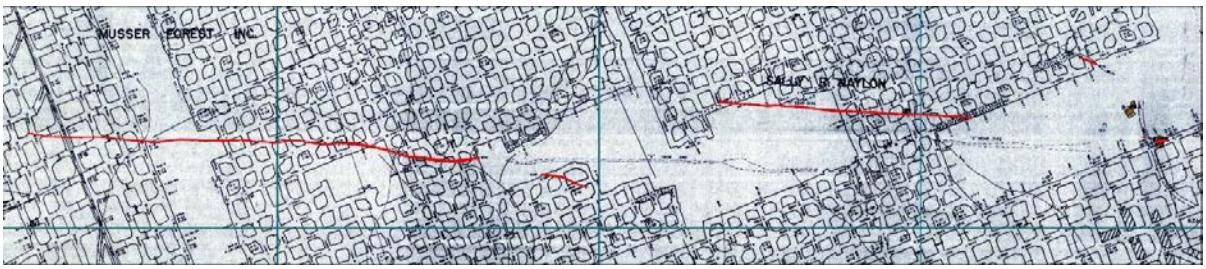

Figure 4. Tanoma Mine map showing exposure of Dixonville Dike in the Lower Freeport workings. Map courtesy of Michael Moore (2016).

DCNR geologists Robert Smith and Viktoras Skema visited the mine on October 13, 1984 and recorded a 16-22 cm thick kimberlite dike, striking N87°W, with a 7-cm coke margin exposed over a strike length of 20 m. Analyses of samples of coal/coke are included in the National Coal Resource Data System (N.C.R.D.S.). A second visit by them (3/1/88) was to the Main D, L2 Entry 30+000 where the dike, 7.5 to 8 cm thick, was seen to trend S88°W. A study of garnets revealed that 42 of 56 analyzed were classified as G9 group (Smith and Barnes, 2006). Projections of the dike 0.9 miles north of Tanoma Village, and a cluster of six E-W dikes, said to project to the surface approximately 0.25 miles south of the Village of Barr Slope, have not been verified (Smith, Skema and Dague, Pers. Comm., 2016).

Joseph Tedeski, a geology student at IUP, working part time in the Tanoma Coal Mine as an Assistant Mine Foreman/Fireboss, started mapping the dikes, communicating with interested professionals, and distributing samples for scientific study. We are indebted to the manager of the Tanoma Mine (Scott Britton, 1991) not only for encouraging Tedeski to map the dike in the underground workings (Figure 3), but also for facilitating excursions underground for interested parties from the University of Pittsburgh (Michael Bikerman, Henry Pellwitz), Penn State University (Duff Gold, Peter Deines, Gary Mitchell, Andy Sicree, Barry Scheetz and David Eggler, and Temple University (Gene Ulmer and Natalie Flynn). A Mini-Conference on the Pennsylvania kimberlites was convened at Penn State on May 11, 1994. Most subsequent studies on the Tanoma kimberlite dikes stem from samples collected during these excursions, the private collection of Joseph Tedeski and samples acquired by James G. Tilton, of the Equitable Gas Company. After joining the Pennsylvania Geological Survey in Pittsburgh in 1992, Tedeski worked his notes and photographs into a CD (Tedeski, 2002). In these, he chronicles underground exposures, thickness and orientation changes, and the unusual habit of the intrusion in the coal seam over a strike length of 7200 feet. These notes highlight locations of the megacrysts of garnet (up to 3.8 cm), phlogopite (12 x 18 cm), and Cr-diopside (10 to 12 cm long). Coke from the metamorphic aureole was taken from Section D5 track entry, between the airlock doors for reflectance studies in the Coal Characterization Laboratory of Penn State University. The petrography of the Tilton samples is included in the summary chapter on Jurassic Kimberlite Dikes in the Geology of Pennsylvania (1999) by Charles H. Shultz, of Slippery Rock University.

A tapered brick size sample collected by Bill Bragonier while with Rochester and Pittsburgh Coal Company, shows a thin bioclastic limestone bed 4-5 cm thick separating 1-cm thick beds of khaki-colored siltstone in the hanging wall of the coal (Figure 5). A cursory examination of the fossils (Roger Cuffey, Pers. Comm., 2016) suggest they are shrimp clam shells (*Estheriids* and *Conchonstrids*). They occur as delicate curved shells in cross section, and some of these are preserved in a granular textured coquina.

Figure 5. Dark gray bioclastic limestone in khaki colored, calcareous siltstone, with fossil shrimp clams exposed on top surface. W. Bragonier collection. (Photograph by C. Miller)

The Ernest Mine Kimberlite

The Ernest Mine in White and Rayne Townships produced Upper Freeport (Upper E) coal in 1903 and left a "refuse pile of some 9.0 million tons of abandoned coal waste over an area of 94 acres" (Stant *et al*., 2007). There is no record of dikes in the archived maps examined. Initially a Rochester and Pittsburgh Company operation, it closed under Consolidation Coal Company. A reclamation permit was issued to Cambria Reclamation Company November 1995. Although the Ernest Mine is mentioned in the 1960's Penn State kimberlite correspondence, it was not until 2007 that Brent Means, a PA-DEP Mine Inspector, found the first recorded specimen (identified by Robert Smith at DCNR). Subsequent searches focused on the Ernest No. 3 Mine portal area, specifically in an excavation as part of the Americkohl Reclamation program (Figure 6). Reclamation included refuse re-mining and dumping (1998 to 2004) of 1,437,282 tons of FBC fly ash from the Cambria co-generation plant (Stant *et al*., 2007).

Figure 6. Ernest No. 3 Mine showing location of kimberlite specimen and part of the Americkohl Reclamation program. Image courtesy of R.C. Smith, 2016.

In August, 2009, Jeanne Dague "found an excellent, 2- to 3-kg specimen (Figure 7a) with ≥2.5 cm of coked coal attached to both contacts of a 9 ±0.5 cm-thick dike section" (Smith et al., 2016). Note the "rounded" megacryst of fresh phlogopite (Figure 7b) embedded in the kimberlite matrix. Thin sections were cut (D.P. Gold) in June, 2016 and examined by Arnold Doden. A 2-mm red garnet with a 0.6 mm kelyphitic alteration rim was extracted, cleaned and fragments were analyzed by SEM/EDS in the DCNR laboratory by Smith and Barnes (Pers. Comm., 9/1/2016). The preliminary results (refer to Table 1, Mineralogy and Petrology section in this document) are interpreted as a high calcium G-9 pyrope rather than a subcalcic G-10 garnet.

Figure 7a. Jeanne Dague sample collected on waste dump at Ernest No 3 Mine, (Photograph by J. Dague)

Figure 7b. Phlogopite megacryst in Jeanne Dague sample. Background grid is 1/10 inch.

Location of the Jeanne Dague sample is recorded as 40° 40' 21" N, -79° 11' 00" W, not far from the entrance to the No. 3 portal (Figure 6) at approximately: 40° 40' 25"N, 79° 10' 50"W (Smith e*t al.,* Pers. Comm., 2016).

A geological reconstruction by Viktoras Skema placed the dike in the Upper Freeport coal that remained intact in support pillars around the mine entrance, until the 2009 reclamation. Smith, Skema, and Dague, (Pers. Comm., 2016) conclude "that the kimberlite came from the relatively small re-mined area on the north and northeast edge of the site (near the creek) and not from the dark deep mine spoils on the south end". Neither the attitude nor location of the dike in the Ernest Mine is known, but it is suspected to be in the support pillar at No. 3 portal.

The Sandy Ridge Kimberlite

Doden and Gold (2000) recorded another outlier in Sandy Ridge Quarry, 4.5 miles south-southeast east of Philipsburg, in Clearfield County Pennsylvania (see Figure 30, later this text). Here Butler sandstones between Lower and Upper Freeport coals, and the overlying Lower Mahoning sandstone, up to the Mahoning coal seam, are mined and crushed on site for aggregate. This kimberlite is an enigma because the only samples came from an aggregate stockpile. Despite days of searching by at least 6 different geologists, no dikes or sills have been identified in the sandstones and siltstones exposed in the highwalls, or floor, nor have any magnetic anomalies been found on the property. This kimberlite could be restricted to intrusions in one of the Freeport coals?

Spatial and Thermal Nature of the Intrusions

Habit, Temperature, and Intrusive Mode

Similarity in traces of Dixonville/Tanoma dikes demonstrates their vertical continuity (Figures 1, 3 and 4), as thin dikes, rarely more than a few feet thick. Their apparent absence in surface crop is an enigma. The most striking attribute of the Dixonville, and Gates-Adah dike is the very large length-to-thickness ratio and rarity of satellite intrusions despite a well-jointed host. These are not swarms but rather segments of dikes along the same strike trend. Other unusual habits exposed in the Tanoma Mine are the wedge-shaped dikes and sills terminating in the coal, and bulbous dikes (or cylindrical sills).

Late carbonated veins, some with fibrous calcite, point to a shear component adjacent to and within the intrusion. Except for a coked aureole up to 8 inches thick in the coal, no hornfels is noted adjacent to shale or around shaley inclusions. Law *et al*., (2004) note flow fabric (aligned phenocrysts and xenocrysts), and subparallel fracture alignment through xenocrysts and matrix, as petrographic evidence for an "instant freeze". Implications are that there was little or no volumetric transport of magma through the fissures. They note the consistent orientation of shear and tensional fractures penetrating minerals and matrix, and conclude solidification during a phreatomagmatic (presumably outgassing?) event. Agglomeratic textures and flow fabric apparent in some samples suggest a local fluidized condition for the magma, where the only vesicles noted are in coke inclusion (see Figure 22, later this text).

The dike intruded a well-developed east-west joint set (Figure 8) locally parallel to calcite veins and a strike-slip fault. The relationships are shown in more detail in Figure 9a.

Figure 8. Dike (left), joints and fault (top right corner) in roof (Tedeski, 2002)

Late shear zones, some with transverse fiber calcite veins near the contact and in the chilled contact (Figures 9b & c) suggest both a shear and tensional component post emplacement.

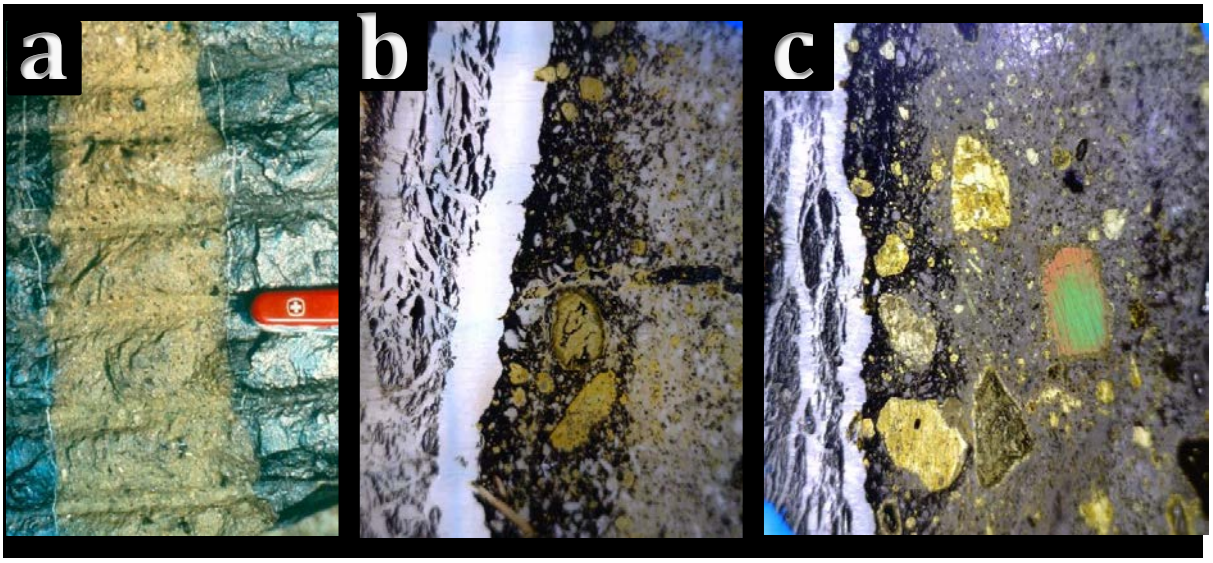

Figure 9a. Dike and calcite veins in roof (Gold, 1994)

Figure 9b. Shear with cross fiber calcite (thick vein) in "chilled margin." Sample PC1-1A.

Figure 9c. Sigmoidal calcite stringers in thick vein and cross-fiber calcite veins along dike contact. Sample TK-3.

Narrowness of the conduits and paucity of thermal metamorphism of shale and sandstone adjacent to, or as inclusions within the Tanoma dikes, indicates a highly fluid medium and relatively low emplacement temperature.

Incompatibility of high-temperature minerals and low thermal metamorphism is a paradox for kimberlite emplacement that has intrigued geologists for more than a century. However, estimating emplacement temperature is no trivial exercise. Thermal metamorphic effects are strongly dependent on the duration heat flowed from the dike into the country rock (Jaeger, 1961), and the latent heat of crystallization (heat capacity) of the magma (Szekely and Reitan, 1971). Szekely and Reitan (1971) modelled the distance a melt can travel in tabular conduits

before freezing and conclude that the heat loss from a 1 meter-thick dike of "normal" silicate magma under hypabyssal conditions would freeze less than 10 km from its source. A 10-m thick dike could be as long 28 km. Intrinsic and positional properties of magmas are density, viscosity, magma pressure, heat capacity, latent heat of fusion, heat loss and thermal diffusivity between the magma and adjacent country rock, liquidus and solidus temperatures, and depth. Other critical factors include flow rate (velocity), time to solidify (freeze), and tectonic setting. A dike or fissure emplacement mode is favored in terranes under tectonic tension (high vertical stress) and sills in compressional regimes, where $\sigma 1$ is essentially horizontal.

Emplacement temperature are greater than those indicated by metamorphic changes in wall rock, and this discrepancy decreases with longer residence time and slow rate of magma cooling (Jaeger, 1961). The best estimates of emplacement temperature are likely to come from metamorphism of wall rock inclusions in the kimberlite. An innovative approach for estimating emplacement temperature uses Color Alteration Indices (CAI) for conodonts (Pell *et al*., 2015). Paleozoic carbonate xenoliths from the Chidliak kimberlite field on Baffin Island, Canada suggest heating temperatures of 460°C to 735°C, with some outliers 700°C to 935°C. A distillation study on tar, hydrogen, oxygen and nitrogen on unaltered coal and coke adjacent to the Masontown (aka Gates-Adah) dike in southwestern Pennsylvania, led Sosman (1938) to deduce (sans burial-depth corrections) that the maximum temperature reached by the coke was between 440°C and 520°C, and an emplacement temperature not exceeding 600°C. Based on carbonate content he speculated on a state of "hot plastic stiff mud" for the magma. An attempt to apply metamorphic grade on Tanoma Mine samples (Dobransky, 1986) found changes in fixed carbon, ash and volatiles correlate with a logarithmic rise in vitrinite reflectance from 1.0% to 4.5%, but Dobransky was able only to constrain the temperature to >325°C for the transformation of kaolinite/illite in shales, 60 cm from the dike, to kaolinite/smectite closer to the contact. Preliminary studies by Mitchell and Davis (1996) and (Mitchell *et al*., 2015) using reflectance data suggest an emplacement temperature of approximately 500°C for coke from Main A Entry l-3. A refinement of their data is presented in Part II.

Geology of the Dixonville Dike

Honess and Graeber (1926) describe the dike as a porphyry with phenocrysts of olivine, phlogopite, light-green pyroxene (diallage), jet-like crystals of "glassy" ilmenite, "massive to rounded or subangular crystals of dolomite", and serpentine-rich patches in a carbonate/serpentine matrix. Accessory minerals include rutile, perovskite, titaniferous magnetite, pyrrhotite, rare spinel and red garnets (up to 4 mm). At least three stages of carbonate mineralization are noted, and the authors suggest hydrothermal alteration for the high CO_2 and water content (the quench values in Table 1 are a lower limit). Although they call attention to the lack of metamorphosed shale inclusions, and only an 8-inch thick coke aureole, they do not address an emplacement temperature.

A resurgence of interest in igneous carbonates during the 1960's led Peter Deines to examine the carbon and oxygen isotopic composition of calcite and dolomites in freshly collected samples. Deines (1968) found (a) an extreme variability of the C^{13} concentration over short distances, (b) the heaviest terrestrial carbon (12 to 24.8‰) in any geologic environment, (c) a striking correlation between the carbon and oxygen isotopic composition, except for the lighter carbon

values, and (d) a systematic gradient from light carbon at the margin to heavy in the middle of the dike.

Geology of the Tanoma Dike

The kimberlite intrusions in the Tanoma Mine are exposed in the gently dipping seam of the lower Kittanning Coal (Figure 2) in the Allegheny Group, at a depth of 180 to 400 feet below the surface. Tedeski (2002) provides detailed observations on the dike. Most exposures reveal a steeply dipping single dike oriented 264°/84°. Local offsets impart an overall pattern of *en echelon* sheets (vertical to horizontal) from 1 to 18 inches thick that extend through the mine working for some 7200 feet. In most places the dike is apparent both in the roof and floor, with segments of the intrusion transecting as well as terminating (up, down and sideways) in coal and overlying shale. Flow textures indicate upward, lateral, and downward movement. The dikes appear to intrude along mode 1 fractures (joints) rather than adjacent strike-slip faults with the same attitude.

Figure 10. Dikes from floor and roof terminating in 48-inch coal seam. Main Drive L-1 west (Tedeski, 2002)

Tedeski (2002) mapped the westernmost exposure as a dike 6 inches thick in the Main A, R1 entry, near Station 1352, with an attitude of 264°/84°. At station 1348, the dike changes to a sill (wedge) 37 inches long, tapering to the southeast, pinching out after 6 feet in the roof, and reappears 3 feet to the north as an 8-inch thick dike that is continuous along strike over the next three entries. Near Main Drive L-1 *en echelon* dikes from the roof and floor terminate in the coal (Figure 10).

At the L-3 Entry, the dike is 12 -13 inches thick in the roof, tapers towards the floor and forms a sill, 15 inches thick and 52 inches long in the coal, (Figure 11). The floor to roof height is 48 inches, and the coked aureole is at least 4 - 8 inches thick. This was selected as the main sampling site for coke and coal because of the limited volume of kimberlite dike to have flowed through this terminal sill. Coal and coke samples from this setting, sampled by Mbalu-Keswa and Gold in 1994, are identified as I-94 1 to 1-94.15 in the sketch (Figure 12). Note the small steeply dipping appendage at the distal end of the sill. Some coal balls were recovered from 3 to 6 inches beneath the sill. The coal balls occur in mesophase coke 3-6 inches from the contact. Five textural zones, extending for 7.5 inches from an 18-inch thick dike, are apparent in the metamorphic

Figure 11. Dike from roof, to a sill in the coal, and wedging out in the floor. The white coating (top left) is rock grout (Gold, 1994)

aureole in the coal exposed in the D-6 track entry. These grade from 2.5 inches of hard coke and calcite, to "baked" coke (2 inches), then into mesophase, "coal ball" zone 2 inches thick, and into shiny, weakly cleated coal (±1-inch), and back to normal coal with cleats preserved. Maceral changes are likely to be more refined.

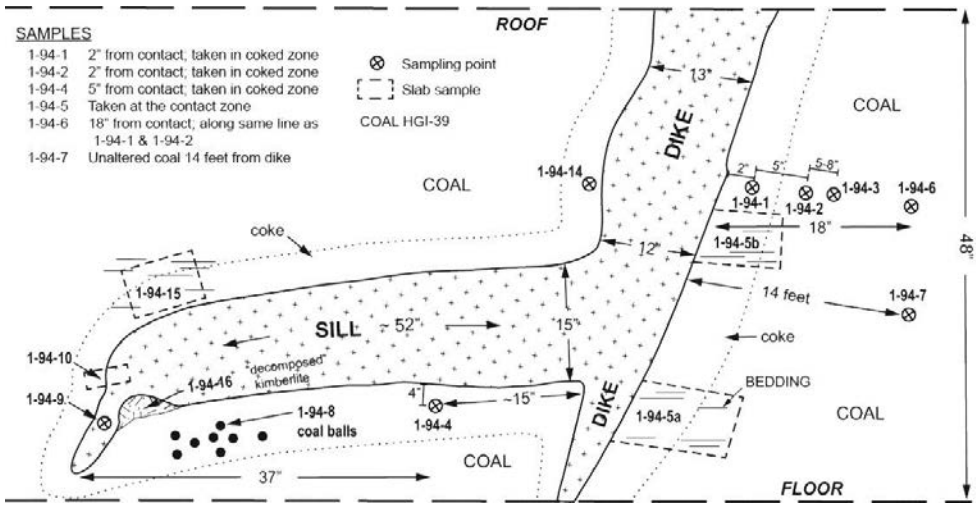

Figure 12. Sketch of wall at MD L-3 entry, the main sampling site for coke and coal (Mbalu-Keswa and Gold, 1994)

A 16-inch thick dike through the floor, coal, and roof is exposed for 410 feet again in Section D2 near Station 4822, disappears in a blind cut of 20 feet and reappears without change for another 350 feet. The strike of the changing dike is N84°W with a lateral shift 4 feet to the north. However, there is a change east of the pillar to N76° E and a bifurcation into a 12-inch northern and 5-inch southern fork, 5 feet apart. The next pillar exposes the dike trending N83°W split into a 10-inch thick northern and 2-3 inches thick southern segment. Both segments enter a barrier block of coal approximately 40 feet apart, where a garnet megacryst (1.5 inches across) was recovered from weathered kimberlite. At the next entry the dike is exposed for 4.5 feet above the coal seam in the "intake air belt overcast", where it splits and jogs through the hanging wall sandstone sub-parallel to a strike-slip fault at Main D R 2-3 (Figure 13)

Figure 13. Dike in coal and fractures adjacent to strike-slip fault in H/W shales and siltstones. Main Drive R 2-3 (Tedeski, 2002)

Along Main D are single and *en echelon* dike segments as well as dikes from the floor and roof that terminate in the coal. Single and multiple dikes, ranging from thin selvages to 8 inches, were exposed in a highly weathered state along several Main D entries. In the L1 entry, near section D5, a polished garnet 1.5 inches across (Figure 14) was recovered. Coal balls (Figure 15) and elongate forms of mesophase coke in the metamorphosed aureole were collected at the D5 track

entry. At Section D6 airlocks the dike is 19 inches thick in the roof and floor, 36 inches in the coal, with phenocrysts of phlogopite 5 by 7 inches, chrome diopside up to 5 inches long, and dolomite nodules 3 by 4 inches. Garnets are abundant.

Figure 14. Megacrysts of garnet from weathered (decomposed) kimberlite. L-1 Entry, near D-5. (Tedeski, 2002)

Figure 15. Meso-state balls (apples) of coke 6-8 inches from contact. D-5 track entry. (Tedeski, 2002)

Dike segments are exposed in Main D, between D6 and D5. At the left rib of the belt entry "fingers" in the coke (mesophase thermoplastic deformation?) are exposed in decomposed (weathered?) kimberlite. The "fingers" point slightly upward to N85°W (Figure 16) and appear to have been incorporated in a kimberlite melt flowing eastward.

Figure 16. Finger of coke pointing upward to west in decomposed kimberlite. Left rib of belt entry, Main Drive. (Tedeski, 2002)

At the Entry to D5 airlock door, two dikes 9 inches and 7 inches thick are exposed in the roof, separated by 5.5 feet of coke and coal in the coal seam, and by 5.5 feet of shale in the roof. Along Main D belt a pod of breccia is exposed adjacent to the dike (top left and bottom right in Figure 17). The "breccia" consists of angular fragments of coke and coal shot through by carbonate veins, many of which are lens–shaped.

Figure 17. Breccia consisting of coal and coke fragments in a matrix of carbonate veins, along contact with dike (top left and bottom right). Main D belt. FOV 3 feet. (Tedeski, 2002)

These dikes thicken (bulge) to 29 and 26 inches respectively in the coal. In the next Entry D5B, on MD R-2, the dike, 18 inches thick in the floor and 17.5 inches in the roof, bulges smoothly into an oval-shaped cylinder approximately 104 inches wide in the center (Figure 18; looking east).

Figure 18. Bulbous sill in coal, looking east. Note only a single dike in floor and roof. Axis of sill is 104 inches. MD R-2. The overlapping circular pattern are scour marks from the continuous miner. (Tedeski, 2002)

A quasi conformable relationship of an incipient kimberlite "sill" overriding thin (1-3 cm) layers of coke on well-bedded underclay is apparent (Figure 19). The feeder dike is exposed in the lower right corner. Apart from an increase in the number of calcite veins and stringers, the dike to sill transition in the coal is a remarkably simple, perhaps even passive event.

Figure 19. "Sill" of kimberlite, quasi-conformable to the underlying underclay bed, marked with the pencil. Note the coke wedge on the left side between the carbonate veined kimberlite and the underclay, and the dike phase in the lower right corner (Tedeski, 2002)

This "bulbous sill" can be traced for at least 50 feet along strike. The view to the west (Figure 20) shows a single dike in the floor, "ballooning" in the coal to 109 inches, and two dikes, respectively 11 inches (north) and 9.5 inches (south) in the roof.

Figure 20. Bulbous sill in coal seam, looking west. Note the two dikes on the left and the thin apophysis offset by a bedding fault on the right. For scale the hammer is 13 inches long: the long axis of the "sill" is 109 inches. (Tedeski, 2002)

In addition there is an intrusive stringer (top right) of kimberlite that is offset along a bedding fault in the hanging wall of the coal seam (Figure 21). We deduce that the displacement occurred during the expansive phase of sill development.

Figure 21. Apophysis of kimberlite off "bulbous sill", truncated on bedding fault in roof. The displacement is in the direction of sill propagation. (Tedeski, 2002)

The last exposures (3 segments of dike) are at the end of the rooms to the left of D5, the limit of the mining.

Mineralogy and Petrology

Samples from all Indiana County dikes are porphyritic micaceous kimberlites hosting olivine, phlogopite and chrome-diopside, and picro-ilmenite and garnet (including G9 varieties) as phenocrysts, megacrysts and microcrysts. The term megacryst is preferred because many of the phenocrysts are broken fragments. Other accessory minerals typical of kimberlites are titaniferous magnetite and perovskite. Despite the variation in texture, distribution, concentration and type of phenocrysts/megacrysts apparent in mapping, as well as in hand specimens, there is a commonality of a distinctive mineralogy. These are summarized in **Table 1**.

Olivine (mostly pseudomorphed by serpentine and calcite) dominates the megacryst assemblage. The matrix minerals include euhedral olivine, phlogopite, perovskite, spinel, diopside, monticellite, apatite, zircon, calcite, and late-stage serpentine (Mbalu-Keswa, 1995). The most common xenoliths are local country rocks and coke, some as rounded vesicular clasts with carbonate infill (Figure 22), and rare dolomitic nodules (Figure23). The contact (upper left corner in Figure 23) shows cleated coal adjacent to agglomeratic kimberlite (Figure 24). A coarse-grained dolomite(?) nodule occurs less than 50 cm from the contact (Figures 23 and 24).

Kimberlites are composite assemblages of minerals and rocks from both the source and transit localities entrained during emplacement. Their brecciated nature and porphyritic texture inhibits the development of equilibrium assemblages and complicates radiometric age-dating measurements. A porphyritic texture signifies an interrupted emplacement history with significant residence time for some crystallization of phenocrysts in an intermediate magma chamber(s). Compositional differences between phenocrysts and their kindred species in the matrix are likely.

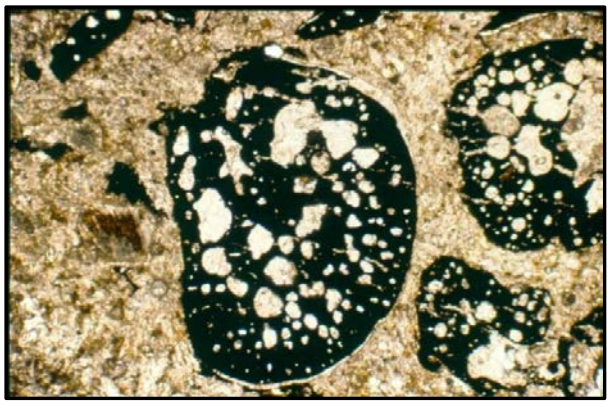

Figure 22. Vesicular coke pellets in kimberlite. FOV 1.5 cm. (Mbalu-Keswa, 1995)

Polymineralic lithic inclusions (xenoliths) represent the equilibrium assemblages amenable for petrogenetic analysis, but no suitable specimens were found at Tanoma. However, a proxy for these may be the assemblages in the "bleb" inclusions in the pyroxene and garnet megacrysts.

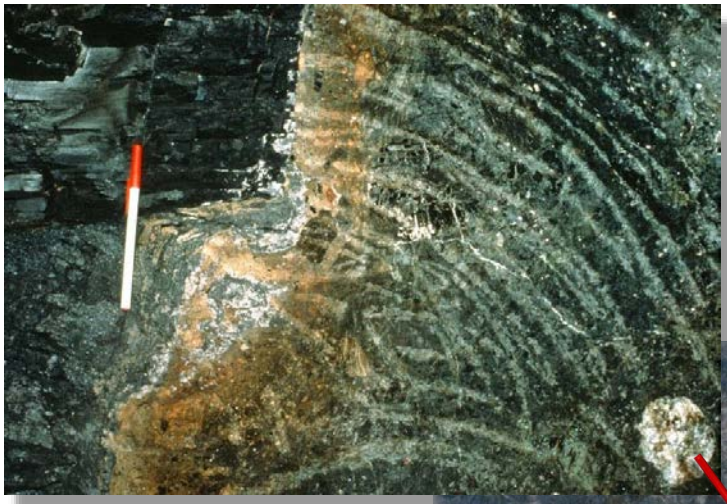

Figure 24. Cleated coal (top left) in contact with kimberlite. Details on texture surrounding dolomite nodule (lower right) are shown in Figure 24 below. D-6 track (Tedeski, 2002)

Figure 23. Dolomitic xenolith (white) in kimberlite agglomerate (Tedeski, 2002)

TABLE 1. Chemical Analyses and Mineral Components of Pennsylvania Kimberlites

	Whole Rock						Mineral
Major	I		II	III	IV	V	VI
	Dixon-		Tanoma	Tanoma	Sandy	Mason-	Ernest
(wt %)	ville		D5	D6	Ridge	town	garnet
SiO2	14.48		23.28	27.15	24.09	28.83	44.60
TiO2	1.56		1.82	2.32	1.58	5.67	0.48
Al2O3	5.44		1.78	1.69	3.52	2.94	20.54
Fe2O3	7.23		9.24	9.96	7.62	9.30	
FeO	3.13						4.40
MnO	0.27		0.17	0.18	0.19		0.28
MgO	22.53		26.40	24.69	15.26	24.31	21.40
CaO	18.21		12.43	12.26	21.39	11.24	4.84
Na2O	0.53		0.21	0.22	0.15	0.75	
K2O	0.45		0.59	0.54	1.35	1.31	
P2O5	0.39		1.22	0.87	0.64	0.77	
H2O+	8.46				4.41	3.96	
H2O-	0.38	LOI	23.04	19.64	2.48	0.83	
CO2	17.51				15.5	11.34	
S	0.28						
Total	100.86		100.18	99.52	98.44	100.98	99.99
Cr2O3							3.35
NiO							0.1
Trace Elements in ppm							
	Ba		856	695	1663		
	Cr		1187	1420	1150	185	
	Nb				166		
	Ni		493	588	564	700	
	La				144	142.5	
	Ce				368	270	
	Nd				114	85	
	Sm				15.7	13.35	
	Eu				4.23	3.25	
	Gd				9.75		
	Dy		493	588	5.11	3.4	
	Rb		18	19	45		
	Sr		382	321	1372		
	V		155	163	181		
	Y		7	8			
	Zr		122	93	269	13.75	
	Th				23.4	17	

Tanoma Samples (after Mbalu-Keswa, 1995)		
MINERALS IDENTIFIED (Relative Abundance)		
Mineral	***Common***	***Rare***
XENOCRYST:		
Dolomite?		*
MEGACRYST:		
Olivine	XX	
Ilmenite	XX	
Garnet	X	
Diopside	X	
Phlogopite	XX	
Spinel		*
GROUNDMASS		
Olivine	X	
Phlogopite	XX	
Spinel	X	
Carbonate	XX	
Serpentine	XX	
Perovskite	X	
Apatite		*
zircon		*
Monticellite		*
Pyroxene		*
BLEBS (inclusions in pyroxenes and garnets)		
Phlogopite	X	
Ilmenite	X	
Calcite	X	
Olivine	X	
Perovskite		*
Apatite		*
Spinel		*

I = Dixonville Dike,Barr Slpe Mine (Wet chemical analysis from Honess and Graeber, 1926)

II = Tanoma D5 (XRF analysis from Mbalu-Keswa, 1995)

III = Tanoma D6 (XRF analysis from Mbalu-Keswa, 1995)

IV = Sandy Ridge ACT-Labs, Ontario, Canada (from Gold and Doden)

V = Masontown. Majors from Kemp and Ross (1907). Trace elements from Shervais et al., (1987). Minerals include: pyrrhotite, pentlandite, chalcopyrite, and Pt-iron alloy in olivine megacrysts (Stone and Fleet, 1990)

VI = An average of 6 red garnets from Ernest sample: normalized to 100% (Smith and Barnes, 9/01/2016)

An interesting feature in the Tanoma dikes are "blebs" of polymineralic assemblages within megacrysts of pyroxene and garnet (Figure 25). The "blebs" range from a few microns to 1 mm in diameter, are circular, semi-polygonal to irregular in shape and do not appear to mimic the host's shape. Most of the "blebs" are spherical and are completely enclosed by the host, but a few irregular "blebs" occur as embayments on the margin. The blebs are interpreted as entrapped magma during the growth of the host (Mbalu-Keswa *et al.,* 1994). A phlogopite inclusion was noted in an olivine megacryst.

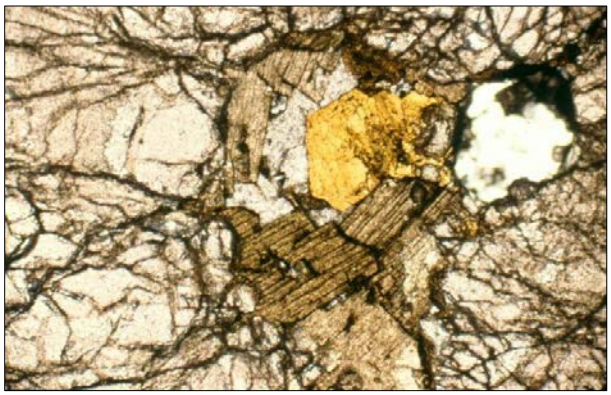

Figure 25. Polymineralic inclusion in garnet megacryst. Plain light. FOV 2.5 mm. (Mbalu-Keswa, 1995)

The following description on selected minerals in the Tanoma kimberlite are taken from the thesis by Chuma Mbalu-Keswa (1995).

Olivine

Olivines and its pseudomorphs are the most obvious mineral in the Tanoma kimberlite. They occur as megacrysts, microcrysts in the matrix, and in polymineralic "blebs" in pyroxene megacrysts.

Megacrysts ranging from 1-8 cm long, as well as fragments with rounded margins. Many exhibit marginal reaction rims and some show compositional zoning (Fe enrichment) on backscatter electron (BSE) images.

Euhedral and subhedral microcrysts in the matrix, range from 100 to 500 microns across. Most are altered to serpentine.

Olivines in the polymineralic "blebs" in pyroxene are 100-350 microns long and are distinctly enriched in MgO (Fo_{88} to Fo_{91}).

Pyroxene

Two distinct varieties of clinopyroxenes are apparent:

An emerald green, well-cleaved euhedral Cr-rich pyroxene (chrome diopside) up to 6 cm across (Figure 26).

A lighter greenish-gray, Cr-poor variety as large as 10 cm across. The latter contain polymineralic inclusion or "blebs" consisting mainly of phlogopite, ilmenite, and titanomagnetite in a carbonate matrix. Despite their physical difference their chemistry is similar.

Figure 26. Polymineralic inclusion in garnet megacryst. Plain light. FOV 2.5 mm. (Mbalu-Keswa, 1995)

Other clinopyroxenes occur within the "blebs", and these differ from those in the host kimberlite matrix in their greater TiO_2 content.

Orthopyroxenes are suspected amongst the altered and serpentinized megacrysts and microcrysts, particularly those with euhedral and subhedral outlines. They may have been more abundant than the 0.4% noted by Shultz (1999) in Tanoma samples.

Ilmenite

Tanoma ilmenites are glassy magnesium-rich ilmenites (picro-ilmenites of a bygone generation), with relatively constant MgO values ranging from 9.4 to 11.46%. Four paragenetic types have been recognized (Mbalu-Keswa, 1995).

1. Large (up to 5cm across) rounded to irregular-shaped single crystals with carbonate veinlets and fractures containing small phlogopite crystals similar to those in the matrix (Figure 27). These are interpreted to be xenocrysts rounded by abrasion during transportation.
2. Large subhedral crystals up to 3 cm across.
3. Small (50 to 100 µm) euhedral to anhedral crystals dispersed in the groundmass. No chemical data are available.

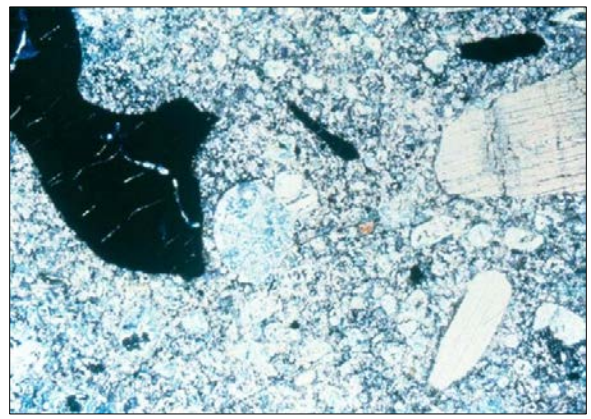

Figure 27. Ilmenite, olivine and phlogopite megacrysts in globular textured matrix. Plane Light. FOV 2 cm (Mbalu-Keswa, 1995)

4. (a) Small rounded grains, 50-100 µm across, occur in the multiphase "blebs" in pyroxenes, and more rarely in garnet megacrysts, where they occur as one of the most abundant phases. The trend in the ilmenites within the "blebs" is low MgO with increasing Cr_2O_3, in contrast to larger crystals in the matrix with higher MgO and a decrease in Cr_2O_3 with an increase in MgO. A possible chemical discriminator is "low chrome, low magnesium".
   (b) Small euhedral (rectangular) grains in a similar setting and association as 4a, are Cr-poor relative to their round neighbors.

Chemically there is a separation between Cr- rich and Cr-poor ilmenites megacrysts at approximately 2.5 % Cr_2O_3. In the latter Fe is enriched at the expense of Mg. The cores of the subhedral megacrysts analyzed show remarkably uniform Ti, Fe and Mg content. However the reaction rinds preserved on some of the more regular faces show a marked enrichment in iron, and in some also alumina (Cassidy, 2015).

The reaction rims, ranging from 5-30 µm thick (Figure 28), are enriched in Al, Mg and Fe and depleted in Ti and Cr: and contain discrete spinel phases of titanomagnetite and magnetite (Borella, 1997). A non-uniformity of reaction rim development around all or part of the megacrysts is interpreted as local fragmentation of a late iron-enrichment oxidation trend of relatively short duration (Borella, 1997). Pre- and syn- reaction rim developments in micro-veins

are consistent with fragmentation events prior to and during emplacement. Elemental components in the EDEX spectrum of the veins (and their likely mineral phases) include: Fe (magnetite); Mg + Si (olivine); Ca + Mg +C (calcite/dolomite), Ba + S (barite). The late veins are composed primarily of carbonates and are clearly post-emplacement phenomena.

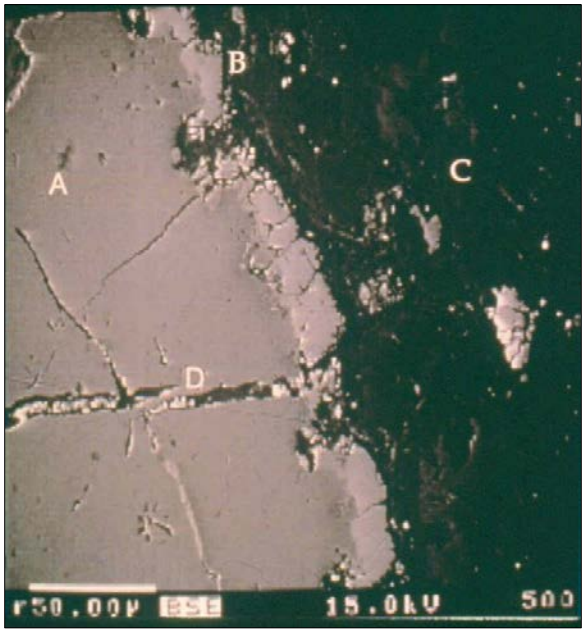

Figure 28. Back-scatter image of ilmenite, spinel in rim and matrix. FOV 5500 µm. (Borella 1997)

Phlogopite

The most distinctive mineral characterizing the Tanoma kimberlite is phlogopite. It occurs as megacrysts and microcrysts in the groundmass, and the polymineralic "blebs" in garnets and pyroxenes, and modally are second only to olivine. All are titanium rich (TiO_2 values from 1.74 to 2.70%), with SiO_2 steady in the range of 38.59 to 41.97%. There is no obvious chemical discriminant between matrix and "bleb" phlogopites except for a slightly greater chrome content (> 0.5% Cr_2O_3) in the latter. The megacrysts crystals have yet to be analyzed.

Dark brown to bronze-colored phlogopites are ubiquitous as megacrysts, as well as microcrysts in the matrix. They occur as large euhedral crystals typically less than 8 cm across (Mbalu-Keswa, 1995), but Tedeski (2002) records some from 12 -18 cm across. The booklets typically are intergrown with carbonate along the cleavage planes. Many of the larger crystals are distorted and kinked (Figure 29), and generally have corroded margins.

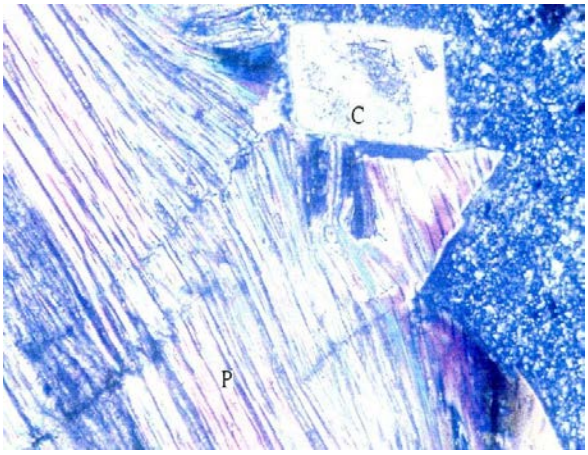

Figure 29. Phlogopite megacryst, with calcite laminae on cleavage. Crossed Nicols. FOV 2 mm. (Mbalu-Keswa, 1995)

The groundmass phlogopites occur as small laths that only locally show a flow-alignment fabric.

Phlogopites also populate the polymineralic "blebs" in clinopyroxenes and garnet, and may occur as single crystals in olivine. The former occur as laths up to 5 mm long and are well-preserved with sharp outlines. In some pyroxene hosted "blebs" the laths are distorted and exhibit reaction margins. Others are intergrown with an unidentified, Mg-rich silicate phase (37.3 % MgO; 34.5% SiO_2; depleted in Al_2O_3 (0.3%) and CaO (0.18%)).

Garnets

Most of the garnets are reddish brown and range in size from 0.1 mm to 5 cm. They typically occur as rounded isolated crystals or as irregularly-shaped fragments. Less than 25% of the analyzed samples have a corona of kelyphite (see Appendix 1 image 8). They are mainly titan pyropes, or G1 garnets in the Dawson and Stevens (1975) classification. Borella (1997) examined the reaction rinds, typically 5 to 20 μm thick, around G-1, Cr-poor pyrope. These showed a decrease in silica and alumina and a marked increase in K_2O and H_2O in the rims.

Polymineralic inclusions in garnet consist mainly of phlogopite and calcite with accessory amounts of pyrite (?), apatite, sphalerite, ilmenite and zircon. From a limited number of analyses, garnets with inclusions appear to be slightly enriched in Cr_2O_3 and depleted in TiO_2.

Unusual pyrope garnets exhibiting color changes from daylight to fluorescent lighting conditions (alexanderite effect) were collected from the Gates-Adah kimberlite (Smith and Barnes, 2006). Embedded in a supplement to this report are SEM analyses of 58 pyrope garnets from Tanoma (collected on the Smith and Skema excursions in 1982 and 1984). This population contained six G1, six G3, and forty four G9's (16 were judged normal, 4 as low Ca and 9 as low Fe, 14 with both low Ca and Fe, and 2 with low Ti. There were two anomalous garnets with high Mg. These compositions are not favorable for the preservation of diamonds (Doden *et al.,* 1998).

Spinels

The spinels, mostly titanomagnetites occur as:

(1) Relatively rare rounded megacrysts up to 1 cm in diameter.
(2) Very small (< 1 μm) crystals in the matrix. No analyses are available, but reddish outlines on some grains suggest incipient oxidation.
(3) Clusters of small (100-500 μm) magnetite crystals along the margin of serpentinized olivines.
(4) Micron-size crystals of magnesian-rich titanomagnetites(?) occur in polymineralic inclusions in pyroxenes. They exhibit some unusual chemistries. High MgO in the 5-6% range, TiO_2 (11.25 to 16.21%), FeO (33.74 to 37.79%), $Fe2O_3$ (37.13 to 44.42%), and less than 0.3% Al_2O_3. Cr_2O_3, typically in the 1.18 to 1.98% range, reaches a value of 10.38% in one analysis.

Micro-veins

Several stages of micro-veins are apparent in many of the megacrysts of garnet, pyroxene and ilmenite. Early veins in the garnets occur wholly within the megacryst, a second set that pierces or occurs between the reaction rim and the host, and later veins that extend through the megacrysts in to the matrix.

Barite was detected in some early stage internal veins; carbonate (calcite and dolomite) in the late through-going veins. The former may represent deformation during, and the latter post emplacement (Borella, 1997).

Emplacement Depth and FO_2 Considerations

The coal resources in the Appalachian foreland basin have stimulated many studies on the coal rank and the thermal regimes. White's (1925) regional carbonization map (fixed carbon, dry, ash-free) shows the 65-75 isocarbs for Indiana County. The burial depth at the time of

kimberlite emplacement (assumed 160 to 180 Ma) is variously estimated as 2.1 to 2.9 km from fission track annealing data on apatites (Blackmer, 1992), and 3.4 km from vitrinite reflectance of coal (Zhang, 1992). Paxton (1983) concluded that coal rank and reflectance were produced before folding and thus supported a burial depth of approximately 3-4 km over the High Plateau. Bulk density/porosity/compaction measurements on Lower Allegheny sandstones (Chou, 1985) showed a steep gradient over the High Plateau, consistent with the isocarb data, and Paxton's estimate. A variable heat flow is inferred for blocks within the basin (Blackmer, 1992) who notes an elevated thermal anomaly in the vicinity of the Gates-Adah kimberlite. From fission track annealing dates in apatites, and vitrinite reflectance temperatures, Blackmer (1992) and Blackmer *et al.,* (1994) were able to reconstruct the following unroofing history of the Appalachian foreland basin. From the end of the Alleghenian Orogeny into the Jurassic unroofing was rapid and greater in the east than the west. This was followed by a quiet period of relatively little erosion into the Miocene, and then rapid unroofing to the present (Blackmer, 1992). The unroofing history is important because vitrinite reflectance data record maximum temperature and not the temperature adjusted for the amount of erosion at the time of kimberlite emplacement. The probable burial depth of 2.3 to 2.9 km for a mid-Jurassic age for intrusion coincides with a tensional regime of drift and subsidence of the North American passive margin.

Temperature and log f_{O2} data were attained from Fe-Ti geothermometry and geobarometry calculations using the Andersen and Lindsley (1988) model for ilmenite-spinel pairs in pyroxene-hosted "inclusions". These range from 788°C to 882°C and from -12.5 to -14.5 atmospheres respectively (Mbalu-Keswa, 1995). With inferred emplacement conditions more oxidizing than either the FMQ and MW buffers, the preservation of any carbon polymorphs is negligible.

Tectonic Setting and Age of Emplacement

A Jurassic event is favored for the emplacement of these Pennsylvania kimberlites, based on stratigraphy and radiometric age dates (Shultz, 1999). Despite mineral equilibration difficulties a 167 ±3 Ma date from U-Pb in perovskites, in the Masontown dike, is considered tight (Smith, Pers. Comm., 2016), and in good agreement with the K/Ar dates of 176±10 and 188 ± 10 Ma, by Pimental *et al.*, (1975). In a later study (Bikerman *et al.,* 1994) found the fine-grained, matrix phase phlogopite to be younger (147±1.5 Ma) than the phenocrystic phlogopite (353.2±2.2 Ma). The Dixonville/Tanoma dikes intrude Alleghenian Group strata and are clearly post-Pennsylvanian in age.

Current attempts to determine $^{40}Ar/^{39}Ar$ crystallization ages on phlogopite megacrysts, as well as microcrysts in the matrix, from the Tanoma intrusion, are described below. Samples were hand-picked and 0.1 gm aliquots were measured by Chris Hall at the Argon Geochronology Laboratory at the University of Michigan, following the protocol of Hall and Farrell (1995). The Tanoma phlogopites yielded total gas ages of 551.2 ± 1.4 Ma for the megacrysts and 516.2 ± 1.4 Ma for the microcrysts. Their plateaus are relatively flat and yield similar (within the reported error) ages to the total gas ages. The MSWD (mean square weighted deviation) for the age calculations are less than 1.5. Interpretation for these ages is complicated by their complex petrogenesis and because they pre-date the host strata. Other studies of phlogopite in kimberlite occurrences have yielded similar geologically older than host rock ages. Phillips and Onstott (1988) demonstrated that phlogopites from kimberlites have zoned age determinations within

crystals and attribute the disequilibrium to acquisition, by diffusion, of excess argon during and after crystallization. This excess argon anomaly in the Tanoma samples has yet to be resolved. Most likely the reported ages here possess the same isotopic disequilibrium.

The alignment of isolated kimberlites in a northeast trending belt from Tennessee through New State coincide with the axis of the Appalachian foreland basin (Figure 30).

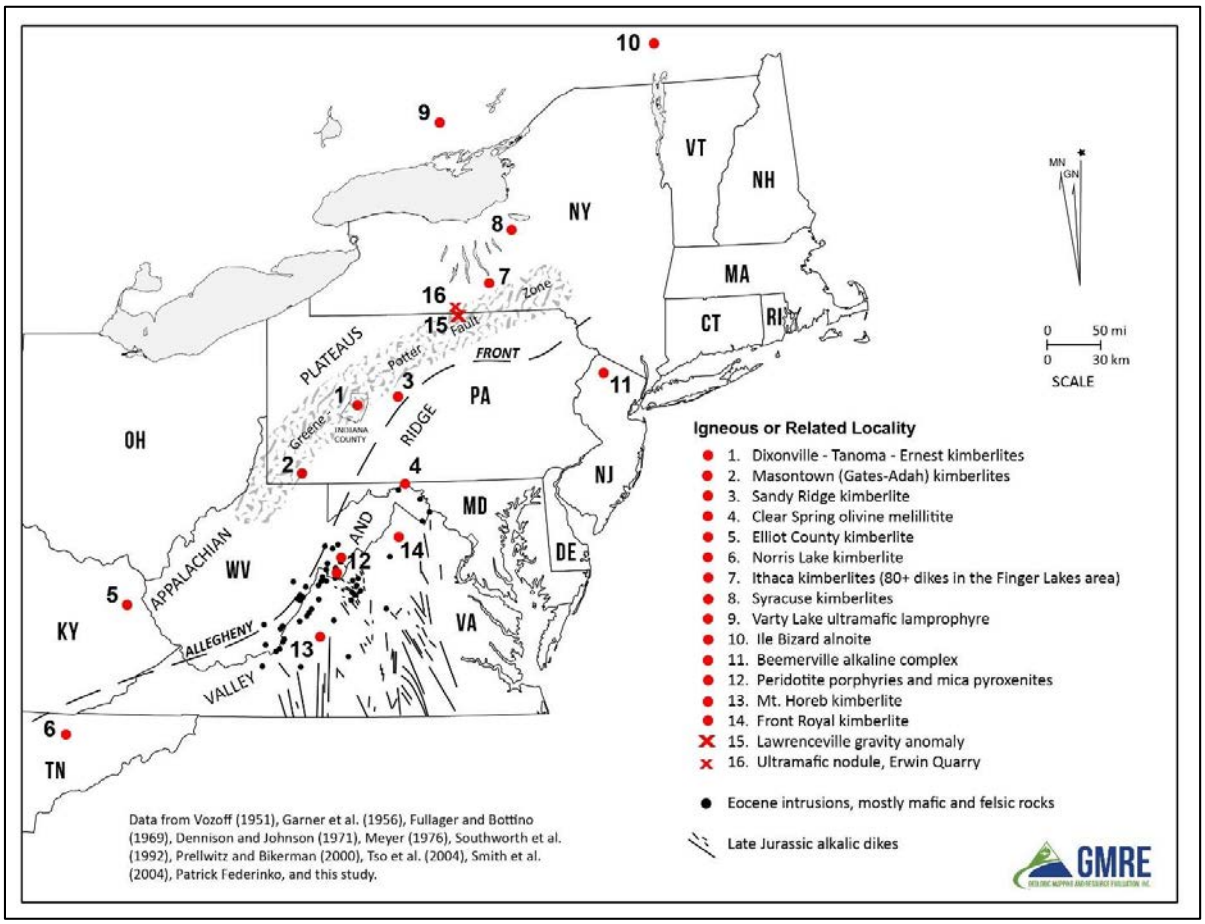

Figure 30. Regional map showing locations of kimberlites and other ultramafic/alkaline rocks in Pennsylvania and nearby states. Greene-Potter fault zone adapted from Root (1978) and Parrish and Lavin (1982). Also illustrated is the Allegheny structural front that marks the boundary between the Appalachian Plateaus and Valley and Ridge Provinces.

Sub-surface structures include the Rome Trough graben and the Greene-Potter fault zone (Root, 1978), which overlie Grenville Basement. The basin-axis trend from Mannheim, Syracuse and Ithaca, New York to Dixonville and Masontown, Pennsylvania is reinforced if one infers that a 15-milligals anomaly approximately 12 miles in diameter, that is centered on Lawrenceville, Tioga County, Pennsylvania (Vozoff,1951) represents a local, high density intrusion. No surface exposures have been reported, but a garnet lherozolite nodule approximately 30 cm across was recovered by Pat Federenko from the nearby G.O. Hawbaker, Inc., sand and gravel quarry at Erwin, New York. An emplacement age of 139 Ma (Basu *et al.,* 1984) for kimberlites near Syracuse in New York, and Ile Bizard in Quebec (spatially associated with the Oka Carbonatite Complex, dated as 117 Ma) may define a northward younging trend.

A more diverse variety of relatively small intrusive centers is exposed east of the Allegheny Front (see Figure 30). These include clusters of Eocene alkali plugs in Virginia and West Virginia and swarms of Jurassic dikes, as well as some older ultramafic bodies such as kimberlite at Mount Horeb, Virginia, olivine melilitite flows and tuffs at Clear Springs, Maryland (433± 3 Ma and 436±4 Ma) (Smith, 2004), and a 435±20Ma age for an alkali complex at Beemersville, New Jersey (Zartman *et al.*, 1967). However, all occur in significantly different allochthonous hosts.

G-9 garnets have been recovered (Smith and Barnes, Pers. Comm., 2016) from a number of these sites (Ile Bizard, Portland Point, N.Y., Tanoma, Gates-Adah, Mount Horeb, and the Clear Spring diatreme tuff) on both sides of the Allegheny Front. It is noteworthy that high Cr pyropes in the Gates-Adah dike are inferred to come from a peridotitic environment (ibid).

Cross-strike, essentially vertical discontinuities in the crystalline basement terrane are apparent in the regional gravity and magnetic maps (Alexander *et al.,* 2005). Parrish and Lavin (1982) suggest that deep-seated, cross-strike basement fractures were reactivated during the Jurassic reopening of the Atlantic Ocean. There are convincing correlations for Ile Bizard, as part of the Monteregian Hills intrusive trend along the Ottawa-Bonchere Graben (Krumapelli, 1970), and the Lawrenceville gravity anomaly on the Attica-Lawrenceville lineament (Parrish and Lavin, 1982). The Gates-Adah dike parallels but does not coincide with the basement, Highlandtown fault zone on the Pittsburgh-Washington lineament, but Roen (1968) concluded the dike intruded a preexisting strike-slip fault of minimal left-lateral movement. He called attention to "northwest-trending transcurrent structural lineaments, -…- considered to be reflections of differential movement along the margin of a subsurface decollement". The Dixonville/Tanoma Dike overlies the 140° trending Home-Gallitzen basement lineament (Alexander *et al.,* 2005). However, the 086° strike of the Dixonville/Tanoma dike is not consistent with basement fractures trajectories, nor is it apparent in the overlapping sets of physiographic lineaments (110° and 140°) mapped from LANDSAT imagery (Gold, 1999). The kimberlite "intrusion" at Sandy Ridge (# 12) is included despite its "phantom" nature, because it is close to the Tyrone–Mt Union lineament. Intuitively, this model for the Appalachian Foreland Basin does not apply to the Clear Springs olivine melilitite and the Beemersville alkali complex in allochthonous tectonic settings.

The kimberlite has been emplaced through Proterozoic basement (Grenville crust of ± 1 billion year age) and Phanerozoic cover after at least the deposition of the Allegheny Group during the Pennsylvanian. In a recent study of the Gates- Adah dike Schultze and Hearn (2015) call attention to the presence of SiO_2-enriched spinels and speculate a buried UHP (ultra-high pressure) terrane beneath the Grenville. A diamond potential is indicated from the G9 garnets, and the equilibrium condition of the clinopyroxenes with respect to a steady-state subcratonic geothermal gradient to a surface heat flow of 40 mW/m^2 in the diamond stability field, despite its off-cratonic tectonic setting in the Appalachian foreland basin (Schultze and Hearn, 2015).

The fact that minerals in many kimberlites yield a crystallization age that predates emplacement and a porphyritic texture suggests a residence time below the Ar-blocking temperatures in a secondary magma chamber, or preservation of mantle argon. A gas-fluidization system is envisaged in which a reduction in temperature during upward migration triggers exsolution and outgassing of volatile components and promotes a large pressure build

up, sufficient to develop cracks and erode fissures through the crust, particularly in regions of tectonic tension (Gold, 1972).

Summary and Conclusions

- The rogue intrusions in Indiana County are carbonatized hypabyssal kimberlites.
- The Dixonville dike and the Tanoma dike are the same intrusion, and extend almost continuously from the lower Kittanning coal to the Lower Freeport coal through a vertical distance of approximately 180 feet.
- With a demonstrated vertical extent of several hundred feet in the underground workings, there should be surface crops. Their apparent absence is an enigma.
- The singularity of the Dixonville dike and the Masontown (Gates-Adah) dike is remarkable. They are essentially single-fissure, small volume events.
- The kimberlite dikes in Indiana County provide an opportunity to address problems of kimberlite emplacement relative to emplacement temperatures and habit of intrusion. Novel terms such as "bulbous sills" and "blades dikes" represent well-documented underground exposures, in which nearly flat-lying coal seams have played an important role. Relatively cold intrusion and long reach are part of this genre.
- The off-craton setting in the Appalachian foreland basin coincides with an extensional tectonic regime during the Jurassic and the opening of the Atlantic Ocean.
- Dike and sill habits suggest that magma pressure may have been in balance with lithostatic load; a condition that would have promoted a lateral (quasi- horizontal) component to crack development with only limited upward migration towards the surface. We propose that the coal seams provided a convenient escape sink for the outgassing volatile phases from the magma, stifling their upward migration.
- A volatile-rich kimberlite melt is inferred from the high H_2O and CO_2 content of emplaced kimberlite. We conclude that a fluid-rich melt, with a low heat capacity, was necessary for the emplacement of these thin dikes (cm scale) a long distance from their source.
- We propose that intrusion-induced hydraulic fracturing augments the emplacement of kimberlites in the thicker foreland basins coal seams.
- Heavy isotope work by Shank (1992) indicated a Sr^{87}/Sr^{86} ratio of 0.750 (quoted from Mbalu-Keswa, 1995), which is well within the Bristow et al., (1987) field for micaceous Group II kimberlites.
- The potential for diamonds is low.

Acknowledgements

Elizabeth and Frank Verterano, New Wilmington, Pa., and Timothy H. Folkomer, Springfield, Pa., for financial support of the age dating effort.

References

Andersen, D.J., and Lindsley, D.H., 1988, Internally consistent solution models for Fe- Mg- Mn- Ti oxides: Fe-Ti oxides: American Mineralogist, v. 73, p.714-726.

Basu, A.R., Rubury, E., Mehnert, H., and Tatsumato, M., 1984, Sm-Nd, K-Ar and petrologic study of some kimberlites from eastern United States and their implication for mantle evolution: Contributions to Mineralogy & Petrology, v.86, p. 34-44.

Bikerman, M., Prellwitz, H.S., Dembosky, J., Simonetti, A., and Bell, K., 1997, New phlogopite K-Ar dates and the age of southwestern Pennsylvania kimberlite dikes: Northeastern geology and environmental Sciences, v. 19, no. 4, p. 302-308.

Blackmer, G.C., 1992, Post-Alleghanian thermal and unroofing history of the Appalachian Basin, Pennsylvania: University Park, Pa., The Pennsylvania State University, Ph.D. thesis, p. 172.

Blackmer, G.C., Omar, G.I., and Gold, D.P., 1994, Post-Alleghanian unroofing history of the Appalachian Basin, Pennsylvania, from Apatite Fission Track Analysis and thermal models: Tectonics, v. 13, # 5, p. 1259-1276.

Borella, M.W., 1997, The Significance of Megacrysts and Xenocrysts in the Tanoma Kimberlite Dikes: B.S. thesis, p. 46.

Bristow, J.W., Allsop, H.L., Smith, C.B., and Skinner, E.M.W. 1987: Nuclear Active. Jan. p. 21-26.

Cassidy, P.H., 2015, A Study of Ilmenites from Tanoma Kimberlite: an assessment of diamond-bearing potential: University Park, Pa., The Pennsylvania State University, B.S. thesis p. 43.

Cassidy, P.H., Gold, D.P., Mitchell, H.D., and Feineman, M.D., 2015, An EPMA study of Ilmenite from the Tanoma Kimberlite, Indiana County, PA: Abstract and Poster, Materials Today Symposium, Penn State University.

Chou, N.H., 1985, An analysis of factors controlling the variation in porosity of Pennsylvanian Aged Sandstone of the Allegheny Plateau of Western Pennsylvania, *in*: Central Pennsylvania Geology Revisited, Annual Field Conference of Pennsylvania Geologists, 50th, State College, PA., Guidebook, p. 260-262

Coopersmith, H., P.G., 2014, Diamond Exploration in the USA: Prospectors and Developers Association of Canada: Power Point Presentation at Convention, Toronto, Canada.

De Wit, M., 2014, "World-class diamond deposits; Can we find them or are there no more?" Power Point Presentation at Convention, Toronto, Canada.

Dawson, J. B., and Stevens, W. E., 1975, Statistical Classification of Garnets from Kimberlites and Associated Xenoliths: Journal of Geology, v.83, p. 589-607.

Deines, P., 1968, The Carbon and Oxygen Isotopic Composition of Carbonates from a Mica Peridotite Dike near Dixonville, Pennsylvania: Geochemica et Cosmochemica Acta, v. 32, p. 613-625.

Dobransky, D.W., 1986, Coal and Clay Mineral Metamorphism Associated with the Dixonville Kimberlite Dike, Pennsylvania: Abstracts Geological Society of America, v. 18, no. 4, p. 286.

Doden, A.G., Mbalu-Keswa, C., and Gold, D.P., 1998, Geology and mineralogy of the Tanoma kimberlite, SW PA: Evaluation of diamond potential: Geological Society of America Program with Abstracts, v. 30, no. 1, Northeastern Section Meeting, Portland, ME, March 18-20, p. 14-15.

Doden, A.G., Altamura, R.J., and Gridwood, K.R., 2000, Mineralogy and chemistry of the Clear Spring Olivine Melilitite Intrusion and Associate Diatreme, Western Maryland: Abstracts Geological Society of America, New Brunswick, N.J., v. 32, no. 1, p. A-14.

Fullagar, P.D. and Bottino, M.L., 1969, Tertiary felsite intrusions in the Valley and Ridge Province, Virginia: Geological Society of America Bulletin, v. 80, p. 1853-1858.

Garner, T.E., Jr., 1956, The igneous rocks of Pendleton County, West Virginia: Report of Investigation No. 12, Geological and Economic Survey, State of West Virginia. 31 p.

Glover, A.D., 1981a, Commodore quadrangle, *In* Berg, T.M. and Dodge, C.M., eds., Atlas of preliminary geologic quadrangle maps of Pennsylvania: Map 61, Bureau of Topographic and Geologic Survey, PA DCNR.

Glover, A.D., 1981b, Clymer quadrangle, *In* Berg, T.M. and Dodge, C.M., eds., Atlas of preliminary geologic quadrangle maps of Pennsylvania. Map 61, Bureau of Topographic and Geologic Survey, PA DCNR.

Glover, A.D., 1981c, Ernest quadrangle, *In* Berg, T.M. and Dodge, C.M., eds., Atlas of preliminary geologic quadrangle maps of Pennsylvania: Map 61, Bureau of Topographic and Geologic Survey, PA DCNR.

Gold, D.P., 1968, Natural and Synthetic Diamonds and the North American Outlook: Earth and Mineral Sciences Bulletin, The Pennsylvania State University, v. 37, No. 5, p. 37-43.

Gold, D.P., 1972, Monteregian Hills: Diatremes, Kimberlite, Lamprophyres and Intrusive Breccias west of Montreal. Excursion B-10: 24th International Geological Congress, Montreal, Canada, Guidebook, p. 32.

Gold, D.P., 1994, The Nature of Kimberlite Intrusions in the Appalachian Foreland Basins: Lecture, and Abstracts with Program, Pittsburgh Geological Society, v. XLVII, no. 2. Oct. 19, 1994.

Hall, C.M., and Farrell, J.W., 1995, Laser ^{40}Ar-^{39}Ar ages of tephra from Indian Ocean deep-sea sediments: Tie-points for the astronomical and geomagnetic polarity time scales: Earth and Planetary Science Letters, v. 133, no. 3-4, p. 327-338.

Harris, P.G., and Middlemost, A.K., 1969, The Evolution of Kimberlites: Lithos, v.3, p.77-88.

Honess, A.P., and Graeber, C.K., 1924, A New occurrence of an Igneous Dike in Southwestern Pennsylvania: American Journal of Science, v. 7, no. 5, p. 313-315.

Honess, A.P., and Graeber, C.K., 1926, Petrography of the Mica Peridotite Dike at Dixonville, Pennsylvania: Mining and Metallurgical Experimental Station Bulletin, no. 2, p. 1-16. The Pennsylvania State College.

Hower, J.C., and Davis, A., 1981, Application of vitrinite reflectance anisotropy in the evaluation of coal metamorphism: Geological Society of America Bulletin, Part 1. v. 92, p. 350-366.

Jaeger, J.C., 1961, The Cooling of Irregular Shaped Igneous Bodies: American Journal of Science, v. 259, p. 721-734.

Kemp, J.F., and Ross, C.G., 1907, A Peridotite Dike in Coal Measures of Southwestern Pennsylvania: New York Academy of Science Annals, v. 17, p. 509-518.

Kumarapeli, P.S., 1970, Monteregian Alkalic Magmatism and the St. Lawrence Rift System in Space and Time: Canadian Mineralogist, v. 10, p. 421-431.

Law, E., Bear, S and Van Horn S., 2004, Petrographic Evidence of an Instant Freeze of Kimberlite Diatreme: Abstracts Geological Society of America, Northeast and Southeast Section Meeting, Tysons Corner, v. 36, no. 2, p. 71.

Marks, W.J., 1999, Generalized Geologic Columnar Section Bituminous Coal Measures.

Mbalu-Keswa, C., Gold, D.P., and Tedeski, J.R., 1993, Mineralogy of the Tanoma Kimberlites, Indiana County, Pennsylvania: Abstracts with Program, Friends of Mineralogy: Annual meeting & Symposium on World Class Mineral Deposits, p. 9-10.

Mbalu-Keswa, C., Gold, D.P., and Tedeski, J.R., 1994, Polymineralic "blebs" in pyroxene megacrysts from the Tanoma Kimberlites, Indiana County, Pennsylvania: Abstracts Geological Association Canada - Mineralogical Association of Canada, Annual Meeting, Waterloo, v.19, p. A-72.

Mbalu-Keswa, C., Gold, D.P., and Tedeski, J.R., 1994, Inclusions in clinopyroxene xenocrysts from the Tanoma Kimberlite, Indiana County, Pennsylvania: Abstracts Geological Society of America, Northeast Section Meeting, Binghamton, v. 26, no. 3, p. 60.

Mbalu-Keswa, C., 1995, Nature and occurrence of polyphaser crystalline inclusions in garnet and pyroxene megacrysts from the Tanoma kimberlite, southwestern Pennsylvania: University Park, Pa., The Pennsylvania State University, M.S. thesis, p. 73.

Meyer, H.O.A., 1976, Kimberlites of the continental United States: a review: Journal of Geology, v. 84, p. 377-403.

Mitchell, R.H., 1986, Kimberlites: Mineralogy, Geochemistry, and Petrology: New York, Plenum Press, 442 p.

Mitchell, G.D., Davis, A., Gold, D.P. and Cassidy, P.C. 2015, Coked Coal marginal to Kimberlite Intrusions in the Tanoma Mine, Indiana County, Pennsylvania: Abstract 264071, Session 236, Baltimore, Meeting Geological Society of America, v. 47, no. 7, p. 389.

Mitchell, G.D., Davis, A., Gold, D.P. and Cassidy, P.C. 2015, Coked Coal marginal to Kimberlite Intrusions in the Tanoma Mine, Indiana County, Pennsylvania: Abstract 264071, Session 236, Baltimore, Meeting Geological Society of America, v. 47, No. 7, p. 606.

Nelly, P., Bikerman, M., and Flint, N.K., 1975, A new K-Ar date on the Masontown dike, southwestern Pennsylvania: Pennsylvania Geology, v. 6/3, p. 5-7.

Parrish, J.B., and Lavin, P.M., 1982, Tectonic Model for Kimberlite Emplacement in the Appalachian Plateau of Pennsylvania: Geology, v. 10, p. 344-347.

Paxton, S.T., 1983, Relationships between Pennsylvanian-age Lithic Sandstone and Mudstone Diagenesis and Coal Rank in the Central Appalachians: University Park, Pa., The Pennsylvania State University, Ph.D. Thesis, p. 503.

Pell, J., Russell, J.K., and Zhang, S., 2015, Kimberlite Emplacement Temperatures from Conodont Geothermometry: Earth and Planetary Science Letters, v. 411, p. 131-141.

Phillips, D., and Onstott, T.C., 1988, Argon isotopic zoning in mantle phlogopite: Geology, v. 16, # 6, p. 542-546.

Prellwitz, H.S. and Bikerman, M., 2000, The petrography and geochronology of the Masontown, PA kimberlite intrusion: a summary, *in:* Harper, J. A., ed., Pittsburgh at the millennium: The impact of geoscience on a changing metropolitan area: Annual Conference of Pennsylvania Field Geologists, 65th, Pittsburgh, Pa., Guidebook, p. 50-55.

Radomski, S., 1975, Coal Apples associated with the Kimberlite Intrusions at the Tanoma Coal Mine: University Park, The Pennsylvania State University, B. S. thesis, p. 17.

Rock, N.M.S., 1991, Lamprophyres: Glasgow, Blackie and Son, Ltd., 285 p.

Root, S. I., [1977], Possible recurrent basement faulting, Pennsylvania—Part 1, Geologic framework: Pennsylvania Geological Survey, unpublished manuscript on file at the Bureau of Topographic and Geologic Survey, Middletown, Pa., 23 p.

Schulze D.J., and Hearn, B.C., Jr., 2015, Mantle Xenoliths from the Masontown, Pennsylvania Kimberlite: an Ordinary Mantle with Si-enriched Spinel: The Canadian Mineralogist, v. 53 p. 767-773.

Shervais, J.W., Taylor, L.A., and Laul, J.C., 1987, Magma mixing and kimberlite genesis; mineralogic, petrologic, and trace element evidence from eastern U.S.A. kimberlites, *in:* E.M. Morris and J.D. Pasteris eds., Mantle Metasomatism and Alkaline Magmatism: Geological Society of America Special Paper 215, p. 101-114.

Shultz, C.H., 1999, Jurassic Kimberlite Dikes, chap. 13 *of* Shultz, C,H., ed., The geology of Pennsylvania: Pennsylvania Geological Survey and Pittsburgh Geological Society, 4th ser., Special Publication 1, p. 211-217.

Smith, R. C. II., 1984, Dixonville Kimberlite: Commonwealth of Pennsylvania Department of Environmental Resources, Internal Report, 5 p.

Smith, R. C. II., Foland, K.A., Nickelsen, R.P., 2004, The Lower Silurian Clear Springs Volcanic Suite: Sword Mountain olivine Melilitite (433± 3Ma) and Hanging Rock Diatreme, Washington County, Maryland: Abstracts Geological Society of America Joint Northeast and Southeast Section Meeting, v. 36, no. 2, p. 71.

Smith R. C., Skema, V., and Dague, J., 2016 Ernest No. 3 Mine Kimberlite, Wayne Township, Indiana County, PA. Some Unedited and Unreviewed History and Interpretation.

Smith, R. C. II., and Barnes, J.H., 2006, Blue Gray by Day and Pinkish Purple by Night: Pennsylvania's Pyrope Garnets: Pennsylvania Geology, v. 36, No. 4, p. 2-10.

Sosman, R.B., 1938, Evidence of the Intrusion-Temperature of Peridotites: American Journal of Science, v. 35, p. 353-359.

Southworth, C.S., Gray, K.J., and Sutter, J.F., 1992, Middle Eocene intrusive igneous rocks of the Central Appalachian Valley and Ridge Province – Setting, chemistry, and implications for crustal structure, In Principal oil and gas plays in the Appalachian basin (Province 131): U.S.G.S. Bulletin 1839 -I, J. p. J1-J24.

Stant, J., Evans, L., Gadinski, R., and Norris, C., 2007, Impacts on Water Quality from Emplacement of Coal Combustion Waste in Pennsylvania Cola Mines: Pennsylvania Minefill Study – Clean Air Task Force, August 2007, 59 p.

Szekely, J., and Reitan, P.H., 1971, Dike Filling by Magma Intrusion and by Explosive Entrainment of Fragments: Journal of Geophysical Research, v. 76, # 11, p. 2602-2609.

Tedeski, Joseph R., 2002, Tanoma/Dixonville Kimberlite Dike and other Geologic Features found in the Tanoma Coal Mine: CD Pennsylvania Geological Survey, Pittsburgh office.

Tso, J.L., McDowell, R.R., Avary, K.L., Matchen, D.L., and Wilkes, G.P., 2004, Middle Eocene igneous rocks in the Valley and Ridge of Virginia and West Virginia, *in* Geology of the National Capital Region – Field Trip Guidebook, p. 137-161.

White, D., 1925, Progressive regional carbonization of coals: AIME Transactions, v 71, p. 253-281.

Wyllie, P.J., and Tuttle, O.F., 1960, The System CaO-CO_2-H_2O and the Origin of Carbonatites: Journal of Petrology v. 1, p. 1-46.

Zartman, R.E., Brock, M.R., Heyl, A.V., and Thomas, H.H., 1967, K-Ar and Rb-Sr ages of some alkali intrusive rocks from the central and eastern United States: American Journal of Science, v. 265, p. 848-870.

Zhang, E., 1992, Coalification patterns of the Pennsylvania coal measures in the Appalachian foreland basin, western and southcentral Pennsylvania. University Park, Pa., The Pennsylvania State University, M. S. Thesis, p. 76.

THE ROGUE KIMBERLITE DIKES IN INDIANA COUNTY, PENNSYLVANIA PART 2. COKED COAL MARGINAL TO KIMBERLITE INTRUSION IN THE TANOMA MINE

GARETH D. MITCHELL, EMS ENERGY INSTITUTE AND ALAN DAVIS (EMERITUS PROFESSOR OF GEOLOGY), EARTH AND MINERAL S ENERGY INSTITUTE, THE PENNSYLVANIA STATE UNIVERSITY, UNIVERSITY PARK. PA 16802

Introduction

The Tanoma Mine is located approximately 5 km west of Dixonville, in Indiana County Pennsylvania, where a kimberlite dike was exposed while mining in the Lower Freeport or "D" coal (Honess and Graeber, 1926) in the Barr Slope Mine (Figure 1). *En echelon* dikes striking E-W were exposed for over 2 km in the Tanoma Mine tending towards Dixonville, and there is little doubt these represent the same dike swarm, albeit in a different seam, the Lower Kittanning or "B" coal, approximately 50 meters stratigraphically below. The Tanoma kimberlite was formally noted in a Pennsylvania Department of Environmental Resource internal report (Smith II, R.C, 1984). However, no detailed petrologic or mineralogic studies were undertaken for comparison with the Dixonville intrusion until now. Besides characterization of an igneous intrusion in workings of the Tanoma coal mine, Indiana County, Pennsylvania, an investigation of the contact metamorphism with the coal was initiated in an attempt to use maximum reflectance measurements to estimate the temperature of intrusion. (Figure 1).

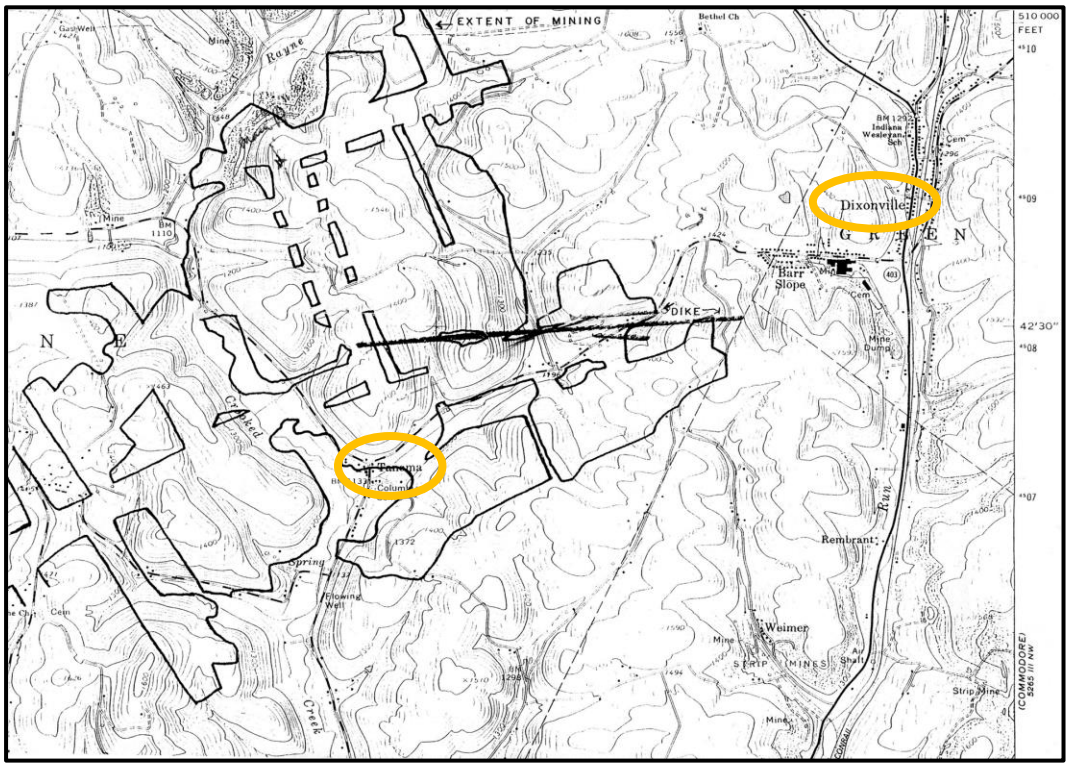

Figure 1. Location of the Tanoma Mine Workings and the East-West Trending Intrusion West of Dixonville, Bar Slope Mine on the Clymer, 7.5' quadrangle.

Evaluation of Thermal History

Figure 2 portrays a 24-30 cm thick dike intruding the full height of the Lower Kittanning coal seam and that was composed mostly of serpentine, but containing large megacrysts (phlogopite shown), remnants of olivine as well as unaltered kimberlite. A chill zone beside the contact with the natural coke was observed along with the characteristic shrinkage fractures in the coke that form parallel with the thermal gradient and are generated from thermoplastic deformation and devolatilization of the coal. These coke structures strongly suggest that the coal had reached bituminous rank at the time of intrusion and likely had reached its current medium volatile rank (i.e. 1.11% mean max. vitrinite reflectance, ASTM D388). However, the question being asked at the time this work was conducted (1994), "can the temperature of the intrusion be determined by optical microscopic techniques, specifically using coke reflectance?" Textural and reflectance evaluations of metallurgical coke suggest useful information could be derived using these techniques, although application to the thermal metamorphism of coal would be more complicated in accounting for a long list of unknown influences of geological setting and variable reaction conditions.

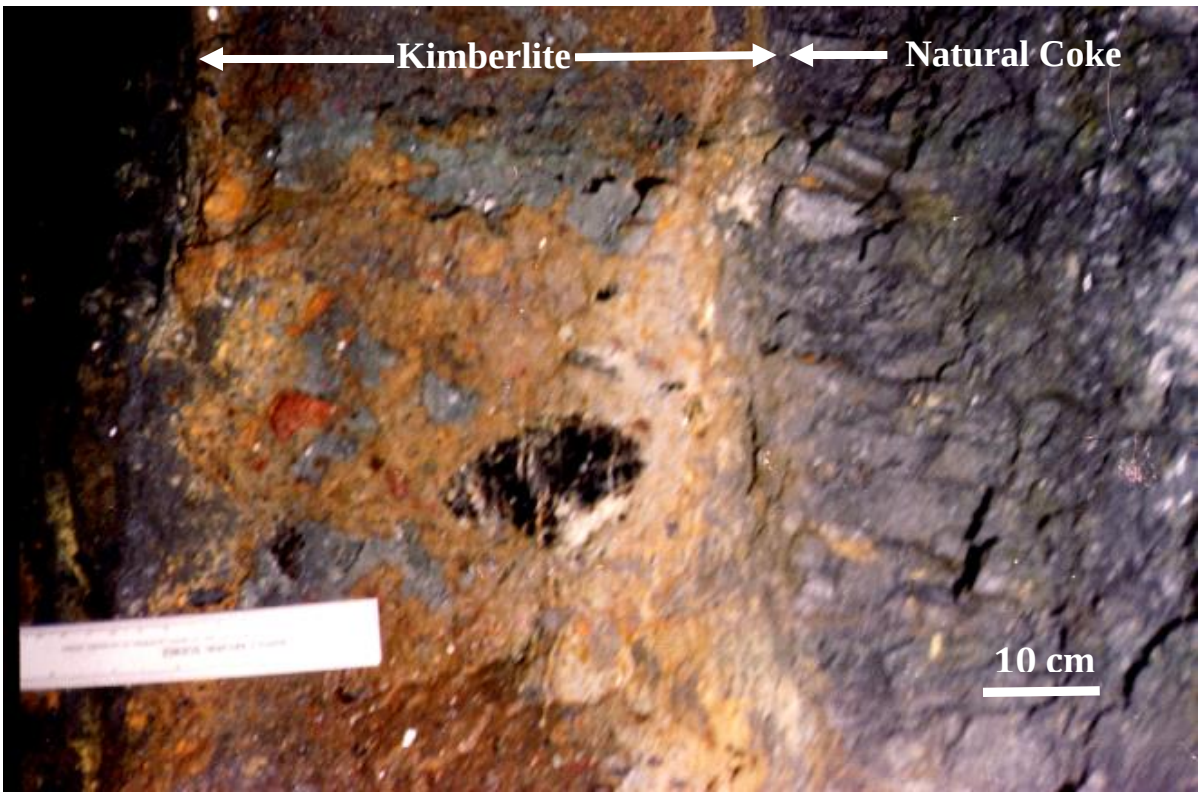

Figure 2. Photograph of contact between kimberlite dike (left) and natural coke (right). Note the phlogopite megacryst (center) and shrinkage cracks perpendicular to the intrusion.

Thin dikes of a highly fluid magma like those encountered at the Tanoma Mine would probably result in fairly rapid heating for a limited time period and may be influenced by the latent heat of crystallization of the magma, groundwater circulation and expulsion of volatile matter, as well as thermal conductivity and diffusivity of rocks, etc., (Delaney 1987). Bostick and Pawlewicz, 1984; Stewart et al., 2005 used kinetic solutions (Carslaw and Jaeger, 1959) to estimate temperature across intrusions and wall rock as well as laboratory carbonization in an

attempt to determine maximum dike temperature. Spear (1993) suggests that thin dikes of <1 meter may cool in a matter of days, making the maximum temperature achieved during intrusion a dominant factor in defining morphological changes such as the size and shape of optical textures and measured reflectance values (Cooper et al., 2007; Baker et al., 1998; Price, 1983). Using fluid inclusions, vitrinite reflectance, apatite fission track analyses of Gippsland Basin dikes, Barker et al., (1998) found that cooling next to relatively thin dikes may interfere with development of an incipient conversion systems. The cooling causes estimates of maximum temperature determined by reflectance techniques to be lower than those estimated by fluid inclusions.

A more direct approach is taken in our investigation based on the assumption that the maximum temperature attained by the coal at the contact is determined by subjecting the contact coke to progressively high temperatures in the laboratory to determine the temperature below which thermal treatment fails to induce a change in the measured reflectance. Using one of the contact samples to generate a reflectance profile from contact to unaffected coal establishes (a) whether the coal had been heated though it's thermoplastic phase, and (b) whether it developed a coalesced mesophase and a solid anisotropic carbon, thereby producing a partially condensed and crosslinked aromatic carbon. This means that exposing the natural coke to further increases in temperature will only result in additional condensation of the pseudo-lattice by the shedding of small aromatic and aliphatic compounds. In support of this approach, not only will a reflectance profile of the natural coke be necessary, but laboratory carbonization of the coal at progressively high temperatures will be needed to provide template of how the coal would react to thermal input in a manner similar to Bostick and Pawlewicz, (1984).

Samples *(see Part 1, Figure 12)*

Two block samples (~ 8x10x14cm) of the natural coke were obtained for general characterization and to determine contact temperature using quantitative reflectance techniques. Each block contained a thin layer of kimberlite and the complete aureole along with some unaltered coal. One block sampled from the top surface of a sill (I-94-15), and the other block used to extract contact coke for direct carbonization was collected from a ~30 cm thick dike (I-94-5b). Finally, a sample of unaltered coal 4.3 m from the dike was employed to obtain background reflectance values as well as coal for laboratory carbonization measurements at progressively higher temperatures.

(Figure 12 from Part I, which is a map showing the sample locations, is reproduced here for your convenient reference):

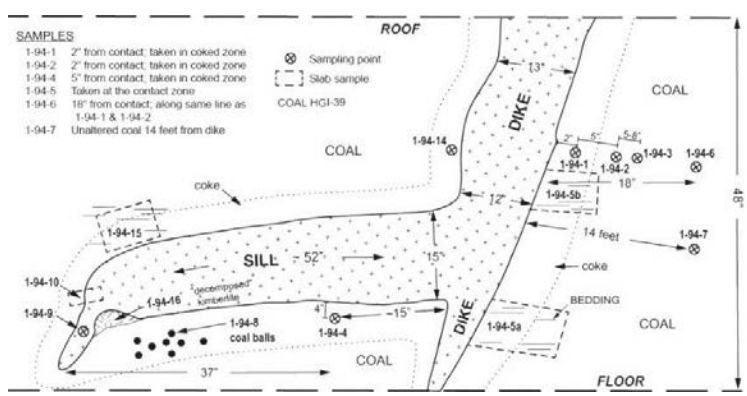

Polished specimens were prepared from block sample (I-94-15) containing natural coke after an initial vacuum impregnation with a cold-setting epoxy resin. A cross-sectional surface measuring approximately 8 by 14 cm sized from the original block was cut into six smaller subsamples of 2 by 7 cm (Figure 3). These were re-impregnated in epoxy for added stability, and then ground using 400 and 600 grit silicon carbide papers and polished, using 0.3 µm and 0.05 µm alumina slurries, for reflected-light optical microscopy. The other, smaller block sample (I-94-5b) containing kimberlite material sampled from a vertical dike was used in laboratory coking experiments. In addition, a representative sample of the coal was crushed and prepared into briquettes for petrographic analysis. This control sample yielded background reflectance values as well as powdered coal (minus 0.25 mm, or 60 mesh) for micro-carbonization tests.

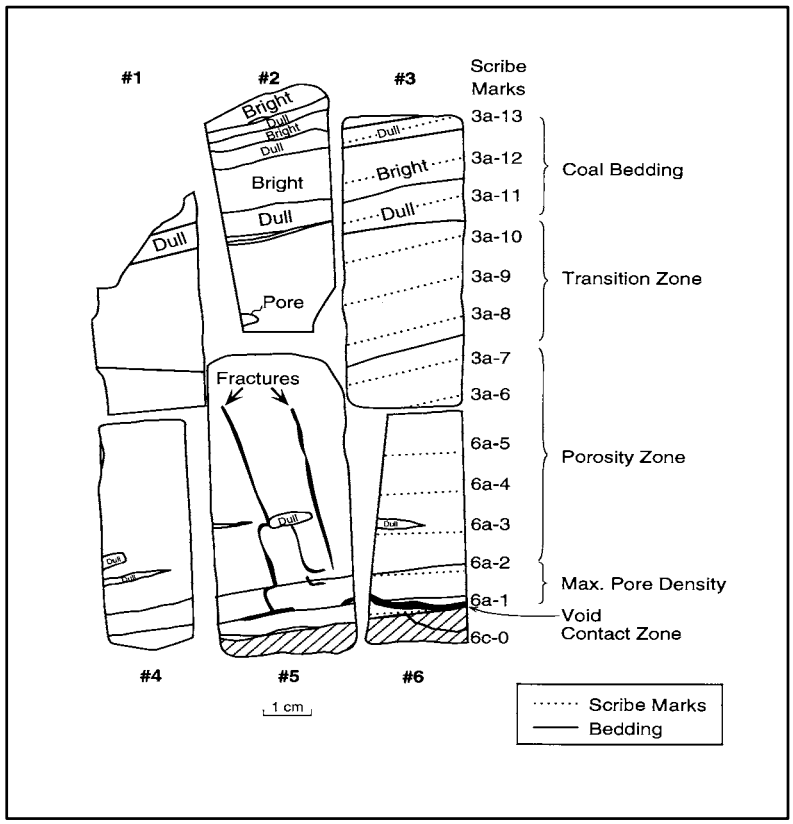

Figure 3. Sample preparation of larger large block (I-94-15) containing contact zone (bottom), natural coke and marginally reacted coal (top). Orientation of bedding planes suggest this sample was collected from the top surface of a connecting sill 1.3 m from the dike.

Analytical Protocol

Reflectance analyses were performed using a Leitz MPV 2 research microscope with white-light illumination and a 50 X oil-immersion objective for a total system magnification of 625 X. The incident light was polarized at 45°. Light from the polished surface was passed through a 1.9 µm diameter limiting aperture and then through an interference filter centered around 546 ±5 nm. For measurement of reflectance the photomultiplier system was standardized using optical glasses of 1.009% and 1.662% reflectance. Calibrated neutral density filters were used to reduce light intensity of the natural coke into the reflectance range of the glasses, the optimal stability

range of the photomultiplier, then reflectance values were calculated based on the transmittance of the filter at 550 nm.

Mean maximum (R_{max}) and mean minimum (R_{min}) reflectance values were collected on all samples by rotating the specimens through 360° and recording the highest and lowest values measured by the photomultiplier, respectively for 100 individual readings. Typically, random reflectance is employed for temperature profiling of igneous/coal contacts. This is understandable when measuring reflectance values on fine size or immature dispersed organic matter in sedimentary rocks, but not from coal that developed a mesophase and solidified into fairly large isochromatic textures.

To establish a reflectance/temperature profile for this Lower Kittanning coal carbonized under atmospheric pressure, small aliquots of coal were heated using a micro-carbonization technique. The procedure involved loading ≈1.0 g of <0.25 mm coal into a quartz tube stopped with quartz wool, and placed into a small stainless steel reaction tube. Samples were set into a programmable laboratory furnace and carbonized under a slight over-pressure of nitrogen at a heating rate of about 5°C/min to the desired maximum temperature and allowed to soak at that temperature for 2 hours. Carbonization temperatures between 200° and 900°C were employed at 100°C increments with runs at 350° and 450°C added later to complete the thermal/reflectance profile. This procedure was not used to simulate coking conditions occurring at depth during intrusion. Rather it provides a correlation between temperature and reflectance for this coal under uniform coking conditions.

Carbonization runs using the same procedures were performed on material retrieved from the contact zone from the second block sample (I-94-5b) containing natural coke. A particulate sample of natural coke was obtained by removing the contact zone containing kimberlite material and then cutting a 5 mm thick slab from the end of the specimen. The recovered material was crushed to minus 0.25 mm and carbonized as describe before. Four carbonization tests were made at 100°C increments from 400° to 700°C. Samples of the contact coke and those from micro-carbonization were prepared for reflectance microscopy.

Results and Discussion

Under the polarizing microscope using oil immersion, the contact zone (6c-0, Fig. 3) was seen to be composed of serpentine with significant rounded porosity and small amounts of irregularly shaped coke fragments commonly possessing a 2-12 µm mosaic texture. The first competent coke layer (6c-1, Fig. 3) also possessed rounded porosity and was composed predominantly of irregularly shaped mosaic carbon of 2-10 µm with minor 1-3 µm circular mosaic carbon. Rounded porosity within the contact zone suggests the presence of a fluid phase being trapped in a more viscous melt, gas or liquid. For the next 3 cm beyond the contact zone, slightly lenticular mosaic carbon of 8-40 and 8-25 µm was observed. Farther away from the contact zone, mosaic size diminished and approximately 7 cm from the contact 1-5 µm mosaic textures (more characteristic of the current coal rank), were found along with a fairly high concentration of partially coalesced spherical mesophase in an isotropic pitch (3a-7, Fig. 3) similar to that observed by Brooks and Taylor (1961 & 1968). In contrast to the pitch matrix, the size and concentration of mesophase spheres decreased until the first vitrinite containing bands of liptinite and inertinite macerals was observed, at 10.75 cm from the contact (3a-10, Fig. 3).

Beyond this point, normal coal features with bedding structures were observed oriented parallel to the contact, which would be consistent with a sill. The vitrinite reflectance values in aureole remained higher (1.22% ±0.02) than the mean reflectance of the background coal specimen (1.11% ±0.02). Based upon these results the reflectance profile for the upper contact of a thin sill showed a gradual decrease equal to one half of the width of the intrusion from the contact. Similar results have been reported by Cooper et al., (2007) for stills and dikes of lamprophyric composition intruding 1.0% reflectance coal in the Raton Basin.

Mean reflectance values relative to distance from the intrusion are plotted in Figure 4 which shows that the greatest maximum reflectance was measured for anisotropic material intimately associated with the kimberlite within the contact zone. As distance from the contact increased, maximum reflectance decreased, whereas minimum reflectance remained about the same. At 6.75 cm from the datum, measurements became possible on the pitch phase, initially found in low concentration and trapped within an anisotropic carbon matrix. The pitch had reflectance values that were similar to, but slightly higher than, the present-day unaltered coal (1.11% Ro). Reflectance values measured on vitrinite from the region 10.75 cm from the datum also were only slightly higher than that measured for the unaltered coal.

Coals of medium volatile bituminous rank produce lenticular isochromatic mosaic units of ≈1-4 μm and with maximum reflectance values between 7.0-10.0% when carbonized to 1000°C (Gray,1976: Gray & DeVanney, 1986, ASTM D5061, 2015). The mosaic units observed in the thermally metamorphosed coal were much larger and the maximum reflectance lower compared to metallurgical cokes. These differences probably result from the influences of factors such as time, low thermal conductivity, maximum temperature, cooling rate, influence of a liquid phase, possible incorporation of higher molecular weight aromatic volatiles and the confining pressure that existed during the magmatic intrusion.

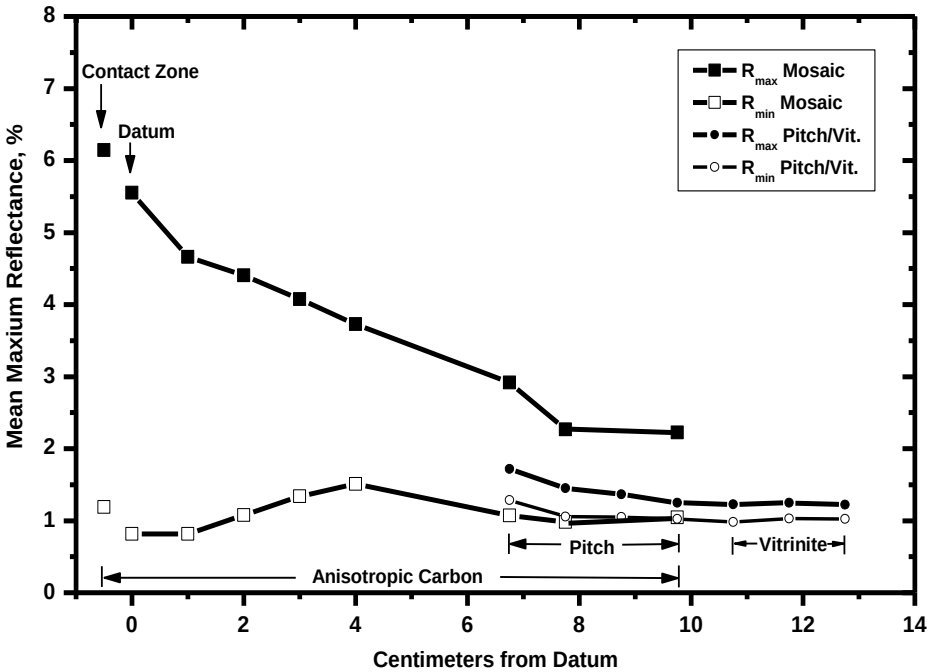

Figure 4. Mean Apparent Maximum and Minimum Reflectance of Natural Coke from the Lower Kittanning Coal, Tanoma Mine, Indiana Co., PA (I-94-15)

Laboratory Carbonization Experiments

Reflectance results of the carbonization experiments from 200° to 900°C are plotted in Figure 5. Maximum and minimum reflectance was measured on the anisotropic mosaic, pitch-like material and recognizable vitrinite. During these tests, a significant weight-loss rate was recorded between 400° and 500°C, which corresponding to the coal fluid temperature range. Laboratory carbonization of the coal at 900°C resulted in a maximum reflectance and a bireflectance (B_i, difference between maximum and minimum reflectance) nearly double that measured from the contact zone with the intrusive (Figure 4). Also, the mosaic units observed from the 900°C test were considerably smaller (1-4 μm) and more uniform than those derived from thermal metamorphism with little change in all carbonization runs between 450° - 900°C. At 400°C a pitch-like material was observed in which there was evidence of thermoplasticity and devolatilization. For lower temperature runs (350° - 200°C) no sign of plasticity was observed. Therefore, measurements were taken on vitrinite. Plotting of the reflectance distribution measured from the Tanoma aureole (Figure 4) on the laboratory temperature distribution in Figure 5, revealed temperature distributions in the range of 585° to 408º C. Taking into consideration the pressure effects described by Chandra (1965), the mosaic sizes and the level of bireflectance measured on these laboratory cokes suggest the coal had attained its present-day rank at time of intrusion. Also, coke material in direct contact with the kimberlite had progressed through the development of coalesced mesophase and had become a partially condensed, solid anisotropic carbon.

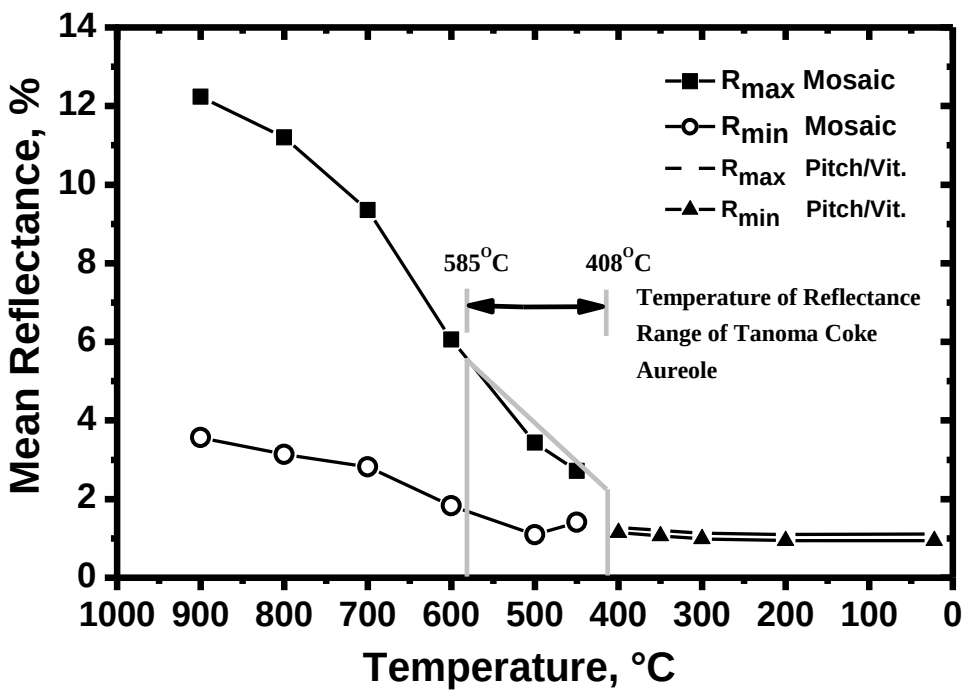

Figure 5. Reflectance results from laboratory semi-cokes using the Tanoma coal showing the temperature range of the aureole based upon reflectance of the natural coke

To complete direct temperature evaluation at the intrusive/coal contact, a sample of the thermally metamorphosed coke was removed from the datum region of dike sample I-94-5b.

Laboratory carbonization of this material was performed at 100°C increments in the 400° - 700°C range to define the temperature at which thermal treatment no longer changes reflectance of the material. Reflectance values measured on the material removed from block I-94-5b compare well with those values measured from the datum region of the sill sample, i.e., 5.64% vs 5.55%, respectively. R_{max} and B_i values for the 700°C product were similar to those values measured from the laboratory carbonization of the coal at 900°C (11.04 & 8.78 vs 12.24 & 8.67, respectively). However, a rapid linear decrease in R_{max} was observed for the natural coke carbonization products as the temperature dropped to 500°C. At 400°C, there was no significant difference between the reflectance of the starting material and the carbonization product. Using the reflectance values obtained from the 500° - 700°C products as a basis for linear regression, the temperature at which the regression line intersected the reflectance of the starting material was determined. As shown in Figure 6, coal adjacent to the intrusion at the datum was estimated to have reached a maximum temperature of at most 494 ±5°C. Using the maximum reflectance value measured for the carbonaceous material included within kimberlite a temperature of 514 ±9°C was estimated for the contact zone. These estimates closely correspond to the upper level of the fluid temperature range and maximum devolatilization measured for the coal under ambient conditions.

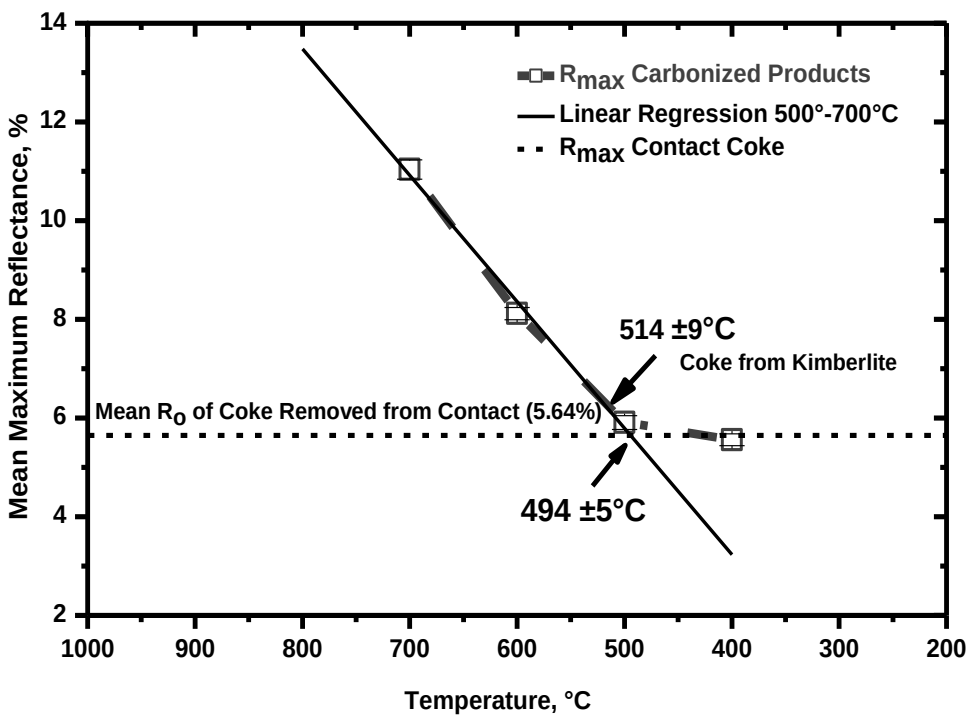

Figure 6. Mean max. reflectance distribution of heat treated contact coke from I-94-5b

Conclusions

Using reflected-light optical microscopic and laboratory carbonization techniques, natural and laboratory coke samples were evaluated to reveal that:

- The Lower Kittanning coal of the Tanoma Mine had attained its current rank of medium volatile bituminous by the time of intrusion.
- The contact coke had been exposed to sufficient temperature to cause resolidification of a coalesced mesophase.
- Progressive laboratory carbonization of the current Tanoma coal suggested that contact temperature could have reached 508ºC, but
- Laboratory carbonization of coke removed from the contact zone provided a temperature of 514 ±9°C for the material intimately mixed with the kimberlite and a temperature of 494 ±5°C for material adjacent to the contact.

References

American Society for Testing and Materials (ASTM), 2015a, D 5061 - Standard Test Method for Microscopical Determination of Volume Percent of Textural Components in Metallurgical Coke, American Society for Testing and Materials, Book ASTM Standards 05.06, p. 660-664.

American Society for Testing and Materials (ASTM), 2015b, D 388 - Standard Classification of Coals by Rank, American Society for Testing and Materials, Book ASTM Standards 05.06, 448-454.

Barker, C.E., Bone, Y., Lewan, M.D., 1998, Fluid inclusions and vitrinite reflectance geothermometry to heat-flow models of maximum paleotemperatures next to the dikes, Western onshore Gippsland Basin, Australia: International Journal of Coal Geology, v. 37, no. 73-111.

Bostick, N.H. and Pawlewicz, M.J., 1984, Paleotemperatures based on vitrinite reflectance of shales and limestones in igneous dike aureoles in the upper Cretaceous Pierre shale, Walsenburg, Colorado, Hydrocarbon Source Rocks of the Great Rocky Mountains Region: Rocky Mountain Association of Geologists, p. 387-392.

Brooks, J.D. & Taylor, G.H., 1968, The Formation of Some Graphitizing Carbons *in:* Walker, P. L., ed., Chemistry and Physics of Carbon: New York, Marcel Dekker, Inc., v. 4, p. 243-286.

Brown, H.R. & Taylor, G.H., 1961, Some Remarkable Antarctic Coals: Fuel, London, v. 40, p. 211-224.

Carslaw, H.S. and Jaeger, J.C., 1959, Condition of heat in solids, 2nd. Ed.: New York, Oxford University Press, 509 p.

Chandra, D., 1965, Reflectance of Coals Carbonized under Pressure: Economic geology, v. 60, p. 621-629.

Cooper, J.R., Crelling, J.C., Rimmer, S.M., and Whittington, A.G., 2007, Coal metamorphism by igneous intrusion in the Raton Basin, Co and NM: Implications for generation of volatiles: International Journal of Coal Geology, v. 71, p. 15-27.

Delaney, P.T., 1987, Heat transfer during emplacement and cooling of mafic dykes, *in:* Hall, H. C., and Fahrig, W. F., eds., Mafic Dyke Swarms, Geologic association of Canada, v. 34, p. 31-46.

Gray, R.J., 1976, A System of Coke Petrography: Proceedings of the Illinois mining institute, p. 20-47.

Gray, R.J. & DeVanney, K.F., 1986, Coke Carbon Forms: Microscopic Classification and Industrial Applications: International Journal of Coal Geology, v. 6, p. 277-297.

Honess, A.P. and Graeber, C.K., 1926, Petrography of the Mica Peridotite Dike at Dixonville, Pennsylvania: American Journal of Science, 5th Series, v. 12, p. 484-494.

Price, L.C., 1983, Geologic time as a parameter in organic metamorphism and vitrinite reflectance as an absolute paleogeothermometer: Journal of Petroleum Geology, v. 6, p. 5-38.

Smith, R.C. II, 1984, Dixonville Kimberlite: Commonwealth of Pennsylvania Department of Environmental Restoration, Internal Report, p. 5.

Spear, F.S., 1993, Metamorphic phase equilibria and pressure-temperature-time paths, Mineralogical Society of America Monograph 1, p. 43-46.

Stewart, A.K., Massey, M., Padgett, P.L., Rimmer, S.M. and Hower, J.C., 2005, Influence of a basic intrusive on the vitrinite reflectance and chemistry of the Springfield (No. 5) coal, Harrisburg, Illinois: International Journal of Coal Geology, v. 63, p. 58-67.

PALEOSOL DEVELOPMENT ALONG THE MISSISSIPPIAN-PENNSYLVANIAN UNCONFORMITY NEAR JOHNSTOWN, PENNSYLVANIA[1]

MICHAEL C. RYGEL[2], SUNY POTSDAM
JACK D. BEUTHIN[3], WEATHERFORD LABORATORIES

Abstract

The Mississippian–Pennsylvanian boundary near Johnstown, Pennsylvania is marked by an iron-rich "boundary mudstone" that grades downward into a quartzose "subjacent sandstone" at in the Mauch Chunk Formation (Mississippian). Field, micromorphological, geochemical, and mineralogical characteristics of these strata indicate that they constitute a well-developed paleosol (the "Route 56 paleosol) with a complex pedogenic history. The boundary mudstone contains evidence for waterlogged conditions (sphaerosiderite) consistent with a gleyed underclay and evidence of intense tropical weathering (abundant kaolinite, ferric iron, and runiquartz) under well-drained conditions. These contrasting mineralogical and micromorphological characteristics indicate the Route 56 paleosol experienced a complex, polygenetic history involving contrasting soil-forming regimes. Specifically, the Route 56 paleosol is interpreted as having formed in a tropical rainy climate on an interfluve of the Mississippian–Pennsylvanian unconformity. This study demonstrates how detailed geochemical and micromorphological analyses can be used to provide sedimentological evidence for an otherwise cryptic unconformity surface.

Introduction

The Mississippian–Pennsylvanian unconformity in the Appalachian Basin is a regional surface that records both a mid-Carboniferous eustatic event (Saunders and Ramsbottom, 1986; Beuthin, 1997) and tectonic activity within the basin (Quinlan and Beaumont, 1984; Ettensohn and Chesnut, 1989; Chesnut, 1990; Ettensohn, 1994). The Mississippian–Pennsylvanian unconformity is marked by pronounced erosional relief associated with paleovalleys (Rice, 1984, 1985; Rice and Schwietering, 1988; Chesnut, 1988; 1992; Beuthin, 1994; Yang, 1998). Although paleosols would be expected to occur on interfluves along the unconformity surface, they have been reported at only a few locations throughout the basin (Smyth, 1984; Williams and Bragonier, 1985; Cecil and others, 1992; Chesnut and others, 1992; Beuthin, 1997; Humbert, 2001). Interfluve paleosols are often subtle features that are difficult to identify using field evidence alone and it is likely that they have been overlooked in many locations. McCarthy and Plint (1998) showed that paleopedology can be used to recognize interfluve paleosols associated with sequence boundaries and that these features typically have a complex, polygenetic origin.

---

[1] This contribution is largely derived from Rygel, M.C. and Beuthin, J.D., 2002, Paleopedology of a residual clay associated with the Mississippian-Pennsylvanian (mid-Carboniferous) unconformity, southwestern Pennsylvania; Southeastern Geology, v. 41, no. 3, p. 129-143.

[2] Department of Geology, SUNY Potsdam, Potsdam NY 13676, rygelmc@potsdam.edu

[3] Weatherford Laboratories, 16161 Table Mountain Parkway, Golden, CO 80403, jack.beuthin@weatherfordlabs.com

We use this approach to provide insight into the nature and origin of the Mississippian–Pennsylvanian boundary in the central Appalachian Basin.

The Mississippian–Pennsylvanian boundary and associated strata are well exposed in a roadcut along Pennsylvania Route 56 just to the north of the city of Johnstown (Figures 1 and 2).

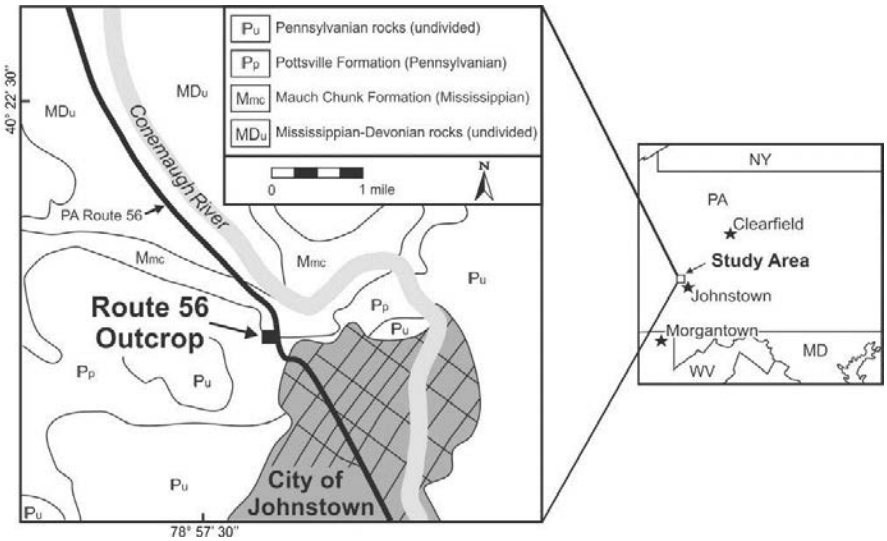

Figure 1. Location of the Route 56 paleosol near Johnstown, Pennsylvania (bedrock geology after Glover and Edmunds, 1981). Other paleosols associated with the Mississippian Pennsylvanian boundary have been reported near Clearfield, Pennsylvania (Williams and Bragonier, 1985) and Morgantown, West Virginia (Cecil and others, 1992).

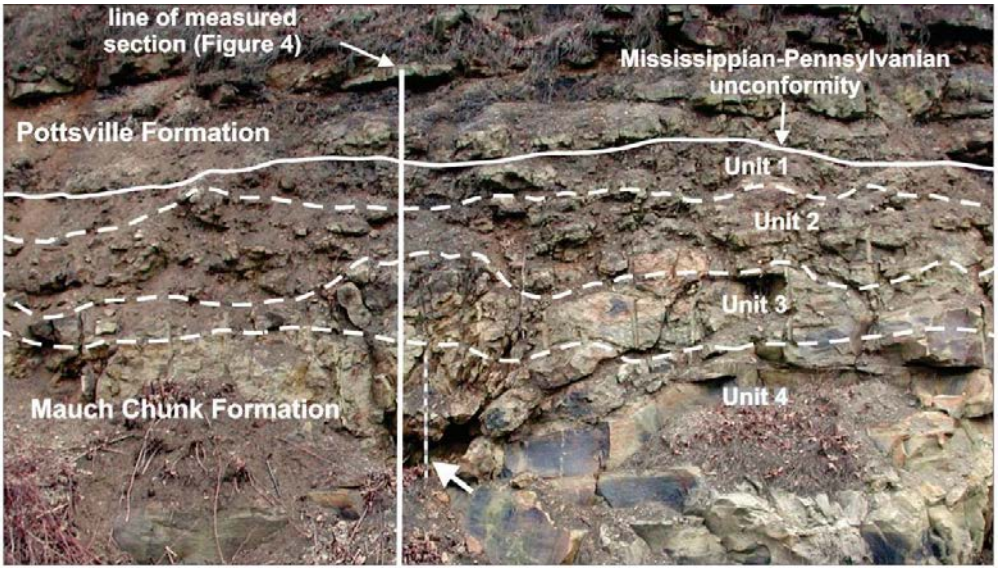

Figure 2. Outcrop photograph and interpretive stratigraphy of the Route 56 paleosol. Position of the Mississippian Pennsylvanian unconformity (Mauch Chunk Pottsville contact) is indicated by the bold solid horizontal line; contacts between units within the paleosol shown with dashed lines. Units 1 and 2 comprise the boundary mudstone, Units 3 and 4 comprise the subjacent sandstone. Exact position of the measured section shown is with thick vertical line. Note that unit thicknesses vary across the outcrop. Photoscale (measuring staff indicated by bold arrow) is 1.7 m tall with 0.1 m gradations.

The boundary is marked by an iron-rich mudstone with characteristics of a semi-flint to plastic clay. This mudstone, which is overlain by strata of the Pottsville Formation (Pennsylvanian),

grades down into a subjacent sandstone of the Mauch Chunk Formation (Mississippian). In this paper, the boundary mudstone and underlying Mauch Chunk sandstone are collectively termed the "Route 56 paleosol." Mudstones in the Pennsylvanian System with similar lithologic characteristics were interpreted by Williams and others (1965) as residual clays formed on well-drained interfluves of cyclothem-bounding unconformities. In this study we use paleopedology to test the hypothesis that the "boundary mudstone" at the study site is a residual soil formed on an interfluve associated with the Mississippian–Pennsylvanian unconformity.

Stratigraphic Setting

Strata exposed in the study interval belong to the upper part of the Mauch Chunk Formation (upper Mississippian) and the lower part of the Pottsville Formation (middle Pennsylvanian) (Figure 3). Below the Route 56 paleosol about 30 m of the Mauch Chunk Formation is exposed; common lithologies include red mudstone, green siltstone, and gray sandstone. This middle Chesterian unit records a regional transgression in southwestern Pennsylvania (Horowitz and Rexroad, 1972; Brezinski, 1989; Edmunds, 1993; Stamm, 1997). Above the Route 56 paleosol about 4 m of the Pottsville Formation are exposed, comprising carbonaceous mudstone and a gray sandstone that are likely part of the Mercer shale member of Phalen (1910). Although biostratigraphic control on the age of the basal Pottsville strata in this exposure are lacking, palynomorphs and megaflora from the Mercer interval elsewhere in the basin indicate a Bolsovian (Atokan) age (Peppers, 1996; Blake and others, 2002). The formation contact is an irregular erosional surface with about 1.0 m of relief across the outcrop face.

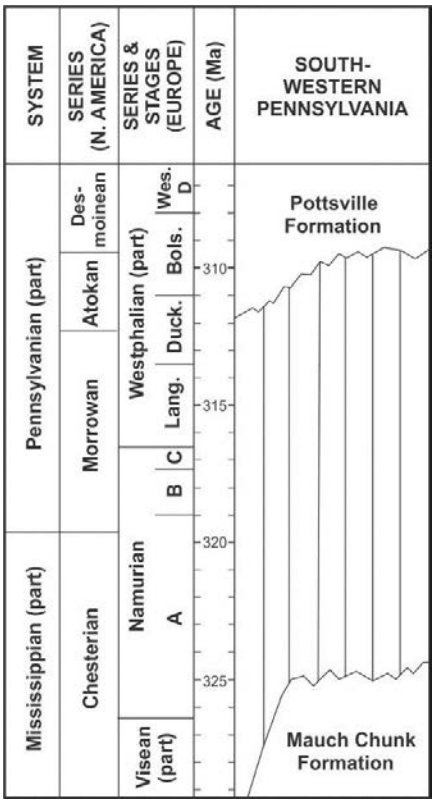

Figure 3. Upper Mississippian lower Pennsylvanian stratigraphy of southwestern Pennsylvania showing hiatus associated with the Mississippian Pennsylvanian unconformity. Chronostratigraphy after Edmunds (1993); numerical dates from Menning and others (2000). European stage names are abbreviated as follows: Langsettian (Lang.), Duckmantian (Duck.), Bolsovian (Bols.), and Westphalian D (West. D).

The Mississippian–Pennsylvanian unconformity in southwestern Pennsylvania omits strata of uppermost Mississippian-lower Pennsylvanian age (upper Chesterian-Morrowan or Namurian-lower Westphalian) and may represent as much as 16 million years of missing time (Edmunds, 1993; Menning and others, 2000). In the Appalachian Basin the Mississippian–Pennsylvanian boundary records both a prolonged lowstand and a major climate change from wet-dry/monsoonal conditions in the Mississippian to tropical rainy conditions during the Pennsylvanian (Cecil and others, 1985; Cecil, 1990). The record of climate change is evident in the paleosol record throughout the Appalachian Basin. Vertic and calcic paleosols are ubiquitous in the Upper Mississippian succession (Cecil and others, 1985; Cecil, 1990; Cecil and Dulong, 1992; Caudill and others, 1992; Caudill and others 1996; Beuthin, 1997; Greb and Caudill, 1998; Miller and Eriksson, 1999, 2000). Although thin, impure

Mississippian coals are present locally, these organic-rich horizons are probably the products of topographic control, rather than climate control (Beuthin and Blake, 2002). In contrast, the lower Pennsylvanian succession comprises thick coals (paleo-Histosols), but lacks vertic and calcic paleosols (Donaldson and others, 1985; Cecil and others, 1985; Cecil, 1990; Cecil and Dulong, 1992).

The Route 56 Paleosol

Outcrop Description

Within the line of section, the boundary mudstone is 1.5 m thick and the subjacent sandstone is 5.5 m thick (Figure 4). Four horizon-like units are recognized in the paleosol, two in the boundary mudstone (Units 1 and 2) and two in the subjacent sandstone (Units 3 and 4). Laterally, the units vary in thickness and the boundary mudstone is locally truncated at the base of the Pottsville Formation. Unit descriptions are as follows:

Unit 1: 50 cm thick; light-olive-gray; silty mudstone with isolated lenses of muddy, very fine- to fine-grained sand; internally massive; slight vuggy texture with yellowish-orange iron staining common around vug margins; basal contact wavy and gradational.

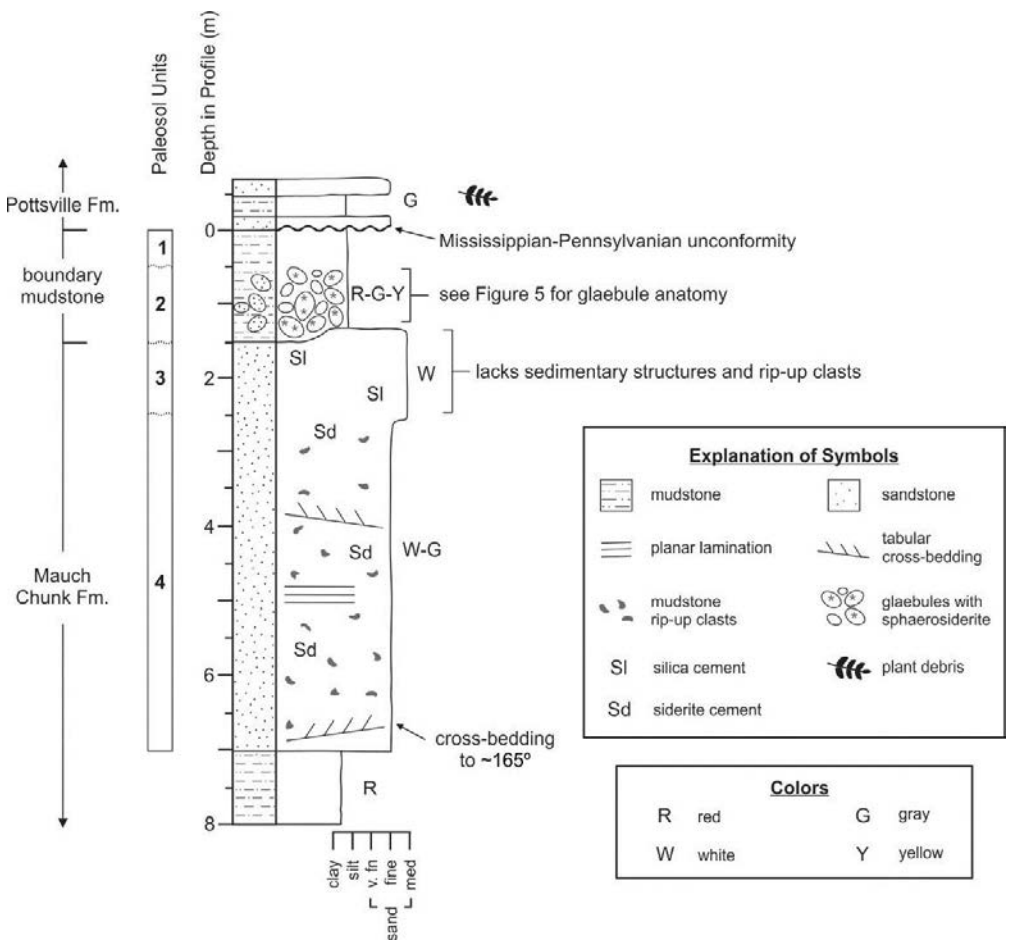

Figure 4. Sedimentological log of the Route 56 paleosol and associated strata.

Unit 2: 100 cm thick; light-gray to reddish-yellow; silty mudstone; massive; numerous iron-rich glaebules ranging from 5 to 26 cm in diameter; glaebules have a tripartite concentric structure consisting of a siderite-rich core, iron-depleted middle layer, and a ferruginous outer rind (Figure 5); silty to sandy cores have abundant reddish-brown sphaerosiderite rosettes (0.1-1.0 mm in diameter); clayey middle layers have a well-developed vuggy texture (vugs ranging from 0.1-1.0 mm in diameter); reddish-brown rinds are silty; small glaebules lack siderite-rich cores; basal contact wavy and gradational.

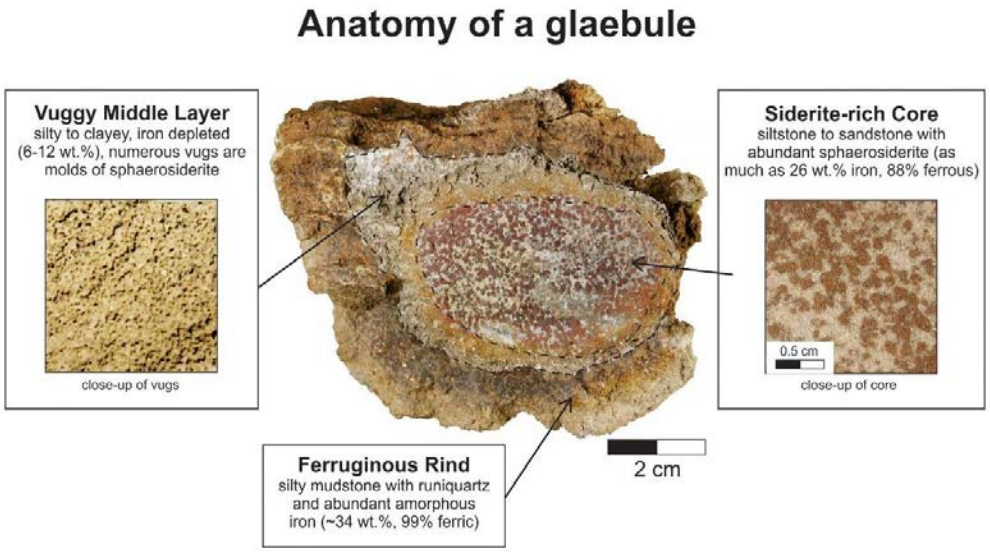

Figure 5. Tripartite concentric structure of a glaebule from Unit 2 of the boundary mudstone.

Unit 3: 100 cm; white to very-light-gray; medium-grained sandstone; quartzose and silica-cemented; internally massive, lacks primary sedimentary structures and labile clasts; basal contact wavy and gradational.

Unit 4: 450 cm; light-gray; fine-grained sandstone; argillaceous; scattered siderite cement; very thick- to massive-bedded; planar-laminated to cross-bedded; contains pebble-sized rip-up clasts of gray-green mudstone; contact with subjacent red beds is sharp and flat.

Micromorphology and Petrography

Boundary Mudstone (Units 1 and 2): The micromorphological terminology used in this section is after Brewer (1976). The relative abundance of skeleton grains (silt and sand) and plasma (clay) ranges from skeleton grains floating in plasma to skeleton grains that are in contact or linked by intergranular braces. The plasma fabric is mostly asepic (weakly/randomly oriented clay, dull plasma) with scattered patches of sepic fabric (oriented, bright clay). In patches of sepic fabric, bright clay is aligned in isolated to interconnected streaks (insepic and mosepic fabrics, respectively). Where plasma forms intergranular braces, bright clay commonly jackets skeleton grains (skelsepic fabric). In contrast to the rest of the boundary mudstone, the cores and vuggy middle layers of the glaebules exhibit sepic fabric with patches of densely woven bright clay (omnisepic fabric) (Figure 6A). Skeleton grains are almost exclusively composed of quartz and

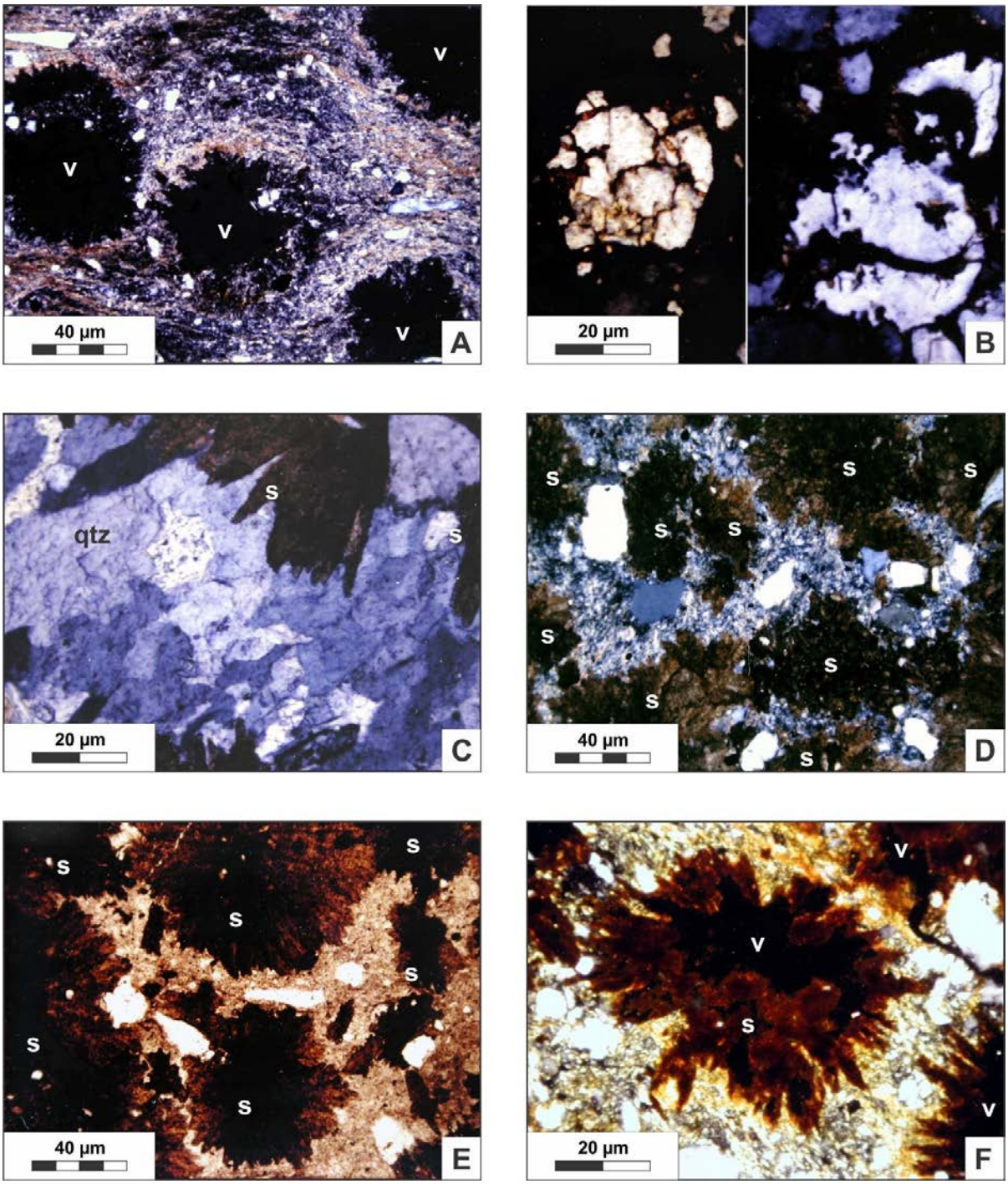

Figure 6. Selected photomicrographs from the Route 56 paleosol. (A) Sepic plasmic fabric surrounding vugs (v) in sample 0.75V (middle layer of a glaebule; cross polarized light). (B) Fractured and corroded quartz grains (runiquartz) from sample 1.00R (glaebule rind; plane polarized light). (C) Sphaerosiderite (s) embaying quartz (qtz) in sample 1.00C (glaebule core; cross polarized light). (D) Sphaerosiderite rosettes (s) in muddy matrix from sample 1.00C (glaebule core; plane polarized light). (E) Sphaerosiderite rosettes (s) in silty sandy matrix of sample 1.00C (glaebule core; cross polarized light). (F) Vug (v) with radial margin and relict sphaerosiderite (s) in sample 1.00V (middle layer of a glaebule; circular polarized light).

range in size from silt to medium-grained sand. Glaebule rinds are clayey; any clay fabric present is generally obscured by amorphous iron. Scattered quartz grains in the rinds are fractured and corroded, with microveins of ferric material frequently lining the fractures (Figure 6B); they are nearly identical to runiquartz as described by Stoops (1983). Many quartz grains in the cores of the glaebules are etched and embayed by siderite (Figure 6C). Cutans are uncommon, but where present they typically are stained by iron (ferri-argillans) or composed of densely packed plasma (embedded grain argillans). Some ferri-argillans coat collapsed voids. Glaebule cores generally lack cutans and contain spherical aggregates or siderite with a radiating crystal habit (Figures 6D and 6E). These sphaerosiderite rosettes range in diameter from 0.6-1.0 mm although they locally coalesce to form intergrown masses up to 1 cm in size. The radial form of many vugs indicates that they are molds of sphaerosiderite rosettes (Figure 6F). A few segregations of material resemble voids filled with skeleton grains (granotubules), some of which are lined with streaks of plasma (isotubules).

Subjacent Sandstone (Units 3 and 4): Skeleton grains are typically in contact with one another and interstitial plasma is rare. Where present, plasma forms intergranular braces. Skeleton grains in Unit 3 are composed of fine- to medium-grained, subangular to subrounded monocrystalline (90%) quartz sand. Grain contacts in Unit 3 are commonly flat or concave-convex. Quartz overgrowths are common in Unit 3 and can be regarded as embedded grain quartzans. Polycrystalline quartz grains and mudstone rip-up clasts become common near the base of Unit 4. In Unit 3 and the top part of Unit 4, cherty silica fills many interstitial voids and euhedral siderite cement (not sphaerosiderite) is present locally. In the upper part of Unit 4, a few plane argillans and embedded grain argillans are present.

Bulk Mineralogical and Geochemical Features of the Boundary Mudstone

Bulk XRD analysis shows that clay content of the boundary mudstone ranges from 25.7 to 70.6% (Table 1). Kaolinite and illite were the only detectable clays and the kaolinite:illite ratio ranged from 1.6 to 3.5. Quartz is the only other abundant silicate mineral and its abundance ranges from 24.2 to 57.3%. A glaebule core sample contained 15.0% siderite; no other carbonate phases were detected. XRD analysis failed to detect iron-bearing minerals in the glaebule rinds, an anomaly that is consistent with the presence of amorphous iron in thin section.

Silica, iron, and alumina are the primary constituents of the boundary mudstone (Table 2). Silica is the most abundant, with values ranging from 41.95 to 88.84% by weight. Total iron ($FeO + Fe_2O_3$) reaches a maximum value of 33.8% in a glaebule rind from Unit 2. Ferric iron predominates in the rinds (99% of total iron) and ferrous iron is most abundant in the cores (88%). Alumina reaches a maximum value of 24.4% in Unit 1.

Abundance of leachable bases ($MgO + CaO + Na_2O + K_2O$) ranges from 0.35 to 2.80%. The ratio of alumina to bases ($Al / MgO + CaO + Na_2O + K_2O$) can be used to measure the degree of leaching in a paleosol (Retallack, 2001); values in the boundary mudstone range between 13 and 23.

Table 1. Whole rock XRD data for the Route 56 paleosol *(data are normalized).*

Common minor minerals include rutile, plagioclase, K-feldspar, diaspore, anatase, and hematite. Multiple samples from 0.50 m represent the sandy (0.50-1) and clayey (0.50-2) lithologies present at this depth. Glaebular samples are identified as having come from either the siderite-rich core (C), the middle vuggy layer (V), or the ferruginous rind (R). XRD samples were analyzed using a Scintag X-1 diffractometer; diffractogram peaks were analyzed using lab software available at the U.S. Geological Survey in Reston, VA.

UNIT		Depth in Profile (m)	Quartz (%)	Siderite (%)	Illite (%)	Kaolinite (%)	Minor Minerals (%)
Boundary mudstone	1	0.00	35.5	0.0	16.9	45.4	1.6
		0.25	52.8	0.0	12.8	28.8	5.6
		0.50-1	67.8	0.0	9.4	19.1	1.8
		0.50-2	24.2	0.0	16.5	57.1	2.1
	2	0.75 V	85.3	0.0	3.6	9.5	1.7
		0.75 C	57.3	15.0	6.9	18.8	2.1
		1.00 R	24.8	0.0	21.6	49.0	1.3
		1.00 V	69.2	0.0	8.5	19.7	2.7
		1.00 C	87.3	0.4	2.0	6.9	3.4
		1.25	95.7	1.1	0.0	3.0	0.2
Subjacent sandstone	3	1.50	95.5	1.5	0.0	1.9	0.0
		1.75	89.5	0.0	4.5	4.6	1.4
		2.00	92.5	0.0	0.0	6.6	0.9
		2.50	90.6	0.0	3.7	4.8	1.0
	4	3.00	84.0	0.0	6.1	6.2	3.3
		3.50	87.1	0.0	2.6	9.2	1.1
		4.00	84.9	0.0	6.5	7.1	1.5
		4.50	82.0	0.0	5.8	11.0	1.2
		5.00	80.8	0.0	5.8	10.5	2.8
		5.50	76.5	0.7	5.0	11.6	6.1
		6.00	83.4	0.9	3.2	7.9	4.7
		6.50	81.3	1.4	3.0	5.6	8.7
		7.00	83.7	0.2	4.6	8.0	2.5

Table 2. Whole-rock geochemical data for the Route 56 paleosol *(given in weight percent).* Multiple samples from the same depth in the profile are identified using the nomenclature described in Table 1. Alumina/bases ratios were calculated using the methodology of Retallack (2001). Samples were prepared and analyzed (using X-ray fluorescence) by a commercial laboratory.

Unit		Depth in profile (m)	SiO_2 %	TiO_2%	Al_2O_3 %	Total Fe %	MnO %	MgO %	CaO%	Na_2O %	K_2O%	P_2O_5 %	Cr_2O_5 %	LOI %	Total %	Al/bases ratio
Boundary mudstone	1	0.00	62.07	1.35	23.27	1.49	0.01	0.37	0.08	0.16	2.19	0.05	0.03	7.89	98.93	21
		0.25	80.15	0.97	10.74	1.17	0.01	0.17	0.05	0.08	1.04	0.03	0.03	3.53	97.94	20
		0.50-1	82.69	0.88	9.11	0.66	0.01	0.15	0.05	0.07	0.86	0.03	0.05	2.98	97.47	20
		0.50-2	59.89	1.24	24.40	1.18	0.02	0.36	0.01	0.16	2.15	0.07	0.03	8.31	97.89	23
	2	0.75 V	78.92	0.70	6.97	6.12	0.04	0.10	0.06	0.05	0.57	0.06	0.08	3.73	97.40	22
		0.75 C	50.55	0.45	4.64	25.79	0.29	0.20	0.29	0.03	0.38	0.22	0.04	14.20	97.09	13
		1.00 R	41.95	0.57	9.84	33.78	0.42	0.15	0.04	0.06	0.95	0.30	0.03	9.23	97.32	20
		1.00 V	67.24	0.84	9.42	11.52	0.11	0.17	0.12	0.07	0.90	0.10	0.06	7.47	98.00	19
		1.00 C	70.46	0.46	4.22	13.90	0.15	0.12	0.14	0.03	0.39	0.15	0.06	7.29	97.37	15
		1.25	88.84	0.34	2.10	3.49	0.05	0.08	0.04	0.02	0.21	0.03	0.07	1.98	97.22	15
Subjacent sandstone	3	1.50	89.82	0.58	3.15	1.85	0.03	0.06	0.02	0.02	0.24	0.03	0.08	1.63	97.47	23
		1.75	91.37	0.54	2.78	1.29	0.01	0.03	0.01	0.02	0.22	0.03	0.10	0.89	97.25	25
		2.00	89.44	0.44	5.05	0.87	0.01	0.03	0.01	0.01	0.14	0.03	0.08	1.87	97.97	66
		2.50	90.90	0.58	4.10	0.63	0.01	0.04	0.01	0.02	0.33	0.03	0.06	1.24	97.92	25
	4	3.00	90.81	0.67	4.66	0.48	0.01	0.07	0.02	0.03	0.53	0.03	0.04	1.34	98.66	18
		3.50	90.57	0.69	5.67	0.60	0.01	0.07	0.03	0.04	0.62	0.03	0.06	1.69	100.07	18
		4.00	91.23	0.67	5.34	0.47	0.01	0.08	0.02	0.05	0.72	0.03	0.04	1.62	100.23	15
		4.50	91.62	0.45	5.42	0.64	0.01	0.07	0.01	0.04	0.57	0.03	0.06	1.69	100.56	19
		5.00	90.57	0.44	5.17	1.21	0.04	0.09	0.02	0.04	0.56	0.03	0.04	1.97	100.17	18
		5.50	85.97	0.48	5.60	3.99	0.15	0.18	0.07	0.04	0.65	0.06	0.06	3.35	100.59	15
		6.00	90.24	0.43	4.38	2.31	0.09	0.13	0.02	0.03	0.48	0.03	0.05	2.27	100.45	16
		6.50	87.60	0.24	3.28	4.39	0.17	0.25	0.04	0.02	0.32	0.03	0.03	3.34	99.68	13
		7.00	90.70	0.52	4.39	1.45	0.04	0.10	0.06	0.03	0.49	0.08	0.05	1.88	99.79	16
		Detection Limit (%)	0.01	0.01	0.01	0.01	0.01	0.01	0.01	0.01	0.05	0.03	0.01	0.05	0.01	

Discussion

Evidence of Intense Pedogenesis

The complexity documented in the Route 56 paleosol supports our interpretation of these rocks as a well-developed paleosol with a complex pedogenic history. Although the complexity of the paleosol makes it impossible to use standard soil horizon nomenclature, it is still possible to interpret the pedogenic processes that created each unit.

The subjacent sandstone exhibits varying degrees of pedogenic alteration. The presence of bedding and labile rip-up clasts in the lower part of the sandstone (Unit 4) implies that it consists of relatively unaltered parent material. In contrast, the upper part of the sandstone (Unit 3) possesses several characteristics of a well-leached, pedogenic ganister including quartz-rich sand, silica cement, absence of sedimentary structures, and a downward transition into a compositionally less mature sandstone (Percival, 1983).

Numerous aspects of Units 1 and 2 indicate that boundary mudstone is a clayey residuum composed of strongly altered parent materials. Abundant kaolinite and quartz suggests removal of unstable constituents by intense hydrolysis and leaching consistent with what would be expected in modern Oxisols (Soil Survey Staff, 1998; Birkeland, 1999; Retallack, 2001) or ferruginous soils (Duchaufour, 1982). Intense weathering is also supported by the presence of runiquartz, a common feature of modern Oxisols (Stoops, 1983). Sepic fabrics observed within Unit 2 glaebules are likely relict features inherited from an earlier stage of pedogenesis. The oxidized rinds and reduced cores of these glaebules suggest a complex history of iron mobilization and redoximorphism (Vepraskas, 1999). Although it is difficult to determine the nature of the parent material of the boundary mudstone, common coarse silt and sand suggest that at least some of the parent material was sandy (Loughnan and Bayliss, 1961).

Geochemical data also indicate that the boundary mudstone is a deeply weathered residual clay. Alumina/bases ratios of 13 to 23 indicate strong base depletion consistent with modern Oxisols (Retallack, 2001). Even though iron is in both an oxidized and reduced state, total iron values (up to 33.78%) compare well with that of some modern Oxisols (Birkeland, 1999). Like other paleosols associated with major geological unconformities, the Route 56 paleosol is enriched in resistant elements such as iron, aluminum, and silica (Retallack, 2001).

The absence of root traces and lack of clay coatings is consistent with evidence for extreme weathering because organic matter has low preservation potential in the strongly oxidizing conditions.

A Polygenetic History

The Mineralogical and micromorphological disparities described above suggest a polygenetic origin involving contrasting soil-forming regimes. For example, abundant kaolinite in the boundary mudstone indicates hydrolysis associated with a well-drained land surface but sphaerosiderite in the same part of the paleosol suggests gleying associated with a poorly-drained environment. Altogether, the features of the paleosol are interpreted to record three phases of development, as outlined below and in Figure 7.

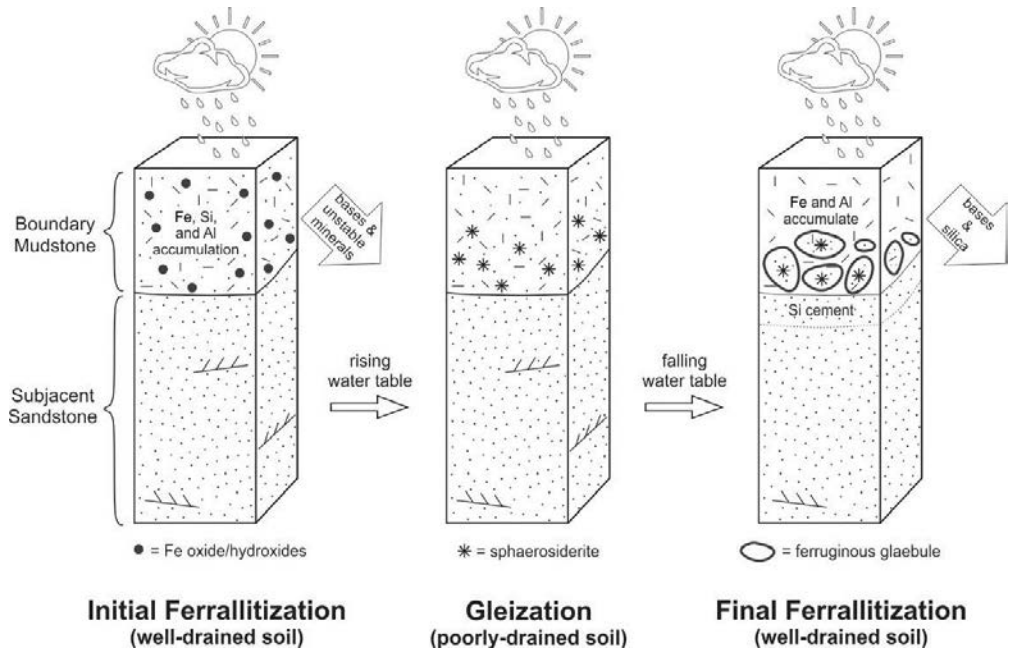

Figure 7. Three phase pedogenic model for the Route 56 paleosol illustrating development of ferruginous glaebules in the boundary mudstone.

Phase 1(Initial Ferrallitization): This phase was characterized by good drainage and intense hydrolysis. Abundant rainfall and good drainage allowed for the leaching of bases and the destruction of unstable minerals by chemical weathering. The residuum of kaolinite and quartz is preserved as the kaolinitic matrix of the glaebule cores. The presence of sphaerosiderite in globule cores indicates that the hydrolysis phase was followed by gleization. Given the evidence for an initial phase of intense chemical weathering, it seems likely that iron oxides/hydroxides also accumulated as a residual product of deep weathering. During this initial phase, the Route 56 paleosol approached a state of development comparable to that of an Oxisol.

Phase 2 (Gleization): During this phase drainage conditions deteriorated as the water table rose. The iron oxides/hydroxides concentrated during Phase 1 were transformed into sphaerosiderite by during gleying by alkaline, reducing water (Curtis and others, 1975; Ludvigson and others, 1998; Ufnar and others, 2001). These waters were probably meteoric rather than marine because the presence of sulfide in the system would have favored the formation of pyrite over sphaerosiderite.

Phase 3 (Final Ferrallitization): During this final phase, the glaebules in Unit 2 of the boundary mudstone were created by lowered or seasonally fluctuating water levels. Oxidation of sphaerosiderite created the iron-rich materials in the glaebule rinds. Much of this iron appears to be derived from the iron-depleted, vuggy middle layer of the glaebules. The siderite-rich cores of the glaebules represent pedorelicts of the gleization phase. Fractured runiquartz in glaebule rinds suggests intense physical and chemical destruction of quartz. The solubility of quartz in the upper part of the paleosol may have increased significantly by redoximorphic reactions involving iron (Morris and Fletcher, 1987). This final phase of pedogenesis was followed by deposition of Pottsville sediments during onlap of the mid-Carboniferous land surface.

Relationship to the Mississippian-Pennsylvanian Unconformity

The Route 56 paleosol is interpreted as an interfluve expression of the Mississippian–Pennsylvanian unconformity. Unlike many floodplain paleosols, those developed on interfluves typically are polygenetic and have complex drainage histories related to changes in base level (Gardner and others, 1988; McCarthy and Plint, 1998; McCarthy and others, 1999; Plint and others, 2001). Given the complexity seen within the Route 56 paleosol, it is difficult to unequivocally attribute polygenesis of the Route 56 paleosol to a single base-level event. Although likely formed in association with the mid-Carboniferous eustatic event that impacted much of the basin (Saunders and Ramsbottom, 1986; Beuthin, 1997; Driese and others, 1998; Blake and others, 2002), the hiatus in the study area is large enough that the paleosol may also have been impacted by tectonic activity, climate change, and landscape evolution.

The Route 56 paleosol probably does not record the entire weathering history of the unconformity. The deeply leached and weathered character of the paleosol suggests development during the tropical rainy conditions of the early Pennsylvanian Period (Cecil and others, 1985; Cecil, 1990). In contrast, paleosols formed under the seasonal climate of late Mississippian time in the Appalachian Basin are typically vertic and/or calcareous (Cecil and others, 1985; Cecil, 1990; Cecil and others, 1992; Caudill and others, 1992, 1996; Beuthin, 1997; Beuthin and Blake, 2002). Much like the Olive Hill clay of eastern Kentucky, the Route 56 paleosol probably records Pennsylvanian weathering of exposed Mississippian strata in the aftermath of a "Mississippian–Pennsylvanian" event. Regardless of exactly when weathering began, the Route 56 paleosol provides sedimentological evidence for a pronounced unconformity between the Mississippian and Pennsylvanian systems at this site.

The Route 56 paleosol provides important data for assessing regional variations in soil formation associated with the Mississippian–Pennsylvanian unconformity. The Mercer clay near Clearfield, Pennsylvania (Figure 1) is also interpreted as a residual clay developed in association with the unconformity (Williams and Bragonier, 1985). In contrast to the iron-rich Route 56 paleosol, the Mercer clay is a more deeply weathered alumina-rich residuum that contains diaspore, boehemite, and gibbsite. Just east of Morgantown, West Virginia (Figure 1), the unconformity is marked by a clayey paleosol that appears to be a paleo-Ultisol (Cecil and others, 1992). Taken together, these paleosols indicate a south-to-north increase of paleopedogenesis across the northern flank of the basin that likely resulted from differences in the duration of subaerial exposure related to paleotopography on the unconformity surface.

Conclusions

In many cases, identification of residual clays related to the Mississippian–Pennsylvanian unconformity may requires more than just field observation. In this case, abundant siderite might lead one to infer that it was formed entirely in a poorly-drained environment. However, micromorphological and geochemical analysis indicates a complex, polygenetic developed during the large time gap represented by the Mississippian–Pennsylvanian unconformity.

Despite its stratigraphic importance, the Mississippian–Pennsylvanian unconformity remains a cryptic feature at many localities in the Appalachian Basin (Brezinski, 1985; Edmunds, 1993). Although the erosional features of the unconformity are much more obvious, this study adds to the growing body of evidence that paleosols can be equally diagnostic features (Cecil and

others, 1992; Beuthin, 1997). Given the insights from this study, it seems likely that the unconformity should be marked by more residual clays and mature paleosols on the northern and western flanks of the basin where prolonged exposure occurred. Continued analysis of paleosols associated with the Mississippian–Pennsylvanian boundary may yield better evidence for the unconformity and additional details of soil-forming processes related to unconformity development.

Acknowledgments

This contribution is largely derived from Rygel, M.C. and Beuthin, J.D., 2002, Paleopedology of a residual clay associated with the Mississippian–Pennsylvanian (mid-Carboniferous) unconformity, southwestern Pennsylvania; Southeastern Geology, v. 41, no. 3, p. 129-143.The original manuscript benefited from thoughtful reviews by Steven Driese (University of Tennessee) and Stephen Greb (Kentucky Geological Survey). We thank Bascombe M. Blake (West Virginia Geological & Economic Survey) for reviewing an early draft of this manuscript and Frank Dulong (U. S. Geological Survey, Reston) for providing technical guidance and lab facilities for XRD analysis.

References Cited

Beuthin, J.D., 1994, A sub Pennsylvanian paleovalley system in the central Appalachians and its implications for tectonic and eustatic controls on the origin of the regional Mississippian Pennsylvanian unconformity, *in* Dennison, J.M., and Ettensohn, F.R., eds., Tectonic and eustatic controls on sedimentary cycles: SEPM (Society for Sedimentary Geology) Concepts in Sedimentology and Paleontology, v. 4, p. 107 120.

Beuthin, J.D., 1997, Paleopedological evidence for a eustatic Mississippian Pennsylvanian (mid Carboniferous) unconformity in southern West Virginia: Southeastern Geology, v. 37, p. 25 37.

Beuthin, J.D., and Blake, B.M., Jr., 2002, Scrutiny of a global climate model for Upper Mississippian depositional sequences in the central Appalachian foreland basin, U.S.A.: Journal of Geology.

Birkeland, P.W., 1999, Soils and geomorphology (3rd edition): New York, Oxford University Press, 430 p.

Blake, B. M., Jr., Cross, A. T., Eble, C. F., Gillespie, W. H., and Pfefferkorn, H. W., 2002, Selected plant megafossils from the Carboniferous of the Appalachian Region, Eastern United States: Geographic and Stratigraphic Distribution: *in* Hills, L.V., Henderson, C.M., and Bamber, E.W., eds., Carboniferous and Permian of the World: Canadian Society of Petroleum Geologists, Memoir 19, p. 259-335.

Brewer, R., 1976, Fabric and mineral analysis of soils (2nd Edition): New York, R.E. Krieger, 482 p.

Brezinski, D.K., 1989, Upper Mississippian, *in* Harper, J.A., ed., Geology in the Laurel Highlands, southwestern Pennsylvania: Annual Field Conference of Pennsylvania Geologists, 54th, Johnstown, PA, Guidebook, p. 205 210.

Caudill, M.R., Mora, C.I., Tobin, K.J., and Driese, S.G., 1992, Preliminary interpretations of paleosols associated with Late Mississippian marginal marine deposits, Pennington Formation, Monterey, TN, *in* Driese, S.G., Mora, C.I., and Walker, K.R., eds., Paleosols, paleoweathering surfaces, and sequence boundaries: University of Tennessee Department of Geological Sciences Studies in Geology 21, p. 57-77.

Caudill, M.R., Driese, S.G., and Mora, C.I., 1996, Preservation of a paleo Vertisol and an estimate of Late Mississippian paleoprecipitation: Journal of Sedimentary Research, v. 66, p. 57 78.

Cecil, C.B., 1990, Paleoclimate controls on stratigraphic repetition of chemical and siliciclastic rocks: Geology, v. 18, p. 533 536.

Cecil, C.B., Stanton, R.W., Neuzil, S.G., Dulong, F.T., Ruppert, L.L., and Pierce, B., 1985, Paleoclimate controls on Late Paleozoic sedimentation and peat formation in the central Appalachian Basin: International Journal of Coal Geology, v. 5, p. 195 230.

Cecil, C.B., and Dulong, F.T., 1992, Stop 10: West Virginia Turnpike section, *in* Cecil, C.B., and Eble, C.F., eds., Paleoclimate controls on Carboniferous sedimentation and cyclic stratigraphy in the Appalachian Basin: U.S. Geological Survey Open-File Report 92-546, p. 45.

Cecil, C.B., Eble, C., and Dulong, F.T., 1992, Stop 1 Mississippian Pennsylvanian unconformity, Exit 15, I 68, *in* Cecil, C.B., and Eble, C.F., eds., Paleoclimate controls on Carboniferous sedimentation and cyclic stratigraphy in the Appalachian Basin: U.S. Geological Survey Open File Report 92 546, p. 7 11.

Chesnut, D.R., 1988, Stratigraphic analysis of the Carboniferous rocks of the central Appalachian Basin [Ph.D. dissertation]: Lexington, University of Kentucky, 297 p.

Chesnut, D.R., 1990, Timing of Alleghenian tectonics determined by central Appalachian foreland basin analysis: Southeastern Geology, v. 30, p. 203 221.

Chesnut, D.R., 1992, Stratigraphic and structural framework of the Carboniferous rocks of the central Appalachian Basin in Kentucky: Kentucky Geological Survey Bulletin 3, 42 p.

Chesnut, D.R., Greb, S.F., Eble, C., and Rice, C., 1992, Stop 9 – Gregoryville exposure on I 64 in Kentucky – an examination of two middle Carboniferous depositional models, *in* Rice, C.L., Martino, R.L., and Slucher, E.R., Regional aspects of Pottsville and Allegheny stratigraphy and depositional environments (Ohio and Kentucky): U.S. Geological Survey Open File Report 92 558, p. 47 55.

Curtis, C.D., Pearson, M.J., and Somogyi, V.A., 1975, Mineralogy, chemistry, and origin of a concretionary siderite sheet (clay ironstone band) in the Westphalian of Yorkshire: Mineralogical Magazine, v. 40, p. 385 393.

Donaldson, A.C., Renton, J.J., and Presley, M.W., 1985, Pennsylvanian deposystems and paleoclimates of the Appalachians: International Journal of Coal Geology, v. 5, p. 167-193.

Driese, S.G., Caudill, M.R., and Srinivasan, K., 1998, Late Mississippian to Early Pennsylvanian paleokarst in east central Tennessee: Field, petrographic, and stable isotope evidence: Southeastern Geology, v. 37, p. 189 204.

Duchaufour, P., 1982, Pedology: London, George Allen and Unwin, 449 p.

Edmunds, W.E., 1993, Regional aspects of the Mauch Chunk Formation: the hard luck delta revisited, *in* Shaulis, J.R., Brezinski, D.K., Clark, G.M., and 13 others, Geology of the southern Somerset County region, southwestern Pennsylvania: Annual Field Conference of Pennsylvania Geologists, 58th, Somerset, PA, Guidebook, p. 11 19.

Ettensohn, F.R., 1994, Tectonic control on formation and cyclicity of major Appalachian unconformities and associated stratigraphic sequences, *in* Dennison, J.M., and Ettensohn, F.R., eds., Tectonic and eustatic controls on sedimentary cycles: SEPM (Society for Sedimentary Geology) Concepts in Sedimentology and Paleontology, v. 4, p. 217 242.

Ettensohn, F.R., and Chesnut, D.R., 1989, Nature and probable origin of the Mississippian Pennsylvanian unconformity in the eastern United States, *in* Yugan, J., and Chun, L., eds.,

Compte Rendu, Onzième Congrès International de Stratigraphie et de Géologie du Carbonifère: Nanjing, Nanjing University Press, v. 4, p. 145 159.

Gardner, T.W., Williams, E.G., and Holbrook, P.W., 1988, Pedogenesis of some Pennsylvanian underclays; Ground-water, topographic, and tectonic controls: in Reinhardt, J., and Sigleo, W.R., Paleosols and weathering through geologic time: Principles and applications: Geological Society of America Special Paper 216, p. 81-101.

Glover, A.D., and Edmunds, W.E., 1981, Johnstown quadrangle, in Berg, T.M., and Dodge, C.M., compilers, Atlas of preliminary geologic quadrangle maps of Pennsylvania: Harrisburg, Pennsylvania Geologic Survey, Map 61, p. 295.

Greb, S.F., and Caudill, M.R., 1998, Stop 5: Well-developed paleosols of the upper Pennington Formation, *in* Eble, C.F., Greb, S.F., and Dever, G.R., Jr., eds., Geology of the Pound Gap roadcut, Letcher County, Kentucky: 1998 Annual Field Conference of the Kentucky Society of Professional Geologists Guidebook, p. 37-41.

Horowitz, A. S., and Rexroad, C. B., 1972, Conodont biostratigraphy of some United States Mississippian sites: Journal of Paleontology, v. 46, p. 884 891.

Humbert, S.E., 2001, Subaerial paleokarst in the upper Pennington Formation (Upper Mississippian) limestones at Leatherwood Ford, Big South Fork, Tennessee [M.S. Thesis]: Knoxville, University of Tennessee, 143 p.

Loughnan, F.C., and Bayliss, P., 1961, The mineralogy of the bauxite deposits near Weipa, Queensland: The American Mineralogist, v. 46, p. 209 217.

Ludvigson, G.A., Gonzalez, L.A., Metzger, R.A., Witzke, B.J., Brenner, R.L., Murillo, A.P., and White, T.S., 1998, Meteoric sphaerosiderite lines and their use for paleohydrology and paleoclimatology: Geology, v. 26, p. 1039 1042.

McCarthy, P.J., and Plint, A.G., 1998, Recognition of interfluve sequence boundaries: integrating paleopedology and sequence stratigraphy: Geology, v. 26, p. 387 390.

McCarthy, P.J., Faccini, U.F., and Plint, A.G., 1999, Evolution of an ancient coastal plain: paleosols, interfluves and alluvial architecture in a sequence stratigraphic framework, Cenomanian Dunvegan Formation, NE British Columbia, Canada: Sedimentology, v. 46, p. 861 891.

Menning, M., Weyer, D., Drozdzewski, G., van Amerom, H.W.J., and Wendt, I., 2000, A Carboniferous time scale 2000 – discussion and use of geological parameters as time indicators from Central and Western Europe: Geologie en Mijnbouw, v. A 156, p. 3 44.

Miller, D.J., and Eriksson, K.A. 1999, Linked sequence development and global climate change: The Upper Mississippian record in the Appalachian Basin: Geology, v. 27, p. 35–38.

Miller, D. J., and Eriksson, K. A. 2000, Sequence stratigraphy of Upper Mississippian strata in the central Appalachians: A record of glacioeustasy and tectonoeustasy in a foreland basin setting: American Association of Petroleum Geologist Bulletin, v. 84, p. 210–233.

Morris, R.C., and Fletcher, A.B., 1987, Increased solubility of quartz following ferrous ferric iron reactions: Nature, v. 330, p. 558 561.

Percival, C.J., 1983, A definition of the term ganister: Geological Magazine, v. 120, p. 187 190.

Phalen, W.C., 1910, Description of the Johnstown Quadrangle: U.S. Geological Survey Geologic Atlas of the United States, Folio 174, 15 p., 4 pl.

Plint, A.G., McCarthy, P.J., and Faccini, U.F., 2001, Nonmarine sequence stratigraphy – updip expression of sequence boundaries and systems tracts in a high resolution framework, Cenomanian Dunvegan Formation, Alberta foreland basin, Canada: American Association of Petroleum Geologists Bulletin, v. 85, p. 1967 2001.

Quinlan, G.M., and Beaumont, C., 1984, Appalachian thrusting, lithospheric flexure, and the Paleozoic stratigraphy of the Eastern Interior of North America: Canadian Journal of Earth Sciences, v. 21, p. 973 996.

Retallack, G.J., 2001, Soils of the past, an introduction to paleopedology (2nd edition): Oxford, Blackwell Science, 404 p.

Rice, C.L., 1984, Sandstone units of the Lee Formation and related strata in northeastern Kentucky: U.S. Geological Survey Professional Paper 1151 G, 53 p.

Rice, C.L., 1985, Terrestrial vs. marine depositional model a new assessment of subsurface Lower Pennsylvanian rocks of southwestern Virginia: Geology, v. 13, p. 786 789.

Rice, C.L., and Schwietering, J.F., 1988, Fluvial deposition in the central Appalachians during the early Pennsylvanian: U.S. Geological Survey Bulletin 1839, p. B1 B10.

Saunders, W.B., and Ramsbottom, W.H.C., 1986, The mid Carboniferous eustatic event: Geology, v. 14, p. 208 212.

Soil Survey Staff, 1998, Keys to soil taxonomy: Blacksburg, Pocahontas Press, 328 p.

Smyth, A.L., 1984, Pedogenesis and diagenesis of the Olive Hill Clay Bed, Breathitt Formation (Carboniferous) Northeastern Kentucky [M.S. thesis]: Cincinnati, Ohio, University of Cincinnati, 201 p.

Stamm, R.G., 1997, Late Mississippian conodont biostratigraphy of the Appalachian Basin, preliminary correlations to the Eastern Interior basin and eustatic curves: Geological Society of America Abstracts with Programs: v. 29, no. 2, p. 48.

Stoops, G., 1983, Micromorphology of oxic horizons, *in* Bullock, P., and Murphy, C.P., eds., Soil Micromorphology: Berkhamstead, U.K., A.B. Academic, p. 419 440.

Ufnar, D.F., Gonzalez, L.A., Ludvigson, G.A., Brenner, R.L., and Witzke, B.J., 2001, Stratigraphic implications of meteoric sphaerosiderite δ18 values in paleosols of the Cretaceous (Albian) Boulder Creek Formation, NE British Columbia Foothills, Canada: Journal of Sedimentary Research, v. 71, p. 1017 1028.

Vepraskas, M.J., 1999, Redoximorphic features for identifying aquic conditions: North Carolina Agricultural Research Service Technical Bulletin 301, 33 p.

Williams, E.G., and Bragonier, W.A., 1985, Origin of the Mercer high alumina clay, *in* Gold, D.P., Central Pennsylvania geology revisited: Annual Field Conference of Pennsylvania Geologists, 50th, State College, PA, Guidebook, p. 204 290.

Williams, E.G., Guber, A.L., and Johnson, A.M., 1965, Rotational slumping and the recognition of disconformities: Journal of Geology, v. 73, p. 534 547.

Yang, C., 1998, Basin analysis of the Carboniferous strata in central and southern West Virginia using sequence stratigraphic principles [Ph.D. dissertation]: Morgantown, West Virginia University, 350 p.

GENETIC STRATIGRAPHY: LATE PLEISTOCENE THROUGH THE HOLOCENE PALEOCLIMATES AND PALEOENVIRONMENTS OF PENNSYLVANIA

FRANK J. VENTO, PH.D., PROFESSOR EMERITUS, DEPARTMENT OF GEOLOGY, CLARION UNIVERSITY OF PENNSYLVANIA
ANTHONY VEGA, PH.D., PROFESSOR, DEPARTMENT OF GEOLOGY, CLARION UNIVERSITY OF PENNSYLVANIA
HAROLD ROLLINS, PH.D., PROFESSOR EMERITUS, DEPARTMENT OF GEOLOGY, UNIVERSITY OF PITTSBURGH

Introduction

The following paper will be published (Chapter 1: Genetic Stratigraphy: Late Pleistocene through the Holocene Paleoclimates and Paleoenvironments of Pennsylvania) in an upcoming book: The Archaeology of Native Americans in Pennsylvania edited by Kurt W. Carr, Christopher A. Bergman, Christina B. Reith, Bernard K. Means, and Roger W. Moeller. This represents a detailed synthesis of Pennsylvania archaeology including the geomorphology of archaeological sites and paleoenvironmental reconstruction of the last 16,000 years for the region. All citations to this paper should acknowledge the material above. The chapter presents a synthetic organization of the geomorphology of Pennsylvania as it relates to Native American archaeological sites. First, using genetic stratigraphy, we reconfigure the geomorphology of the major drainage systems into chronostratigraphic units, focusing upon dated paleosols from cultural deposits. Relevant sites within each of the major drainage basins are discussed and characterized, noting the specific geomorphic traits signaling potential stratified cultural deposits along various sections of the evolving drainage systems. To achieve environmental reconstruction, the chronostratigraphic units are then correlated within and between drainage basins. In addition, a standardized descriptive terminology is presented for the stratigraphy of Pennsylvania's drainage systems as they relate to climatic and cultural strata.

Secondly, we offer a paleo-environmental and paleoclimatic reconstruction that extends from Late Pleistocene to the present. This enables cultural events to be positioned on an ecological stage, in sufficient detail that they can (where appropriate) be related to such environmental and climatic events as the Younger Dryas, the Sub-Boreal, the Neo-Atlantic/Medieval Warming and the Little Ice Age (Figure 1).

Introduction to Genetic Stratigraphy

Work on the stratigraphic correlation of marine units led to the recognition of genetic units (Walker, 1980; Goodwin and Anderson 1985; Busch and West, 1987). These genetic units were categorized according to their lateral extent (Figures 2 and 3). Some genetic units were the transgressive-regressive products of sea level change and could be correlated widely, presumably reflecting a depositional signature that affected a broad geographic area (allogenic event). Other genetic units were locally developed (such as the products of delta switching and destruction) and were termed autogenic. The latter were of limited use in regional stratigraphic correlation.

Genetic units, wherever identified (e.g. in exposures, cores, etc.), are of unknown lateral extent prior to correlation. The scale of allogenicity and autogenicity is relative and is dependent upon the scale of observation of lateral extent. Allogenic events, for example, may be global or confined to a single depositional basin or drainage system. Autogenic events may be similarly

scaled, ranging from local tectonism down to delta switching, storm scour, or channel avulsion. In order to establish the geographic extent of a genetic unit one must assume initially that it is extensively correlatable (Figure 4).

Years B.P.	Blytt-Sernander Climatic Episodes	Pollen Zones	Forest Type	Climatic Conditions	Fluvial Conditions	Genetic Stratigraphic Horizons	Archaeological Cultural Periods	Stratigraphic Discontinuities
Present	Modern							
500	Neo-Boreal "Little Ice Age"	C-3b	Spruce-Pine Rise	Cool moist to cool dry	Rapid alluviation	A-C	Late Woodland	Little Ice Age Disconformity 750 B.P.
	Pacific							
1,000	Neo-Atlantic	C-3a	Oak Hemlock Chestnut	Warm moist	Floodplain stability	Owasco Paleosol	Middle Woodland	Scandic Disconformity 1750 B.P.
1,500	Scandic			Cool moist	Rapid alluviation	Weak Bw/BC/C		
2,000								
2,500	Sub-Atlantic			Warm moist	Floodplain stability	Fox Creek Paleosol	Early Woodland	
3,000								
3,500	Sub-Boreal	C-2	Oak Hickory	Warm dry	Severe to modest later channel migration (small tributaries) with alluviation dominant over incision along major tributaries; zonal flow and Bermuda High	Bw	Transitional Archaic	Sub Boreal
4,000								
4,500	Atlantic	C-1	Mid-Point Hemlock Decline	Warm and slightly moister	Atlantic II Increased meridional flow and increased rates of vertical accretion	Upper Atlantic I paleosol (incipient)	Late Archaic	Disconformity 4200 B.P.
5,000						Bw		
5,500						Middle Atlantic II paleosol (incipient)		
6,000			Oak Hemlock		Atlantic I Primarily zonal flow and slow continuous vertical accretion, strong soil weathering/ development of Bw, Bt Btx, Bx	Bw, Bt, Btx, Bx	Middle Archaic	
6,500								
7,000								
7,500								
8,000								
8,500	Boreal	B	Pine Oak	Warm dry	Zonal circulation and rapid alluviation	Boreal paleosol (incipient)		
9,000						BC/CB/C, lamellae bands (stacked A-C horizons)		
9,500	Pre-Boreal						Early Archaic	
10,000								
10,500	Younger Dryes	A-4	Spruce Pine	Cool dry	Initiation of meandering	C		YD Disconformity 10,100 to 10,900 B.P.
					Braided			
11,000	Allerod	A-3/A-2	Spruce Pine		Renewed vertical accretion, absent on low terraces due to erosion during YD	A-B horizon development	Paleoindian	
	Intra-Allerod Cold Period (IACP)							
11,500	Allerod							
12,000	Older Dryas							
12,500	Bolling		Spruce Parklands					
13,000	Oldest Dryas			Warm and wet	Braided conditions	Lateral accretion/ outwash		Late Wisconsin Disconformity
13,500		T	Tundra				PreClovis	
14,000								
14,500								

Figure 1. Diagrammatic Table Showing Relationship of Climate Episodes with Pollen Zones, Climatic and Fluvial Response, Stratigraphic Discontinuities and Genetic Horizons

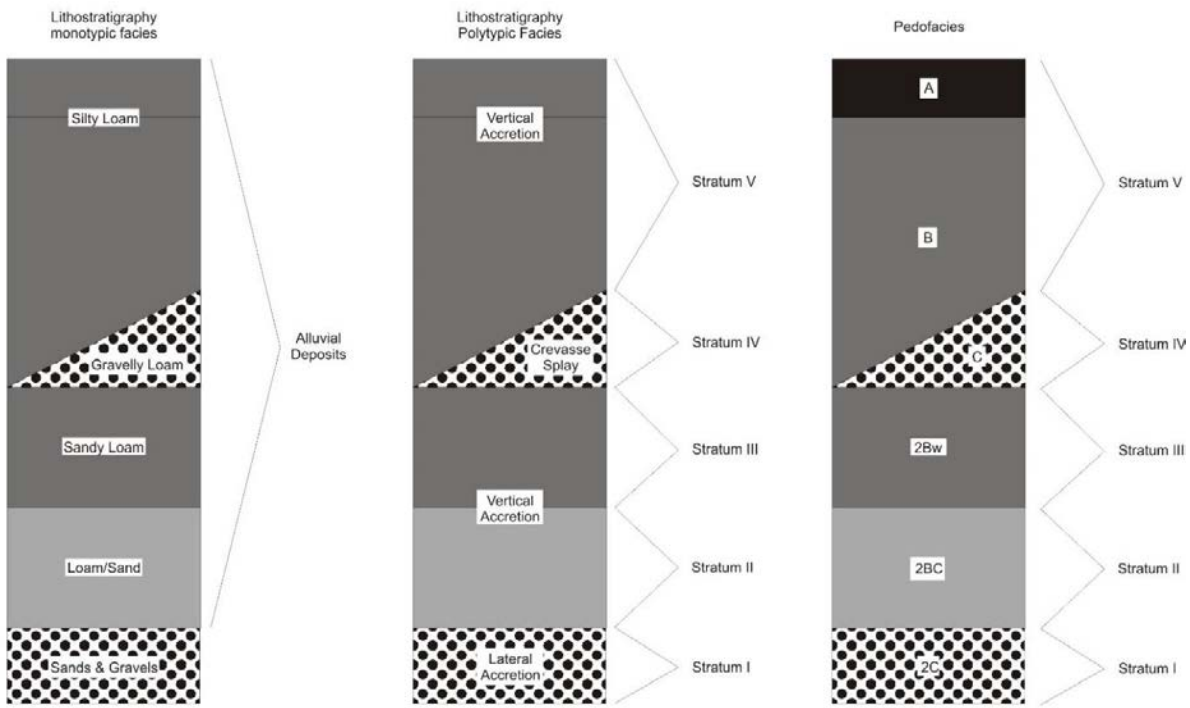

Figure 2. Schematic Profile Illustrating Monotypic and Polytypic Facies and Pedostratigraphic Horizons

In Pennsylvania and, in general, the Mid-Atlantic region, alluvial paleosols (now buried cumulic A horizons) document prolonged episodes of terrace stability. As such, they are excellent chronostratigraphic marker horizons (allogenic genetic units) that can be recognized and utilized in both inter-basinal and intra-basinal stratigraphic correlations. On the other hand, alluvial strata that are products of events that are environmentally and geographically circumscribed are local (autogenic genetic units) and generally not as useful for stratigraphic correlation. A sand horizon deposited as a result of a large flood event over several days is a classic autogenic unit that is effectively time-parallel. While such events are temporally constrained, their geographical expressions (or recognition) within an alluvial package are quite limited.

Genetic stratigraphy, as applied to marine sequences, can be readily adapted to alluvial sequences containing paleosols (buried soils). Alluvial sequences are now viewed as representing long intervals of stasis (indicated by buried soils), punctuated by brief episodes of deposition or erosion (Kraus and Brown 1986; Kraus 1987; Retallack 1984). As such, paleosols are ideal genetic units for establishing a chronostratigraphic framework. Because they reflect extensive temporal stability, paleosols, in general, are allogenic genetic units traceable over considerable distances. The degree of temporal stability, or time interval represented by the paleosols, varies widely. A-horizons may form on alluvial deposits in humid regions in only a few hundred years (Scully and Arnold 1979, 1981). On the other hand, paleosol formation may take tens of thousands of years or more in arid regions (Kraus and Brown 1986, and references therein).

The bulk of the physical alluvial record is, in a sense, a record of the punctuational events - the brief and episodic deposition of channel and splay deposits, channel avulsion, migration, etc.

Thus, alluvial facies are predominantly autogenic units, untraceable over extensive geographic areas. Alluvial sequences commonly vary greatly in thickness and contained facies over short lateral distances, making lithofacies correlation virtually impossible. However, such pronounced facies development is likely to be absent within very distinct genetic surfaces connected with the thin paleosols. Paleosols can thus be treated like the transgressive surfaces and climate-change surfaces in marine genetic stratigraphy. The complexities of Walther's Law will only be present within the boundaries of the allogenetic genetic surfaces of the paleosols.

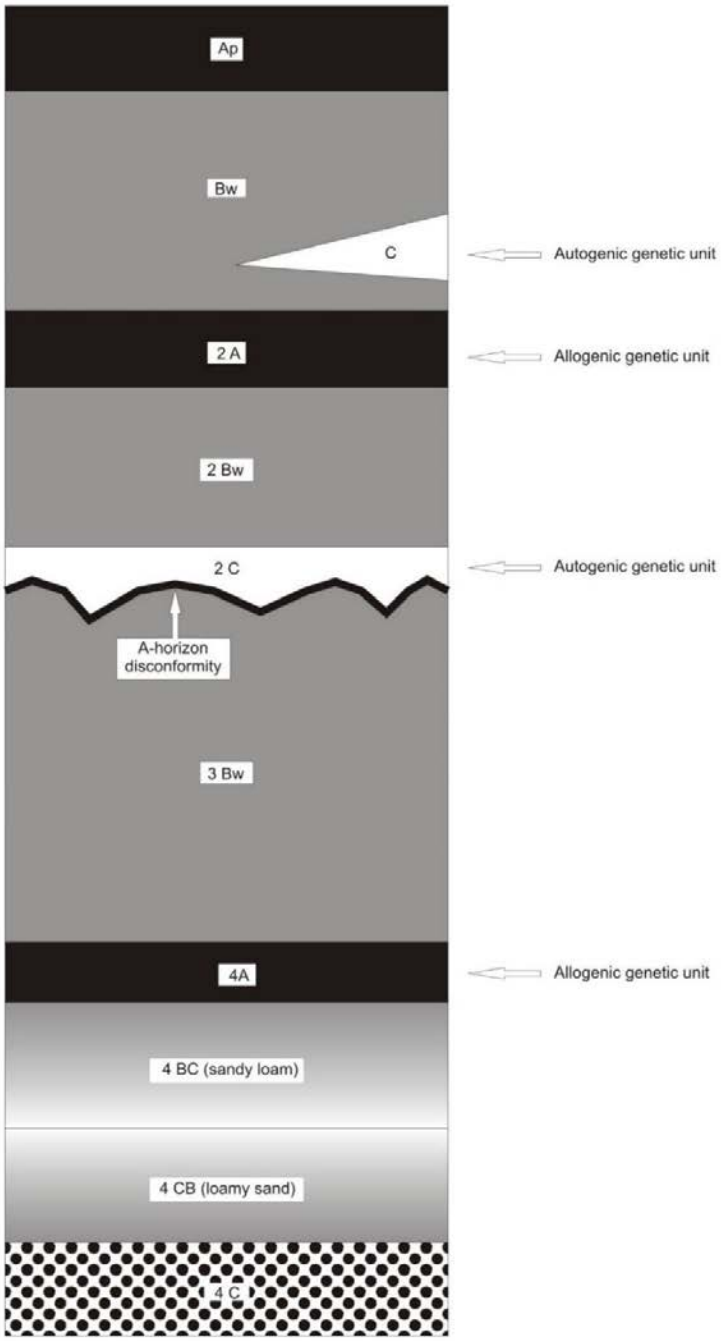

Figure 3a. Idealized Soil Stratigraphic Profile Showing Allogenic and Autogenic Horizons

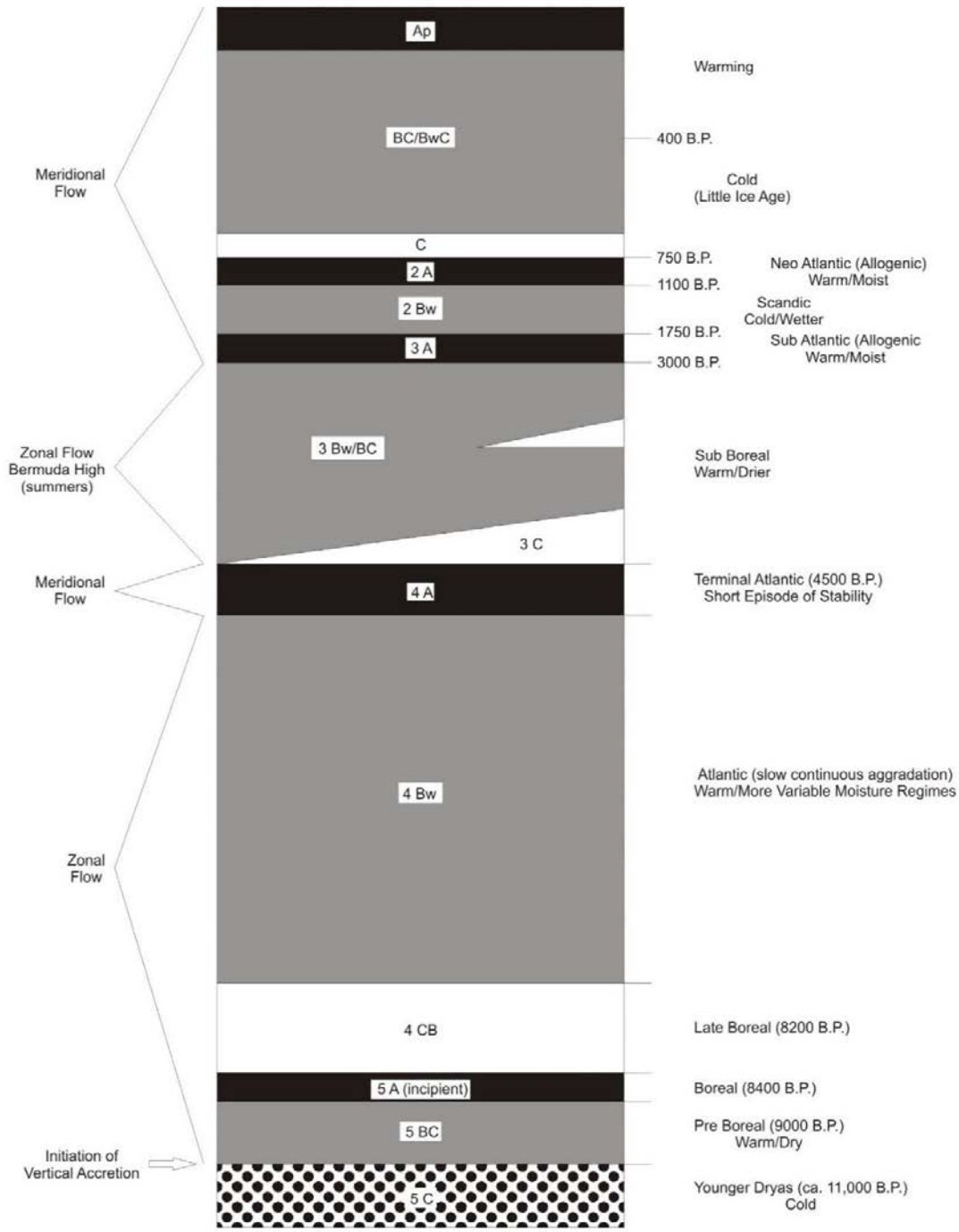

Figure 3b. Idealized Soil Stratigraphic Profile for the Susquehanna River Valley

The lateral changes in the distinguishing characteristics of marine allogenic surfaces also have an analog in alluvial sequences. In the stratigraphic record of marine basins, proximal (marginal) hard grounds may grade distally basinward into cryptic time-averaged shell lags. Similarly, Brown and Kraus (1986) and Kraus (1987) described morphological variation in

laterally developed paleosols ("pedofacies") in early Eocene overbank deposits in the northern Big Horn Basin. Pedogenic sequences near channel margins (proximal) developed only incipient (stage 1) paleosols, whereas those in flood plain areas (distal) tended to exhibit relatively more mature (stage 2 or stage 3) paleosols. The more mature distal paleosols will usually be more easily traced over wide areas, but the more cryptic immature proximal paleosols will provide greater details of autogenic overprinting (episodic channel migration, avulsion, etc.). In practice both the more mature distal and cryptic/immature proximal paleosols represent "marker" or "event" horizons that permit the floating of adjacent stratigraphic sections into a meaningful integrated chronostratigraphic framework. The application of this high-resolution chronostratigraphic framework will facilitate predictive stratigraphy (Figures 2 – 4). Genetic units thus can provide important information on the responses of fluvial systems to Holocene climate change and can aid in archaeological site prediction. The recognition of allogenic genetic surfaces that "punctuate" small-scale allogenic units permits refined chronostratigraphy at archaeological sites. The basic genetic units can often be combined into a hierarchical framework of allogenic genetic units, leading to an integrative type of stratigraphic analysis (Busch and West, 1987; Rollins *et al.* 1989; Vento *et al.* 1994, Vento *et al*. 2008).

In fact, any carefully constructed chronostratigraphic framework using paleosols should investigate the merits of a hierarchical approach. Temporally extensive alluvial sequences are likely to record more than a single level of allogenic genetic units. Kraus (1987) subdivided the early Eocene Willwood alluvial deposits into third-order sequences (small paleosol sequences, 3-7 m thick), second-order sequences (tens of meters thick and harboring a number of vertically stacked, third-order cycles), and first-order sequences (hundreds of meters thick, containing several second-order sequences). The larger genetic units (first-order) probably reflect such events as basin-wide climatic and/or tectonic change. Smaller genetic units (third-order and second-order) are likely controlled by such factors as channel migration, avulsion, overbanking, etc. (Kraus 1987).

There can be intimate interfacing of marine and terrestrial genetic units in drainage basins that adjoin coasts. For example, the Delaware drainage system which possesses only minor falls at the Coastal Plain/Piedmont transition, is affected by fluctuations in base level resulting from changes in relative sea level. A dramatic reduction in the rate of floodplain accretion at the head-of-tide and in lower elevational portions of the Delaware Valley, at approximately 5000 BP. to 4500 BP., correlates with a major change in rate of sea level rise in Delaware Bay (Kraft and John 1987). Conversely, middle and upper sections of the Valley exhibit high rates of alleviation during the same interval. Cycles of relative sea level change along the northeast coast of the U.S. might control via episodic alluviation or incision, for example, the development of paleosol sequences.

Prolonged changes in the fluvial regimes in the northeast were related to ablation of the Laurentian ice sheet and concomitant changes in atmospheric circulation. For example, from 10,000 BP. to 6000 BP. the Holocene was dominated by strong zonal flow which favored relatively slow but continuous vertical accretion along the major drainage routes in the region (Figure 5). After 6000 BP. the continued ablation of the ice sheets engendered more frequent meridional circulation and the penetration of warm and moist air masses, and larger cyclonic storms (Vento *et al.* 1994). Paleosols on aggrading terraces within the Middle Atlantic region reflect these changes in atmospheric circulation. The interval 6000 BP. to present displays a

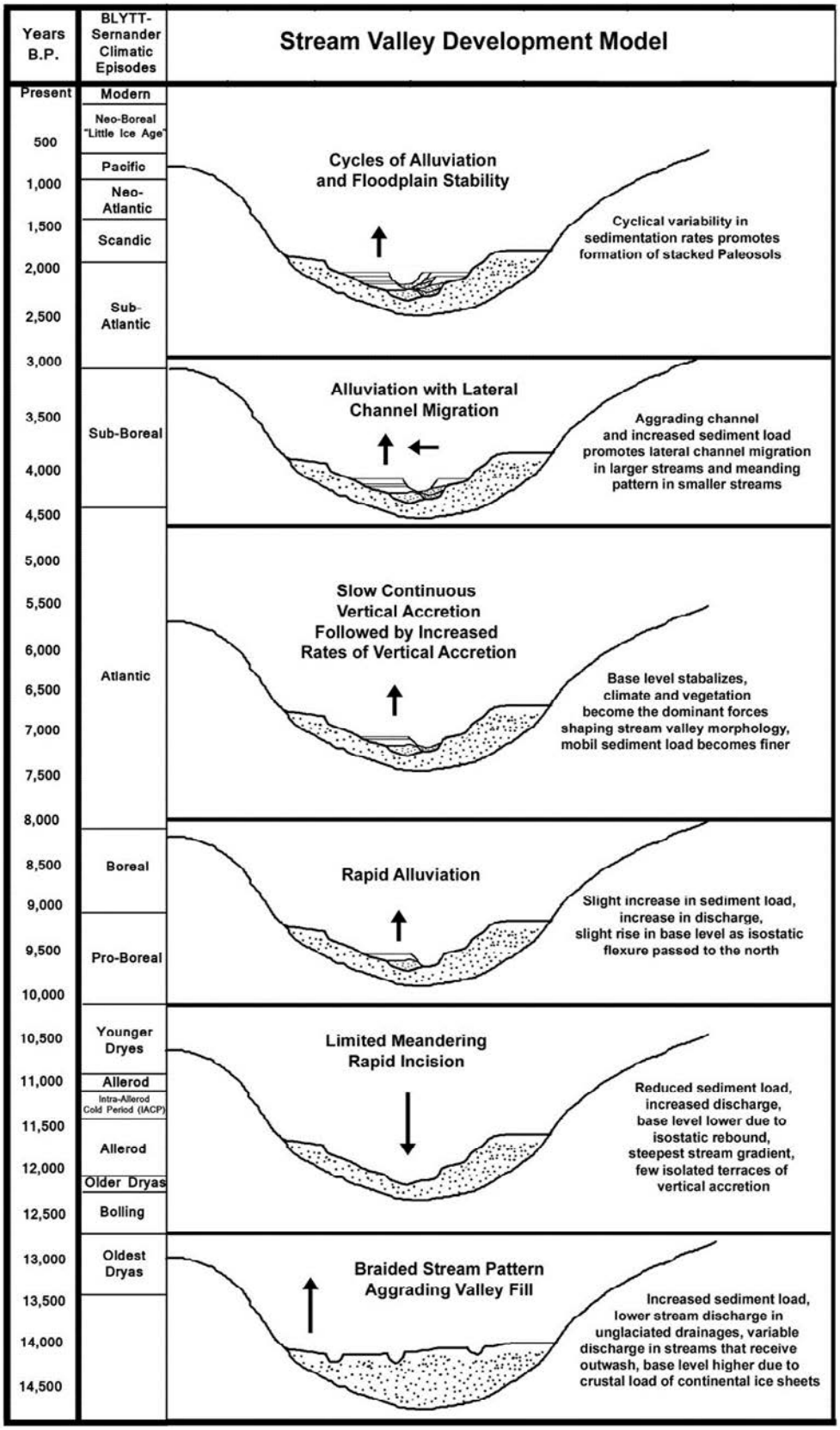

Figure 4. Stream Valley Development Model for Pennsylvania

record of varying periods of flood plain stability interrupted by periods of frequent over banking events and active lateral channel migration. The interval 700 BP. to present, spanning the Little Ice Age and the period of historic deforestation was a time favoring active overbank deposition as well as lateral channel migration and flood scouring (Vento *et al.* 1994; Vento *et al.* 2008; Figure 5).

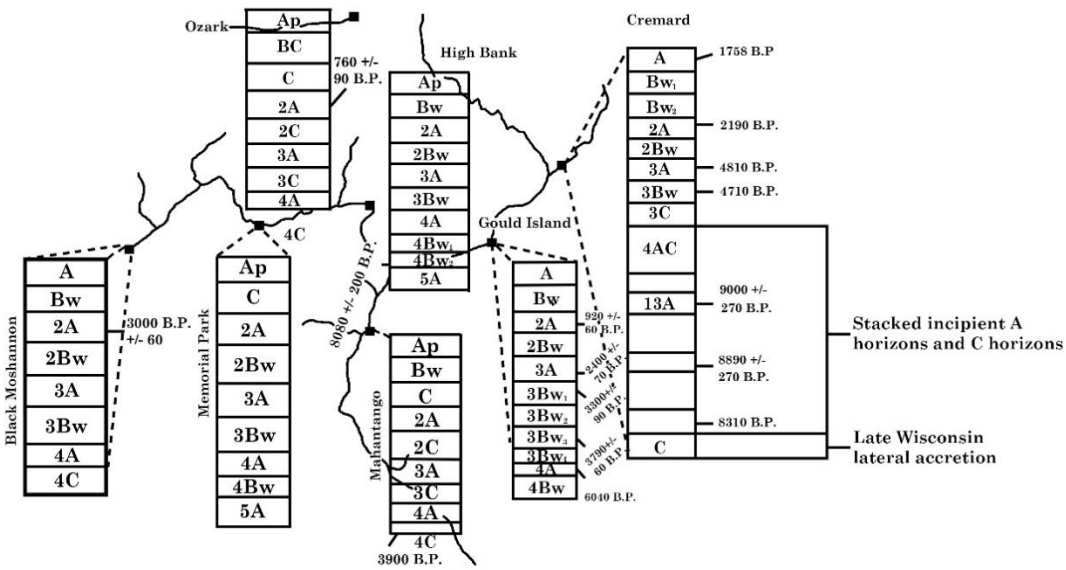

Figure 5. Penecontemporaneous Soil Stratigraphic Profiles Showing Paleosols Genetic Units) within the Susquehanna River Drainage Basin

Paleosols, as documented episodes of terrace stability, are found not only across drainage divides throughout Pennsylvania and the greater Middle Atlantic region but, recently, similar buried A horizons have been found at St. Catherines Island, Georgia (Vento and Stahlman, 2011) and provide an even more extended temporal opportunity (22,800 BP. to 10,000 BP.) for correlation by such allogenic genetic units. In the latter situation, burial of the paleosols was a result of increased aeolian deposition, not overbank deposition.

Methodological Application and Implementation of Genetic Stratigraphy - Pennsylvania and the Middle Atlantic Region

We suggest that ongoing research on the chronostratigraphy of the Delaware, Ohio, and Susquehanna drainage basins will soon lead to the development of an integrated genetic stratigraphic framework. The recognition of multiple, buried Holocene age genetic sola sequences (Vento and Rollins, 1989; Vento *et al.* 1994), based on data from over 480 stratigraphic sections in the Susquehanna, Delaware and Ohio drainage basins, permit preliminary evaluation of use of genetic stratigraphy for intrabasinal and interbasinal correlation (Figures 6 and 7 and Figure 8).

This extended stratigraphic database has led to more precise formulation of the methodology and practice of genetic stratigraphy in alluvial sequences in the northeastern United States, as follows:

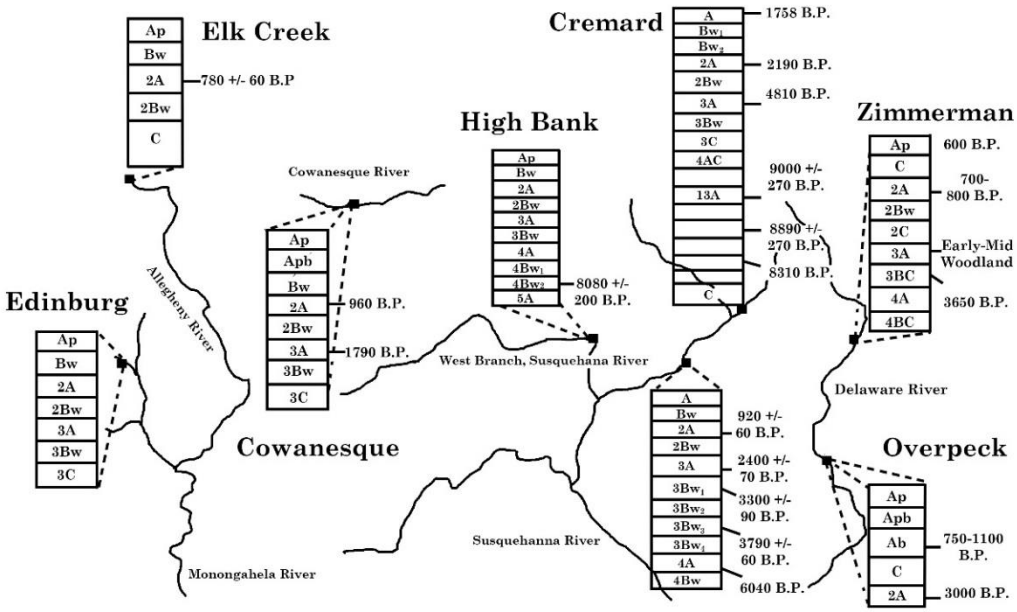

Figure 6. Soil Stratigraphic Profiles Showing Penecontemporaneous Paleosols (Genetic Units) in Geographically Separated Drainage Basins

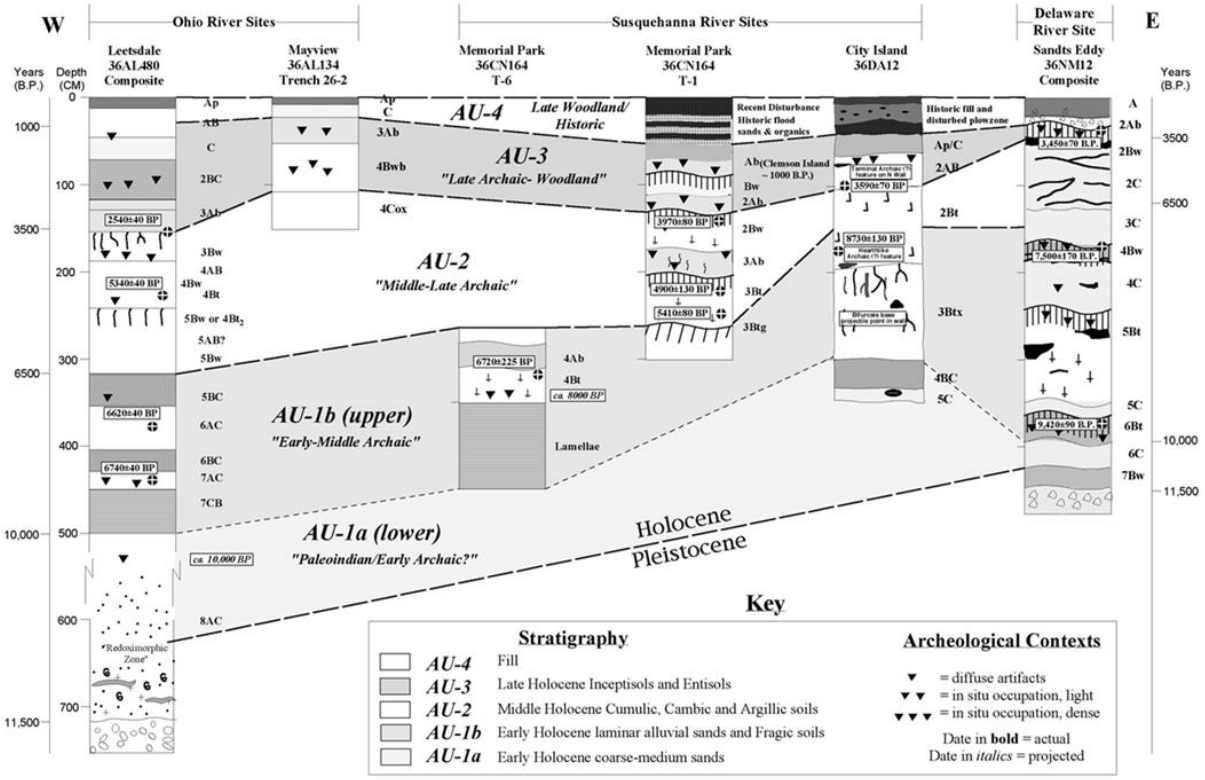

Figure 7. Stratigraphic correlations across Pennsylvania trunk stream for the Ohio, Susquehanna and Delaware River Basins (taken from Schuldenrein, Vento and Selby 2003).

(1.) Stratigraphic Sections:

Detailed stratinomic (stratum-by-stratum) description and measurement of individual alluvial sequences is essential. Particular attention must be paid to identification of all types of soil horizons.

(2.) Paleosols as Allogenic Units:

Buried soil horizons serve as the basic units in the application of genetic stratigraphy to alluvial sequences. Of particular value are the buried cumulic A-horizons, which reflect conditions of temporal stability in humid regions. A-horizons are frequently traceable over wide areas of a single drainage basin, and even among multiple drainage basins. As such, they can be ideal allogenic units, as useful as seismically determined unconformities are to Atlantic and Gulf coastal plain chronostratigraphy (Galloway 1989; Poag and Schlee, 1984). As is often the case with marine unconformities, alluvial soil horizons may encompass the bulk of time represented by a stratigraphic sequence (see Kraus 1987). In this regard genetic stratigraphy of alluvial sequences departs from the use of transgressive surfaces in high-resolution genetic stratigraphy of marine glacio-eustatic cycles (Busch and West 1987; Rollins *et al.* 1989). In the latter situation, the transgressive surfaces may be more geologically "instantaneous" and are allogenic because of the interconnected physical "forcing" of sea level change and the "shallowing upward units formed as a result of minor rises of sea level punctuating longer period of sea level stasis during which aggradation (and progradation) occurs gradually" (Busch and West 1987:).

In genetic stratigraphy of alluvial sequences the paleosol proper is the basic genetic unit, but even these buried soil horizons may reflect varying durations of accumulation (i.e. variable temporal stability) ranging from hundreds of years in humid regions (Scully and Arnold 1971, 1981) to tens of thousands of years under more arid conditions (Kraus and Brown, 1986). Radioactive dates approximately bracketing the buried cumulic A-horizons at sites along the Upper Ohio, Allegheny, Upper Delaware and Susquehanna River valleys provide a time of accumulation of about 250 years, consistent with pedogenic rates in humid regions of the northeast U. S. (Scully and Arnold 1979, 1981).

(3.) Initial Assumption of Allogenicity:

Genetic stratigraphy depends upon the initial assumption of allogenicity. Operationally, one must "expect" to detect and trace buried A-horizons among all sections. In practice, of course, individual sections may not contain specific A-horizons. This reflects autogenic (local) influence, which, in the case of alluvial sequences may be a result of:

(3a) local erosion or revilement along stream channels;

(3b) tributary order (1st and 2nd order tributaries may not have been present during formation of some older paleosols associated with stretches along the main stream). These would include those smaller consequent, insequent, or subsequent streams which have a direct confluence with either the main river channel or one of its major tributaries;

(3c) position within the alluvial "landscape", frequent flooding, active lateral channel migration and rapid overbanking may not provide the temporal stability for the formation of an A-horizon proximal to the stream channel, whereas one may have accumulated on a slightly higher, less frequently flooded, terrace (Figures 8 and 9). For example, many of the major rivers

in Pennsylvania exhibit a low-lying (less than 2m above the present channel) discontinuous late Holocene age terrace (designated T0) which is comprised entirely of coarse-grained flood deposits or incipient A horizons inter fingered with stacked C-horizons. The frequency and degree of overbanking and active channel migration precludes the development and preservation of buried solas. Conversely, as noted by Vento and Rollins (1989:8) and Vento *et al.* (2008), "The absence of any multiple allogenic genetic surfaces (paleosols) on …stable, higher, older terraces…is an indication that very late Pleistocene and Holocene overbank deposition has rarely reached the heights of the higher Binghamton…and Olean…age terraces". Limited amounts of Holocene alluvium can be found in the Ohio and Delaware River basins on terraces equivalent to the persistent Binghamton Sub-age Terrace present along the main stem of the Susquehanna River (Peltier 1949). On occasion, modern large flood events have reached this and higher terraces. The low rates of vertical accretion on these high terraces allows for a compressed artifact assemblage with potentially Paleoindian through Late Woodland artifacts occurring with the upper part of the sola (Ap/Bw).

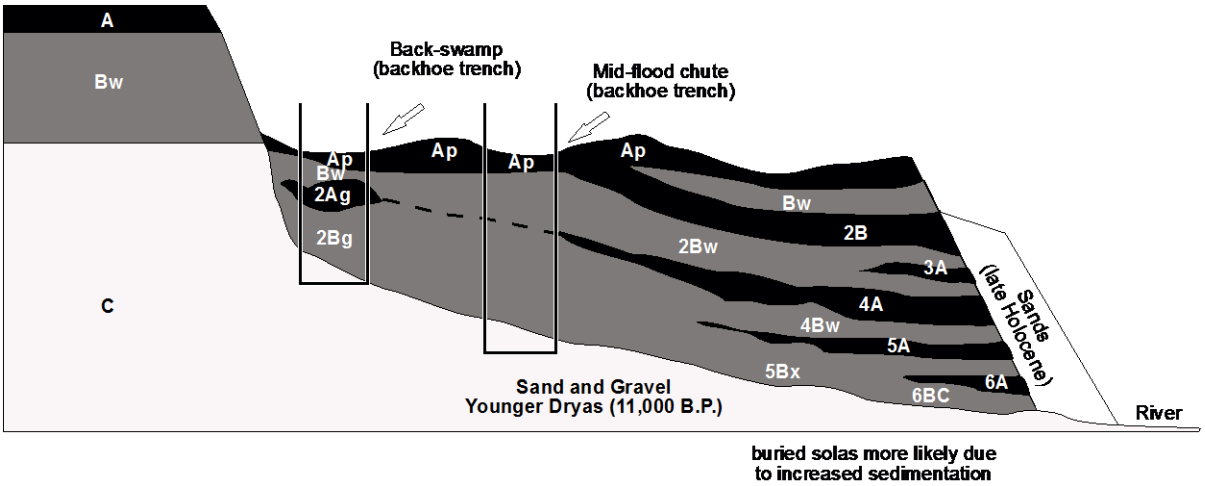

Figure 8. Schematic cross-section showing paleosol development on a Late Wisconsin Terrace (taken from Vento, Rollins, Vega et al. 2008).

In virtually all examined stratigraphic sections, the highly time-averaged and condensed mature A-horizons (A/Ap horizon) present on these higher (often outwash) terraces have great allogenic "reach" but exhibit very limited chronostratigraphic resolution. Decreasing allogenicity, however, accompanies buried A-horizons on the lower aggrading terraces (Port Huron and Valley Heads), but these genetic units are nevertheless correlatable across drainage divides within a given drainage basin (Figure 6), as well as between drainage basins (Figures 7). Figure 8 is a genetic soil stratigraphic cross section showing correlation of horizons at deeply stratified sites across trunk streams within the Ohio, Susquehanna and Delaware River valleys (Schuldenrein, Vento and Selby 2003). The chronostratigraphic persistence of these genetic units has been corroborated by radiocarbon dating, Optical Luminescence dating (OSL), as well as temporally diagnostic artifact types.

(3d) Because of valley morphology and associated stream dynamics, underfit streams with V-shaped cross section and poorly developed floodplains rarely display multiple paleosols. In the Susquehanna, Ohio, and Delaware drainage basins, the number of buried multiple sola

(allogenic genetic units), which may or may not contain *in situ* archaeological materials, correlates directly with the size of the drainage basin and varies with valley morphology (Figure 9). Although small first-order consequent streams appear to be associated with no, or only one, paleosol, the larger, higher discharge, second- and third-order tributaries are also rarely associated with more than one buried sequence. Discounting historic period alluvium, tributary streams tend to be associated with one or two soil sequences, although two or more buried sequences are the rule on most reaches of lower terraces along the main stem of the Ohio, Allegheny, Delaware and Susquehanna Rivers.

An interesting observation from these ongoing geological investigations is that the lower terrace (Port Huron Sub-age T1 terrace) along the main stem of the Delaware River does not generally exhibit a sequence of buried soils as well developed as those encountered along the similar reaches of the Allegheny River, upper Ohio River, and upper and central Susquehanna River. The pedogenic immaturity of the buried soils and restricted occurrence of stacked, buried cumulic A-horizons in the Upper Delaware River Valley may be a function of: 1) the constricted profile along much of the Valley, affecting the magnitude and frequency of overbank events and/or 2) the relatively coarse-grained, quartz-rich sediment load (as compared to the Susquehanna River) carried and deposited by the river which does not readily lead to clear depositional stratification (fining-upward sequences), and/or (3) post-depositional diagenesis.

The lower reaches of both the Delaware and Susquehanna Rivers contain few large or small tributaries entering the main channel. Both also exhibit persistent broad valley profiles indicating more efficient flow (greater competence and capacity) and, hence, less likelihood for significant flood-scouring of the low terraces or for active channel avulsion.

The presence or absence of buried soils along a given section of a river is, partly, a function of: (1) valley size and shape, (2) the potential for back-flooding and rapid vertical accretion, such as that which occurs at stream confluences, and (3) stream velocity, as controlled by channel size and shape, rate of discharge, and gradient development (Figure 9). This leads to the following generalizations:

(1) All small, first-order tributaries are actively downcutting and eroding headwardly, adjusting toward temporary base level and grade.

(2) Low-order streams are less likely than higher-order streams to migrate laterally or aggrade their valleys. These smaller streams typically exhibit low discharges, steep gradients, and bedrock-defended channels. Because of their hydrology and thin alluvial soil packages, small tributary streams are less likely to contain artifact-bearing buried soil horizons (Figure 9). In addition, small streams have been more affected by historic deforestation and urbanization than have larger drainage channels.

(3) The V-shaped valley form, steep gradient, and accompanying smaller floodplains of first-order streams promote rapid scouring by large flood events of any previously emplaced overbank deposits. In addition to the effects of historic deforestation which favored channel migration and flood scouring, the Little Ice Age (700 BP. to 150 BP.) allowed for increased flood frequency during much of the year, due to higher effective precipitation from rainfall and snowmelt and less evapotranspiration.

(4) Multiple buried soils tend to be preserved along large fourth- and fifth-order streams in the region, in part because these streams have essentially been fixed in their present channels since the end of the Younger Dryas (circa. 10,100 BP.).

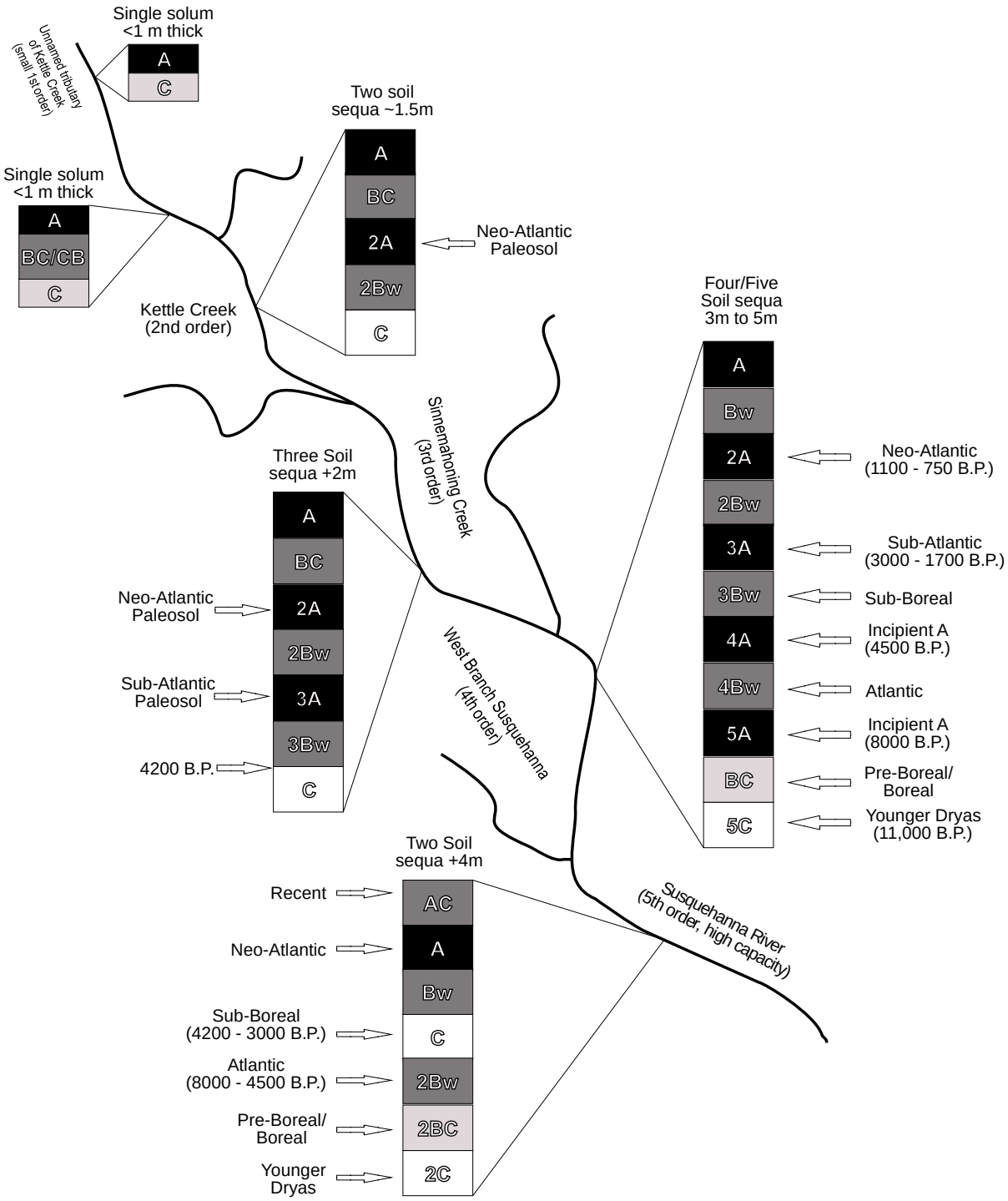

Figure 9. Schematic showing relationship of stream order to the age and number of soil generations (taken from Vento, Rollins, Vega et al. 2008)

(5) If we ignore the effects of base level, isostasy and tectonism, changes in climate, and the expansion (headward erosion) in the number of tributaries carrying increased sediment load to major drainage lines become the more obvious controls on the phases of Holocene aggradation and alluviation along the major rivers in the region. Interpretation of isostatic effects on streams, especially those well south of the glaciated area, is confounded by difficulty determining what part of the terrace riser is related to climate or changes in base level, and what part of the terrace scarp or riser is relate to isostatic uplift or epierogeny. Furthermore, the relaxation rate is rapid initially, but decreases with time as well as with distance from the ice margin. This is analogous to a compound fault scarp where it is difficult to determine what part of the fault scarp is directly related to faulting versus what portion is due to post-fault erosion along the fault line.

(6) The pattern of paleosol occurrence and the record of climate change in the Susquehanna, Ohio and Delaware drainage basins indicate that allogenic genetic units (paleosols) are more easily preserved and traceable along the higher, better-drained levee or bank-edge areas of the floodplains and along reaches of straight channel between rapidly accreting point bars. Predictably, the autogenic effects of rapidly accreting point bars often prevent the development of A-horizons, although cryptic immature paleosols might be discernible. This is especially true along first- through third-order streams in the basin. Farther from the actual channel, the thickness of the overbank deposits decreases as does the number of buried soil generations (Figure 9). This is the result of decreased sedimentation rates away from the active channel. For example, a time line on the levee along the T1 terrace of the Delaware and Susquehanna Rivers, at a depth of 3 m below ground surface may be only 50 cm below ground surface at a distance of 50 m from the levee. Furthermore, as one moves away from the active river channel, the buried cumulic A -horizons will typically rise to intersect the present ground surface, or pinch out (Figures 9 and 10). Interestingly, this was noted at the Gould Island Site (36Lu90) on the North Branch Susquehanna River and along French Creek at the Wilson Shute Bridge (36Cw170) (Figure 11). On the high central portion of the island, a buried cumulic A-horizon containing Owasco artifacts was identified approximately 50 cm below ground surface. On the distal edge of the island the Owasco materials were identified in a poorly developed B horizon at a depth of 3.5 m below ground surface, documenting high rates of sedimentation on the lower aggrading margin of the island.

Buried paleosols on low terraces (Port Huron and/or Valley Heads) near bank-edge and levees within the Susquehanna, Ohio and Delaware drainage document intervals of terrace/floodplain stability, punctuated by episodes of overbank discharge and channel avulsion. The presence of each cumulic A-horizon attests to at least hundreds of years of fluvial stability (little overbank deposition) under probably warm and moist climatic conditions. These warm-moist intervals, which are controlled by changes in atmospheric circulation, include the early Archaic, terminal Atlantic (Archaic), Sub-Atlantic (late Broadspear Tradition, Early and Middle Woodland) and Neo-Atlantic (Clemson Island-Oswaco) climatic episodes of the Holocene (Figures 1 and 4).

It would appear useful, at this time, to formally name the paleosols that date to the Neo-Atlantic (1100 BP. to 750 BP.), Sub-Atlantic (3000 BP. to 1900 BP.), terminal Atlantic (4500 BP. to 6000 BP.), Boreal (circa 8000 BP.), and Pre-Boreal (10,000 BP. to 11,000 BP.) as the Owasco, Fox Creek/Orient, upper Atlantic I, Boreal I and Post Younger Dryas paleosols, respectively.

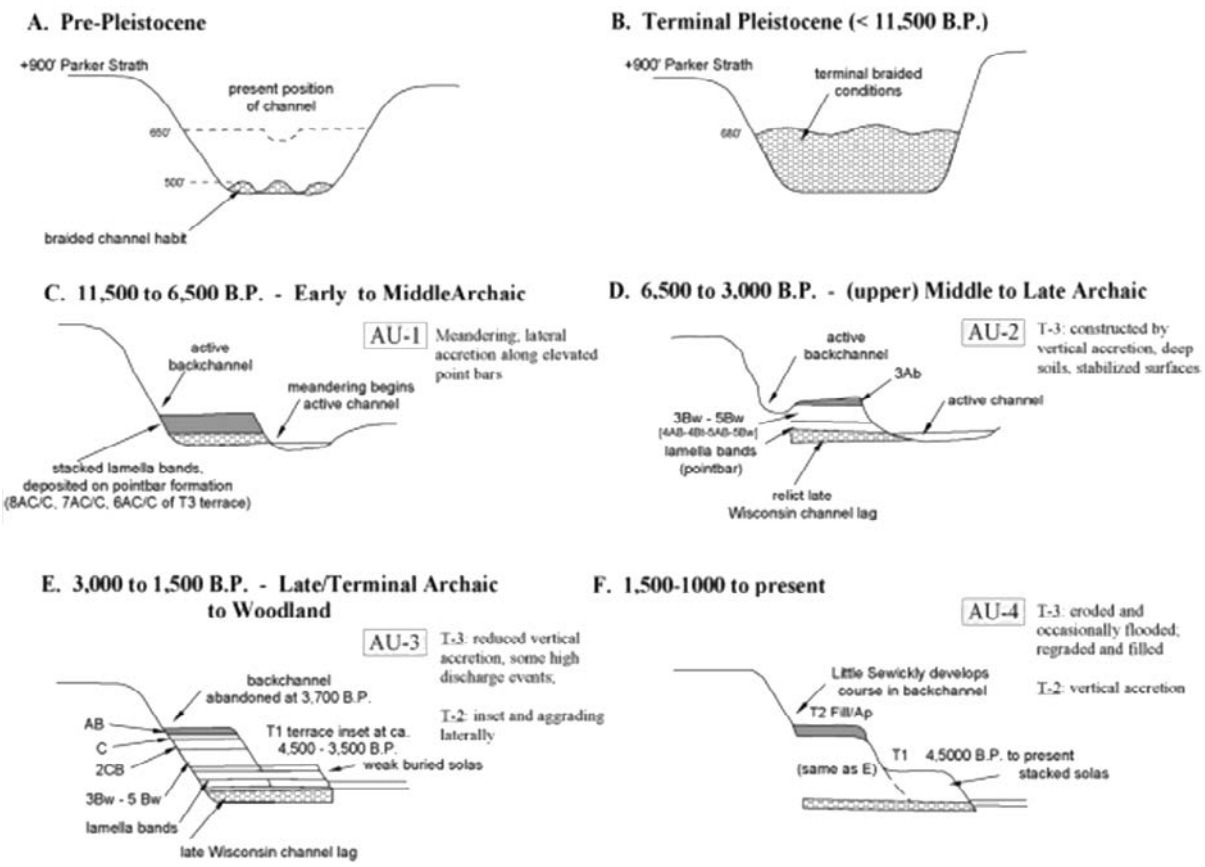

Figure 10. Terrace evolution along the Allegheny River, Pennsylvania.

Frequently, the allogenic A-horizons are stratigraphically separated by cambic B-horizons, poorly developed argillic B-horizons, and/or coarse-grained flood depots (C-horizons-autogenic units) of varying thicknesses. These texturally variable B and C-horizons reflect changes in flood intensity and valley bottom stability during principally cool/moist and warm/dry intervals of the Holocene (Figure 1). Such variable paleoclimatic conditions may have affected vegetational cover and led to increased rates of surface runoff, mass-wasting and to more frequent floods, favoring vertical accretion. This would have inhibited A-horizon development. These more rapid or continuous rates of terrace or floodplain aggradation (thick B-horizons) appear to correlate with the Boreal/Atlantic (Archaic), Sub-Boreal (late Archaic-Broadspear), Scandic (post-Fox Creek and pre-Owasco/Clemson Island materials), and Pacific (McFate, Quiggle, Shenks Ferry) paleoclimatic intervals of the Holocene.

(4.) A and B Horizons in Alluvial Sequences:

Stacked A and B horizons (i.e., multiple soil generations) on aggrading terraces afford different opportunities to archaeologists. The frequently thick early to middle Holocene age cambic B horizons often encountered on terraces provide surfaces which were available for human occupation for shorter intervals of time. The slow but constant aggradation and thickening of the profile enhances vertical separation of temporally distinct occupations (Schuldenrein, Vento and Selby 2003). Such sites as Shawnee Minisink (36Mr43) on the Delaware, Leetsdale (36A1480) and Point State Park (36Al581) on the Ohio and City Island

(36Da12) and Memorial Park (36Cn164) on the Susquehanna River have thick moderately well-developed B horizons dating from early Archaic through Middle Archaic times (Figure 11). A-horizons, on the other hand, reflect greater landform stability and were exposed to human occupation for decades or centuries, and therefore are more likely to contain mixed multiple occupations. Horizontal patterning of artifacts and features may in some cases be meaningless because of overlapping (palimpsested) occupations. Although B-horizons may contain fewer artifacts and features per level, they are more likely to represent single occupations.

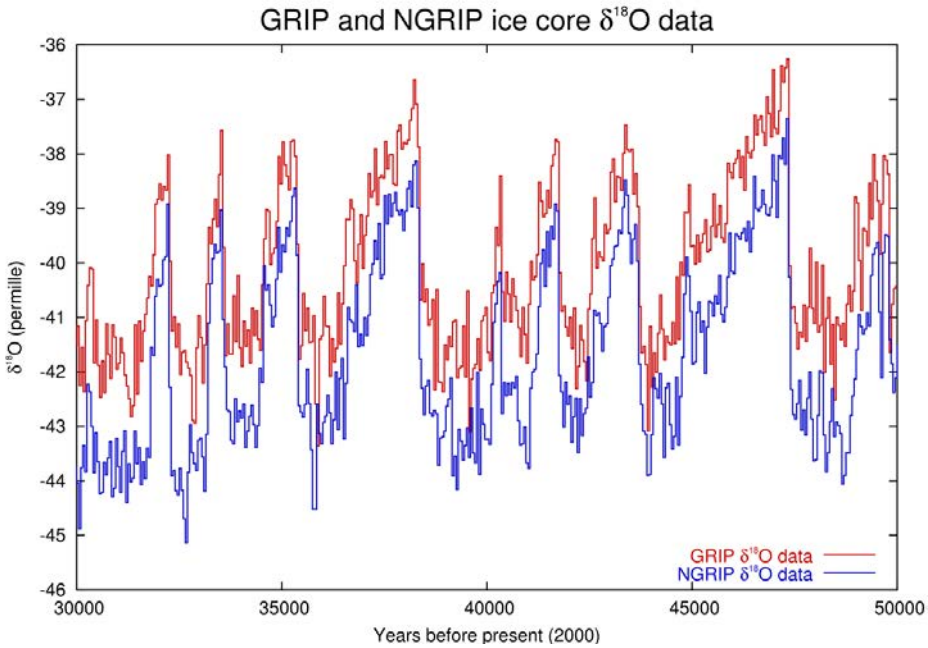

Figure 11. Dansgaard-Oeschger (DO) Cycles (Wanner et al., 2008)

(5.) Floating Sections and Use of Marker Horizons:

Stratigraphic sections are compared by tracing and matching genetic units. In alluvial sequences this involves correlating stacked A-horizons, wherever possible. Relative stratigraphic thicknesses play little or no role in the process of "floating" stratigraphic sections. However, "marker horizons", in the broadest sense, play an essential role in establishing a pedostratigraphic or chronostratigraphic framework.

Stratigraphic Disconformities over the Last 12,000 Years

Over the last 12,000 years there have been at least five major stratigraphic discontinuities or erosional disconformities that appear in the alluvial stratigraphic record. Most of these disconformity events are identifiable along major drainage lines because of the extended time span of that alluvial record, but the more recent disconformities are clearly discernible even along the smaller internal and external drainage links and have extensive geographic reach across the region.

The first and earliest disconformable event was the one connected with the Younger Dryas cold interval (10,100 BP)- a time of increased precipitation promoting high flow velocities, extensive flood scouring and active lateral channel migration along all drainage lines in the

region. The paucity or absence of Bolling-Allerod vertical accretion deposits along low terraces was largely due to erosional removal during the Younger Dryas. Most of the identifiable Paleoindian sites which have stratigraphic integrity occur immediately on or just above the Younger Dryas lateral accretion deposits. To date, only the Shawnee Mininsink site on the main stem of the upper Delaware River contains a thick (>2m) package of vertical accretion deposits which predates the Younger Dryas interval.

The second and nearly as widespread disconformity is associated with the warm and dry conditions of the Sub-Boreal climate phase (4200 BP. to 3000 BP.). Recorded pedostratigraphic evidence of this event varies, based upon stream maturity, drainage basin size, valley morphology and channel dynamics. For example, along smaller first-order and second-order streams the warm and dry conditions were sufficient to remove, if present, any earlier Holocene age valley fills. Along these drainage lines this interval was marked by active lateral channel migration and associated deposits comprise the basal sequence encountered along the valley bottom zone. Along the larger drainage lines in the region, the Sub-Boreal was marked by slow but continuous vertical accretion permitting development of a cambic B-horizon. On occasion these thickening profiles were truncated or scoured by large cyclonically induced flood events that penetrated into Pennsylvania with the continuing ablation of the Wisconsin ice sheets.

Probably least well-expressed in the alluvial stratigraphic record is the disconformity associated with the Scandic climatic phase (1900 BP. to 1100 BP.) which is stratigraphically positioned between the warm and moist record of the earlier Sub-Atlantic and the later Neo-Atlantic climate phases. The colder and wetter conditions of the Scandic climatic interval encouraged increased flood frequency and magnitude. In places, this led to erosional removal of the cumulic A-horizon that is often associated with the Sub-Atlantic interval. The Scandic disconformity is best expressed along major aggrading streams (e.g., Susquehanna, Ohio, Allegheny and Delaware Rivers).

The Little Ice Age (circa 700 BP. to 150 BP.) is associated with cold and wet conditions that favored lateral channel migration and flood scouring along most drainage lines in the region. Along small external links (first-order streams and rills) the flood intensity during the Little Ice Age was sufficient to remove earlier late Holocene deposits such that the entire profile along the flood plains of these small drainage lines is often less than 700 years in age. Along larger drainage lines, this cold and wet period led to the termination and subsequent burial of the cumulic A-horizon which was formed during the previous warm and moist Neo-Atlantic climate phase. Record of the Little Ice Age interval can be observed in many profiles by a coarsening upward sediment sequence overlying finer-grained sediments (Figure 5).

The final (latest) disconformity is associated with historic deforestation of the region during the late 18th through mid-19th centuries, and subsequent urbanization along many of the large drainage lines (Figure 1). There is little doubt that smaller streams in the region were more affected by historic deforestation, urbanization (impervious cover and sewer systems), and the construction of numerous small dams and mill ponds than larger drainage lines and have therefore removed in places earlier late to middle Holocene valley fills. However, even along large streams like the Ohio, Susquehanna and Delaware Rivers, there is typically a surface horizon comprised of a thick (but variable) package of somewhat coarse-grained sediments

overlying earlier late Holocene deposits. These coarser vertical accretion deposits reflect the effects of deforestation that permitted higher sediment yields to streams and higher rates of surface runoff with higher flow velocities (Figure 10).

Paleoclimatology and Paleoenvironments

We present next a paleoenvironmental reconstruction of the region extending from just before the Last Glacial Maximum (LGM) to the present, in sufficient detail that the history of environmental and climatic change can be tied to geomorphological and cultural events. We realize that such a synthesis is limited by the paucity of information on centennial and decadal climate change in the region. Our focus is on the Late Pleistocene and the Holocene epochs, as this is the time interval coinciding with the appearance of human societies in the region.

Pleistocene to Holocene Transition

Long-term climatic changes, such as those related to the shift from the last glacial interval to the Holocene, have been directly correlated to perturbations in the earth's orbit, axis, and wobble - the so-called Milankovitch cycles (Rohli and Vega 2014), which affect the amount of solar radiation reaching the earth's surface. For late Quaternary climates, the 100,000 year orbital variation cycle, the 23,000- and 19,000-year precession cycles and the 41,000-year obliquity cycles are particularly important (see Grootes and Stuiver 1997). Marine records indicate a shift from cold dry conditions during the LGM to warmer conditions beginning approximately 17,000 BP. (Leyden 1985; Lowell *et al.* 1995; Thompson *et al.* 1995; Wright *et al.* 2005).

By 10,000 BP. the earth's axial tilt maximized while the precession cycle placed perihelion on June 24 (Ruddiman, 2001). Shorter-term climatic cycles on millennial scales of about 1540 years (Dansgaard-Oeschger [D/O)] cycles; Figure 12) and about 1500 years (Bond cycles; Figure 12) have also been recognized in proxy records from ice cores and from cores taken from the ocean and larger continental lakes (Ruddiman 2001). Bond cycles refer to quasi-periodic Holocene climatic cycles but as yet it is unclear how these shorter-term cycles may relate to the celestial mechanics and feedback cycles that drive the longer cycles. There is some indication that they are primarily caused by variation in solar output (e.g. Denton and Karlen 1973; Finkel and Nishiisumi 1997; Bjorck *et al.* 2001; Bond *et al.* 2001; Neff *et al.* 2001; Ruddiman 2001; Kodera 2002; Rahmstorf 2003).

There are a number of posited explanations and currently no consensus regarding the cause of these shorter cycles, particularly the D/O cycles (e.g., Rind and Overpeck 1993; McIntyre and Molfino 1996; Clark *et al.* 1999; Keeling and Whorf 2000; Clement *et al.* 2001; Broecker, 2003). Some large-scale climate changes correlate with stochastic events such as volcanic eruptions and catastrophic floodwater outflows and tend to either enhance or dampen the expression of the solar-based climatic cycles (Magny and Begeot 2004). Three such events, related to the sudden collapse of proglacial Lake Agassiz, occurred ~10.9, ~9.9, and ~7.7 14C ka (~12.85, ~11.3, and ~8.4 cal ka), and fed large quantities of cold, fresh water into the North Atlantic, temporarily shutting down the ocean conveyor system that largely structures Northern Hemisphere climates. This dramatically enhanced the scale of D/O cycles at these times (Teller, *et al,* 2002). A number of other similar floodwater events occurred throughout the early Holocene, but were of smaller scale with reduced impacts on climate.

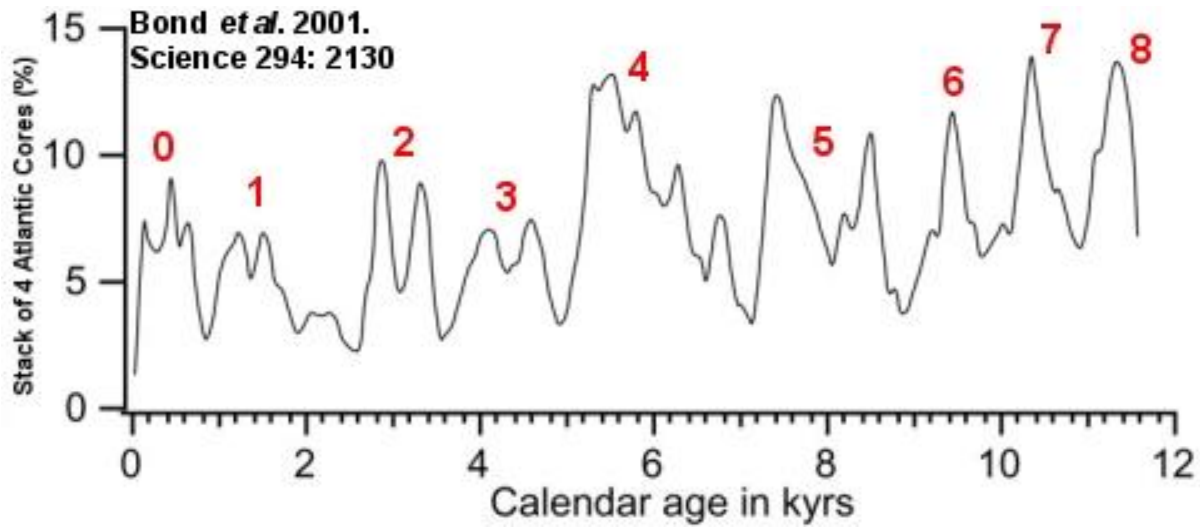

Figure 12. Bond Cycles (Bond et al., 2001)

Regardless of cause it is becoming increasingly clear that the transitions between the steady-state conditions that characterize these millennial-scale cycles are relatively abrupt, often occurring on the order of a decade or less, and certainly within the lifetime of an individual (Schulz and Paul 2002; Willard et al. 2007). In the North Atlantic, and apparently throughout the Northern Hemisphere (Sirocko *et al.* 1996; Wilkins and Currey 1997; Ding *et al.* 1998; Schulz *et al.* 1998; Bianchi and McCave 1999; Grafenstein *et al.* 1999; Brown *et al.* 2000; Leuschner and Sirocko 2000; Courty and Vallverdu 2001; Norenet al. 2002; Benson *et al.* 2003; Burns *et al.* 2003; Gupta *et al,* 2003; Wang *et al.* 2003), the D/O and Bond cycles are synchronous and take a characteristic form (Alley 1998). Although they range in duration from 1000 to 2000 years, they average about 1500 years long (more precisely, ~1470 years [Rahmstorf 2003]), and are initiated by a rapid rise in temperature in a matter of decades (5-8 degrees C during the glacial period and 1-3 degrees C during the Holocene), with a gradual return to moderate conditions over the course of ~1000 years, ending with a rapid return to very cold temperature prior to the start of a warming event and the initiation of a new cycle. Currently, nine cycles have been recognized in the detailed core records spanning the last 12,000 years (e.g. Bond *et al.* 1997; Ruddiman 2001) (Figure 11 and 12).

Although it is becoming evident that environmental change in eastern North America is correlated with millennial-scale cycles present in the ice core records (e.g. Willard *et al.* 2005), all nine of the Holocene cycles have yet to be recognized at local scales. Other, even shorter, climatic cycles, such as those associated with the El Nino-Southern Oscillation (Robell *et al*. 1999; Moy *et al.* 2002; Goman and Leigh 2004) and the North Atlantic Oscillation (and associated fluctuations in the Bermuda High [Gamble and Meentemeyer 1997; Vega 1998; Goman and Leigh 2004; Willard *et al.* 2007]) range in duration from a few decades to several centuries and are also evident in a variety of proxy records. They may also relate to variation in solar output (e.g. Grafenstein *et al.* 1999; Chapman and Shackleton 2000; Clement *et al.* 2001; Berger and von Rad 2002; Kunzendorf and Larsen 2002; Menking and Anderson 2003; Takahashi *et al.* 2003; Gagan *et al.* 2004). Unfortunately, these shorter cycles are within the range of variation of most

radiocarbon dates, making records of these events difficult to correlate with one another or with environmental and archaeological changes.

The chronology or the more complete and well-controlled North Atlantic core records may eventually be used in defining cycles of environmental change in the eastern U.S., although there are currently chronological differences of 50 years, or less, between the marine and the ice core records, due to depositional discontinuities and differences in chronological techniques (Stapor *et al.* 1991). Significantly, perhaps, there appears to be a lag in the response of vegetational communities to the climate change events that are recorded in the North Atlantic records (Viau *et al.* 2002). The disparate response times are short, consistently less than 200 years and often less than 100 years (Williams *et al.* 2002). This suggests that there may be similar consistent disparities between the North Atlantic core records and the alluvial records, or it may indicate a delay in vegetational zone response to climate change. For this reason, and also because the stratigraphic sequence does not yet afford sufficient resolution to identify all the millennial-scale cycles evident in the core records, we here employ the Blytt-Sernander climatic sequence (Cronin *et al.* 2000; Davis *et al.* 1994, 1998; Grimm and Jacobson 1992; Harrison *et al.* 2003; Hu, *et al.* 1999; Jackson and Whitehead 1991) to order Holocene environmental change in eastern North America (Figure 1).

Currently, two models of chronostratigraphy are commonly used in Pennsylvania - the Blytt-Sernander model and the Pollen Zone model. The Blytt-Sernander model was developed during the study of Danish peat bog formation in the late 19th and early 20th Centuries (Blytt 1876; Sernander 1908). The Pollen Zone model was developed in New England during the first half of the 20th Century (Deevey 1939; Davis 1965). Both models subdivide the late Pleistocene and Holocene into a series of chronozones of varying duration (Figure 1). The Blytt-Sernander system uses names that indicate the dominant climatic conditions in Northern Europe (e.g., Boreal and Atlantic), the chronostratigraphic system for New England is subdivided on dominant types of pollen found in the strata. From oldest to youngest, these include the Herb (Zone T); Spruce (Zone A-1 to A-4); Boreal (Zone B), Oak and Hemlock (C-1), Oak and Hickory (C-2); and Oak and Chestnut (C-3) pollen zones (Deevey 1939; Davis 1965:386-397). Pollen Zone C-3 has subsequently been subdivided into two parts (C-3a and C-3b), and Zone C-3b refers to a later (upper) portion that contains more spruce and pine pollen (Figure 1).

As portrayed in Figure 1, there are strong similarities between the Blytt-Sernander and Pollen Zone chronostratigraphic systems. Although developed for northern Europe, the climatic sequences described in the Blytt-Sernander model have been used effectively to interpret trends in climate change and alluvial deposition along major stream in Pennsylvania (Vento and Rollins 1989; Vento *et al.* 1992; Vento *et al.* 2008), and the model is commonly referred to by archaeologists working in and around Pennsylvania (e.g., Carr 1998a; 1989b; Coppock 2009a; 2009b; Raber *et al.* 2004; Wall *et al.* 2003).

Thus, our discussion of regional paleoenvironments is organized according to the Blytt-Sernander chronozones, cross-referenced with the appropriate New England Pollen Zone designation (Figure 1). Individual climatic episodes include the Bolling-Allerod interstadial, Younger Dryas, the Pre-Boreal, the Boreal, the Atlantic, the Sub-Boreal, the Sub-Atlantic, Scandic,

Neo-Atlantic, Pacific, and the Little Ice Age. Much of the following discussion is taken or adapted from Coppock *et al.* (2011) and from Miller *et al.* (2007).

The Quaternary Period of the Cenozoic Era began approximately 1.8 million years ago with the onset of a glacial phase embedded within the larger Ice Age, which began during the Tertiary Period, 65 million years ago. The Quaternary Period is divided into two distinct Epochs - the Pleistocene and the Holocene (Recent) (Figure 1). Although there is much discussion regarding its lower boundary, in the last few years that portion of the Quaternary impacted by human activity is frequently designated as the Anthropocene.

The Pleistocene is subdivided into four major ice advances - the Nebraskan, Kansan, Illinoian, and Wisconsin, which are separated by warmer interglacial phases known as the Aftonian, Yarmouthian, and Sangamon. The Sangamon ended approximately 100,000 BP. with the terminal Wisconsin ice advance.

The Pleistocene Epoch peaked approximately 18,000 years ago when permanent ice covered most of North America north of the Ohio River and extended across the pole covering much of Europe and Asia. This glacial maximum (Figure 13) is termed the Wisconsin Glacial Phase in North America, the Weichselian in Western Europe and the Wurm in the Alps (Crowley and North 1991). The Wisconsin was characterized by cold temperatures, expanding continental ice sheets, and subsequent sea level change. According to Willard, et al. (2007), temperatures during the Wisconsin peak were approximately 3-4 degrees C cooler than present with eustatic sea level as much as 120 m to 170 m below present level. This exposed large sections of the continental shelves and extended the coastline up to 200 km from present (Willard *et al.* 2007).

The Wisconsin phase ended with significant shrinking and collapse of the Laurentide ice sheet beginning about 16,000 BP., resulting in reorganization of atmospheric circulation patterns (Knox 1993; 2000; Foreman *et al.* 1995; Leigh and Feeney 1995; Dwyer *et al.* 1996; Noren *et al.* 2002) due to changes in energy from a wide array of climatic forcing (Berger 1978; Robell *et al.* 1999; Bard 2002, 2003; Moy *et al.* 2002).

Surprisingly, seasonal insolation levels approximated those of the present (Ruddiman, 2001). However, lower summer insolation levels led to glacial expansion, peaking between 21,000 and 17,000 BP. At that time the North American ice sheets, the Laurentide in the east and the Cordilleran in the western mountains, were the largest on Earth.

The Last Glacial Maximum (22,000-14,000 BP.

Depending on geographic location, the Last Glacial Maximum (LGM) occurred between 22,000 and 14,000 BP. (Crowley and North 1991; Taylor *et al.* 1997; Jackson *et al.* 2000; Goman and Leigh 2004; Mayewski *et al.* 2004; Willard *et al.* 2007; Wanner *et al.* 2008; LaMoreaux *et al.* 2009). For practical purposes, we can assume that the LGM occurred approximately 18,000 BP (Figure 14) in North America. A variety of techniques have been used to reconstruct the paleoclimatic history of this time period. The most extensive reconstruction was the CLIMAP project (Climate/Long Range Investigation, Mapping and Prediction) which utilized glacial moraine analyses, pollen analyses, analyses of lake levels, varves, records of biogenic and non-biogenic deep sea sediments, ice cores, and a wide range of dating techniques including extensive analyses of C14 (Crowley and North 1991).

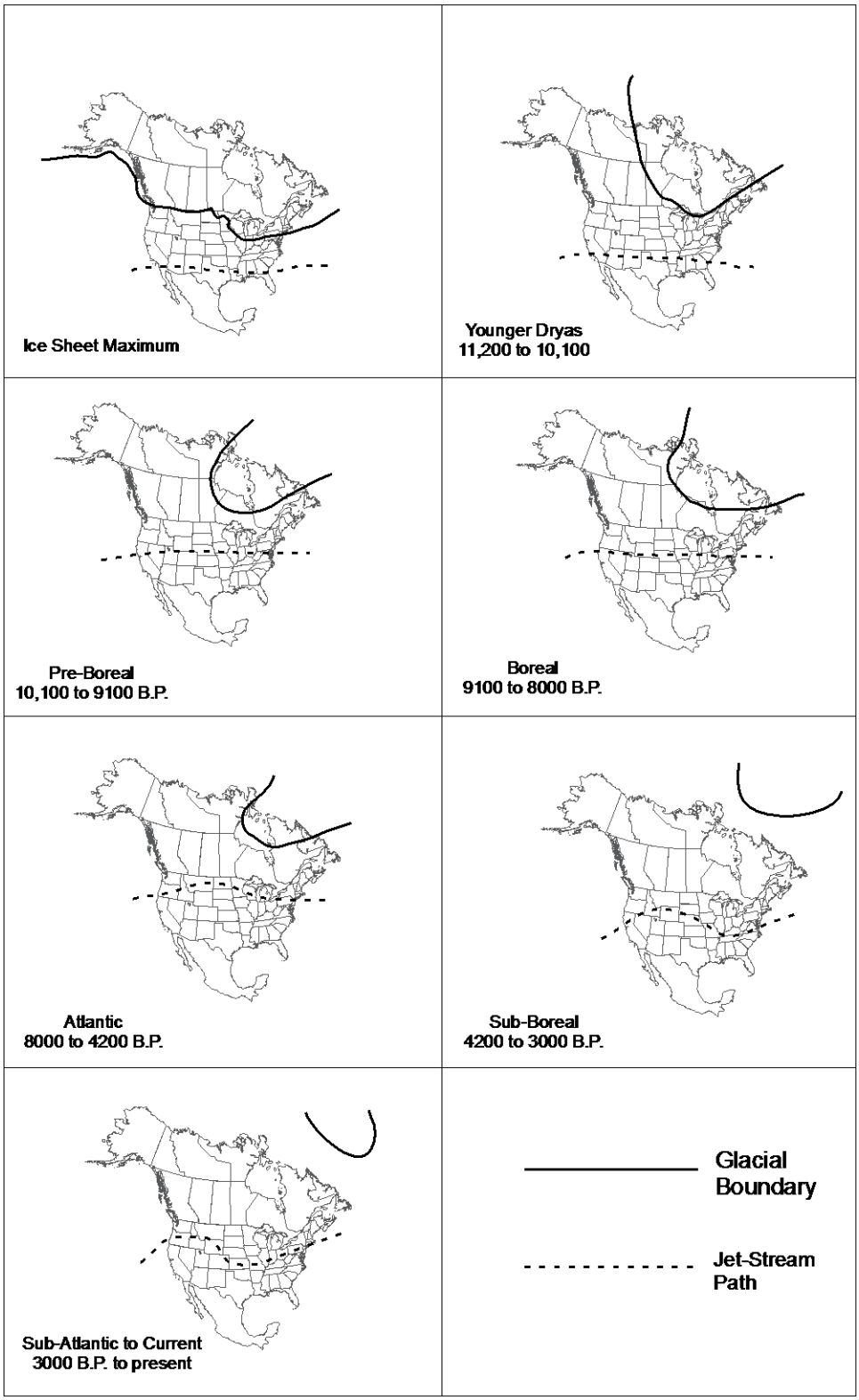

Figure 13. Glacial Boundary and Jet-Stream Path changes from the Ice Sheet's Maximum through the Present

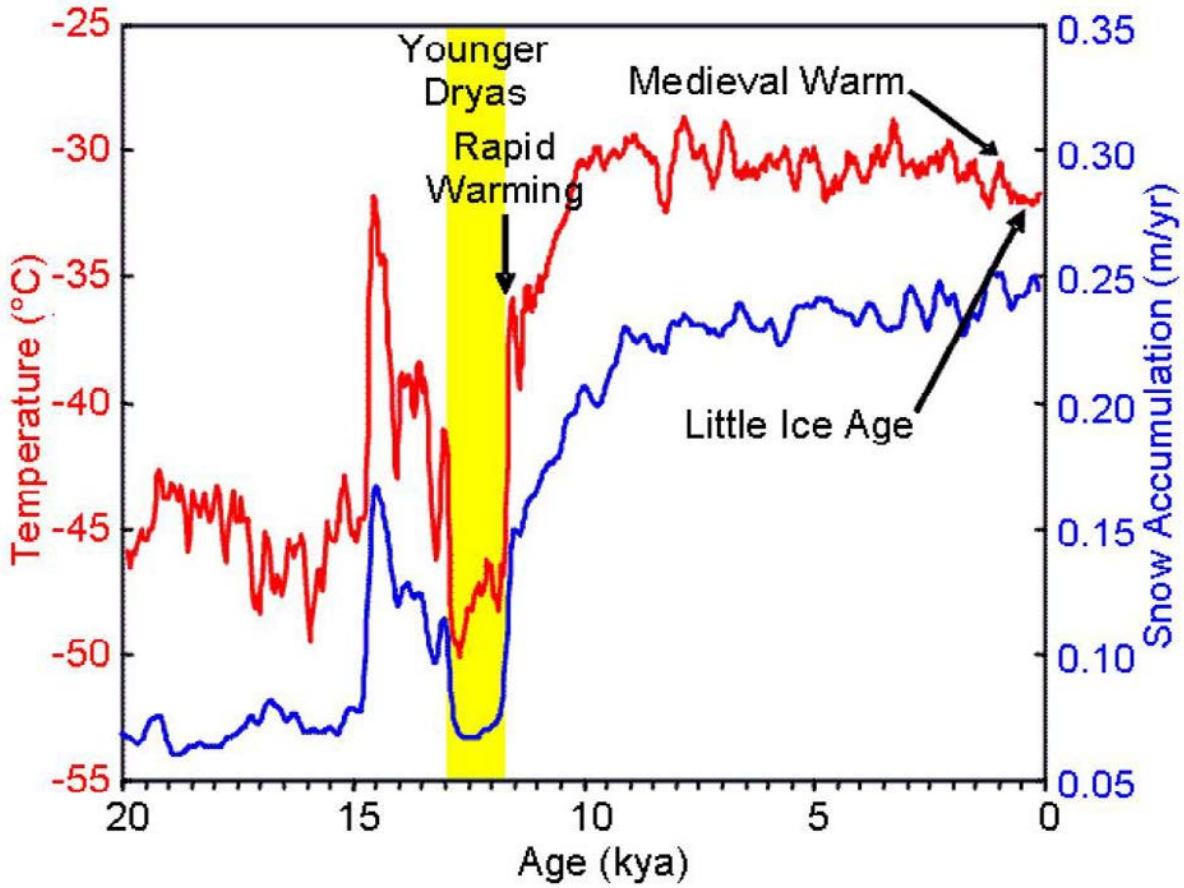

Figure 14. Temperature variations over the past 20,000 Years

As our focus is on North America, our discussion of paleoenvironments centers on the Laurentide ice sheet. This ice sheet was the most extensive in North America and its thickness varied between 3500 and 4000 meters. The weight of the ice sheet depressed the continental crust as much as 700-800 meters. Measurable isostatic rebound, as much as 9 mm per year in Hudson Bay, is still ongoing in many locations as a result of deglaciation.

During the LGM, major circulation patterns were radically altered. The ice sheet caused extensive expansion and strengthening of the circumpolar vortex in the Northern Hemisphere (Mayewski, *et al.* 2004). This led to an equator-ward offset of the atmospheric and oceanic polar fronts, and considerable equator-ward extension of the "D" and "C" climatic types (Koppen climate classification) throughout North America (Rohli and Vega, 2014). The present day position of the oceanic front in the North Atlantic occurs as high as 78 degrees N latitude (as a result of the Gulf Stream). During the glacial maximum, the oceanic front had an average position of about 45 degrees N latitude. Furthermore, the average position of the atmospheric mean polar front (jet stream) was approximately 1200 km south of present location, extending to 34 degrees N, very near the Gulf Coast of the U.S. The combined effect of the polar front displacements and circumpolar vortex expansion was a mean reduction in average air temperatures of about 10 degrees C near the ice margin. Proxy evidence indicates that mean temperature changes were most severe during the cool season rather than during the warm season. Winters in Tennessee,

for example, were approximately 15-20 degrees C cooler than present (Crowley and North 1991) leading to widespread differences in flora and fauna, compared to the present. In North America tundra consisted of a relatively thin strip adjacent to the Laurentide ice sheet. This meant that the spruce-pine boreal forest was restricted, compared to that of Europe at the time, or to the present (Crowley and North 1991).

As a result of the ice advances, drainage systems were altered in western Pennsylvania. Pre-glacially, drainage was through the Upper and Middle Allegheny Rivers into the Lake Erie Basin and to the south into the Monongahela-Beaver River system. Because of glaciation, some of the northern valleys were infilled with glacial deposits but others were diverted southward to form the present-day Ohio River.

The presence of the ice sheet dramatically affected the North American mean atmospheric circulation. Present-day circulation features generally light mean winds from the southwest. Glacial maximum winds were primarily from the northwest and with average velocity approximately 50-80% above present (Crowley and North 1991). This positioned most of North America in very cold and dry conditions, as the bulk of the continent lay poleward of the mean polar front. Further, the stronger air speeds and different direction had a dramatic effect on oceanic circulation, upwelling, and sea ice formation. For example, sea surface temperatures were approximately 6-10 degrees C lower than present for the North Atlantic. These features combined to force circumpolar vortex expansion into a positive oceanic/atmospheric feedback loop.

During the late Wisconsin, periglacial landscapes formed adjacent to the Laurentide ice sheet edge and extended throughout northwestern and central Pennsylvania and into New York State (Ciolkosz *et al.* 1986). In fact, most of the landforms lying outside the glacial boundary in Pennsylvania reflect periglacial climatic conditions. These include the large in-situ and float-block rock shelters along the Allegheny and Clarion Rivers, the shale chip rubble terraces and rock strewn lower valley slopes in the and the boulder rock fields (felsemeers) which cap the ridges underlain by the Silurian Tuscarora Sandstone and the Devonian Oriskany Sandstone in the Valley and Ridge Province.

Periglacial landscapes form near the edge of glacial areas typically form from the freezing and thawing of water over time (Gardner *et al.* 1991). Areas that are subjected to intense freeze/thaw cycles (both seasonal and over time through climatic fluctuations) produce distinctive terrain and landscape features as products of weathering and erosion (Gardner *et al.* 1991). Such features include unsorted irregular mixed deposits resulting from a combination of ice wedging, solifluction, gelifluction, frost creep, rockfalls, and slides.

In order for periglacial environments to form, mean annual air temperatures of less than 0 degrees C are required. This permits the development of permafrost and other periglacial features (Carson and Kirby 1972; Washburn 1976; Washburn 1980; Pewe, 1983). Solifluction and gelifluction require mass wasting of material during warm months (Benedict 1976). During such times, topsoil thaws and becomes waterlogged over the subsurface permafrost. Unconsolidated materials may move significant distances, even on the shallowest of slopes. U-shaped lobes of materials, patterned ground landscapes of stone circles, polygons, and/or stone stripes form through this process, in combination with frost heaving. Other features include

block fields and rock streams in which large angular blocks form through repeated freeze/thaw action and frost wedging, and these are common features along the mountain tops and slopes where the Silurian Tuscarora Sandstone crops out in the Valley and Ridge physiographic province. These features demonstrate the vastly altered climate of the LGM.

During the late Wisconsin, the dynamic response of hill slopes to the extremes of seasonal climates resulted in the deposition and post-depositional modifications of locally extensive slope strata (Gardner *et al.* 1991). Incipient orientation and grain size stratification is discernible in these deposits associated with valley side slopes (French 1976; Washburn 1980, van Steijn *et al.* 1984, Clark 1988).

According to Watts (1979), landscapes within 65 km of the maximum glacial limit consisted of tundra, dominated by boreal forest and jack pine forest ecotones. Pollen assemblages from late glacial deposits in the eastern United States contain large quantities (up to 40%) of sedge, indicating tundra environments (Bartlein *et al.* 1984; Davis *et al.* 1975; Delcourt 1979; King 1980). Microbotanical data from a number of locations in Pennsylvania provide insight into the floral community of this area during the late Pleistocene. These include Rose Lake in Potter County, Kings Gap Pond #1, and Crider's Pond in Cumberland County, Longswamp in Berks County, and Tannersville Bog in Monroe County. At Longswamp, immediately south of the late Wisconsin ice front, tundra vegetation with grasses, ericaceous shrubs and dwarf birch were present, suggesting a cold, dry, and windy environment (Watts 1979). Similar vegetation, with no evidence of spruce ["generally perceived to be one of the first arboreal plants to colonize deglaciated regions" (McWeeney and Kellogg 2001: 193)] or other trees, occurred at Kings Gap Pond #1, located along the northern edge of South Mountain in Cumberland County, between 16,080 BP. and 14,410 BP. (Delano *et al.* 2002). However, evidence of a contemporaneous non-tundra, spruce forest occurs at Crider's Pond, Cumberland County, in a similar setting, ca. 28 km to the southwest, in sediments as old as 15,000 BP. (Watts 1979). Pollen cores from Crider's Pond indicate that this area, more than 145 km south of the glacial boundary, was dominated by spruce (*Picea sp.*), dwarf birch (*Betula glandulosa*), and various herbs between 15,000 BP. and 13,000 BP. (Watts 1979).

Near the end of the Pleistocene, between 13,000 BP. and 9000 BP. (Watts 1983: 179), at Tannersville Bog, the demise of sedge, aspen (*Populus tremuloides*), and green alder (*Alnus crispa*), is followed by spruce (*Picea sp.*), fir (*Albies sp.*), jack pine (*Pinus banksiana*), gray birch (*Betula populifolia*), and pitch pine (*Pinus rigida*). At 12,000 BP., spruce woodland replaced tundra in western Maryland, western and central New York, and southern New England (Davis, 1983). The occurrence of spruce over such a wide area indicates both the rapid migratory capability of spruce and a climatic amelioration at 12,000 BP. permitting spruce to grow in regions where it was previously limited by climate (Davis 1983: 179).

In addition, investigations at Corry Bog, in northwestern Pennsylvania, by Cotter (1983), Cotter and Crowl (1984), and Karrow *et al. (*1984), indicate that the spruce pollen zone in Pennsylvania occurs between 14,250 BP. and 11, 250 BP. Cotter (1983) and Cotter and Crowl (1984) state that the herb pollen zone lasted from 18,500 PB. to 14,250 BP., and that the earliest occurrence of the spruce pollen zone at sites near the Woodfordian drift border of Pennsylvania was approximately 14,250 BP., rather than 12,600 BP. as suggested by Karrow *et al.* (1984).

The first major deglaciation of the ice sheet occurred between about 14,000-9000 BP., coincident with rapid and extreme climatic change. This deglaciation, which was initiated over a very short 200-300 year warming interval (Crowley and North 1991; Taylor *et al.* 1997), triggered massive ablation over the 5,000-year interval and a subsequent rise in sea level. By 12,000 BP., summer temperatures were about as warm as they are today (Atkinson *et al.* 1987). Remnants of the Laurentide ice sheet persisted until 6000-7000 BP., but the ice sheet was vastly reduced in size. Within this time interval, the most dramatic deglaciation occurred at about 13,000 BP., associated with the Bolling-Allerod climatic interval.

The Bolling-Allerod Interstadial (LGM to 11,200 BP.)

The end of the LGM experienced warming conditions that approximated those of the present (Willard *et al.* 2007). This interval of increasing temperature is known as the Bolling-Allerod interstadial (BA). This interval lies between the late Pleistocene and the abrupt cold period that followed, termed the Younger Dryas. A short-lived cold interval, the Older Dryas, occurred during the middle of the BA (Yu and Eicher 2001).

With the final retreat of the Wisconsin ice sheets, Holocene climatic conditions that affected weather patterns over much of eastern North America were drastically different from those that existed during glacial advances. Climatic forcing during the BA relates to orbital variations (Milankovitch cycles) which enhanced mean summer insolation in the Northern Hemisphere (Berger 1978; Wanner *et al.* 2008). This was at a maximum around 11,000 BP. due to the coincidence of precession and obliquity cycles, and lasted until about 9000 BP. Kutzbach (1983) calculated that global radiation was approximately 7% greater than today during this interval. The increase in global radiation caused profound changes in the circulatory systems of the hemisphere. Downstream cooling effects occurred in the North Atlantic and Eurasia due to the large remnant ice sheet over North America and the influx of cold water into the North Atlantic (Wanner *et al.* 2008). This affected oceanic circulation as well as the overlying atmosphere.

As the glacier retreated, temperatures increased and organic soil horizons developed. Watts (1979) suggests that vegetation of this interval may have been a mosaic - stands of spruce, dwarf shrubs, and wet meadows would have occupied areas free of permafrost and local areas of tundra would have occurred on permanently frozen sites. This environment would have offered few edible plant resources for human populations. However, large, cold-adapted herbivores, such as mastodon, buffalo, and caribou would have been available human prey.

During this interval, stronger circulation occurred over North America as the climate shifted from cold dry conditions to warmer, wetter regimes (Willard *et al.* 2007). Such warming also promoted a rapid rise in sea level, significantly inundating low elevation global coastlines (Parkinson, 1989). Sea level rise during this interval constituted the most significant global physical change of the entire Holocene, reaching about 1 m/100 yrs (Parkinson 1989). Much of the continental shelf was inundated during this time interval. The effects on the landscape were dramatic as coastlines, nearshore regions, and inland areas responded to rising seas.

Atmospheric circulation strengthened, shifting from predominantly zonal flow during the LGM when it was extensively forced by the presence of the Laurentide ice sheet, and concomitant expansion of polar climates through the mid-latitudes, to predominantly meridional flow

(Foreman *et al.* 1995; Leigh and Feeney 1995; Dwyer *et al.* 1996; Knox 2000; Noren *et al.* 2002; Figure 13). This strengthened the Bermuda high which largely controls moisture advection into the southeastern U.S. (Gamble and Meentemeyer 1997; Vega 1998). During times when there is predominantly meridional flow, mean moisture advection increases over the eastern U.S. This is supported by Noren *et al.* (2002), who show an increase in the frequency of storm-related floods in the northeastern U.S.

Despite warming conditions, the BA was predominantly cold and dry, due to the significant but diminishing presence of the Laurentide ice sheet (Otvos 2005; Goman and Leigh 2004). Lower latitude regions of North America show increasing wetness over time, as the ice sheet retreated triggering a concomitant shift in the mean position of the polar jet stream as well as a change in strength and position of the Bermuda High (Liu and Fearn 2000).

Currently, the Bolling-Allerod dated soils that occur on low terraces have been identified at the Shawnee-Minisink site (36Mr43) along the Delaware River and at the Millstone site (36El204) along the Clarion River in Elk County. At the Shawnee-Minisink site, 200 cm of alluvial deposits date to the Bolling-Allerod interval. At the Millstone site, test excavations revealed 160 cm of soil and sediment resting on former channel lag deposits of late Wisconsin age (Fritz 2011; Figure 10). At that site the upper part of a reddish-brown (7.5 YR) coarse prismatic 2Bw horizon had an OSL date of 16,520 +/- 1645 years BP (Beta-288326 and UIC 286). Sediments within the lower portion of the 2Bw horizon yielded an OSL date of 17,750 +/- 1680 years BP (Beta-245308, UIC 2862). Although the date ranges are broad, the evidence is sufficient to conclude that sediments found at the top of the 2Bw horizon (80 to 85 cm) represent a stable alluvial surface during the Bolling-Allerod climate episode.

At about 13,000 BP., jack pine (*Pinus banksiana*), balsam fir (*Abies balsamea*), and speckled alder (*Alnus rugosa*) were present, forming a diverse environment containing both tree and shrub species. Red spruce (*Picea rubens*) was present by 11,500 BP., with white pine (*Pinus strobus*) appearing shortly thereafter (Watts 1979). Watts (1979) suggests that mosaic vegetation communities of this period would have featured stands of pine, dwarf shrubs, and wet meadows in permafrost-free zones.

The Pleistocene fauna of Pennsylvania can be characterized as a combination of currently extinct mega-vertebrates and extant temperate mega-vertebrates, in association with now disjunct large and small northern species (Semken 1983: 192). During the late Pleistocene, the development of open grazing lands and boreal forests would have supported a wide array of mammals adapted to cool climates (Cleland 1966). For example, the Marshalls Creek mastodon, Newton mammoth, Saltillo mastodon, Pleasant Lake mammoth and Conneaut Lake mammoth all date to the BA interval, and suggest a mosaic of open grazing and boreal forests. Evidence suggests that these types of biomes along the glacier's southern margins were exploited by megafauna indigenous to these areas, specifically the woodland musk ox (*Ovibos moschatus*), mastodon and woolly mammoth (*Mammut sp.*), barren ground caribou (*Rangifer tarandus*), giant beaver (*Castoroides sp.*), and moose-elk (*Cervacles scotti*) (Cleland 1966: 91-92; Prufer and Baby 1963: 55; Ritchie and Funk 1973). Recent studies at Sheridan Rockshelter in Wyandot County, Ohio, note the presence of flat-headed peccary and giant beaver at 11,060 BP. and 10,850 BP.,

respectively. The dates for these now extinct fauna overlap the date on Clovis age bone point recovered during excavation of the rock shelter (Redmond and Tankersley 2005).

The Younger Dryas (11,000 BP. - 10,100 BP.)

The Younger Dryas (YD) (Figure 13), also known as the Nahangan Stadial, the Loch Lomond Stadial, or the Greenland Stadial, marked a distinct and significant climatic reversal from the previous rapid deglaciation phase (Figures 15 and 16). The YD was characterized by a rapid decrease in temperature which lasted approximately 900 (C14) years. Pollen analysis shows the results of this brief but dramatic temperature plunge as it records an expansion of boreal taxa including spruce, fir, larch, paper birch, and alder (Peteet *et al.* 1990; Kneller and Peteet 1999). Ice core data place this 900-year-long interval, which began and ended abruptly, between 11,000 and 10,100 years ago (Fiedel 1999). At Alpine Swamp, in northern New Jersey, radiocarbon dates place the boreal expansion between 11,000 and 10,000 BP. (Peteet *et al.* 1990).

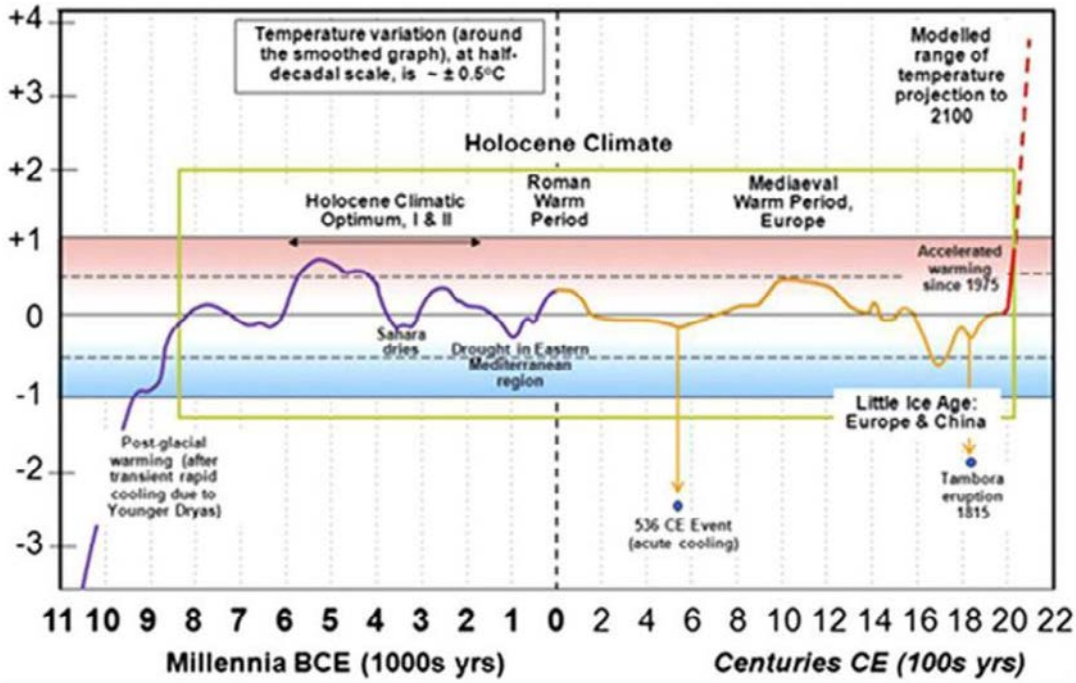

Figure 15. Climatic Periods of the Holocene

During the YD, the circumpolar vortex expanded toward the equator while strengthening significantly and extending boreal conditions equatorward (Ritchie 1979). This offset atmospheric and oceanic circulation regimes that were established during the previous ablation period. The cause of the YD, although debated in the literature, was likely centered on atmospheric and oceanic circulation changes induced by cold meltwaters from the retreating Laurentide ice sheet. Before about 11,000 BP. virtually all meltwaters were carried to the Gulf of Mexico via the Mississippi River (Marchitto and Wei 1995). By 11,000 BP. the ice sheet retreated to a point where the St. Lawrence River opened allowing the large freshwater lake, Lake Agassiz, to drain significant quantities of cold meltwater into the North Atlantic Ocean (Broecker 2006; Willard *et al.* 2007). This caused an extensive cold low-salinity lens in the North Atlantic which significantly altered the oceanic circulation. This hypothesis is supported by Bond (2005) who

showed that major Holocene climatic shifts were accompanied by a 1 - 2-degree C drop in sea surface temperatures (SSTs). These lower SSTs triggered a positive feedback loop that altered the overlying atmospheric circulation pattern leading to circumpolar vortex expansion and cooling over much of North America and Europe.

This expansion brought cold, dry air over portions of eastern North America which had previously been undergoing significant ecotone changes stemming from a circulation regime that supported warmer and increasingly wetter conditions. Along the major drainage lines in the region, the YD was a time of more effective precipitation which favored active lateral channel migration and higher stream discharges (Figure 5). The blocking anticyclone that developed over the North Atlantic also resulted in a decrease in the advection of warm moist air into Europe. This led to a major drop in temperature and increased aridity over that continent. Furthermore, a cold water lens in the North Atlantic disrupts the formation of North Atlantic Deep Water (NADW) which inhibits heat transport (Crowley and North 1991).

In the Middle Atlantic region, the basal sands and gravels that consistently underlie early Holocene age vertical accretion deposits on low terraces date to the Younger Dryas. The renewed activity of rivers during the YD may in part be responsible for the general paucity of recorded Pre-Clovis and Clovis sites along low terraces. In addition, because of the low heights of very late Wisconsin and early Holocene terraces above active river channels, many of these sites may have been eroded during the YD erosional interval through early Holocene flood events and channel migrations. We can conclude that the YD was responsible for a significant erosional disconformity in alluvial sequences along major rivers throughout eastern North America (Figure 1). It is interesting to note that Bolling-Allerod paleosols correlated with climate warming have been identified along the east coast in association with barrier islands, such as St. Catherines Island, Georgia (Vento and Stahlman 2011; Rich *et al.* 2011) and within segments of the Chesapeake Bay and the Delmarva Peninsula. Again, the absence of these buried cumulic A horizons and B horizons dating to the BA on terrace contexts within Pennsylvania likely reflect their removal by active lateral channel migration, braided stream activity and flood scouring during the cold and dry Younger Dryas interval.

During the Inter-Allerod-Younger Dryas transition, at 11,000 BP., the climate in the northeastern interior deteriorated and experiences broad scale changes in vegetation regimes and dynamic temperature fluctuations (Bartlein *et al.* 1984; Davis 1983). Although there is no evidence of glacial ice advancing into the United States in association with the Younger Dryas (11,000 - 10,100 BP.), cold dry climatic conditions and boreal forests were present in Pennsylvania during the interval, 10,800 BP. to 10,000 BP. (Wright 1987). Bernabo and Webb (1977) estimate that pollen in southwestern Pennsylvania at 11,000 BP. consisted of about 30% spruce, 20% pine, and slightly less than 10% oak and herbs. Microbotanical remains indicate that the terrestrial environment of this region at that time would have contained both boreal and deciduous tree species. Deciduous species would have been initially restricted floodplains and other favorable settings before gradually expanding into more diverse environments.

The Younger Dryas in Pennsylvania is characterized by an expansion of boreal taxa including spruce, fir, larch, paper birch, and alder (Peteet *et al.* 1990; Kneller and Peteet 1999). In contrast, the pollen record at Browns Pond in the central Appalachians of Virginia suggests a brief cold

reversal at 12,260 BP., possibly correlating with the Older Dryas, identified in Europe. But, there is no evidence of a climatic reversal between 11,000 BP. and 10,100 BP., suggesting that the Younger Dryas cooling may not have extended as far south as Virginia (Kneller and Peteet 1999). In Pennsylvania there must have been a significant variation in floral communities based upon soil type, slope/aspect and topographic position with for example the higher ridges in the Valley and Ridge containing a higher percentage of Boreal taxa that the more southerly unglaciated sections of the State.

During the Late Pleistocene, the flora and fauna pattern was a mosaic of rapidly changing ecological settings with no modern analogs. According to Carbone (1976), along with the general north/south trend in the Late Pleistocene vegetational pattern, there also would have been east/west physiographic donation. Grasslands were most extensive on the Coastal Plain, with an addition of conifers in the Piedmont. According to Carbone (1976), the Valley and Ridge physiographic region probably displayed the greatest ecological diversity, the most deciduous trees, and the more plentiful human food resources. Using the terminology of Jochim (1976), the food resources along the rivers of the Valley and Ridge section can be described as evenly distributed and continuous. The Appalachian Plateau provided a combination of conifers and grasses, with moderately frequent deciduous elements in sheltered riverine settings. Lepper (1989: 244) argues that "a complex deciduous forest, surprisingly modern in character, would have been present" on the unglaciated Appalachian Plateau throughout the Paleoindian period, suggesting that food resources were at least as plentiful as in the Valley and Ridge. The glaciated Plateau probably contained fewer food resources and, based on Paleoindian site distribution, such resources were more dispersed and in upland settings. Jochim (1976) describes this as a patchy distribution of food resources.

In summary, the Paleoindian environment south of the glaciated zone and the adjacent coastal plain contained a mosaic of boreal, deciduous, and arboreal species. Initially, the deciduous trees would have been restricted to the more favorable settings such as lower elevation well-drained floodplains, and they would have gradually dispersed from these regions as the climate warmed. The deciduous elements increased to the south and the arboreal species increased to the north. Large mammals, such as deer and elk, would have tracked the mast-producing deciduous species and were likely more plentiful in the floodplain settings. In contrast, the vegetation of the glaciated Appalachian Plateau was more open in character, and the flora and fauna were less diverse (Dirkmaat *et al.* 1990). Site distributions in this region suggest that upland glacial features, such as bogs and swamps, probably also contained a variety of food resources. However, the floral and faunal components of specific ecological settings are not well understood, and more site specific data needs to be collected.

The YD ended as a new atmospheric/oceanic equilibrium was attained. Further ice sheet ablation eventually permitted contraction of the circumpolar vortex and expansion of the Bermuda High. The poleward shift of these general circulation features caused net poleward migration of the polar front (jet) and allowed the advection of warmer, moister air masses to penetrate the higher latitudes over eastern North America.

Meridional Jet Flow (+ PNA) Across North America.

Zonal Jet Flow (- PNA) Across North America.

The Reverse PNA (trough to ridge; strongly - PNA) Pattern.

Figure 16. Jet Flow Patterns

The Pre-Boreal (10,100-9100 BP.) and Boreal (9100-8000 BP.)

After the YD, temperatures quickly climbed, reaching, and ultimately surpassing those of the BA. The Pre-Boreal was characterized by warmer and drier climate, overall (Figure 1). Changes in forest composition in the northeast around 10,000 BP confirm that the opening of the Holocene was marked by near modern climatic conditions (Carbone, 1976; Davis, 1983) with warmer-than-present temperatures reflected in the vegetation. The expansion of white pine, which is an excellent temperature and moisture marker, occurred at this time in both upland and lowland elevations in the northeast (Davis 1983). Interestingly, Kutzbach stated that, based upon the results of his orbital variation models, the radiation curves for tilt and precession reinforced each other and resulted in a 7% increase (over that of present) in July global radiation at 9,000 BP. during the Boreal climatic phase. Graetzer (1986) and Watts (1979) show net decreases in the number of low-order streams, low water volumes, decreases in biomass and decreases in the height of the water table during this time. For more southern areas of the United States, Goman *et al.* (2004) found evidence of increased precipitation in North Carolina in the form of a significant number of identified large overbank floods (frequency of about 5 major floods per 1000 years) occurring during this time period. In contrast, only 6 major floods occurred in the study region during the following 6100 years. Superimposed on the record of generally warming temperatures was a brief 150-250 year cooling event known as the Pre-Boreal Oscillation, the result of a second flood of Lake Agassiz waters, beginning about 11,355 BP (Fischer *et al.* 2002).

During the Boreal, another release of cold fresh water from Lake Agassiz occurred at around 8200, when approximately 163,000 km3 of freshwater spilled through the Hudson Straits into the Labrador Sea (Barber *et al.* 1999; Mayewski 2004). This event is thought to have added a low-salinity freshwater lens to the North Atlantic, reducing the rate of formation of North Atlantic Deep Water (NADW). In turn, this may have reduced rates of northward heat transport, facilitating a short-term climatic shift to cooler temperatures around 8200 BP. in areas of Europe and northern North America.

Evidence of this 8200 BP. event is apparent in several high resolution, well-dated records: the Greenland ice cores (Alley *et al.* 1997; Johnson *et al.* 2001), speleothems in Ireland (Baldini *et al.* 2002), tree rings and lacustrine sediments in northern and eastern Europe (Klitgaard-Kristenson *et al.* 1998; Veski *et al.* 2004) and the Cariaco Basin sediments (Hughen *et al.* 1996). These records suggest the event lasted 100-200 years, beginning at 8250 BP. (Johnson *et al.* 2001). This event is most evident in Europe and Greenland, although there is some evidence for aridity in the tropics (Alley and Agustsdottir 2005; Morrill and Jacobsen 2005).

Because of the event's limited duration, there is some debate concerning its effect on climate and associated vegetational change. Some have argued that even a 200 year long event may have been adequate at that time to cause environment change, in concert with other mechanisms (e.g. solar fluctuations). As such, it may represent a centennial-scale event causing environmental (and vegetational) changes that may have persisted for some time after the termination of the event, itself. Many studies, in particular those of low-resolution, emphasize multi-centennial climatic change centered around 8200 BP. (Dean *et al.* 2002). Rohling and Palike (2005) however argue that the vast majority of high resolution climate proxy records indicate the event started at or before 8400 BP. and most imply an age before 8500 BP. They contend it would be incorrect to attribute all climate anomalies to the 8200 BP. event; instead they suggest climatic

deterioration between 8500 BP. and 8000 BP is more likely part of a broad pattern of longer-term anomalies in the Holocene, probably related to solar fluctuations.

Overall, during this time, hemispheric warming likely triggered a decrease in the latitudinal thermal gradient and continental/oceanic contrast as the cold water lens of the Younger Dryas diffused. This would reduce variation in the polar jet stream creating a more zonal mean atmospheric flow regime and overall drier conditions during this time (Figures 13-15). It is likely that fewer large magnitude precipitation events occurred, a condition supported by zonal flow (Figure 16). As the region warmed from the colder Younger Dryas, increased vegetational growth would have mitigated overbank deposition in concert with the transition to a warmer and moister climatic regime.

These conditions likely extended into the Boreal period (9100-8000 BP.), which marked a transitory phase from the Pre-Boreal to the wetter Atlantic period. Warmer and drier conditions would predominate as the atmosphere sought a new equilibrium to shifting latitudinal energy gradients. Such changes would increase the strength of the Bermuda High pressure system, inducing significant increase in moisture advection over North America east of the Rocky Mountains. Greater moisture advection leads to not only wetter climatic regimes, but also to increased air temperatures through low-latitude air mass advection.

During this interval, most of the rivers in the eastern United States established a clear meandering channel habit, and began the long phase of Holocene aggradation. Along most of the major drainage lines the warmer and drier conditions of the early and middle Holocene (Pre-Boreal and Boreal) is marked by frequent low magnitude overbanking events and the formation of thick, often well-developed cambic B-horizons which overlie the basal sands and gravels deposited during the Younger Dryas. The cultural history of most sections of the northeast shows trends consistent with the northward retreat of coniferous forest, containing relatively meager food resources compared to the nuts, berries and herbs of the deciduous forests (Stoltman and Baerries 1982).

The work of Knox (1983) supports the interpretation of dry conditions for the Boreal climate phase. Runoff and sediment yields are principal determinants of the physical properties of alluvial channels and flood plains, and the frequency and magnitude of water and sediment yields are adjusted to climate, vegetative cover and physiography. Knox's (1983) seminal paper discusses the adjustments of river systems as they relate to the direct effects of climatic events (storms and floods) and the indirect effects of vegetation as it controls runoff and erosion. Knox (1983) propose that fluctuations in the atmospheric circulation pattern (i.e. jet stream) from zonal (de-amplified west to east flow) during the Boreal climatic phase to mixed zonal-meridional (amplified flow, allowing cross latitudinal advection) during the Atlantic through Sub-Boreal climatic phases were responsible for significant changes in stream regime (e.g. large floods, aggradation vs. incision) (Figure 17). Langbrin and Schumm (1958) also emphasized the strong influence of vegetative cover on surface runoff and subsequent bankfull discharges. To date, there is no strong evidence for the replacement of forest by prairie vegetation in the Middle Atlantic region (even during the warm and dry Sub-Boreal climatic phase). This indicates that changes in forest communities, though important, were apparently secondary to climate change in effecting fluvial responses.

Within the Upper Ohio, Delaware and Susquehanna River drainage basins the early Holocene (Pre-Boreal and Boreal) was a time of active alluviation/aggradation. Since both base-level and tectonic controls can effectively be ignored, the most likely cause of this alluviation was the expansion of tributary streams supplying an increase in sediment yields to the river and its main tributaries, as well as a change in atmospheric circulation patterns.

Holocene Environments

Watts (1979) has examined the pollen record for central Appalachia and the New Jersey Coastal Plain, and divides the post-glacial time span into four intervals: (1) the late Pleistocene, influenced by the proximity of the glacial front and ending about 13,000 BP., (2) the early Holocene, characterized by the immigration of tree species from southern refugia, ending about 9000 BP., (3) the Hypsithermal, a warm, dry interval lasting until 3500 BP., and (4) the late Holocene, when a relatively stable primary forest became established (Miller *et al.* 2004; Watts, 1979; Figure 15). We note that this is a broader climatic classification than the Blytt-Sernander scheme described earlier, but it incorporates greater variation and facilitates interpretation of larger-scale paleoenvironmental trends that might be more unequivocally registered in the stratigraphic record.

Earlier interpretations of the pollen record focused on the concept that the environment of 10,000 years ago resembled the modern Boreal forest, and was dominated by pine and lacked the deciduous food-bearing species that were abundant in the forest after 5000 BP. (Fitting 1968; Ritchie 1979). More recent data show a post-glacial proliferation, in pollen profiles, of deciduous elements such as oak. This is presumed to be evidence, at least locally, of colonization of deciduous species in the early Holocene forest (Davis *et al.* 1975; Dincauze and Mulholland 1977; Eisenberg 1978; Miller *et al.* 2007). Delcourt and Delcourt (1980) present evidence of conifer-hardwood forests in the Middle Atlantic region at 10,000 BP. In addition to conifers and oak, these forests included cold-adapted, mesic species such as birch, elm, ironwood, maple, and beech. Oak and hickory pollen are well-represented at 10,000 BP. in a core from Browns Pond (Kneller and Peteet 1999). Carbonized grape, plum, and hackberry occur in a Paleoindian hearth at the Shawnee Minisink site on the Delaware River and indicate that understory vegetation common in temperate forests was present during this early interval (Dent and Kauffman 1985). In sum, conifers dominated throughout the glaciated region and deciduous species were most common in the unglaciated regions to the south of the late Wisconsin terminal moraine.

Pre-Boreal Climatic Episode (10,100 BP. - 9000 BP.)

The Pre-Boreal (10,100 BP. - 9000 BP.) environments, however, were comprised primarily of conifers with mixed deciduous elements (lower part of Pollen Zone B) from 10,100 - 9000 BP. Most of Pennsylvania was characterized by a closed forest comprised of pine, fir, oak, hemlock, alder, and birch. Although the Laurentide ice sheet had receded to the north, weather patterns remained influenced by ongoing deglaciation. At this time, the dominant atmospheric circulation pattern for North America was zonal (west to east), which resulted in an increased frequency of cyclonic storms (Knox 1983: 30-31); Vento *et al.* 2008: 16). Eastern Canada, however, remained covered by massive glacial ice, and sea level was approximately 20 m below its present level.

Delcourt and Delcourt (1981) have documented the presence of conifer-oak forests in the Middle Atlantic region at 10,000 BP. that included cold-adapted, mesic species such as birch, elm, ash, ironwood, maple, and beech. Oak and hickory pollen are well-represented at 10,000 BP at Browns Pond in Virginia. Hemlock was present in central Pennsylvania by 9600 BP. (Watts 1979: 462).

Although the data suggest that the Pre-Boreal forest likely contained a substantial component of temperate hardwoods, these species were probably restricted to favorable topographic and edaphic niches, initially occurring as patches within a predominantly coniferous forest. In the southern section of the modern conifer-hardwoods found on the Appalachian Plateau, deciduous species have migrated northward along major valleys and their tributaries (Braun 1950), a situation that may resemble the early to mid-Holocene immigration of deciduous species along stream valley from glacial refugia in the south. Faunal data also support the existence of a temperate forest. At Hosterman's Pit, Centre County (Guilday 1967), faunal remains dated to approximately 9000 BP. are mostly temperate forest species such as squirrel, pine mouse, rabbit, and deer.

The Holocene fauna of Pennsylvania is generally assignable to Semken's (1983) second category. He states that the reduction in the number of species has led authors (e.g. Martin, 1967; Martin and Webb 1974; Semken 1974) to regard the Holocene biotic record (especially the megafauna) as impoverished, compared to the high species diversity of the Late Pleistocene (Graham 1979). This faunal change has been used to define the Pleistocene/Holocene transition. Clearly, the megafaunal species of the late Pleistocene suffered extensive extinction. Moreover, the temporal response of vertebrate species to deglaciation and associated climate change was highly variable (Guilday and Parmalee 1965); Guilday *et al.* 1966, 1977). Nevertheless, the viewpoint of a vertebrate transition within a few hundred years after deglaciation appears to be valid (Semken 1983).

The faunal assemblage that is radiocarbon dated to 11,300 BP. + - 1000 at New Paris No. 4, a cave in Bedford County, revealed that a transition occurred from predominantly boreal species to an admixture of temperate forest species (Guilday *et al.* 1964). Fauna associated with temperate conditions were present at Meadowcroft Rockshelter in western Pennsylvania, levels dated approximately 11,300 BP. (Adovasio *et al.* 1985). Included species were box turtle, turkey, eastern mole, and pine or woodland vole.

Boreal Climatic Episode (9000 BP. - 8000 BP.)

The Boreal chronozone (9000 BP. - 8000 BP.) (upper half of Pollen Zone B) marks the beginning of a warm interval that has been referred to as the North American climatic optimum, the Altithermal, or the Hypsithermal period (Deevey and Flint 1957; Figure 1). Climatic regimes of the Hypsithermal include the warm and dry Boreal episode (9000 BP. - 8000 BP.) and the warm and wet Atlantic episode (8000 BP. - 4200 BP.).

During the Hypsithermal there was a dramatic expansion of white pine into both uplands and lowlands (Watts 1979). Because pine is an excellent indicator of temperature and moisture, this reveals that the climate was both warmer and drier than during the previous thousand years, or any time after (Davis 1983). The increase in pine pollen during the Boreal climatic episode

provides important evidence of the prevailing climate and biotic environment. Watts notes that "pines flourish on acid sandy soils where natural fires are frequent and where competition for the larger canopy-forming deciduous trees is restricted, " adding that pines become established on sites where forest has been destroyed by fire, storm blow downs, or forest clearance, all of which make "light gaps" (Watts 1979: 462). Although oak, hickory, beech, and elm were present, they did not reach peak distributions until about 5000 BP. (Prentice *et al.* 1991: Figure 1).

Pollen evidence also signals the change to warmer and drier climates (compared to present) over the interval between 9000 BP. and 5500 BP. Within this time interval the data for the Hypsithermal are strongest in the Midwest where pollen profiles argue for advance of the prairie eastward into Illinois, reaching its maximum extent about 7000 BP. (Bartlein *et al.* 1980; King, 1980). In the eastern United States, evidence for a warmer, drier period at this time (as summarized by Graetzer 1986), includes a peak in grasses at Bear Meadows in Centre County, Pennsylvania (Kovar 1965), and xeric vegetation on the Cumberland Plateau in Tennessee (Delcourt 1979) Davis *et al.* (1980) point out that an increase in the altitudinal range of hemlock and white pine is evidence of a warmer, drier period between 9000 BP. and 5000 BP. in New England. Watts (1979), in his examination of pollen diagrams in the Middle Atlantic region, supports the hypothesis of a warmer, drier climate between 8500 BP. and 5500 BP. (Miller *et al.* 2004). Klippel and Parmalee (1982) note that even with this warming trend the climate the climate during the early Holocene was considerably cooler than at present on the Allegheny Plateau, with conditions most closely resembling the more northerly boreal forest regions. Bernarbo and Webb (1977) note that, by 9000 BP., however, the pollen in southwestern Pennsylvania consisted of almost no spruce, 30 percent pine, 35 percent oak, and slightly less than 10 percent herbs, indicating the northward retreat of the boreal forest (Coppock *et al.* 2010; Coppock *et al.* 2011).

Effects of the warmer, drier climate included a decrease in the number of low-order streams, a general lower water volume in streams, a decrease in biomass on ridges, and a lowering of the water table (Braetzer 1986; Watts 1979). Evidence, provided by correlations of pollen core data with pollen taken from surface samples of known vegetational type, suggests that the overall composition of the vegetation did not change radically (Bradstreet and Davis 1975). Changes in hydrology and decreases in productivity would likely have had some effect on the distribution of prehistoric populations. Specifically, upland areas would have become relatively less suitable, whereas major riverine areas such as the Ohio, Delaware, and Susquehanna flood plains and terraces would have been relatively more suitable (Miller *et al.* 2007).

The warm, dry Boreal climate had a detrimental effect on ponds and low-order streams. Oxidized soils containing damaged or destroyed pollen at sites from Georgia to New Jersey, (including Big Pond, Bedford County, Pennsylvania) indicate that the ponds and bogs dried out more frequently during the mid-Holocene Hypsithermal than in subsequent times (Watts 1979: 263). By 6500 BP., the last remnant of the Laurentide ice sheet had melted on the Quebec-Labrador Plateau, and the Atlantic Ocean had reached its current level (Vento *et al.* 2008). This retreat of the ice sheets effectively allowed for the penetration of cyclonic storms into Pennsylvania from the Gulf of Mexico and Atlantic Ocean.

Faunal studies have indicated that a modern array of species was present in central Pennsylvania by 9290 BP. (Guilday 1967). Faunal assemblages from Sheep Rock Shelter (36Hu1) in Huntingdon County, Pennsylvania, and Meadowcroft Rockshelter (36Wh297) in Washington County, Pennsylvania, show no evidence of a significant shift of animal species distribution during the Hypsithermal (Guilday and Parmalee 1965; Figure 10). However, evidence for a change from forest (Pre-Boreal episodes) species has been reported in the upper Mississippi Valley (McMillan and Klippel 1981; Purdue and Styles 1986), and in other parts of eastern North America (Semken 1983). Faunal remains from Sheep Rock Shelter indicated that whitetail deer, elk, raccoon, beaver, rabbit, muskrat, grey squirrel, and turkey were important in the diet of Native American groups in the Juniata Valley throughout the Holocene (Guilday and Parmalee 1965).

Atlantic Climatic Episode (8000 BP. – 4200 BP.)

Reexamination of stratigraphic sequences across Pennsylvania indicates that the Atlantic climatic episode can be divided into two parts: 1) the early Atlantic (8000 BP. to 6000 BP.) which records a period of slow vertical accretion and the subsequent formation of strong cambic, weak argillic, and, in places, fragic soil profiles and 2) the late Atlantic which records greater frequency of larger overbanking events, more rapid vertical accretion, and distinct coarsening upward profiles associated with the continued ablation/retreat of the Wisconsin ice sheets, allowing for the penetration of warm and moist air masses into Pennsylvania from the Gulf of Mexico.

During the Hypsithermal rapid increases in temperatures occurred across much of the Northern Hemisphere, but with most warming in the high latitudes. Tropical locations were approximately 1-degree C warmer than at present, while temperatures near the North Pole were approximately 4 degrees C warmer. In terms of seasonal change, winter temperatures changed more than summer temperatures, +3-9 degrees C and +2-6 degrees C, respectively. Data from the southern hemisphere indicates cooling during this time interval, as well.

Causes of the Hypsithermal's rapid temperature increases across much of the Northern Hemisphere apparently relate to orbital variations, or Milankovitch cycles (Wanner *et al.* 2008). At about 9000 BP. the earth's axial tilt was maximized at 24 degrees. This, combined with perihelion during Northern Hemisphere summer drove solar radiation levels upward by approximately 8%. Circulation changes included either a northward expansion of the polar vortex or an enhanced meridional circulation during the Hypsithermal (Wanner *et al.* 2008). These events are not likely mutually exclusive with both occurring simultaneously. This is suggested by Greenland cores which show increased levels of sea salt and terrestrial dust. Wanner *et al.* (2008) also discuss a southward shift of the Intertropical Convergence Zone (ITCZ) throughout the mid to late Holocene. They also posit that the NAO index shifts to more positive values (zonal flow conditions) during the mid-Holocene, and shifts to negative values (meridional flow) during the late Holocene.

The pollen record for the Upper Ohio, upper and central Delaware and Susquehanna River drainage basins shows a rapid decrease in pine and an accompanying increase in both oak and hemlock. This change in the pollen spectra was likely the result of transition from the warmer and drier conditions of the Pre Boreal - Boreal climatic phases to moister conditions during the Atlantic climatic phase. The basal dates from many research sites document the beginning of the

Atlantic climatic phase at approximately 8000 BP. At these sites, buried A-horizons, if present, are overlain by a rather thick package of fine-grained overbank deposits that document a lengthy episode (8000 BP. to 4200 BP.) of continuous low magnitude flood deposition induced by strong zonal atmospheric circulation. Throughout the region the presence of a thick, moderately well-developed B horizon attests to this episode of slow continuous vertical accretion during the Atlantic climatic phase.

Although Knox (1983) and Vento and Rollins (1989) had argued for the prevalence of a more meridional circulation regime during this period, it is more likely that zonal conditions prevailed, with the mean jet increasing in latitude, permitting warmer and wetter air masses to occupy the study region. This is supported by the long-term stability of floodplains through the early part of the Atlantic period (Vento *et al.* 2008). Climatically, precipitation stability is more indicative of zonal circulation regimes. Meridional circulations (Figure 16) are triggered during periods of extreme latitudinal thermal gradients. This occurs when polar latitudes are much colder than the less variable and more consistent low latitude temperatures. An increased latitudinal thermal gradient triggers circumpolar vortex expansion which, in turn, triggers increases in polar front amplitude. Embedded within the meridional circulation are mid-latitude (frontal) cyclones. These cyclones tend to be of greater frequency and magnitude than during zonal flow periods, as upper air vorticity is enhanced under the highly amplified flow regime. The increase in vorticity occurs as a result of large latitudinal differences in the position of the ridge and trough axes. Strong positive vorticity advection occurs relative to deepened troughs in a meridional circulation regime as air motions follow constant absolute vorticity trajectories (CAVT). This supports strong, deep, and long-duration frontal cyclones which are normally associated with significant precipitation events.

The PNA and the NAO indices are inversely correlated as the positive PNA indicates meridional flow as does the negative NAO. The two indices, used in conjunction, provide an approximation of mean upper-atmosphere flow from the central North Pacific Ocean to Western Europe. The prevailing forcing mechanisms of upper-atmospheric flow suggest that the long-term floodplain stability present throughout the 4000-year Atlantic climatic episode stems from primarily zonal flow conditions. It is climatically plausible that the warming conditions and Laurentide ice sheet ablation forces a net poleward adjustment in the mean polar jet as documented by Watts (1979), Bartlein *et al.* (1984), and King (1980). The adjustment to this new flow regime likely occurred abruptly (Wendland and Bryson 1974) with fluvial systems responding directly to the climatic change and indirectly to the slower associated vegetation shift (Knox 1983). As Knox (1983) suggests, vegetation would transition to the new climatic forcing within 50-200 years. The sudden increase in both oak and hemlock during the Atlantic climatic episode supports the idea of a rapidly changing climatic regime to warm-moist conditions circa. 8000 BP. to 4200 BP. (Figure 1). As explained above, a transition to an increased meridional flow regime would be coincident with frequent, strong, and slow-moving frontal cyclones. This should be reflected in the fluvial sedimentological record by frequent and well-developed overbank deposits, but such does not occur in the fluvial record of this interval. We therefore conclude that the meridional scenario is inapplicable, on the basis of the available record and present-day atmospheric flow analysis.

As mentioned earlier, the forests of the Atlantic climatic phase (Pollen Zone C-1; Prentice *et al.* 1991; Vento *et al.* 2008: 17) are characterized by a rapid decrease in pine and concomitant increase in both oak and hemlock. Although mast-bearing trees continued to increase in abundance during the Atlantic episode, they did not reach their historic levels until the late Holocene or Neoglacial period (i.e., post-5000 BP.). Chestnut, an extremely slow migrant, does not occur in central Pennsylvania until around 5500 BP. Many of the arboreal species that reached dominance at that time (e.g. oak and chestnut) provided fruits and nuts known to have consumed both by humans and by human prey such as deer, elk, bear, and various small mammals (Davis 1976).

The Sub-Boreal Climatic Episode (4200 BP. - 3000 BP.)

Increasing frequency of cyclonic storms occurred during the continuing northward ablation of the Laurentide ice sheet after the Atlantic climatic episode (beginning as early as 6000 BP.). Abundant resultant alluvial deposition is supported by data from the Upper Ohio and Upper and Middle reaches of the Susquehanna and Delaware River drainage basins. Stratigraphic evidence, in the form of channel avulsion and deposition of coarse-grained vertical and lateral accretion deposits, especially along the first-, second-, and third-order streams within the basin, documents the increased occurrence of large storms after 6000 BP (Figure 5). Similar stratigraphic evidence in the northern Midwest supports the idea of more frequent large floods after 6000 BP. (Knox *et al.* 1981; Figure 1).

Not surprisingly, the incision of the Pre-Boreal and early Atlantic valley-fill deposits in most areas of the basin occurred about 6000 BP. This was coincident with increased meridional circulation - a condition that promoted strong cyclonic storms via the lifting and mixing of warm, moist Gulf air masses by cool, dry air masses out of Canada (Vento and Fitzgibbons 1987; Grissinger *et al.* 1981; Figure 17). This episode of middle Holocene incision and more frequent large floods may be responsible for the general paucity or near absence of in situ, Paleoindian, Early Archaic and Middle Archaic sites in low terrace contexts along many of the streams in the Commonwealth.

During the period 4200 BP. to 3000 BP. (Sub-Boreal to Historic Contact), the genetic stratigraphic package deposited on the lowermost Port Huron and Valley Heads terraces in the Susquehanna and Delaware basins is marked by various occurrences of erosion and deposition that can be attributed to atmospherically induced changes in climate. The typically thick cambric B-horizons and/or C-horizons of the Sub-Boreal were emplaced during warm and dry conditions, probably in association with meridional stabilization of the Bermuda-Azores anticyclone over eastern North America and/or the increased importance of warm/dry zonal flow (much like the 1930s) which reduced vegetative cover, increased surface runoff and promoted vertical accretion on low terraces within the basin. This situation occurs when the Bermuda-Azores High becomes especially large and strong, and/or retrogrades westward over the eastern portion of North America. These conditions result in a positive PNA and a negative NAO index, indicative of highly meridional flow with the mean jet trough position westward of normal. In many cases, the PNA will "reverse" through displacement of the normal ridge to trough (from west to east) to a trough to ridge flow regime. Eastern North America falls under the presence of a ridge and subsequent high pressure. This decreases the likelihood of precipitation while simultaneously advecting

warm, dry air from the southwest. Such conditions occur with relative frequency during present-day summers.

The decline of hemlock during the Sub-Boreal lends support to the assignation of warm-dry conditions during this time. The absence of well-developed cumulic A-horizons and associated flood plain instability may also be attributed to these conditions (Figure 1). Archaeologically, the observed low numbers of Transitional Archaic sites along small to moderate-sized drainage lines in the region may reflect a prehistoric preference for larger streams where discharges would have been less affected by the warm-dry conditions due to base flow (ground water) contribution. Perhaps significantly, this warm-dry interval is also well documented at Meadowcroft Rockshelter in deposits dated to the same time interval (Campbell *et al.* 2008). Additionally, as noted by Stinchcomb (2012), pollen and lake-level data from the region indicate a warm dry interval from 5500 BP. to 3000 BP., accompanied by the well-documented Eastern Hemlock (*Tsuga canadensis*) decline (Watts 1979; Davis 1983; Shuman *et al.* 2004, 2009). Coeval dry conditions were documented in nearby Lake Grinnel, New Jersey (Li *et al.* 2007), upstate New York (Mullins *et al.* 2011, and Davis Pond, Massachusetts (Newby *et al.* 2011). West Virginia speleothem Sr/Ca ratios also indicate a dry interval around 3000 BP. (Springer *et al.* 2009).

To date, the most detailed and exhaustive studies within the Upper Delaware and Middle Delaware River valley has been completed by Stinchcomb *et al.* (2012) and Stinchcomb (2013). The Transitional Archaic period coincides with the late-middle Holocene reworking and aggradation phase (Phase IV) along the upper Delaware River valley (Stinchcomb *et al.* 2012). Following middle Holocene (6000 BP. - 5000 BP.), average flood deposit grain size decreases and a widespread soil formed along the higher T2a alluvial terrace. Adjacent to the T2a is a lower T2b terrace that contains evidence of rapid sedimentation and multistory, weakly developed buried soils. Because overbank sediment was accumulating along the lower surface (active floodplain), the higher, less flood-prone, T2a surface became a more suitable habitation site. This T2a buried soil often holds evidence of Late and Transitional Archaic occupation. Carbon isotope composition of soil organic matter from Delaware alluvial soils suggests that the Transitional Archaic period follows a shift from higher to lower C4:C3 plants, centered at 4500 BP. (Stinchcomb *et al.* 2013). This shift may be related to major climate reorganization (the 4200 BP. event, and middle to late Holocene transition), post 6000 BP. - 5000 BP. incision and riparian development, or both (Stinchcomb *et al.* 2012; Stinchcomb *et al.* 2013).

The beginning of the Sub-Boreal climatic episode (Pollen Zone C-2) marks the end of the Hypsithermal and the beginning of the Neoglacial period (Vento *et al.* 2008:4; Figure 1). The forest of this time was dominated by oak and hickory, and there is a marked reduction in pine, birch, and alder (Prentice *et al.* 1991: 2047). A dramatic decline in hemlock that began around 5000 BP. (Hass and McAndrews 2000:81) continued throughout this interval (Coppock *et al.* 2010, 2011).

There are competing hypotheses to explain the reduction of hemlock during the Sub-Boreal interval. Knox (1983), Vento and Rollins (1989), and Vento *et al.* (1992; 2008) suggest that the decline of hemlock and its continued suppression during the Sub-Boreal (ca. 4500 BP. - 3000 BP.) indicate that warm and dry conditions prevailed at this time. They argue that this warm-dry pattern resulted from meridional stabilization of the sub-tropic high zone over Pennsylvania or

increased warm-dry zonal flow (much like conditions in the 1930s). This pattern led to a reduction in vegetative cover and greater surface runoff, which promoted vertical accretion on low terraces within stream basins. Although others have proposed that the hemlock decline was the result of disease or insect infestations (e.g. Bhiry and Filion 1996; Davis 1981; Filion and Quinty 1993), most of the evidence suggests that the decline can be attributed to drought (e.g. Haas and McAndrews 2000; Niering 1953; Valero-Garces *et al.* 1997; Yu *et al.* 1997). Regardless of whether the overall climate during this period was warm and dry, or more like today's, it is clear that the rapid deposition of coarse sediments along rivers and streams during the Sub-Boreal period was the result of frequent cyclonic storms causing severe to moderate lateral channel migration of tributaries, with alluviation dominant over incision.

Although there is some disagreement regarding the occurrence of a mid-Holocene climatic optimum in the Northeast, there is even greater debate regarding the climate following 5000 BP. A number of researchers argue in support of environments affected by severe climatic fluctuations, including a warm, dry, or xerothermic, period between 5000 BP. and 2600 BP. (Carbone 1976; Custer 1988; Curry and Custer 1982; Vento and Rollins 1989; Vento *et al.* 2008). Joyce (1988) notes that the xerothermic has been assigned various dates within this time interval. Curry and Custer (1982) argue that the xerothermic corresponded to the warm, dry conditions of the late Atlantic and the Sub-Boreal periods in the Blytt-Sernander construct. Others contend that, although there were undoubted fluctuations in temperature and moisture after 5000 BP., these were no more than low amplitude fluctuations of short durations (Beckerman 1986; Joyce 1988; Watts 1979).

According to Miller *et al.* (2003) and Miller *et al.* (2007), impacts on vegetation were likely minimal and the species composition of the forest habitat, as a result, was similar to that of present-day in many respects. Custer (1984; 1988) points to a decrease in hemlock and an increase in hickory as evidenced by many of the major pollen studies in the northeastern United States. Hickory, in these studies, is considered to be an indicator of relatively dry conditions. However, as both Custer (1988) and Carbone (1976) remark, the difficulties of species-level identification of pollen samples renders such interpretations problematical. Moreover, mesic species of hickory exist (*Carya cordiformis*, *Carya ovata*), and are common in the modern biota (Joyce 1988). Most xeric hickory species also grow and thrive on moist fertile soils. The sudden and synchronous decline of hemlock across a wide range of latitudes, often interpreted as due to dry conditions resulting from climate change, better favors causation from disease (Bhilry and Filion 1966; Davis 1983; Watts 1979, 1983). Also, pollen profiles do not exhibit significant increases in non-arboreal pollen, such as grasses, amaranth, and chenopod that would suggest a significant decline in over story vegetation resulting from decreased precipitation and increased temperatures (Miller *et al.* 2004; Miller *et al.* 2007; Coppock *et al.* 2010).

Carbone's (1976) quantitative analysis of data from the Shenandoah Valley is often cited to support the proposition that warm and dry conditions were present in the Middle Atlantic during the late Holocene. That study followed a statistical methodology developed by Webb and Bryson (1972), based on modern pollen samples and modern climatic data from 73 sample locations in the Midwest. Carbone (1976) applied this methodology to raw data from Hack Pond, located in the Shenandoah Valley of Virginia, to support the existence of warm, dry period, culminating around 4350 BP. (Carbone 1976; Miller *et al.* 2004). According to Carbone (1976; 106), this

involved "increased temperatures, increased desiccation, and moisture stress". Carbone's discussion does not make clear when temperature and precipitation reached modern conditions, although Carbone states that the "climatic shifts of the last 4000 to 5000 years can be better understood as perturbations of the modern pattern rather than as actual long-term shifts (Carbone 1976: 107). Problems in projecting the effective spatial ranges (from the Midwest eastward) and timing of climatic change for this widely utilized model stem from ecological variability, on both regional and local scales.

Alluvial stratigraphy has also been used to support warm, dry conditions in the late Holocene. Increases in overbank deposition rates have been attributed to increased runoff resulting from decreased vegetative cover. Such an interpretation is based in part on Knox's (1972) study of the morphology of stream channels and flood plains in southwestern Wisconsin. Knox interpreted increased aggradation prior to 6000 BP. to result from a warm, dry period when climate was primarily influenced by dry westerly winds. This interval is well document in the pollen profiles of the Midwest, which indicate an eastward migration of the Midwestern prairie prior to 6000 BP. (King 1980). After 6000 BP., Knox theorized that increased rainfall and vegetation resulted in a decrease in the magnitude and frequency of peak stream flows, resulting in less overbank deposition. Knox (1983) noted that the period of greatest sediment yield during the climatic progression from humid to arid to humid conditions would have been at the end of the warm, dry period, when vegetative cover was at a minimum, but when rainfall increased. Again, the difficulties of transferring mechanisms (climatic or otherwise) across interregional settings of alluvial deposition remain (Miller *et al.* 2007).

Nevertheless, studies of alluvial stratigraphy in the Middle Atlantic region do indicate that overbank deposition was rapid between approximately 5000 BP. and 3000 BP. Vento and Rollins (1989) and Vento *et al.* (2008) identified a record of rapid vertical accretion in the Ohio and Susquehanna River basins, consisting of sediments with Late Archaic and Transitional Period cultural material. Scully and Arnold (1981) found evidence of increasing vertical accretion in the upper Susquehanna drainage basin after 4900 BP. Schuldenrein *et al.* (2003) found somewhat similar, although slightly more subdued, trends along the Delaware. Carbone (1976) pointed to the rapid deposition of culturally sterile, sandy clay loam between 5000 BP. and 2700 BP. as an indication that vegetation cover was at a minimum as a result of increased temperatures and decreased rainfall.

Hydrological studies cast additional light on the link between sediment yield, climate, and vegetation cover. Langbein and Schumm (1958) demonstrated that the degree of precipitation decrease required to substantially affect the sediment yield and magnitude of floods is quite large. Their data show that the decline in precipitation required to cause a forest to grassland transition would result in only a 30 percent increase in sediment yield. Late Archaic and Transitional Period over bank deposition apparently increased at least this much, yet there is no evidence in pollen profiles of grassland vegetation during this period (Vento and Rollins 1989; Vento *et al.* 2008). Data presented by Knox (1972) indicate that changes in mean annual precipitation above 650 mm mean annual precipitation have little effect on flood size. Present day precipitation in the Susquehanna, Delaware, and Ohio River basins is approximately 900 mm annually (Vento *et al.* 2008). Thus, for decreased rainfall to affect either the sediment yield of drainage basins or the magnitude of overbank flooding, arid conditions would have been

required. As noted above, there is no evidence of vegetation changes in the late Holocene pollen record of the Middle Atlantic region that would indicate a shift in overstory composition involving an increase in xeric species. However, as noted above, this interpretation of the pollen profile is not irrefutable (Miller *et al.* 2004).

Vento and Rollins (1989) and Vento *et al.* (2008) support the hypothesis of a warm, dry Sub-Boreal (4200-3000 BP.), and they attribute rapid vertical accretion to changes in atmospheric circulation patterns. Based on Knox's (1983) discussion of the effects of zonal vs. meridional circulation, Vento *et al.* (2008) and Joyce (1988) point to an increase in meridional circulation resulting in more frequent cyclonic storms and more frequent overbank flooding. Miller *et al.* (2004) emphasize that such an interpretation does not depend upon an overall decrease in precipitation and/or decrease in vegetation in order to explain the increase in alluvial deposition. Although there are, to date, no independent supporting data for this hypothesis, in contrast to that of severe climatic change, it is not in conflict with the pollen data (Miller *et al.* 2003).

Miller *et al.* (2003) further note that there is not conclusive evidence of a widespread warm, dry climate such as hypothesized by Carbone (1976) and Curry and Custer (1982) for the period between 5000 BP. and 2600 BP. Rather, data suggest that modern levels of temperature and precipitation prevailed in the eastern United States and the Ohio River drainage basin in general. Cyclonic storms, as evidenced by flood scouring and the deposition of coarse-grained material on the flood plain, likely were more common than in the previous period. Flood plain and terrace soils supported mesophytic species such as beech, oak, tulip tree, ash, sugar maple, and walnut. Upland soils supported forest communities dominated by chestnut, hickory, and oak. The late Holocene forest differed from the modern forest primarily in age structure, comprised of tree communities with variable ages, of various stages of regeneration, and containing internal gaps caused by falls of senescent trees. These gaps supported a variety of edible resources that thrived in the open, including berries such as blackberries, raspberries, and a variety of tubers. These would have been available subsistence resources (Miller *et al.* 2004; Miller *et al.* 2007).

The Sub-Atlantic Climatic Episode (3000 BP. - 1750 BP.)

The Sub-Atlantic is recognized by some in North America as a period that included many small climatic shifts. Overall, it was one characterized by fairly warm temperatures and slowly rising sea levels (Goodbred *et al.* 1998). By 3000 BP. the mean climate abruptly transitioned to a warm and moist condition. The Sub-Atlantic and Neo-Atlantic/Medieval Warm Period (1100 BP. to 750 BP.) climatic episodes mark a sequential transition from warm and moist, to cool and moist, and then to warm and moist conditions. In contrast to the previous climatic episode, this transition provided several hundred years of flood plain stability leading to long-term A-horizon development (Figures 1, 4 and 5). Clearly, the effects of meridional circulation and the associated cyclonic and convectional storms were much reduced during these climatic periods. A subsequent return to a record of more abundant hemlock pollen, from low levels during the warm-dry Sub-Boreal indicates lowered rates of evapotranspiration and more effective precipitation.

The climate and forests inferred from the record of the Sub-Atlantic chronozone (lower Pollen Zone C-3a) were very similar to those present at the time of European contact. That Sub-Atlantic forest is characterized as an association of oak and chestnut, with local variation

controlled by slope and altitude. Ridge tops were typically dominated by scarlet, black and chestnut oaks; the upper slopes by red oak; the lower slopes by white oak, red oak, hickory, and hemlock; the valley floors and river terraces supported white oak, sugar maple, hemlock, white pine, and pitch pine (Braun, 1950). Chestnut was a dominant species, although it has since been eliminated by the chestnut blight of the early twentieth century. The forest contained pockets of other climax associations that reflected the region's mountainous character and altitudinal variation (Braun, 1950). Of these, the mixed mesophytic cove forests were particularly well developed.

Scandic (1750 BP. - 1250 BP.)

The forest during the Scandic period (middle Pollen Zone C-3a) appears to have been similar to that of the preceding Sub-Atlantic phase. Cooler and moister climatic phases, such as the Scandic, as well as the subsequent Pacific (700- 500 BP.) and Neo-Boreal (500 - 50 BP.) phases, effectively arrested A-horizon development while the increased frequency of tropical storms (hurricanes) led to increased runoff, floodplain instability, and the formation of Bw and BC horizons on floodplains and low terraces (Figure 1).

These cooler and moister climatic phases favored rapid vertical accretion and very poorly developed B-horizons and coarse-grained C-horizons (autogenic units) on low terraces within the region. As, noted this was likely the result of an increase in the frequency of tropical storms (hurricanes) and/or more common cool season flood events associated with increased meridional flow conditions. Precipitation from intensive low pressure cells similar to the 1955 and 1972 tropical cyclone induced floods could have been rather common during these climatic phases, as the atmosphere approached modern flow characteristics.

An interesting observation from pollen studies within the region is the high percentages of grass, vetch, and chenopodium (both pollen and seed) occurring in alluvial deposits less than 2000 years old. Grass, vetch and chenopodium are often associated with various types of disturbance events. Their occurrence here may either indicate a cultural alteration of the natural floodplain or be the result of natural deforestation followed the invasion of these colonizing taxa. Scully and Arnold (1981), Alexander and Prior (1981), Gooding (1971) and Nelson (1966) have suggested that Amerinds may have been an important geomorphic agent, due to burning, clearing, and cultivating forest lands before European cultivation. The reported high percentages of *Ambrosia* and *Rumex* pollen in the C3a zone may be attributable to aboriginal clearing. In addition, the presence of ubiquitous charcoal flecks in the late Holocene alluvium on the Port Huron and Valley Heads terraces may reflect increased aboriginal utilization and occupation of the valley bottoms during this time. Interestingly, recent re-analysis of the molluscan fauna from Meadowcroft Rockshelter (Campbell *et al.* 2008) reveals the same anthropogenic clearance "signature" at the same time interval.

Neo-Atlantic (1100 BP. - 750 BP.)

The Neo-Atlantic is also referred to as the Medieval Climate Optimum or the Medieval Climatic anomaly. It was a warm period in North America and Europe. In fact, excluding present day temperature levels, this period was the warmest of the last 2000 years. Temperatures were only 0.1 - 0.2 degrees Centigrade below those of today.

The forest during the Neo-Atlantic period (upper Pollen done C-3a) was similar to that of the preceding Sub-Atlantic and Scandic phases. As during the Sub-Atlantic, an increase in floodplain stability during the warm moist Neo-Atlantic period resulted in the formation of an often persistent cumulic A-horizon (Owasco paleosol) which is typically capped by a variably thick package of late Holocene sediments emplaced at the onset of the following Little Ice Age (Vento and Fitzgibbons 1986, Figure 1). Interestingly, during the late Holocene there is clear evidence for increasing local disturbance of vegetation, probably in response to increased human land use (e.g., horticultural and agricultural activities). At the Gallipolis site along the Ohio River in eastern Ohio, the pollen record shows increasing local disturbance of vegetation beginning about 4850 BP. (Fredlund, 1989). Supporting data from the study of pollen and wood charcoal from Cliff Palace Pond in Jackson County, Kentucky, indicates a forest dominated, around 1250 BP., by fire-tolerant taxa such as oak and chestnut (Delcourt *et al.* 1998).

Little Ice Age (Neoglacial) 750 BP. - 150 BP.

Definition of the Little Ice Age (LIA) has been, and remains, controversial but for the purposes of this chapter the LIA began at approximately 750 BP with the end of the Neo-Atlantic (Medieval Warm Period) and ended at roughly 150 BP. At its height, growing seasons in the northern regions of North America and Europe were shortened by as much as 20 percent, leading to frequent crop failures and forcing both human migration and increased hunting/gathering activities in affected regions. Recently dated records of ice-cap growth from Arctic Canada suggests that a succession of strong volcanic eruptions forced an abrupt onset of the Little Ice Age between A.D. 1275 and 1300 (Miller et al. (2012).

The term Little Ice Age was originally coined by F. Matthes in 1939 to describe a series of mountain glacier advances and retreats, analogous to, though considerably more moderate than, the Pleistocene glacial fluctuations (Mann 2002). This relatively prolonged period has now become known as the Neoglacial period. The term Little Ice Age is, instead, reserved for the most intensive recent period of mountain glacier expansion and is conventionally defined as the 16th–mid 19th century period during which European climate was most strongly impacted (Mann 2002). The coldest historically recorded portion of the LIA was the Mauder Minimum, a period between A.D. 1645 and A.D. 1715, when the number of observed sunspots decreased, indicating a reduced level of solar activity.

During this cooling period, the tilt of the earth's axis also changed. Such changes may profoundly affect ocean circulation, which, in turn, affects climate. Still other scientists have suggested that volcanic eruptions—such as one in the southern Philippines in A.D. 1642 may have had an impact on the cooling, causing chemical reactions in the atmosphere that blocked or redirected sunlight (Mann 2002). During the Maunder Minimum mean temperatures were 1.2 to 1.4 degrees Centigrade cooler than those of the Neo-Atlantic (Medieval Warm Period). Mann (2002) appropriately states that the Little Ice Age should be considered a time of modest cooling of the Northern Hemisphere and that the LIA may have been more significant in causing increased variability of the climate, rather than directional change in the average climate itself. The most dramatic climate extremes were less associated with prolonged multiyear periods of cold than with year to year temperature changes, or even particularly prominent individual cold

spells, and these events were often quite specific to particular seasons (Grove 1988; Bradley and Jones 1993; Jones *et al*. 1998; Mann *et al*. 1998; 1999)

The interpretation of the climatic effects recorded in the latter part of the LIA record is confounded by the fact that European settlement of the northeastern United States occurred during this interval. Starting in the 18th century much of the climatic record has been overprinted by this dominance of historic human land use and by A.D. 1830, more than 80% of central New England had been converted to either open pasture or tilled fields. Interestingly by A.D. 1850, much of this area had been over-exploited agriculturally and subsequently left open to natural reforestation, as the focus of agricultural activity shifted westward, and much of the human population shifted to urban areas. Currently, 65% to 90% of central New England is reforested, but whereas vegetational patterns prior to settlement were dominated by natural physiography, climate, and disturbance, the post-settlement forest recovery does not mimic that of pre-settlement New England (Francis and Foster, 2000).

There are many hypotheses pointing to a change in ocean circulation as causation for the LIA and most of these centered on shifts in the oceanic conveyor in the North Atlantic Ocean (OLIVER, 1992). The (NAO) conveyor is responsible for large-scale heat transport and storage in the deep ocean. Other purported causal mechanisms were large volcanic events during the early part of the 19th century (such as the Tambora Eruption of 1815) that inhibited solar radiation by sulfate aerosols and caused extensive cooling in North American as well as cycles of changes in sunspot activity as proposed for the Mauder Minimum.

With regard to influence on sites in alluvial settings, the LIA would have caused higher rates of effective precipitation, greater amounts of spring snow melt, decreased annual amounts of evapotranspiration, all of which would have resulted in higher rates of sediment input to streams and higher stream discharges leading to more frequent flooding events. The effects of the LIA would have been more pronounced on sites situated on low aggrading flood plains, as a result of flood scouring and active lateral channel migration. On larger drainage lines (i.e., Allegheny, Delaware, Ohio and Susquehanna Rivers) the increased frequency of overbank deposition is recorded by the burial of the Owasso paleosol and a coarsening upward sediment suite emplaced by frequent high magnitude flood events.

Modern (150 BP. - present)

The forest type associated with the Little Ice Age and Modern periods (Pollen Zone C-3b) was similar to that of the preceding Sub-Atlantic through Neo-Atlantic stages but with an increase in spruce and pine. Nearly all the original forest cover in Pennsylvania was removed by the end of the nineteenth century, as a result of urbanization, lumbering, mining and agricultural activities. The forests of today are exclusively secondary communities which bear little resemblance to the original forest association (Casselberry and Paull 1967; Gifford and Whitebread 1951). As noted earlier, the effects of historic deforestation allowed for higher sediment yields to streams, higher discharges and associated more frequent flood events of greater magnitude. In conjunction with large cyclonic events (Hurricane Agnes 1972) many flood plains and low terraces exhibited extensive flood scouring and subsequent impact to surficial or near surface prehistoric archaeological resources.

Current Stratigraphic Practices in Geoarchaeology

For the most part, the current practices of archaeological stratigraphy (Stein, 1980) and pedology in archaeology (Holliday 1990) ignore the use of soils as tools in the construction of a chronostratigraphic framework and illustrate the general lack of understanding and appreciation of the advantages of genetic stratigraphy in archaeological research.

Previous attempts in the Middle Atlantic Region to correlate depositional phenomena among drainage basins often linked them with climate. The landmark study of Carbone (1976) combined the results of palynological, faunal, and depositional studies into a comprehensive view of paleoenvironments for the region, but stopped short of identifying chronostratigraphic units. Custer (1978) applied a similar approach on a site-specific basis, comparing archaeological localities occurring in the region's Valley and Ridge province. Most attention has been accorded studies of aeolian soils and archaeological deposits of the region's Coastal Plain (Curry 1980; Curry and Custer 1982; Custer and Watson 1987; Stewart 1983, 1986, 1991). In non-floodplain settings, thick aeolian deposits burying archaeological sites have been viewed as a region-wide fingerprint of a mid, post-glacial warm/dry climate. Tentative connections between buried A-horizons and region-wide environmental conditions have been suggested (e.g. Stewart 1991), but never formalized into a comprehensive framework.

These studies have been criticized from a number of perspectives (e.g., Cavallo and Joyce 1985; Joyce 1988), including the restricted nature of the database and the assumption that sedimentary sequences are the result of such a myriad array of local variables that any linkage with regional environmental/climatic trends must be fortuitous. Over the last 10 years there has been a heightened awareness of the application of genetic stratigraphy at archaeological sites. Archaeologists and geoarchaeologists (Creemens *et al* 1998; Schuldenrein and Vento 2011; Vento *et al.* 2008; Schuldenrein *et al.* 2003; Coppock, *et al.* 2011; Fritz, 2012; Stinchcomb *et al.* 2012; Stinchcomb *et al* 2013) now working in the region have been impressed by recurrent patterning in sedimentary sequences and have sought some means of integrating these data with models of changing climate and vegetation. The concept of genetic stratigraphy now provides a coherent means of evaluating these patterns and distinguishing between local and regional variation in sedimentary records.

References

Adovasio, J.M, Carlisle, R.C., Cushman, K.A., and others, 1985, Paleoenvironmental reconstruction at the Meadowcroft, Rockshelter, Washington County, Pennsylvania, *in* Mead, J.I. and Meltzer, D.J., eds., Environments and Extinctions: Man in the Late Glacial North America: Center for the Study of Man, Orono, University of Maine, p. 73-110.

Alexander, C. S., and Prior, J. C., 1971, Holocene Sedimentation Rates in Overbank Deposits in the Black Bottom of the Lower Ohio River, Southern Illinois: American Journal of Science, v. 270, p. 361-372.

Alley, R.B., 1998, Icing the North Atlantic: Nature, v. 392, p. 335-336.

Alley, R.B., and Ágústsdóttir, A.M., 2005, The 8K Event; Cause and Consequences of a Major Holocene Abrupt Climate Change: Quaternary Science Reviews, v. 24, p. 1123-1149.

Alley, R.B., Mayewski, P.A., Sowers, and others, 1997, Holocene Climatic Instability: A Prominent, Widespread Event 8200 Yr Ago: Geology, v. 25, p. 483-486.

Atkinson, T.C., Briffa, K.R., and Coope, G.R., 1987, Seasonal temperatures in Britain during the past 22,000 years reconstructed using beetle remains: Nature, v. 325, p. 587-592.

Baldini, J.U.L, McDermott, F., and Fairchild, I.J., 2002, Structures of the 8200-year Cold Event Revealed by a Speleothem Trace Element Record, Science, v. 296, p. 2203-2206.

Barber, D.C., Andrews, J.T., Bilodeau, G., and others, 1999, Forcing of the Cold Event of 8200 Years Ago by Catastrophic Drainage of Laurentide Lakes: Nature, v. 400, p. 344-348.

Bard, E., 2002, Abrupt Climate Changes over Millennial Time Scales: Climate Shock: Physics Today, v. 55, p. 32-38.

Bard, E., 2003, North-Atlantic Sea Surface Temperature Reconstruction: Boulder, Co., IGBP PAGES/World Data Center for Paleoclimatology Data Contribution Series No. 2003-026.

Bartlein, P.J., Webb, T., and Fleri, E.C., 1984, Holocene Climatic Change in the Northern Midwest: Pollen-Derived Estimates: Quaternary Research, v. 22, p. 361-374.
Beckerman, Ira B., 1986, Prehistoric Settlement and Subsistence in Piedmont, North Carolina: University Park, Pennsylvania State University, Ph.D. Dissertation.
Benedict, J.B., 1976, Frost Creep and Gelifluction Features: A review: Quaternary Research, v. 6, p. 55-76.
Benson, L., Lund, S., Negrini, R., and others, 2003, Response of North American Great Basin Lakes to Dangaard-Oeschger Oscillations: Quaternary Science Reviews, v. 22, p. 2239-2251.
Berger, A.L., 1978, Long-Term Variations of Caloric Insolation Resulting from the Earth's Orbital Elements: Quaternary Research, v. 9, p. 139-167.
Berger, W.H. and von Rad, U., 2002, Decadal to Millennial Cyclicity in Varves and Turbidites from the Arabian Sea: Hypothesis of Tidal Origin: Global and Planetary Change, v. 34, p. 313-325.
Bernabo, J.C. and Webb, T., 1977, Changing Patterns in Holocene Pollen Record of Northeastern North America: A Mapped Survey: Quaternary Research, v. 8, p. 64-96.
Bhiry, N. and Filion, L., 1996, Mid-Holocene Hemlock Decline in Eastern North America Linked with Phytophaeous Insect Activity: Quaternary Research, v. 45, p. 312-320.
Bianchi, G.G. and McCave, I.N., 1999, Holocene Periodicity in North Atlantic Climate and Deep-ocean Flow South of Iceland: Nature, v. 397, p. 221-244.
Björck, S., Muscheler, R., Kromer, B., and others, 2001, High-resolution Analyses of an Early Holocene Climate Event May Imply Decreased Solar Forcing as an Important Climate Trigger: Geology, v. 29, p. 1107-1110.
Blytt, A., 1876, Essay on the Immigration of the Norwegian Flora during Alternating Rainy and Dry Periods: Cammermeyer, Kristiania.
Bond, G., 2005, Are Dansgaard-Oeschger Cycles and Multicentennial Cycles of the Holocene and the Last Glacier Interconnected?: Geophysical Research Abstracts, v. 7, p. 06038.
Bond, G., Komer, B., Beer, J., and others, 2001, Persistent Solar Influence on North Atlantic Climate during the Holocene: Science v. 294, p. 2130-2136.
Bond, G., Showers, W., Cheseby, M., and others, 1997, A pervasive Millennial–scale Cycle in North Atlantic Holocene and Glacial Climates: Science, v. 278, p. 1257–1266.
Bradley, R. and Jones, P., 1993, Little Ice Age Summer Temperature Variations: Their nature and Relevance to Recent Global Warming Trends: Holocene, v. 3, no. 4, p. 367-376.
Bradstreet, T.E. and Davis, R.B., 1975, Mid-Postglacial Environments with Emphasis on Maine: Arctic Anthropology, v. 12, no. 2, p. 7-22.
Braun, E.L., 1950, Deciduous Forests of Eastern North America: New York, Hafner, 596 p.
Broecker, W.S., 2003, Does the Trigger for Abrupt Climate Change Reside in the Ocean or in the Atmosphere?: Science, v. 300, p. 1519-1522.
Broecker, W.S., 2006, Was the Younger Dryas Triggered by a Flood?: Science, v. 312, p. 1146-1148.
Brown, R. D., 2000, Northern Hemisphere Snow Cover Variability and Change, 1915–1997: Journal of Climate, v. 13, p. 2339–2355.
Burns, S.J., Fleitmann, D., Matter, A., Kramers, J., and Al-Subbary, A., 2003, Indian Ocean Climate and an Absolute Chronology over Dansgaard/Oeschger Events 9 to 13: Science, v. 301, p. 1365.
Busch, R.M., and West, R.R., 1987, Hierarchical Genetic Stratigraphy: A Framework for Paleoceanography: Paleoceanography, v. 2, p. 141-164.
Campbell, J.M., Gallup, K.M., Vento, F.J., and Adovasio, J.M., 2008, Reinterpretation of the Molluscan Fauna of Meadowcroft Rockshelter (36WH297) in Relation to Holocene Millennial-scale Climate Variation: Paper presented at the 73rd annual meeting of the Society for American Archaeology.
Carr, K.W., 1998, The Early Archaic Period in Pennsylvania: Pennsylvania Archaeologist, v. 68, no. 2, p. 42-69.
Carbone, V.A., 1976, Environment and Prehistory in the Shenandoah Valley: Washington D.C., The Catholic University of America, PhD. dissertation, University Microfilms, Ann Arbor.
Carson, M.A. and Kikby, M.J., 1972, Hillslope Form and Process: London, Cambridge University Press, 476 p.
Cassellberry, S.E., and Paull, G., 1967, The Ecology of the Sheep Rock Shelter Site, *in* Michels, J. and Smith III, I.F., eds., Archaeological investigations of the Sheep Rock Shelter Site: Occasional Papers in Anthropology Nos. 1-2. Department of Anthropology, The Pennsylvania State University, University Park.
Cavallo, J.A. and Joyce, A.A., 1985, Explanatory Models of Late Archaic Culture Change in the Middle Atlantic Region: An Evaluation: Paper presented at the 1985 Middle Atlantic Archaeological Conference, Rehoboth Beach, DE.
Chapman, M.R. and Shackleton, N.J., 2000, Evidence of 550-year and 1000-year Cyclicities in North Atlantic Circulation Patterns during the Holocene: The Holocene, v. 10, p. 287-291.
Ciolkosz, E.J., Cronce, R.C., and Sevon, W.D., 1986, Periglacial features in Pennsylvania: Penn State Agronomy Series, no. 92, p. 15.
Clark, M.J., (Ed.), 1988, Advances in Periglacial Geomorphology, Wiley, New York, pp. 481.
Clark, P.U., Webb, R.S., and Keigwin, L.D., 1999, Mechanisms of Global Climate Change at Millennial Time Scales: American Geophysical Union Geophysical Monographs 112, Washington D.C.
Cleland, C.E., 1966, The Prehistoric Animal Ecology and Ethnozoology of the Upper Great Lakes Region: Ann Arbor, University of Michigan.
Clement, A.C., Cane, M.A., and Seager, R., 2001, An Orbitally Driven Tropical Source for Abrupt Climate Change: Journal of Climate, v. 14, p. 2369-2375.
Coppock, G.F., 2009, Phase III Data Recovery Investigations: The Martin Site (36Hu187), SR 0453, Section 003, Improvements Project, Morris Township, Huntingdon County, Pennsylvania, Byways to the Past Technical Series, Volume 15, The Pennsylvania Department of Transportation and the Federal Highway Administration.
Coppock, G.F., Stiteler, J.M., and Vento, F.J., 2011 Assessing Intra-watershed Paleoenvironment and Landform Development: A Case Study from South-Central Pennsylvania: North American Archaeologist, v. 32, p. 193-247.
Cotter, J.F., 1983, The Minimum Age of the Woodfordian Deglaciation of Northeastern Pennsylvania and Northwestern New Jersey: Bethlehem, Pa., Lehigh University, Ph.D. dissertation, p. 151.

Cotter, J.F. and Crowl, G.H., 1984, The Paleolimnology of Rose Lake, Potter Co., Pennsylvania: A Comparison of Palynologic and Paleo-pigment Studies, *in* Romans, R.C., ed., Geobotany II, New York, Plenum, p. 91-122.

Courty, M.A. and Vallverdu, J., 2001, The Microstratigraphic Record of Abrupt Climate Changes in Cave Sediments of the Western Mediterranean: Geoarchaeology, v. 16, p. 467-499.

Cremeens, D., Hart, J.P., and Darmody, R. G., 1998, Complex Pedostratigraphy of a Terrace Fragipan at the Memorial Park site: Geoarchaeology, v. 13, no. 4, p. 339-360.

Cronin, T.M., Willard, D., Karlsen, A., and others, 2000, Climatic Variability in the Eastern United States over the Past Millennium from Chesapeake Bay Sediments: Geology, v. 28, p. 3-6.

Crowley, T.J. and North, G.R., 1991, Paleoclimatology: Oxford Monographs on Geology and Geophysics #18, New York, Oxford University Press, p. 349.

Curry, D.C., 1980, Burial of Late Archaic Coastal Plain Sites as a Result of Aeolian Deposition: Presented at 10th Annual Middle Atlantic Archaeological Conference, Dover, Delaware.

Curry, D.C. and Custer, J. F., 1982, Holocene Climatic Change in the Middle Atlantic Area: Preliminary Observations from Archaeological Sites: North American Archaeologist, v. 3, p. 275-285.

Custer, J.F., 1984, The paleoecology of the Late Archaic: Exchange and Adaptation: Pennsylvania Archaeologist, v. 54, no. 3-4, p. 32-48.

Custer, J.F., 1988, Late Archaic Cultural Dynamics in the Central Middle Atlantic Region: Journal of Middle Atlantic Archaeology, v. 4, p. 39-59.

Custer, J.F. and Watson, S., 1987, Making Cultural Paleoecology Work - An Example from Northern Delaware: Journal of Middle Atlantic Archaeology, v. 3, p. 81-84.

Davis, M.B., 1965, Phytogeography and palynology of Northeastern United States, *in* Wright, H.E. Jr., and Frey, D.G., eds., The Quaternary of the United States: A Review Volume for the VII Congress of the International Association of Quaternary Research, Princeton, NY, Princeton University Press, p. 377-401.

Davis, M.B., 1976, Pleistocene Biogeography of Temperate Deciduous Forests: Geoscience and Man, v. 18, p. 13-26.

Davis, M.B., 1983, Holocene Vegetation History of the Eastern United States, *in* Wright, H.E. Jr., ed., Late Quaternary Environments of the United States, Vol. 2, The Holocene, Minneapolis, MN, University of Minnesota Press, p. 166-181.

Davis, M.B., Sugita, S.S., Calcote, R.R., Ferrari, J.B., and Frelich, L.E., 1994, Historical Development of Alternate Communities in a Hemlock-hardwood Forest in Northern Michigan, USA, *in* May, R., Webb, N., and Edwards, P., eds., Large-Scale Ecology and Conservation Biology, Blackwell Science, Oxford p. 19-39.

Davis, M.B., Calcote, R.R., Sugita, S., and Takahara, H., 1998, Patchy Invasion and the Origin of a Hemlock-hardwoods Forest Mosaic: Ecology, v. 79, p. 2641-2659.

Davis, M.B., Sugita, S.S., Calcote, R.R., Ferrari, J.B., and Frelich, L.E., 1994, Historical Development of Alternate Communities in a Hemlock-hardwood Forest: in May, R., Webb, N., and Edwards, P., eds., Northern Michigan, USA. Large-Scale Ecology and Conservation Biology, Blackwell Science, Oxford, p. 19-39.

Davis, R.B., Bradstreet, T.E., Stuckenrath, R. Jr., and Borns, H.W. Jr., 1975, Vegetation and Associated Environments During the Past 14,000 Years Near Moulton Pond, Maine: Quaternary Research, v. 5, p. 435-465.

Dean, W.E., Forester, R.M., and Bradbury, J.P., 2002, Early Holocene Change in Atmospheric Circulation in the Northern Great Plains: An Upstream View of the 8.2 ka Cold Event: Quaternary Science Reviews, v. 21, p. 1762-1775.

Deevey, E.S., 1939, Studies on Connecticut Lake Sediments: 1 – a Postglacial Chronology for Southern New England: Quaternary Research, v. 14, p. 240-250.

Deevey, E.S. and Flint, R.F., 1957, Postglacial Hypsithermal Interval: Science, v. 125, p. 182-184.

Delano, H.L., Miller, N.G., and Potter, N., Jr., 2002, Plant Fossil Evidence for Late Pleistocene Tundra Conditions in South-Central Pennsylvania: Abstract for paper presented at the Annual Meeting of the Northeast Section of the Geological Society of America, Halifax, Nova Scotia. Geological Society of America, v. 34, no. 1, p. A-27.

Delcourt, Hazel R., 1979, Late-Quaternary Vegetation History of the Eastern Highland Rim and Adjacent Cumberland Plateau of Tennessee: Ecological Monographs, v. 49, p. 255-280.

Delcourt, P.A. and Delcourt, H.R., 1981, Vegetational Maps for Eastern North America: 40,000 YR BP to the Present, *in* Romans, R.C., ed., Geobotany II, New York, NY, Plenum Publishing, p. 123-165.

Delcourt, P.A., Delcourt, H.R., Ison, C.R., Sharp, W.E., and Gremillion, K., 1998, Prehistoric Human Use of Fire, the Easter Agricultural Complex, and Appalachian oak-Chestnut Forests: Paleoecology of Cliff Palace Pond, Kentucky: American Antiquity, v. 63, no. 2, p. 263-278.

Dent, R.J. and Kauffman, B.E., 1985, Aboriginal Subsistence and Site Ecology as Interpreted from Microfloral and Faunal Remains, *in* McNett, C.W., Jr., ed., Shawnee Minisink: A Stratified Paleoindian-Archaic Site in the Upper Delaware Valley of Pennsylvania, New York, NY, Academic Press, p. 55-79.

Denton, G.H. and Karlén, W., 1973, Holocene Climatic Variations – Their Patterns and Probable Cause: Quaternary Research, v. 3, p. 155-205.

Dincauze, D.F. and Mulholland, M.T., 1977, Early and Middle Archaic Site Distributions in Southern New England, *in* Newman, W.S. and Salwen, B., eds., Amerinds and Their Paleoenvironments in Northeastern North America,. Annals of the New York Academy of Sciences, Volume 288, New York, p. 439-456.

Ding, Z.L., Rutter, N.W., Liu, T.S., and others, 1998, Correlation of Dansgaard-Oeschger Cycles Between Greenland ice and Chinese loess: Paleoclimates, v. 4, p. 281-291.

Dwyer, T.R., Mullins, H.T. and Good, S.C., 1996, Paleoclimatic Implications of Holocene lake-level fluctuations, Owasco Lake, New York: Geology, v. 24, p. 519-522.

Eisenberg, L., 1978, Paleo-Indian Settlement Pattern in the Hudson and Delaware River Drainages, *in* Occasional Publications in Northeastern Anthropology, No. 4, Rindge, New Hampshire.

Fabio, G., Arseneault, D., Nicault, A., Perreault, L., and Begin, Y., 2014, Volcano-induced Regime Shifts in Millennial Tree-Ring Chronologies from Northeastern North America: Proceedings of the National Academy of Sciences, v. 111, no. 28, p. 10077-10082

Fairbanks, R.G., 1989, A 17,000-year Glacio-eustatic Sea Level Record: Influence of Glacial Melting Rates on Younger Dryas Event and Deep-ocean Circulation: Nature, v. 342, p. 637-642.

Fiedel, S.J., 1999, Older Than We Thought: Implications of Corrected Dates for Paleoindian: American Antiquity, v. 64p. 95-115.

Filion, L. and Quinty, F., 1993, Macrofossil and Tree-ring Evidence for a Long-term Forest Succession and Mid-Holocene Hemlock Decline: Quaternary Research, v. 40, no. 1, p. 89-97.

Finkel, R.C. and Nishiizumi, R., 1997, Beryllium 10 Concentrations in the Greenland Ice Sheet Project 2 Ice Core from 3-40 ka: Journal of Geophysical Research, v. 102, p. 26699-26706.

Fisher, T. G., Smith, D., and Andrews, J. T., 2002, Preboreal Oscillation Caused by a glacial Lake Agassiz Flood: Quaternary Science Review, v. 21, p. 873–878.

Foreman, S.L., Oglesby, R., Markgraf, V., and Stafford, T., 1995, Paleoclimatic Significance of Late Quaternary Eolian Deposition on the Piedmont and High Plains, Central United States: Global and Planetary Change, v. 11, p. 35-55.

Francis, Donna R. and David R. Foster, 2001, Response of Small New England Ponds to Historic Land Use. Holocene 11(3):301-312

Fredlund, G.G., 1989, Holocene Vegetational History of the Gallipollis Locks and Dam Project Area, Mason County, West Virginia: Cultural Resources Analysts, Inc. Contract Publication Series 89-01, Lexington, Kentucky.

French, H.M., 1976, The Periglacial Environment: London, Longman, 309pp.

Fritz, Michael, 2011, Late Quaternary Environmental Dynamics of the Western Canadian Arctic–Permafrost and Lake Sediment Archives at the Eastern Beringian Edge: Potsdam, University of Potsdam, PhD. Dissertation, p. 121.

Gagan, M.K., Hendy, E.J., Haberle, S.G., and Hantoro, W.S., 2004, Post-glacial Evolution of the Indo-Pacific Warm Pool and El-Niño-Southern Oscillation: Quaternary International, v. 118-119, p. 127-143.

Galloway, W.E., 1989, Genetic Stratigraphic Sequences in Basin Analysis I: Architecture and genesis of flooding-surface Bounded Depositional Units: AAPG Bulletin, v. 73, p. 125-142.

Gamble, D.W. and Meentemeyer, V.G., 1997, A Synoptic Climatology of Extreme Unseasonable Floods in the Southeastern United States, 1950-1990: Physical Geography, v. 18, p. 496-524.

Gardner, T.W., Ritter, J.B., Shuman, C.A., and others, 1991, A Periglacial Stratified Slope Deposit in the Valley and Ridge Province of Central Pennsylvania, USA: Sedimentology, Stratigraphy, and Geomorphic Evolution: Permafrost and Periglacial Processes, v. 2, p. 141-162.

Gifford, C.L., and Whitebread, R., 1951, Mammal Survey of South-Central Pennsylvania Final Report: Pittman-Robertson Project 38-R, Pennsylvania Game Commission, Harrisburg.

Goman M., Joyce, A., Mueller, R., and Paschyn, L., 2004, Multiproxy Paleoecological Reconstruction of Prehistoric Land-use History in the Western Region of the Lower Rio Verde Valley, Oaxaca, Mexico: The Holocene Online First 1-12.

Goman, M., and Leigh, D., 2004, Wet Early to Middle Holocene Conditions on the Upper Coastal Plain of North Carolina: Quaternary Research, v. 61, p. 256-264.

Goodbred, S.L., Hine, A.C., and Wright, E.E., 1998, Sea-level Change and Storm Surge Deposition in a Late Holocene Florida Salt Marsh: Journal of Sedimentary Research, v. 68, p. 240-252.

Gooding, A.M., 1971, Postglacial Alluvial History in the Upper Whitewater Basin, Southeastern Indiana, and Possible Regional Relationships: American Journal of Science, v. 271, p. 389-401.

Goodwin, P.W. and Anderson, E.J., 1985, Punctuated Aggradational Cycles: A General Hypothesis of Episodic Stratigraphic Accumulation: Journal of Geology, v. 93, p. 515-533.

Graetzer, M.A., 1986, Settlement Patterns and Paleoclimatic Modeling: A Preliminary Study of Data from the Bald Eagle Watershed of Central Pennsylvania: University Park, Pennsylvania State University, Master's thesis.

Grafenstein, U. von, Erlenkeuser, H., Brauer, A., Jouzel, J., and Johnsen, J.A., 1999, A Mid-European Decadal Isotope-climate Record from 15,000 to 5000 year B.P.: Science, v. 284, p. 1654-1657.

Graham, R.W., 1979, Paleoclimates and Late Pleistocene Faunal Provinces in North America, *in* Humphrey, R.L., and Stanford, D., eds., Pre-Llano Cultures of the Americas: Paradoxes and Possibilities, The Anthropological Society of Washington, Washington, D.C, p. 49-69.

Grimm, E.C., and Jacobson, G.L., Jr., 1992, Fossil-pollen Evidence for Abrupt Climate Changes during the Past 18,000 Years in Eastern North America: Climate Dynamics, v. 6, p. 179-184.

Grissinger, E.H., Little, W.C., and Murphey, J.B., 1981, Erodibility of Stream Bank Materials of Low Cohesion: Transactions of the American Society of Agricultural Engineers, v. 24, p. 624-630.

Grissinger, E.H., Murphy, J.B., and Little, W.C., 1981, Late-Quaternary Valley-fill Deposits in North-central Mississippi: Unpublished manuscript, U.S. Department of Agriculture, Agricultural Research Service, Oxford, Mississippi.

Grootes, P.M. and Stuiver, M., 1997, Oxygen 18/16 Variability in Greenland Snow and Ice with 10-3-to 105-year Time Resolution: Journal of Geophysical Research, v. 102, p. 26,445-26,470.

Grove, Jean, 1988, The Little Ice Age, Methuen, The University of Michigan, p. 498.

Guilday, J.E., 1967, The Climatic Significance of the Hosterman's Pit Local Fauna, Centre County, Pennsylvania: American Antiquity, v. 32, p. 231-232.

Guiday, J.E., Martin, P.S., and McCrady, A.D., 1964, New Paris No. 4: A Pleistocene Cave Deposit in Bedford County, Pennsylvania: Bulletin of the National Speleological Society, v. 26, p. 121-194.

Guiday, J.E. and Parmalee, P.W., 1965, Animal Remains from the Sheep Rock Shelter (36Hu1), Huntingdon County, Pennsylvania: Pennsylvania Archaeologist, v. 35, p. 34-49.

Guilday, J.E., Parmalee, P.W., and Hamilton, H.W., 1977, The Clark's Cave Bone Deposit and the Late Pleistocene of the Central Appalachian Mountains of Virginia: Bulletin of Carnegie Museum of Natural History, v. 2, p. 1-87.

Gupta, A.K., D.M. Anderson, and J.T. Overpeck, 2003, Abrupt Climate Changes in the Asian Southwest Monsoon During the Holocene and their Links to the North Atlantic Ocean. Nature 421:354-357.

Haas, J.N. and McAndrews, J.H., 2000, The Summer Drought Related Hemlock (Tsuga Canadensis) Decline in Eastern North America 5,700 to 5,100 years ago, *in* McManus, K.A., Shields, K.S., and Souto, D.R., eds., Proceedings: Symposium on Sustainable Management of Hemlock Ecosystems in Eastern North America. General Technical Report NE-267, U.S. Department of Agriculture, Forest Service, Northeastern Forest Experiment Station 81-88, Newton Square, Pennsylvania.

Harrison, S.P., Kutzbach, J.E., Liu, Z., and others, 2003, Mid-Holocene climates of the Americas: a dynamical response to changed seasonality: Climate Dynamics, v. 20, p. 663-688.
Holliday, V.T., 1990, Pedology in Archaeology, *in* Lasca N.P., and Donahue, J.D., eds., Archaeological geology of North America: Boulder, Colorado. Geological Society of America Centennial Special Vol. 4, p. 525-540.
Hughen, K.A., Overpeck, J.T., Peterson, J.T., and Trumbore, S., 1996, Rapid Climate Changes in the Tropical Atlantic Region during the Last Deglaciation: Nature, v. 380, p. 51-54.
Jackson, S.T., Webb, R.S., Anderson, K.H., and others, 2000, Vegetation and Environment in Eastern North America during the Last Glacial Maximum: Quaternary Science Reviews, v. 19, p. 489-508.
Jackson, S.T. and Whitehead, D.R., 1991, Holocene Vegetation Patterns in the Adirondack Mountains: Ecology, v. 72, p. 641-653.
Johnson, S.J., Dahl-Jensen, D., Gundestrup, N., and others, 2001, Oxygen Isotopy and Paleotemperature Records from Six Greenland Ice-core Stations; Camp Century, Dye-3, GRIP, GISP2, Renland, and NorthGRIP: Journal of Quaternary Science, v. 16, no. 4, p. 299-307.
Jones P.D., Briffa, K.R., Barnett, T.P., and Tett, S.F.B., 1998, High-Resolution Paleoclimatic Records for the Last Millennium: Interpretation, Integration and Comparison with General Circulation Model Control-Run Temperatures: Holocene, v. 8, no. 4, p. 455-471.
Joyce, A., 1988, Early/Middle Holocene Environments in the Middle Atlantic Region: A Revised Reconstruction, *in* Nicholas, G.P. ed., Holocene Human Ecology in Northeastern North America, New York, NY, Plenum Press p. 185-214.
Karrow, P.F., Warner, B.G., and Fritz, P., 1984, Corry Bog Pennsylvania: A Case Study of Radiocarbon Dating of Marl: Quaternary Research, v. 21, p. 326-336.
Keeling, C.D. and Whorf, T.P., 2000, The 1,800-year Oceanic Tidal Cycle: A Possible Cause of Rapid Climate Change: Proceedings of the National Academy of Sciences, v. 97, p. 3814-3819.
King, J.E., 1980, Post-Pleistocene Vegetational Changes in the Midwestern United States, *in* Johnson, A.E., ed., Archaic Prehistory of the Prairie-Plains Border, Publications in Anthropology No. 12, University of Kansas, Lawrence, p. 3-11
Klippel, W. and Parmalee, P.W., 1982, Diachronic Variation in Insectivores from Cheek Bend Cave and Environmental Change in the Midsouth: Paleobiology, v. 8, p. 447-458.
Klitgaard-Kristensen, D., H., Sejrup, P., Haflidason, H., Johnsen, S., and Spurk, M., 1998, A Regional 8200 Cal. YR BP Cooling Event in Northwest Europe, Induced by Final Stages of the Laurentide Ice-sheet Deglaciation?: Journal of Quaternary Science, v. 13, p. 165-169.
Kneller, M. and Peteet, D., 1999, Late-Glacial to Early Holocene Climate Changes from a Central Appalachian Pollen and Macrofossil Record: Quaternary Research, v. 51, p. 133-147.
Knox, J.C., 1972, Valley Alluviation in Southwestern Wisconsin: Annals of the Association of American Geographers, v. 62, p. 401-410.
Knox, J.C., 1983, Responses of River Systems to Holocene Climates, *in* Wright, H.E., ed., Late Quaternary Environments of the United States, Volume 2, The Holocene, Minneapolis, University of Minnesota Press, p. 26-41.
Knox, J.C., 1993, Large Increases in Flood Magnitude in Response to Modest Changes in Climate: Nature, v. 361, p. 430-432.
Knox, J.C., 2000, Sensitivity of Modern and Holocene Floods to Climate Change: Quaternary Science Reviews, v. 19.1, no. 5, p. 439-457.
Knox, J.C., McDowell, P.F. , and Johnson, W.C., 1981, Holocene Fluvial Stratigraphy and Climate Change in the Driftless Areas, Wisconsin, *in* Mahaney, W.C., ed., Quaternary Paleoclimate, Geological Abstracts Limited, Norwich, England, p. 107-127.
Kodera, K., 2002, Solar Cycle Modulation of the North Atlantic Oscillation: Implication in the Spatial Structure of the NAO: Geophysical Research Letters, v. 29, p. 14557-14560.
Kovar, A.J., 1965, Pollen Analysis of the Bear Meadows Bog of Central Pennsylvania: Pennsylvania Academy of Science, v. 38, p. 16-24.
Kraus, M.J, 1987, Integration of Channel and Floodplain Suites; II, Vertical relations of alluvial paleosols: Journal of Sedimentary Research, v. 57, p. 602-612.
Kraus, M.J. and Bown, T.J., 1986, Paleosols and Time resolution in Alluvial Stratigraphy, *in* Wright, V.P., ed., Paleosols: Their Recognition and Significance, Blackwell, Oxford, p. 180-207.
Kunzendorf, H. and Larsen, B., 2002, A 200-300 Year Cyclicity in Sediment Deposition in the Gotland Basin, Baltic Sea, as deduced from geochemical evidence: Applied Geochemistry, v. 17, p. 29-38.
Kutzbach, J.E., 1983, Modeling of Holocene Climates, *in* Wright, H.E., Jr., ed., Late Quaternary Environments of the United States, Vol. 2, The Holocene, University of Minnesota Press. CCR #503, p. 271-277.
LaMoreaux, H.K., Brooks, G.A., and Knox, J.A., 2009, Late Pleistocene and Holocene Environments of the Southeastern United States from the Stratigraphy and Pollen Content of a Peat Deposit on the Georgia Coastal Plain: Paleogeography, Paleoclimatology, Paleoecology, v. 280, p. 300-312.
Langbein, W.B., and Schumm, S.A., 1958, Yield of Sediment in Relation to Mean Annual Precipitation: Transactions of the American Geophysical Union, v. 39, p. 1,076-1,084.
Leigh, D.S. and Feeney, T.P., 1995, Paleochannels Indicating Wet Climate and Lack of Response to Lower Sea Level, Southeast Georgia: Geology, v. 23, p. 687-690.
Leuschner, D.C. and Sirocko, F., 2000, The Low-latitude Monsoon Climate during Dansgaard-Oeschger Cycles and Heinrich Events: Quaternary Science Review, v. 19, p. 243-254.
Leyden, B.W., 1985, Late Quaternary Aridity and Holocene Moisture Fluctuations in the Lake Valencia Basin, Venezuela: Ecology, v. 66, p. 1279-1295.
Li, Y.X., Yu, Z.C., and Kodama, K.P., 2007, Sensitive Moisture Response to Holocene Millennial-scale Climate Variations in the Mid-Atlantic Region, USA: The Holocene, v. 17, no. 1, p. 3-8.
Liu, K.B. and Fearn, M., 2000, Reconstruction of Prehistoric Landfall Frequencies of Catastrophic Hurricanes in Northwestern Florida from Lake Sediment Records: Quaternary Research, v. 54, p. 238-245.
Lowell, T.V., Heusser, C.J., Anderson, B.G., and others, 1995, Interhemispheric Correlation of Late Pleistocene Glacial Events: Science, v. 269, p. 1541-1549.
Matthes, F., 1939, Report of Committee on Glaciers: Transactions, American Geophysical Union, v. 20, p. 518–535

Mann, M., 2002, Little Ice Age Volume 1, The Earth System: Physical and Chemical Dimensions in Global Environmental Change, *in* MacCracken, M. C. and Perry, J. S., eds., Encyclopedia of Global Environmental Change, Chichester, John Wiley & Sons, Ltd, p. 504-509.

Mann, M., Bradley, R.S., and Hughes, M.K., 1998, Global-Scale Temperature Patterns and Climate Forcing Over the Past Six Centuries: Nature, v. 392, p. 779-787

Mann, M., Bradley, R.S., and Hughes, M.K., 1999, Northern Hemisphere Temperatures during the Past Millennium: Inferences, Uncertainties, and Limitations: Geophysical Research Letters, v. 26, p. 759-762.

McIntyre, A. and Molfino, B., 1996, Forcing of Atlantic Equatorial and Subpolar Millennial Cycles by Precession: Science, v. 274, p. 1867-1870.

McMillan, R.B., and Klippel, W.E., 1981, Environmental Changes and Hunter-Gatherer Adaptation in the Southern Prairie Peninsula: Journal of Archaeological Science, v. 9, p. 215-245.

McWeeney, L. and Kellogg, D.C., 2001, Early and Middle Holocene Climate Changes and Settlement Patterns along the Eastern Coast of North America: Archaeology of Eastern North America, v. 29, p. 187-212.

Magny, M. and Bégeot, C., 2004, Hydrological Changes in the European Midlatitudes Associated with Freshwater Outbursts from Lake Agassiz during the Younger Dryas Event and the Early Holocene: Quaternary Research, v. 61, p. 181-192.

Marchitto, T.M, and K.Y. Wei, 1995, History of Laurentide Meltwater Flow to the Gulf of Mexico During the Last Deglaciation, as Revealed by Reworked Calcareous Nannofossils: Geology 23:779-782.

Martin, P.S., 1967, Prehistoric Overkill, *in* Martin, P.S. and Wright, H.E., Jr., eds., Pleistocene Extinctions: The Search for a Cause, New Haven: Yale University Press, p. 75-120.

Martin, R.A. and Webb, S.D., 1974, Late Pleistocene Mammals from the Devil's Den Fauna, Levy County, *in* Webb, S.D., ed., Pleistocene Mammals of Florida, University Presses of Florida, Gainesville, p. 114-145.

Mayewski, P.A., Rohling, E.E., Staer, J.C., Karlen, W, and others, 2004, Holocene Climate Variability: Quaternary Research, v. 62, p. 243-255.

Menking, K.M. and Anderson, R.Y., 2003, Contributions of La Niña and El Niño to Extreme Mid-Holocene Drought and Late Holocene Moisture in the American Southwest: Geology, v. 31, p. 937-940.

Miller, P.E., Marine, J.T., and Vento, F.J., 2007, Archaeological Investigations, Route 11/15 Improvements, (SR 0011, Section 008), Juniata and Perry Counties, Pennsylvania, ER No. 1989-0381-042, Volume II: 36Pe16. Prepared by KCI Technologies, Prepared for: Pennsylvania Department of Transportation, Engineering District 8-0.

Miller, P.E., Vento, F.J., Marine, J.T., and Pollack, E.A., 2004, Phase III Archaeological Data Recovery, Route 11/15 Improvements (SR 0011, Section 008), Juniata and Perry Counties, Pennsylvania. Volume III: 36Pe60. Submitted to the Pennsylvania Department of Transportation, Engineering District 8-0, Harrisburg.

Morril, C. and Jacobsen, R.M., 2005, How Widespread Were Climate Anomalies 8200 years ago?: Geophysical Research Letters, v. 32:19:10.1029/2005GL02536.

Moy, C.M., Seltzer, G.O., Rodbell, D.T., and Anderson, D.M., 2002, Variability of El Niño/Southern Oscillation Activity at Millennial Timescales during the Holocene Epoch: Nature, v. 420, p. 162-165.

Mullins, H.T., Patterson, W.P, Teece, M.T., and Burnett, A.W. 2011, Holocene Climate and Environmental Change in Central New York (USA): Journal of Paleolimnology, v. 45, p. 243–256.

Neff, U., Burns, S.J., Mangini, A., and others, 2001, Strong Coherence between Solar Variability and the Monsoon in Oman Between 9 and 6 kyr ago: Nature, v. 411, p. 290-293.

Nelson, C. A., 1966, Geologic Map of the Blanco Mountain Quadrangle, Inyo and Mono counties, California: U.S. Geol. Survey Map GQ-529.

Newby P, Shuman, B.N., Donnelly, J.P., and MacDonald, D., 2011, Repeated Century-scale Droughts over the Past 13,000 Yr Near the Hudson River Watershed, USA: Quaternary Research, v. 2011, p. 75:523-530.

Niering, W.A., 1953, The Past and Present Vegetation of High Point State Park, New Jersey: Ecological Monographs, p. 127-148.

Noren, A.J., Bierman, P.R., Steig, E.J., Lini, A., and Southon, J., 2002, Millennial-scale Storminess Variability in the Northeastern United States during the Holocene Epoch: Nature, v. 419, p. 821-824.

Oliver, J. E., 1992, The Past as a Guide to the Future, *in* Majumdar, S.K., ed., Global Climate Change: Implications, Challenges, and Mitigation Measures , Pennsylvania Academy of Science, p. 14-26.

Otvos, E.G., 2005, Holocene Aridity and Storm Phases, Gulf and Atlantic Coasts, USA: Quaternary Research 63:368-373.

Parkinson, R.W., 1989, Decelerating Holocene Sea-level Rise and its Influence on Southwest Florida Coastal Evolution: A Transgressive/Regressive Stratigraphy: Journal of Sedimentary Petrology, v. 59, p. 96-972.

Peltier, L.C., 1949, Pleistocene Terraces of the Susquehanna River, Pennsylvania: Pennsylvania Geological Survey, 4th Series, Bulletin G 23, Department of Internal Affairs, Harrisburg.

Peteet, D.M., Vogel, J.S, Nelson, D.E., and others 1990, Younger Dryas climatic reversal in Northeastern USA? AMS Ages for and Old Problem: Quaternary Research, v. 33, p. 219-230.

Pewe, T.L., 1983, The Periglacial Environment in North America during Wisconsin Time, *in* Wright, H.E., ed., Late Quaternary Environments of the United States, edited by H.E. Wright, Minneapolis, MN, University of Minnesota Press, p. 157-189.

Poag, C. W., and Schlee, J.S., 1984, Depositional Sequences and Stratigraphic Gaps on Submerged United States Atlantic Margin, *in* Schlee, J.S., ed., Interregional Unconformities and Hydrocarbon Accumulation, AAPG, v. 36, p. 165-182.

Prentice, I.C., Bartlein, P.J., and Webb, T. III, 1991, Vegetation and Climate Change in Eastern North America since the Last Glacial Maximum: Ecology, v. 72, p. 2038-2056.

Prufer, O.H. and Baby, R.S., 1963, Paleo-Indians of Ohio: Ohio Historical Society, Columbus, Oh.

Purdue, J.R. and Styles, B.W., 1986, Dynamics of Mammalian Distribution in the Holocene of Illinois: Illinois State Museum Report of Investigations, v. 41, p. 1-63.

Raber, P.A., Burns, J.A., Byra, P.L., and others, 2004, Phase III Archaeological Data Recovery Investigations, Sites 36Ju104 and 36Mi192, S.R. 0022, Sections A09 and A11, Lewistown Narrows, Juniata and Mifflin Counties, Pennsylvania, Byways to the Past Technical Series, Volume 9: The Pennsylvania Department of Transportation and the Federal Highway Administration.

Rahmstorf, S., 2003, Timing of Abrupt Climate Change: A Precise Clock: Geophysical Research Letters, v. 30, p. 1510-1513.

Redmond, B.G. and Tankersley, K.B., 2005, Evidence of Early Paleoindian Bone Modification and use at the Sheridan Cave Site (33WY252), Wyandot County, Ohio: American Antiquity, v. 70, p. 503-526.

Retallack, G.J., 1984, Completeness of the Rock and Fossil Record: Some Estimates using Fossil Soils: Paleobiology, v. 10, p. 59-78.

Rich, F.J., Vega, A.J., and Vento, F.J., 2011, Evolution of Late Pleistocene-Holocene Climate and Environments of St. Catherines Island and the Georgia Bight, *in* Bishop, G.A., Rollins, H.B., and Thomas, D.H., eds., Geoarchaeology of St. Catherines Island, American Museum of Natural History Anthropological Papers, no. 84, p. 67-77.

Rind, D. and Overpeck, J., 1993, Hypothesized Causes of Decade-to-century-scale Climate Variability: Climate Model Results: Quaternary Science Reviews, v. 12, p. 357-374.

Ritchie, W.A. and Funk, R., 1973, Aboriginal Settlement Patterns in the Northeast: Albany, NY, University of the State of New York, p. 378.

Ritchie, W.A., 1979, Some Ecological Factors in the Prehistory of Man: Bulletin of the New York State Archaeological Association, v. 75, p. 23-37.

Rohli, R.V. and Vega, A.J., 2014, Climatology, Third edition: Sudbury, Massachusetts, Jones and Barlett, p. 443.

Rohling, E.J. and Pailke, H., 2005, Centennial-scale Climate Cooling with a Sudden Cold Event around 8,200 Years Ago: Nature, v. 434, no. 7036, p. 975-979.

Rollins, H.B., West, R.R., and Busch, R.M., 1989, Field Recognition of Small-scale Genetic Surfaces, *in* Franseen, K. and Watney, W.L., eds., Sedimentary Modeling: Computer Simulation of Depositional Sequences: Subsurface Geology Series 12, Kansas Geological Survey, p. 43.

Ruddiman, W.F., 2001, Earth's climate, past and future: New York, NY, W.H. Freeman and Company, 465 p.

Schuldenrein, J., Vento, F.J., and Crowley, S.S., 2003, Interim Geomorphological Report for Archaeological site 36AL480, Area 3 South, Leetsdale Industrial Park, Leetsdale, Allegheny County, Pennsylvania. Geoarchaeology Research Associates and Clarion University. Submitted to U.S. Army Corps of Engineers, Pittsburgh District, Contract No. DACW 59-01-T-0028. Copies available from Geoarchaeology Research Associates, Yonkers, New York.

Schuldenrein, J. and Vento, F.J., 2011, Chapter 2, Environmental Context, Data Recovery at Site 36AL480, Leetsdale, Pennsylvania, Monongahela Locks and Dams Numbers 2, 3, and 4 Modernization Project. Pittsburgh, PA: United States Corps of Engineers, Pittsburgh District.

Schultz, H., Erlenkeuser, H., and von Rad, U., 1998, Correlation between Arabian Sea and Greenland Climate Oscillations of the Past 110,000 Years: Nature, v. 393, p. 54-57.

Schultz, M. and Paul, A., 2002, Holocene Climate Variability on Centennial-to-millennial Time Scales: 1. Climate records from the North-Atlantic realm, *in* Wefer, G., Berger, W.H., Behre, K.E., and Janson, E., eds., Climate Development and History of the North Atlantic Realm, Berlin, Heidelberg, Springer p. 41-54.

Scully, R.W. and Arnold, R.W., 1979, Soil-geomorphic Relationships in Postglacial Alluvium in New York: Soil Science Society of America Journal, v. 43, p. 1014-1019.

Scully, R.W. and Arnold, R.W., 1981, Holocene Alluvial Stratigraphy in the Upper Susquehanna River basin, New York: Quaternary Research, v. 15, p. 327-344.

Semken, H.A., 1974, Micromammal Distribution and Migration during the Holocene: American Quaternary Association Abstracts, v. 3, p. 25.

Semken, H.A., Jr., 1983, Holocene Mammalian Biogeography and Climatic Change in the Eastern and Central United States, *in* Wright, H.E., Jr., ed., Late-Quaternary Environments of the United States: Volume II: The Holocene, Minneapolis, University of Minnesota Press, p. 182-207.

Sernander, R., 1908, On the Evidence of Postglacial Changes of Climate Furnished by the Peat-mosses of Northern Europe: Geologiska Foreningens I Stockholms Forhandlingar, v. 30, p. 467-478.

Shuman B., Newby, P., Huang, Y., and Webb, T., III, 2004, Evidence for the Close Climatic Control of New England Vegetation History: Ecology, v. 85, no. 5, p. 1297-1310.

Shuman B., Henderson. A., Colman, S.M., and others, 2009, Holocene Lake-Level Trends in the Rocky Mountains, USA: Quaternary Science Reviews, v. 28, p. 1861-1879.

Sirocko, F., Garbe-Schönberg, D., McIntire, A., and others, 1996, Teleconnections between the Subtropical Monsoons and High-latitude Climates during the Last Deglaciation: Science, v. 272, p. 526-529.

Springer, N.M., Ying, K., Fu, Y., and others, 2009, Maize Inbreds Exhibit High Levels of Copy Number Variation (CNV) and Presence/absence Variation (PAV) in Genome Content: PLoS Genetics, 5.11: e1000734.

Stapor, F.W. Jr., Matthews, T.D., and Lindfors-Kearns, L.E., 1991, Barrier-island Progradation and Holocene Sea-level History in Southwest Florida: Journal of Coastal Research, v. 7, p. 815-838.

Stein, J.K., 1980, Geoarchaeology of the Green River shell mounds, Kentucky, Minneapolis, MN, University of Minnesota, PhD. Dissertation.

Stewart, M.R., 1983, Soils and the Prehistoric Archaeology of the Abbott Farm: North American Archaeologist, v. 4, p. 27-49.

Stewart, M.R., 1986, Inferences from intra-site lithic distributions: Journal of Middle Atlantic Archaeology, v. 2, p. 93-116.

Stinchcomb, G.E., Driese, S.G., Nordt, L.C., and Allen, P.M., 2012, A Mid to Late Holocene History of Floodplain and Terrace Reworking along the Middle Delaware River Valley, USA: Geomorphology, v. 169-170, p. 123-141.

Stinchcomb, G.E., Messner, T.C., Williamson, F.C., Driese, S.G., and Nordt, L.C., 2013, Climatic and Human Controls on Holocene Floodplain Vegetation Changes in Eastern Pennsylvania Based on the Isotopic Composition of Soil Organic Matter: Quaternary Research, v. 79, p. 377-390.

Stoltman, J.B. and Baerreis, D.A., 1983, The Evolution of Human Ecosystems in the Eastern United States, chap. 16 of Wright, H.E., Jr., ed., Late Quaternary Environments of the United States, Volume 2, The Holocene: Minneapolis, MN, University of Minnesota Press, p. 252-268.

Takahashi, T., Sutherland, S.C., Freely, R.A. and Cosca, C.E., 2003, Decadal Variation of the Surface Water PC02 in the Western and Central Equatorial Pacific: Science, v. 302, p. 852-856.

Taylor, K.C., Mayewski, P.A., Alley, R.B., Brook, E.J., and others, 1997, The Holocene/Younger Dryas Transition Recorded at Summit, Greenland: Science, 278, p. 825-827.

Teller, J.T., Leverington, D.W., and Mann, J.D., 2002, Freshwater Outbursts to the Oceans from Glacial Lake Agassiz and their Role in Climate Change During the Last Deglaciation: Quaternary Science Reviews, v. 21, p. 879-887.

Thompson, L.G., Mosley-Thompson, E., Davis, and others, 1995, Late Glacial Stage and Holocene Tropical Ice Core Records from Huascarán, Peru: Science, v. 269, p. 46-50.

Van Steijn, H., van Brederode, L.E., and Goedheer, L.E., 1984, Stratified Slope Deposits of the Greze Litee type in the Ardeche Region in the South of France: Geografiska Annaler 66A, p. 295-305.

Vega, A.J., 1998, Generalized Western North Atlantic Circulation and Southern United States Precipitation Variability: Journal of the Mississippi Academy of Sciences, v. 43, no. 4, p. 174-187.

Vento, F.J., and Fitzgibbons, P.T., 1987, Archeological and Geoarchaeological Investigations in Cowanesque River Valley: Open File Report submitted to the Baltimore District Corps of Engineers.

Vento, F.J. and Rollins, H.B., 1989, Genetic Stratigraphy, Climate Change and the Deep Burial of Archaeological Sites in the Susquehanna River drainage Basin: Grant report submitted to the Pennsylvania Bureau for Historic Preservation.

Vento, F.J., Rollins, H.B., Adovasio, J.M., and others, 2008, Development of a Late Pleistocene-Holocene genetic stratigraphic framework for the Mid-Atlantic region: Implications in archaeology. Paper presented at the 73rd annual meeting of the Society for American Archaeology, Vancouver, British Columbia (26-30 March 2008). *In* A Geoarchaeological and Paleoenvironmental Investigation of the Aughwick Creek Watershed (Watershed 12C), Alternative Mitigation, Sites 36Hu199 and 36Hu200, SR 0522, Section 05BN, Vento and G.F Coppick (2010), Appendix E. Report submitted to the Pennsylvania Department of Transportation, Engineering District 9-0. Heberling Associates, Inc., Alexandria, Pennsylvania. (BHP ER No. 1983-0424-061).

Vento, F.J., Rollins, H.B., Stewart, M., Raber, P., and Johnson, W., 1992, Genetic Stratigraphy, Climate Change, and Deep Burial of Archaeological Sites in the Susquehanna, Ohio, and Delaware River Basins: Report prepared for the Pennsylvania Historical and Museum Commission, Harrisburg.

Vento, F.J., Rollins, H.B., Johnson, W., and Raber, P., 1994, Genetic Stratigraphy, Climate Change and the Potential for the Burial of Archaeological Sites in Alluvial Contexts in the Delaware, Ohio and Susquehanna River drainage basins: Grant report submitted to the Pennsylvania Museum and Historical Commission.

Vento, F.J. and Stahlman, P., 2011, Development of a Late Pleistocene-Holocene Genetic Stratigraphic Framework for St. Catherine's Island: Archaeological Implications, in Bishop, G.A., Rolling, H.B., and Thomes, D.H., eds., Geoarchaeology of St. Catherines Island, Georgia, New York, NY, American Museum of Natural History, , p. 99-112.

Veski, S., Seppa, H., and Ojala, A.E.K., 2004, Cold Event at 8200 yr B.P. Recorded Annually in Laminated Lake Sediments in Eastern Europe: Geology (Boulder), v. 32, p. 681-684.

Viau, A.E., Gajewski, K., Fines, P., Atkinson, D.E., and Sawada, M.C., 2002, Widespread Evidence of 1500 yr Climate Variability in North America during the Past 14000 yr: Geology, v. 30, p. 455-458.

Walker, R.G., 1990, Facies Modeling and Sequence Stratigraphy: Perspective: Journal of Sedimentary Research, v. 60, p. 777-786.

Wall, R.D., Verney, R., Gould, R., and Luhman, H.E., 2003, Hunters to Horticulturalists: The Archaeology of the Mansfield Bridge Site, S.R. 6015, Section D52, Tioga County, Pennsylvania: Byways to the Past Technical Series, Volume 7. The Pennsylvania Department of Transportation and the Federal Highway Administration.

Wanner, H., Beer, J., Butikofer, J., and others, 2008, Mid- to late Holocene Climate Change: An Overview: Quaternary Science Reviews, v. 27, p. 1791-1828.

Wang, Y.J., Cheng, H., Edwards, R.L., and others, 2003, A High-resolution Absolute-dated Late Pleistocene Monsoon Record from Hulu Cave, China: Science, v. 294, p. 2345-2348.

Washburn, A.L., 1976, Periglacial Indicators of Permafrost: Quaternary Research, v. 6, p. 1-124.

Washburn, A.L., 1980, Geocryology, New York, Wiley, p. 406.

Watts, W.A., 1979, Late Quaternary Vegetation of the Central Appalachia and the New Jersey Coastal Plain: Ecological Monographs, v. 49, p. 427-469.

Watts, W.A., 1983, Vegetational History of the Eastern United States 25,000 to 10,000 years Ago, in Wright, H.E., Jr., ed., Late Quaternary Environments of the United States, Volume II: The Holocene, Minneapolis, MN, University of Minnesota Press, p. 294-310.

Webb, Thompson III and Bryson, R.A., 1972, Late- and Postglacial Climatic Change in the Northern Midwest, USA: Quantitative Estimates Derived from Fossil Pollen Spectra by Multivariate Statistical Analysis: Quaternary Research, v. 2, p. 70-115.

Wendland, W.M. and Bryson, R.A., 1974, Dating Climatic Episodes of the Holocene: Quaternary Research, v. 4, p. 9-24. Also IES Report #21, Institute for Environmental Studies, University of Wisconsin-Madison. CCR #327.

Wilkins, D.E. and Currey, D.R., 1997, Timing and Extent of Late Quaternary Paleolakes in the Trans-Pecos Closed Basin, West Texas, and South-central New Mexico: Quaternary Research, v. 47, p. 306-315.

Willard, D.A., Bernhardt, C.E., Korejwo, D.A., and Meyers, S.R., 2005, Impact of Millennial-scale Holocene Climate Variability on Eastern North American Terrestrial Ecosystems: Pollen-based Climatic Reconstruction: Global and Planetary Change, v. 47, p. 17-35.

Willard, D.A., Bernhardt, C.E., Brooks, G.R., and others, 2007, Deglacial Climate Variability in Central Florida, USA: Paleogeography, Paleoclimatology, Paleoecology, v. 251, p. 366-382.

Williams, J.W., Post, D.M., Cwynar, L.C., Lotter, A.F., and Levesque, A.J., 2002, Rapid and Widespread Vegetation Response to Past Climate Change in the North Atlantic region, Geology, v. 30, p. 971-974.

Wright, E.E., A.C. Hine, S.L. Goodbred, Jr., and S.D. Locker, 2005, The Effect of Sea-level and Climate Change on the Development of a Mixed Siliciclastic-carbonate, Deltaic Coastline: Suwannee River, Florida, USA. Journal of Sedimentary Research 75:621—635.

Wright, Herbert E., 1987, Synthesis: The Land South of the Ice Sheets, in Ruddiman, W.F. and Wright, H.E., Jr., eds., North American and Adjacent Oceans during the Last Deglaciation, The Geology of North America, v. K-3: Geological Society of America, Boulder, Colorado, p. 479-488.

Yu, S-B, Chen, H-Y., and Kuo, L-C., 1997, Velocity Field of GPS Stations in the Taiwan area: Tectonophysics. v. 274, no. 1, p. 41-59.

Yu, Z. and Eicher, U., 2001, Three Amphi-Atlantic Century-scale Cold Events during the Boelling-Allerod Warm Period: Geographie Physique et Quaternaire, v. 55, no. 2, p. 171-179.

DAM-BREACH HYDROLOGY OF THE JOHNSTOWN FLOOD OF 1889 CHALLENGING THE FINDINGS OF THE 1891 INVESTIGATION REPORT

NEIL M. COLEMAN AND ULDIS KAKTINS, UNIVERSITY OF PITTSBURGH AT JOHNSTOWN,
DEPARTMENT OF ENERGY & EARTH RESOURCES
STEPHANIE WOJNO, NORTHWEST MISSOURI STATE UNIVERSITY,
DEPARTMENT OF HUMANITIES AND SOCIAL SCIENCES

Unedited excerpts from the paper by Coleman, Kaktins, and Wojno (2016), including key figures and a table of data for the South Fork dam and watershed. The work illustrates how it is possible to reevaluate a historic disaster using modern data and analyses and careful review of historical records. The paper has been published "open access" (Creative Commons CC BY-NC-ND license) in the Elsevier journal ***Heliyon****, and therefore the full paper can be obtained without cost from the following website:* ***http://www.heliyon.com/article/e00120?via=sd%3D&***

Abstract

In 1891 a report was published by an ASCE committee to investigate the cause of the Johnstown flood of 1889. They concluded that changes made to the dam by the South Fork Fishing and Hunting Club did not cause the disaster because the embankment would have been overflowed and breached if the changes were not made. We dispute that conclusion based on hydraulic analyses of the dam as originally built, estimates of the time of concentration and time to peak for the South Fork drainage basin, and reported conditions at the dam and in the watershed.

We present a LiDAR-based volume of Lake Conemaugh at the time of dam failure (1.455×10^7 m^3) and hydrographs of flood discharge and lake stage decline. Our analytical approach incorporates the complex shape of this dam breach. More than 65 minutes would have been needed to drain most of the lake, not the 45 minutes cited by most sources. Peak flood discharges were likely in the range 7200 to 8970 $m^3 s^{-1}$. The original dam design, with a crest ~0.9 m higher and the added capacity of an auxiliary spillway and five discharge pipes, had a discharge capacity at overtopping more than *twice* that of the reconstructed dam. A properly rebuilt dam would not have overtopped and would likely have survived the runoff event, thereby saving thousands of lives.

We believe the ASCE report represented state-of-the-art for 1891. However, the report contains discrepancies and lapses in key observations, and relied on excessive reservoir inflow estimates. The confidence they expressed that dam failure was inevitable was inconsistent with information available to the committee. Hydrodynamic erosion was a likely culprit in the 1862 dam failure that seriously damaged the embankment. The Club's substandard repair of this earlier breach sowed the seeds of the dam's eventual destruction.

1. Introduction

On May 31, 1889, between 2:50 and 2:55 p.m., the South Fork dam breached, releasing the torrent now known as the Johnstown Flood (Kaktins et al., 2013). More than 2200 lives were lost and hundreds of the victims were never recovered. An outstanding historic account of the flood was written by McCullough (1968). In the aftermath, on June 5th, 1889 a committee led by the esteemed James B. Francis was appointed by the American Society of Civil Engineers (ASCE) to

visit the South Fork dam and investigate the cause of its failure. Francis was a hydraulic engineer best known for his work in flood control, turbine design, canal work, dam construction, and weir discharge calculations. He was a founding member of the ASCE and served as its president from November, 1880 to January, 1882. Other committee members included Max J. Becker, ASCE President in 1889, Alphonse Fteley, ASCE Vice President, and William E. Worthen, a past president of the ASCE. The committee visited the South Fork dam and downstream locations, reviewed the original design of the dam and subsequent modifications made during repairs, commissioned an elevation survey of the dam remnants, interviewed eyewitnesses, and performed various hydrologic calculations. In the end they determined the dam would have failed even if it had been maintained within the original design specifications. The committee concluded that:

> "The [South Fork] Hunting and Fishing Club [sic], in repairing the breach of 1862, took out the five sluices [drainage pipes] in the dam, lowered the embankment about 2 feet, and subsequently, partially obstructed the wasteway [spillway] by gratings, etc., to prevent the escape of fish. These changes materially diminished the security of the dam, by exposing the embankment to overflow, and consequent destruction, by floods of less magnitude than could have been borne with safety if the original construction of 1851-1853 had been adhered to; but in our opinion they cannot be deemed to be the cause of the late disaster, as we find that the embankment would have been overflowed and the breach formed if the changes had not been made. It occurred a little earlier in the day on account of the changes, but we think the result would have been equally disastrous, and possibly even more so…." (Francis et al., 1891, p. 456).

This claim that the dam, even as originally constructed, would have failed bears scientific scrutiny. We have analyzed the time of concentration (t_c) for the drainage basin and flood inflows to the lake on May 30-31. We examined whether two spillways (an original auxiliary spillway on the southwest abutment was missed by the committee) and the drainage pipes together, along with greater storage capacity behind a higher impoundment, could have prevented overtopping of the dam if it had not been lowered as much as 0.9 m when the South Fork Fishing and Hunting Club (SFFHC) rebuilt the dam. Our analysis is supported by river level observations that stream inflows to the lake had peaked hours before the dam breach.

Our research relies on many 19th century publications and more recent work that document historic data using English units rather than SI units. For most of our calculations we use the always preferable SI units, but where we highly depend on old data sources we report the original English units. We believe this approach will help confirm our appropriate use of the 19th century data and will aid future workers who may further analyze this dam breach disaster.

2. Background

2.1 Changes made to the South Fork dam

The South Fork dam and its impoundment, Lake Conemaugh (also known as the Western Reservoir), were located near the present-day small towns of St. Michael and Sidman, in Cambria County, Pennsylvania (Figure 1). The impoundment was originally built by the Commonwealth of Pennsylvania to supply water during low-flow periods by way of the Little Conemaugh River

to the downstream canal system in Johnstown. The design and construction history of the South Fork dam and reservoir are discussed by Francis et al. (1891) and reviewed by Kaktins et al. (2013). A view of the dam in cross section is shown in Figure 2. After the state of Pennsylvania sold the canal properties to the Pennsylvania Railroad in 1857, the dam and reservoir were of no direct use to the railroad and were left with minimal oversight. In July of 1862 the dam breached gradually, draining the lake in half a day. The history of this breach is further discussed in the file of online supplementary content. The Pennsylvania Railroad no longer needed the dam and in 1875 they sold the land parcel including the dam and former lake to John Reilly, a former congressman from Altoona. In 1879 Reilly came to an agreement with Benjamin Ruff for transferring the property, but the formal sale was directly to the SFFHC in March 1880 (McGough, 2007).

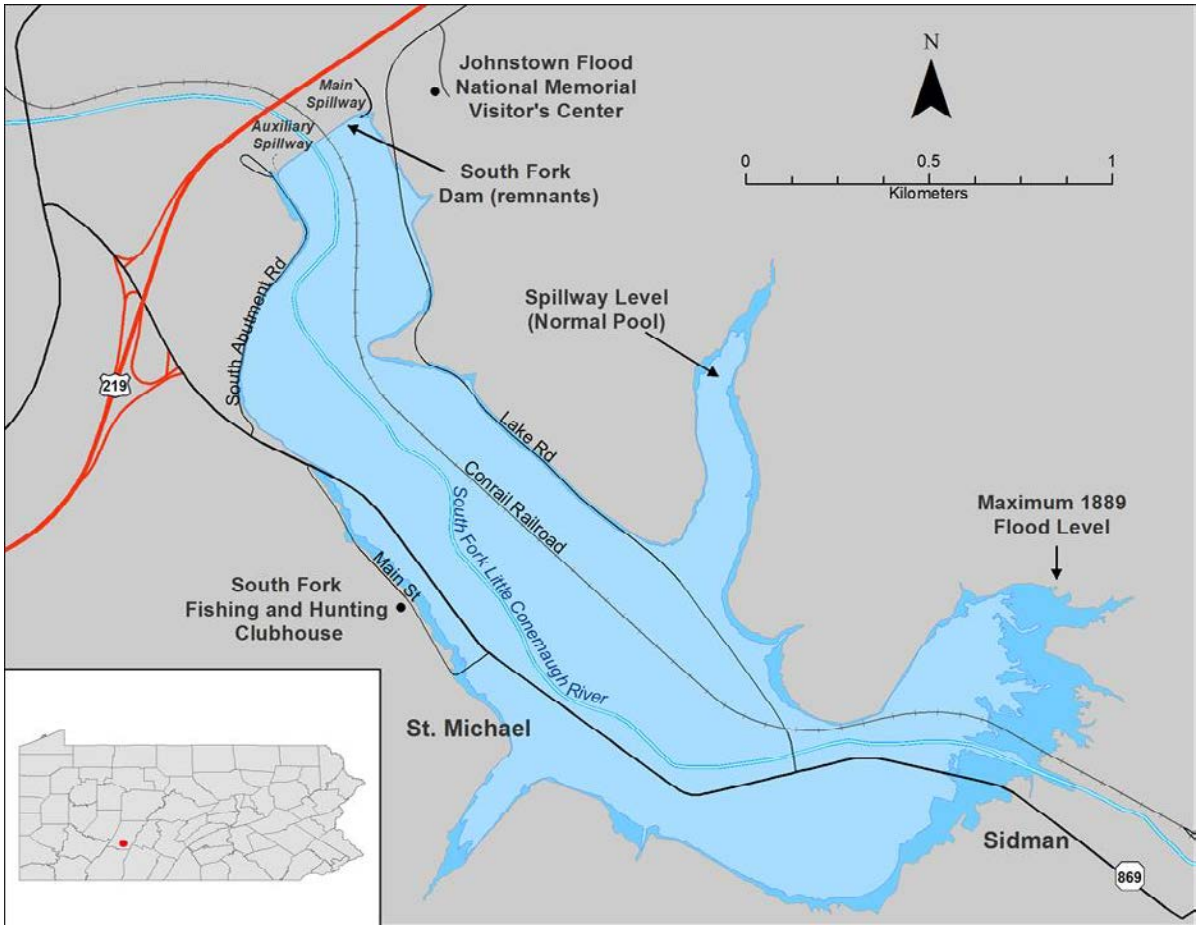

Figure 1. *Location map of the South Fork dam and Lake Conemaugh. The towns of St. Michael and Sidman and the Conrail branch line in the former lakebed did not exist at the time of the flood.*

Ruff intended to establish a resort. But the 1862 failure set the stage for the dam breach disaster in 1889 because when the dam was rebuilt by the SFFHC significant changes were made to the original design. The changes, such as lowering the dam crest, the omission of low-permeability puddled clay that had originally been emplaced on the upstream half of the embankment, and the use of mining wastes containing plastic clays, are discussed by Kaktins et al (2013). A very significant change was the removal of the sluice or discharge pipes at the base

of the dam and blocking the opening of the remaining stone culvert portion with hemlock planks. It is unclear when this occurred. McCullough (1968, p. 55) states that although Congressman Reilly sold the property at a slight loss, he made up for it by first removing the old cast iron discharge pipes and selling them for scrap. This statement differs from Francis et al. (1891, p. 445 and 456) who wrote that the SFFHC removed the pipes. They also documented that the dam repairs began in April 1880, several months before the property was conveyed to the SFFHC. In any case, the rebuilt dam now had no mechanism to control the lake water level except for discharge through the main spillway.

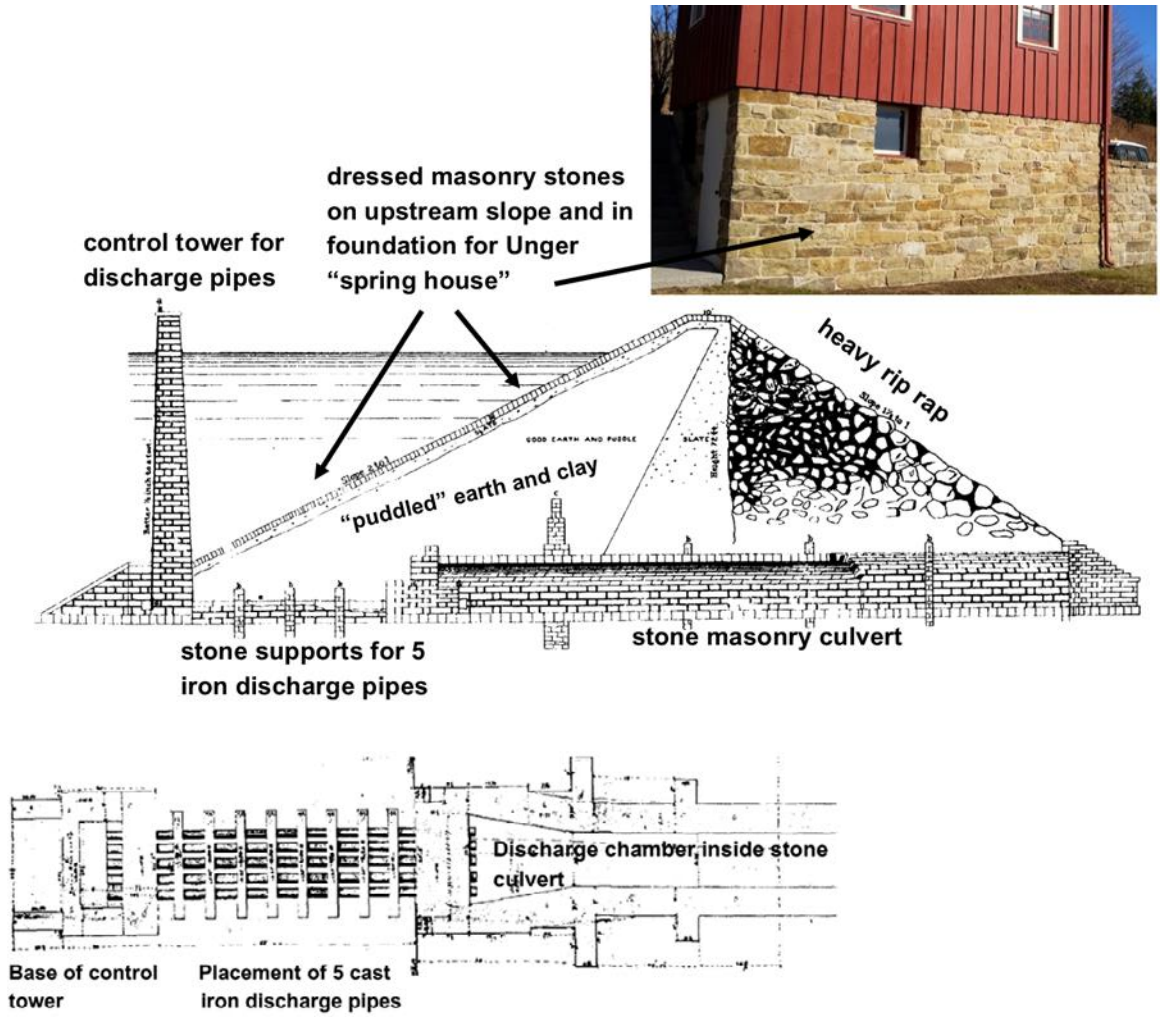

Figure 2. *View of the original design of the South Fork dam, showing heavy riprap on the downstream face, a broad "puddled" clay section on the upstream side, slope wall of dressed stone on the upstream face, and a masonry culvert beneath the dam center fed by cast-iron pipes to discharge water and control the lake level. In 1846, in Morris' revised plan, the masonry control tower was replaced with a wooden frame tower (Francis et al., 1891, p. 444). Modified from Plates LI and XLVIII of Francis et al. (1891). Photo inset at upper right: dressed masonry stones in the foundation of the Unger "spring house" at the Johnstown Flood National Memorial (photo by N. Kaktins).*

Another change relates to the masonry stones that were originally placed on the upstream side ("slope wall") of the dam (Figure 2). As shown in Figure 3 of Kaktins et al. (2013), the placement of these dressed stones on the northeastern side of the dam seemed to be incomplete

at the time of dam failure. According to Benjamin Ruff, in a written reply to an engineering report from Daniel J. Morrell (Cambria Iron Company), the face of the dam on the lake side was not covered with riprap, but was covered with a "slope wall" (McGough, 2002, p. 24). Therefore the masonry cover that comprised the slope wall may well have been complete for the original dam, but some of those dressed stones were apparently removed during or before the dam reconstruction. A National Park Service (NPS) photograph reproduced in McGough (2007, Illustration #9) clearly shows that, at least on the northern side, the original dressed stones have been replaced by riprap on the rebuilt dam. We found masonry stones that appear similar in size to the original specifications incorporated in the foundation of the house and spring house of the former F. J. Unger property, on the north side of the dam (Figure 2, inset top right). Unger was the last president and manager of the SFFHC. The former barn reportedly also had dressed stones in its foundations. They may have been scavenged from the dam before it was rebuilt because photos of the lake side of the dam after the flood show that the remaining original slope wall covered less than the bottom fourth of the slope on the northern remnant of the dam. It would certainly have been unusual in the 1800's to fabricate dressed stones to use in the foundations of a barn or spring house, unless such stones were already available. It should be noted that the spring house foundation shown in Figure 2 is not entirely original. Parts were restored by the NPS to repair damage. The present foundation is likely a good representation of the original, given the NPS's goal of working to accurately preserve historic sites.

Figure 3. *Large sandstone riprap on the western (left) and eastern (right) remnants of the dam. These represent the downstream side of the dam and illustrate the excellent riprap used in the original construction, obtained mostly from excavation of the main spillway (photos by U. Kaktins). Large riprap like this was not used in reconstruction efforts by the SFFHC.*

One of the key changes was that the large riprap originally used to cover the downstream slope of the dam (see Figure 3) *was not used* to cover the repaired section. Smaller riprap was used, and this is evident in plate LIIIA of Francis et al. (1891) (also see Figure 4). Despite this photographic evidence to the contrary in their own report, Francis et al. (1891, p. 446) state that

"heavy" riprap was used to cover both sides of the repaired embankment. Also the original dam, instead of a heart wall, relied on "puddled" clay layers to ensure a low permeability integrity of the embankment. But the puddled layers were not replaced during the repairs.

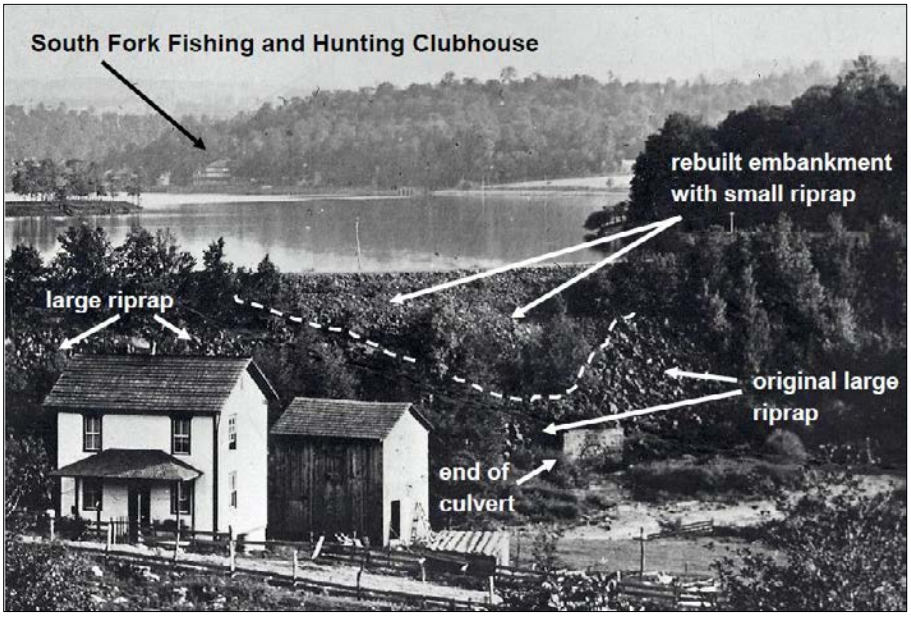

Figure 4. *Undated photo taken after the 1862 partial dam failure but before the 1889 flood. View is toward due south. After the repairs, large riprap is missing from the downstream center of the dam but is clearly seen on the eastern (left) and western (right) sides of the original embankments. Note the lesser amount of vegetation on the repaired section (zone above dashed white line). The house site at lower left now lies beneath a bridge foundation on Interstate 219. Base image modified from Plate LIIIA of Francis et al. (1891) and also available from the Johnstown Heritage Association at: http://jaha.org/edu/flood/why/img/dam_gallery/pages/southfork_dam.html. [Accessed 3/2/2016]*

Another major change was the lowering of the dam crest, reportedly to widen the carriage road on top (Francis et al., 1891, p. 446), but the lowering of the crest was also an obvious expedient to quickly get material to begin repair the partial breach of 1862 (Kaktins et al., 2013). We believe that was the primary reason for lowering the crest. The lowering of the dam crest is nicely shown even today by the fact that large riprap boulders on the intact eastern embankment stand higher than the present-day crest (Figure 5). Only a few large riprap remain near the crest on the western dam remnant. That area was accessible by road in later years, and we believe most of the boulders along that crest were long ago removed for other purposes. Unfortunately for the SFFHC, the initial material stripped from the dam crest and used to fill the 1862 breach was

Figure 5. *View along crest of the eastern dam remnant, looking westward toward the observation platform. This part of embankment represents original construction. Large riprap from the original construction is still in place, standing more than 0.6 m higher than present crest, as a result of the embankment crest being lowered as much as 0.9 m by the SFFHC. White ruler on rock is 0.33 m long (photo by N. Coleman).*

washed out by heavy rains in December 1879. Additional changes included the construction of a bridge over the mouth of the spillway and the installation of a boom and fish screens at the bridge. These features would have had the effect of somewhat reducing the main spillway discharge capacity.

[See full paper for details on the development of the following figures]

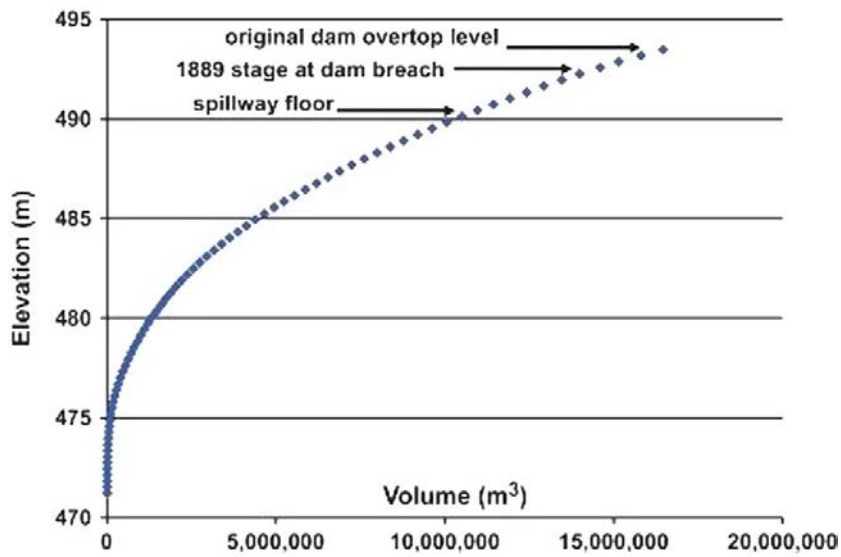

Figure 9. *LiDAR-based storage-elevation curve for Lake Conemaugh. The highest point on the curve represents an overtopping level of 493.5 m for the South Fork dam as originally built. Data Source: PASDA (2013a, b).*

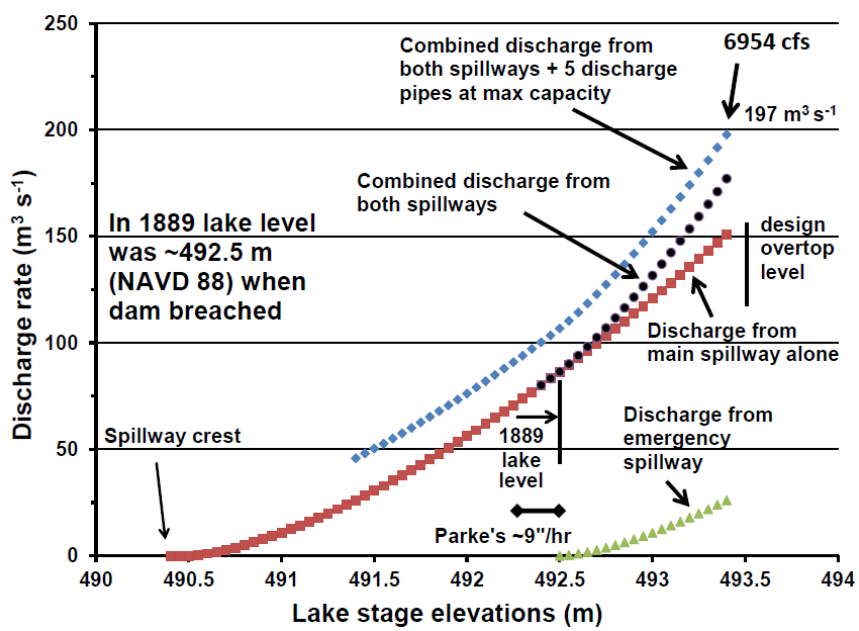

Figure 12. *Discharge capacity for the South Fork dam as originally designed, with crest ~1 m higher. The base level of this chart is ~490.4 m which is our estimate of the modern-day elevation of the subsoil spillway crest (see Section 2.3.2 of full paper). Overtopping would have occurred at ~493.5 m (NAVD 88) if the dam had been rebuilt to its original crest height. The spillway flow level would have been ~0.1 m less.*

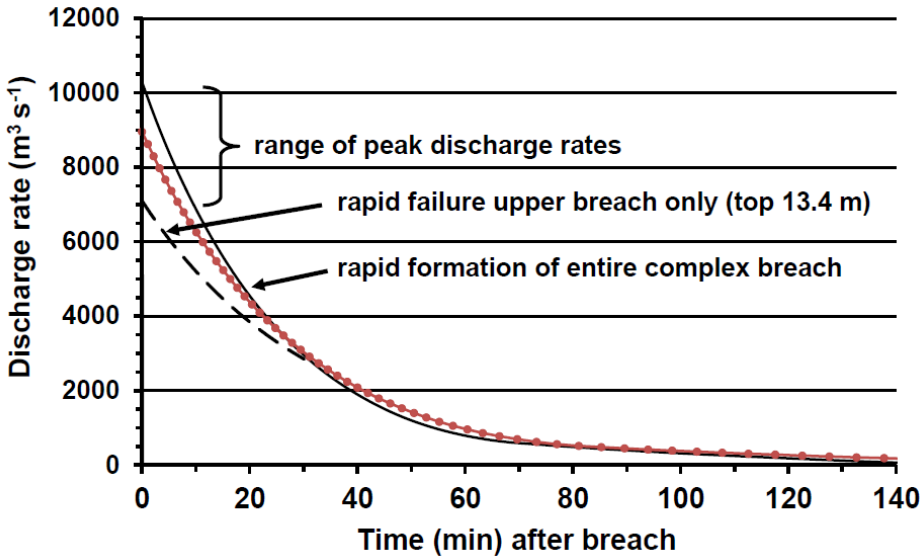

Figure 15. *Dam breach discharge hydrographs for the 1889 flood. Red dotted line represents scenario where the entire breach formed instantly. Solid black line includes 15% increase in initial discharge to incorporate uncertainty (see text of full paper). These calculations represent maximum theoretical discharge through the breach and spillway, with Q_p ~8970 to 10,300 $m^3 s^{-1}$. Dashed black line represents early-time discharge from only the top 13.4 m of the breach. This line intersects the vertical axis at ~7100 $m^3 s^{-1}$. Adding ~100 $m^3 s^{-1}$ for the spillway and ditch yields the minimum Q_p of ~7200 $m^3 s^{-1}$.*

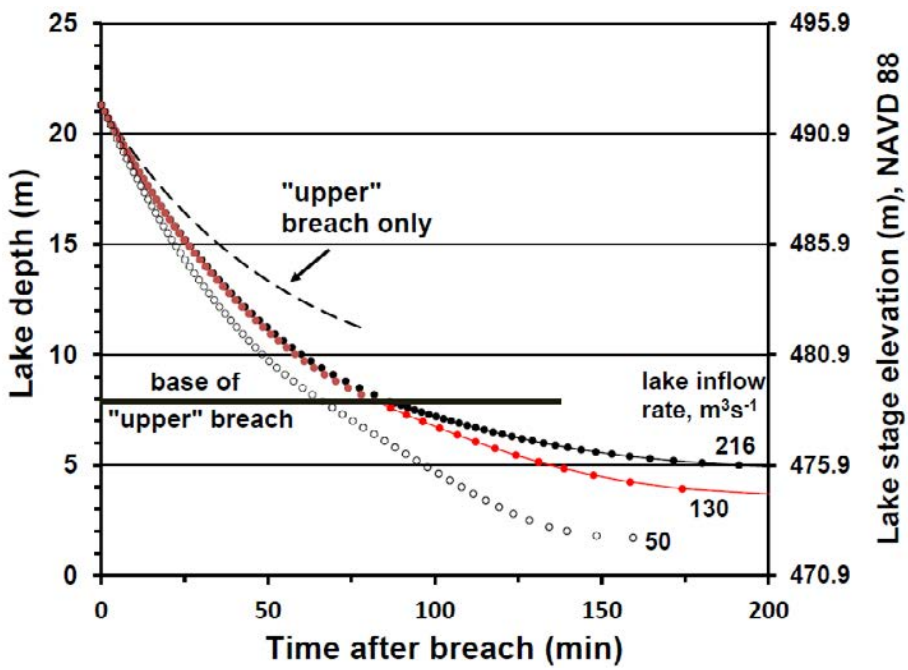

Figure 16. *Lake stage hydrographs for Johnstown Flood of 1889. Curves are plotted for three different lake inflow rates. Dotted lines represent cases where the entire complex breach formed rapidly, which would have drained the lake in the shortest time. Plot of open circles includes 15% increase in initial discharge rate to incorporate uncertainty (see text of full paper). Dashed line shows hypothetical lake stages if only the upper 13.4 m of the breach had formed. The zone between the dashed and dotted lines represents a family of curves for all plausible erosion times for the lower 7.9 m of the inner breach.*

Table 4. Summary of key data for the South Fork dam and watershed.

Dam comparisons	**Original dam**	**Rebuilt dam**
Embankment height	72 ft (22 m)	≤70 ft (~68-69 ft in center)
Overtopping elevation (NAVD 88)	~493.5 m	~492.5 m (~1616 ft); lake level at time of dam breach
Discharge capacity (Q) at overtopping		
Main spillway	~151 $m^3 s^{-1}$	~86 $m^3 s^{-1}$
Auxiliary spillway	~26 $m^3 s^{-1}$	ditch ~ <10 $m^3 s^{-1}$
Five discharge pipes	~20 $m^3 s^{-1}$	0 $m^3 s^{-1}$
Total *Q*	~197 $m^3 s^{-1}$ (6954 cfs)	~96 $m^3 s^{-1}$ (3430 cfs)
Estimated time of embankment overtopping	Would not have overtopped	~11:30 a.m. (actual)
Spillway floor elevation (NAVD 88)	~490.4 m (crest)	~490.4 m (crest)
Hydraulic and basin data		
Basin drainage area above Lake Conemaugh	~53 mi^2 (137 km^2) (Brua, 1978)	
Time of concentration (t_c), South Fork of the Little Conemaugh R.	3.6 to 7.3 hr	
Time to peak inflow to lake after period of most intense rainfall	2.5 to 5.1 hr (≤7.3 hr in extreme events)	
Rate of lake rise ~10:30-11:30 a.m. just before initial overtopping of dam	~9 in hr^{-1} (J. Parke; Francis et al., 1891, p. 449) [corresponds to lake inflow of 115 $m^3 s^{-1}$ beyond main spillway capacity of rebuilt dam]	
Estimated peak lake inflow before 11:30 a.m.	201 $m^3 s^{-1}$ [spillway (86) + excess inflow (115)] [inflow of 216 $m^3 s^{-1}$ used in our analysis to reduce chance of underestimating inflow]	
Volume of lake at time of 1889 dam breach	1.455×10^7 m^3 (below stage 492.56 m, NAVD 88)	
Time to drain lake to base of the upper breach	≥ 65 minutes	

5. Discussion

We respectfully disagree with the ASCE committee that reviewed the cause of the failure of the dam (Francis et al., 1891). They had concluded that the modifications to the dam by the SFFHC "…cannot be deemed to be the cause of the late disaster as we find that the embankment would have been overflowed and the breach formed if the changes had not been made." We question the committee's conclusions for five reasons:

First, if the drainage pipes had been replaced they would have been opened early on May 31st to their maximum capacity, which would have reduced the rate of rise observed by Parke. The issues noted earlier about possible hydrodynamic damage to the pipes and culvert would not have been a concern because releases from the dam were no longer needed to supply water to a canal. Therefore newly installed pipes and a repaired culvert would only have been used during floods or to lower lake levels to allow embankment repairs. Second, the committee failed to recognize that the dam likely had been lowered by the SFFHC more than 0.6 m, probably as much as 0.9 m, including settling of the embankment. The storage-elevation curve (Figure 9) shows that an added 0.9 m of lake stage could have stored an additional 1.6 million m^3 of water without overtopping. Third, in the original design the main spillway would have had much greater discharge capacity and the discharge pipes and auxiliary spillway would have been functional, but the committee never acknowledged that this smaller spillway even existed. Fourth, contrary to the committee's claims of an increasing rate of rise of the lake stage until dam failure, there is evidence that flood levels in both the South Fork and the Little Conemaugh River had stabilized and begun to fall, if only slightly, by 12:00-1:00 pm, suggesting that the time of concentration and peak in the runoff hydrograph had occurred hours before the dam breach. And fifth, the poor reconstruction of the older dam breach did have several adverse consequences. Apart from the fatal lowering of the dam crest, the random-fill technique used to fill the previous breach (rather than the clay "puddling" method) was a major factor in the disaster by making it possible for a large portion of the dam's core to become saturated during high lake stands. The committee itself reported (Francis et al., 1891, p. 454) that "All the material put in [by the club]…to repair the breach of 1862, appears to have been washed out, together with part of the old embankment…" They also reported (p. 454) that exposed parts of the *original* dam showed that they "…offered great resistance to washing and that [the work] was originally selected and put in with the requisite care to make a sound embankment."

We prepared Figure 18 to clearly show how the dam as originally built would have resisted overtopping on May 31, 1889. Even if extremely high lake inflows had continued unabated, overtopping of the dam at its original design height would have been averted for 14 hrs. In the absence of alternate failure mechanisms such as piping, the dam would have been preserved because lake inflows would have substantially diminished during the afternoon and evening. In the actual event, if the estimated peak inflow had time to fall just 9%, from ~216 to ≤197 $m^3 s^{-1}$, overtopping would have been entirely prevented had the dam been rebuilt to its original height. Figure 18 also reveals that had the reconstructed dam been built only 0.6 m higher, overtopping would have been delayed more than 7 hrs. even at the high and constant inflow rate assumed to develop this figure.

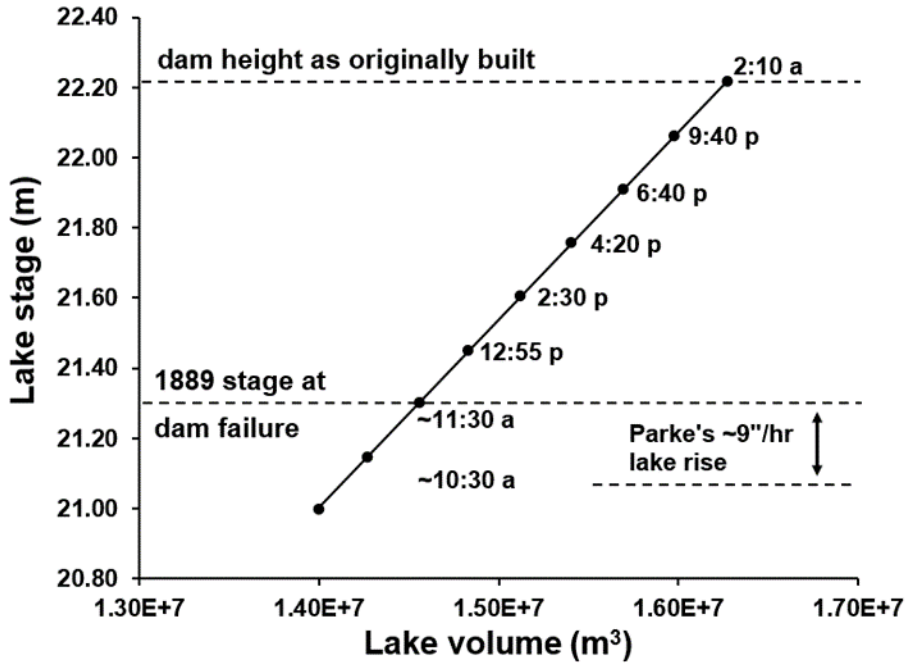

Figure 18. *Graph showing time needed to reach various hypothetical lake stages. Graph was prepared using the discharge capacity curves in Fig. 12 with the storage elevation curve in Fig. 9. The plotted times assume that a constant lake inflow of ~216 $m^3 s^{-1}$ would continue for many hours. Even in this extreme and unrealistic scenario, the nonlinear increase in spillway and pipe flow capacities and rise in lake storage would have averted overtopping for ~14 hours. In reality the dam would never have been overtopped.*

It is not well known that the reliability of the South Fork dam was tested just a few years after it was completed, when in the spring of 1856 the reservoir overflowed at an unspecified place after a rapid snowmelt (Unrau, 1980, p. 51). We have not found details about where the overflow occurred, but given the higher dam crest it must have flowed through the auxiliary spillway on the western abutment. With the dam at it design height the reservoir appears to have performed as intended, with two functioning spillways and the discharge pipes also probably opened. A leak in the dam was reported at that time but was soon repaired. In fact, the Pennsylvania State Engineer inspected the South Fork dam later that year. "The Western Reservoir [Lake Conemaugh] was examined and found to be in excellent condition. It furnished a sufficient supply of water to keep up the [canal] navigation when other sources had entirely failed" (Gay, 1856, p. 16). He had reported that the spring floods severely damaged other impoundments in the region, including Piper's and Raystown dams on the Juniata River. Eighty-foot breaches occurred in both of these dams.

There are useful insights to be gained from the resilience of another earthen dam in the region that was built with a "puddled" clay core. This dam was on Mill Creek four miles from Johnstown, and it survived the May 1889 event. We know this from the minutes of the Board of Trade and Citizens Meeting, June 19, 1891, which state that the dam was 310 ft long and 25 ft high, built in 1834 with a spillway 44 ft wide and a "puddle wall" 7.5 ft wide within the center of the dam. The minutes go on to document that a "freshet" [flood] occurred on July 2, 1889 and that the spillway was insufficient to carry the flow. The *whole dam* was overtopped by this flood but it did not fail, providing an example of the resilience of the original "puddle wall" construction technique.

Unfortunately, the SFFHC did not use this technique to repair the South Fork dam. Kaktins et al. (2013) argue that the fill contained plastic clays, which when wetted would have had very low shear strength. Therefore, liquefaction effects may have been largely responsible for the very rapid upper breach formation. Francis et al. (1891, p. 446) commented that hauling fill by [horse] teams over the freshly deposited material "…made a fairly compact embankment on the upper side of the stone embankment." But since there was a definite sag in the central, filled portion of the embankment any compaction was of a limited nature.

It is interesting to compare the committee's conclusions about the South Fork dam (Francis et al., 1891) to their earlier investigation of the Mill River dam failure in Massachusetts (Francis et al., 1874; Sharpe, 2004). James Francis and William Worthen served on both committees. The members criticized the material used to make the Mill River embankment, and that it could not be relied on to make the structure water-tight. During the construction there "…was no sufficient inspection, so peculiarly important in a work of this description…" "The remains of the dam indicate defects of workmanship of the grossest character." In the discussion section, member Worthen went on to write:

> Men were employed who were ignorant of the work to be done, and there was nothing like an inspection, although money and life depended upon it. I do not believe, however much we are an evolved species, that we are derived from beavers; a man cannot make a dam by instinct or intuition.

Neither Worthen nor Francis reflect this philosophy in their role 16 years later as investigators of the South Fork dam failure. The need for engineering inspection and water-tight embankments was equally important during the SFFHC's repair of the South Fork dam. And yet, when confronted with the many changes made to that dam and the poor methods used to repair the embankment, including lack of engineering inspection, Francis et al. (1891) concluded that the changes and repairs to the dam were not responsible for the disaster. They even went so far as to conclude that if the embankment had been rebuilt to its original height the result may have been *greater* loss of life. Clearly there were inconsistencies in philosophy between the ASCE reviews of the South Fork and Mill River dam failures.

Despite numerous lawsuits, the SFFHC was never found financially liable for losses of life or damages. One reason for this was that Benjamin Ruff, who supervised the rebuilding of the dam, had died two years before the 1889 dam breach and could not be held accountable. Most of the legal actions ended before publication of the ASCE report by Francis et al. (1891).

6. Conclusions

We calculate a LiDAR-based volume of 1.455×10^7 m^3 for Lake Conemaugh at the time of the 1889 dam breach. The peak discharge was likely in the range from 7200 to 8970 m^3 s^{-1}, with the lower part of this range being more likely because the deepest part of the complex breach may have formed gradually. Considering uncertainty, we estimate an upper limit on the peak discharge of 10,300 m^3 s^{-1}. The reservoir took more than an hour to drain, contrary to older claims that the lake drained in 45 min. If the entire complex breach formed rapidly, more than 65 min would have been needed to drain the lake to the floor of the upper breach. Part of the lake would still have been nearly 8 m deep at that time.

In analyzing topographic surveys at the site we found that the 1889 dam survey elevations are systematically 1.9 m (6.2 ft) lower than the modern GPS reference frame. Another of our findings is that soil genesis on the bare rock spillway has produced as much as half a meter of soil in >120 years following the dam breach. The average rate of soil accumulation exceeds 4 mm yr^{-1}.

Although Francis et al. (1891) stated that the mode of repairing the breach was not according to best practice, they nonetheless concluded that "…failure of the dam cannot be attributed to any defect in its construction. The failure was due to the flow of water over the top of the earthen embankment, caused by the insufficiency of the wasteway…" However, we find that the changes made to the South Fork dam were indeed responsible for the disaster, having altered its original design and rendered it highly vulnerable to overtopping. The dam could indeed have survived the rainfall event of May 30-31, 1889 had it been maintained as built in 1853 with a higher crest, a functioning second spillway, five drainage pipes, proper well-compacted fill with puddle layers, riprap replacement of proper size, and no bridge or fish screens across the main spillway. The discharge capacity of the original dam was more than *twice* that of the reconstructed dam. The dam as originally designed could have averted overtopping for as much as 14 hours even under extreme conditions of inflow duration and rate. Such extreme conditions did not exist because observations of local streams indicate that flows into Lake Conemaugh peaked hours before the dam breach. We therefore disagree with the main conclusion of Francis et al. (1891), that the dam failure was inevitable. They placed too much reliance on several estimates for the rate of rise of the water and the implied excess flow into the reservoir. This seems unusual given James Francis' expertise in flood control and weir calculations and his practical knowledge of river behavior in flood, from the rapid rise to peak discharge and the relative speed of flood recessions. The committee assumed flow depths in the spillway that were implausible, based on evidence from the dam remnants that they themselves visited (i.e., preserved plow furrow on crest). Their unsupported assumption of protracted, extreme lake inflow before and after the dam breach led to their conclusion about the non-survivability of the dam.

We believe the investigation report represented state-of-the-art in 1891, with review of the embankment design and history, careful surveys and photographic documentation of the dam site, hydrologic analyses, and the inclusion of alternate views of the dam failure and site characteristics. However, we are puzzled that the 1891 conclusions are not consistent with evidence easily available to the committee. Their report (Francis et al., 1891) contains no reference to a second spillway. We find it difficult to believe that the original auxiliary spillway at the southwest abutment was unknown to the committee, given their review and documentation of the engineering specifications for the dam. They visited the dam site at a time when the original excavations on the western abutment should still have been apparent, and, most importantly, obtained a detailed post-flood survey of the dam remnants (Figs. 6 and 7 – *see full paper*) that clearly showed the southwest abutment was lower than the dam crest, even after the entire crest had been lowered by the SFFHC. In fact, Francis commented that "…near the ends [of the dam] there were ascents to the level of the top of the dam." (Francis et al., 1891, p. 468). The committee also received a report of the magnitude of flow that occurred over the left abutment after the digging of a shallow ditch, before flow had overtopped the crest. Yet, it appears none of the committee members perceived this clear evidence of an auxiliary spillway which would have functioned effectively given the original, higher dam breast. This spillway

would have been more apparent before the construction of a parking lot at the western abutment circa 1977.

The confidence with which the committee stated the dam would have failed in any event was unwarranted. They made no comment about the smaller riprap used on the downstream face of the dam, even though the size difference was obvious in photographic Plate LIIIA of their report. The committee went so far as to conclude that had the dam been rebuilt to its original height, the dam breach could possibly have been more disastrous due to the larger impounded volume. They even suggested that lowering the dam widened the crest, and that its use as a road must have increased its resistance to breaching. But any improvement in resistance from using the crest as a road would have been insignificant compared to the unparalleled benefits of maintaining the higher crest. The combination of increased storage and more than doubled discharge capacity would have prevented overtopping long enough to protect the South Fork dam.

The ASCE review of the South Fork dam (Francis et al., 1891) and supporting calculations appear to us to have been biased in favor of the dam owners, thereby helping to shield the SFFHC, in a historic engineering sense, from subsequent liability claims or even the perception of liability in the wake of the disaster. We believe an injustice was thereby done to the more than 2200 people who lost their lives and to the survivors. The ASCE publication by Frank (1988) provided an updated perspective on the cause of the flood, but did not include supporting hydraulic calculations. J. Wesley Powell (1889), director of the U.S. Geological Survey, wrote "The Lesson of Conemaugh" in which he discussed the importance of dams and factors to consider in their design, including basin analysis and gaging of precipitation and streams. The disaster thereby brought new attention to the safety of existing and future dams, undoubtedly saving many lives in the future.

Acknowledgements

We thank Dr. Rex Wescott and an anonymous reviewer for their comments on our paper, which helped to significantly improve the manuscript. We thank Musser Engineering, Inc. of Central City, Pennsylvania, and Professor Brian Houston (University of Pittsburgh at Johnstown) for their GPS analyses of key elevations at the South Fork dam. We appreciate the field work assistance of Dr. Carrie Davis Todd, now at Baldwin Wallace University, and her contributions to an earlier paper on historical aspects of the 1889 flood. We are grateful to the Johnstown Area Heritage Association for helping us access material at the Johnstown Flood Museum library. We thank the National Park Service Johnstown Flood Memorial for access to their archived materials and for a 2011-2012 research permit to investigate the soils that occupy the former lakebed and spillway.

References

Brua, S.A., 1978. Floods of July 19-20, 1977 in the Johnstown area, western Pennsylvania. U.S. Geological Survey Open File Report 78-963, 62 p.

Francis, J.B., Ellis, T.G., Worthen, W.E., 1874. The failure of the dam on Mill River. ASCE Transactions, v. III, no. 4, p. 118-122.

Francis, J.B., Worthen, W.E., Becker, M.J., Fteley, A., 1891. Report of the Committee on the cause of the failure of the South Fork dam. Transactions of the American Society of Civil Engineers, v. XXIV, pp. 431 – 469.

Frank, W.S., 1988. The cause of the Johnstown flood: A new look at the historic Johnstown flood of 1889. *Civil Engineering—ASCE*, Vol. 58, No. 5, May 1988, pp. 63-66. Also see: http://www.smoter.com/flooddam/johnstow.htm. [Accessed 2/13/2016]

Gay, E.F., 1856. Report of the [Pennsylvania] State Engineer for the fiscal year ending November 30, 1856. Report dated Dec. 23, 1856. In: Reports of the heads of departments. Transmitted to the Governor in pursuance of law, for the financial year ending Nov. 30, 1856. Harrisburg.

Kaktins, U., Davis Todd, C., Wojno, S., Coleman, N.M., 2013. Revisiting the timing and events leading to and causing the Johnstown flood of 1889. Pennsylvania History: a Journal of Mid-Atlantic Studies, v. 80, no. 3, 335–363.

McCullough, D., 1968. The Johnstown Flood. New York, Simon and Schuster, 302 p.

McGough, M.R., 2002. The 1889 flood in Johnstown, Pennsylvania. Thomas Publications, Gettysburg, PA, 180 p.

McGough, M.R., 2007. The club and the 1889 flood in Johnstown, Pennsylvania. 124 p.

NPS (National Park Service), 2012. Investigator's annual report, permit number JOFL-2011-SCI-0001.

Powell, J. W., 1889. The lesson of Conemaugh. The North America Review, CXLIX (August 1889), 154–156. Online at: http://www.lakepowell.org/page_two/information/THE%20LESSON%20OF%20CONEMAUGH.pdf. [Accessed 1/27/2016]

Unrau, H.D., 1980. Historic Structure Report: The South Fork dam historical data, Johnstown Flood National Memorial, Pennsylvania. Package no. 124, U.S. Department of the Interior, National Park Service (1980): 242.

HARPER'S GEOLOGICAL DICTIONARY

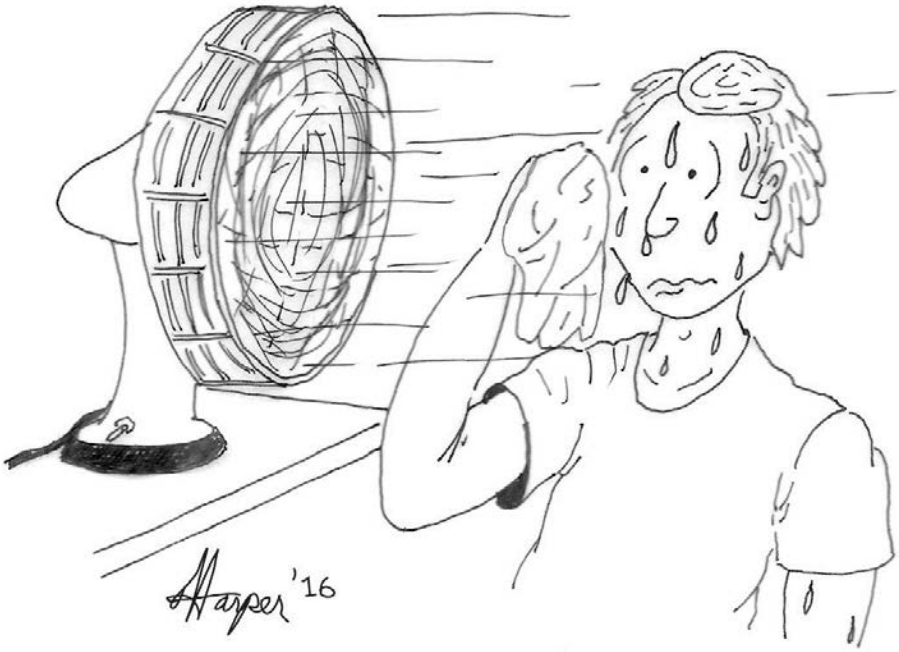

THERMAL METAMORPHISM - the pronounced change in atmospheric temperatures resulting from heated political disagreements over the scientific validity of climate change.

refer to Stop 1 description & paper in the Guidebook: Lucerne Coal Refuse Site Cambria Reclamation Corp. Center Township, Indiana County – Reclamation via Coal Refuse Fired Electric Generation Units

APPENDIX A

ARIPPA WHITE PAPER ON COAL REFUSE

What is coal refuse?

The Environmental Protection Agency (EPA) describes coal refuse as waste products of coal mining, physical coal cleaning, and coal preparation operations containing coal, matrix material, clay, and other organic and inorganic material. Others have described coal refuse as a by-product of coal mining activities, not including overburden, which has been spread on the land. Coal refuse piles vary from a few to hundreds of acres of unreclaimed mine lands.

Pennsylvania regulations define coal refuse as "…any waste coal, rock, shale, slurry, culm, gob, boney, slate, clay and related materials, associated with or near a coal seam, which are either brought aboveground or otherwise removed from a coal mine in the process of mining coal or which are separated from coal during the cleaning or preparation operations. The term includes underground development wastes, coal processing wastes, excess spoil, but does not mean overburden from surface mining activities."

Where was and is coal refuse placed?

Because it is a by-product of coal mining operations, coal refuse is located throughout the coal regions of Pennsylvania and other coal producing states. Pennsylvania's coal regions are shown below:

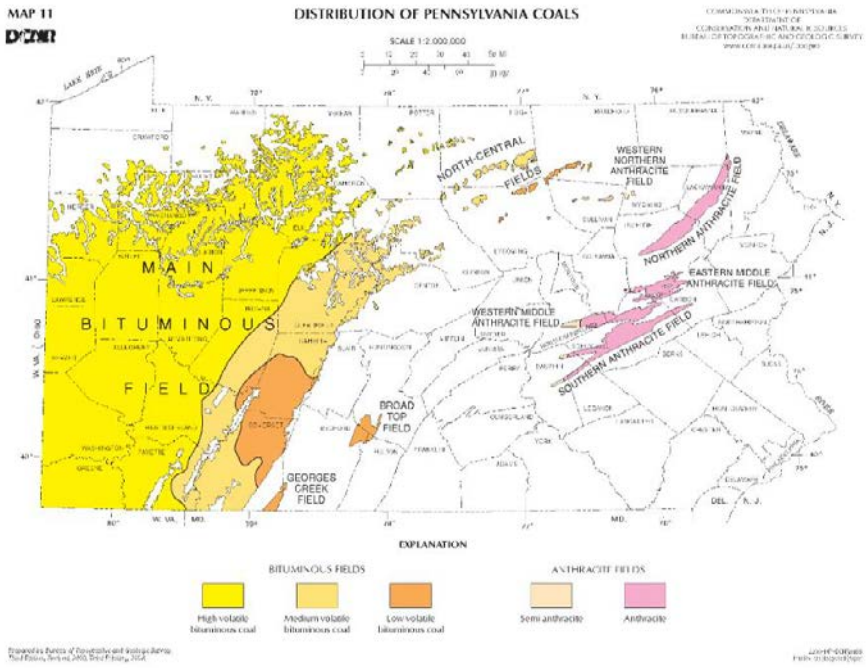

Pennsylvania's coal miners have extracted approximately 16.3 billion short tons of anthracite and bituminous coal from the state's mines since commercial mining began in 1800. While mines permitted under the 1997 Surface Mining Control and Reclamation Act (SMCRA) are required to be reclaimed after the coal is extracted and processed, many pre-SMCRA mines were abandoned without any reclamation. These sites are referred to as Abandoned Mine Lands (AML).

Typical coal refuse pile on abandoned mine lands. This site is Mine 37 located near Windber, PA along the Paint Creek.

In Pennsylvania, there are more than 5,000 abandoned, unreclaimed mining areas covering approximately 184,000 acres. The coal refuse piles at these abandoned mine lands cover an aggregated area of 8,500 acres and contain a total volume of more than 200 million cubic yards.

The total amount of coal refuse in Pennsylvania is unknown. Based on the known amount on abandoned mine lands and estimates of the amount of coal refuse associated with historical mining operations, the amount is between 200 million and 8 billion cubic yards. It has been speculated that the amount of coal refuse is approximately 2 billion cubic yards split almost equally between the anthracite and bituminous coal regions.

What problems do unreclaimed coal refuse sites cause?

Land

The coal refuse piles are scattered across the landscape next to communities, rivers and streams and sometimes fill entire valleys. These piles are unsightly and scar the landscape and some areas look like moonscapes. The piles also tend to attract dumping and other activities increasing the potential for nuisances such as starting the coal refuse piles on fire. Abandoned coal mines and coal refuse piles cause many adverse impacts to surrounding land. Unstable coal refuse piles may collapse and threaten the safety of nearby communities and the scenic and recreational quality of the landscape is ruined. Properly reclaimed coal refuse sites can and have returned the land to productive uses including wildlife habitat, recreational opportunities and commercial development.

Large coal refuse pile on an abandoned mine land located directly in the community of Nanty Glo, PA. These piles often attract use of recreational vehicles and other dangerous activities, which causes a safety concern.

Water

More than 3,300 miles of streams in Pennsylvania are impacted by Acid Mine Drainage (AMD), according to the United States Geological Survey (USGS). This is the result of AMD from both mine discharges as well acid runoff from coal refuse piles, as shown in this photograph. The acid mine drainage discharges, resulting from the oxidation of pyrites and maracites (iron-sulfide minerals), significantly impact water quality in the streams into which these contaminated waters flow. The acidic discharges contain iron, manganese, aluminum along with other metals and materials which become more readily soluble due to the increased acidity. The run-off from precipitation in addition to being acidic and contaminated by metals, contains silt which is a pollutant as well. This acidic contaminated discharge creates water pollution and negatively affects the ability of a stream to support and aquatic life. The chemistry of oxidation of pyrites in a coal refuse pile is very complex. Although a host of chemical processes contribute to acid mine drainage, pyrite oxidation is by far the greatest contributor. The net effect of these reactions is to release hydrogen ions (H^+), which lowers the pH and maintains the solubility of the ferric ion in the water. These reactions can occur spontaneously or can be catalyzed by microorganisms that derive energy from the oxidation reaction.

AMD entering a stream from a nearby coal refuse pile causes the stream to turn orange in color due to the iron precipitating out of solution as the solid iron hydroxide ($Fe(OH)_2$). In many streams affected by AMD, the iron hydroxide covers the entire stream bed and rocks.

During 200 years of coal mining, Pennsylvania produced more than 25 percent of the nation's total coal output and presently ranks fourth in the nation in annual coal production by state. Pennsylvania's coal regions are located within, or extend into, the four major river basins in Pennsylvania – the Ohio, Susquehanna, Potomac, and Delaware River Basins. Bituminous coal deposits underlie western and north-central Pennsylvania, and anthracite deposits underlie east-central and northeastern Pennsylvania.

As noted in the DEP Citizens Advisory Council's Transition Report to the incoming State administration, Pennsylvania faces a documented abandoned mine land inventory cost of $16.1 billion. Of this amount, reclaiming coal refuse piles represents approximately $2 billion or more.

By comparison, federal abandoned mine land (AML) funding grants fell by 15% last year, and in 2014 only provided around $50 million toward abatement of such hazards. Under the current federal AML program, coal refuse piles receive relatively low priority and very limited funding; and the finding from the federal AML program is expected to continue to fall as reclamation fees from ongoing mining diminish.

Air

Coal refuse sites historically and currently catch fire. Coal refuse fires typically start as a smoldering, oxygen starved fire producing the necessary oxygen from the generation of steam from the moisture in the coal refuse. Slowly, as the fire continues to develop, avenues for oxygen migration through the refuse expand resulting in flames. Combustion of the coal refuse allows uncontrolled toxic air pollutants and greenhouse gases to be emitted into the atmosphere. The toxic air pollutants are a particular health and safety problem in the proximity of the coal refuse fires.

Depiction of uncontrolled combustion byproducts commonly referred to as "red-dog".

The oxidation of pyrites produces an exothermic reaction which produces the heat that causes the carbonaceous material in the coal refuse pile to ignite and burn. The temperature within a coal refuse pile (or portions of a pile) will increase when more oxygen is available to cause oxidation but the amount of air circulating in the pile is insufficient to provide for the dissipation of heat. The temperature of the refuse increases until the ignition temperature of the carbonaceous material in the refuse is reached. At this point the coal refuse pile spontaneously combusts releasing the various uncontrolled air pollutants into the air of the near-by community.

Pennsylvania has identified more than 40 coal refuse piles that are currently burning and at some point will need to be addressed. This does not include underground mine fires. In 2014, the PADEP's Abandoned Mine Land Program spent $2,213,477.80 in emergency funds to extinguish and reclaim the Anthracite Region's Simpson Northeast coal refuse fire located in Fell Township, Lackawanna County.

Pennsylvania was the first state to pass a law to address the air pollution associated with coal refuse disposal entitled "The Coal Refuse Disposal Control Act, Act of September 24, 1968, P.L. 1040, No. 318." This has allowed the Commonwealth to address active coal refuse pile fires and to attempt to prevent additional coal refuse piles from catching fire. While the efforts have met with success, new coal refuse fires continue to occur.

The EPA (1978 Study) identified the uncontrolled emissions from burning coal refuse piles. The following pollutants were listed:

(1) criteria pollutants (total particulates, respirable particulates, nitrogen oxides, sulfur dioxide, sulfur trioxide, hydrocarbons, carbon monoxide, and mercury);
(2) non-criteria pollutants (ammonia, hydrogen sulfide, polycyclic organic materials); and
(3) trace elements (arsenic, boron, silicon, iron, manganese, magnesium, aluminum, calcium, copper, sodium, titanium, lead, tin, chromium and vanadium)

The USGS Report entitled "Emissions from Coal Fires and Their Impact on the Environment" identified the following:

> "…Self-ignited, naturally occurring coal fires and fires resulting from human activities persist for decades in underground coal mines, coal waste piles, and unmined coal beds. These uncontrolled coal fires occur in all coal-bearing parts of the world (Stracher, 2007) and pose multiple threats to the global environment because they emit greenhouse gases—carbon dioxide (CO2), and methane (CH4)—as well as mercury (Hg), carbon monoxide (CO), and other toxic substances…"

> "…In the United States, the combined coast of coal fire remediation projects, completed, budgeted, or projected by the Office of Surface Mining Reclamation and Enforcement, exceeds $1 billion, with about 90% of that in two States—Pennsylvania and West Virginia… Altogether, 15 States have combines cumulative OSM coal-fire project costs exceeding $1 million…."

> "…Direct hazards to humans and the environment posed by coal fires include emission of pollutants, such as CO, CO2, nitrogen oxides, particular matter, sulfur dioxide, toxic organic compounds, and potentially toxic trace elements, such as arsenic, Hg, and selenium (Finkleman, 2004). Mineral condensates formed from gaseous emissions around vents pose a potential indirect hazard by leaching metals from mineral-encrusted surfaces into nearby water bodies…"

What is Pennsylvania's experience with reclaiming coal refuse sites?

Over the last 50 years, Pennsylvania's experience has evolved. The commonwealth established and implemented "Operation Scarlift" in the 1960s and 1970s to address environmental damage from mining operations and today participates in the U.S. Department of the Interior's Abandoned Mine Land Reclamation Program, which utilizes money from industry to reclaim abandoned mine lands.

Reclamation costs, based on PADEP AML Program experience, varies between $40,000 per acre to $100,000 per acre. These costs are tied to the physical reclamation (grading, covering with soil, and planting vegetation) of a site. **These costs do not address the treatment of AMD**

or the elimination of the threat of future fires. Using these cost-per-acre projections to reclaim sites, the physical reclamation of coal refuse sites of different acreage would be:

a. 20 acres $800,000 to $2,000,000
b. 50 acres $2,000,000 to $5,000,000
c. 100 acres $4,000,000 to $40,000,000

To reclaim these sites properly requires more than just planting vegetation such as beach grass. The sites need to be examined and plans developed to address water pollution problems, proper grading and controls and the proper use of vegetative sustaining cover using indigenous vegetation.

Frequently the PADEP's Abandoned Mine Land Program must utilize emergency funds to remediate coal refuse piles that have become a health or safety hazard. Examples include unstable or literally collapsed coal refuse piles as well smoldering or open flame fires. One experience occurred in 2014 with the Simpson Northeast Refuse Fire, Fell Township in Lackawanna County when the coal refuse pile that had been smoldering ignited in flames. The department had to expend $2,213,477.80 in emergency funds to extinguish the fire and reclaim the pile by grading, covering with soil and planting vegetation.

To extinguish a coal refuse fire, the burning coal refuse must be removed, spread out, and water or other chemicals used to quench the flames. After the fire is extinguished, the coal refuse is re-deposited by spreading and compacting, with the addition of alkaline materials as necessary to neutralize the residual acidic materials. The site is then covered with soil and re-vegetated. Hydrologic controls are also constructed, however, there is no money allocated to provide long-term discharge treatment for pollutants that have not been remediated.

What must be considered in the reclamation of coal refuse piles?

To properly reclaim coal refuse piles, the following, at a minimum, need to be addressed:

- water pollution from run-off and acid mine drainage discharges
- site stabilization including re-grading to insure the stability of the site as well as properly managed water run-off
- covering with vegetative supporting material
- planting with vegetation to support the final land use

The reclamation engineering design must include:

- ✓ Installation of hydrologic controls
- ✓ Installation of wet land treatment systems for small volume discharges
- ✓ Grading and compacting
- ✓ Covering of the site with 1 to 4 feet of soil
- ✓ Adjusting the soil acidity with alkaline materials
- ✓ Addition of fertilizers
- ✓ Vegetate consistent with the local flora

As the photograph shows, even after several years the site is still void of vegetation. Reclamation of a coal refuse site requires far more effort and expenditures than simply planting a species such as beach grass that may survive in that hostile environment. In that situation, the surface water, ground water and air pollution issues still would exist. The only problem that may be addressed by that solution is purely a cosmetic one in that the view of the coal refuse pile is not as stark.

The photograph also shows water pollution in the form of run-off and mine drainage (orange tinted water to the right and bottom of the pile) that is being caused by this abandoned coal refuse site. It is a site that previously experienced a fire, as evidenced by the red-dog (red color material on the top and right side of the pile). The site also has steep slopes that are eroding and will cause future stability concerns. Further, water accumulates on the pile and causes concentrated mine drainage to flow in the nearby stream.

Alternative Solution for reclaiming coal refuse impacted areas

Another approach to reclamation of coal refuse piles and the areas affected by them is through the utilization of coal refuse as a fuel. This solution addresses water pollution, potential coal refuse fires, and reclamation of coal refuse affected sites. Coal refuse can be an effective fuel in facilities designed to burn coal refuse in a controlled manner minimizing environmental impacts. If coal refuse from these sites is used as fuel, the coal refuse is removed, processed, burned and the resultant ash beneficially used to remediate the residual acidity at the site. When reclaimed in this fashion, all of the problems associated with coal refuse piles are permanently addressed. The EPA has described the benefits of coal refuse-fired electric generating units:

> "Coal refuse (also called waste coal) is a combustible material containing a significant amount of coal that is reclaimed from refuse piles remaining at the sites of past or abandoned coal mining operations. Coal refuse piles are an environmental concern because of acid seepage and leachate production, spontaneous combustion, and low soil fertility. Units that burn coal refuse provide multimedia environmental benefits by combining the production of energy with the removal of coal refuse piles and by reclaiming land for productive use. Consequently, because of the unique environmental benefits that coal refuse-fired EGUs provide, these units warrant special consideration so as to prevent the amended NSPS from discouraging the construction of future coal refuse-fired EGUs in the U.S."

Following are examples of before and after pictures of coal refuse pile reclamation projects performed by coal refuse fired plants:

GALLITZIN SITE – Allegheny Township, Blair County

BEFORE RECLAMATION

AFTER RECLAMATION

ERNEST SITE – Rayne Township, Indiana County

BEFORE RECLAMATION

AFTER RECLAMATION

ACOSTA SITE -- Jenner Township, Somerset County Permit

BEFORE RECLAMATION

AFTER RECLAMATION

NORTHAMPTON'S HUBER SITE – Hanover Township, Luzerne County

BEFORE RECLAMATION

AFTER RECLAMATION

PANTHER CREEK – Nesquehoning Borough, Carbon County

BEFORE RECLAMATION

AFTER RECLAMATION

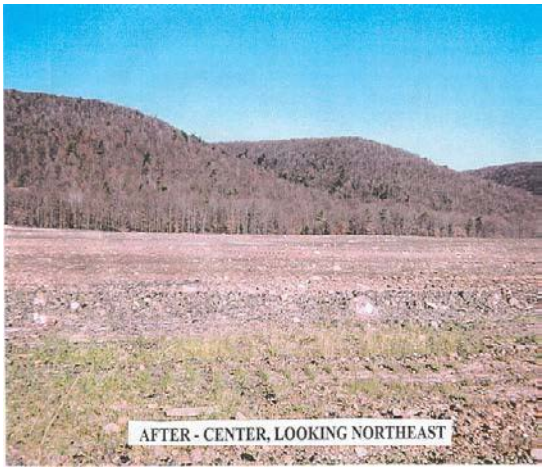

What processes do coal refuse-fired units use to solve the problems associated with abandoned coal refuse sites?

The re-mining of coal refuse piles in accordance with surface mining regulations provides for the reclamation of the energy remaining in this material. Because these sites had discharges to surface and ground waters, the companies are required to develop abatement plans. These abatement plans rely upon the use of acid-forming coal refuse being used as fuel in a fluidized bed combustion boiler or circulating fluidized bed boiler (CFB). The removal of the coal refuse results in the elimination of the AMD. The CFB Units are designed to fire coal refuse with limestone to control acid gas emissions, primarily sulfur dioxide (SO_2), while producing an alkaline byproduct (coal ash) that can be beneficially used for mine land reclamation.

The figure below depicts the typical processes used to reclaim a coal refuse site using a coal refuse-fired CFB boiler. The coal refuse material is processed at the mine site by screening to remove rock and other inert materials. The finer material is used as fuel for the alternative energy power plant where limestone is added to the furnace to control acid gas emissions. The resulting ash material, which meets the beneficial use criteria, is returned to the mine site and mixed with any unusable coal refuse material as a means to neutralize any remaining acidic materials. The materials are then compacted in place to contours as described in the surface mining permit.

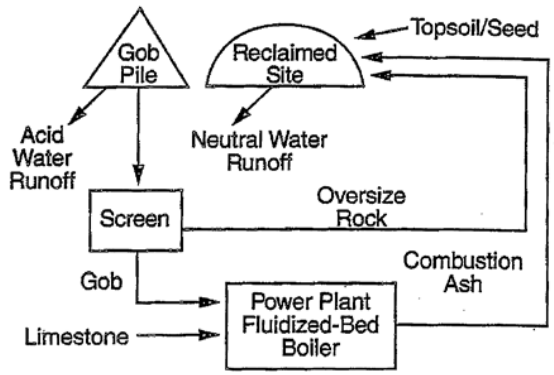

The reclamation of the piles remediates the acidic drainage that comes from the coal refuse pile in two ways. Typically 75 percent or more of the coal refuse is moved off site as fuel for the alternative energy plant meaning the majority of the acidic materials and the resultant water pollution is removed from the nearby waterways. The remaining acidic material is neutralized by the beneficial use ash and compacted in place according to the contours defined in the surface mining permit. In addition, most of the water runoff in the area is diverted to flow around the reclaimed area rather than through the site. Consequently, the previous pollution released from an unreclaimed coal refuse pile is addressed both by reducing the quantity of water flow from the now reclaimed pile as well as by the improved quality of the runoff. The quality of the runoff is improved by removing the acidic materials that would normally dissolve the metals that exist in the coal refuse piles as well as through the change in the solubility of these materials due to the change in acidity at the site. As such the concentration of the acidity as well as the metals such as iron, aluminum, and manganese in surface and groundwater releases are significantly reduced.

What is the air emission profile of a coal refuse-fired CFB boiler?

Coal refuse-fired units convert coal refuse into steam and electricity by burning the fuel in a highly controlled and regulated fashion, using a specialized type of technology, circulating fluidized bed boiler (CFB) with limestone injection for acid gas control. These units are also equipped with fabric filter systems to control filterable particulate matter (FPM) emissions. The coal refuse-fired units control emissions of SO_2, nitrogen oxides (NOx), air toxics, FPM and total particulate matter (TPM).

These units are some of the lowest emitters of mercury and FPM. That is evidenced in their use in the development of the MATS rule. Multiple coal refuse-fired units were included in Maximum Achievable Control Technology (MACT) Floor calculations (top 12% performing units)

used to establish the emission standards for mercury and non-mercury metals. The result of the inclusion of these coal refuse-fired units resulted in lower MATS emission standards for mercury and non-mercury metals (including the FPM surrogate) than would have otherwise been established. While the coal refuse may be higher in mercury content, coal refuse fired units are very low emitters of mercury and are a primary reason why the MATS mercury emission rates are low for all coal-fired units.

In addition, the emissions of greenhouse gases from these units can be considered as offset due to the eventual in-place burning of the coal refuse piles. Coal refuse fires also result in the uncontrolled release of the same pollutants that these plants control with high removal rates. Because these units provide electricity to the grid they also reduce emissions from other fossil fuel-fired EGUs which otherwise would be operating. The reclamation and re-vegetation of coal refuse sites also results in the expansion of green spaces which aids in the sequestration of GHGs.

What are coal ash or Coal Combustion Residuals (CCR) and how can they be beneficially used for reclamation of coal refuse sites?

EPA has classified coal combustion residuals (CCRs), also called coal ash, as non-hazardous. Further, EPA has stated that due to the unique characteristics of surface mine reclamation the regulations are not applicable to the utilization of coal ash in coal mine land reclamation but EPA will be working with the Federal Office of Surface Mining Reclamation and Enforcement in the development of their rules. This office has been reviewing and analyzing various state programs including Pennsylvania as part of their process to develop rules that reflect best practices. Under the Pennsylvania Regulatory Program, the beneficial use of coal ash in coal mine land reclamation is a two-fold program.

The first component of Pennsylvania regulatory program is the certification and ongoing recertification of the coal ash for having a beneficial use in coal mine land reclamation. The coal ash certification process involves a comprehensive review of the source of the coal ash and an ongoing evaluation of the physical, chemical and leaching properties of the ash both at the point of generation and the where the coal ash is placed. Coal ash and coal ash leachate are analyzed for 37 different chemical constituents and properties. The ash leachate must consistently contain concentration levels lower than the certification requirements set forth in the regulations in order to be approved for statewide beneficial use at coal mine sites.

The second component of this regulatory program is integrating the beneficial use of the coal ash in coal mine land reclamation through Pennsylvania's Coal Mine Primacy Regulatory Program or through contract when the utilization is tied to the reclamation of abandoned mined lands. The programs are designed to insure that the management of the coal ash at the coal mine site will result in the reclamation of the land and improve water quality.

Over the past fifty years, Pennsylvania's program has demonstrated its effectiveness. This is especially true for the coal refuse sites that have been re-mined and reclaimed.

Are there examples of the benefits provided by this reclamation?

There are numerous case studies regarding the reclamation of coal refuse sites and the benefits achieved. The Revloc Site and Maple Coal Site are two such examples:

REVLOC, PENNSYLVANIA

Revloc, PA is located in Cambria County approximately 90 miles east of Pittsburgh in the heart of the western Pennsylvania coalfields. The mining town centered the Revloc mine built in 1916-17. The Revloc mine later became Bethlehem Steel's Mine 32 and Beth Energy operated the mine until it was closed in the 1980s.

REVLOC Site – Pre-1989

In 1989, Ebensburg Power Company obtained a surface mining permit from the PA DEP for the re- mining and reclamation of the western side of the Revloc coal refuse pile. The reclamation project required the processing of the coal refuse to produce usable fuel by separating out some reject material that could not be burned in the CFB. The larger sized reject material consisted of the rock, clays, and "red dog", or the material left from the in-place burning of the coal refuse over the last century.

The fuel was trucked to Ebensburg Power Company's coal refuse-fired power plant and used for the production of alternative electric energy. The fuel was combusted with limestone, which controls acid gases in a circulating fluidized bed boiler. The ash that that is produced meets all criteria for beneficial use for coal mine land reclamation. This beneficial use ash was returned to the Revloc site and mixed with the reject material, compacted and contoured as defined in the surface mining permit.

In 1997, at the request of the local townspeople and the PADEP, Ebensburg submitted and received a surface mining permit for the re-mining and reclamation of the eastern side of the Revloc coal refuse pile. This part of the coal refuse pile was burning and on days when the wind was blowing from the east, the fumes would inundate the Revloc community. As part of the re-mining and reclamation work, Ebensburg Power Company extinguished the fires and ended the air pollution from the coal refuse pile that had occurred over the last century.

That coal refuse pile contained approximately 4,120,000 tons of material and covered approximately 56 acres of land. The eastern and western parts of the pile were separated by the

South Branch of the Blacklick Creek. The runoff from the coal refuse pile would all flow into this creek resulting in the stream being devoid of aquatic life. The runoff from the coal refuse pile before reclamation discharged 226 tons per year of acidity, 0.5 tons per year of iron, 1 ton per year of manganese and 33 tons per year of aluminum.

The reclamation project was completed in 2011. During the project life, approximately 3,200,000 tons of usable coal refuse was removed from the site, and approximately the same number of tons of beneficial use ash was returned to neutralize the remaining acidic compounds contained in the reject material. The cost of the project was approximately $24 million.

The process reclaimed about 56 acres, of which 20 acres are available for industrial development. The coal refuse piles and fires are gone forever and approximately six miles of the South Branch of the Blacklick Creek has returned to a quality which supports aquatic life, including trout. The reclamation process reduced the acidity from the baseline by 93 percent, reduced iron by 92 percent, reduced manganese by 71 percent and reduced aluminum by 95 percent.

REVLOC Reclaimed

On December 12, 2008, the local paper, the Johnstown Tribune-Democrat, described and proclaimed the Revloc Reclamation Project as a "huge success".

MAPLE COAL SITE

Maple Coal Company – Colver Refuse Site, Barr and Blacklick Townships, Cambria County, PA

Elk Creek (North Branch of Blacklick Creek; Blacklick Creek; Conemaugh River; Kiskiminetas River; Allegheny River; Ohio River)

Maple Coal Company (Maple), a wholly owned subsidiary of Inter-Power/AhlCon Partners, LP, provides coal refuse fuel to the Colver Power Plant (located in Cambria County, Pennsylvania). The Maple Coal Company currently has three surface mining permits to mine coal refuse for use in their circulating fluidized bed boiler at the Colver Power Plant, the resulting alkaline ash is

beneficially utilized to reclaim the area previously occupied by the acidic coal refuse. During the mining and reclamation activities, "red dog" was encountered providing evidence that the coal refuse had previously burned in-place.

Site reclamation of the Colver refuse site began in 1995 and has continued to this date. The majority of the coal refuse has been removed and the vast majority of the alkaline coal ash placement has been completed in the areas that were producing the AMD related to the first two Surface Mining Permits (SMP). Maple is now developing the area related to third SMP which will address the last remaining source of AMD in this portion of the drainage basin.

Pre-1965 Coal Refuse Mining and Reclamation

The Subchapter "F" monitoring stations (SW-2B, SW-4A and SW-23) on the Colver Refuse Site SMP #11900201 and the Rail Yard Refuse Site SMP #11970201 provide evidence that the water quality was severely impacted by AMD prior to the commencement of Maple's reclamation operations. At the time of the original permit application, it was assumed that the removal of the acidic coal refuse and the beneficial use of the alkaline coal ash during their reclamation activities would improve the quality of the receiving stream (Elk Creek) by improving the water quality of the Subchapter "F" water monitoring stations (SW-2B, SW-4A and SW-23).

The pre-mining water quality from abandoned mine discharges to Elk Creek and its tributaries from the above referenced surface mining permits (abandoned coal refuse sites) accounted for 843.5 total tons of acidity, iron, manganese, and aluminum for the water samples collected and analyzed April 13, 1995, through April 8, 1996. The loadings in pounds per day is the average for the entire year based on twenty five samples/bi-monthly monitoring at each monitoring point.

Pre-Mining Loading on Elk Creek		
April 13, 1995 through April 8, 1996		
Acidity	689,149 lb/yr	344.6 tons/year
Iron (Fe)	23,932.9 lb/yr	11.97 tons/year
Manganese (Mn)	3,952.95 lb/yr	1.98 tons/year
Aluminum (Al)	47,779 lb/yr	23.89 tons/year
	TOTAL	**382.44 tons/year**

The most current data (December 18, 2013 through December 8, 2014) collected at these same monitoring stations indicate that the total tonnage of acidity, Fe, Mn, and Al is 1.0 tons or a reduction of 381.44 tons (99.73%). The loadings pounds per day is the average for the entire year based on thirteen samples, one sample per month per sampling point.

Post Refuse Removal – Site Utilization of Beneficial CFB Ash Placement		
December 18, 2013 through December 8, 2014		**% Improvement Over Baseline**
Acidity		99.9%
Iron (Fe)		97.6%
Manganese (Mn)		99.2%
Aluminum (Al)		99.9%
	TOTAL	**99.73%**

Present Coal Mining and Reclamation Activities

Homer City generating station, Lucerne Mines reclamation in foreground

refer to paper in the Guidebook: The Rogue Kimberlite Dikes in Indiana County, Pennsylvania
Part 1. Unusual Intrusive Habit of Kimberlite Dikes in Coal Seams

APPENDIX B

PETROGRAPHY OF THE TANOMA AND ERNEST KIMBERLITES

Thin sections of kimberlite collected from the Tanoma and Ernest mines were examined as a supplement to this paper. The rocks exhibit inequigranular, porphyritic textures of variable modal composition, including sedimentary xenoliths. In thin section the rock matrix is generally light gray to yellowish-gray, fine-grained and somewhat porous. A broad range of mineral sizes exists for those crystals not part of the rock matrix (groundmass), including olivine, phlogopite, garnet, picroilmenite, and orthopyroxene, all of which range from ~ 250 μm up to 8+ mm. The larger sizes can be extended up to 4+ cm if one includes crystals found in hand specimens. We refer to the non-matrix crystals as megacrysts and microcrysts to defer any genetic connotations; some of the large minerals are probably xenocrysts (crystals that grew earlier in a foreign magma) and others are likely kimberlite phenocrysts but their distinction is beyond the scope of this paper.

The predominant megacrysts observed in samples available in this work are olivine, phlogopite, and less commonly, picroilmenite. Garnet and orthopyroxene megacrysts have been reported previously (Mbalu-Keswa, 1995; Shultz, 1999) but none were recognized confidently in the thin sections examined here. Several serpentine pseudomorphs could be euhedral pyroxene crystals. The megacrysts are set in a matrix of mostly carbonate, opaque minerals (magnetite and perovskite), serpentine, and minor apatite. For olivine and phlogopite a continuum of size ranges occurs, along with a range of crystal forms (anhedral to rarely euhedral) for both minerals.

Olivine is almost entirely replaced by serpentine and subsequently by calcite. In a few serpentine pseudomorphs quartz was observed as a partial and latest stage replacement mineral. The rare patches of original olivine remaining in some cases contain a few needles of rutile that are likely to be primary inclusions (see discussion in Honess and Graeber, 1926). Iron oxides occur along fractures and, on some pseudomorphs margins.

Larger phlogopite crystals are better preserved than the olivines, although most also exhibit extensive replacement by serpentine, calcite, and less commonly by chlorite and late quartz. These crystals are commonly kinked and/or sheared, are generally anhedral with ragged margins, and commonly have magnetite and possibly other iron oxide minerals concentrated at their margins. Smaller phlogopite crystals (microcrysts) tend to be poorly preserved and most are completely replaced by chlorite (Honess and Graeber, 1926).

Picroilmenite megacrysts range in size from 1 to 7 mm, exhibit a jet black color, and show indications of conchoidal fracture under reflected light. Most crystals are generally well preserved.

The matrix of thin sections examined in this study is dominated by carbonate, most of which is calcite, although local dolomite crystals exist. Opaque minerals include magnetite and perovskite, irregularly distributed but common in the rock matrix. Both minerals are commonly 5-20 μm size, with larger clusters up to ~100 μm. Opaques can be concentrated

locally up to 10-15% or more in the matrix. The other major component of the Tanoma/Ernest kimberlite matrix is serpentine. A few prisms of partially replaced apatite were also observed. Shultz (1999) reported calcite-filled vesicular margins to some shale and coke inclusions as well as interstitial, irregular micro-vesicles. Several thin sections examined in our study have irregularly-shaped interstitial voids now filled with cryptocrystalline quartz and clusters of coarse calcite crystals. These probably correspond to Shultz's micro-vesicles.

Thin sections (TK-1b and TK-2b) from the Bragonier sill specimen (Figure 5a, 5b) shows an anomalous composition and texture. The rock consists mostly of subspherical grains (50-150 μm) set in a matrix of coarse-grained calcite. Although not well preserved, some grains resemble volcanic lapilli. Other grains are subangular and may be kimberlite and country rock fragments. A few long, arcuate fossil shells containing fibrous calcite crystals also are present. Their occurrence, and the fact that some subspherical grains exhibit complex internal structures (see Photograph 10), warrants a tentative classification as lapilli. Photograph 11 shows a fossil shell incorporated into the kimberlite sill. Clearly, further study of this rock is required.

No detailed point counting analysis was made in this work, but Schultz (1999) provided the following summary of modes for Tanoma, with textural components grouped into three broad categories and normalized to 100% by volume:

1.	**Megacrysts (26.1% total volume of rock)**	
	Olivine	52.4
	Garnet	11.7
	Mg Ilmenite	2.1
	Phlogopite	33.3
	Orthopyroxene	0.4
2.	**Matrix (64.7% total volume of rock)**	
	Olivine microphenocrysts	24.8
	Phlogopite	0.0[a]
	Magnetite + Perovskite	13.3
	Combined matrix minerals[b]	61.9
3.	**Carbonate veins + xenoliths (9.2% total volume of rock)**	
	[a] Small matrix phlogopite crystals were observed in the present study of Tanoma kimberlites.	
	[b] These include "pseudomorphous bodies of calcite, rare dolomite rhombs, sparse apatite prisms, and minor serpentine within very irregular web-like patches of calcite".	

Shultz's (1999) modal analysis is considered generally representative of the Tanoma specimens examined in this study. Typical of kimberlites, the proportions of minerals varies from sample to sample. The Ernest Mine kimberlite is comparable petrographically to the Dixonville rocks (Honess and Graeber 1926) and Tanoma dike (Mbalu-Keswa, 1995).

A distinct characteristic of the Tanoma kimberlite is the prolific amounts of carbonate present, an observation made by previous studies (e.g., Honess and Graeber, 1926; Mbalu-Keswa, 1995; Shultz, 1999). The most obvious concentration of carbonate occurs in the rock matrix, but it also exists as partial replacements of phlogopite and olivine megacrysts (and to a lesser extent in microcrysts) and as veins (see photos in Plate 1). In their examination of the Dixonville kimberlite ("mica peridotite") Honess and Graeber (1926) described carbonate occurrences in three categories, listed in order of abundance:

1. A fine-grained, almost structureless calcite that comprises the groundmass.
2. A massive, uniform carbonate, probably dolomite, possessing perfect rhombohedral cleavage and occurring as irregular, rounded to subangular patches, somewhat suggestive of crystal outline.
3. Small amounts of a coarsely granular aggregate of calcite or dolomite, forming pseudomorphs after olivine.

In our Tanoma specimens the matrix calcite (category #1) also forms veins that cut olivine and phlogopite macrocrysts.

The petrographic relationships described above lead to several conclusions. Kimberlites in general have substantial amounts of carbonate minerals (mostly primary, some secondary), with volume percents commonly in the 10-30% range (see Mitchell, 1985). In contrast, the Tanoma/Dixonville/Ernest kimberlites contain anomalous quantities of carbonates, with volumes of 30-40% being a conservative estimate and several samples exceed 50%. However, such concentrations are not unique among rare igneous rocks. Ultramafic lamprophyres, for example, are petrographic relatives to kimberlites and many also have large quantities of carbonate (Mitchell, 1985; Rock, 1990). With such high concentrations and the petrographic relationships described above the rocks are considered carbonatized (Rock, 1990). That much of this carbonate is primary magmatic calcite and/or dolomite is confirmed by isotopic data (e.g., Deines, 1968) and, therefore, it is not related to secondary sources such as groundwater. At Tanoma/Dixonville/Ernest the extensive amounts of matrix calcite, some of which cuts macrocrysts as veins, as well as the adjacent wall rocks, argues for late-stage carbonatization in dike and sill emplacement. The presence of excess volatiles (CO_2, H_2O?) is consistent with possible lapilli observed in some of the Tanoma sill specimens and vesicles. Given the large amounts of primary carbonates present, the Tanoma/Dixonville/Ernest rocks can be recognized as carbonatized kimberlites.

Examples of minerals and textural relationships in the Ernest and Tanoma kimberlites are described below for the accompanying images in Plate 1.

Photograph 1, Image 095833, Sample Ernest-3. Anhedral olivine megacryst completely replaced by serpentine and later calcite. Lath-shaped crystals are microcrysts and macrocrysts of phlogopite set in a calcite-rich matrix. Macroscopic view of thin section using reflected light. FOV = 9.7 mm wide.

Photograph 2, Image 171254, Sample Tanoma TK-7. Anhedral olivine macrocrysts and microcrysts set in a matrix of calcite, opaque minerals, and serpentine. Light blue area in the upper right corner is thin section epoxy. Macroscopic view of thin section using transmitted plane light. FOV = 9.7 mm wide.

Photograph 3, Image 170245, Sample Tanoma TK-4. Large altered phologpite macrocryst with minor shears and anhedral form at edge of sample. Macroscopic view of thin section using transmitted polarized light. FOV = 16.5 mm wide.

Photograph 4, Image 171004, Sample Tanoma TK-5. Olivine, phlogopite, and picroilmenite (mostly black anhedral crystal) macrocrysts. Macroscopic view of thin section using transmitted polarized light. FOV = 9.7 mm wide.

Photograph 5, Image 130531, Sample Tanoma TK-5. Jet black picroilmenite macrocryst. Matrix is calcite-rich and contains magnetite and minor perovskite, some of which forms partial rims on serpentinized olivines. Macroscopic view of thin section using transmitted plane light. FOV = 9.7 mm wide.

Photograph 6, Image 115604, Sample Tanoma PC1-1A. Phlogopite macrocryst replaced by serpentine, iron oxides, and matrix calcite. Macroscopic view of thin section using transmitted plane light. FOV = 9.7 mm wide.

Photograph 7, Image 132600, Sample TK-3. Phlogopite macrocryst with magnetite-rich rim and calcite veins (left arrow). Other crystals are enveloped in thick rims of calcite (right arrow). Macroscopic view of thin section using transmitted plane light. FOV = 9.7 mm wide.

Photograph 8, Sample 29. Olivine (upper left), garnet (lower center), and phlogopite (upper right) in a serpentine and calcite-rich matrix. Microscopic view in plane light, FOV = 3 mm wide.

Photograph 9, Sample Ernest 2. Phlogopite macrocryst (right), phlogopite microcryst (upper center), and degraded olivine (upper left) in a matrix of largely serpentine and calcite. Microscopic view in plane light, FOV = 3 mm wide.

Photograph 10, Image 115011, Sample PC1-1A. Olivine macrocrysts replaced and enclosed by thick mantles of calcite. Macroscopic view of thin section using transmitted polarized light. FOV = 9.7 mm wide.

Photograph 11, Image 172946, Sample TK-1b. Contact between kimberlite and siltstone wall rock. Arrows point to fossils (shrimp clam shells) in overlying siltstone and possible shell in the kimberlite. Macroscopic view of cut slab with reflected light. FOV = 21.3 mm wide.

Photograph 12, Image 171657, Sample TK-2b. Coquina with calcite matrix. Macroscopic view of cut slab with reflected light. FOV = 9.7 mm wide.

PLATE 1

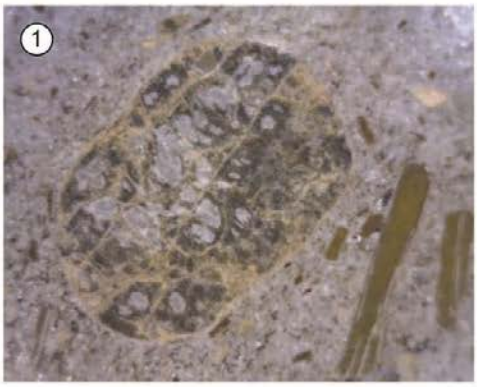

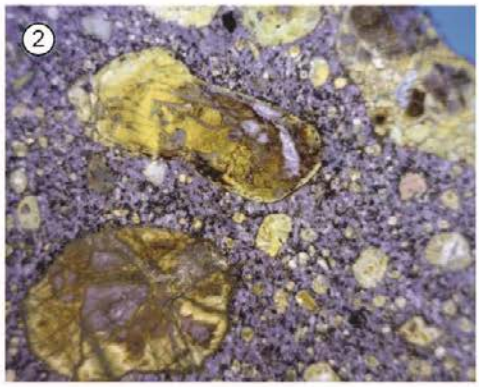

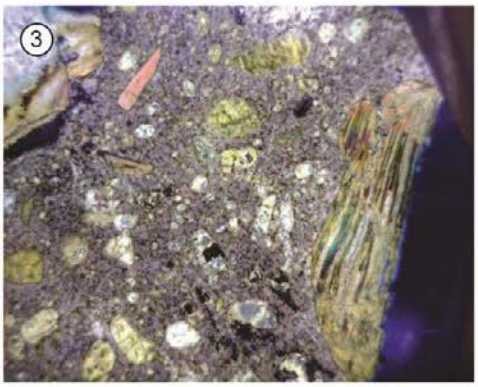

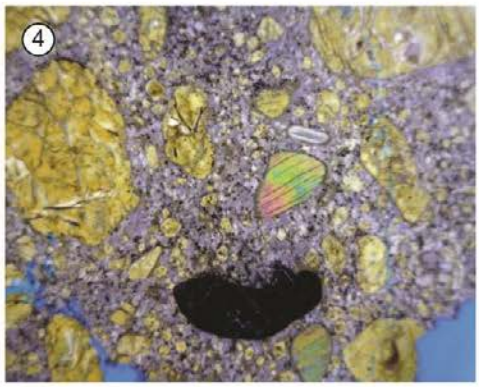

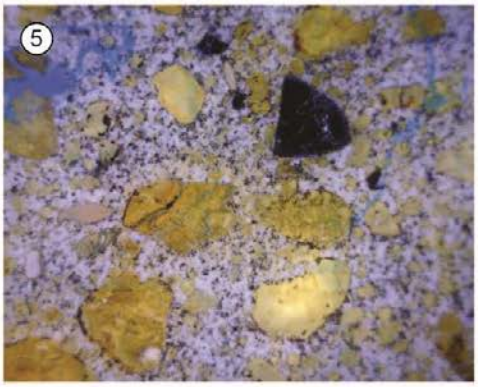

PLATE 1 continued

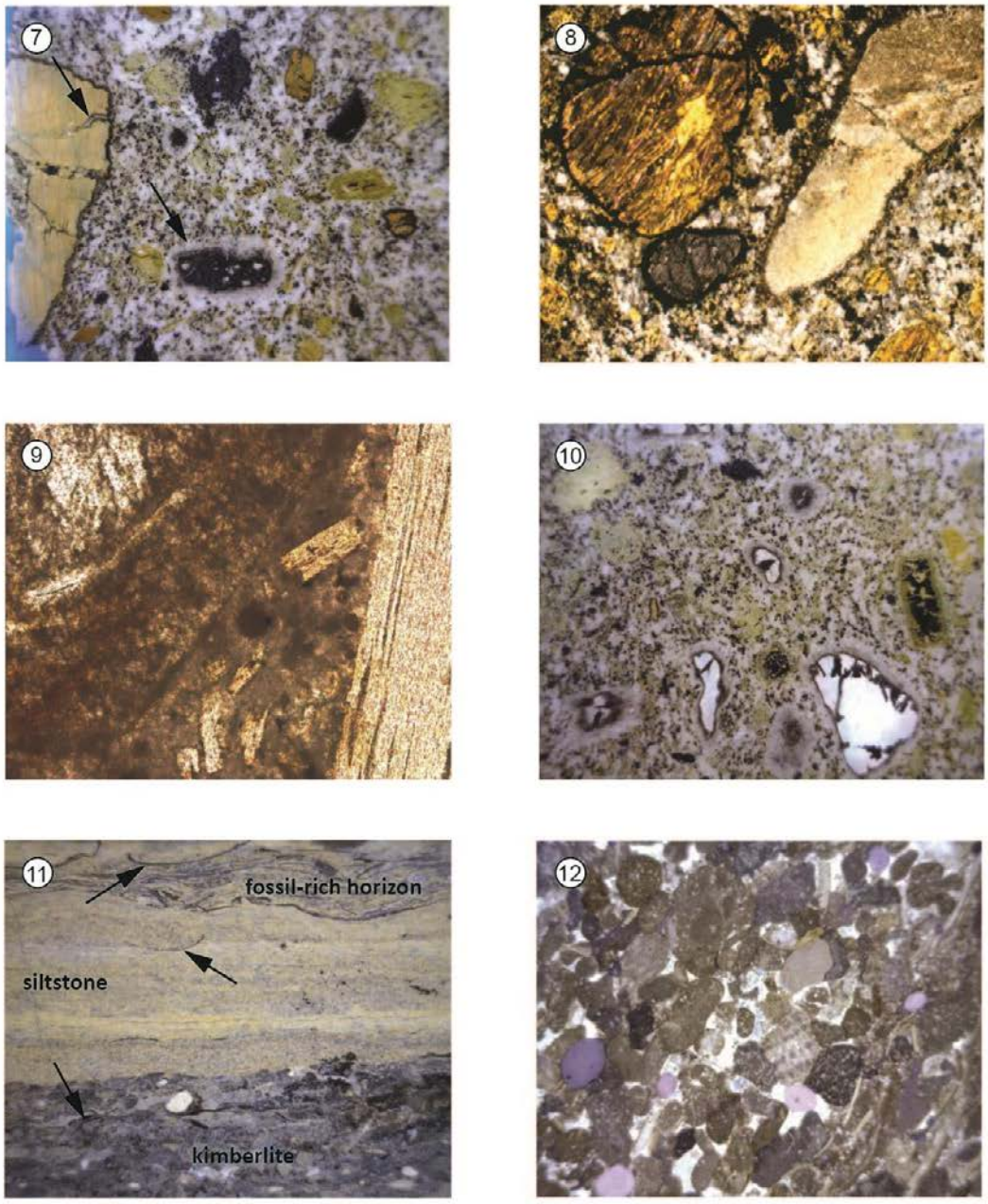

A SPECIAL THANK YOU TO OUR MANY INDIVIDUAL SPONSORS!

Kris Carter (Veronica Reynolds Fund)
Gary Ball
David Behringer
Emmanuel Charles
John Clarke
Marco Droese
Ellen Fehrs
John Giziewicz
John Harper*
Don Hoskins
Mark Ioos* (Skelly & Loy)
Ryan Kerrigan
Gary Kribbs*
Kent Littlefield*
Toni Markowski
Edgar Meiser*
Cole Miller
Don Monteverde*
Yuriy & Victoria Neboga/Vasyl Bohdanov
Sally Newcomb
Beverly Phillips
Barbara Rudnick (Bernice Pasquini Fund)
Stephen Urbanik
John Neubaum
Steve Shank
Jacqueline Hockenberry
Frank Pazzaglia
Patrick G. Bowling
William Bragonier
Susan Brown
William Bruck
Michael Campagna
Cliff Dodge
Mark Eschbacher
Kurt Friehauf
Andrew Frishkorn
William Gough*
Barbara Hanes*
Jon Inners
Andy Jenkins
John Kubala
Joseph Lee*
Walter Leis
George Love
Paul Martino
John Mason
Aaron O'Hara*
Charles Scharnberger
Vic Skema
Mindi Snoparsky*
John Stefl
Bill Stephens
Dakota Valle
Jay Winter

AND OUR GENEROUS CORPORATE SPONSORS!

Pennsylvania Mining Professionals (PMP)
McNaughton Bros / Allied Van Lines
Pennsylvania Council for Professional Geologists
(Recognition of Kris Carter)
American Geotechnical & Environmental Services
Mountain Research, LLC

**Denotes an individual who donated to both the Scholarship Fund and the General Fund*

80TH FCOPG 2015 GROUP PHOTO

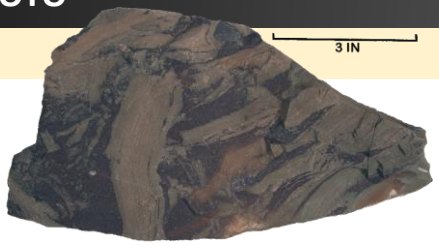

Brecciated Flint Clay from STOP 6